THE STRUCTURE AND PETROLOGY OF THE GULA GROUP, CENTRAL NORWEGIAN CALEDONIDES, WITH SPECIAL REFERENCE TO SULFIDE MINERALISATION - IMPLICATIONS TO THE GEOLOGY OF THE TRONDHEIM NAPPE.

David Ian Rainey, B.Sc.(Edinburgh).

Thesis submitted for the degree of
Doctor of Philosophy
University of Edinburgh
1980

DECLARATION

I hereby declare that this thesis has been composed by myself, and that the work contained is my own, except where specifically stated.

David I. Rainey.

ABSTRACT

The Trondheim Nappe outcrops over the greater part of the Trondelag region of central Norway, within which it is the highest unit of the Caledonian allochthon. The nappe is cored by the Gula Group, which outcrops centrally in Trondelag, and which is flanked by the stratigraphically equivalent Eastern and Western Trondelag successions. Immediately adjacent to the Gula Group, on its eastern and western margins respectively, are the metamorphosed basic volcanics of the Fundsjo and Storen Groups. The geological and geochemical characteristics of the Gula Group suggest close association with an island-arc system, while those of the Fundsjo and Storen Groups are consistent with an origin at a submarine spreading centre (possibly in a marginal basin). Juxtaposition of the Gula Group, and the Fundsjo and Storen Groups, by tectonic processes, may have occurred during the pre-Tremadocian Trondheim Orogeny. Subsequent to this event, the younger units of the Eastern and Western Trondelag successions were deposited, and emplacement of the Trondheim Nappe onto the Baltoscandian platform took place during the post-Llandoverian main Scandinavian Orogeny, as a result of closure of the Iapetus Ocean. North American faunas in the Western Trondelag succession indicate derivation from the Greenlandian continental margin.

Both copper-zinc and nickel-copper sulfide mineralisation occur in the Gula Group. The copper-zinc mineralisation is generally associated with metabasaltic horizons and is of volcanogenic origin. Application of the sphalerite geobarometer to deposits in the central parts of the Gula Group in southern Trondelag suggests metamorphic pressures of at least 6 kb, probably related to the Trondheim Orogeny. In contrast, pressures of 5 kb or less have been obtained from deposits in the Storen and Fundsjo Groups. Low pressure re-equilibration during the main Scandinavian Orogeny probably took place and pressures in excess of

9 kb may have been attained in the central parts of the Gula Group.

Nickel-copper sulfide mineralisation is associated with rare metagabbroic and ultramafic intrusions. The metagabbroic complexes were intruded before or during the Trondheim Orogeny. Where primary magmatic silicate assemblages have been found, mineral chemistry is consistent with available data from other gabbroic intrusions of tholeiitic character. The ultramafic bodies were emplaced after the metamorphic peak associated with the Trondheim Orogeny, but before the end of the main Scandinavian Orogeny. Petrological observations, together with consideration of whole-rock and mineral chemistry, suggest intrusion of a crystal-liquid mush containing olivine (with minor clinopyoxene) and a highly-magnesian liquid. The nickel-copper sulfide mineralisation is of magmatic origin, and assimilation of country-rock sulfur was probably responsible for saturation of the silicate magmas with respect to sulfur, and hence for the precipitation of the immiscible sulfide liquids. In many cases, however, subsequent metamorphism and deformation have resulted in considerable textural and chemical modification of the original ores.

CONTENTS

ILLUSTRATIONS

TABLES

CHAPTER 1

INTRODUCTION

1.1 The Scandinavian Caledonides.

The eastern part of the North Atlantic Caledonides is exposed in western Scandinavia over a longitudinal distance of about 1500 km and a width of 200-300 km (inset Map 2). It is underlain by Baltoscandian Precambrian crystalline basement from 1800 to 1000 my old. The Caledonides are known for the most part as a result of reconnaissance survey, and in general investigations are insufficiently advanced to give a safe foundation for a regional synthesis. The situation is further complicated by the Norwegian-Swedish border, which over a large area more or less symmetrically divides the orogen, and across which fundamental differences in stratigraphic and structural interpretation have evolved. It is now generally accepted, however, that a sequence of major nappe units have been translated from west to east onto the Baltoscandian Platform, with higher parts of the nappe pile being derived from west of the present Norwegian coast.

The area of south-central Scandinavia, from Ostersund in Sweden to Trondheim in Norway (Fig. 1.1), has been the subject of a special study in the context of the Inter-Union Commission on Geodynamics (Annersten, 1973). Gee (1975a, b, 1978) has attempted to present a coordinated model for this "geotraverse", which extends westwards from the eastern Caledonian Front to the Norwegian coast. He follows the convention established by earlier workers in the Scandinavian Caledonides (e.g. Hogbom, 1909) in treating the various rock units in two major categories: the Eastern Complex, and the Western Complex.

The Eastern Complex is composed of Precambrian crystalline basement overlain by a late Precambrian to Silurian sequence of sediments up to 2 km thick, and extends from the Caledonian Front to the Norwegian coast. The Western Complex, entirely allochthonous on the Eastern Complex, is

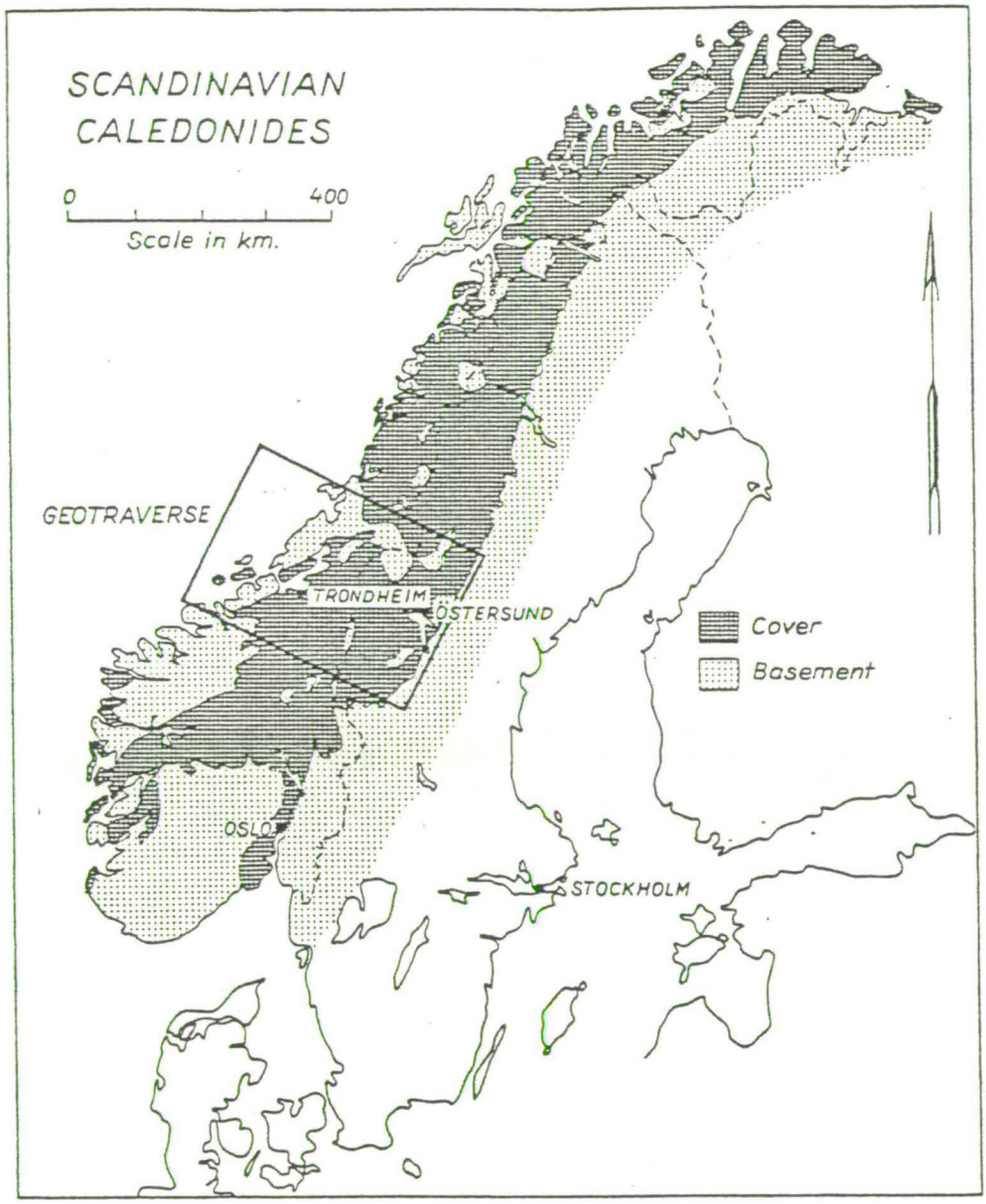

Fig. 1.1 Basement-cover relationships in the Scandinavian Caledonides and location of the "geotraverse" area. (Taken from Gee, 1978).

composed of a basal unit, the Sarv Nappe; a central unit, the Seve-Koli Nappe complex; and an upper unit known variously as the Upper Nappe (Springer-Peacey, 1964; Gee, 1975a, b; 1978) and the Trondheim Nappe (Kulling, 1961; Wolff, 1967a; Roberts et al., 1970). Table 1.1 summarises the tectonic and stratigraphic units in the "geotraverse" area.

The major allochthonous units, the Offerdal and Western Complex Nappes, have been displaced eastwards from environments along, and to the west of the present Norwegian coast. Gee (1978) suggests that nappe displacement distance is in the order of 1000 km, although he emphasises that actual translation may account for only about one half of this amount, the rest being achieved by stretching of the nappes. He suggests that a nappe pile was built up in the west from Early to Mid Silurian, which lead subsequently to a gravitational collapse and stretching of the nappes together with continued displacement eastwards onto the Baltoscandian Platform during the Late Silurian to Early Devonian. From Early to Mid Devonian the Caledonian Frontal zone was affected by decollement tectonics with cover shortening in the Eastern Complex in excess of 70 km (the parautochthon - Table 1.1).

1.2 The Gula Group

The highest unit in the allochthon outcrops in the western part of the "geotraverse" area over the greater part of the Trondelag region (Map 1), and will hereafter be referred to as the Trondheim Nappe after Kulling (1961) and Wolff (1967a).

The regional stratigraphy within the Trondheim Nappe, comprising the Trondheim Supergroup (Table 1.1), was initially established in the classical Holanda-Horg area in western Trondelag by Vogt (1945) who described five groups:

TECTONIC UNITS			STRATIGRAPHY and LITHOLOGIES	
LATE-OROGENIC SEDIMENTS			HITRA FORMATION and overlying Ludlovian (?) to Middle Devonian sediments	
WESTERN COMPLEX	Low meta. grade	"Upper Nappe"	TRONDHEIM SUPERGROUP	Silurian (?), Ordovician, Cambrian (?), and (?) older sediments and volcanic rocks
	High meta. grade			
	Low meta. grade	Seve-Köli Nappe Complex	KÖLI SUPERGROUP	Silurian, Ordovician, and (?) older sediments and volcanic rocks
	High meta. grade		SEVE SUPERGROUP	
	Low meta. grade	Särv Nappe	SÄRV GROUP (locally on basement)	Late Precambrian sediments Dolerite dike-swarm Precambrian crystalline rocks
EASTERN COMPLEX	Allochthon	Offerdal (Granite-mylonite, Alsen and Fuda) Nappes	CRYSTALLINE BASEMENT and RISBÄCK GROUP	Late Precambrian sediments and Precambrian crystalline rocks
	Parautochthon	Lower nappes of Jämtland including Olden Nappe	JÄMTLAND SUPERGROUP (locally on basement)	Silurian, Ordovician, Cambrian, and late Precambrian sediments Precambrian crystalline rocks
	Autochthon	Stable platform	JÄMTLAND SUPERGROUP BASEMENT	Ordovician and Cambrian sediments Precambrian crystalline rocks

TABLE 1.1 Summary of tectonic and stratigraphic units in the "geotraverse" area.

(Taken from Gee, 1975b).

a) Gula Group - age uncertain but pre-Tremadocian

b) Storen Group - age uncertain but pre-Tremadocian

c) Lower Hovin Group - Lower to Upper Ordovician

d) Upper Hovin Group - age uncertain, assumed Upper Ordovician to Lower Silurian

e) Horg Group - age uncertain, assumed Lower Silurian.

In eastern Trondelag probable stratigraphic correlatives of these groups are known (Wolff, 1967a) as the Sonvatn Group (Gula); Fundsjo Group (Storen); Sulamo Group (Lower Hovin); Kjolhaugen Group (Upper Hovin); and Slagan Group (Horg). These successions are known as the Western and Eastern Trondelag successions respectively and are shown on Map 1.

The Gula Group occupies the central part of the Trondelag region, resting on the Fundsjo Group in the east and in contact with the Storen Group in the west (Map 1). It crops out over some 300 km from the district of Snasa in the north to that of Dombas in the south, and has its maximum E-W extent of over 50 km in the area of Gauldalen (place names are located on Map 2). In western Trondelag there is considerable controversy over the possible outcrop of the Gula Group. However, it will be suggested later in this thesis (Chapter 3) that a thin sliver of Gula Group less than 1 km in thickness, discontinuously separates the younger part of the Western Trondelag succession from the lower tectonic units of the Seve-Koli Nappe complex further to the west (Map 1).

The Gula Group consists of intensely deformed psammitic, calcareous, graphitic, and pelitic schists, with subordinate amphibolites and rare bodies of metagabbroic and ultramafic affinities. Sulfide mineralisation occurs dominantly in association with the amphibolites and the metagabbroic and ultramafic masses, and rarely in the schists themselves. Fossil remains are lacking but a Cambrian age has previously been assumed by reason of Tremadocian graptolites reported from the Sulamo Group in

eastern Trondelag, close to the contact with the Fundsjo Group (Vogt, J. H. L., 1889; Vogt, T., 1941; Stormer, 1941; Wolff, 1967b, 1976).

The Storen and Fundsjo Groups consist dominantly of metamorphosed basic volcanics while the overlying units of the Eastern and Western Trondelag successions are composed of a variety of metasediments and more felsic volcanics.

In the Trondheim Nappe metamorphism reaches upper amphibolite facies in the central parts of the Gula Group, and decreases symmetrically outwards and upwards through the nappe to lower amphibolite/greenschist facies in the Storen and Fundsjo Groups and greenschist or lower facies in the higher units.

At present there is considerable controversy over:

a) the regional outcrop distribution of the Gula Group

b) the structural relationships between the various units of the Trondheim Nappe, and

c) the large scale structure of the nappe itself.

In general the Gula Group is poorly exposed. The terrain has been dissected by a series of deep glacial valleys, which in general trend NW-SE. Valley floors are intensely cultivated and sparsely but continuously populated. In contrast, the valley slopes have a dense covering of pine forest while the intervening high ground, although unforested, is commonly blanketed with a thick covering of glacial debris.

1.3 Sulfide Mineralisation

Sulfide mineralisation in the Gula Group may be divided conveniently into two types: copper-zinc mineralisation of amphibolite association; and nickel-copper mineralisation of metagabbroic and ultramafic association.

1.3.1 Copper-zinc mineralisation.

Ores of this type have been mined from many small deposits within the Gula Group. From 1632 when the deposits at Kvikne were first exploited two main periods of production occurred.

Between 1650 and 1750 three independent smelting works, at Kvikne, Soknedal and Budal, were established for the production of copper. The Kvikne works became the largest industrial enterprise in the region, with twelve smelters operating on the River Orkla during this first era. The Naverdal smelter was finally closed down in 1872. First mention of the ores was by Voss (1783) in a review of Norwegian ore deposits, while Helland (1902), Falck-Muus (1932); Enmo (1935); and Storen (1951) provide historical accounts of the development of the mining and smelting industry in the region.

Following a decrease in activity in the 19th century, a second period of mining was initiated at the beginning of this century. A number of old mines were revived, including those at Kvikne, and new mines, such as those at Rostvangen, were brought into operation. Production ceased abruptly during the world-wide recession of the nineteen-twenties, until the Undal mine was reopened in 1952. Since 1971, when the Undal mine was finally abandoned, there has been no exploitation of Gula copper-zinc sulfide mineralisation.

The origin of the Gula copper-zinc deposits has been the subject of extensive arguement in the geological literature. In general two schools of thought have prevailed. Authors such as Nilsen and Mukherjee (1972) emphasise the structural control of the orebodies, together with the presence of wall-rock alteration, and suggest an epigenetic origin; while others such as Vokes and Morton (1973) argue that such features are not inconsistent with deformed and metamorphosed syngenetic volcanogene deposits. More recently the syngenetic model has received general acceptance (Nilsen, 1978).

1.3.2 Nickel-copper mineralisation.

A number of small metagabbroic and ultramafic bodies in the Gula Group are associated with nickel-copper mineralisation. Minor production has taken place from the Skjaekerdalen metagabbro complex in northern Trondelag, and from the Olkar and Vakkerlien metagabbros and the Kaltberget ultramafic in southern Trondelag.

The petrology and some aspects of the geochemistry of the host rocks has been described by Nilsen (1974) who suggests a primary magmatic origin for the sulfide mineralisation. The Vakkerlien metagabbro has been the subject of a detailed study by Thompson (1978), who proposes a model involving the intrusion and differentiation of a basic sheet containing an immiscible sulfide magma. Subsequent deformation and metamorphism control the present shape, orientation, and spatial relationships of the various rock types.

1.4 The Project.

During the nineteen-sixties Falconbridge Nickel Mines Limited set up a small exploration company, A/S Sulfidmalm, to explore for base metals in Norway. The Gula Group drew immediate attention. Initial exploration was centred around the old mines and showings of amphibolite association. A short drilling programme, however, revealed no ore of economic potential and attention moved to the showings of metagabbroic and ultramafic association. In 1974 grab samples from the Vakkerlien showing returned good nickel assays and intensive geophysical exploration was instigated over the area. This resulted in a drilling programme in the summer of 1975 which proved a mineralised zone of 1250 m length with an elliptical cross-section of average width 25 m and average depth 5 m, lying down the centre of a similarly shaped and aligned metagabbro body. Using a 0.4% Ni cut-off, a body of 380000 tonnes of average

grade 1.08% Ni and 0.39% Cu was outlined. The success of this drilling lead to an extension of the exploration programme to cover all known metagabbro and ultramafic bodies within the Gula schist.

At this stage a research programme was initiated to describe the various types of sulfide mineralisation occurring in the Gula Group and to investigate their origin. The programme consists of two parts. Thompson (1978) has investigated the systematically cored Vakkerlien prospect, while the project forming the basis of this thesis involves a regional investigation of the Gula Group with particular reference to the sulfide mineralisation.

The objectives of the project are summarised as follows:

a) To investigate the regional geology of the Trondheim nappe with special reference to the Gula Group, and its relationship to adjacent units.

b) To describe the various types of sulfide mineralisation and their host rocks, and to elucidate their origin.

A total of seven months field work was carried out during the summers of the years 1976-1978. As a result of the vast area over which the Gula Group outcrops, it has not been possible to achieve the first objective on anything but a reconnaissance basis. To this end five profiles across the Gula Group and adjacent units have been mapped at a scale of 1:50000. The profiles, the localities of which are indicated on Map 2, follow the major NW-SE trending valleys previously described, allowing utilisation of good exposure offered by road and railway construction. The results of this investigation are presented in Chapter 3, together with implications to the geology of the Trondheim Nappe which is reviewed in Chapter 2. To compliment this study the petrology and geochemistry of the copper-zinc mineralisation associated with the Gula amphibolites has been compared with similar mineralisation

occurring in the metavolcanics of the adjacent Storen and Fundsjo Groups. A reconnaissance investigation of host-rock geochemistry has also been carried out. These aspects form the basis of Chapter 4. Structural relationships between the metagabbroic and ultramafic host rocks to nickel-copper mineralisation and their enclosing country rocks have been investigated, where exposure permitted, by mapping over their areas of outcrop at 1:10000 or 1:5000 scales, and by logging of drill core where available. Collection of samples for petrological and geochemical investigation was carried out from surface exposure, dumps, and where possible, from drill core. The petrology and geochemistry of the host rocks are presented in Chapter 5, together with consideration of ore genesis. The geochemistry of the sulfide mineralisation is presented and discussed in Chapter 6, and the conclusions of the thesis are summarised in Chapter 7.

This project has been carried out at the Grant Institute of Geology, University of Edinburgh, under the supervision of Dr. K. R. Gill.

CHAPTER 2

THE GEOLOGY OF THE TRONDHEIM NAPPE - A REVIEW

Wolff (1960, 1964) and Springer-Peacey (1964) pointed out that the Cambro-Silurian rocks in the northern Trondelag region are separated from the basement by a major thrust plane. Springer-Peacey (1964) interpreted the rocks above this thrust as constituting an "upper nappe" with a higher tectonic level than the Seve-Koli Nappe Complex, the highest tectonic unit outcropping in Sweden (Gee, 1975 a, and b). Wolff (1967a) extended this thrust to surround all of the Cambro-Silurian rocks of the Trondelag region and suggested the name "Trondheim Nappe" for the rocks lying above it (after Kulling, 1961). The extent of the nappe and its relationship to underlying units are shown on Map 1.

To the south and southeast the Trondheim Nappe rests on the Eocambrian felspathic sandstone sequence known as "the sparagmites" (Skjeseth, 1963; Bjorlykke, 1974; Roberts, 1978). Gee (1975a) broadly correlates this sequence with the basal part of the Jamtland Supergroup of Sweden. The sediments are apparently autochthonous on the Precambrian crystalline basement (Gee, 1975a). To the east the nappe is underlain by both basement and Jamtland Supergroup sediments which are locally allochthonous, while to the northeast it lies on the high-grade Seve amphibolites of the Seve-Koli Nappe Complex (Table 1.1; Gee, 1975 a, and b, 1978). At its most northern extent the Trondheim Nappe is cut out by the Grong-Olden culmination, bringing it in contact with the allochthonous basement of the Offerdal and associated nappes (Gee, 1974). To the west, the Cambro-Silurian sequence rests largely on Seve amphibolites, but locally on parautochthonous crystalline basement (Gee, 1975 a, and b, 1978).

The Trondheim Nappe is the principal tectonic unit outcropping in

the Trondelag region. The distribution of the various stratigraphic units within the nappe, comprising the Trondheim Supergroup (Table 1.1), are shown on Map 1. The central zone is occupied by the high-grade schists of the Gula Group, and flanked by lower-grade volcanics and sediments, which in general, dip to the west in the east, and to the east in the west beneath it. These are the Eastern and Western Trondelag successions respectively.

2.1 The Gula Group.

On its eastern and western flanks the Gula Group structurally overlies the metavolcanics of the Fundsjo and Storen Groups respectively. It is composed of psammitic, pelitic, calcareous, and graphitic schists with subordinate amphibolites and intrusive bodies of ultramafic and metagabbroic affinities. Intense deformation, high-grade Barrovian metamorphism, and local migmatisation have obscured most of the internal stratigraphy. However, despite this, Nilsen (1978) describes the Gula Group in southern Trondelag as composed of a central core of calcareous quartz-biotite schists and gneisses, often interlayered with calc-silicate horizons and graphitic quartzites. This central Singsas Formation is flanked by zones of grey, commonly graphitic, biotite-phyllite, the Asli Formation in the east and the Undal Formation in the west. Olesen et al. (1973) report a similar distribution of lithologies in the area between Selbu and Tydal but refrain from suggesting any formational subdivisions.

The Guda conglomerate (Wolff, 1964), included in the Asli Formation by Nilsen (1978), outcrops in the valley of the River Stjora (Map 2) some 2-3 km west of the Gula/Fundsjo contact, and has been traced northwards as far as the Inna valley, where it occurs adjacent to this boundary (Dudek et al., 1973). Olesen et al. (1973) report a

conglomeratic zone in a similar position in the Selbu-Tydal area and suggest a correlation. The conglomerate is in general polymict, containing quartzite, metabasic, and marble pebbles. Olesen et al. (1973) have recorded a similar conglomeratic lithology at Blomlia, near the Gula/Storen contact.

Amphibolite horizons are common throughout the Gula Group, and are found at any position within it.

The Gula Group has generally been accepted as being older than the flanking volcanics by reason of its higher metamorphic grade, and the evidence for age relationships within the adjacent Eastern and Western Trondelag successions. In general these suggest younging away from the Gula Group.

At Nordaunevoll, in eastern Trondelag, a single exposure of black shale has yielded the Tremadocian graptolite Dictyonema flabelliforma (Vogt, J. H. L., 1889; Vogt, T., 1941; Stormer, 1941). The locality occurs some 300 m eastwards of the eastern limit of the Fundsjo Group (Maps 1 and 2) in an area included in the Gula Group by Rui (1972), but regarded by Wolff (1967b, 1976) as part of the Sulamo Group. According to Rui (1972), the metavolcanics of the Fundsjo Group close to the Nordaunevoll locality are dominated by a blue-green hornblende and a sodium-rich plagioclase together with minor epidote, chlorite, carbonate, and biotite. This assemblage is typical of epidote-amphibolite facies metamorphism (Miyashiro, 1968), and the preservation of graptolite remains in the adjacent black shales is therefore problematical. However, it will be suggested later in this chapter and in Chapter 3 that the boundary between the Fundsjo and Storen Groups and the higher units of the Trondelag successions represents a non-conformity; the Gula, Storen and Fundsjo Groups having suffered earlier deformation and metamorphism. With this proviso, if the Nordaunevoll

locality is included in the Sulamo Group, the problem of the high-grade Fundsjo volcanics no longer arises. Wolff's (1967b, 1976) correlation is therefore favoured in this thesis, and consequently the Gula Group, together with the Fundsjo and Storen Groups is regarded as pre-Tremadocian in age.

There has been considerable argument in the literature as to the possible outcrop of the Gula Group at the base of the Trondheim Nappe in western Trondelag, and on the flanks of the Tommeras basement window (Map 2). Wolff (1967b) identified the high-grade rocks outcropping on the shores of Trondheimsfjord between Buvika and Orkanger, and extending southwestwards towards Surnadal, as garnet-bearing mica schists. He considered them direct equivalents of the Gula Group and part of the Trondheim Nappe. Similar relationships are suggested for apparently identical rock-types separating the Storen metavolcanics from the Lekstalsvann sediments (Springer-Peacey, 1964) exposed in the Tommeras basement window (Wolff, 1964, and in Springer-Peacy, 1964). With regard to the controversial rocks in Western Trondelag, Wolff (1976) subsequently preferred to regard them as high-grade equivalents of the Storen Group. These proposals are refuted by Gee (1977, 1978), who prefers to correlate these high-grade lithologies with the Seve Supergroup of the Seve-Koli Nappe Complex, on the basis of lithological similarity (both composition and metamorphic grade) and structural continuity. These possibilities have been investigated in the field and will be discussed in more detail in Chapter 3.

2.2 Stratigraphy.

2.2.1 Stratigraphy of the Western Trondelag succession.

Vogt (1945) established the stratigraphy of the Western Trondelag succession in the classical Holanda-Horg area (Table 2.1). The succession

lies in an isoclinal structure, the Horg Syncline, and is dominated in its lower part by the basaltic metavolcanics of the Storen Group, and in its upper part by the sediments and subordinate volcanics of the Hovin and Horg Groups.

2.2.1.1 The Storen Group - The Storen Group is dominated by metabasaltic greenstones, often displaying pillow structures, with lesser pyroclastics and acid volcanics. Cherts, limestones, and other intercalated sediments occur locally. Trondhjemite and gabbroic intrusives are common and serpentinites have been reported (Gee, 1975b).

Fossils have not been recorded from the Storen Group; its age is therefore inferred from fossil evidence in the adjacent Lower Hovin Group. Blake (1962) considered the Lower Krokstad shale (Table 2.1) as being of middle Arenigian age on the basis of its graptolite fauna. Berry (1968) drew attention to the American affinities of this fauna and correlation elsewhere suggests a latest Arenig or lowermost Llanvirnian age (Dewey et al., 1970). Further, Newman and Bruton (1974) have described Llanvirnian faunas from the Holanda limestone near the base of the Lower Hovin Group. The Storen must therefore be Arenigian or pre-Arenigian in age. Correlation with the Fundsjo Group in eastern Trondelag, however, suggests a pre-Tremadocian age.

2.2.1.2 The Lower Hovin Group - The base of the Lower Hovin Group is dominated by boulder conglomerates which have been given various local names, for instance, the Stokvola and Venna conglomerates. Clasts are angular and appear to be derived from the Storen Group, being dominated by greenstones with lesser felsic volcanics, cherts and other sediments. These boulder conglomerates pass upwards into pebbly horizons interspersed with finer volcanogenic sediments, themselves giving way to the parallel-bedded volcaniclastic turbidites of the Krokstad Formation, which are intercalated with the fossiliferous shales (Blake, 1962) and limestones (Strand, 1948; Newman and Bruton,

Table 2.1 Stratigraphies of the Eastern and Western Trondelag successions. F - denotes fossiliferous unit.

			Western Trondelag Holanda-Horg (Vogt, 1945)		Eastern Trondelag Meraker (Chaloupsky, Fediuk , Siedlecka, Wolff, 1967)
SILURIAN	Llandoverian		HORG GROUP - Sanda shale and sandstone; Lyngestein conglomerate at base.	(F)	SLAGAN GROUP - black phyllite and sandstone.
ORDOVICIAN			UPPER HOVIN GROUP - Hovin sandstone and Grimas rhyolite; Volla conglomerate at base		
	Caradocian	(F)	LOWER HOVIN GROUP - Tomme beds and rhyolitic tuff.		SULAMO GROUP - grey and black phyllites with
	Llandeilian		Svarttjern limestone; Krokstad sandstone and Upper Krokstad shale.		calcareous sandstones
	Llanvirnian		Holanda andesite		basic volcanics
		(F)	Holanda limestone		
	Arenigian	(F)	Lower Krokstad shale and breccia		
	Tremadocian			(F)	(Dictyonema) black shales (Roros district, Vogt, 1941)
			Venna conglomerate at base		Lille Fundsjo conglomerate at base
? CAMBRIAN ?			STOREN GROUP - dominantly basic volcanics and pyroclastics, subordinate terreginous sediments, limestones and cherts.		FUNDSJO GROUP - basic volcanics and pyroclastics.
			GULA GROUP Undal Formation Singsas Formation		GULA GROUP (SONVATNE GROUP) Asli Formation Singsas Formation

1974) previously mentioned.

Higher in the Lower Hovin succession limestones, shales, rhyolitic tuffs, and conglomerates occur. The Tomme shale marks the top of the Lower Hovin Group and has yielded the graptolites Dicranograptus clingani and Pleurograptus linearis of Caradocian age (Vogt, 1945; Strand, in Strand and Kulling, 1972, pp. 56).

2.2.1.3 The Upper Hovin Group - The Upper Hovin Group consists of a basal polymict conglomerate, referred to as the Volla conglomerate, which contains clasts of both Storen and Precambrian basement derivation. The conglomerates, locally overlain by rhyolitic volcanics, give way to the turbiditic greywackes of the Hovin sandstones. Fossils are unrecorded in the Upper Hovin Group, but a late Caradocian or younger age is inferred from those occurring in the underlying Lower Hovin Group (Vogt, 1945).

2.2.1.4 The Horg Group - The Horg Group consists of a basal nearly monomict quartzite conglomerate (the Lyngestein conglomerate) which passes upwards into the greywacke sandstones of the Sanda Formation. Fossil evidence is lacking but a Llandoverian age is inferred from faunas in the Lower Hovin Group (Vogt, 1945), and by correlation with the Slagan Group in eastern Trondelag (Chaloupsky and Fediuk, 1967; Siedlecka and Siedlecki, 1967; Wolff, 1967a).

2.2.2 Stratigraphy of the Eastern Trondelag succession.

The Eastern Trondelag succession has been established in its northern part by Chaloupsky and Fediuk (1967), Siedlecka (1967), and Siedlecka and Siedlecki (1967); and in its southern part by Rui (1972). The sequences are directly correlatable and will be described using the terminology of Chaloupsky and Fediuk (1967). A summary of the stratigraphy, together with a suggested correlation with the Western Trondelag succession is shown in Table 2.1.

Fossil evidence in the Sulamo (2.1) and Slagan Groups together with evidence of sedimentary structures, such as graded bedding, load casts, and small-scale cross-bedding requires that this westerly dipping sequence is inverted (Wolff, 1967a; Siedlecka, 1967; Chaloupsky and Fediuk, 1967; and Rui, 1972). The oldest part of the succession is represented by the Fundsjo Group (Hersjo Formation - Rui, 1972) basic volcanics which give way to the sediments and rare volcanics of the Sulamo, Kjolhaugen, and Slagan Groups (Kjurundal and Saetersjo Formations, Roros Group, and Hummelfjell Formation respectively - Rui, 1972).

2.2.2.1 The Fundsjo Group - The Fundsjo Group consists of a suite of meta-volcanic rocks of generally basic character and locally with relict pillow structures. Keratophyric lithologies are common, but as these can often be traced into pyroclastic horizons they probably represent original tuffaceous lithologies (Oftedahl, 1967, 1968). The Fundsjo Group is believed to be older than Tremadocian in age on the basis of the Dictyonema-bearing black shales at the base of the Sulamo Group (2.1).

2.2.2.2 The Sulamo Group - East of the Fundsjo Group, and structurally underlying it, the Sulamo Group is dominated by grey-green phyllites and greywacke sandstones. Limestones and conglomerates are locally present. A basal conglomerate, the Lille Fundsjo conglomerate serves to separate the two groups. According to Sturt (1975), this horizon is dominated by foliated clasts of Fundsjo Group metavolcanics; the foliation is randomly orientated. The implications of these observations will be discussed later in this chapter. The Dictyonema-bearing black shales, close to the contact with the Fundsjo Group at Nordaunevoll, have already been described (2.1), and a Tremadocian and younger age is indicated for this group.

2.2.2.3 The Kjolhaugen Group - Siedlecka (1967) has described this unit in some detail. It lies structurally below the Sulamo Group and consists of greywackes, sandstones, phyllites and minor conglomerates. The upper part of the Group is intruded by concordant metagabbros.

2.2.2.4 The Slagan Group - This unit is dominated by black phyllites intercalated with greywacke sandstones and shales. The contact between this group and the Kjolhaugen Group is probably transitional (Siedlecka, 1967). Getz (1890) recorded the presence of Silurian graptolites in the Slagan phyllites. Examples of the species Monograptus and Rastrites have been identified (Kiaer, 1932) indicating a Llandoverian age.

2.3 Metamorphism.

In general the metamorphism of the Trondheim Nappe may be described as decreasing symmetrically about the central parts of the Gula Group, where the higher grades of amphibolite facies metamorphism are attained, together with local migmatisation. A summary map, compiled from the data presented below, is given in Fig. 2.1.

Goldschmidt's (1915) map of the southern and central parts of the Trondelag region, in which he delineated metamorphic zones based on the index minerals chlorite, biotite, and garnet, has yet to be superceded. These zones lie symmetrically about a central region of calc-silicate bearing schists corresponding to the Singsas Formation defined by Nilsen (1978). Strand (1960) suggested that the chlorite zone corresponds to greenschist facies metamorphism, the biotite and garnet zones to epidote-amphibolite facies, and the calc-silicate schists to almandine-amphibolite facies. Amphibolite facies has thus been attained in the central parts of the Gula Group, but only upper epidote-amphibolite facies (garnet zone) on its flanks. The Storen and Fundsjo Groups lie

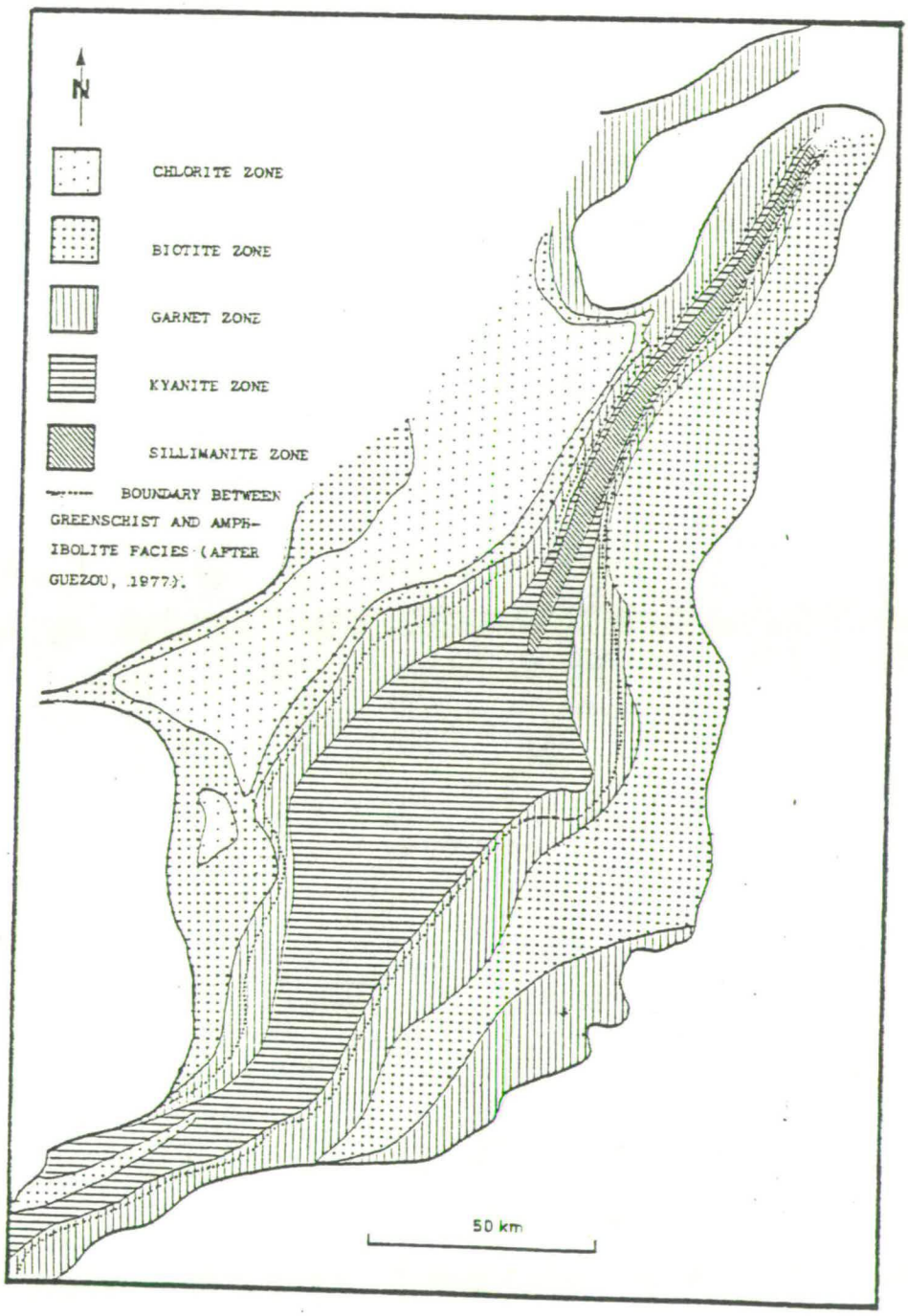

Fig. 2.1 Metamorphic zonal map of the Trondheim Nappe. Data from: Goldschmidt (1915); Strand (1960); Wolff (1960); Chaloupsky and Fediuk (1967); Siedlecka (1967); Roberts (1968); Dudek et al., (1973); Olesen et al., (1973); Guezou (1977).

dominantly in the lower epidote-amphibolite (biotite zone) or greenschist facies. The Hovin and Horg Groups of the Western Trondelag succession, and the Sulamo, Kjolhaugen, and Slagan Groups of the Eastern succession usually exhibit lower epidote-amphibolite or greenschist facies metamorphism.

Olesen et al. (1973) have investigated the metamorphism of the Gula Group and adjacent units in the area between Selbu and Tydal in central Trondelag. They delineate a central sillimanite zone, in the interior of the Gula Group, flanked by symmetrical staurolite-kyanite, garnet-hornblende, and biotite zones. The Storen and Fundsjo Groups lie in the biotite zones. On the basis of mineral assemblages and particularly on the direct replacement of kyanite by sillimanite, they suggest that pressures of 7-8 kb and temperatures of 600-700^{o}C were reached.

In a study of the Gula Group in central Trondelag, Roberts (1968) pointed out that while in many places hornblende is the sole porphyroblastic mineral, garnet, staurolite, and kyanite may also occur. Furthermore, in a study of the Stjora valley he reports the occurrence of a narrow sillimanite bearing zone some 3 km to the west of the Gula/Fundsjo contact. From the mineral assemblages he suggests derivation in the highest temperature sillimanite-almandine-orthoclase sub-facies of the almandine-amphibolite facies.

Chaloupsky and Fediuk (1967) in a detailed study of the Eastern Trondelag succession in the Meraker area confirm the observations of Goldschmidt (1915), and Strand (1960). They conclude that the succession has attained the quartz-albite-epidote-biotite sub-facies of the greenschist facies with a general decrease in grade eastwards. Siedlecka (1967) in a related study slightly to the south and east of that of Chaloupsky and Fediuk (1967) points to an increase in biotite and epidote

westwards towards the Fundsjo Group and suggests the possibility that this group has attained epidote-amphibolite facies.

The metamorphism of the Gula Group between the Stjora and Inna Rivers has been described by Dudek et al. (1973). A central sillimanite zone, up to 5 km across, and associated with local migmatisation, coincides with the central parts of the Gula Group, and is flanked by zones of lower metamorphic grade. This pattern extends northwards into the valley of the River Helgaa, as described by Wolff (1960).

A review of the variation in metamorphism exhibited by the Trondheim Nappe has been presented by Guezou (1977).

2.4 Structure.

The structure of what is now regarded as the Trondheim Nappe has been disputed by many authors. A summary of the various models is presented in Fig. 2.2.

Early descriptions of Trondelag geology were given by Keilhau (1850) and Kjerulf (1871) who considered that the rocks were folded in a large synclinal synform, the Gula Group forming the core and representing the youngest rocks (Fig. 2.2a). Kjerulf (1878) in a later publication discussed the possibility that the system was inverted, the Gula schists thereby representing the oldest rocks in the core of an anticlinal synform (Fig. 2.2b). Svenonius (1885) retained the idea that the Gula schists were the oldest rocks, but suggested, on the basis of observations in central Trondelag, that they had been squeezed up in the core of an antiformal structure (Fig. 2.2c). Bugge (1910) in a study of the Rennebu area, rejected these views in favour of the earlier hypothesis that the Gula Group was the youngest stratigraphic unit, lying in the core of a synform. Wegmann (1925) in a refinement of Kjerulf's (1878) model, considered the Gula as allochthonous on the

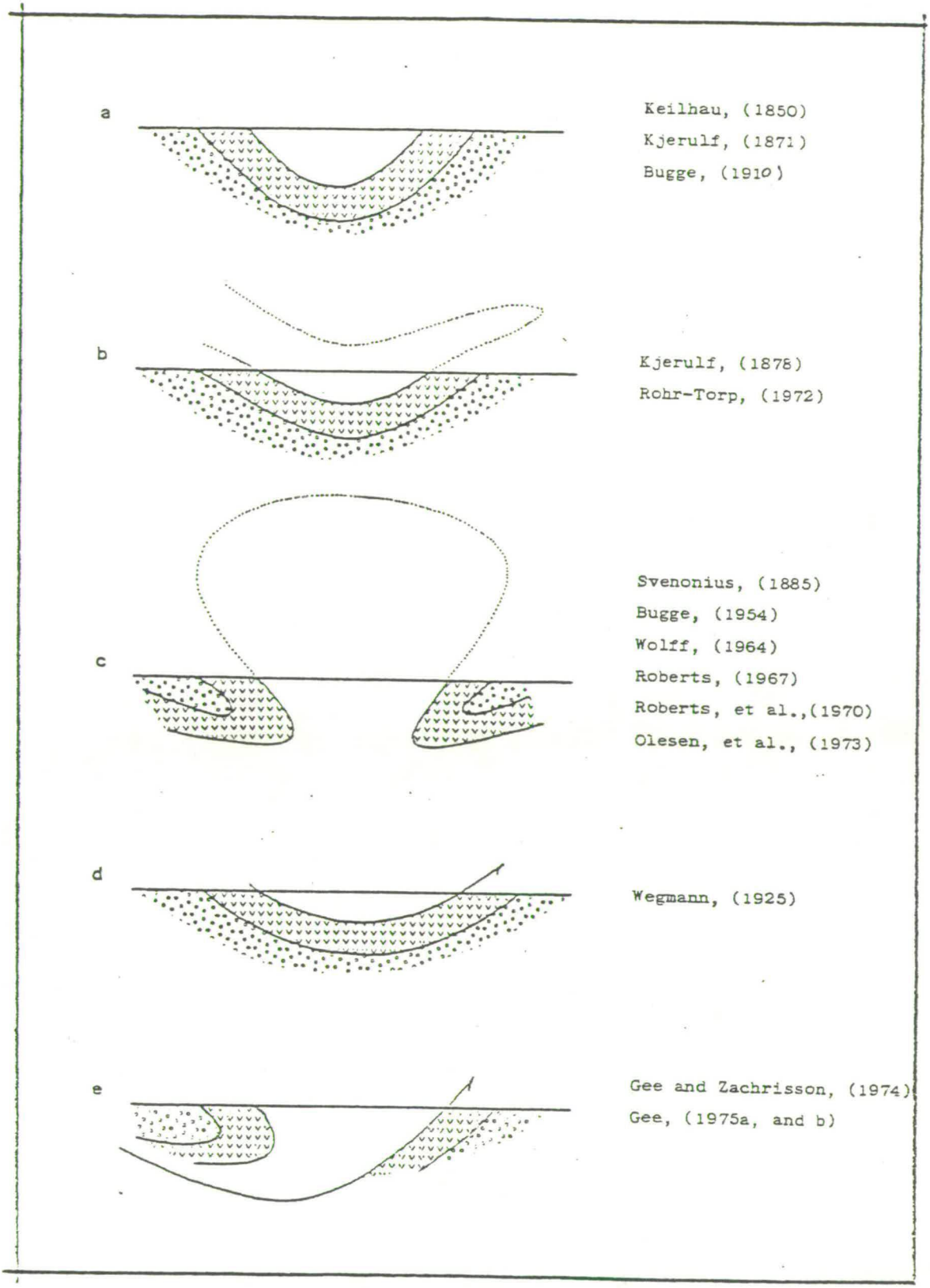

Fig. 2.2 Previous interpretations of Trondelag structure. Unshaded - Gula Group; V - Storen and Fundsjo Groups; circles - higher units of the Eastern and Western Trondelag successions.

volcanic Storen and Fundsjo Groups (Fig. 2.2d). In a reversal of his earlier views, Bugge (1954) favoured the hypothesis initially suggested by Svenonius (1885). This model is essentially similar to those proposed by Wolff (1964), Roberts (1967), Roberts et al. (1970), and Olesen et al. (1973), who suggest that central Trondelag geology is dominated by an upright fan-shaped antiform, cored by the Gula Group, and flanked by recumbent folds of the younger volcanics and sediments.

There are, however, problems in correlating this proposed structure from one area to another. For instance, Roberts (1967) and Roberts et al. (1970), basing their conclusions on observations in the Stjora valley, regard this antiformal structure (referred to as the Stjordalen Anticline) as a product of a first phase of deformation, and responsible for the development of the regional foliation. In contrast, Olesen et al. (1973), in their study of the Selbu-Tydal area, some 25 km to the south, described an earlier phase of isoclinal folding giving rise to the regional foliation. They suggest that subsequent deformation of this foliation lead to the development of the major antiformal structure, in this area known as the Selbu Antiform.

A refinement of the antiformal model has been provided by Gale and Roberts (1974), who propose a tectonic contact between the Gula Group and the Storen and Fundsjo Groups on the basis of the oceanic trace-element geochemistry of the Storen volcanics and the apparently miogeosynclinal nature of the original Gula sediments.

Rohr-Torp (1972) made a detailed study of the Gula, Storen and Lower Hovin Groups in the area around Innset. From way-up evidence in the Hovin sediments ("cross-lamination" and graded bedding), and in the Storen metavolcanics (shapes of pillows), and their relationships to observed fold closures, he suggests that the easterly dipping sequence is characterised by a series of tight to isoclinal folds in which the

antiforms young towards their cores. He regards this as strong evidence against the "mushroom-shaped" antiform described above and favours a model similar to that of Kjerulf (1878) in which the entire Trondelag succession is inverted in an early recumbent isocline and subsequently refolded (Fig. 2.2b).

The most recent interpretation of Trondelag structure is that suggested by Gee and Zachrisson (1974). This model involves different nappe units for the Eastern and Western Trondelag successions. The western succession occupies the nose of a typical recumbent-fold nappe, the surface of decollement being the contact between the Gula and Fundsjo Groups. The model is illustrated in Fig. 2.2e. The evidence presented for this interpretation is distinctly ambiguous and not convincing. Largely on the basis of a literature survey: "It is concluded that there are greater similarities between the Jamtland-Vasterbotten (Koli Supergroup) successions and those of the eastern part of Trondheimfaltet (Eastern Trondelag succession) than between the latter and the classical stratigraphy of the Holanda-Horg area (Western Trondelag succession)." The American affinities of faunas in the Western Trondelag succession are noted (Berry, 1968; Neuman and Bruton, 1974) together with the dominantly Baltic affinities of fossil assemblages in the Otta serpentinite conglomerate (Jaanusson, 1973), outcropping to the south of the Trondheim Nappe as defined by Wolff (1967a). An earlier correlation of this conglomerate with the serpentinite conglomerates of the Swedish Koli is also mentioned (Kulling, in Gavelin and Kulling, 1955). The Baltic affinities of the Otta conglomerate are suggested as further evidence for not correlating the Eastern Trondelag succession with that of western Trondelag. The argument is circular, involving both the proposed correlation of the Swedish Koli with the Eastern Trondelag succession, and its correlation with the

Otta conglomerate. The hypothesis therefore rests solely on a lithological correlation based largely on examination of the literature. A slightly modified version of this hypothesis has been presented subsequently by Gee (1975a).

A number of later structures have affected the rocks of the Trondheim Nappe together with the underlying nappes of the Eastern and Western Complexes (Roberts et al., 1970; Gee, 1975a). Among them are the Tommeras Antiform and the Snasavatn Synform to the west, and the Sylarna Antiform and the Helags-Tanfors Synform to the east (Map 1). In southern Trondelag, an open synform, known as the Singsas Synform (Nilsen, 1978), or the Trondelag Synform (Gee, 1975a), has been recognised. All of these structures are late-stage folds influencing both the Eastern and Western Complexes together. They therefore developed after the emplacement of the nappes.

The structural history of the Trondheim Nappe has been investigated in northern Trondelag by Roberts et al. (1970); in the Selbu-Tydal area of central Trondelag by Olesen et al. (1973); and in the Dombas-Lesja area of southern Trondelag by Guezou (1978). As with the major structures, problems arise when correlations of minor structures are attempted from one area to another. A tentative correlation of the various descriptions of minor structures will be presented in Chapter 3, in the light of the present study.

2.5 Timing of Orogenic Deformation and Metamorphism.

Most authors are agreed that some early deformation took place before the peak of regional metamorphism (Roberts, 1967; Roberts et al., 1970; Olesen et al., 1973; Gee, 1975a). Subsequent major refolding was probably related to nappe translation.

Wilson et al. (1973), on the basis of K-Ar ages of metamorphic minerals and whole rocks (phyllites) from the Stjora valley, propose a minimum age for the regional metamorphism of 438 ± 12 my, regarding ages in excess of this value as anomalous. In an extension of this study into Sweden, Gee and Wilson (1974) suggest that this Silurian event was responsible for the main orogenic deformation in the greater part of the Scandinavian Caledonides. In support of this they appeal to the lack of evidence for a major unconformity within the Lower Palaeozoic sequence of the Scandinavian Caledonides. However, on the island of Soroy in northern Norway, Pringle and Sturt (1969) had drawn attention to a Rb-Sr isochron on an anatectic vein associated with the syntectonic Hasvik gabbro. The age of 530 ± 35 my indicated that this area (the Kalak Nappe) was affected by an early orogenic event approximating in time to the Grampian event in Scotland (Dewey and Pankhurst, 1970). This possibility was extended by Sturt et al. (1975) who demonstrated that the internal metamorphic fabrics of the main nappe sequence of Finnmark developed during an early Ordovician phase of deformation. The final emplacement of the thrust-nappe sequence, however, belongs to a later phase of Caledonian orogenic development, probably in the Upper Silurian. In addition Sturt and Thon (1976), in a discussion of Gee and Wilson (1974), describe a major unconformity in the Bergen Arc System between the Moberg conglomerate, and its overlying Ashgillian limestones (Kolderup and Kolderup, 1940), and the underlying metavolcanics. They suggest at least two major phases of folding associated with upper greenschist or almandine-amphibolite facies metamorphism prior to the deposition of the conglomerate, and conclude that at least two phases of orogenic development occurred within the Caledonides of western Norway. A correlation of the Moberg conglomerate with Lower Hovin and Sulamo Group conglomerates is

suggested (after Vogt, 1945), together with a tentative correlation of the pre-Ashgillian orogenic event with the Grampian event in Scotland.

The early orogenic development has now become established in the literature as the Finnmarkian phase and accepted as affecting the Finnmark nappe sequence and the Bergen Arc system (Sturt, 1978; Sturt and Roberts, 1978). Sturt and Roberts (1978) suggest on the basis of Rb-Sr isochrons that this event may extend back as far as the Lower Cambrian (552 my).

Sturt (1975) has tentatively proposed that this early orogenic phase might be extended to include the lower part of the Trondheim Nappe. He notes, firstly, the opinions of Vogt (1928; 1945) and Strand (1960) that the conglomerates at the base of the Lower Hovin Group represent a major stratigraphic break, named by Strand (1960) the Trondheim disturbance. He then recalls Spjeldnes' (in Sturt et al., 1967) suggestion that abundant detrital fragments of hornblende in the Caradocian Kalstad limestone (Lower Hovin Group - Strand, in Strand and Kulling, 1972, page 56) were derived from a previously metamorphosed Storen Group. Further convincing evidence is provided by the Lille Fundsjo conglomerate (Table 2.1) which he believes is dominated by foliated fragments of Fundsjo volcanics in which the foliation has random orientation. He concludes that the Fundsjo Group had undergone deformation, metamorphism, and considerable erosion prior to the deposition of the Lille Fundsjo conglomerate. The argument is developed further by consideration of the K-Ar mineral ages obtained by Wilson et al. (1973). A number of dates in excess of 450 my were obtained, but were dismissed as being due to excess argon contained in the minerals concerned. Sturt, however, points out that these "anomalous" ages represent hornblendes from the Gula, Storen, and Fundsjo Groups.

He concludes that these dates represent blocking temperature ages for a Cambro-Ordovician orogeny which in the Trondelag region affected only the Gula, Storen, and Fundsjo Groups.

In a study of the Dombas-Lesja area, Guezou (1978) states:

"The Trondheim Nappe rocks were subjected to five tectonic episodes in the Stakahoi Group (Gula Group), but only four in the other groups."

Although he has not recognised the earliest deformation in the Storen or Fundsjo Groups, this does, however, lend further credence to Sturt's (1975) proposals for an extension of the early Cambro-Ordovician orogenic event into the Trondelag region.

2.6 Summary.

The review presented above illustrates that the various interpretations of the regional geology of the Trondheim Nappe depend on the related problems of stratigraphic correlation, interpretation of the major structures, and timing of the orogenic deformation and metamorphism.

Most authors regard the Eastern Trondelag succession as directly equivalent to the Western Trondelag succession. Gee and Zachrisson (1974), however, prefer a correlation of the Eastern Trondelag succession with the Koli successions of lower tectonic level.

The internal structure of the Trondheim Nappe has been variously interpreted as being synformal (e.g. Rohr-Torp, 1972); antiformal (e.g. Wolff, 1964; Roberts, 1967; Roberts et al., 1970; Olesen et al., 1973); or as being the wedge-shaped nose of a recumbent fold -nappe (Gee and Zachrisson, 1974; Gee, 1975a).

The age of orogenic deformation and metamorphism in Trondelag has generally been accepted as being mid-Silurian and synchronous with nappe emplacement. However, Sturt (1975) has presented very strong arguments

in favour of the Gula, Storen, and Fundsjo Groups having suffered a Cambro-Ordovician orogenic episode, probably related to the Grampian of Scotland, and the Finnmarkian of northern and southwestern Norway.

CHAPTER 3

THE GEOLOGY OF THE TRONDHEIM NAPPE - A CONTRIBUTION

The regional geology of the Trondheim Nappe has been the subject of long and intensive investigation (Chapter 2). The stratigraphies of the Eastern and Western Trondelag successions have been well established and are generally accepted throughout their areas of outcrop. In contrast, the majority of structural models are based on detailed studies of relatively small areas. Fundamental differences of interpretation have thus evolved. For instance, of the models illustrated in Fig. 2.2, many of those advocating the antiformal structure (Svenonius, 1885; Wolff, 1964; Roberts, 1967; Roberts et al., 1970; Olesen et al., 1973) are based on studies in central Trondelag, while those favouring the synformal structure are commonly the result of studies in southern Trondelag (Keilhau, 1850; Bugge, 1912; Rohr-Torp, 1972). The problems encountered in the correlation of both major and minor structures between adjacent areas of central Trondelag (Roberts et al., 1970; Olesen et al., 1973) have also been mentioned.

The possibility of a more consistent regional structure within the Trondheim Nappe has been investigated by the examination of five traverses across the Gula Group, and adjacent units. Each traverse follows a major NW-SE trending river valley after which it has been named. Map 2 indicates the locations of the traverses, which are, from north to south:

a) the Helgaadalen traverse;

b) the Inndalen traverse;

c) the Stjordalen traverse;

d) the Gauldalen traverse; and

e) the Orkladalen traverse.

The traverses mapped are largely restricted to the Gula, Storen, and Fundsjo Groups. Consequently, comment on the lithostratigraphic correlation of the Eastern and Western Trondelag successions is based on more general considerations of the regional geology. Some details regarding the internal stratigraphy of the Gula Group, and its possible outcrop in the Tommeras area and in western Trondelag are presented. The structure of the Gula Group and the implications to the structure of the Trondheim Nappe are then discussed.

3.1 Stratigraphy

3.1.1 The Eastern and Western Trondelag successions.

The structural models outlined in Chapter 2, with one exception, assume a correlation of the Eastern and Western Trondelag successions. The interpretation of Gee and Zachrisson (1974), however, is based on a stratigraphic correlation of the Eastern Trondelag succession with the Koli Supergroup of Sweden, and requires that the contact between the Gula and Fundsjo Groups is of major tectonic importance. The rather dubious bases for these arguments have been discussed in Chapter 2. While this interpretation may be "in keeping with the nappe geometry further east in the Geotraverse" (Gee, 1975), it cannot be considered consistent with the geology of the Trondelag region.

Table 3.1 (Columns A, B, and C) illustrates the stratigraphic interpretation preferred by Gee and Zachrisson (1974). A correlation of the Eastern Trondelag succession with the Silurian sequences of central-southern Vasterbotten and northern Jamtland (Zachrisson, 1964, 1969, 1971) is indicated. Inherent in this proposal is the requirement that the Eastern Trondelag succession youngs from the Slagan Group towards the Fundsjo Group, which is in direct conflict with the field based conclusions of other workers (Chaloupsky and Fediuk, 1967;

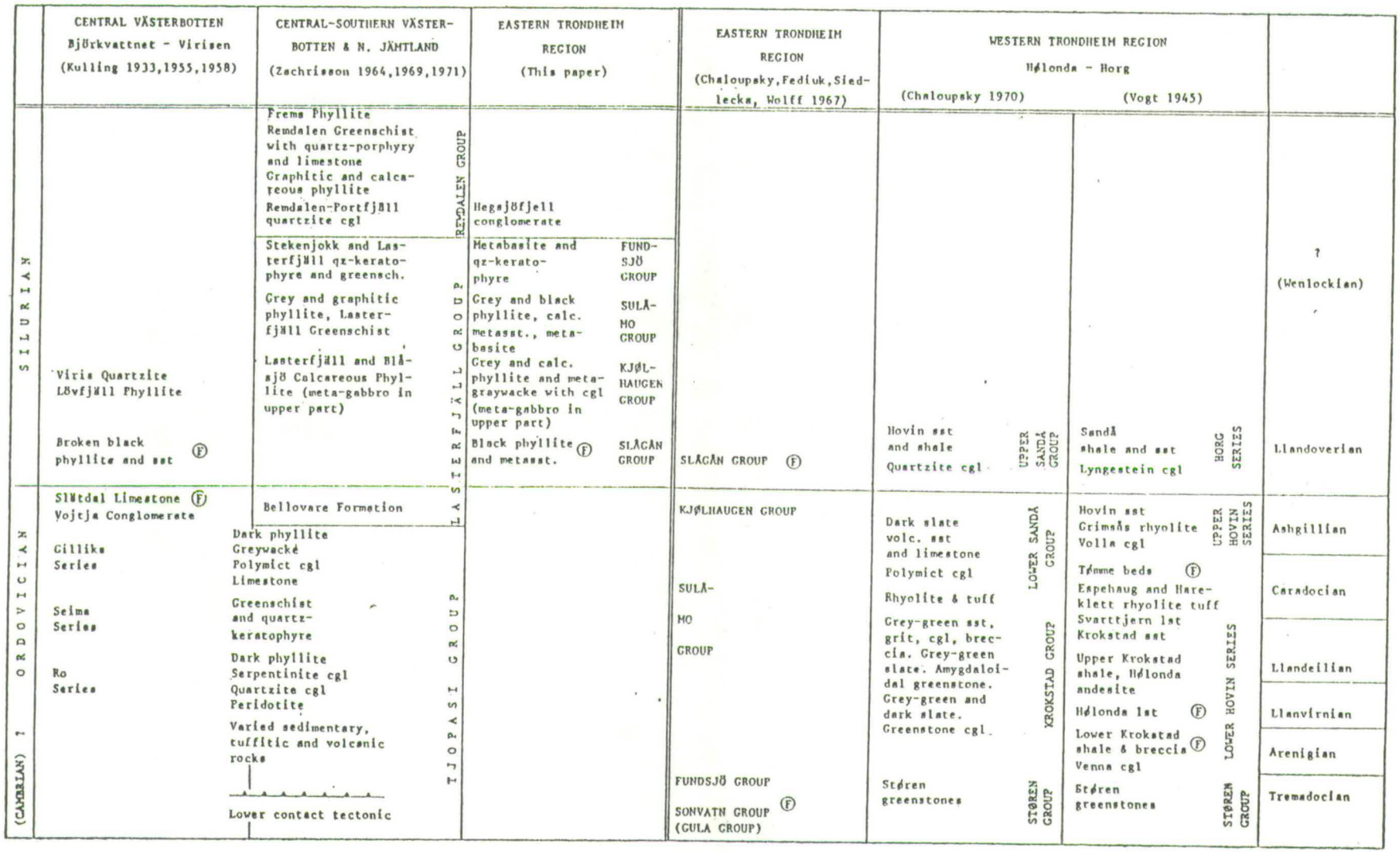

Table 3.1 Stratigraphic correlations of the Eastern Trondelag succession (taken from Gee and Zachrisson, 1974). F - denotes fossiliferous unit.

Siedlecka, 1967; Wolff, 1967a; Rui, 1972). Furthermore, the inclusion of the Dictyonema-bearing black shales at Nordaunevoll in the Sulamo Group, as suggested in Chapter 2, is not compatible with this hypothesis.

The structure proposed by Gee and Zachrisson (1974) involves a simple eastward-facing recumbent isocline. However, the established younging directions in the Western Trondelag succession (to the west away from the Gula Group - Vogt, 1945) suggest that this isocline, if present, must represent the lower part of a larger westward facing structure. Such a geometry is not easily reconciled with the westerly derivation of the Trondheim Nappe, as indicated by the American affinities of faunal assemblages in the Western Trondelag succession (Berry, 1968; Neuman and Bruton, 1974). Moreover, this interpretation fails to explain the structural observations of Rohr-Torp (1972) at Innset (Chapter 2), or the metamorphic zonation of the Trondheim Nappe around the central parts of the Gula Group.

For these reasons, the more widely held correlation of the Eastern Trondelag succession with the Western Trondelag succession is accepted in this thesis.

3.1.2 The Gula Group.

Nilsen (1978) has drawn attention to a broad zonal pattern of lithological distribution within the Gula Group of southern Trondelag. He describes a central zone of quartz-biotite schists with intercalated calc-silicate horizons and graphitic quartzites (the Singsas Formation), flanked by zones of grey, biotite phyllites (the Undal Formation in the west and the Asli Formation in the east). Observations in the northern part of Trondelag indicate that the Undal Formation pinches out between the Selbu-Tydal area (Olesen et al., 1973) and the Stjordalen traverse (Maps 1 and 2). The Asli Formation continues further northwards to pinch out between Inndalen and Helgaadalen (Maps 1 and 2).

The Guda conglomerate, lying within the Asli Formation and reported from Inndalen southwards to the Dovre area (Dudek et al., 1973; Wolff, 1964; Olesen et al., 1973; Pinna, 1973) provides an easily recognisable stratigraphic marker horizon. From the Undal Formation, similar conglomeratic lithologies have been recorded at Blomlia in central Trondelag (Olesen et al., 1973), and in the Folldal area (Nilsen, 1978). The present study has revealed the occurrence of analogous horizons in the Undal Formation on the Gauldalen and Orkladalen traverses. In Gauldalen, the conglomerates are monomict, containing only elongate fragments of quartzites and may represent intraformational breccias. On the Orkladalen traverse, however, fragments of metavolcanics commonly occur amongst those of quartzite and there is no doubt that the lithology represents an original polymict conglomerate.

The overall similarity of the Undal and Asli Formations is notable. They are dominated by grey, biotite phyllites and are commonly associated with conglomeratic lithologies. A correlation of the two units across the central Singsas Formation must therefore be considered.

3.2 Regional Outcrop Distribution Of The Gula Group.

The controversy surrounding the possible outcrop of the Gula Group at the base of the Trondheim Nappe, in western Trondelag, and on the flanks of the Tommeras Antiform has been mentioned in Chapter 2. Wolff (1964, 1967b, and in Springer-Peacy, 1964) considers the high-grade rocks outcropping in these positions as direct equivalents of the Gula Group; while Gee (1977, 1978) and Andreasson et al. (1978) prefer correlation with the Seve Supergroup of the Seve-Koli Nappe Complex.

In a reconnaissance of the Tommeras Antiform, Springer-Peacey (1964) defined the general regional distribution of the main rock units as follows (from the core outwards):

a) the Tommeras Group - largely rhyolitic basement;

b) the Lower Lekstalsvann Group - calcareous sandstones;

c) the Upper Lekstalsvann Group - felspathic sandstones;

d) the Lower Snasa Group - dominantly amphibolite facies metabasics; and

e) the Upper Snasa Group - dominantly greenschist facies metabasics.

Wolff (1964, 1967b, and in Springer-Peacey, 1964) interprets the Tommeras Group as autochthonous basement, and the Lekstalsvann and Lower Snasa Groups as correlatives of the Gula Group, giving way eastwards to the Storen Group (Upper Snasa Group) and Gula Group proper (Fig. 3.1).

Gee (1974) correlated the Leksdalsvann Group with the sediments of the Jamtland Supergroup and proposed that they were allochthonous on the underlying basement (the parautochthon). He considered them as representing the Offerdal Nappe. The overlying Lower Snasa Group metabasics were consigned to the Gula Group (Gee, 1975a), with a major tectonic discontinuity (the base of the Trondheim Nappe) separating them from the underlying sediments of lower metamorphic grade. Gee (1977) further subdivided the Lekstalsvann Groups on the basis of doleritic intrusives observed in the upper unit and correlated with the Ottfjallet dolerites of the Sarv Nappe. The boundary between the Lower and Upper Lekstalsvann Groups was suggested as the contact between the Offerdal and Sarv Nappes. The Lower Snasa Group, dominated by amphibolite facies metabasics, was correlated with the Seve Supergroup of the Seve-Koli Nappe Complex, while the greenschist facies metabasics of the Upper Snasa Group can be followed along strike into the Storen Group of central and southern Trondelag. Gee (1977) based these conclusions on Springer-Peacey's (1964) reconnaissance map. Subsequent field investigations,

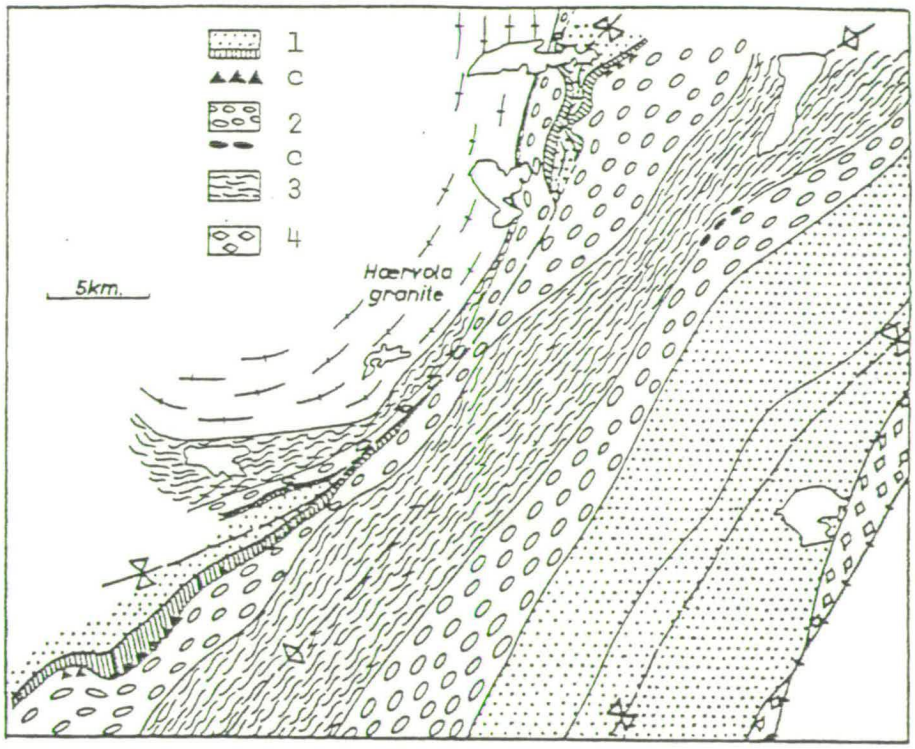

Fig. 3.1 Geology of the eastern flanks of the Tommeras Antiform after Wolff (1964, 1967b, and in Springer-Peacey, 1964).
1 - Hovin Group and eastern correlatives; 2 - Storen and Fundsjo Groups; 3 - Gula Group; 4 - Slagan Group; c - conglomeratic lithologies.

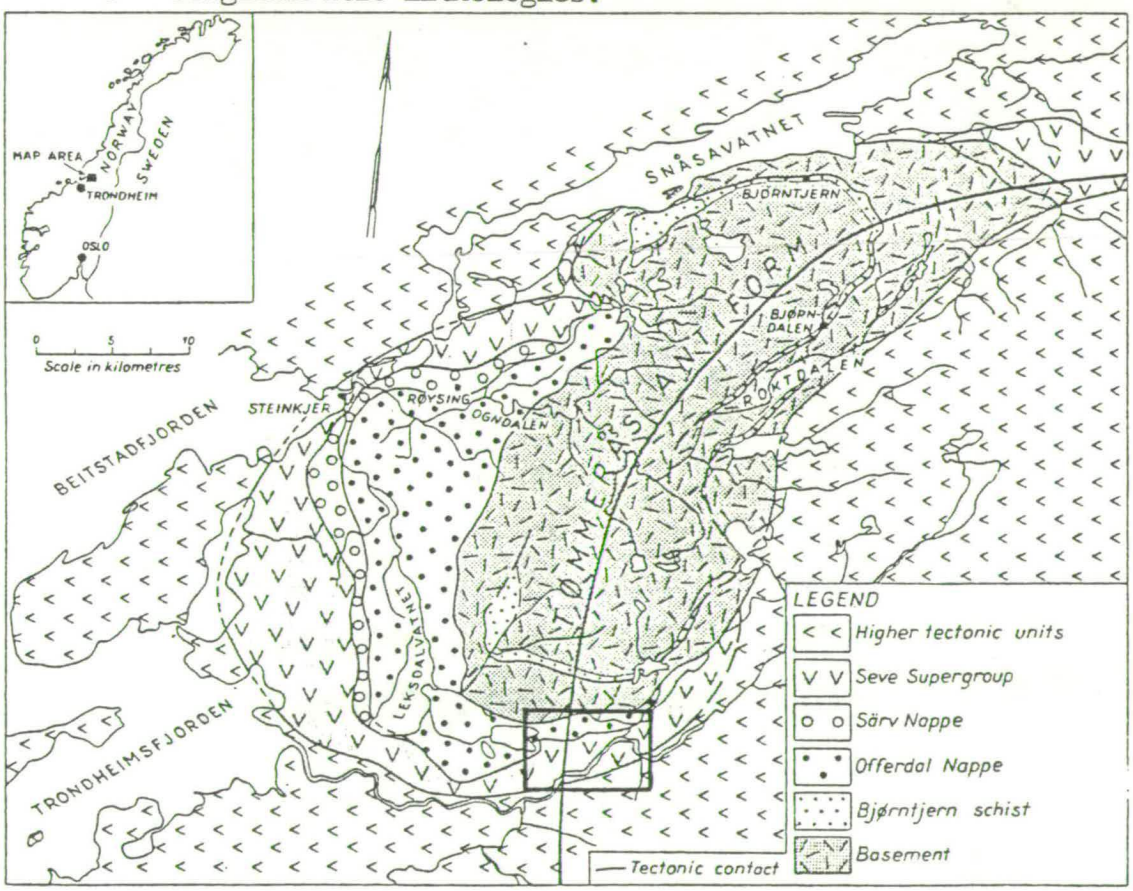

Fig. 3.2 Geology of the Tommeras Antiform after Andreasson et al. (1978).
Area outlined indicates area included in Fig. 3.3.

concentrated to six profiles across the Lekstalsvann Group (Andreasson, 1978) have resulted in modifications to Gee's (1977) map, such that contacts no longer coincide with those of Springer-Peacey (1964). The most recent compilation of the geology of the Tommeras Antiform is that presented by Andreasson et al. (1978) and is shown in Fig. 3.2.

These various interpretations have been investigated by extending the Helgaadalen traverse eastwards into the flanks of the Tommeras Antiform. The area examined is shown in Fig. 3.3.

Sections from the Upper Snasa Group downwards through the Lower Snasa and Lekstalsvann Groups to the Tommeras Group (Springer-Peacey, 1964) are exposed in stream sections running northwards from Ulvilla to Kjesbuvatnet, and from Vollen to Saeter. The Upper Lekstalsvann Group is well exposed along the eastern shores of Kjesbuvatnet. The absence of dolerite intrusives, both here and on the Vollen section, support the correlation of this unit, together with the Lower Lekstalsvann Group, with the Offerdal Nappe as suggested by Andreasson et al. (1978).

The overlying Lower Snasa Group is dominated by garnet amphibolite, in which the garnets commonly exceed 0.5 cm in diameter, with lesser garnet-mica schist. Amphibolitic horizons within the Gula Group are commonly garnetiferous, but this characteristic is always restricted to a narrow metasomatic reaction zone between the amphibolite and the surrounding country-rock schists (Nilsen and Mukherjee, 1972). The garnet-amphibolites on the Ulvilla and Vollen stream sections have no counterpart in the Gula Group, and Gee's (1977) correlation with the Seve Supergroup of the Seve-Koli Nappe Complex is therefore accepted. Towards the contact with the Upper Lekstalsvann Group the amphibolites grade into a chlorite-rich phyllonitic rock, a feature mirrored by an increasingly narrow-spaced fracture cleavage in the Lekstalsvann sediments. The contact (Fig. 3.4) is tectonic, and marks the base of the Seve-Koli Nappe Complex.

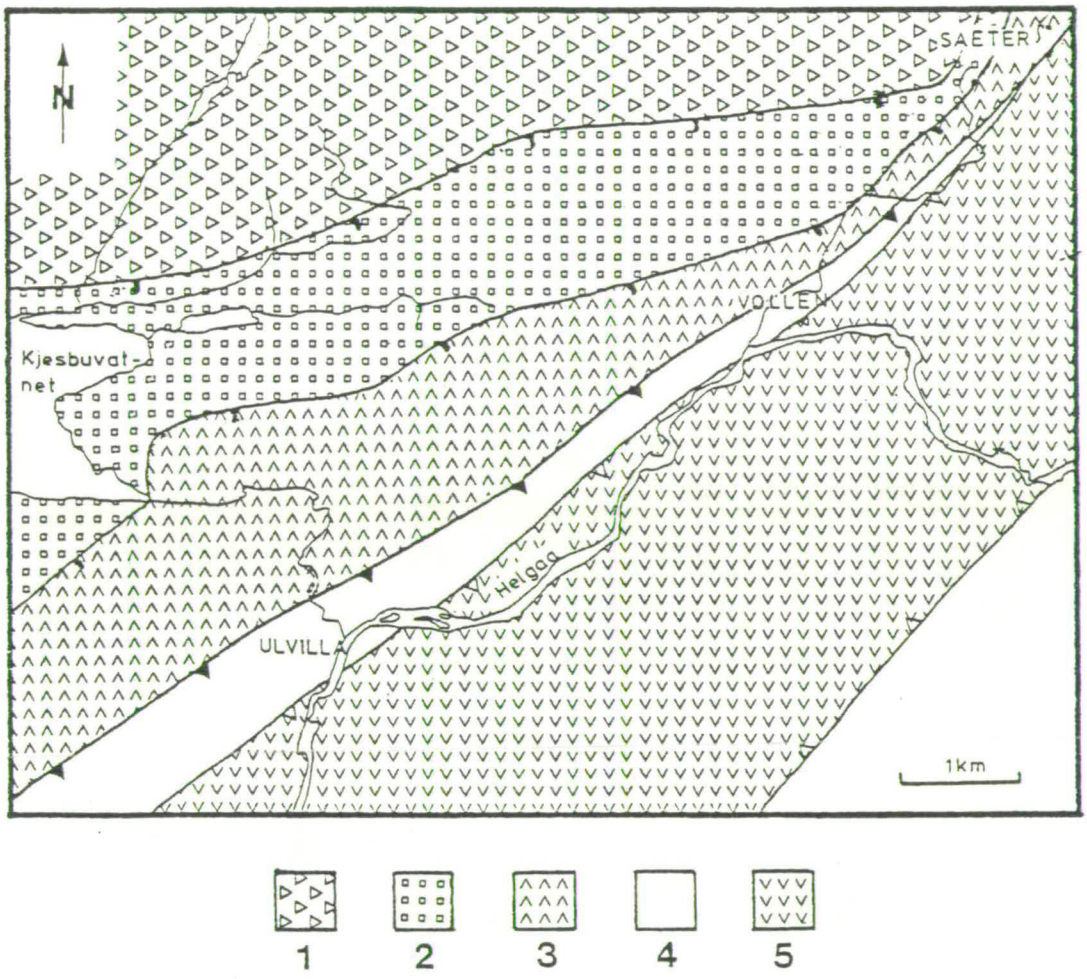

Fig. 3.3 A geological map of the Ulvilla - Vollen area (modified from Andreasson et al., 1978).

1 - Tommeras Group - basement.

2 - Lekstalsvann Group - Offerdal Nappe (Andreasson et al.,1978).

3 - Lower Snasa Group - Seve-Koli Nappe Complex (Andreasson et al., 1978).

4 - Gula Group
5 - Upper Snasa Group (Storen Group)] - Trondheim Nappe.

Contacts as on Map 1.

Fig. 3.4 Contact between the Lekstalsvann Group (Offerdal Nappe - Andreasson et al., 1978) and the overlying Lower Snasa Group (Seve-Koli Nappe Complex - Andreasson et al., 1978).
Note narrow spaced fracture cleavage in Lekstalsvann sediments (bottom), and phyllonitic texture of Seve amphibolites (top).
Contact marked by hammer head.

Fig. 3.5 A D_1 isoclinal fold closure at Graho.
The hinge plunges gently away from the observer towards 150°.

Two distinctive lithologies are poorly exposed in a narrow zone running between Ulvilla and Vollen. These rock-types, which give way eastwards to the massive greenschist facies metavolcanics of the Upper Snasa Group (Storen Group) are best observed on the two streams sections and on the road between the two villages. The exposure is dominated by a parallel-banded calc-silicate gneiss interlayered with more pelitic and psammitic lithologies. At one exposure (Mapsheet Vuku; coord: 32VPR386778) a graphite-bearing quartzite was noted. The calc-silicate gneiss and the graphitic quartzite are characteristic of the Singsas Formation and may be observed frequently further east on the Helgaadalen traverse within the main outcrop of the Gula Group. Furthermore, graphitic lithologies are unknown in the Seve Supergroup (Gee, pers. comm., 1978).

A correlation of these lithologies with the Gula Group is therefore suggested as shown in Fig. 3.3. Their contact with the underlying amphibolities (unexposed in the area investigated) is considered the base of the Trondheim Nappe.

In western Trondelag the high-grade rocks outcropping on the shores of the Trondheimsfjord, between Buvika and Orkanger, and extending southwards towards Surnadal have been identified by Wolff (1967b) as Gula Group mica schists. Subsequently, Wolff (1976) revised this opinion and regarded these lithologies as high-grade equivalents of the Storen Group. Gee (1978), extrapolating from his conclusions in the Tommeras area (Gee, 1977), prefers correlation with the Seve Supergroup. These rocks have been examined on the road and coastal section between Buvika and Borsa, in which the various lithologies are well exposed.

At Borsa, and eastwards towards Buvika, the dominant lithology is a garnet amphibolite similar to that exposed on the flanks of the Tommeras Antiform. The amphibolite is commonly retrogressed and rich

in chlorite. Rare horizons of garnet-mica schist also occur. Approaching Buvika the lithology may be either a finely-laminated garnet amphibolite or an extremely phyllonitic, dark green chlorite schist. Approximately 500 m west of Buvika (Map sheet Orkanger; coord: 32VNR581212) a black graphite-bearing phyllite occurs in two isolated roadside exposures. The next exposure, some 2 km eastwards of this point, is of typical greenschist-facies Storen metavolcanics.

The sequence described above is remarkably similar to that observed in the Tommeras window, and similar correlations are proposed (Map 1). In this case the Gula Group is represented by a graphitic phyllite typical of the Undal Formation outcropping further to the east on the Gauldalen traverse. The unexposed contact between the garnetiferous Seve amphibolite and the Gula phyllite is regarded as the base of the Trondheim Nappe as in Tommeras.

Limited observations around Lokken reveal that in this area Storen greenstones are thrust directly against Seve amphibolites, while Krill (pers. comm., 1978) has found similar relationships between the Seve and the Hovin Group in the area extending southwards from Oppdal. It may be concluded that, in southern Trondelag, the Gula and Storen Groups become successively thrust out against the Seve amphibolites along the base of the Trondheim Nappe (Map 1).

The recognition that the Gula Group outcrops in western Trondelag, and in the Tommeras window, has implications to the regional structure of the Trondheim Nappe, which is discussed in a later section.

3.3 Structure.

Structural observations have been largely restricted to the main outcrop of the Gula Group. The most obvious structure in this unit is the regional foliation which varies from a closely-spaced penetrative

schistosity in pelitic lithologies, to a widely-spaced fracture cleavate in more psammitic horizons. It has a variable orientation which will be discussed further in the context of the regional structure.

3.3.1 Mesoscopic structures.

The earliest recognisable mesoscopic folds are isoclinal and vary in style according to the associated rock-type. In dominantly psammitic lithologies they are represented by rounded fold closures which often dominate whole exposures (Fig. 3.5). In pelitic partings two foliations are commonly recognised on the hinge zone, the first parallel to the compositional banding and a second crenulation foliation axial-planar to the associated fold. In more pelitic lithologies these early isoclines are extremely attenuated and are commonly only recognised as isolated fold hinges of early quartz segregations. In such cases it is not possible to recognise the axial-plane foliation as a crenulation of an earlier structure. The axial direction of these isoclines is variable, as a result of later deformation, and is commonly paralleled by a marked linear structure (Fig. 3.6). This lineation is most commonly defined by a prominent quartz-rodding, but a preferred orientation of porphyroblastic minerals including amphibole, kyanite, and sillimanite may also be responsible (Roberts, 1968; Olesen et al., 1973). Structures of this generation are designated D_1, while the earlier foliation, which may represent an original sedimentary structure or an earlier phase of deformation, is assigned to D_o.

A small number of exposures illustrate that at least one, and possibly two, later phases of folding share the regional foliation. Such an exposure is shown in Fig. 3.7. In this example a thick quartz vein truncates isocline closures of finer quartz segregations, is itself isoclinally folded, and is cut by a Trondhjemite dyke. The regional foliation is axial-planar to the observed fold closures in the quartz

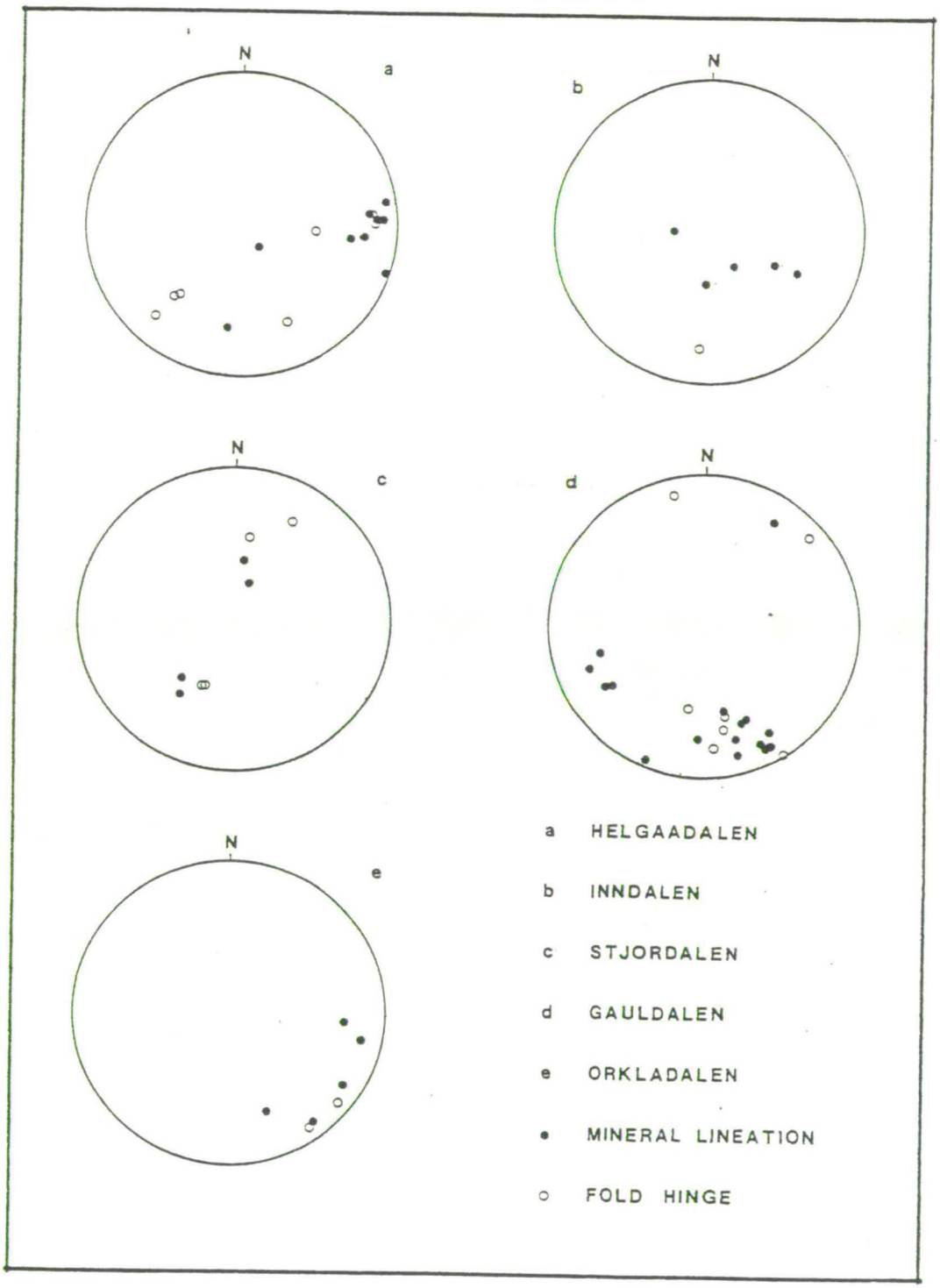

Fig. 3.6 Stereographic projections of D_1 fold hinges and associated linear structures (Schmidt net, lower hemisphere).

Fig. 3.7 Three (?) phases of isoclinal (?) folding affecting the Gula schists - Orkladalen traverse. The D_3 ? foliation is always present at the margins of the dyke on the right-hand side of the field of view. See text for further details.

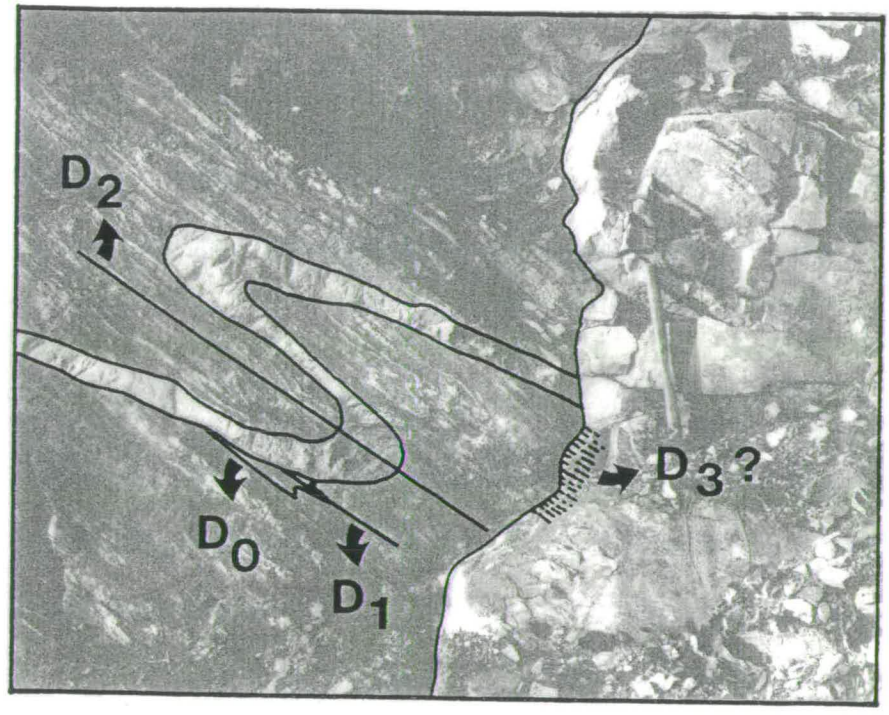
D2
D0
D1
D3?

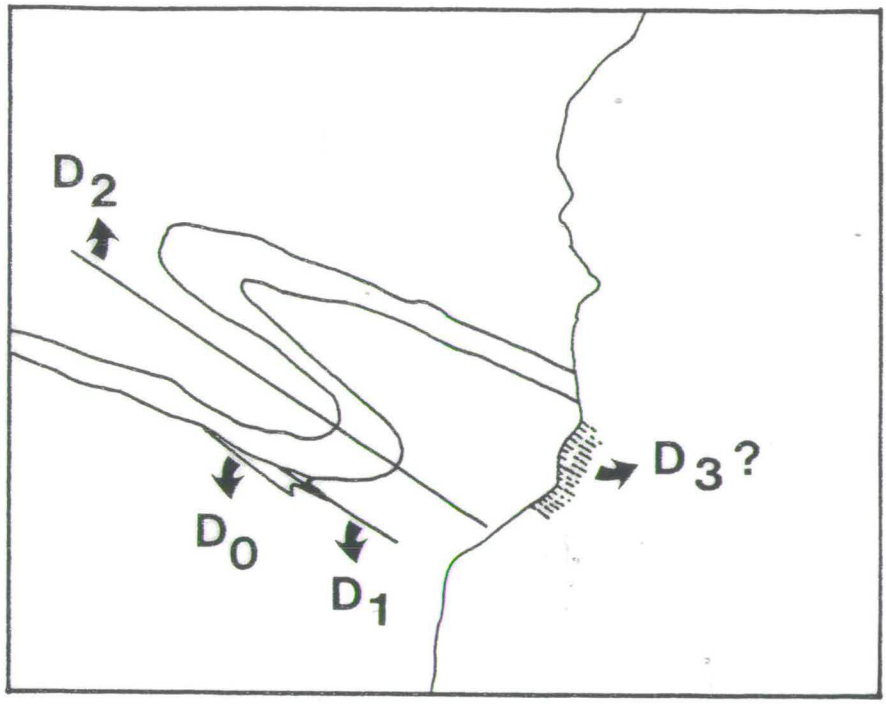
D2
D3?
D0
D1

veins and extends for a few centimetres into the margins of the Trondhjemite dyke. Although the evidence for three distinct fold episodes is not unambiguous, the extreme deformation of the quartz veins relative to that displayed by the dyke strongly suggests this possibility (Rickard, pers. comm., 1976; Gee pers. comm., 1978). If present, the third phase is probably isoclinal as no other fold style has been observed axial planar to the regional foliation. The later generations of isoclinal folds are tentatively designated D_2 and D_3, and where recorded, invariably have an axial direction varying from N-S to NE-SW.

Isoclines are commonly refolded by later (D_4), usually upright folds, with flat-lying approximately N-S hinge directions. The folds are diverse in style from open to tight and in pelitic lithologies the hinge zone may be marked by an axial-plane crenulation cleavage. The intensity of D_4 deformation varies from area to area. For instance, at Gardsjoen, on the Orkladalen traverse, D_4 folds are frequent and commonly tight in style, while further east on the same traverse the area around Graho is characterised by rare undulations of earlier structures.

A suite of upright, N-S trending kink bands has been recorded and probably represents the final episode of deformation. A tentative correlation of the sequential development of minor structures suggested in this study with previous assessments is presented in Table 3.2.

In the Storen and Fundsjo Groups isoclinal fold closures are only rarely observed. However, a foliation paralleling the bedding in the intercalated sediments is always present. In chert horizons chevron-style D_4 folds are commonly well developed.

Limited observations in the Hovin Group on the Stjordalen and Orkladalen traverses indicate that this unit has been isoclinally folded.

This study	Guezou (1978)	Roberts et al. (1970)	Olesen et al. (1973)
D_o			F_1
D_1	F_1	F_1	F_2
D_2	F_2	F_2	Gudbrandegga* Finnkoihogda
D_3	F_3		
D_4	F_4	F_3	Selbu-Tydal
D_5	F_5	F_4	Kink bands

* Uncertain age relationships lead Olesen et al. (1973) to name fold phases after localities rather than chronologically.

TABLE 3.2 A tentative correlation of various assessments of the sequential development of minor structures in the Gula Group.

Between Innset and Naverdal the Hovin greywackes are intruded by a suite of Trondhjemite dykes, one of which truncates an isocline closure in the sediments. Other dykes are themselves isoclinally folded. Assuming one phase of Trondhjemite intrusion, two episodes of isoclinal folding are indicated. A foliation, axial planar to isocline hinges and generally parallel to bedding, is commonly present.

3.3.2 Metamorphism and its relationship to deformation.

The high-grade metamorphism exhibited by the central parts of the Gula Group is related to D_1 as evidenced by the lineation of high-grade minerals, such as kyanite and sillimanite, parallel to D_1 fold axes (Olesen et al., 1973; Roberts, 1968). The zonation of metamorphic grade within the Trondheim Nappe illustrated in Fig. 2.1, suggests a subsequent deformation of this early metamorphism (it will be concluded in Chapter 4 that this zonation is real and not a consequence of any retrogressive effect).

Evidence (Sturt, 1975) suggesting an early orogenic development affecting the Gula, Storen, and Fundsjo Groups, and preceeding the deposition of the overlying, dominantly sedimentary sequences, has been presented in Chapter 2. Support for this proposal is provided by the occurrence of graptolite remains within 300 m of epidote-amphibolite facies Fundsjo metavolcanics at Nordaunevoll (Vogt, J. H. L., 1889; Vogt, T., 1941; Stormer, 1941). The graptolite-bearing lithologies have been assigned to the Sulamo Group, and a major non-conformity, separating them from the higher-grade metavolcanics, has been suggested (Chapter 2).

The early orogenic development will hereafter be referred to as the Trondheim Orogeny, and a tentative correlation with the Finnmarkian Orogeny of northern Norway, and the Grampian Orogeny of Scotland suggested. The timing of this deformation is restricted by: a) the Tremadocian

Dictyonema-bearing shales at Nordaunevoll, regarded here as occurring at the base of the Sulamo Group, and b) the late Arenig or lowermost Llanvirnian graptolites described from the base of the Lower Hovin Group (Berry, 1968). Sturt (1975) pointed out that the maximum "anomalous" hornblende age obtained by Wilson et al. (1973) from the Gula, Storen, and Fundsjo Groups, is consistent with the lowermost limit suggested for the Finnmarkian Orogeny by Sturt et al. (1978) - 572 and 552 my respectively.

It will be shown below that subsequent deformation (D_2-D_5) was associated with the lower-grade metamorphism observed in the higher units of the Eastern and Western Trondelag successions. The metamorphism decreases in grade from epidote-amphibolite facies (garnet-grade), in parts of the Eastern Trondelag succession, to greenschist facies (chlorite-grade) in the Western Trondelag succession (Fig. 2.1). This main Scandinavian Orogeny (Sturt and Roberts, 1978) must be post-Llandoverian, as dictated by the graptolite assemblage of the Slagan Group in eastern Trondelag (Kiaer, 1932). However, as Devonian deposits east of Roros are tectonised (Roberts, 1974) the latest Caledonian deformation affecting the Trondheim Nappe was probably Mid-Upper Devonian in age. The K-Ar ages considered as non "anomalous" by Wilson et al. (1973) range from 420-380 my and are consistent with these arguments.

3.3.3 Regional structure.

Any regionally consistent interpretation of the internal structure of the Trondheim Nappe must account for:

a) the regional outcrop distribution of the various stratigraphic units;

b) the variation in orientation of the regional foliation;

c) the direction of younging in the Eastern and Western Trondelag successions;

d) the metamorphic zonation about the central parts of the Gula Group; and

e) the sequence of tight to isoclinal folds, in which the antiforms young towards their cores, described by Rohr-Torp (1972) from the Innset area on the western end of the Orkladalen traverse (Chapter 2).

Previous interpretations have been reviewed in Chapter 2 (Fig. 2.2). With the exception of that of Gee and Zachrisson (1974), they depend to a large extent on the orientation of the regional foliation.

Observations on the Helgaadalen and Inndalen traverses reveal that the foliation splays in a simple fashion from an easterly dip in the west, through the vertical, to a westerly dip in the east. On the Stjordalen traverse a slightly more complicated pattern is apparent, although a general splaying of the foliation through the vertical is still apparent (Fig. 3.8a).

The variations in the orientation of the foliation observed on the Gauldalen and Orkladalen traverses are almost identical, but differ markedly from those observed to the north. Fig. 3.8b illustrates the orientation of the foliation on the Gauldalen traverse. Moving eastwards from Volla, in the core of the Horg Syncline, the foliation flattens into a broad synform in the central parts of the Gula Group, and then rotates rapidly through 180° to a westerly dip as the Gula/Fundsjo boundary is approached.

These observations suggest an explanation for the contrasting antiformal and synformal interpretations which have evolved in northern and central Trondelag, and in southern Trondelag respectively. A fan shaped antiform is consistent with the splaying foliation on the three northerly traverses, while the pattern displayed on the Gauldalen and Orkladalen traverses accounts for the broad synform favoured by workers in southern Trondelag.

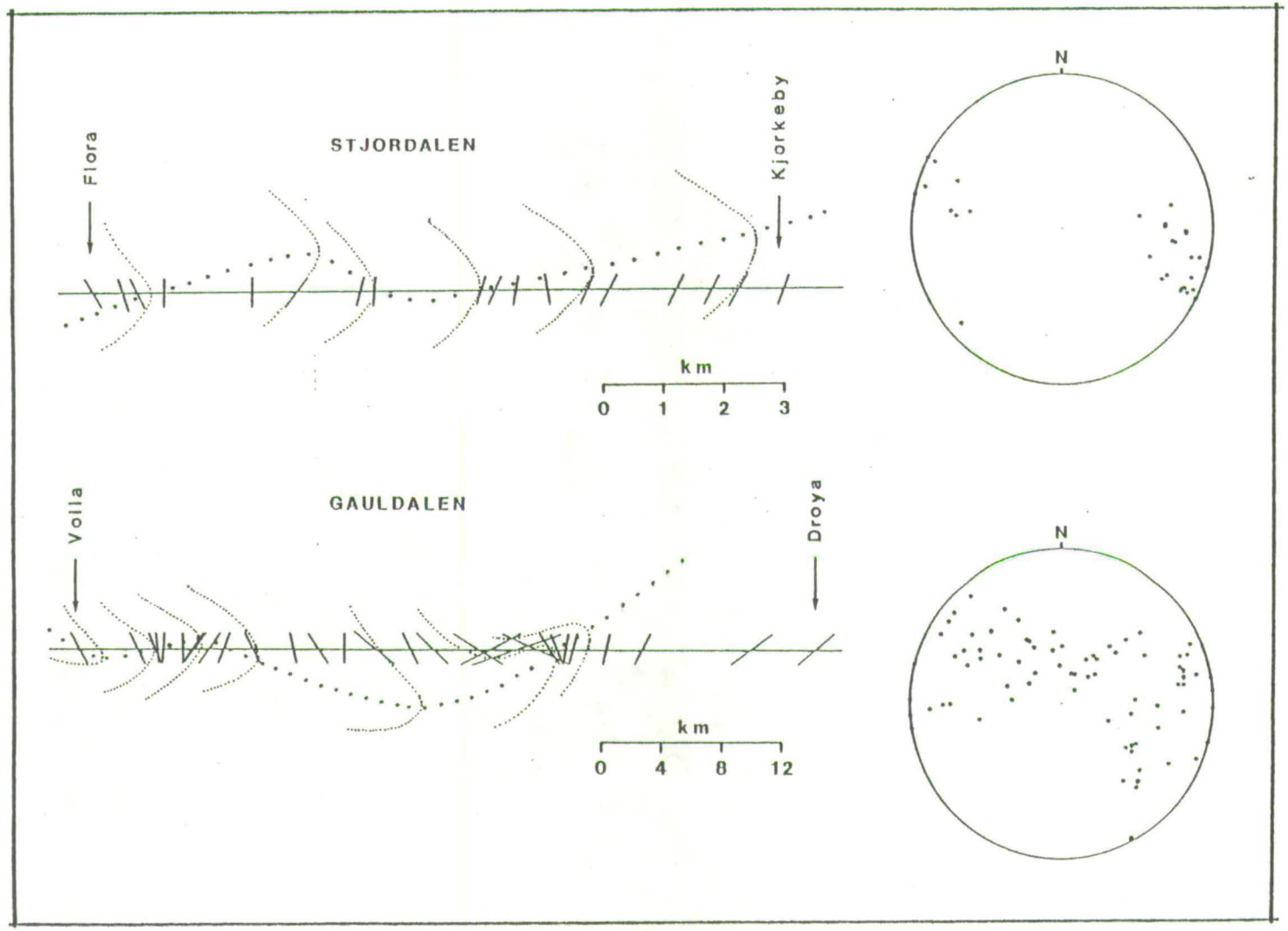

Fig. 3.8 Orientation of the regional foliation across the Stjordalen and Gauldalen traverses, and suggested relationships to major structures. Selected measurements shown on sections, all measurements plotted on stereographs (Schmidt net, lower hemisphere).

The apparently conflicting evidence described above can be reconciled by the interpretation superimposed on Fig. 3.8 a and b. It is suggested that the orientation of the foliation is controlled by a single recumbent isoclinal fold closure, together with an undulation of the associated axial plane superimposed by later folding. On the Gauldalen traverse, the fold closure can be traced westwards from the central parts of the Gula Group into the Horg Syncline (at Volla, Fig. 3.8b). This involvement of the higher stratigraphic units of the Western Trondelag succession demands that the structure does not relate to D_1 minor structures (confined to the Gula, Storen, and Fundsjo Groups), while correlation of the Eastern and Western Trondelag successions demands that it is post-D_2. A correlation of the major structure with D_3 minor structures is therefore favoured. The later, upright folding is probably related to D_4 minor structures, and is correlated with the regional late-stage folding of the Eastern and Western Complexes described in Chapter 2. Emplacement of the Trondheim Nappe must therefore have taken place during or after D_3, but before D_4. The three regional D_4 structures, recognised on the traverses investigated, are here referred to as the Gardsjoen and Singsas Synforms and the Grotli Antiform, and are shown, together with other D_4 structures, on Map 1.

Geological cross-sections, based on field observations and published maps (Wolff, 1967b, 1976; Gee, 1975a, 1978), have been constructed for each of the traverses investigated, and are presented in Fig. 3.9. D_3 and D_4 axial planes are indicated together with a possible position for the regional D_2 axial plane.

The model demonstrated in Figs. 3.8 and 3.9 satisfies all of the restrictions on interpretation imposed by the structural, stratigraphic, and metamorphic features outlined at the beginning of this section. Furthermore, it is consistent with the possibility of a correlation of

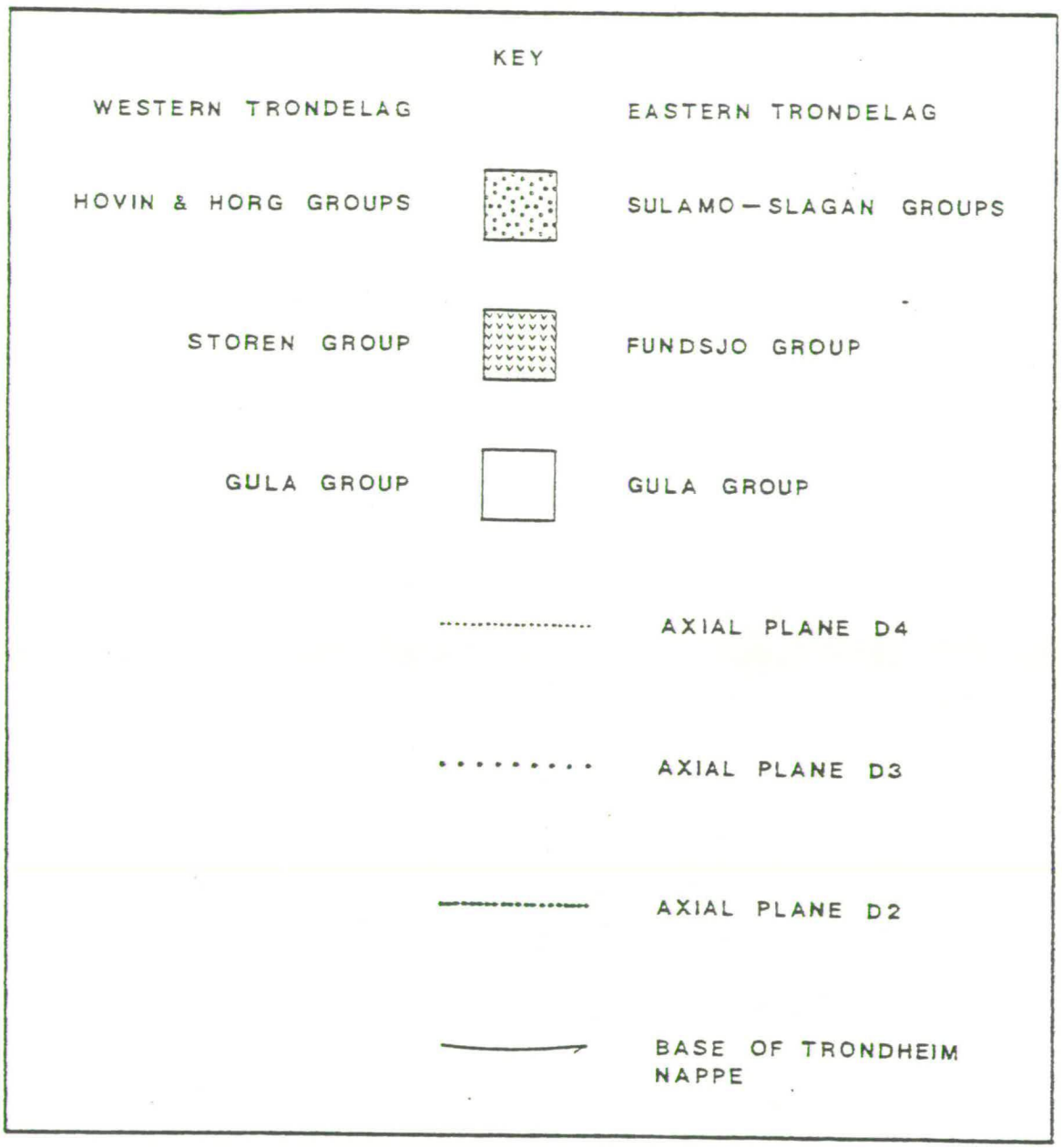

Fig. 3.9 Geological cross-sections through the Trondheim Nappe based on field observations and published maps (Wolff, 1967b, 1976; Gee, 1975a, 1978).
Dashed lines indicate the correlation of the Eastern and Western Trondelag successions.

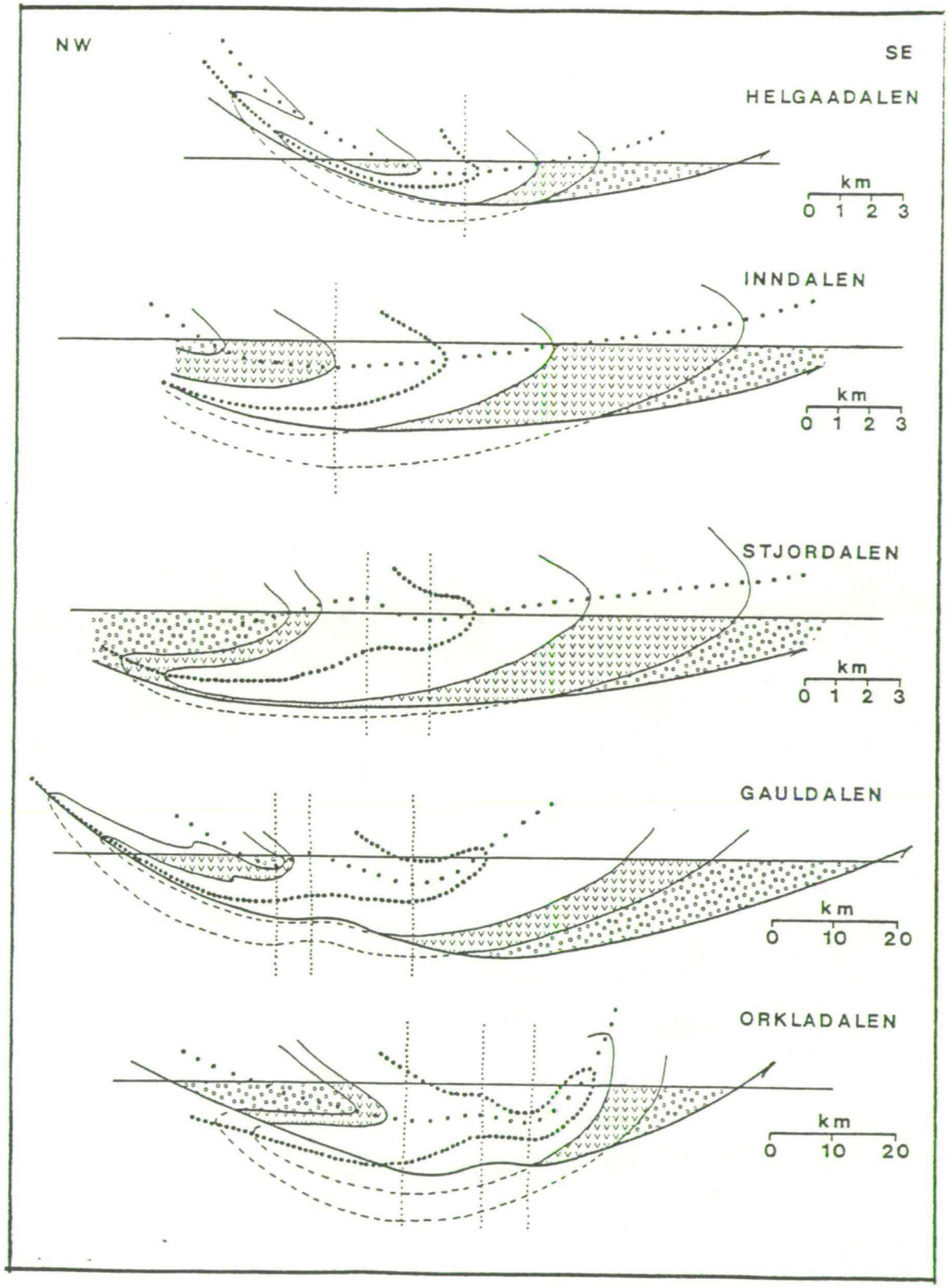
NW
SE
HELGAADALEN
km
0 1 2 3
INNDALEN
km
0 1 2 3
STJORDALEN
km
0 1 2 3
GAULDALEN
km
0 10 20
ORKLADALEN
km
0 10 20

the Undal and Asli Formations within the Gula Group, as suggested in 3.1.2.

3.4 Conclusions.

Gee and Zachrisson (1974) proposed a structural interpretation of the Trondelag region involving a stratigraphic correlation of the Eastern Trondelag succession with the Koli Supergroup of Sweden. This interpretation has been discussed, and is rejected on the basis that it is incompatible with established details of Trondelag geology. The more widely held correlation of the Eastern Trondelag succession with the Western Trondelag succession is favoured in this thesis.

On the basis of lithological similarity, the possibility of a stratigraphic repetition within the Gula Group, involving a correlation of the Undal and Asli Formations, has been suggested.

The controversial outcrop of the Gula Group in western Trondelag, and on the flanks of the Tommeras antiform, has been investigated. A narrow sliver (less than 1 km wide) of typical Gula lithologies has been identified separating the low-grade Storen metavolcanics from the garnetiferous Seve amphibolites of the underlying Seve-Koli Nappe Complex. In southern Trondelag, however, the Gula and Storen Groups are successively thrust out along the base of the Trondheim Nappe, such that the Hovin Group rests directly on the high-grade Seve.

The sequential development of mesoscopic structures within the Gula Group is described. Limited observations have also been carried out on higher stratigraphic units. An early phase of isoclinal deformation (D_1) affects only the Gula, Storen, and Fundsjo Groups, and is associated with an early Cambro-Ordovician orogenic development referred to here as the Trondheim Orogeny. Two subsequent phases of isoclinal folding (D_2 and D_3) and later, less intense deformation (D_4 and

D_5) are related to the main Scandinavian Orogeny (Silurian to Devonian). Major structures probably relating to D_2, D_3 and D_4 dominate the regional geology of the Trondheim Nappe, which was emplaced syn- or post-D_3, but pre-D_4.

CHAPTER 4

COPPER-ZINC SULFIDE MINERALISATION

A brief historical introduction to the principal mining districts associated with copper-zinc mineralisation within the Gula Group has been presented in Chapter 1. Such deposits are largely restricted to the amphibolite horizons interbedded with the Gula schists. Small ($<0.5 \times 10^6$t) massive pyritic bodies constitute the most important ore type and generally have an elongate-lens shape, commonly arranged in an en echelon pattern within any one ore district. The ores are often located at fold hinges, at or near amphibolite schist contacts. Frequent lithological associations are magnetite-rich quartzites, magnetite-amphibole-garnet schists, and garnetiferous quartzites. These rocks have been described in detail by Nilsen (1978) and interpreted by him as metamorphosed cherty iron-formations.

Pyrite is by far the most important sulfide mineral present, with lesser and variable amounts of pyrrhotite, chalcopyrite, sphalerite, and galena. Magnetite is a common accessory constituent. Examples of this type of mineralisation are the Kvikne and Rostvangen deposts (Nilsen and Mukherjee, 1972; Rui, 1973a; Nilsen, 1978).

Less commonly, sulfide deposits occur in association with the various schist lithologies forming the bulk of the Gula Group. The shape, size, structural relationships, and mineralogy of these deposits are similar to those of amphibolite association, and indeed, examination of Nilsen's (1978) map indicates that many are no more than a few hundred metres removed from such horizons. The Undal deposit is an example of mineralisation not far removed from amphibolites, while Flottum and Nordgruve apparently have no such relationship (Nilsen, 1978; Waltham, 1968b).

Many copper-zinc sulfide deposits occur in association with the

metavolcanics and metasediments of the Storen and Fundsjo Groups. While larger tonnages are present (up to 25 x 10^6t), these bodies are similar in shape and structural relationships to those in the Gula Group, and are associated with metavolcanic horizons and metamorphosed cherty iron-formations. The Lokken deposit occurs entirely within metavolcanics of the Storen Group, while those at Tverfjellet and Killingdal occur at metavolcanic/metasedimentary contacts within the Storen and Fundsjo Groups respectively.

An excellent summary of the history of genetic concepts concerning Scandinavian sulfide deposits of this type is given by Vokes (1976). There is now general concensus that the common association with volcanic rocks is not only spatial, but also genetic. The sulfide ores are considered to be metamorphosed volcanogenic massive sulfide deposits resulting from submarine hydrothermal emanations (Oftedal, 1958; Rui, 1973a; Vokes and Morton, 1973; Vokes, 1976; Vokes and Gale, 1976; Nilsen, 1978). When extended to include the Gula Group copper-zinc sulfide/amphibolite association, this model presupposes a volcanic origin for the Gula amphibolites (Rui, 1973a; Vokes and Morton, 1973; Nilsen, 1978). Mineralisation intimately associated with the amphibolites is thought to represent in situ formation, while ores located within Gula schists, but close to the amphibolites may represent transported and resedimented sulfides as initially suggested by Jenks (1971) for deposits such as those on the Japanese island of Shikoku. Strauss and Madel (1974) proposed similar origins for a number of the major deposits of the Iberian pyrite belt (e.g. Tharsis North Lode). The possibility of primary deposition of sulfides, in non-volcanic environments, by migration of metal-rich brines away from a volcanic source (Sato, 1972 ; Turner and Gustafson, 1978) should also be considered. It is less easy to assign a volcanogenic origin to the Gula deposits

with no apparent spatial relationship to amphibolitic horizons, although the sulfide transportation and resedimentation hypotheses mentioned above may explain them, especially when subsequent deformation is taken into account.

Chapter 3 has demonstrated that the Gula, Storen, and Fundsjo Groups have been involved in an early Cambro-Ordovician orogenic event, the Trondheim Orogeny. This chapter presents the results and conclusions of a comparative study of copper-zinc sulfide deposits in these three units. A geochemical investigation of the associated metavolcanics provides clues to their original tectonic environment, while a study of sulfide textures and mineral chemistry provides information on the subsequent metamorphism of the deposits.

4.1 General Comments.

Fundamental to any discussion of the genesis and subsequent history of massive volcanogenic sulfide deposits is the question of original depositional environment. A geochemical study of the associated metavolcanics (4.3) provides valuable insight to this problem, but it must be emphasised that any interpretation must be consistent, not only with the geochemical data, but also with all available geological evidence. This is perhaps especially important in areas of intense deformation and metamorphism where many of the original geochemical characteristics of volcanic rocks may be modified. It is therefore pertinent at this stage to summarise, and emphasise, the more general geological features relating to the Gula, Storen,and Fundsjo Groups.

4.1.1 The Gula Group.

The Gula Group consists of a variety of highly deformed and metamorphosed schistose lithologies including conformable, discontinuous bands and lenses of metabasic material from 1 to 50 m thick. As mentioned previously these Gula amphibolites are generally assumed to be

metamorphosed basic extrusives, although evidence for this is rare. However, the common association of the amphibolites with massive sulfides, and banded ferruginous quartzites (interpreted as metacherts by Nilsen, 1978), together with the pillows, scoriae, and vesicular textures reported by Waltham (1968b) in his study of the Folldal area, is here taken as reasonable justification for ascribing such an origin to these horizons.

The remainder of the Gula Group, consisting of a variety of micaceous schists, ranging from pelitic to psammitic in character is usually regarded as metasedimentary in origin (e.g. Olesen et al., 1973). Primary sedimentary structures are rare but have occasionally been recorded from the more psammitic lithologies (Olesen et al., 1973; Nilsen, 1978).

The possibility that at least a proportion of the Gula schistose lithologies represents original intermediate and more evolved volcanics must also be considered. Waltham (1968b) described the hornblende-bearing schists in the Folldal area, which "by considerable textural and mineralogical variations grades in opposite directions towards micaschist and greenstone", as extrusive or pyroclastic in origin. Sangster and Scott (1976) have drawn attention to the possible metamorphic equivalents of primary rock types commonly associated with Precambrian massive copper-zinc-lead sulfide deposits in North America (Table 4.1). The similarity between these metamorphic equivalents and some of the lithologies occurring in the Gula Group is notable, and may provide an explanation for Gula copper-zinc sulfide deposits with no apparent spatial relationships to amphibolite horizons. However, in view of the general lack of original textures and structures, the proposal that a proportion of the Gula schists represents deformed and metamorphosed intermediate and more evolved volcanics could only be

Primary or Low-Grade Metamorphic Rock	Medium-Grade Metamorphism	High-Grade Metamorphism
Chert	Siliceous schist	Quartzite
Pyritic, cherty iron-formation	Pyrite-pyrrhotite-magnetite mica schist	Pyrrhotite-magnetite mica quartzite
Rhyolite Rhyolite tuff Rhyolite breccia Rhyolite agglomerate	Quartz-feldspar-sericite gneiss	Quartz-feldspar gneiss
Andesitic tuff (chlorite-schist)	Biotite-chlorite-quartz schist	Biotite-quartz gneiss
Andesite (chlorite-schist)	Epidote-plagioclase-amphibolite	Hornblende-plagioclase-amphibolite gneiss
Basalt (chlorite-schist)	Epidote amphibolite	Amphibolite (gneiss)

TABLE 4.1 Possible metamorphic equivalents of primary igneous lithologies (from Sangster and Scott, 1976).

tested by detailed geochemical investigations. An example of such a study is that carried out by Bowes et al. (1971) in the Kylesku Group of the Lewisian of N. W. Scotland. A largely volcanic origin was suggested on the basis of major and trace element abundances.

In conclusion, the Gula Group is a complex system of highly deformed and metamorphosed volcanics and sediments. The amphibolites and possibly a proportion of the schistose lithologies probably represent original extrusive volcanics, interbedded with a mixture of terrigenous and authigenic sediments.

4.1.2 The Storen and Fundsjo Groups.

It has been suggested in Chapter 3 that the Storen and Fundsjo Groups are stratigraphic equivalents. They are dominated by metabasaltic rocks and have a strike length within the Trondheim Nappe of nearly 350 km. A total thickness of 2.5 km has been suggested (Gee, 1975a). If the postulated correlation with similar lithological units at equivalent tectonic level to the north and south is accepted (Strand and Kulling, 1972, page 67; Gale and Roberts, 1974; Halls et al., 1976), a strike length of some 800 km is possible.

Primary structures such as pillows are common (Oftedahl, 1968; Grenne et al., in prep.), while amygdaloidal textures have occasionally been preserved (Bugge, 1910; Chaloupsky and Fediuk, 1967). The metabasaltic rocks, especially in the Fundsjo Group, are frequently associated with sill-like keratophyric horizons (Nilsen, 1978). As such units may often be traced into well defined agglomerates (Oftedahl, 1967) a pyroclastic origin is most likely. Gabbros and ultramafics have been recorded as tectonically emplaced bodies within the metavolcanics (Gee, 1975b; Grenne et al., in prep.).

Various sedimentary lithologies have been recorded in the Storen and Fundsjo Groups. Cherts and volcanogenic sediments are common,

while limestone horizons have occasionally been recorded (Gee, 1975a; Wolff, 1976) and have been noted during this study (Storen Group, Helgaadalen traverse).

A submarine origin is indicated for these rocks by the extensive pillow lavas and their association with cherts, limestones and other subaqueous sediments. The great strike length suggests a linear volcanic axis, while the limestones and pyroclastics imply deposition in a relatively shallow environment.

4.2 Petrology of the Associated Metabasics.

Many detailed petrological descriptions of the metavolcanics of the Gula, Storen, and Fundsjo Group are present in the literature. This section presents a brief resume of these data, and is consistent with the petrological investigation of the samples collected for geochemical analysis during this study (4.3).

Without exception the primary igneous mineralogy has been obliterated by subsequent metamorphism, while the combined effects of metamorphism and deformation have destroyed almost all igneous textures. Mineral assemblages and textures typical of deformed rocks of basaltic composition which have been metamorphosed to greenschist, epidote-amphibolite, and amphibolite facies, now predominate.

4.2.1 The Gula Group.

The basic metavolcanics of the Gula Group have been studied in detail by Nilsen (1974), Nilsen and Mukherjee (1972), and Rui (1973a). They occur as fine grained schistose amphibolites of a dark green to greenish-grey colour. A green hornblende and an oligoclase to andesine plagioclase are the major mineral constituents. Hornblende occurs as elongated prisms up to 2.0 mm in length and generally possesses a preferred orientation, while plagioclase forms a more granoblastic, fine-

grained groundmass (Fig. 4.1). Biotite, chlorite, clinozoisite, carbonate, apatite, sphene, rutile, and ilmenite occur as accessory constituents. At contacts with the enclosing schists, and in thin amphibolite bands, almandine garnet may occur together with calcium-free amphiboles such as cummingtonite and anthophyllite. Nilsen and Mukherjee (1972) suggest that these assemblages are the result of contact metasomatism similar to that described by Tilley (1935) from metamorphosed basic flows in Cornwall.

The assemblage dominated by hornblende and intermediate plagioclase is characteristic of the amphibolite facies of Miyashiro (1968), or the low-rank amphibolite facies of Ernst (1973), and is consistent with the occurrence of kyanite and staurolite in the surrounding schists (Fig. 2.1; Roberts, 1968).

4.2.2 The Storen Group.

The basic metavolcanics of the Storen Group have been described most recently where they outcrop between Stjordalen and Inndalen by Dudek et al. (1973); and around Trondheim and in the Lokken area by Oftedahl (1968). Earlier descriptions are provided by Vogt (1945) for the Holanda-Horg area, and by Wolff (1960) for the Verdal area.

Comparison of Map 1 with Fig. 2.1 indicates that the Storen Group outcrops in areas of variable metamorphic grade. Samples S1, S2, S10, S12, S13 are from areas of greenschist facies metamorphism (Miyashiro, 1967; Ernst, 1973). This is reflected in a mineralogy dominated by chlorite, actinolite, epidote, and albite. Samples S3, S5, S6, S7, S9, and S11 however, contain only minor chlorite and are characterised by hornblende, epidote, and sodic plagioclase, an assemblage characteristic of the epidote-amphibolite facies of Miyashiro (1968), or transitional between the greenschist and low-rank amphibolite facies of Ernst (1973).

Fig. 4.1 Photomicrograph of Gula amphibolite (sample G9). Elongated hornblende in a matrix of plagioclase and sphene. Transmitted light; plane polarised light (ppl); smallest dimension of field of view (f.o.v.) = 1.50 mm.

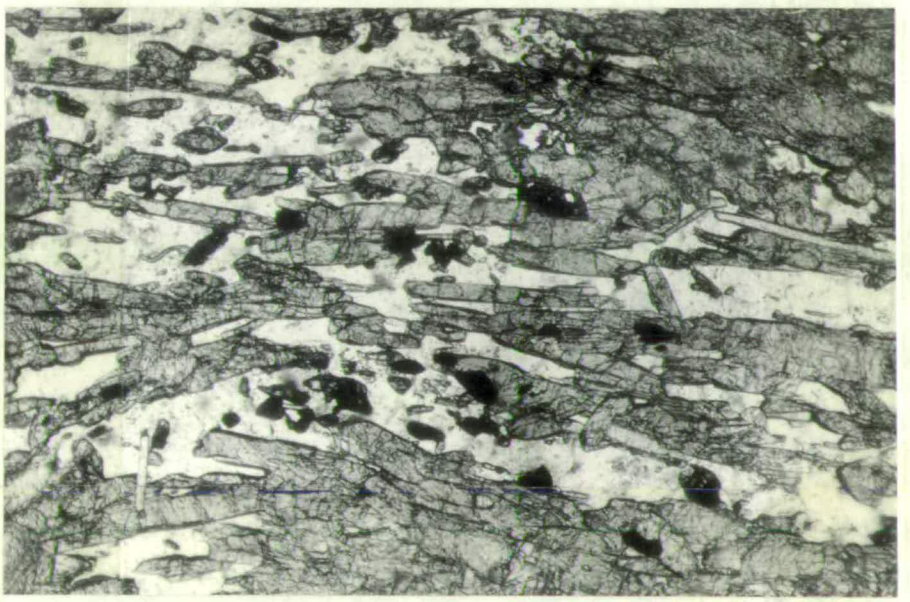

The rocks are commonly foliated, especially in higher-grade localities, and have an apple green to dark green appearance. Amphibole may be porphyroblastic (rarely more than 1.5 mm in length) and generally possesses a preferred orientation which defines the foliation (Fig. 4.2). Chlorite occurs in the lower-grade samples as undulating sheaths often intergrown with actinolite. In higher grades it commonly grows across the foliation suggesting a retrogressive or later metamorphic origin. Epidote and plagioclase form a more granoblastic, fine-grained matrix, except in lower-grade varieties where epidote may occur as well formed porphyroblasts up to 0.5 mm in diameter. Quartz, ilmenite, sphene, apatite, and biotite are common accessories.

In the least deformed of the low-grade samples textures suggesting a primary porphyritic nature have been noted. Probable original phenocrysts (less than 0.75 mm in diameter) are outlined by opaque dust and completely replaced by actinolite and chlorite (Fig. 4.3). Crystal shape is never well preserved but an impression of six- and eight-sided habits is suggested by overall inspection. The possibility of phenocryst enrichment, probably by ferromagnesian minerals such as olivine and pyroxene, has implications to the considerations of geochemistry presented in the following section.

4.2.3 The Fundsjo Group.

The metabasics of the Fundsjo Group have been described in detail from the area around Stjordalen by Chaloupsky and Fediuk (1967), and Siedlecka and Siedlecki (1967); from north of Stjordalen by Dudek et al. (1973) and Wolff (1960); and from southern Trondelag by Rui (1972, 1973b) and Nilsen (1971).

The assemblages and textures are in general very similar to those in the higher-grade Storen samples. Hornblende and sodic plagioclase

Fig. 4.2 Photomicrograph of Storen metabasalt (sample S9).
A well-foliated, fine-grained, hornblende, epidote, plagioclase rock.
Transmitted light; ppl; f.o.v. = 1.92 mm.

Fig. 4.3 Photomicrograph of Storen metabasalt (sample S1).
Possible pseudomorphs after igneous phenocrysts (centre) in actinolite, chlorite, epidote, albite rock.
Transmitted light; ppl; f.o.v. = 2.40 mm.

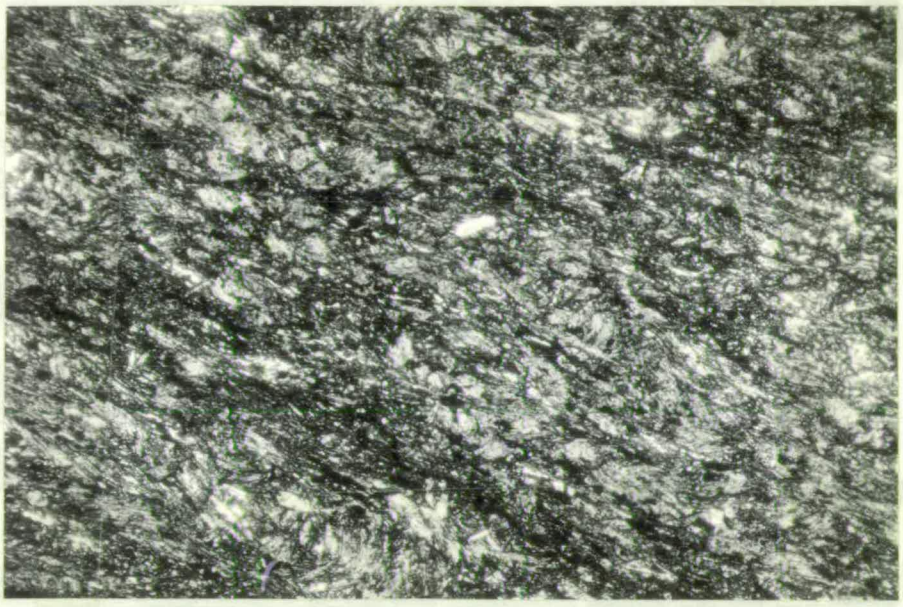

are dominant, with lesser amounts of epidote, and traces of quartz, ilmenite, sphene, apatite, and biotite. These rocks are characteristic of Miyashiro's (1968) epidote-amphibolite facies or the lower part of Ernst's (1973) low-rank amphibolite facies.

4.3 Geochemistry Of The Associated Metabasics.

There is a general lack of geochemical data on the basic metavolcanics of the Gula, Storen, and Fundsjo Groups. One exception to this is the study of all Gula metabasics, including mafic and ultramafic intrusives, carried out by Nilsen (1974). On the basis of 29 major-element analyses, Nilsen (1974) concluded that a tholeiitic fractionation trend genetically relates all basic extrusive and intrusive rocks within the Gula Group. However, evidence to be presented in Chapter 5 indicates that while the metagabbroic intrusions may be genetically related to the apparently extrusive amphibolites, the ultramafics definitely are not. Furthermore, it has long been established that submarine and subaerial weathering, and metamorphism result in considerable modifications to the chemistry of basic igneous rocks (Melson and Van Andel, 1966; Cann, 1969; Hart, 1970; Matthews, 1971). The use of major elements in petrogenetic considerations of metamorphosed basalts such as those of the Gula, Fundsjo and Storen Groups is therefore severely limited.

However, hygromagmatophile elements (Wood, Joron et al., 1979) such as P, Ti, Zr, Y, and Nb, which are characterised by a high charge/radius ratio (field strength) are rarely transported in aqueous fluids and tend to remain unaffected during metasomatic alteration (Pearce and Norry, 1979). These characteristics, together with their systematic variation in fresh lavas, allows these less mobile trace elements to be used to study weathered and metamorphosed basalts whose mineralogy and

chemistry have otherwise been too greatly altered for accurate petrographic interpretation.

Such techniques were initially developed on an empirical basis by investigation of these elements in fresh basalts of different petrological character and tectonic setting. Pearce and Cann (1973) drew attention to the high Y/Nb ratios (>2) of tholeiitic relative to alkali basalts, and developed a series of diagrams which could be used to discriminate basalts erupted in different tectonic environments. Further contributions were provided by Floyd and Winchester (1975); Pearce (1975); and Bloxam and Lewis (1972). A recent attempt to explain the variations in concentration of these elements by consideration of mineral-liquid distribution coefficients and petrogenetic modelling has met with reasonable success (Pearce and Norry, 1979).

These methods have previously been applied to the metamorphosed basic volcanics of the Storen Group. An ocean-floor origin has been suggested by Gale and Roberts (1974), Vokes and Gale (1976), and Pearce and Gale (1977), although consideration of geological as well as geochemical evidence led these authors to prefer deposition in a marginal basin environment. These contributions were based on the same group of analyses.

No trace-element geochemical data has previously been obtained from the metavolcanics of the Gula and Fundsjo Groups. Approximately a dozen samples each of these, and Storen Group metavolcanics were collected for whole-rock analyses. Sample selection was carried out to provide as wide a geographical distribution as possible. The locations of individual samples are shown in Fig. 4.4. Metamorphic veining of quartz and calcite, metasomatic reaction zones (such as those described in 4.2.1) and subaerial weathering were avoided, such that only homogenous, apparently basic rocks were sampled. The analytical techniques are described in Appendix A.

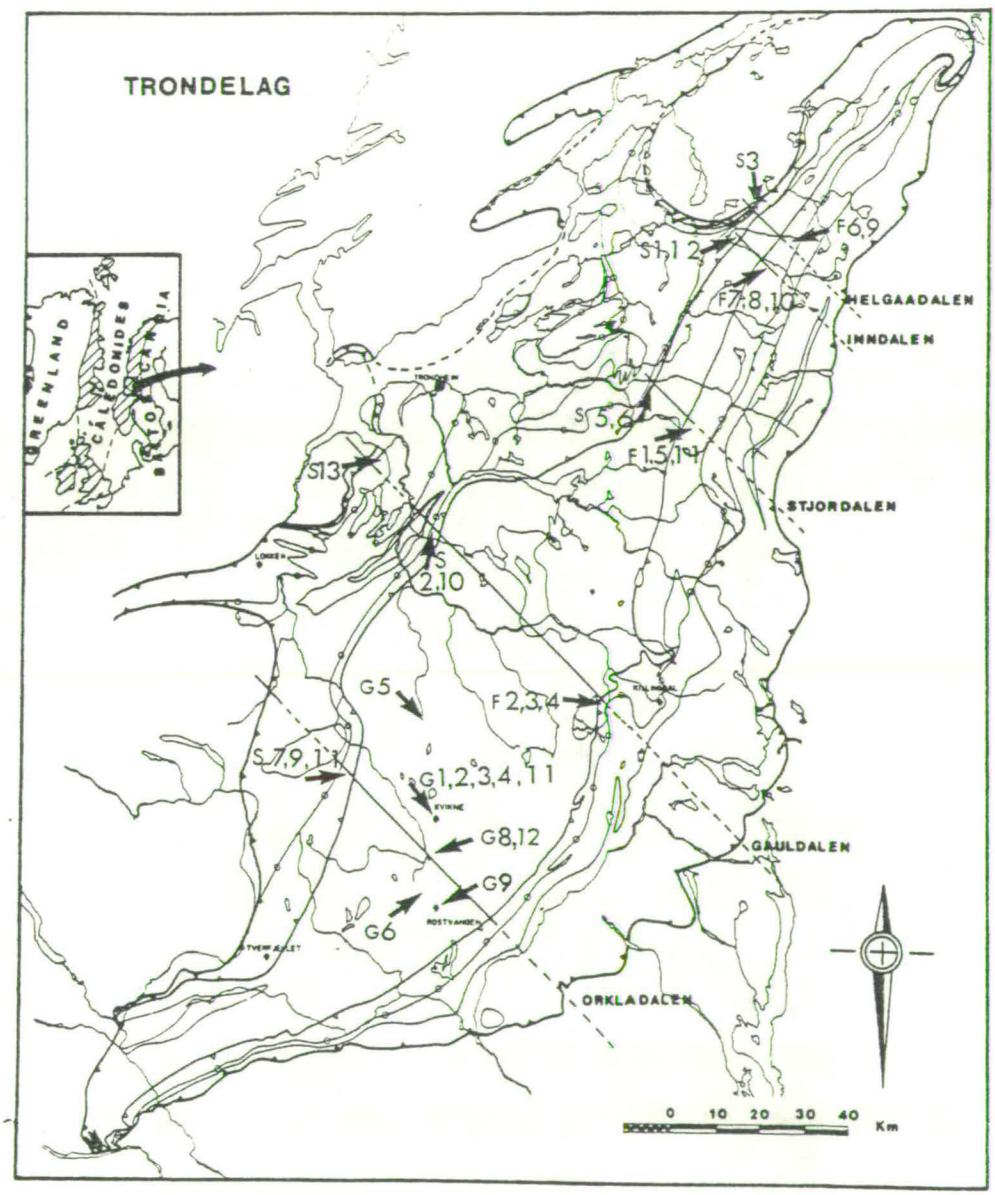

Fig. 4.4 Location of samples of Gula, Storen, and Fundsjo Group metavolcanics analysed in this study.

4.3.1 Major elements.

Major element concentrations of Storen, Fundsjo, and Gula Group metabasics are listed in Tables 4.2, 4.3, and 4.4 respectively. Without exception all analyses fall within the composition limits of basalts (Manson, 1967). However, high Na_2O values relative to CaO as illustrated in Fig. 4.5, suggest that many of these rocks have suffered spilitic alteration (Graham, 1976). The recognition of such alteration, together with the probable effects of metamorphism, restricts the usefulness of major element concentrations to petrogenetic considerations as previously mentioned, and further comment on these data will not be made.

4.3.2 Trace elements.

Trace element data for metabasics of the Storen, Fundsjo, and Gula Groups are presented in Tables 4.2, 4.3, and 4.4. P_2O_5 values are low (usually <0.25 wt %) and Y/Nb and Zr/Nb are high (generally greater than 2.0 and 7.0 respectively) indicating the dominantly tholeiitic nature of all three groups (Pearce and Cann, 1973; Erlank and Kable, 1976; Floyd and Winchester, 1975).

4.3.2.1 The Gula Group - In Gula Group metabasics Ti, Zr, Y and Zr/Y are lower than in typical mid-ocean ridge basalts (MORB). As a consequence, the majority of these rocks plot in the fields of low-K tholeiites of island arcs in Figs. 4.6 and 4.7 (after Pearce and Cann, 1973) and in the field of island arc basalts in Fig. 4.8 (after Pearce and Norry, 1979). In an interpretation of these results it is important to remember that these metabasics have suffered amphibolite facies metamorphism. Although the trace elements quoted in Tables 4.2, 4.3. and 4.4 and plotted in Figs. 4.6, 4.7, and 4.8 have generally been regarded as "stable" under metamorphic conditions, the high pressures indicated for the Gula Group by sphalerite geobarometry (4.4.5)

TABLE 4.2 Analyses of Storen Group metabasalts. Major oxides as wt %; trace elements as ppm.

	S1	S2	S3	S5	S6	S7	S9	S10	S11	S12	S13
SiO_2	46.84	48.09	48.76	46.91	48.14	48.36	48.18	50.13	48.00	46.78	47.42
TiO_2	1.82	1.73	2.24	3.20	2.72	1.77	2.37	1.67	1.40	3.38	0.92
Al_2O_3	12.61	15.11	15.36	12.98	14.53	14.2.	15.50	13.56	14.25	14.23	14.24
Fe_2O_3	12.80	11.11	14.04	15.90	13.35	12.63	10.42	11.74	10.82	14.57	8.74
MgO	14.32	7.86	5.59	7.71	6.21	7.42	8.31	7.63	11.46	6.89	7.63
MnO	0.21	0.17	0.17	0.24	0.17	0.19	0.15	0.18	0.16	0.20	0.19
CaO	8.13	12.62	7.57	7.97	8.52	12.12	10.41	11.07	10.36	9.14	15.24
Na_2O	1.33	2.49	4.76	3.52	4.00	2.68	2.83	3.27	1.77	3.28	5.36
K_2O	1.01	0.12	0.15	0.36	1.10	0.18	0.61	0.29	0.98	0.32	0.08
P_2O_5	0.25	0.19	0.34	0.42	0.38	0.18	0.31	0.16	0.15	0.36	0.11
LOI	4.26	2.34	2.71	2.66	1.45	1.00	0.66	3.02	2.09	3.29	10.66
Cr	1030	351	4	82	22	312	306	382	443	149	211
Zr	78	77	116	132	108	71	67	126	61	110	34
Nb	11	5	7	13	25	6	5	9	5	14	3
Y	17	23	26	30	18	24	22	29	19	22	17
Th	2	1	2	2	4	2	2	2	1	2	3
Y/Nb	1.6	4.6	3.8	2.4	0.7	3.7	3.9	3.1	3.7	1.6	5.6
Zr/Nb	7.3	15.7	16.8	10.4	4.4	11.1	12.1	13.5	12.0	8.0	11.0

TABLE 4.3 Analyses of Fundsjo Group metabasalts. Major oxides as wt %; trace elements as ppm.

	F1	F2	F3	F4	F5	F6	F7	F8	F9	F10	F11
SiO_2	49.06	49.97	48.47	48.08	50.19	50.73	48.71	50.79	52.30	52.47	48.71
TiO_2	1.01	1.36	0.71	1.39	1.33	2.02	1.37	1.22	0.91	1.51	1.89
Al_2O_3	16.70	16.18	16.73	16.28	15.39	14.90	20.72	15.72	15.22	14.77	16.20
Fe_2O_3	7.45	8.92	8.26	12.45	9.55	11.33	7.35	12.16	10.16	12.86	14.15
MgO	6.71	6.12	9.23	7.52	7.89	5.79	6.11	7.63	7.08	7.19	5.42
MnO	0.12	0.16	0.13	0.21	0.15	0.20	0.12	0.26	0.17	0.35	0.16
CaO	12.33	11.09	12.53	8.27	11.39	9.83	10.11	7.49	9.60	5.80	7.43
Na_2O	3.34	5.04	2.70	3.61	3.34	4.31	4.32	3.95	4.10	4.55	5.11
K_2O	0.14	0.18	0.11	1.15	0.09	0.31	0.49	0.10	0.18	0.07	0.43
P_2O_5	0.13	0.19	0.06	0.20	0.17	0.25	0.17	0.11	0.11	0.18	0.21
LOI	0.36	4.15	-0.10	0.48	0.58	0.47	0.51	0.88	0.58	1.17	2.35
Cr	271	162	420	228	89	47	280	141	165	69	-
Zr	63	88	21	75	86	124	68	46	34	76	54
Nb	5	10	3	12	4	5	7	3	3	4	4
Y	17	20	11	26	17	25	19	22	19	27	23
Th	2	3	2	2	1	1	3	0.1	1	3	1
Y/Nb	3.3	2.0	3.3	2.2	4.2	4.8	2.7	6.3	6.0	6.8	5.4
Zr/Nb	11.9	9.1	6.5	6.3	21.6	23.4	9.7	13.1	11.0	18.9	12.5

TABLE 4.4 Analyses of Gula Group metabasalts. Major oxides as wt %; trace elements as ppm.

	G1	G2	G3	G4	G5	G6	G8	G9	$G1_1$	$G1_2$
SiO_2	47.71	47.93	48.04	47.84	48.43	49.90	47.39	47.41	49.39	48.98
TiO_2	0.95	0.86	1.19	1.03	1.24	1.93	1.33	0.97	0.78	0.90
Al_2O_3	15.00	14.68	15.11	15.56	14.74	13.91	16.82	15.65	12.52	12.95
Fe_2O_3	12.77	9.78	10.08	11.08	11.98	13.49	11.12	9.82	21.34	16.66
MgO	9.21	11.82	9.71	10.72	10.59	6.94	7.27	11.44	6.72	8.12
MnO	0.19	0.16	0.21	0.31	0.15	0.23	0.18	0.15	0.34	0.60
CaO	10.88	11.07	11.68	10.11	9.02	9.09	12.81	10.30	5.70	7.98
Na_2O	2.74	3.08	3.01	2.62	3.00	3.92	2.80	3.22	2.53	3.20
K_2O	0.40	0.39	0.59	0.22	0.80	0.30	0.23	0.24	1.50	0.14
P_2O_5	0.06	0.05	0.07	0.09	0.12	0.16	0.08	0.10	0.25	0.17
LOI	0.97	1.20	2.45	1.18	1.54	0.72	1.10	1.65	4.00	1.36
Cr	186	698	439	455	553	105	368	530	279	425
Zr	25	26	47	32	44	66	32	31	39	42
Nb	3	3	3	5	3	6	3	7	6	6
Y	18	15	18	16	16	24	19	16	16	16
Th	2	2	2	3	1	2	1	2	5	4
Y/Nb	5.5	5.1	6.0	3.1	5.1	7.4	6.0	2.2	2.6	2.6
Zr/Nb	7.9	8.6	15.7	6.2	13.8	11.8	10.2	4.1	6.4	6.9

	1		2		3		4		5		6
	a	b									
Zr	77.1	109.8	67	67	80	83	87	65	80	76	84
Ce_N	6.2	30.2	7.0	7.3	19.0	19.0	19.5	17.1	23.8	9.5	15.8
Y_N	11.7	11.4	14.9	13.8	12.3	12.3	10.8	10.8	6.1	4.6	12.3
Ce_N/Y_N	0.5	2.6	0.5	0.5	1.5	1.5	1.8	1.6	3.9	2.1	1.3

1 = Storen samples S_2 (a) and S_{12} (b); 2 = 'N'-type MORB from the Nazca plate (data from Rhodes et al,1976); 3 = 'E'-type MORB from the North Atlantic (data from Tarney et al, 1979); 4 = dykes from the Sarmiento ophiolite complex, southern Chile (data from Saunders et al, 1979); 5 = basalts from the Bransfield Strait marginal basin (data from Weaver et al, 1979); 6 = Basalt from the East Scotia Sea marginal basin (data from Saunders & Tarney, 1979).

TABLE 4.5 Rare-earth element patterns of Storen Group metabasalts compared with mid-ocean ridge and marginal basin basalts. (Values as ppm).

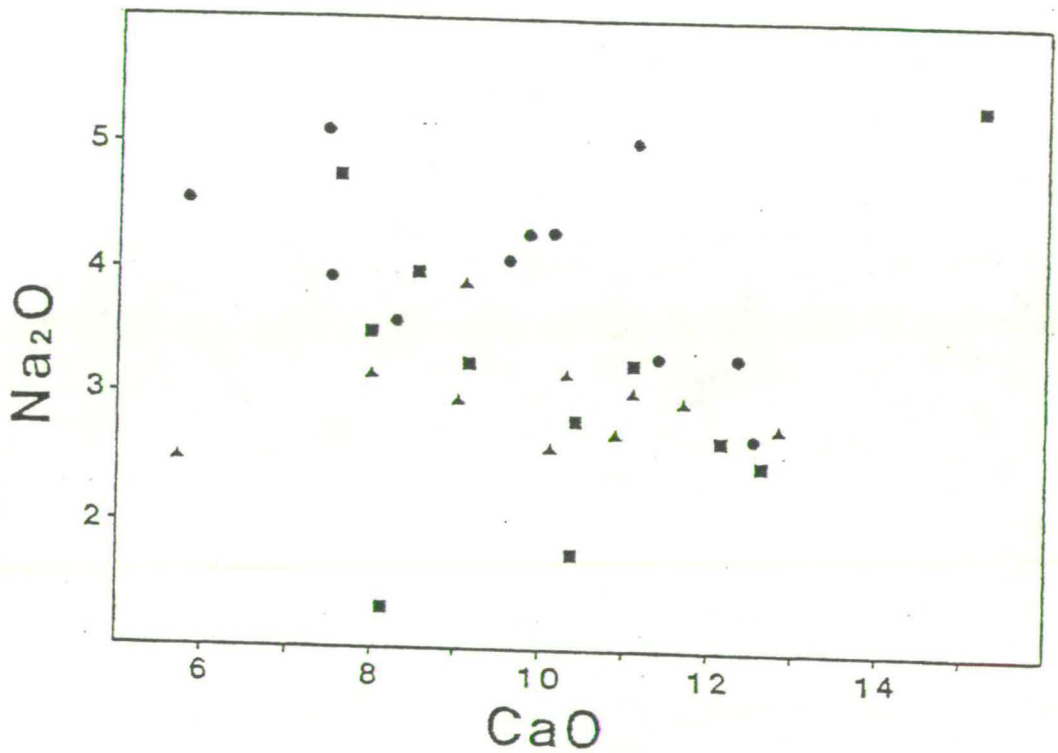

Fig. 4.5 Wt % Na_2O vs CaO for Gula (triangle), Storen (squares), and Fundsjo (circles) Group metabasalts.

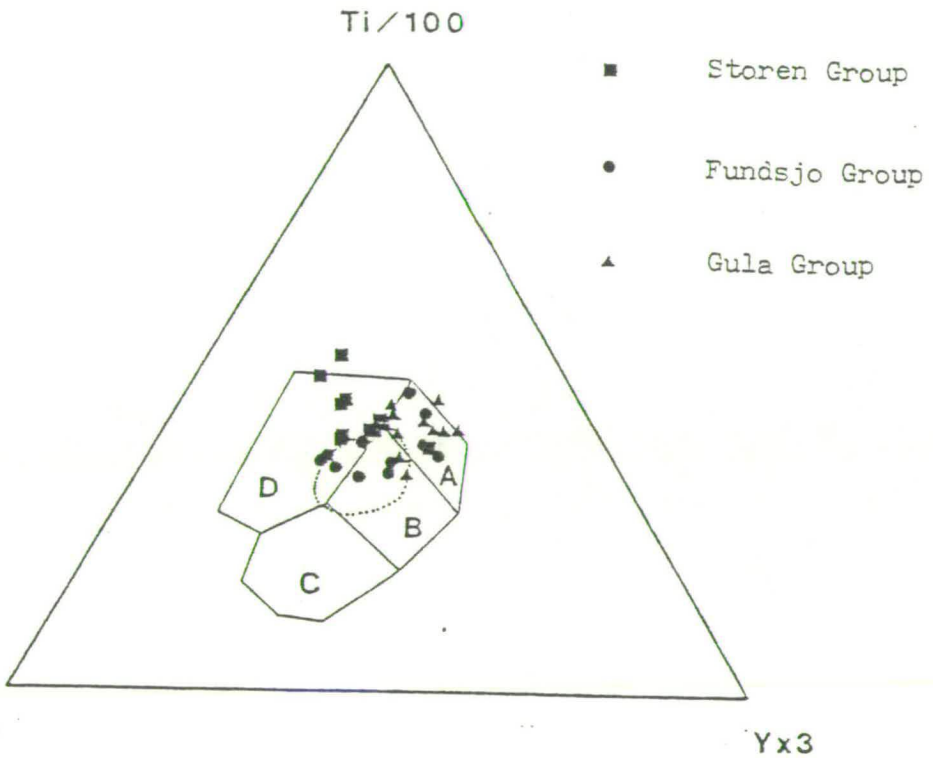

Fig. 4.6 Ti-Zr-Y plot (after Pearce and Cann, 1973) of Gula, Storen, and Fundsjo Group metabasalts. Field A = low-K tholeiites of island arcs; field B = mid-ocean ridge basalts and island-arc volcanics; field C = calc-alkaline basalts and andesites; field D = within-plate basalts. Dotted line = field of analyses published by Gale and Roberts (1974).

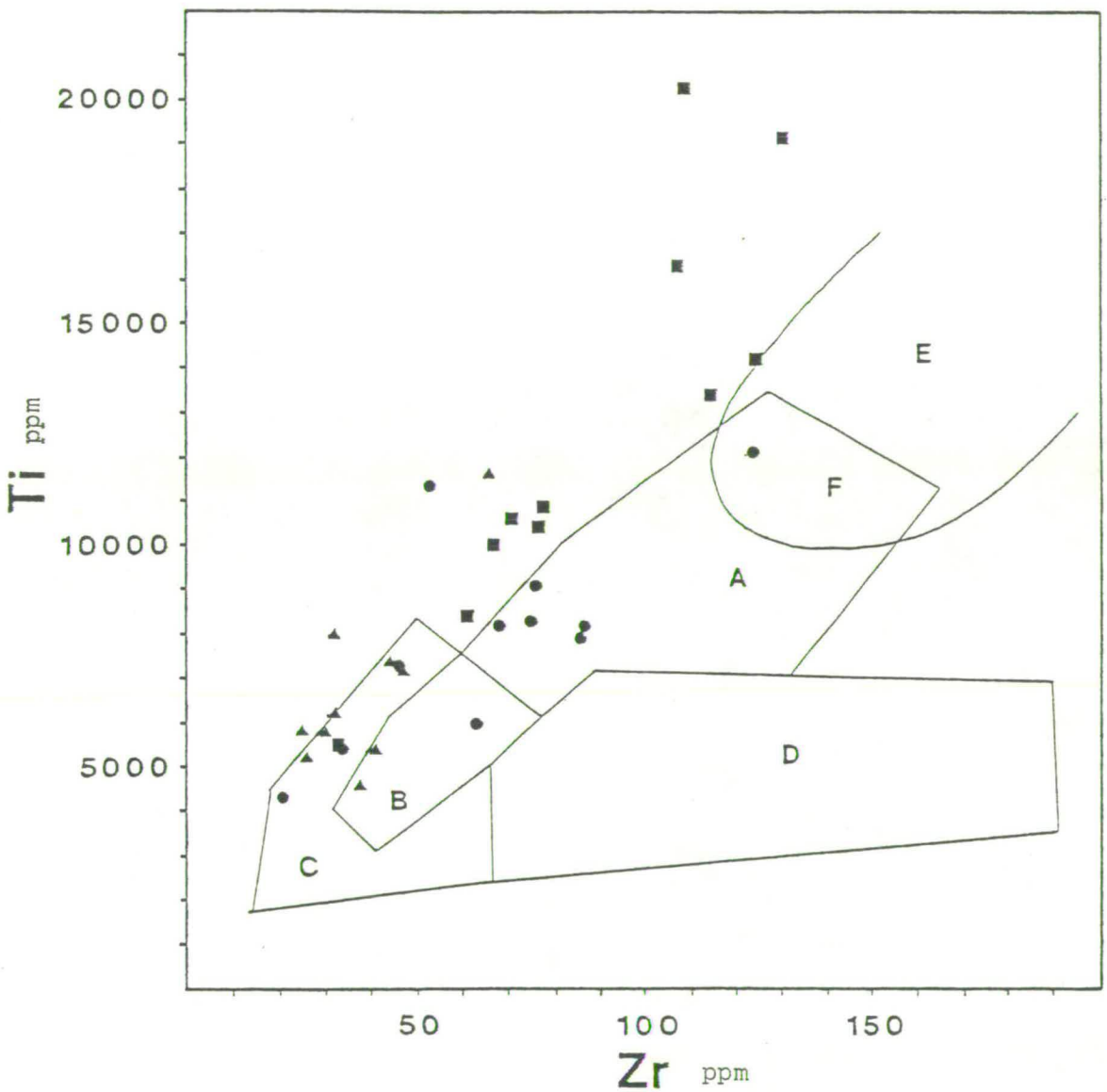

Fig. 4.7 Ti-Zr plot (after Pearce and Cann, 1973) of Gula, Storen, and Fundsjo Group metabasalts. Field A = mid-ocean ridge basalts; field B = mid-ocean ridge basalts and island arc volcanics; field C = low-K tholeiites of island arcs; field D = calc-alkaline basalts and andesites; field E = within-plate basalts (after Pearce and Gale, 1977); field F = mid-ocean ridge basalts and within-plate basalts. Symbols as in Fig. 4.6.

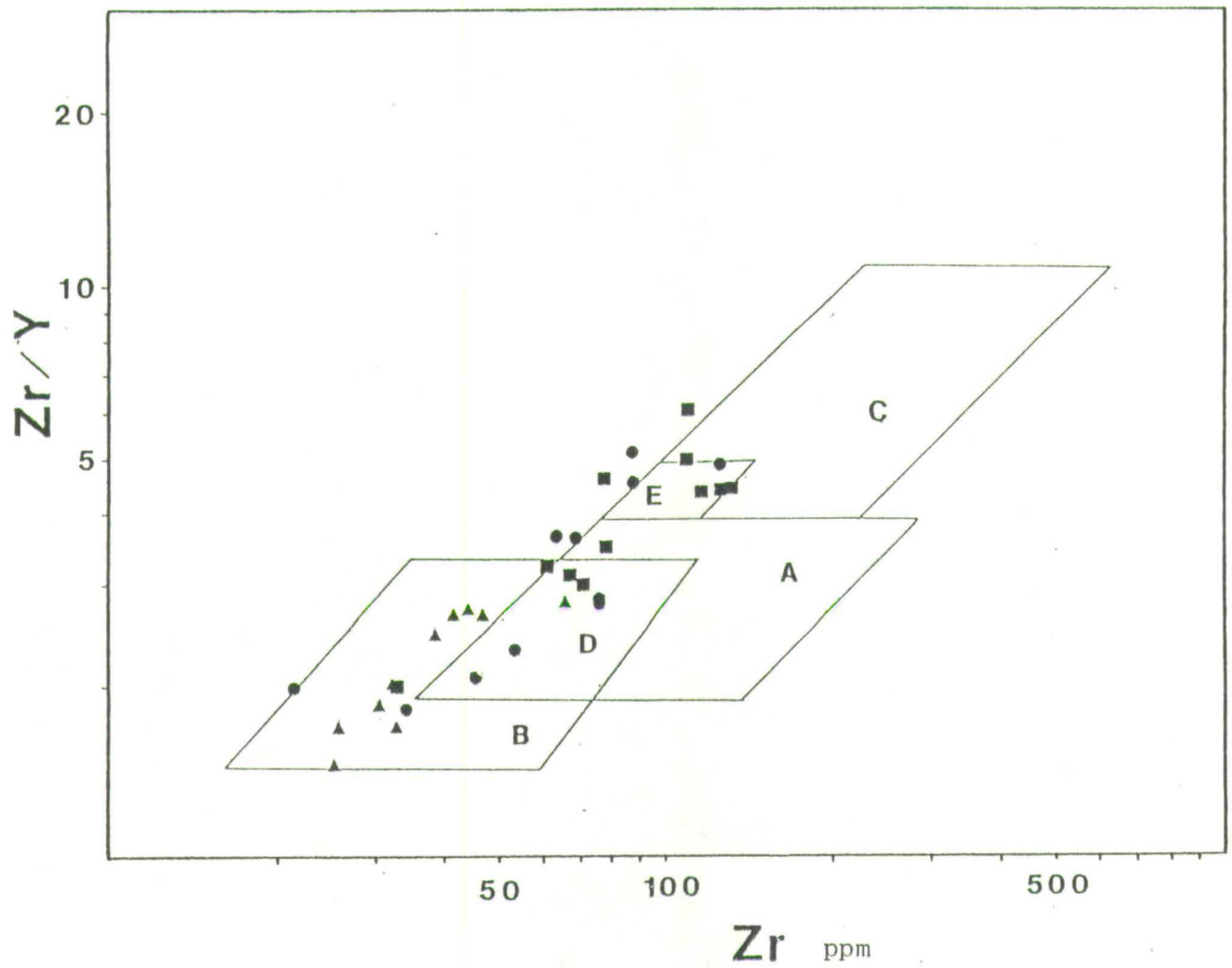

Fig. 4.8 Zr/Y vs Zr plot (after Pearce and Norry, 1979) of Gula, Storen and Fundsjo Group meta basalts. Field A = mid-ocean ridge basalts; field B = island-arc basalts; field C = within-plate basalts; field D = mid-ocean ridge basalts and island-arc basalts; field E = mid-ocean ridge basalts and within-plate basalts. Symbols as in Fig. 4.6.

dictate that any conclusions on tectonic setting based on geochemistry alone should be treated with caution.

4.3.2.2 The Storen and Fundsjo Groups - Metabasics from the Storen and Fundsjo Groups have variable abundances of Zr, Ti, and Y, and variable Zr/Y ratios. On Figs. 4.6 and 4.7 they fall in the MORB field, in the within-plate basalt (WPB) field, and in the field of island-arc tholeiites (IAT); while on Fig. 4.8 they plot largely in the MORB field, with some scatter into the island-arc basalt, and WPB fields. Enrichment of Ti relative to Zr causes many analyses to plot above the fields defined by Pearce and Cann (1973) in Fig. 4.7, perhaps as a result of phenocryst enrichment (4.2.2). Also shown on Fig. 4.6 is the field containing analyses of Storen metabasics published by Gale and Roberts (1974), and Vokes and Gale (1976), and referred to by Pearce and Gale (1977). The difference between these analyses and the results obtained in this study are probably explained by the fact that the earlier analyses represent a large number of samples from only two localities, while the analyses described here represent a much wider geographical distribution.

Trace element abundances such as those displayed in Figs. 4.6, 4.7, and 4.8 have been interpreted by a number of workers as suggesting transitional tectonic environments. For instance, Olsen (in press) has investigated the trace element geochemistry of the host rocks to the Joma massive sulfide deposit, in the Grong area, the Royrvik Group metabasics. He found a similar pattern of trace element abundances, with considerable spread of points across the WPB, MORB, and IAT fields of the Pearce and Cann (1973) Ti-Zr-Y discrimination diagram. He interprets this by suggesting that the Royrvik Group formed in a back-arc basin close to a continental margin (i.e. MORB, formed "within plate", close to a volcanic arc). However, as the fields used to classify basalt tectonically have been defined on a purely empirical basis using fresh basalts of known

and simple tectonic setting (Pearce and Cann, 1973; Pearce and Norry, 1979) there is no evidence to suggest that the model can be extended to suggest that "transitional" trace element distributions imply transitional tectonic environment. However, the possibility that the Storen and Fundsjo Groups represent a fossil marginal basin is worthy of further consideration in view of the geological evidence previously described (4.1.1).

Studies of known marginal basins have shown that their associated basalts are broadly similar to MORB. Gill (1976) noted that Lau Basin basalts displayed a slight enrichment of Sr^{87}; Ba; light rare earth elements (REE); alkalis and water, together with a depletion of heavy REE, Y, Zr, Hf and Ti relative to MORB. He concluded that their geochemistry was transitional from MORB to IAT. More recent studies of basalts from the Mariana (Hart et al., 1972); East Scotia Sea (Saunders and Tarney, 1979); and Bransfield Strait (Weaver et al., 1979) marginal basins, and from the Sarmiento ophiolite complex of Southern Chile (a fossil marginal basin - Saunders et al., 1979) have shown that they tend to be richer in K, Rb, and Ba, and to have higher Ba/Sr and Ce/Yb ratios, and lower K/Rb ratios than MORB.

However, it is now known that some MORB have similar "anomalous" geochemical characteristics (see for instance Tarney et al., 1979; Raschka and Eckhardt, 1976). Basalts from known marginal basins and of "anomalous" MORB are plotted on a Ti-Zr-Y discrimination diagram in Fig. 4.9b and a respectively. In both cases the majority of analyses plot in the MORB field with considerable scatter into the WPB field and the island-arc fields. This diagram (and the others so far presented) therefore fails to discriminate a) between "normal" ('N'-type - Wood, Joron and Treull, 1979) MORB and "anomalous" ('E'-type - Wood, Joron and Treull, 1979) MORB; and b) between MORB in general and marginal-basin

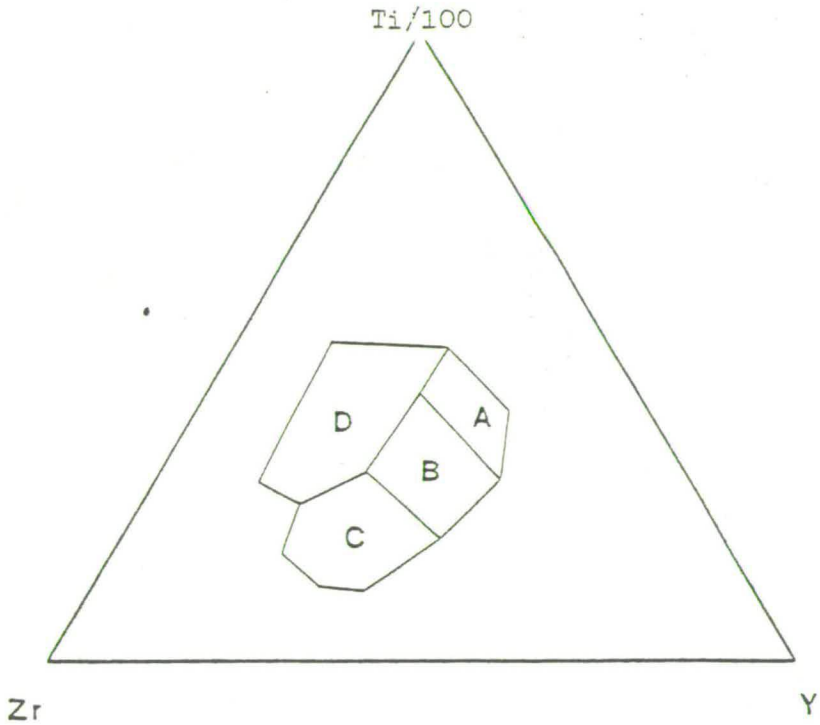

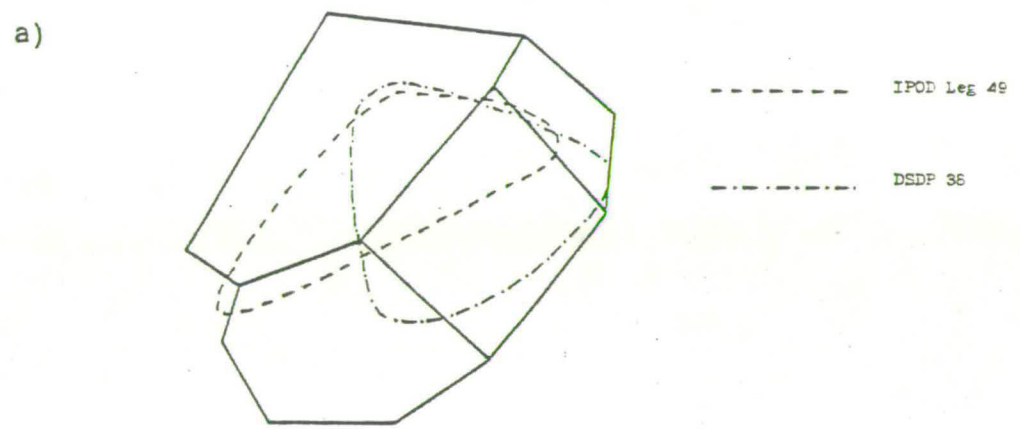

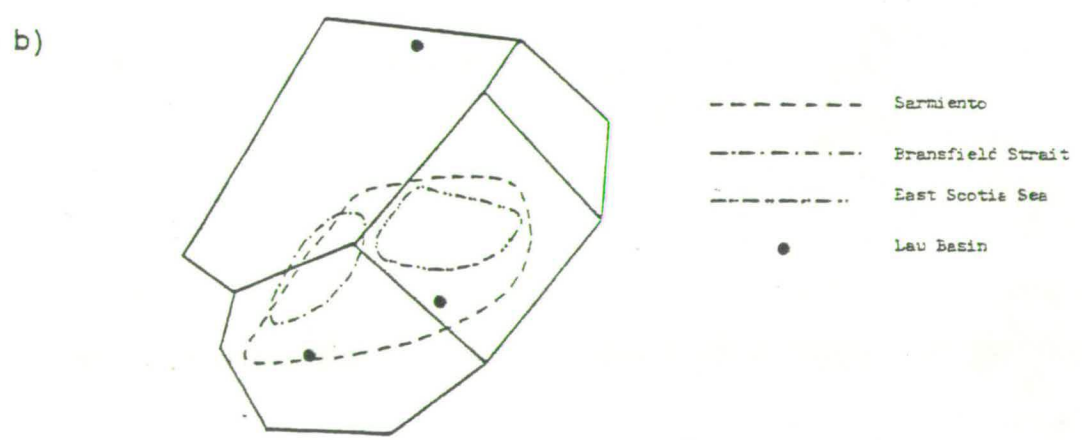

Fig. 4.9 Ti-Zr-Y plot (after Pearce and Cann, 1973) of a) "anomalous" mid-ocean ridge basalt (IPOD 49 - Tarney et al., 1979; DSDP 38 - Raschka and Eckhardt, 1976); and b) basalts of known marginal basins (Sarmiento - Saunders et al., 1979; Bransfield Strait - Weaver et al., 1979; East Scotia Sea - Saunders and Tarney, 1979; Lau Basin - Gill, 1976). Fields as in Fig. 4.6.

basalts (MBB). Furthermore, Figs. 4.6, and 4.9 a and b reveal that the distributions of Ti, Zr, and Y, in Storen and Fundsjo Group metabasics bear strong similarities to those of both 'E'-type MORB and MBB.

REE elements have commonly been used to compare basalts from different tectonic setting (e.g. Herrmann et al., 1974). A difficulty with this method is that absolute REE abundances are dependent on the degree of low-pressure fractionation as well as on conditions of partial melting and nature of the source. This problem can, to a certain extent, be overcome by considering only basalts with similar Zr-contents as there is normally a strong correlation between Zr and both Fe/Mg and REE levels in ocean basalts (Tarney et al., 1977). Table 4.5 (which treats Y as a heavy REE) presents a comparison of Storen Group metabasalts with known MORB and MBB. MBB are slightly enriched in LREE, a feature also displayed by 'E'-type MORB, while 'N'-type MORB show slight depletion of LREE. While REE have commonly been regarded as "immobile" during metamorphism (e.g. Koljonan and Rosenberg, 1975), recent work by Hellman et al. (1979) has thrown considerable doubt on this assumption. Although it is possible that even these have suffered considerable REE mobility, only Storen metabasics of low metamorphic grade have been included in Table 4.5, which demonstrates that both enrichment and depletion of LREE occurs.

The study of the geochemistry of igneous rocks has been extended to include other, supposedly "immobile" trace elements such as Th, Hf, and Ta, by Wood, Joron and Treull (1979). Instrumental neutron activation (INA) provides a technique by which these elements can be "rapidly and precisely" determined (Ta for instance is present in some IAT at concentrations down to 0.01 ppm). Investigation of these elements by INA analysis have shown that 'N'-type MORB; 'E'-type MORB; and WPB can be distinguished on the basis of Ta/Hf ratio; while these basalt types may

be distinguished from those of destructive plate margins by Th/Ta ratio. Wood, Joron and Treull (1979) combine these criteria in the form of the ternary Th-Hf-Ta discrimination diagram presented in Fig. 4.10a. Apparently the discrimination is successful for more fractionated magmas as well as basic rocks, as magma evolution produces only a slight enrichment of Th relative to Hf and Ta.

Only a limited amount of data on Hf and Ta is available at present. Wood, Joron and Treull (1979) point out, however, that Hf and Ta concentrations can be estimated assuming Zr/Hf and Nb/Ta ratios of 39 and 16 respectively. These ratios are apparently constant in terrestrial magmas and on the basis of present knowledge the maximum deviations from these values are ±10 and ±5 for Zr/Hf and Nb/Ta respectively. Wood, Joron and Treull (1979) have included data from the literature where "reliable" X-ray fluorescence (XRF) analyses of Th, Zr, and Nb have been quoted. They claim that such data do not influence the position of the field boundaries in the Th-Hf-Ta diagram. To further test the viability of using XRF Th, Zr, and Nb analyses on this diagram the basalts from IPOD leg 49, Sites 407-410 have been plotted on a Th-Zr/117-Nb/16 diagram using the XRF-analyses of Tarney et al. (1979). These basalts have been analysed for Th, Hf, and Ta by Wood, Tarney et al. (1979) using INA, and have been included in Wood, Joron and Treull's (1979) empirical definition of the fields in Fig. 4.10a. Fig. 4.10b demonstrates that the bulk of analyses from Sites 407-409 plot in the field of 'E'-type MORB, while those from Site 410 plot in the field of WPB. Luyendyk et al. (1979) described evidence suggesting that Site 410 basalts were the product of off-axis volcanism and should be classified as WPB, as further evidenced by their plotting in this field in Wood, Joron and Treull's (1979) Th-Hf-Nb diagram. Plotting XRF analyses of Th, Zr, and Nb on the discrimination diagram defined by INA analyses of Th, Hf, and Ta, therefore appears to give reasonably successful discrimination of basalt types.

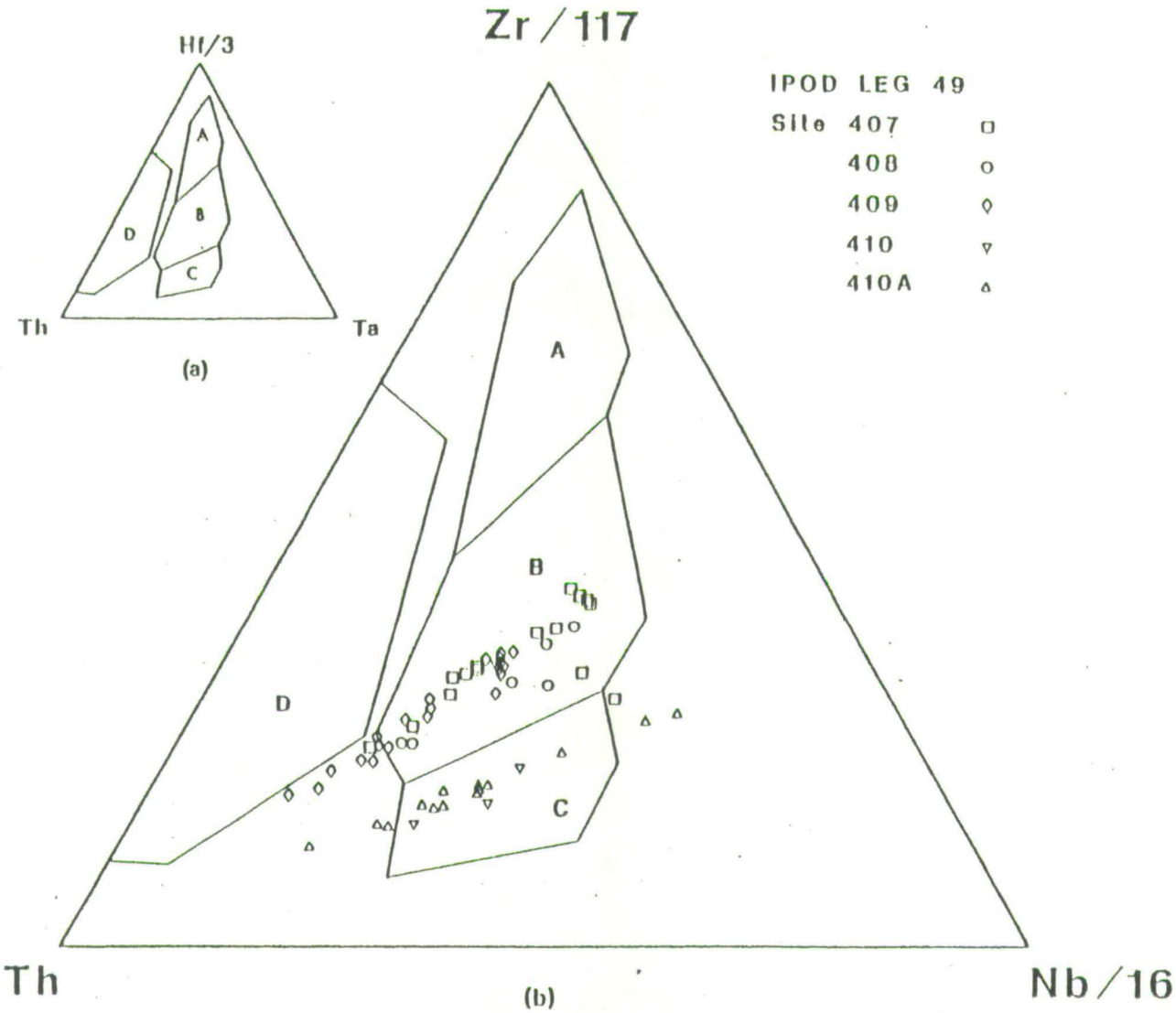

Fig. 4.10 a) The Th-Hf-Ta discrimination diagram of Wood, Joron, and Treull (1979). Field A = 'N'-type mid-ocean ridge volcanics; field B = 'E'-type mid-ocean ridge volcanics; field C = within-plate volcanics; field D = destructive-plate-margin volcanics. b) Th-Zr-Nb plot of IPOD Leg 49 basalts, Sites 407-410. Data from Tarney et al. (1979). Fields as in Fig. 4.10a.

This technique has been extended to include volcanics from known marginal basins. XRF analyses of Th, Zr, and Nb are available for volcanics from the East Scotia Sea (Saunders and Tarney, 1979); Bransfield Strait (Weaver et al., 1979); and from the Sarmiento ophiolite complex (Saunders et al., 1979); and are plotted on a Th-Zr-Nb diagram in Fig. 4.11. It appears that, at least in these cases, MBB have Th/Ta ratios similar to the other magma suites of destructive plate margins. A possible explanation for this is an enhanced stability of a Ti-oxide phase resulting from the high P_{H_2O} and P_{O_2} conditions that might be expected in an island-arc environment (Wood, in press; Saunders et al., in press). Pearce and Norry (1979) have shown that Nb (and Ta) will partition preferentially to the other trace elements considered here into such a phase, thereby causing a relative depletion of Nb (and Ta) in any partial melt produced in this environment. A high P_{H_2O} would also be expected in the source region of MBB; indeed Saunders (pers. comm., 1979) has noted an increased vesicularity in MBB over MORB which he explains by an input of water into the source region (the overlying mantle wedge) from the subducting slab. A similar depletion of Nb (and Ta) would therefore be expected in MBB as in basalts of island-arc affinity. This is an important observation as it may represent a geochemical criterion for distinguishing MORB and MBB.

Storen and Fundsjo Group metabasics are plotted on a Th-Zr-Nb diagram in Fig. 4.12. While accepting that there is some doubt about the stability of Th during alteration and metamorphism (Wood, Joron and Treull, 1979), it is interesting to note that of 22 analyses: 11 plot in the field of destructive-plate-margin volcanics; 7 plot between the destructive-plate-margin volcanics field and the fields of 'E'-type MORB and WPB; and 3 fall in the field of 'E'-type MORB.

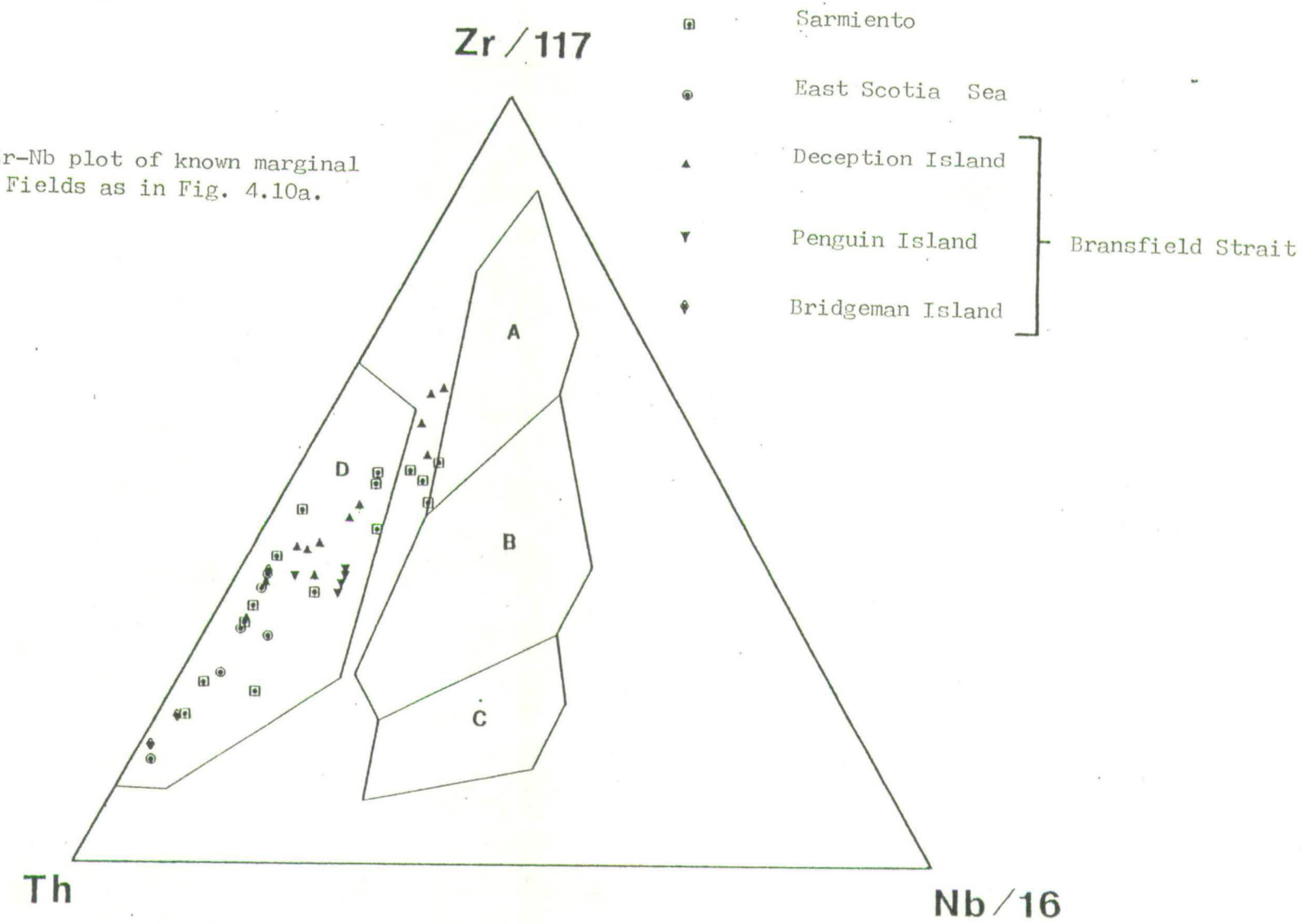

F Fig. 4.11 Th-Zr-Nb plot of known marginal basin basalts. Fields as in Fig. 4.10a.

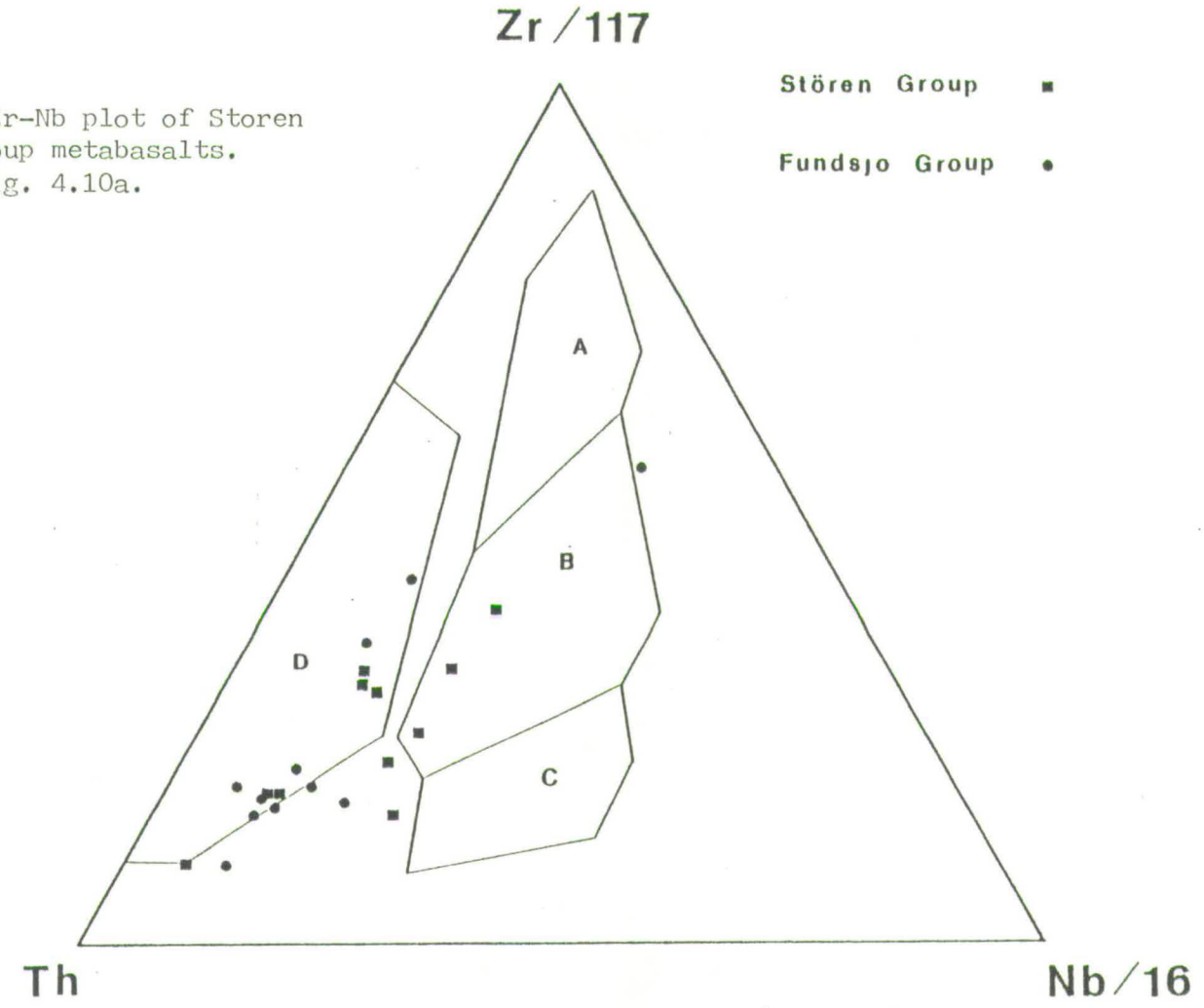

Fig. 4.12 Th-Zr-Nb plot of Storen and Fundsjo Group metabasalts. Fields as in Fig. 4.10a.

If the spread from destructive-plate-margin basalts to MORB is real and not a reflection of analytical error, or secondary processes, it is possible that the scatter of points towards MORB is time controlled. However, the observation that Bransfield Strait volcanics (supposedly a very young marginal basin - Weaver et al., 1979) fall close to the field of MORB in Fig. 4.11 would argue against this. Until much more detailed and accurate geochemical data becomes available such an hypothesis must be purely speculative.

In conclusion, consideration of geochemical data from known marginal basins reveals that they may be depleted in Nb and Ta, possibly as a result of high P_{H_2O} and high P_{O_2} in their source region. For this reason they will tend to plot in the field of destructive-plate-margin volcanics on a Th-Hf-Ta, or a Th-Zr-Nb discrimination diagram. The application of such diagrams obviously requires accurate and precise analyses of the elements involved. Of these, Th, Nb, and Ta are commonly present in such small quantities that even analyses quoted in the literature as "reliable" should be treated with caution. The suggestions outlined above should therefore be regarded as tentative, and pointers for future work rather than definitive conclusions.

Study of the geochemistry of Storen and Fundsjo Group metabasics reveals similarities to basalts formed at mid-ocean ridge and marginal-basin spreading centres. A common depletion in Nb (Table 4.2, 4.3, Fig. 4.12) might favour a marginal basin environment.

4.4 Copper-Zinc Sulfide Mineralisation.

The general geology and some aspects concerning the genesis of the large number of small metamorphosed massive sulfide deposits occurring throughout the Gula, Storen, and Fundsjo Groups have been discussed earlier in this chapter. This section discusses the results of a

comparative investigation of the sulfide petrology and chemistry of five such deposits, paying particular attention to the application of the sphalerite geobarometer. The Lokken and Tverfjellet deposits occur in the Storen Group; the Killingdal deposit in the Fundsjo; and the Kvikne and Rostvangen deposits in the Gula Group.

Petrological investigations of Kvikne, Rostvangen, and Killingdal have previously been carried out (Nilsen and Mukherjee, 1972; Rui, 1973a; Rui, 1973b), but little data on mineral chemistry is available. In contrast, while the Lokken and Tverfjellet deposits have commonly been mentioned in the literature, no detailed descriptions have yet been published. However, some general geological information has been provided by the present mine geologists, and on the basis of this, brief descriptions of the five deposits are presented. While a volcanogenic origin is now generally accepted for Caledonian massive sulfide deposits in Scandinavia (Vokes, 1976) mention is made of any recent debate concerning the genesis of these particular deposits.

4.4.1 The deposits.

4.4.1.1 Lokken - On the basis of present knowledge, Lokken is the largest of the Norwegian Caledonian base-metal sulfide deposits; a total tonnage of 25 x 10^6t has been estimated. The deposit is currently being exploited by A/S Orkla Industrier and the description presented here results largely from discussion with resident geologist G. Grammeltvedt.

The deposit consists of several separate bodies of massive sulfide having the form of elongated lenses of varying cross-sectional shape. The total length is about 4 km while the average width and thickness are about 150-200 m and 50 m respectively (Figs. 4.13 and 4.14). The deposit is orientated E-W, parallel to country-rock fold-axial directions (D_1-Chapter 3).

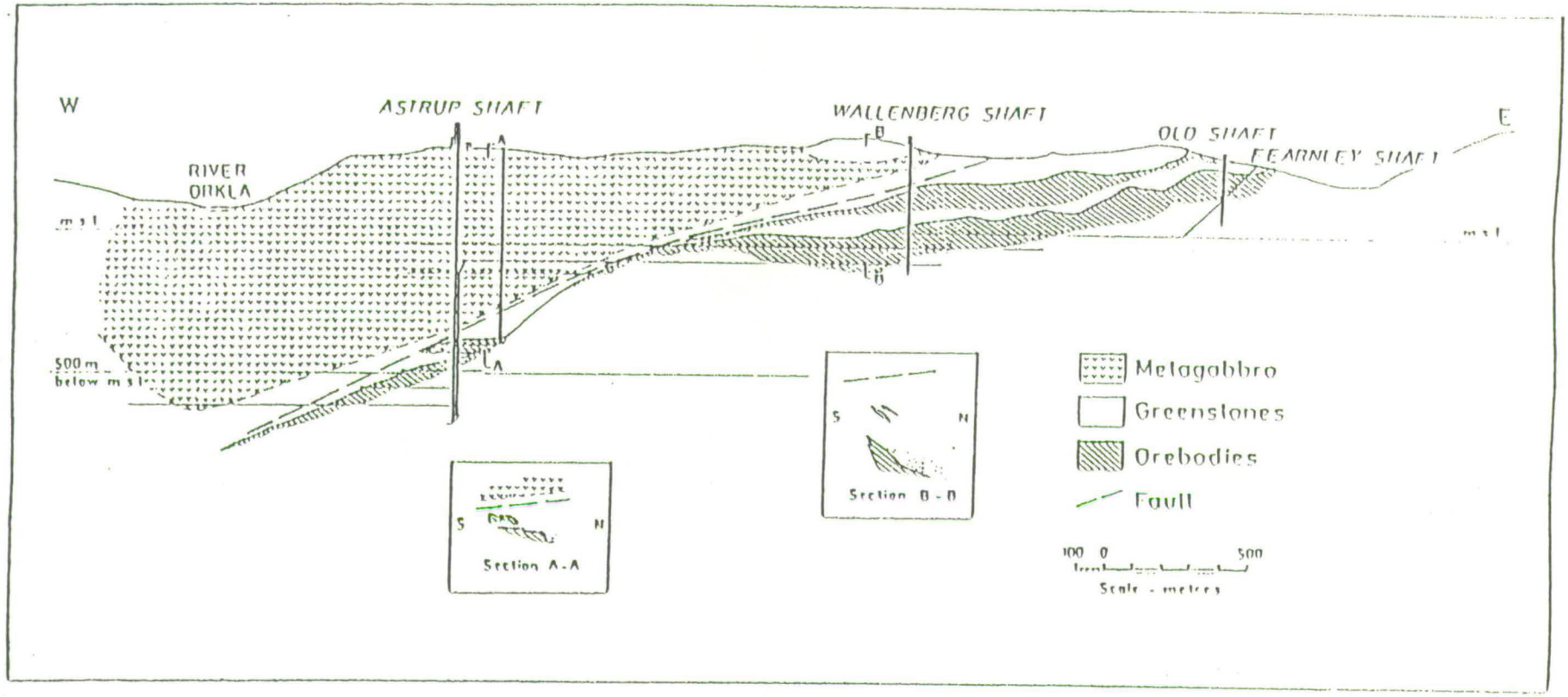

Fig. 4.13 East-west cross-section through the Lokken orebodies (from Grenne et al., in prep.).

Fig. 4.14 Diagrammatic north-south cross-section through the Lokken ore deposit (from Grenne et al., in prep.).

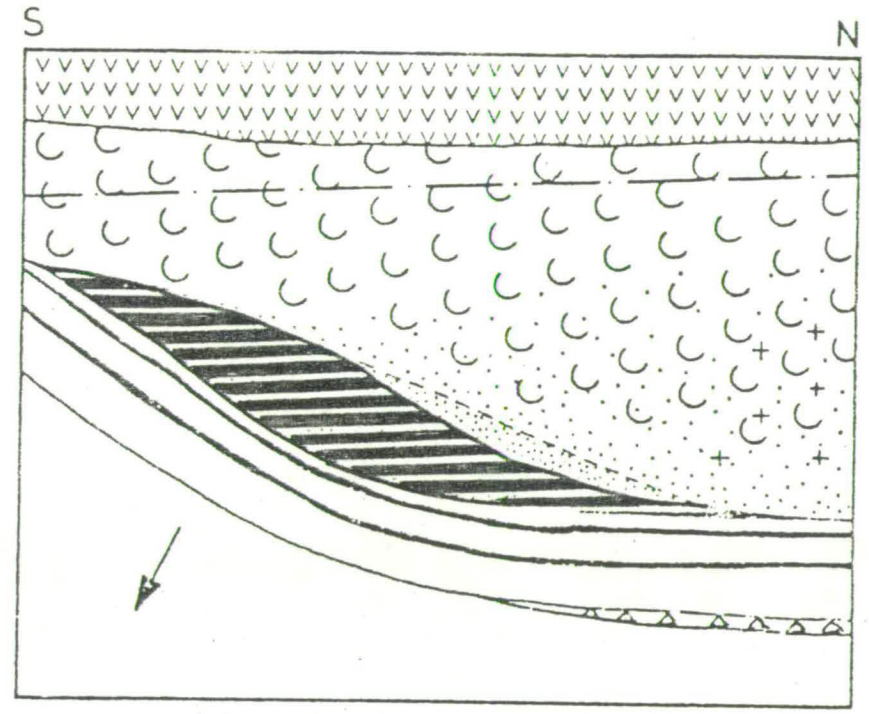

Greenstone, upper subgroup.

Volcaniclastic sediment.

"Vasskis".

Massive sulphide.

Felsite with pyrite dissemination.

Greenstone, lower subgroup.

Greenstone with pyrite dissemination.

Greenstone with pyrite and magnetite dissemination.

Metagabbro.

Fault.

Younging direction.

The ores lie in an inverted sequence of Storen Group lavas, characterised by greenschist facies mineral assemblages and occasionally showing relict pillow structures. As seen from Fig. 4.14 the stratigraphically overlying lavas are interbedded with several red or black cherty horizons, known collectively in Norwegian terminology as "vasskiss". These "vasskiss" horizons are generally 0.5-2.0 m thick and consist of very fine-grained quartz-magnetite-stilpnomelene layers alternating with very fine-grained pyrite-rich layers. Between the ore and the stratigraphically underlying lavas a lenticular unit of "quartz-albite felsite" occurs, often heavily impregnated with pyrite in the form of thin bands and irregular stringers (Fig. 4.14). A large metagabbroic body is present within the stratigraphically underlying lava sequence, but is separated from the ore zone by a westerly dipping fault or thrust plane as shown in Fig. 4.13 and 4.14.

The ore has an average grade of 2.0% Cu; 1.8% Zn; and 42% S; and is dominated by pyrite (75%); chalcopyrite (6%); and sphalerite (3%). Quartz is the main gangue mineral (15% of ore) but minor amounts of calcite, chlorite, and stilpnomelene also occur.

4.4.1.2 Tverfjellet - A total of 20 x 10^6t has been estimated for the Tverfjellet deposit, developed in the late sixties and operated by A/S Folldal Verk. The mine was described in the early stages of its development by Waltham (1968b) but more recent publications are lacking. The description presented here is based largely on discussions with the mine geologist M. Motyse.

The deposit lies in the southern Trondelag outcrop of the Storen Group where mineral assemblages characteristic of epidote-amphibolite facies are dominant (Miyashiro, 1968). The ores occur as steeply inclined elongate lenses, similar to those at Lokken, but in this instance located between metavolcanic and metasedimentary lithologies. An E-W orientation

is related to country-rock fold hinges (D_1 - Chapter 3). Nilsen (1978) suggests that banded magnetite/pyrite ores occurring conformably within the ore lenses (Waltham, 1968, a and b) may be metamorphosed "vasskiss" horizons.

The ore has an average grade of 1% Cu; 1.2% Zn; and 32% S (Nilsen, 1978) and is dominated by pyrite (50%); chalcopyrite (5%); and sphalerite (2%). Quartz is the dominant gangue mineral but calcite, chlorite, mica, hornblende, graphite, and rutile also occur (Waltham, 1968b).

4.4.1.3 Killingdal - The Killingdal deposit contained an estimated 3×10^6t of ore. It has a long history of exploitation, having been discovered in 1674 and operated sporadically until the present day. The mine is now operated by Killingdal Grubeselskap A/S who employ no resident geologist. Recent information on the deposit is therefore lacking. Rui (1973 b), however, provides a comprehensive description of the deposit, as then known, which forms the basis of this resume.

The deposit is composed of two orebodies named the Main Orebody and the North Orebody. Both are strongly elongated, and have lens shaped cross-sections. The orebodies run parallel for a known length of 2.5 km, and have an axial dip of approximately 30° towards the west. The North Orebody is located above and about 50 m to the north of the Main Orebody (Fig. 4.15).

In cross-section the Main Orebody has a maximum width of about 80 m and a maximum thickness of about 10 m. In general the width and thickness decrease towards the deeper parts of the mine. The cross-sectional area of the North Orebody is considerably less than the Main Orebody and consequently it has been exploited to a lesser extent.

The Main Orebody occurs in successive envelopes of quartz-muscovite-schist and chlorite schist at the contact between amphibolite and phyllitic metasediments of the Fundsjo Group. The North Orebody occurs

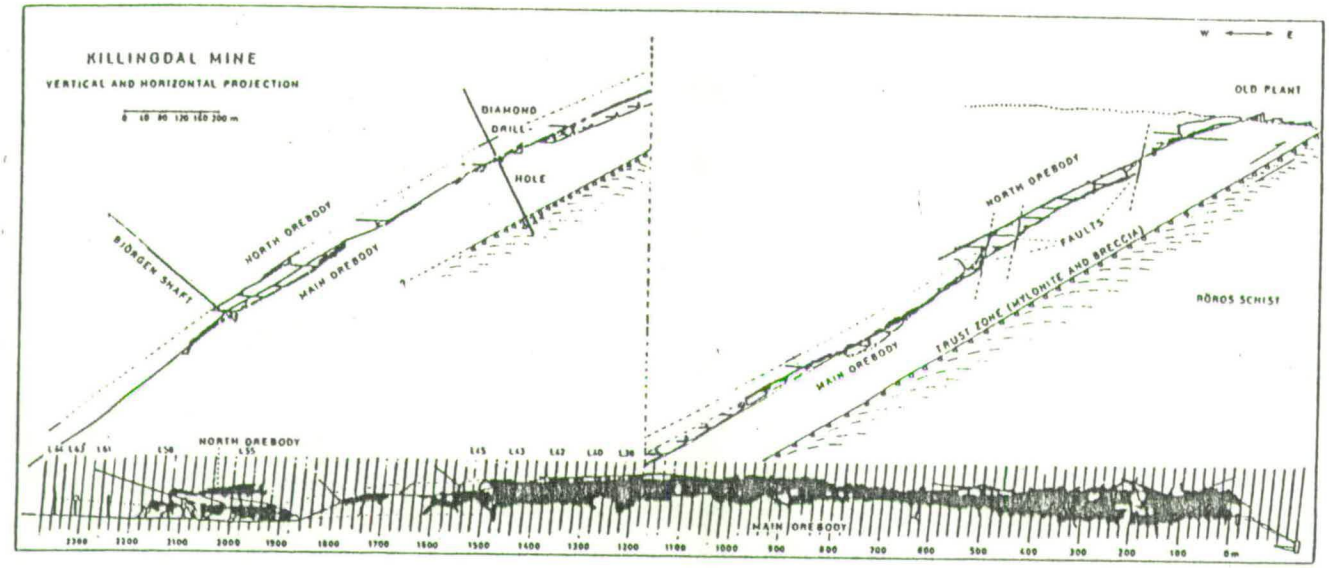

Fig. 4.15 East-west cross-section and plan of the Killingdal orebodies (from Rui, 1973b).

within similar envelopes but entirely within the metasediments. Rui (1973b) interprets these envelopes as representing wall-rock alteration associated with palingenetic epigenetic ore deposition. Vokes (1970, 1974) however, argues strongly that such phenomena are not inconsistent with what would be expected around a "metamorphosed, pre-orogenic ore" either through metamorphism of syngenetic alteration haloes or through metasomatic reaction between the ore and its wall-rocks. A syngenetic origin is now generally accepted for these ores (Nilsen, 1978).

According to Rui (1973b) the Main Orebody has an average grade of 1.9% Cu; 5.9% Zn; 0.4% Pb; and 48.1% S, and is dominated by pyrite (81.1%); sphalerite (9.9%); and chalcopyrite (5.5%); with lesser amounts of galena (0.5%), and traces of pyrrhotite. Quartz and muscovite are the main gangue minerals.

4.4.1.4 Kvikne - The deposits at Kvikne, comprising a large number of workings, were exploited sporadically from 1631 until 1912, although most mining activity occurred before 1812. Little has been published on the geology of the Kvikne mines and the workings are now completely flooded. However, Nilsen and Mukherjee (1972) provide a general description based on examination of dumps and surface exposure. The information presented here is based on this work.

The deposits lie in the central parts of the Gula Group and are confined to amphibolitic horizons. They are usually located at the contacts between the amphibolites and the enclosing mica schist. Old mine records allowed Nilsen and Mukherjee (1972) to suggest an elongated lens, or ruler shape for the largest deposits. The direction of elongation parallels the regional D_1-lineation direction, in this area approximately SE.

On the basis of wall-rock alteration, the apparent tectonic control

of the orebodies, and a constant prevalence of Co over Ni in pyrite, Nilsen and Mukherjee (1972) suggest an epigenetic origin for these ores. However, in a discussion of this paper, Vokes and Morton (1973) argue that these features are typical of metamorphosed volcanogenic deposits and favour such an origin. These veiws have since been accepted by Nilsen (1978).

Between 1631 and 1812 the Kvikne mines produced 7,343 tons of copper. The ore is dominated by pyrite, with lesser amounts of pyrrhotite, chalcopyrite, and sphalerite.

4.4.1.5 Rostvangen - The Rostvangen deposits occur in the Gula Group some 25 km SSE of the Kvikne mines. The deposits were discovered in 1905 and worked from 1908 until 1921, when the world-wide economic crisis lead to the abandonment of the newly developed mine and processing plant after nearly 400,000 tons of ore had been produced.

As at Kvikne, the recent description of the ores by Rui (1973a) was dependent on old mine records and examination of dumps and surface exposure. Rui's (1973a) work forms the basis for this brief introduction.

The orebodies consist of a number of elongated lenses of massive ore "mutually arranged in an en echelon pattern" with their major axes coinciding with the regional SSE D_1-lineation direction. Individual ore shoots have known lengths of 150 to 200 m; widths varying from 15-60 m; and thicknesses of 2-15 m. The mineralisation is confined to the contact between amphibolite horizons and the country-rock schists, and appears to be located at large-scale fold hinges.

According to Foslie (1926) the average grade of the ores was 2.65% Cu; 1% Zn; and 43% S. Pyrite is the dominant sulfide mineral with lesser amounts of pyrrhotite, chalcopyrite, sphalerite, and magnetite.

4.4.2 Petrology.

Approximately a dozen representative samples of Lokken, Tverfjellet, and Killingdal (Main Orebody) were provided by the operating companies, while samples from Kvikne and Rostvangen were selected from dumps by the author.

Vokes (1968) has pointed out that the large stability fields of the common sulfide minerals, coupled with the relatively simple original chemical and mineral compositions of most volcanogenic sulfide ores, results in common and simple mineral assemblages in metamorphosed deposits. This simplicity of assemblage is reflected in this study as shown by Table 4.6, which presents modal analyses of representative samples of each deposit. In all cases the sulfide assemblage is dominated by pyrite, chalcopyrite, and sphalerite. The occurrence of pyrrhotite in metamorphosed massive sulfide deposits has been related to metamorphic grade by Vokes (1969), who suggests that much, if not all, of the pyrrhotite in such ores results from the breakdown of pyrite at about the boundary between greenschist and amphibolite facies metamorphism. While such reactions are obviously controlled by fO_2 and fS_2 (Eckstrand, 1975), the rarity of pyrrhotite in deposits of the Storen and Fundsjo Groups, and its relative abundance in the Gula deposits supports this suggestion. The application of a magnetic colloid (Scott, 1974) indicates that the pyrrhotite present in these deposits is either hexagonal, or an intergrowth of hexagonal and monoclinic phases. As monoclinic pyrrhotite is unstable above 253°C (Kissin, 1974), this intergrowth probably developed on cooling from higher metamorphic temperatures. The presence of magnetite at Tverfjellet and Rostvangen probably relates to metamorphism of pyrite and/or pyrrhotite at higher fO_2.

A number of textural changes relating to progressive regional

TABLE 4.6 Modal analyses of massive volcanogenic ores from the Lokken, Tverfjellet, Killingdal, Rostvangen and Kvikne deposits.

	LOKKEN					TVERFJELLET					KILLINGDAL				
	G6	G7	G8	G9	G10	G1	G2	G3	G4	G5	G11	G12	G13	G14	G15
Py	57	78	74	83	82	34	53	31	51	50	71	77	82	75	84
Po	-	-	-	-	-	3	2	2	t	-	t	2	3	1	3
Cp	1	14	14	5	13	9	10	3	3	1	10	10	13	6	10
Sl	26	1	3	-	t	t	-	-	t	6	17	11	2	18	1
Mt	-	-	-	-	-	22	2	2	22	1	-	-	-	-	-
Gn	-	-	-	-	-	-	-	-	-	-	2	t	t	t	-
Ma	-	-	-	-	-	-	-	-	-	-	-	-	-	-	-
Others	-	-	-	-	-	-	-	-	-	-	t	t	-	-	-
Qtz	16	6	8	13	5	26	17	37	10	42	-	-	t	-	1
Ct	t	-	-	-	-	1	7	13	13	-	-	t	-	-	-
Hbld	-	-	-	-	-	-	-	-	-	-	-	-	-	-	-
Bi	-	-	-	-	-	-	-	-	-	-	-	-	-	-	-
Cl	-	1	-	t	-	4	1	10	-	-	-	-	-	-	1
Stp	-	t	t	t	-	-	-	-	-	-	-	-	-	-	-
Fsp	-	-	-	-	-	1	-	-	-	-	-	-	-	-	-
Musc	-	-	-	-	-	-	7	3	-	-	t	t	-	-	1
Gange	-	-	-	-	-	-	-	-	-	-	-	-	-	-	-
Pore	-	-	-	-	-	-	-	-	-	-	-	-	-	-	-

	ROSTVANGEN					KVIKNE			
	F1	F2	G16	G17	G18	G19	G20	G21	G22
Py	84	25	36	4	31	67	18	49	66
Po	7	8	1	81	6	t	12	2	1
Cp	1	12	9	2	9	t	5	1	6
Sl	3	1	2	t	1	11	2	5	16
Mt	1	20	-	-	18	-	-	-	-
Gn	-	-	-	-	-	t	-	t	-
Ma	-	1	2	-	-	-	18	1	t
Others	-	-	-	-	-	-	-	-	-
Qtz	1	16	48	-	-	6	9	39	8
Ct	-	16	-	-	9	0	t	-	-
Hbld	2	1	-	-	3	t	12	1	1
Bi	-	-	-	5	-	-	-	-	1
Cl	t	-	-	t	1	-	-	-	-
Stp	-	-	-	-	-	-	-	-	-
Fsp	-	-	-	-	-	-	-	-	-
Musc	-	-	-	2	-	t	1	-	-
Gange	1	2	2	1	1	1	23	1	1
Pore	-	-	-	-	-	14	1	1	t

EXPLANATION	
Py	pyrite
Po	pyrrhotite
Cp	chalcopyrite
Sl	sphalerite
Mt	magnetite
Gn	galena
Ma	marcasite
Others	other sulfides
Qtz	quartz
Ct	calcite
Hbld	hornblende
Bi	biotite
Cl	chlorite
Stp	stilpnomelene
Fsp	felspar
Musc	muscovite
Gange	undifferentiated gangue
Pore	pore space

All analyses based on at least 333 points.

metamorphism of massive sulfide deposits have been documented by Vokes (1968, 1969). In general increasing metamorphism results in textures where minerals of high form energy, such as pyrite, arsenopyrite, and magnetite, grow porphyroblastically in a matrix of minerals of lower form energy, such as chalcopyrite, sphalerite, and pyrrhotite. Provided the effects of deformation are not too great, grainsize increases with metamorphic grade. In a study of Scandinavian ore deposits (including Lokken and Tverfjellet) Vokes (1968) concluded that:

> "In the Scandinavian Caledonides it is possible to link the increase in grainsize very closely with the metamorphic grade of the enclosing rocks, without actually being able to equate definite grainsize dimensions with any particular metamorphic grade."

Similar conclusions were reached by Templeman-Kluit (1970), who attempted to quantify the relationship and found fair correlation, especially with regard to pyrite.

The progressive porphyroblastesis and increase in grainsize of pyrite relating to increasing metamorphic grade are well demonstrated by the Gula, Storen, and Fundsjo deposits as illustrated in Figs. 4.16-4.22. The very fine grainsize and restricted recrystallisation of the Lokken pyrites (Fig. 4.16) is consistent with a low metamorphic grade (lower greenschist facies - Vokes, 1968), while the large porphyroblasts typical of Kvikne and Rostvangen (Figs. 4.21 and 4.22) reflect the high-grade metamorphism suggested by their enclosing country-rock schists (Fig. 2.1).

The effects of deformation are variable, presumably according to the associated metamorphic grade and the timing of the deformation relative to metamorphic recrystallisation (Vokes, 1968). At Lokken the very fine grainsize probably relates to cataclastic processes (Vokes, 1968); and later fracturing and subsequent healing by quartz is common (Fig. 4.16). In contrast, the ores of higher metamorphic areas commonly

Fig. 4.16 Photomicrograph of Lokken ore (sample 78.LM.1).
Fine-grained, possibly cataclastic pyrite (light grey) in quartz (dark grey), with minor sphalerite (grey).
Note healing of brittle fractures by quartz.
Reflected light; ppl; f.o.v. = 2.40 mm.

Fig. 4.17 Photomicrograph of Tverfjellet ore (sample 78.FM.7).
Porphyroblastic pyrite (white) and magnetite (grey) in quartz-calcite gangue (dark grey). Minor chalcopyrite (c), and sphalerite (s) also present.
Reflected light; ppl; f.o.v. = 2.40 mm.

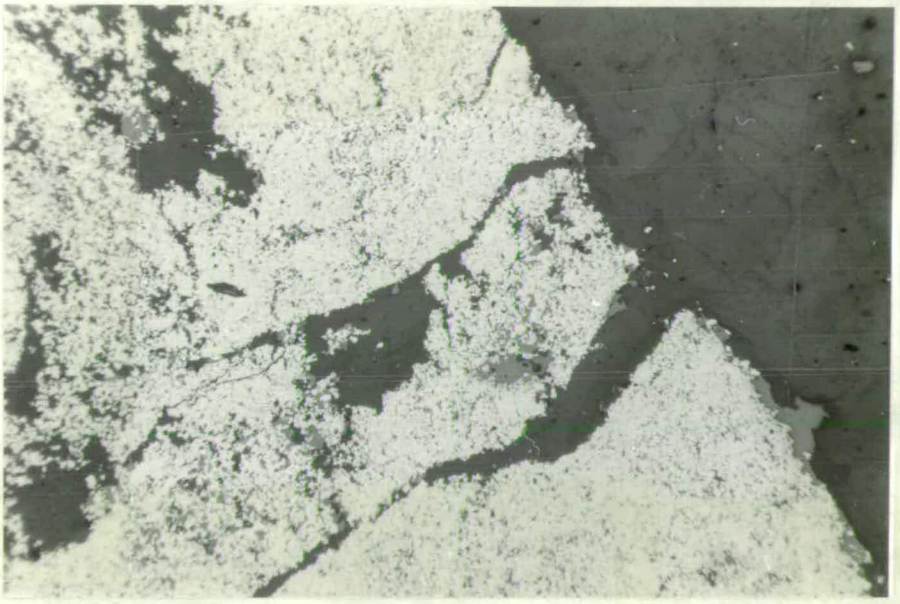

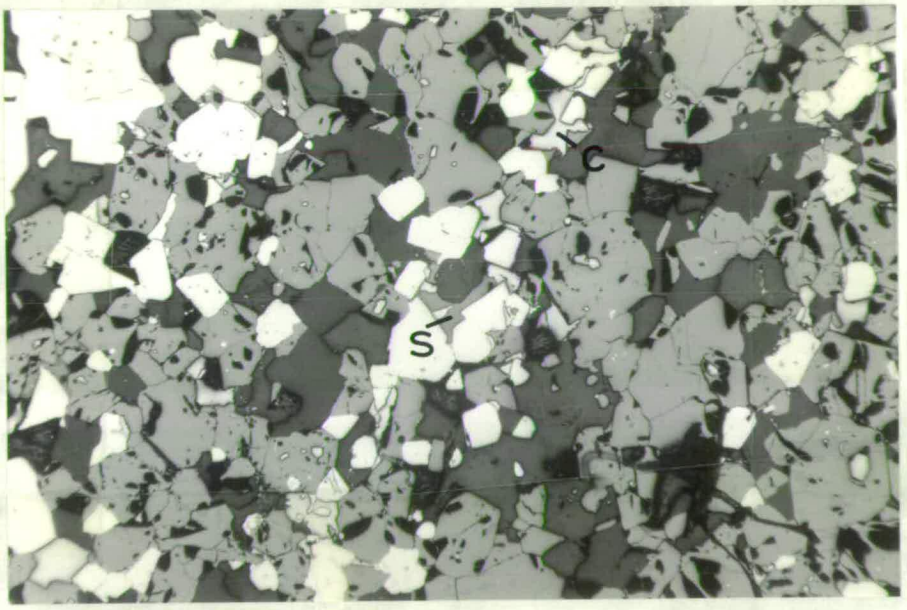
C
S

Fig. 4.18 Photomicrograph of Tverfjellet ore (sample 78.FM.3). Porphyroblastic pyrite (white) in a matrix of pyrrhotite (p) and chalcopyrite (c), and gangue (black).
Reflected light; ppl; f.o.v. = 2.40 mm.

Fig. 4.19 Photomicrograph of Killingdal ore (sample 78.KM.1). Porphyroblastic pyrite (white) and arsenopyrite (a), in a matrix of sphalerite (dark grey), with minor galena (g) and chalcopyrite (c).
Reflected light; ppl; f.o.v. = 2.40 mm

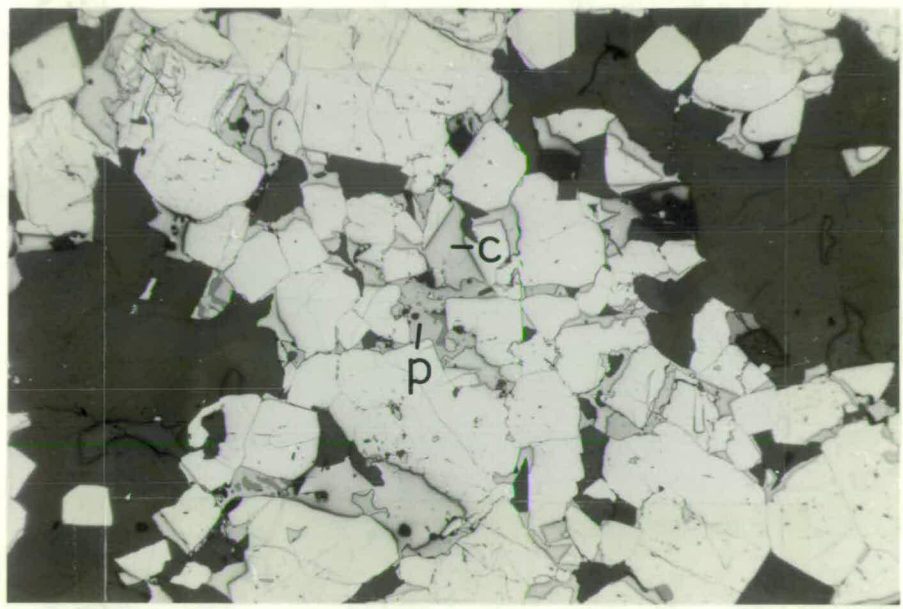
c
p

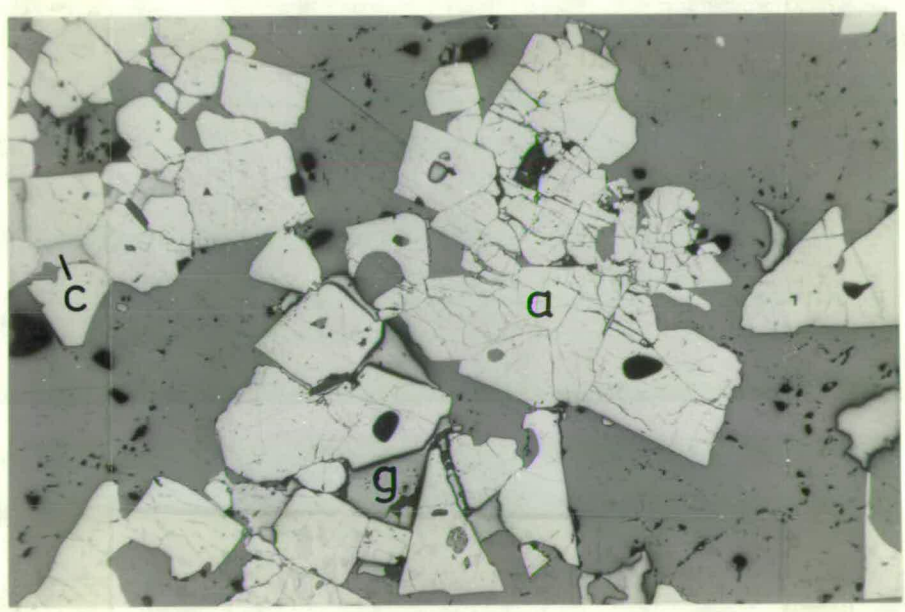
c
a
g

Fig. 4.20 Photomicrograph of Killingdal ore (sample 78.KM.2). Porphyroblastic pyrite (white) in a matrix of chalcopyrite (light grey) and sphalerite (dark grey, centre).
Reflected light; ppl; f.o.v. = 2.40 mm.

Fig. 4.21 Photomicrograph of Kvikne ore (sample 78.KVD.1). Porphyroblastic pyrite (white) with sphalerite (grey) and pore space (dark grey).
Reflected light; ppl; f.o.v. = 2.40 mm.

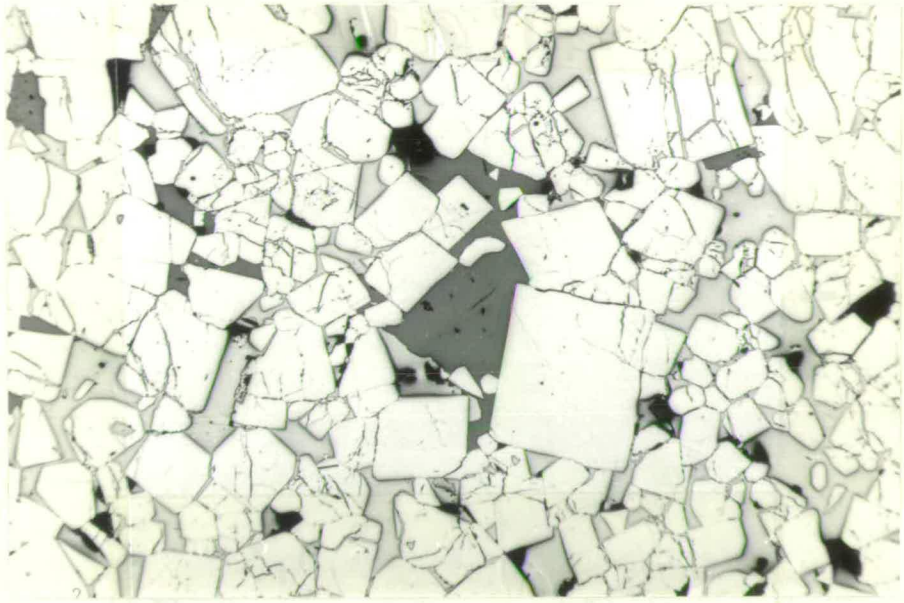

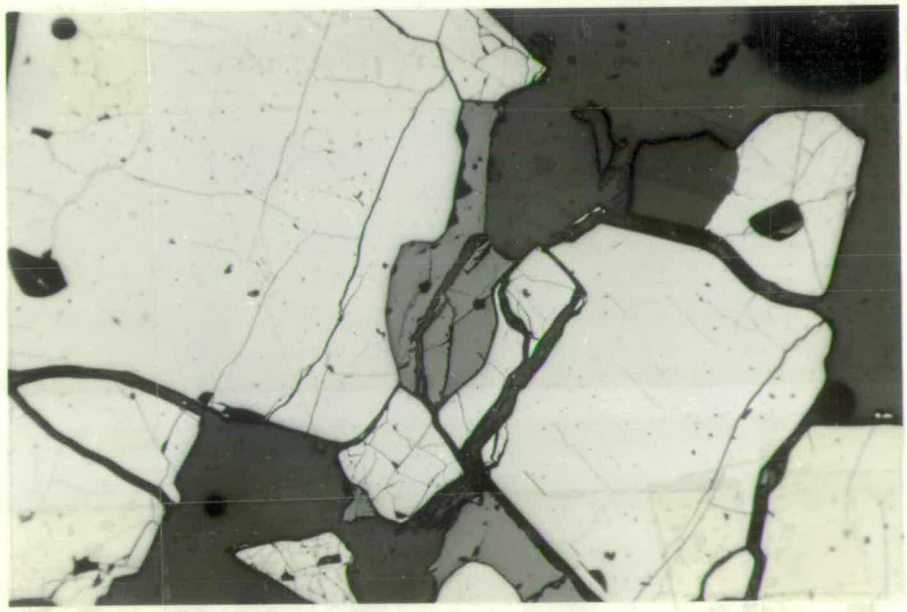

Fig. 4.22 A ground surface of Rostvangen ore (sample 77.RD.1), showing large pyrite porphyroblasts.

Fig. 4.23 Photomicrograph of Rostvangen ore (sample 78.RD.15). Note elongation of pyrite (white) and magnetite (grey) porphyroblasts. Gangue minerals - black.
Reflected light; ppl; f.o.v. = 2.40 mm.

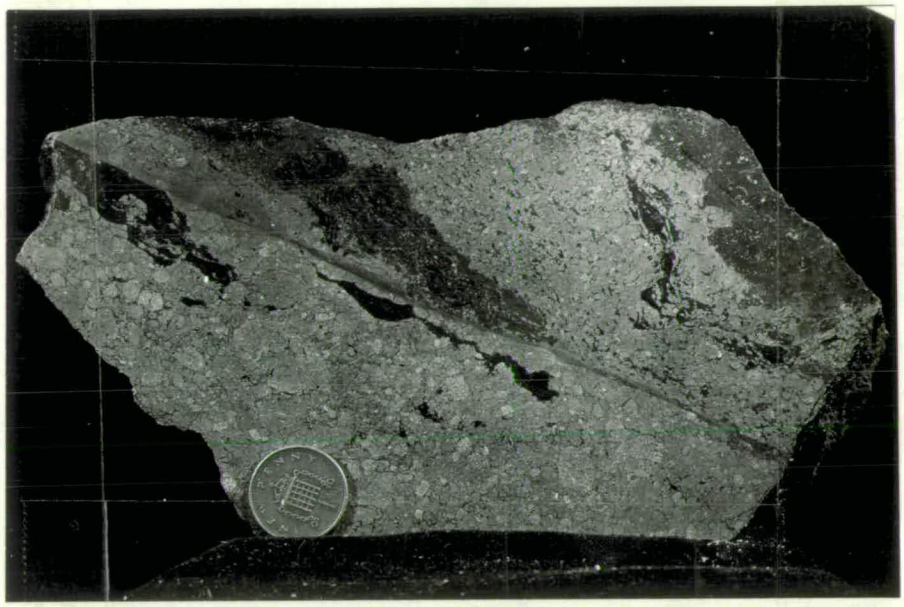

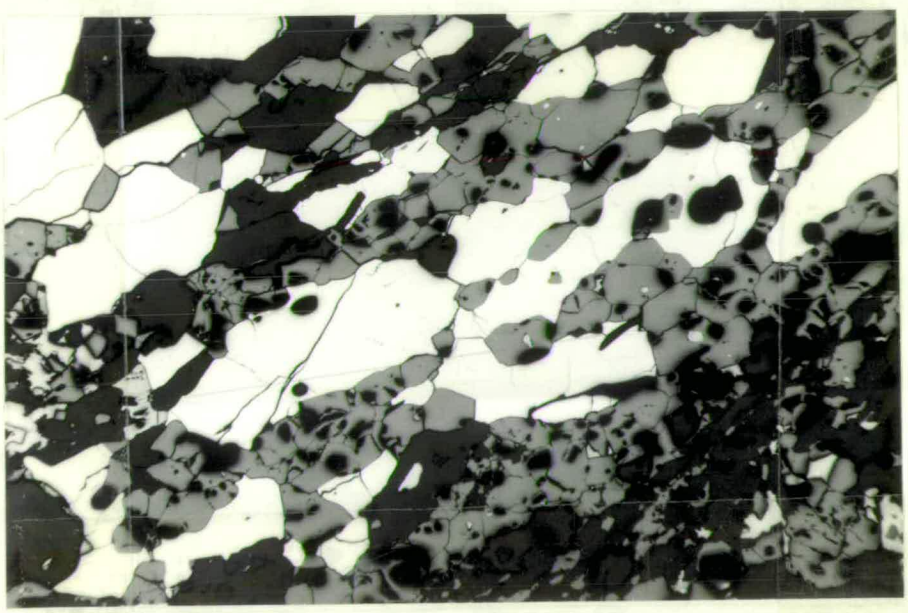

display a sulfide schistosity (Fig. 4.23) defined by elongation of pyrite porphyroblasts (and to a lesser extent, magnetite when present). A cm-scale banding, reflecting variations in the concentration of porphyroblastic pyrite (or magnetite) may also be developed in higher-grade ores (Figs. 4.24 and 4.25).

On the basis of silicate mineralogy, the metamorphic grade within the Trondheim Nappe decreases about the central parts of the Gula Group (Fig. 2.1). As described above this pattern is reflected in the grain-size of porphyroblastic pyrite in metamorphosed volcanogenic sulfide deposits. The possibility that this metamorphic zonation results from a late retrogressive phenomenon related, for instance, to thrusting at the base of the Trondheim Nappe must be considered.

Such a process could account for the observed silicate and sulfide mineralogy and chemistry. The associated deformation would cause re-crystallisation of pyrite porphyroblasts in deposits closest to the thrust zone, resulting in an increase in grainsize towards the central parts of the Gula Group. However, the localisation of the deposits along the D_1- lineation direction in their respective areas suggests that they have not suffered markedly different deformational histories. The metamorphic zonation within the Trondheim Nappe is therefore believed to be real, and not a result of any retrogressive phenomenon. These conclusions support the hypothesis, suggested in Chapter 3, that this zonation is related to deformation of isograds related to an early metamorphic event associated with the Cambro-Ordovician Trondheim Orogeny.

4.4.3 Bulk sulfide chemistry.

The deposits of the Gula, Storen, and Fundsjo Groups are dominantly of the Cu-Zn type. Fig. 4.26 illustrates the relative abundance of copper, zinc, and lead in these deposits based on average grades published in the literature (no data was found for the deposits at Kvikne).

Fig. 4.24 A ground surface of Killingdal ore (sample 78.KM.5) showing banded structure caused by variations in pyrite (light grey) and sphalerite (dark grey) abundances.

Fig. 4.25 A ground surface of Tverfjellet ore (sample 78.FM.7) showing banded structure caused by variations in pyrite (light grey) and magnetite (dark grey) abundances.

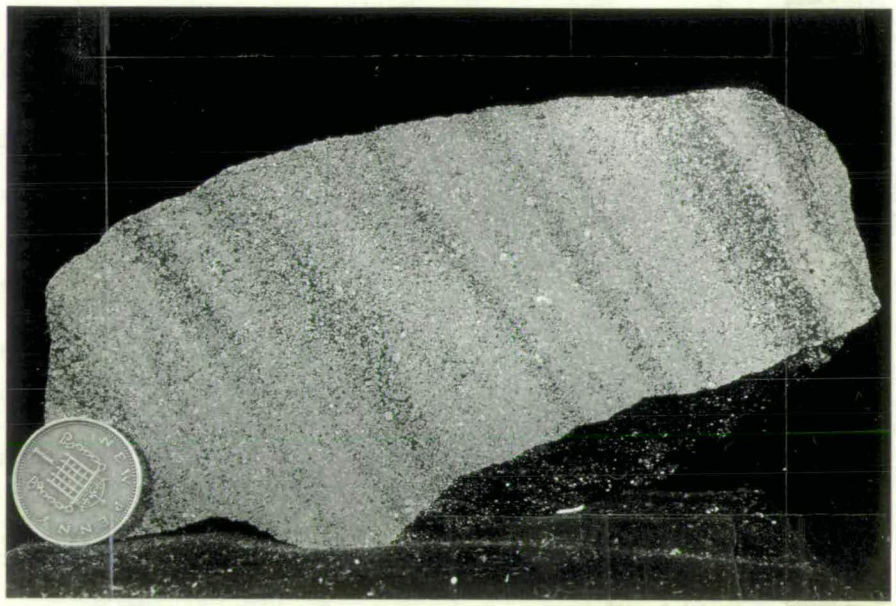

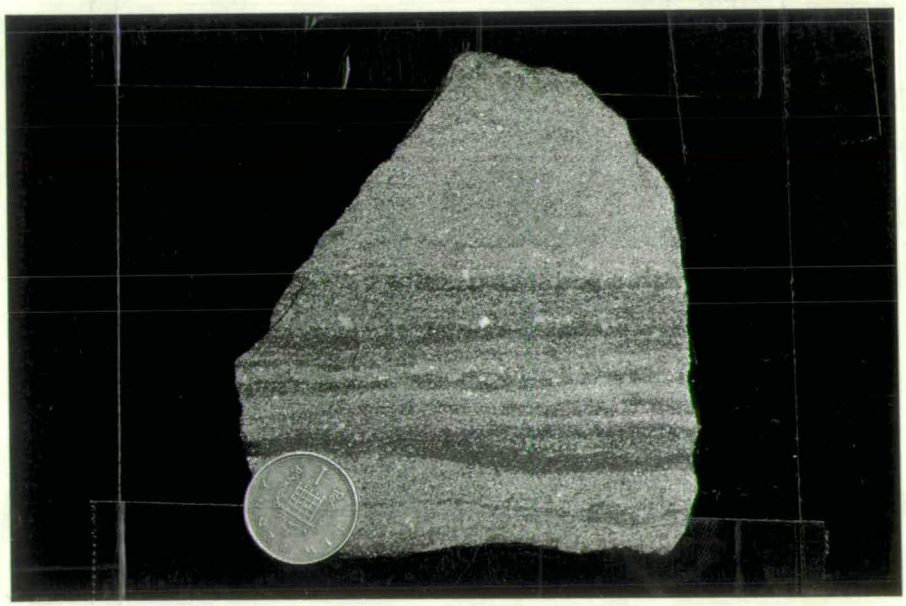

Fig. 4.26 Average composition of Lokken (Grenne et al., in prep.), Tverfjellet (Nilsen, 1978), Killingdal (Rui, 1973b), and Rostvangen (Foslie, 1926) ores (wt %).

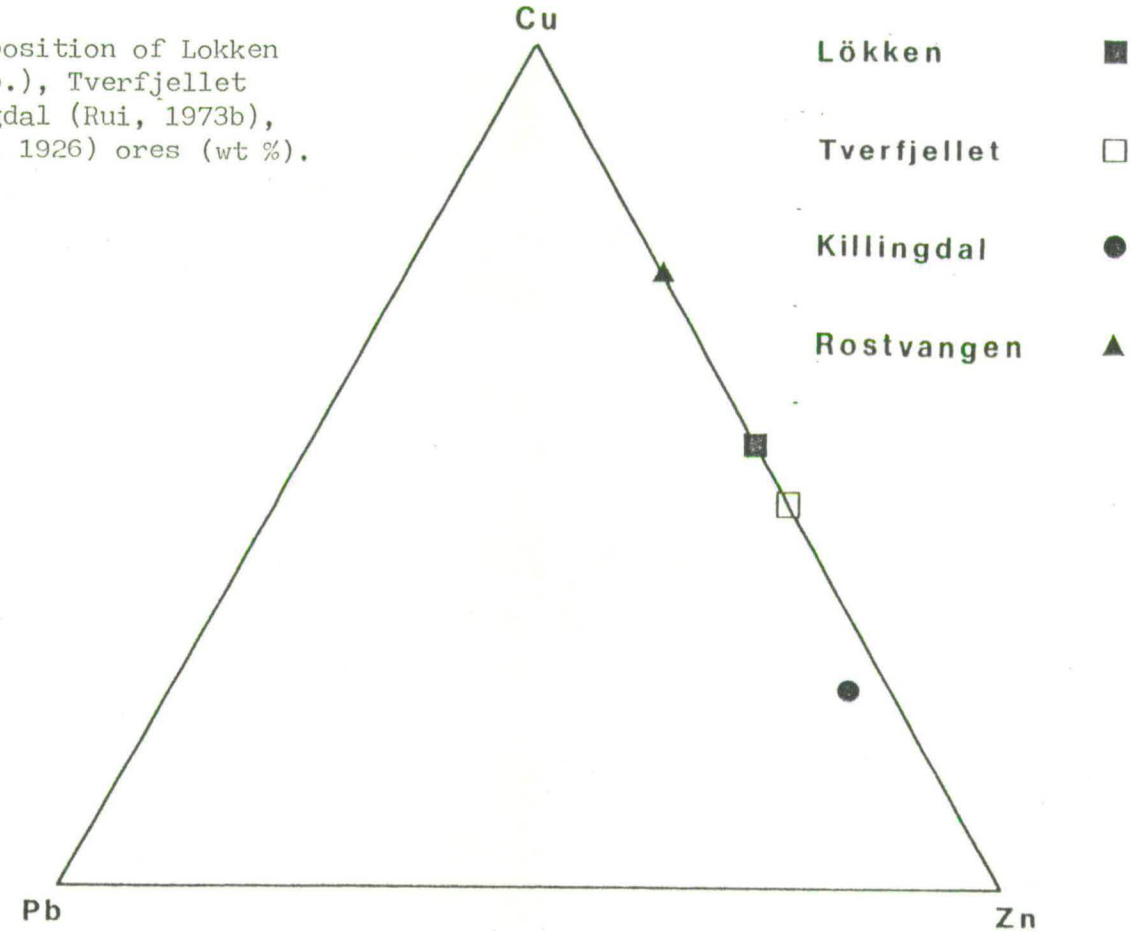

Sawkins (1976) suggested a world-wide classification of massive sulfide deposits. Those of dominantly mafic-volcanic association are referred to as "Cyprus-type" and are characterised by a general lack of lead, and Cu:Zn ratios >1. Less deformed examples commonly display a lithological association typical of ophiolite complexes (Fig. 4.27a), suggesting that they formed at sites of sea-floor spreading. Pearce and Gale (1977), on the basis of geological and geochemical evidence, favour a "behind-arc" environment for this spreading.

Deposits of mixed felsic-volcanic and sedimentary association are known as "Kuroko-type". A generalised cross-section showing the typical lithological setting is presented in Fig. 4.27b. Significant quantities of lead (especially in Phanerozoic deposits), and Cu:Zn ratios <1 are characteristic of this ore type. By analogy with Recent tectonic environments it is suggested that such ores form in a volcanic-arc environment.

A third type of massive sulfide deposit has been recognised by Sawkins (1976). "Besshi-type" deposits occur in structurally complex settings, characterised by thin mafic horizons in thick sequences of "geosynclinal" sediments (Fig. 4.27c). Deformation and metamorphism obscure the original tectonic environments of these ores. However, on the basis of major element geochemistry, Sugisaki et al (1972) suggested that the associated mafic volcanics are similar to present-day mid-ocean ridge volcanics. They proposed that the volcanics were intruded into the sedimentary sequences during an episode of tensional rifting. In contrast Sillitoe (1972) preferred formation at a sub-marine spreading centre and tectonic incorporation into the sediments. Besshi-type ores are generally lead-free and have variable Cu:Zn ratios.

On the basis of these observations, the lead-free nature of Lokken and Tverfjellet, together with their high Cu:Zn ratios supports the

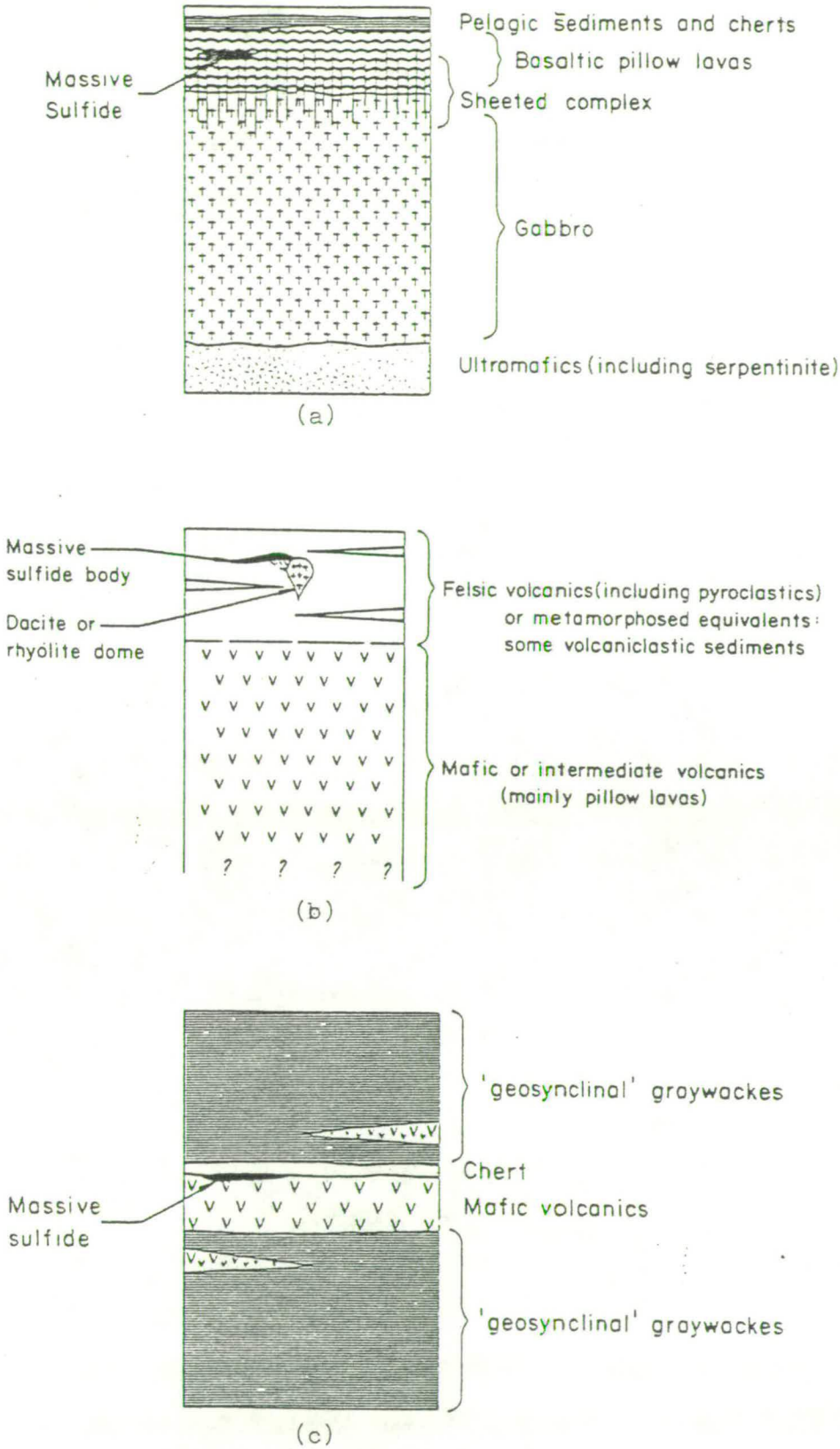

Fig. 4.27 Typical lithological settings of massive volcanogenic sulfide deposits. a) Cyprus-type; b) Kuroko-type; c) Besshi-type. (From Sawkins, 1976).

geological and geochemical evidence suggesting an origin at a submarine spreading centre. In contrast, the lower Cu:Zn ratios and small, but significant quantities of lead at Killingdal suggest affinities with deposits of volcanic-arc environments.

Sawkins (1976) classified the Gula massive sulfide deposits as Besshi-type, on the basis of their lithological association. However, while the possible effects of alteration and high grade metamorphism have been emphasised, the geochemistry of the associated mafic volcanics suggests that they represent original island-arc tholeiites. It is therefore possible that other Besshi-type deposits might reveal similar characteristics if their trace-element geochemistries were to be investigated.

The association of massive sulfide deposits with island-arc tholeiites has not previously been recorded. However, both Mitchell and Bell (1973) and Sillitoe (1973) note the possibility that such an association exists, and suggest that the sulfide deposits would be characterised by metal contents similar to those of spreading-centre deposits. The basis for this hypothesis is the suggestion of Nicholls and Ringwood (1972) that island-arc tholeiites are probably formed by partial fusion, due to hydration, of the mantle wedge overlying a subduction zone, while the calc-alkaline suite results from partial fusion of the subducted slab. While the processes of magma generation at island arcs are now known to be more complicated, and less well understood than previously believed (Graham, 1980), the depletion of light rare earth elements in island-arc tholeiitic magmas relative to the calc-alkaline suite does lend some support to this proposal. The high Cu:Zn ratio and negligible lead content of the Rostvangen deposits (Fig. 4.26) appear to fulfil the predictions of Sillitoe (1973) and Mitchell and Bell (1973) with regard to the composition of massive sulfide deposits associated with arc tholeiites.

4.4.4 Sulfide mineral chemistry.

Average sulfide mineral compositions for the five deposits investigated are shown in Table 4.7. Analytical techniques and conditions are described in Appendix B, and individual analyses listed in Tables B4-B9.

In all cases chalcopyrite is approximately stoichiometric $CuFeS_2$ with very low concentrations of other trace metals. Pyrrhotite contains variable amounts of trace metals, especially lead which reaches a maximum of 0.4 wt% at Tverfjellet. Only in samples from Kvikne is nickel detectable in pyrrhotite, but even here cobalt is prevalent with a Co/Ni ratio of approximately 2. Pyrite has variable amounts of trace metals, notably lead (maximum 0.20 wt%) and Co (maximum 0.26 wt%). Ni is never detectable indicating a high Co:Ni ratio (typical detection limits are shown in Table B.3).

Galena from Killingdal contains minor quantities of iron (average 1.11 wt%) and trace amounts of silver (average 0.37 wt %), arsenic (average 0.12 wt%), and copper (average 0.11 wt%). The solubility of Ag_2S in galena increases with temperature (Boyle, 1968). However, the relationship has not been sufficiently well calibrated to allow its application as a geothermometer.

Arsenopyrite at Killingdal contains trace amounts of lead and cobalt. Clark (1960a and b) reported a temperature and pressure dependence of the arsenopyrite (131) interplanar spacing, also related to the S:As ratio. However, the resulting geobarometer (if temperature can be estimated independently) has been calibrated to only 2kb, and is not applicable to the S:As ratios obtained in this study (1.1:0.9) which suggest much higher pressures.

Inspection of Table 4.7 indicates that the most obvious variable between the five deposits is the iron-content of sphalerite. Barton and Toulmin (1966) and Scott and Barnes (1971) drew attention to the

	LOKKEN			TVERFJELLET				ROSTVANGEN			
	Py	Cp	Sl	Py	Po	Cp	Sl	Py	Po	Cp	Sl
S	53.25	34.93	33.57	53.45	39.37	34.43	33.72	53.56	38.91	34.84	33.54
Pb	0.16	0.09	0.14	0.14	0.49	0.12	0.15	0.19	0.14	0.13	0.10
Fe	47.12	30.72	3.10	47.40	60.94	31.11	6.28	46.55	60.24	30.39	7.18
Zn	0.04	0.14	63.25	nd	0.63	0.04	58.01	nd	0.09	nd	59.64
Cu	0.16	33.76	0.19	0.06	0.10	33.60	nd	0.06	0.10	34.35	0.22
Ni	nd	nd	nd	nd	nd	nd	nd	nd	nd	nd	nd
Ag	nd	nd	nd	nd	nd	nd	nd	nd	nd	nd	nd
Cd	nd	nd	0.22	nd	nd	0.07	0.27	nd	0.10	nd	0.23
Co	0.18	0.05	nd	0.26	0.12	0.06	0.03	0.14	0.08	0.05	0.03
Mn	0.03	nd	nd	ND	ND	ND	ND	nd	nd	nd	0.06
As	ND	ND	ND	ND	ND	ND	ND	ND	ND	ND	ND
A:S	13:5	12:5	9:4	14:5	6:3	14:5	3:2	15:5	15:5	15:5	10:4

	KILLINGDAL						KVIKNE			
	Py	Po	Cp	Sl	Gn	Apy	Py	Po	Cp	Sl
S	53.47	39.29	34.59	33.45	12.97	21.96	53.40	38.97	34.86	33.49
Pb	0.20	0.15	0.09	0.18	85.11	0.12	0.20	0.10	0.15	0.13
Fe	47.20	60.69	30.78	7.96	1.11	35.78	46.69	60.80	30.46	7.88
Zn	0.05	0.10	0.11	56.74	nd	nd	nd	nd	nd	59.05
Cu	0.07	0.07	33.62	0.08	0.11	0.08	nd	0.06	34.16	0,04
Ni	nd	nd	nd	nd	nd	nd	nd	0.03	nd	nd
Ag	nd	nd	nd	nd	0.37	nd	nd	nd	nd	nd
Cd	nd	nd	nd	0.21	nd	nd	nd	nd	nd	0.28
Co	0.14	0.10	0.05	nd	nd	0.11	0.09	0.06	0.03	nd
Mn	nd	nd	nd	0.13	nd	nd	nd	nd	nd	0.15
As	nd	nd	nd	nd	0.12	41.85	ND	ND	ND	ND
A:S	15:5	15:5	15:5	10:5	4:2	5:2	12:4	12:4	12:4	12:4

EXPLANATION

A:S number of analyses : number of samples in average

nd not detectable

ND not determined

Apy arsenopyrite

other symbols as in Table 4.6

TABLE 4.7 Average compositions of sulfide phases in the Lokken, Tverfjellet, Killingdal, Rostvangen, and Kvikne massive volcanogenic sulfide deposits. Individual analyses listed in Tables B.4 - B.9.

relationship between FeS-content of sphalerite coexisting with pyrite and hexagonal pyrrhotite and the dimensions of its cell edge, and hence to its potential use as a geobarometer. Subsequently, Scott (1973) calibrated this sphalerite geobarometer up to pressures of 7.5 kb and demonstrated a temperature independence below 600°C for pressures up to 5 kb. However, he interpreted the results of his 7.5 kb to 8 kb runs as indicating both a temperature and pressure dependence. Lusk et al. (1975) cast doubt on Scott's (1973) inferred 7.5 kb solvus, suggesting that it was in fact T-independent. Scott (1976) conceeded this point and accepted a temperature independence, at least between 500 and 700°C. Lusk and Ford (1978) extended the calibration of the geobarometer to 10 kb, where a temperature independence was demonstrated between 420°C and 700°C. At higher temperature, a slight lowering of FeS-content with increasing temperature was noted. Fig. 4.28 illustrates the variation in sphalerite composition in equilibrium with pyrite and hexagonal pyrrhotite as a function of temperature and confining pressure.

Scott and Barnes (1971) and Scott (1973) demonstrated that, of the minor elements commonly present in sphalerite, Cd and Mn have no effect on the calibration of the geobarometer. Wiggins and Craig (1975), however, found Cu to be potentially effective in modifying the isobars. The sphalerites studied here contain a maximum of 0.56 wt% Cu (Table B.7), and an average of 0.08 wt% (Table 4.7). The common occurrence in ores of this type (but only rarely in this study) of exsolved blebs of chalcopyrite in sphalerite indicate a higher solubility of Cu at greater temperatures and pressures. Toulmin (1960), however, demonstrated that solid solution of CuS in sphalerite was very small (<0.5 mole %) at temperatures up to 600°C, and that solid solution of up to 1.5 mole % CuS (0.9 wt% Cu) at 660°C, and the vapour pressure of the system, had no

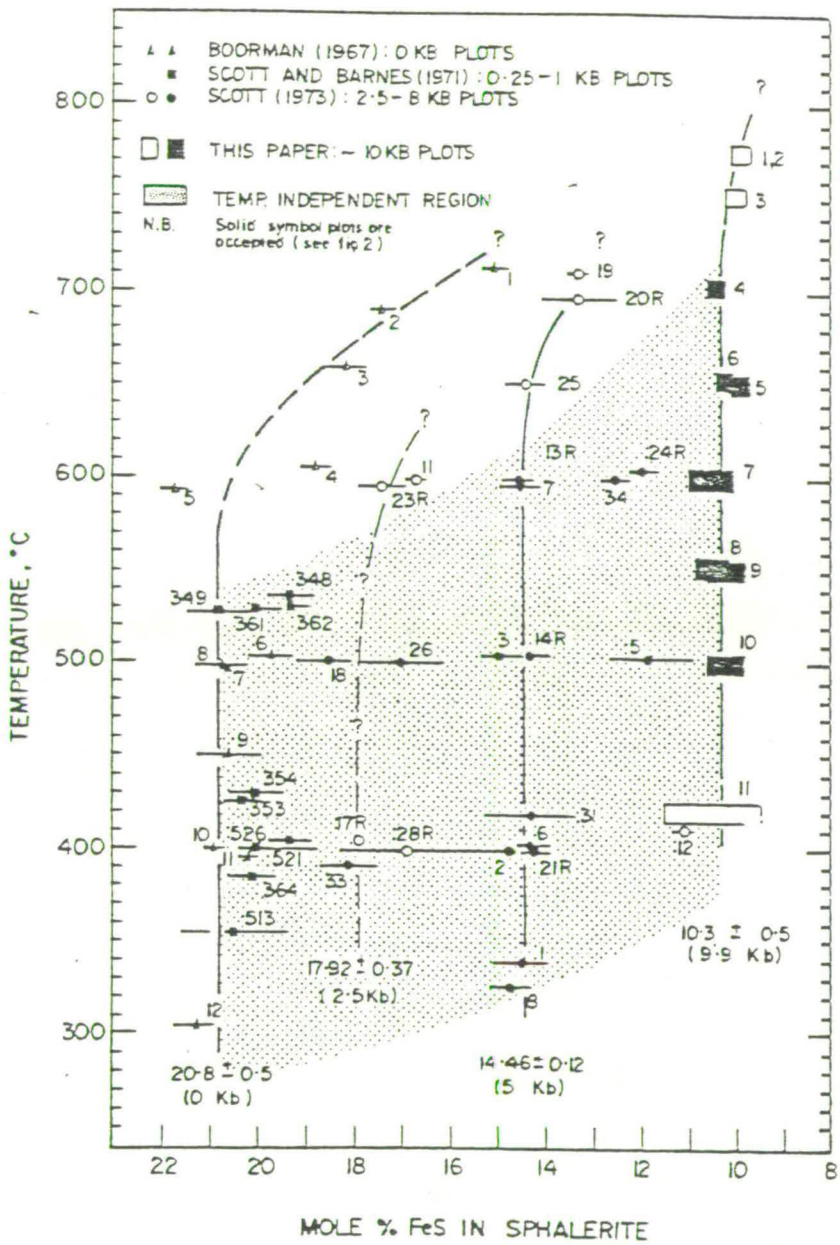

Fig. 4.28 Mole % FeS in sphalerites coexisting with pyrite and hexagonal pyrrhotite as a function of temperature and confining pressure. (From Lusk and Ford, 1978).

effect on sphalerite-pyrite-pyrrhotite phase relations. Thus, the FeS-content of natural sphalerites buffered by pyrite and hexagonal pyrrhotite is a useful and reliable geobarometer, with the possible exception of complications caused by the presence of Cu.

Scott (1976) cited three criteria to be fulfilled for successful application of the sphalerite geobarometer.

1) FeS activity must be buffered by the assemblage pyrite + hexagonal pyrrhotite. While the presence of all three phases in a polished section is suggested as fulfillment of this criterion, mutual contact is preferred, especially at lower metamorphic grade (greenschist facies), where it appears that S is relatively immobile, and FeS activity is variable over quite small distances (centimetres). Retrograde re-equilibration of sphalerite "requires dissolution of FeS", a kinetically unfavourable process compared with exsolution, especially at coarse grain-size (Scott, 1976). Such reactions would produce Fe-rich rims in sphalerites, a feature looked for but not recorded by Scott (1976), in metamorphosed massive sulfide deposits. However, an investigation of a number of Rostvangen sphalerites (Table 4.8) demonstrates that low-pressure re-equilibration has occurred. This process is considered further below.

2) While the isobars are temperature independent over most of Fig. 4.28, for reliable estimates of confining pressure the temperature must be above the reversal in slope of the pyrite-hexagonal pyrrhotite solvus (265^{o}C at 1 bar but not located at higher pressure - Kissin and Scott, 1972; Scott and Kissin, 1973), and lower than the upper stability limit of pyrite (743^{o}C at 1 bar and increasing by 14^{o}C/kb, - Kullerud and Yoder, 1959). Furthermore, at temperatures above 550-700^{o}C, the curvature of the isobars requires accurate determinations of temperature before reliable pressure estimates can be made. The pressure independent region of the calibration is illustrated on Fig. 4.28. In the southern

TABLE 4.8 Compositional zoning in Rostvangen sphalerites. (Full analyses listed in Table B.7).

SPHALERITE	Mole % FeS	
	Core	Rim
472	12.30	13.44
477	12.39	12.84
478	13.42	16.16
479	12.15	12.95
480	11.75	13.70
481	11.00	13.17

TABLE 4.9 Summary of sphalerite geobarometry. Tverfjellet, Killingdal, Kvikne, and Rostvangen deposits.

DEPOSIT	MEAN MOLAR % FeS	STD DEV	MEAN PRESSURE Kb	STD DEV	MAXIMUM PRESSURE Kb
TVERFJELLET	15.16	1.31	4.5	1.3	6.8
KILLINGDAL	14.40	0.51	5.2	0.5	6.5
KVIKNE	13.66	1.03	6.0	1.1	8.1
ROSTVANGEN	13.47	1.31	6.2	1.4	9.5

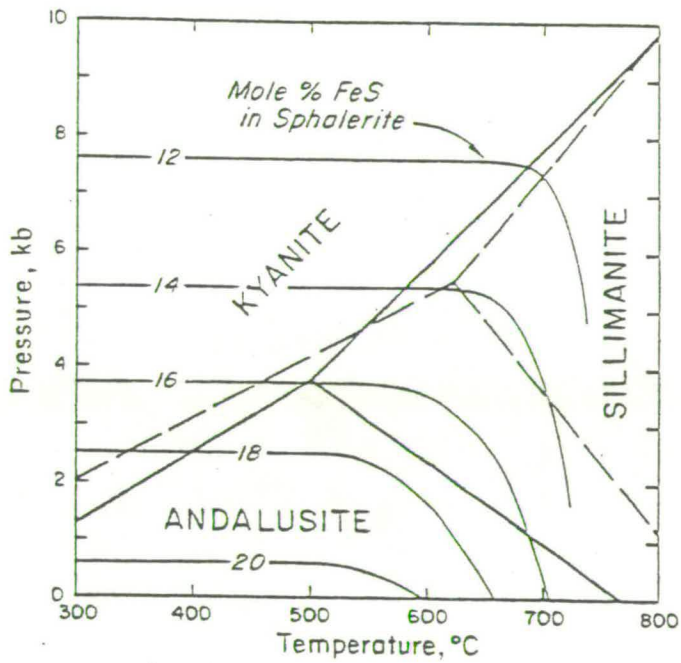

Fig. 4.29 P-T projection of sphalerite isopleths superimposed on the Al_2SiO_5 diagrams of Holdaway (1971) - solid line, and Richardson et al. (1969) - dashed line. Taken from Scott (1976).

part of Trondelag kyanite is the alumino-silicate polymorph occurring in the high-grade parts of the Gula Group (Fig. 2.1). Together with the frequent occurrence of staurolite recorded by Roberts (1968) this suggests that, even at high pressure, temperatures greater than 700°C were not attained (Winkler, 1976, Chapter 14). At lower pressures the occurrence of kyanite alone (Holdaway, 1971; Richardson et al., 1969) restricts the temperature to the temperature-independent region of Fig. 4.28, as shown on Fig. 4.29.

3) Accurate microprobe analyses of sphalerite are required for reliable pressure determinations. Both wavelength-dispersive and energy-dispersive methods were used in this study. Description of techniques and conditions of analyses are presented in Appendix B, and analyses are listed in Table B.7.

Scott (1973) and Lusk and Ford (Lusk, pers. comm., 1979) calculated the mole % FeS of sphalerite directly from the iron analyses. This convertion has been followed here. Equation (2) of Lusk and Ford (1978) has been used to calculate the pressures, as follows:

$$P(kb) = 26.18 - 1.903 \text{ (mole \% FeS)} + 0.0309 \text{ (mole \% FeS)}^2.$$

4.4.5 Application of the sphalerite geobarometer.

Where possible, at least forty analyses of sphalerite were obtained from each deposit where it was found to coexist with hexagonal pyrrhotite and pyrite. The analyses were taken from as close to the centre of the grains as possible. At Lokken no pyrrhotite was found in any of the samples, a feature reflected in the very low FeS-content of the sphalerites (Table 4.7). This deposit is not considered further in this section. Descriptions of the data from each of the remaining four deposits follows and the results are summarised in Table 4.9.

4.4.5.1 Tverfjellet - As shown in Table 4.6, of the samples from Tverfjellet, three (G1, G4, and G5) contained sphalerite, but only G5

contained more than trace amounts. This sample, however, contained no pyrrhotite, and of the others only G4 contained sufficient sphalerite to obtain a small number of analyses.

Fig. 4.30 includes analyses from samples G4 and G5. The analyses fall into two groups. The first group (mole % FeS <10.5) includes analyses from sample G5, which contained no pyrrhotite, while the second (mole % FeS >12.5) includes analyses from G4 where traces of pyrrhotite were present. The lower FeS content of sphalerites from G5 is consistent with the observations of Scott (1976) with regard to sphalerite in contact only with pyrite, as compared with those buffered by both pyrite and pyrrhotite. The small number (10) of analyses from sample G4, of which two are from sphalerites in mutual contact with pyrite and pyrrhotite, show a very wide distribution indicating that a widespread equilibrium of the three phases was not attained. However, this group provides the best available estimate of metamorphic pressure, and indicates a mean of 4.5 ± 1.3 kb as shown in Table 4.9.

4.4.5.2 Killingdal - The five samples of Killingdal ore investigated all contained sphalerite, and all but G11 contained more than trace amounts of pyrrhotite (Table 4.6). Fig. 4.31 illustrates that the analyses fall into two groups. The four analyses with mole % FeS <12.5 are from sample G11 and probably indicate disequilibrium of sphalerite with pyrite and hexagonal pyrrhotite. Ignoring this group, the remaining 42 analyses have a very tight distribution and indicate a mean pressure of 5.2 ± 0.5 kb (Table 4.9). The similarity between the distributions of sphalerite FeS-content of different assemblages (Fig. 4.31) suggests that, in these samples at least, equilibrium was attained on a scale greater than adjacent grains.

4.4.5.3 Kvikne - Of the four samples from Kvikne, all but G19 contain greater than trace amounts of pyrrhotite and all contain sphalerite.

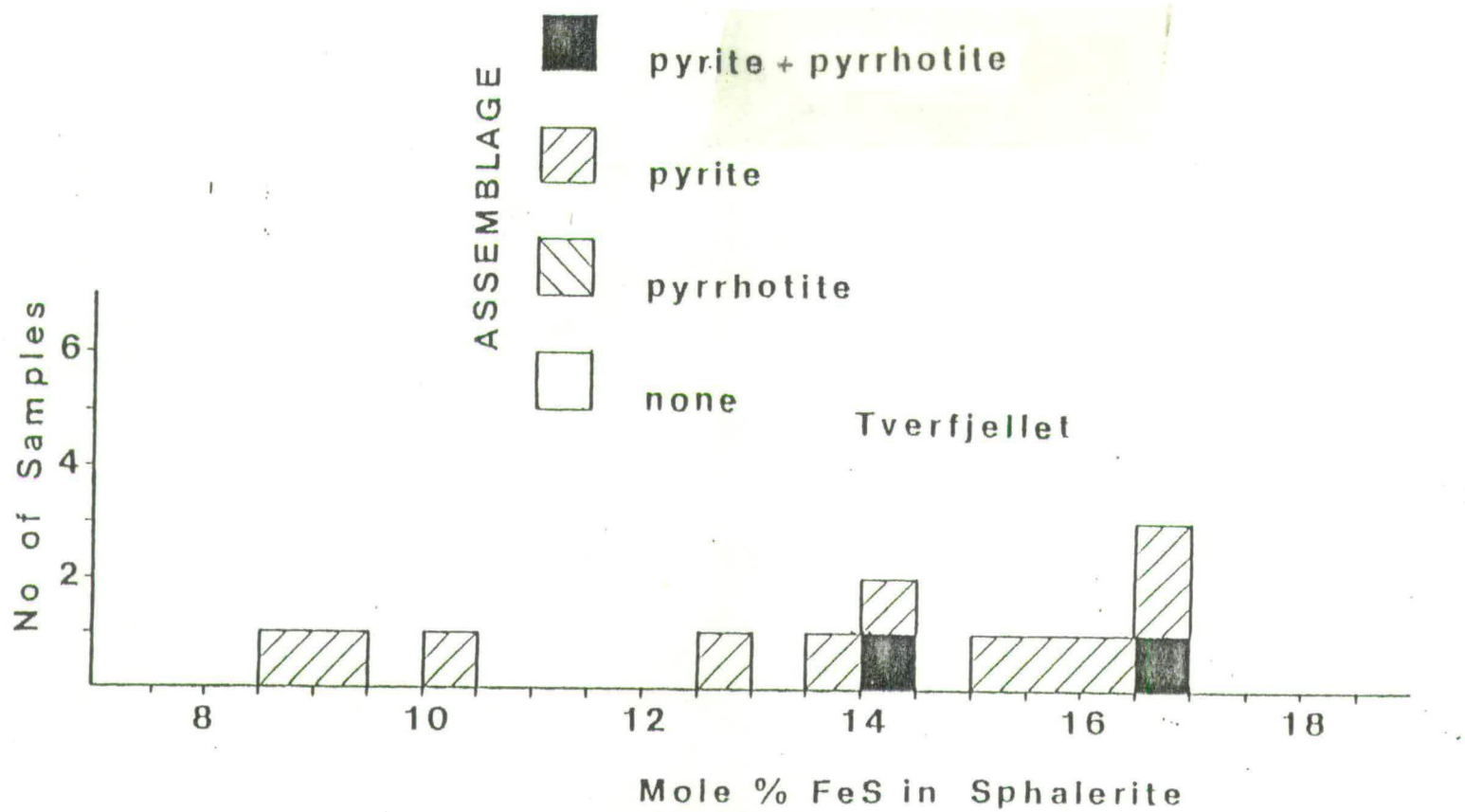

Fig. 4.30 Frequency histogram of mole % FeS in sphalerites from the Tverfjellet deposit. Fe-sulfides in mutual contact with the sphalerites are indicated.

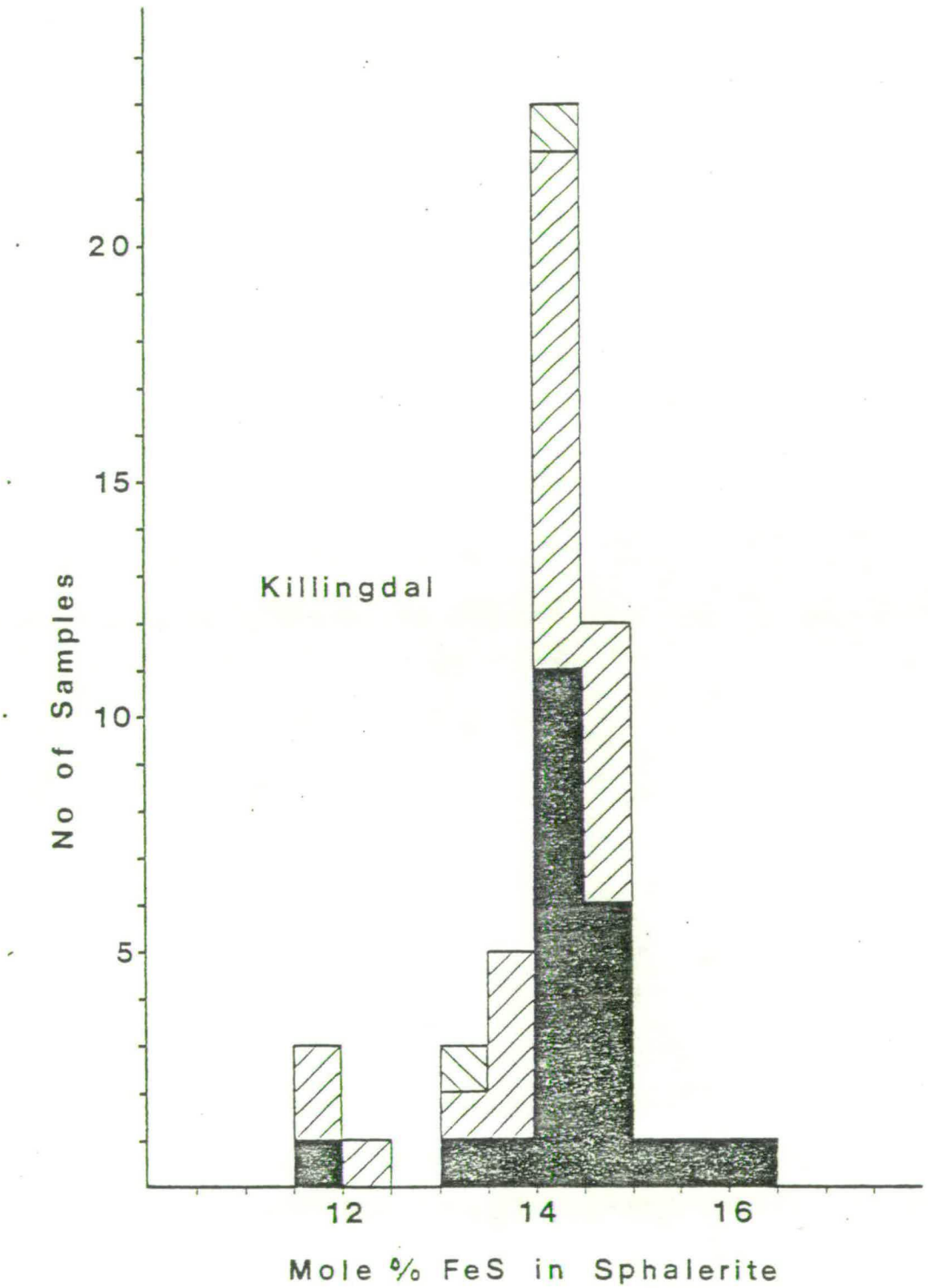

Fig. 4.31 Frequency histogram of mole % FeS in sphalerites from the Killingdal deposit. Annotation as in Fig. 4.30.

Fig. 4.32 illustrates that the 43 analyses have a broad distribution of FeS-content, indicating a mean pressure of 5.9 ± 1.1 kb (Table 4.9). A similar distribution of FeS-contents is noted for sphalerites in mutual contact with different iron-sulfide assemblages, including analyses from sample G19. A relatively widespread equilibrium of sphalerite with pyrite and hexagonal pyrrhotite was therefore probably attained in this deposit.

4.4.5.4 Rostvangen - Table 4.6 demonstrates that of five samples of Rostvangen ore studied all contain more than trace amounts of pyrrhotite. As shown by Fig. 4.33, the sphalerite analyses have a wide distribution with regard to FeS-content. A mean pressure of 6.2 ± 1.4 kb has been calculated from these results. The similar distributions of FeS-contents of sphalerites in equilibrium with different iron-sulfide assemblages suggests a widespread equilibrium of sphalerite with pyrite and hexagonal pyrrhotite.

4.4.5.5 Discussion - In the preceeding sections it has been assumed that sphalerite has not suffered retrogressive re-equilibration. Scott (1976) argues that retrogressive re-equlibration of sphalerite with pyrite and hexagonal pyrrhotite is unlikely as it involves the kinetically unfavourable process of "dissolution", but does not consider the possibility of re-equilibration during a later, prograde metamorphic event. That such "dissolution" occurs is beyond doubt as evidenced by the sharp increase in FeS-content of sphalerite as the pyrite-hexagonal pyrrhotite solvus is approached (compare the analyses of Lokken sphalerites with those from the remaining deposits containing pyrrhotite - Table 4.7). Both the mean and maximum pressures shown in Table 4.9 indicate a higher pressure in the core of the Gula Group (Kivkne and Rostvangen) than in the flanking Storen and Fundsjo Groups (Tverfjellet and Killingdal respectively), which suggests that the sphalerite

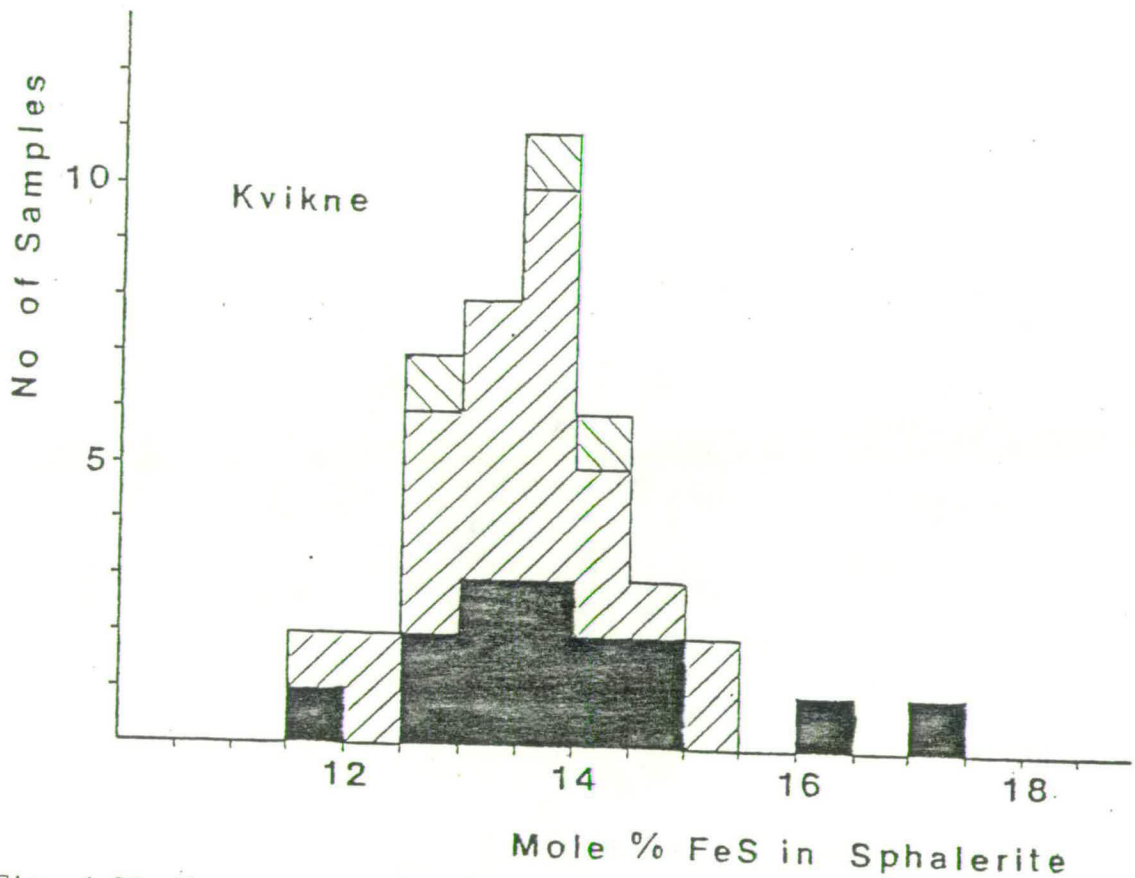

Fig. 4.32 Frequency histogram of mole % FeS in sphalerites from the Kvikne deposit. Annotation as in Fig. 4.30.

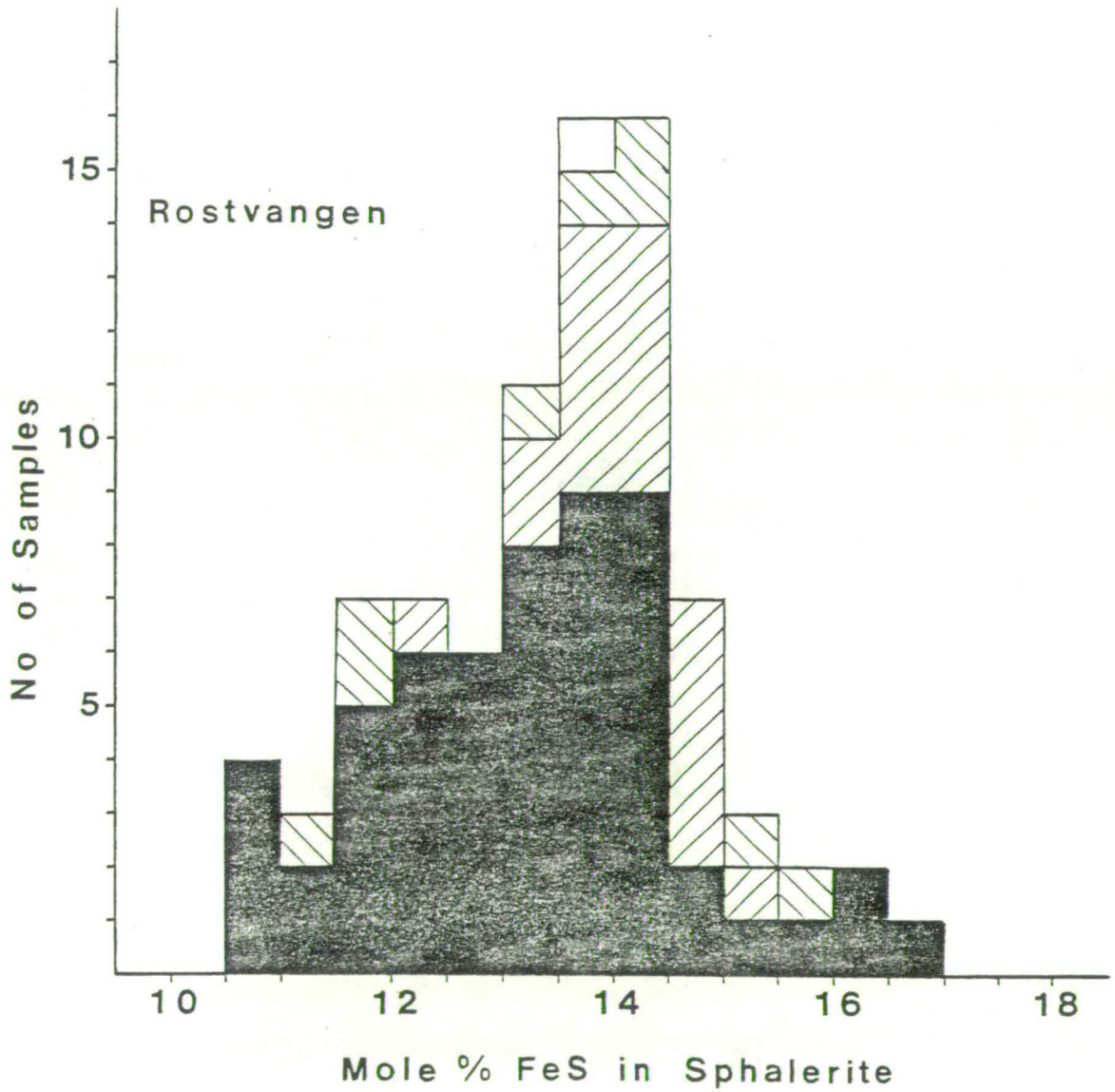

Fig. 4.33 Frequency histogram of mole % FeS in sphalerites from the Rostvangen deposit. Annotation as in Fig. 4.30.

geobarometry is recording, at least in part, the early, Cambro-Ordovician metamorphism of the Trondheim Orogeny (Chapter 3). In which case it is possible that progressive re-equilibration with pyrite and hexagonal pyrrhotite occurred during the later, lower grade, Silurian metamorphism.

A further possibility is that raised by Bristol (1979) who suggested that sphalerite re-equilibrates with monoclinic pyrrhotite when this phase becomes stable below 253°C. Such re-equilibration would result in decreased FeS-content of sphalerite (Scott and Kissin, 1973), such that anomalously high pressures would result from the application of the sphalerite-pyrite-hexagonal pyrrhotite geobarometer. As described in 4.4.2 monoclinic pyrrhotite is commonly present in the ores investigated here as an intergrowth with the more common hexagonal pyrrhotite.

If sphalerite had suffered retrogressive re-equilibration with pyrite and hexagonal pyrrhotite two effects might be noticed:

1) a zoning of sphalerite towards FeS-rich rims; and

2) an increase in FeS-content of sphalerite cores with decreasing grainsize.

In contrast, if re-equilibration with monoclinic pyrrhotite had occurred the opposite effects might be observed. A zoning of sphalerites towards FeS-rich rims has already been described from Rostvangen (Table 4.8).

During the microprobe analyses of sphalerites the approximate average dimension of the individual grains was noted. As sphalerite is complexly intergrown with pyrrhotite and chalcopyrite in a matrix to pyrite porphyroblasts, its shape is commonly irregular and only very general estimates of the "average dimension" were possible.

Fig. 4.34 presents scatter plots of mole % FeS in sphalerite against grainsize. The plots for Tverfjellet, Kvikne, and Rostvangen are

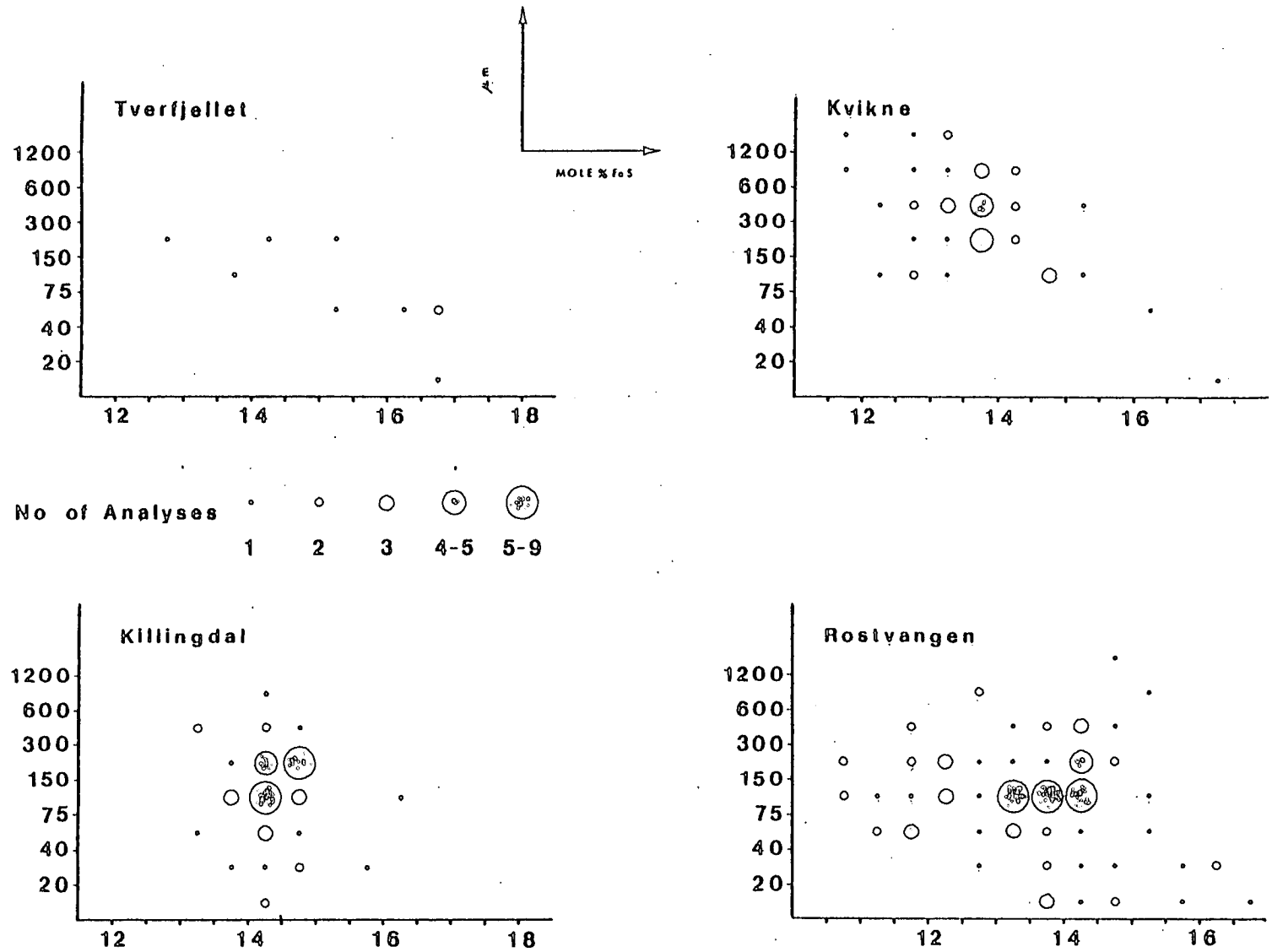

Fig. 4.34 Scatter plots of mole % FeS in sphalerites against grainsize for the Tverfjellet, Killingdal, Kvikne, and Rostvangen deposits.

characterised by diffuse negative correlations. Together with the evidence of zoning in Rostvangen sphalerites, this data suggests that these ores have re-equilibrated from higher pressures, in equilibrium with pyrite and hexagonal pyrrhotite, during the low-grade Silurian metamorphic event. In contrast re-equilibration with monoclinic pyrrhotite does not appear to have been an important process.

The Killingdal scatter plot reveals no correlation between grainsize and composition of sphalerite. This is possibly explained by investigation of Fig. 2.1, where it is demonstrated that the higher parts of the Eastern Trondelag succession are at higher metamorphic grade than their Western Trondelag correlatives. It may be, therefore, that in the vicinity of Killingdal there was little difference in pressure conditions between the early Cambro-Ordovician metamorphism, and the later Silurian event. This would be reflected in the very narrow limits of sphalerite composition, and in the lack of any correlation between composition and grainsize.

In conclusion, the mean value for the pressures calculated from Killingdal sphalerites may represent a close approximation to the conditions prevalent during both the Cambo-Ordovician metamorphism associated with the Trondheim Orogeny, and the more widespread Silurian metamorphic event. In contrast, the mean pressures calculated from Tverfjellet, Kvikne, and Rostvangen, probably represent an attempt to re-equilibrate from higher pressures during the Silurian event. The maximum pressures, relating to greatest grainsize, may give a better estimate of the pressure conditions ambient during the Cambro-Ordovician Trondheim Orogeny.

4.5 Conclusions and Regional Implications.

4.5.1 Metamorphism

Consideration of ore textures reveals that grainsize of porphyroblastic pyrite is greatest in deposits lying in the central parts of the Gula Group. This observation, together with the overall elongation of the orebodies along the D_1-lineation direction suggests that the metamorphic zonation displayed by the Trondheim Nappe is real, and not an effect of retrogression, related for instance to thrusting associated with nappe emplacement.

Application of the sphalerite geobarometer indicates mean pressures of 4.5, 5.2, 6.0, and 6.2 kb for the Tverfjellet, Killingdal, Kvikne, and Rostvangen deposits respectively. The higher pressures obtained from deposits in the central parts of the Gula Group suggest that these values relate to the Cambro-Ordovician Trondheim Orogeny. However, on the basis of variations of composition with grainsize, and an increase in FeS-content towards the rims of sphalerite grains, it is suggested that the sphalerite may have re-equilibrated slightly during the lower-grade main Scandinavian Orogeny.

4.5.2 Geochemistry

While accepting the limitations imposed by the reconnaissance nature of the geochemical investigations, and the possible modifications of primary geochemical patterns by element mobility during metamorphism, the following observations are made.

The trace element abundances of the Gula amphibolite horizons have affinities to those of low-K tholeiites of island arcs. The association of massive sulfide deposits with volcanics of this type has not previously been recorded. However, the average composition of the Rostvangen deposits is consistent with the predictions of Mitchell and Bell (1973) and Sillitoe (1973) that such ores would have a similar bulk chemistry

to those formed at mid-ocean ridges. On this basis, the Gula Group might tentatively be interpreted as part of a fossil volcanic-arc system.

Abundant granitic intrusives are normally associated with arc systems. While such lithologies are common in the Trondheim Nappe as a whole, their occurrence in the Hovin and Horg Groups, and their eastern correlatives, suggest that they are related to the Silurian main Scandinavian Orogeny. The apparent lack of any granitic intrusive activity in the Gula Group, uniquely associated with the Cambro-Ordovician Trondheim Orogeny is a conspicuous problem in interpreting the Gula Group as a fragment of a fossil volcanic-arc system.

However, Jenks (1971) drew attention to the possible effects of early volcanic-arc development in "a tectonically active geosyncline". Gravitational instability results from the deposition of dense, massive volcanics onto less dense, poorly consolidated sediments. Such a system would be susceptible to detachment and gravity sliding, such that the early-arc volcanics may become separated from their source region. Such a process might explain the lack of any granitic intrusives within the Gula Group uniquely associated with the Trondheim Orogeny; and the association of the Gula metabasics of island-arc tholeiitic affinity with an apparently largely sedimentary sequence (although the possibility that a proportion of the less-mafic Gula lithologies represents original intermediate and more evolved volcanics has also been discussed). In similar fashion, massive sulfide deposits, originally associated with the volcanics, might become separated from their host rocks, thus explaining the Gula deposits with no apparent spatial relationship to amphibolite horizons. Subsequent metamorphism and deformation would obscure original relationships still further.

While the complete lithological association which characterises

an ophiolite complex (Fig. 4.27a) is not present, the predominance of mafic, commonly pillowed, volcanics in the Storen and Fundsjo Groups, and their extensive strike length, suggest an origin at a submarine spreading centre. Gabbros and ultramafics are, however, present as tectonically emplaced bodies within the metavolcanics. The close association with limestones and pyroclastics implies deposition in a shallow water environment.

Geochemical investigations of the Storen and Fundsjo metabasics are not inconsistent with these proposals. Similarities to both 'E'-type mid-ocean ridge basalt and marginal-basin basalts have been described, although a common depletion in Nb might favour a marginal-basin origin. While the average bulk-sulfide composition of the Lokken and Tverfjellet deposits are in agreement with these observations, the composition of Killingdal ores bears closer resemblance to deposits of volcanic-arc association.

In Chapter 3 the Cambro-Ordovician Trondheim Orogeny, which affects only the Gula, Storen, and Fundsjo Groups, was tentatively correlated with the Grampian Orogeny in Scotland, and the Finnmarkian Orogeny of northern and southwestern Norway. Wright (1976) and Lambert and McKerrow (1976) have presented speculative attempts to relate the Grampian Orogeny to subduction processes.

Lambert and McKerrow (1976) proposed a model involving the subduction of an active spreading system, suggesting that such a process would explain many of the sedimentalogical, volcanological, structural, and metamorphic features of the Lower Palaeozoic and earlier successions of the northern and northwestern British Isles. Wright (1976), however, drew attention to the abundant basic volcanics (the Tayvallich volcanics) in the Upper Dalradian, which, although they have normal mid-ocean ridge affinities (Graham, 1976), cannot represent slices of oceanic

crust as they lie in a sequence of coarse, shallow water quartzites. He regarded them as marking the "opening stage" of a marginal basin and suggested that the intrusion of the Aberdeenshire gabbros might represent a similar event. He concluded that the Grampian Orogeny marks the closure of such a marginal basin.

The evidence from the Gula, Storen, and Fundsjo Groups could be regarded as consistent with both of these models. Ridge-trench impingement might involve a volcanic arc (the existence of which is now recorded by the Gula Group) above the subduction zone, and would also account for the lithological association of the Storen and Fundsjo Groups, in which pillow lavas are interlayered with shallow-water sediments together with the more typical authigenic sediments associated with deeper-water volcanics. With regard to Wright's (1976) model, the most obvious requirement for a marginal basin is an association with a volcanic arc (now recorded by the Gula Group), proximity to which could result in the assemblage of rock types characteristic of the Storen and Fundsjo Groups.

Whatever the processes involved in the Trondheim Orogeny, the considerable strike length, and dip length (see Fig. 3.9) of the contact between the Gula Group (at least closely associated with a volcanic arc) and the Storen and Fundsjo Groups (of submarine spreading centre origin) probably requires their juxtaposition by tectonic processes. Such processes might also have been responsible for the separation of the Storen and Fundsjo Group volcanic sequences from the ophiolitic assemblage with which they were probably originally associated.

No evidence for a thrust contact between the Gula and the Storen and Fundsjo Groups has been observed in this study. A possible explanation might be the common occurrence of phyllitic lithologies on the

contacts (the Undal and Asli Formations) and the effects of subsequent deformation associated with the main Scandinavian Orogeny. However, Guezou (1978) has mapped a "tectonic contact" between the Gula Group and the overlying metavolcanics in the Dombas-Lesja area. Furthermore, Strand (1951) and Roberts (1967) have recorded "slide zones" close to the margins of the Gula Group in central Trondelag, while Gale and Roberts (1974) point to an increase in strain upwards through the Gula Group towards the boundaries with the Storen and Fundsjo Groups as further evidence for a "conjunctive" tectonic contact.

Following the Trondheim Orogeny, the Hovin and Horg Groups, and their eastern correlatives, were unconformably deposited on the eroded remains of the Gula and Storen/Fundsjo Groups. On the basis of their lithological assemblages, most authors agree that these units originated in an Ordovician to Silurian island arc-marginal basin palaeoenvironment (Gale and Roberts, 1974; Gee, 1975b; Vokes and Gale, 1976; Roberts, 1978).

The existence of a Caledonian ocean, known as the Iapetus Ocean, separating the Baltoscandian and Greenlandian continental platforms during the early Lower Palaeozoic, is now widely accepted (e.g. Gale and Roberts, 1974; Gee, 1975b). North American faunal assemblages in the Lower Hovin Group (Berry, 1968; Neuman and Bruton, 1974) suggest derivation of the entire Trondheim Supergroup from the Greenlandian continental margin. Allochthonous units of lower tectonic level (Western Complex and Offerdal Nappes) were derived from the Baltoscandian margin (Gee, 1975b). Emplacement of the nappe pile onto the Baltoscandian platform took place during the Silurian to Devonian main Scandinavian Orogeny, as a result of closure of the Iapetus Ocean (Gee, 1975b).

CHAPTER 5

NICKEL - COPPER SULFIDE MINERALISATION

Within the Gula Group a small number of basic intrusions have been recorded; they may be divided into two lithological groups - metagabbros and ultramafics. These bodies are occasionally associated with nickel-copper sulfide mineralisation and have been subject to varying degrees of exploration activity during the nineteen-seventies. The various intrusions are listed and classified in Table 5.1, and their locations indicated on Map 2.

Nilsen (1974) carried out a detailed petrological investigation of the intrusions occurring in that part of the Gula Group outcropping to the south of Storen. On the basis of a) the close spatial association of both the metagabbroic and the ultramafic bodies with the Gula amphibolitic horizons, and b) an apparently continuous chemical trend on an AFM diagram ($A = Na_2O + K_2O$, $F = FeO$, $M = MgO$), he suggested that the intrusives are genetically related to the amphibolites. He proposed that they represent ultramafic and mafic cumulate fractions, separated from a tholeiitic basic magma by crystal fractionation, and subsequently extruded together with the basaltic liquid as cognate xenoliths.

The only intrusion considered in this project and not included in Nilsen's (1974) study is the Skjaekerdalen metagabbroic complex in northern Trondelag. Petrological descriptions have been provided by Carstens (1958) and Lovas (1970). Lovas (1970) also investigated the associated sulfide mineralisation by geophysical techniques.

Although small workings are usually present where these intrusions are associated with sulfide mineralisation, the only substantial production has been from the Skjaekerdalen complex where 18750 tonnes of ore, averaging 1.26% Ni and 0.63% Cu, were extracted between 1876 and

Intrusive Body	Type	Mineralised?
Vakkerlien	Metagabbro	Yes
Olkar	Metagabbro	Yes
Gardsjoen	Metagabbro	Yes
Skjaekerdalen	Metagabbro	Yes
Undal	Metagabbro	No
Haukfjellet	Metagabbro	No
Kaltberget	Ultramafic	Yes
Kletten	Ultramafic	Yes
Graho	Ultramafic	No
Plassbekken	Ultramafic	No

Table 5.1 Mafic and Ultramafic intrusions in the Gula Group.

1891. Descriptions of the operations have been provided by A. S. Bachke (1880), and Rosenlund (1915). The only other noteworthy concentration of ore, so far defined, is at Vakkerlien, where an orebody of 379807 tonnes, averaging 1.08% Ni and 0.39% Cu, has been outlined using a 0.4% Ni cut-off (Chapter 1).

This chapter presents brief descriptions of the field relations and petrology of the various intrusions, paying particular attention to sulfide mineralisation where present. Various aspects of silicate mineral and bulk chemistry are described, and a discussion on the origin of the sulfide mineralisation is presented.

Throughout this chapter, and Chapter 6, sulfide mineralisation will be described according to a two-fold classification involving ore-type, and ore-grade.

The ore-type is defined by the textural relationships between the sulfide and silicate phases as follows:

1. Interstitial ores - where the geometry of sulfide/silicate grain boundaries is controlled by silicate minerals.
2. Globular ores - where the sulfides form rounded globules in a silicate matrix.
3. Breccia ores - where sulfides brecciate silicates.
4. Fragmental ores - where silicates brecciate sulfides.

The ore-grade is defined by the proportion of sulfide to silicate phases present as follows (from high grade to low grade):

1. Massive - >50% sulfides.
2. Matrix - 25-50% sulfides.
3. Disseminated - 2-25% sulfides.
4. Finely disseminated - <2% sulfides.

Small veinlets present problems of scale (i.e. they may be massive on a mm or cm scale, but on a larger scale cannot be regarded as such).

They are therefore classified as:

5. Stringer ore.

In an attempt to avoid inconsistencies due to selective sectioning, the classification has been applied to hand specimens rather than to polished or thin sections. It is, however, accepted that sampling from dumps and drill-core does not allow a totally fullproof application.

5.1 Field Relations And Petrology.

5.1.1 The metagabbros.

5.1.1.1 Vakkerlien - The Vakkerlien metagabbro is situated in poorly exposed muskeg terrain above the western slopes of the valley of the River Orkla, and approximately 5 km southwest of the village of Kvikne (Map 2). It has been the subject of extensive investigation by A/S Sulfidmalm, and has been studied in considerable detail by Thompson (1978).

The intrusion consists of two sub-parallel elongated gabbroic bodies known as the Main Body and the Second Body (Fig. 5.1). On the basis of present knowledge, only the Main Body is associated with economically significant mineralisation.

The Main Body may be described as an elongated lens, 1250 m in length, of elliptical cross-section with average dimensions 40 x 80 m. It is exposed at its NW end and plunges at about 4° towards the SE, where it attains a depth of about 40 m (Fig. 5.2). The direction of elongation is parallel to the D_1-lineation direction in the area. The volume of sulfide mineralisation is centrally positioned within the metagabbro having average cross-sectional dimensions of 25 x 5 m. The body is truncated to the SE by a trondhjemite intrusion as shown in Fig. 5.2.

The Second Body is exposed to the south and west of the Main Body

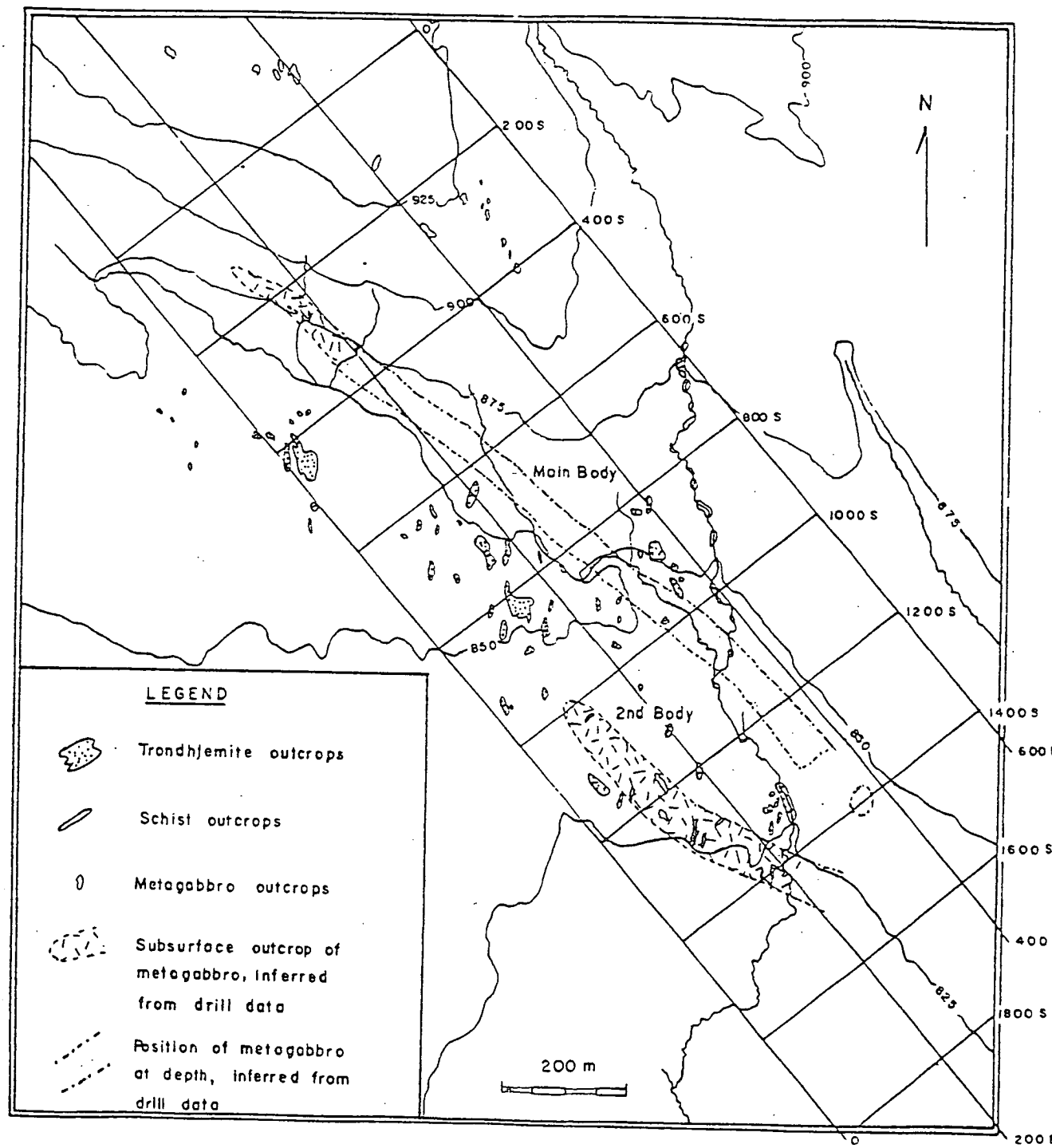

F Fig. 5.1 Geological map of the area around the Vakkerlien metagabbro bodies. (Taken from Thompson, 1978).

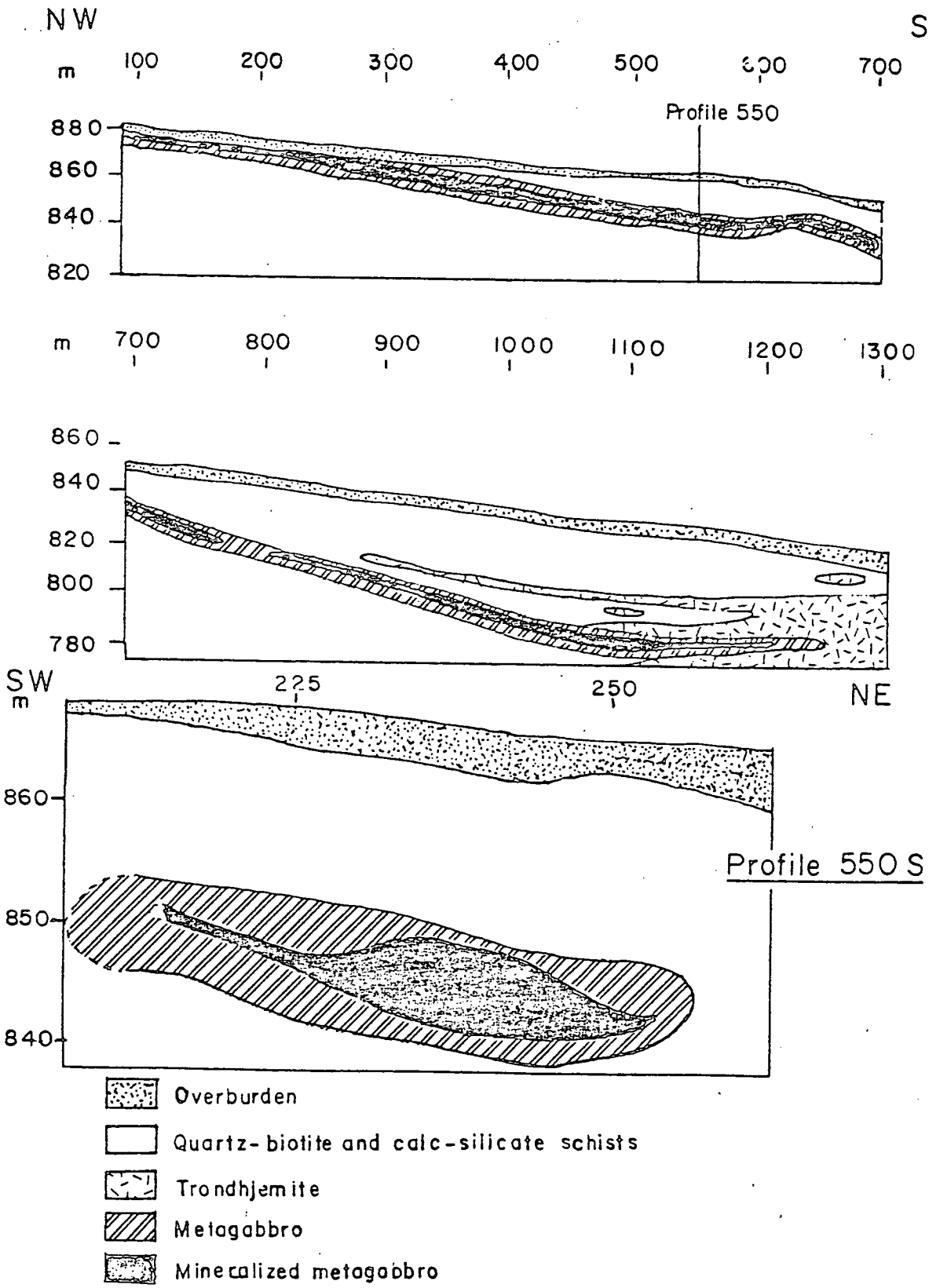

Fig. 5.2 Cross-sections through the Vakkerlien Main Body and ore zone (from Thompson, 1978).

(Fig. 5.1), and from available surface and drill-core data has a similar size, shape, and orientation to the Main Body.

The country rocks consist dominantly of pelitic schist with minor calc-silicate-bearing layers. The schists are barren of sulfides.

The large number of drill-core intersections through the Vakkerlien Main Body enabled Thompson (1978) to investigate lithological and chemical variations throughout the intrusion. He describes two major rock types, which he names Metagabbro and Ultramafic; both have altered and deformed counterparts.

Metagabbro, constituting approximately 50% of the body, consists dominantly of plagioclase (>10%, but generally in the range 40-60%), and amphibole. Accessory minerals are quartz, calcite, biotite, chlorite, epidote group minerals, sphene, rutile, sericite, and sulfides. The grainsize of major minerals varies between 1 and 6 mm (largest dimension). Amphiboles are commonly zoned from brown pleochroic cores to pale green, weakly pleochroic margins. Plagioclase (An_{20} to An_{60}) is generally untwinned and often saussuritised. In deformed varieties a distinct foliation develops, which, together with a mineral recrystallisation may result in a fine-grained, foliated rock with some apparent mineral segregation. In such lithologies chlorite and biotite may be present (<10%) and, together with amphibole, these define the foliation. Plagioclase forms a granoblastic groundmass commonly with minor quartz.

Ultramafic lithologies make up the remaining 50% of the body, and are defined by a plagioclase content of less than 10%. The mineralogy is dominated by amphibole and chlorite which show complete variation in proportions. A foliation is commonly present, especially in chlorite-rich samples. Amphibole occurs as well formed, commonly zoned

porphyroblasts up to 0.8 mm across in a fine grained chlorite, amphibole groundmass. Talc may be present in the more chlorite-rich lithologies. Accessory minerals include quartz, biotite, plagioclase, sphene, rutile, and sulfides. More deformed varieties are characterised by a better developed foliation and by a decrease in the proportion of amphibole porphyroblasts. Biotite becomes increasingly important, generally forming 20-30% of the rock, although at irregular intervals, well defined shear zones consisting of up to 80% biotite occur.

In the margins of the Main Body xenoliths of country-rock schist are common (up to 20% by volume). Close to the metagabbro/schist contact, schist xenoliths predominate. In addition a number of biotite-rich ultramafic inclusions occur. Such ultramafic inclusions are also found in the more gabbroic lithologies in the main part of the body. Although accepting the limitations of drill-core observations, Thompson (1978) uses these varied xenoliths as evidence for a magmatic intrusion of the original gabbro.

Drill-hole profiles across the Vakkerlien Main Body (Fig. 5.3 a, b, and c) show a broad variation from ultramafic in the SW to metagabbroic lithologies dominant in the NE. In general the more deformed lithologies occur at the contacts with country rock schists, and between the different intrusive rock-types.

Lithologically the Vakkerlien Second Body is similar to the Main Body, except that ultramafic types more commonly contain significant amounts of talc and carbonate. Fig. 5.3d shows a drill-hole profile across the Second Body, and illustrates a similar distribution of lithological types to that noted in the Main Body.

According to available data, sulfide mineralisation of Vakkerlien is restricted to the Main Body, where a centrally located orebody of 379807 tonnes, averaging 1.08% Ni and 0.39% Cu, has been defined using

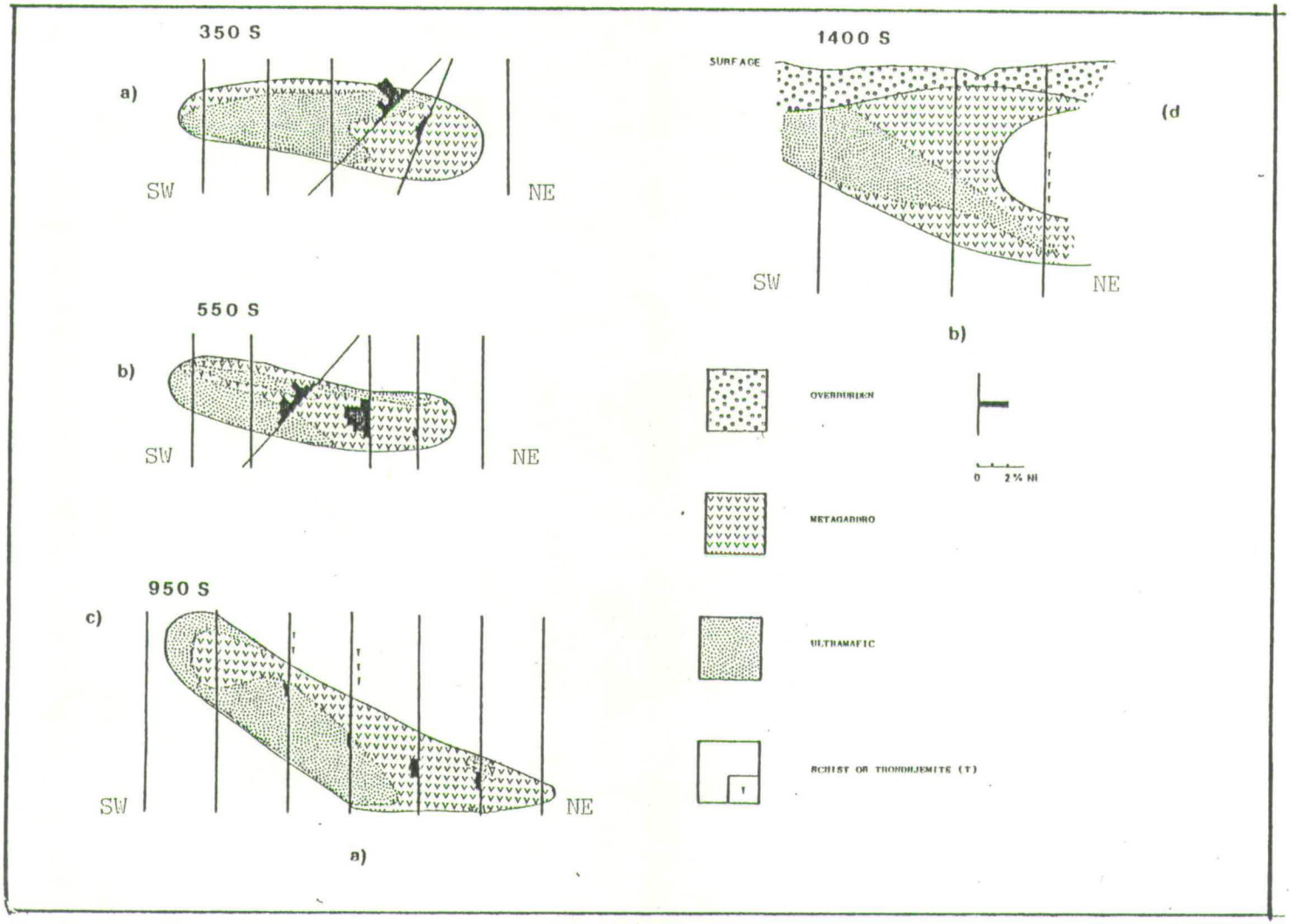

Fig. 5.3 Drill-hole profiles through the Vakkerlien Main Body (a,b, and c) and Second Body (d) showing lithological variation and position of sulfide mineralisation, as indicated by Ni-assays (redrawn from Thompson, 1978).

a 0.4% Ni cutoff. No clear relationship has been found between host-rock lithology and the position of the mineralisation, which is hosted by both ultramafic rock-types and metagabbro (Fig. 5.3).

Thompson (1978) defines three ore types from Vakkerlien.

1. "Massive vein sulfide" occurs as discrete veins up to 30 cm in width, carrying angular clasts of the host rock. According to the classification used in this study, and defined in the introduction to this chapter, these are Massive-Breccia ores.

2. "Disseminated sulfide" is characterised by sulfide, comprising 5-40% of the ore, interstitial to metagabbro or ultramafic silicate phases. According to Thompson (1978) the "host rock for disseminated sulfides, whether metagabbroic or ultramafic, was consistently undeformed, the amphiboles occurring in random orientation". This ore-type is classified here as Disseminated- or Matrix Interstitial ore depending on the proportion of sulfide to silicate present.

3. "Stringer ore" often occurs in "sheared and altered rock types", and is commonly associated with Massive-Breccia ores. Such ore is similarly classified here as Stringer ore.

The sulfide phases in Vakkerlien ores are dominated by pyrrhotite, pentlandite, and chalcopyrite, with minor amounts of pyrite and traces of gersdorffite. Pyrrhotite to pentlandite ratios vary from 10:1 to 3:1 with an average of 5:1. Pyrrhotite to chalcopyrite ratios vary widely from 1:25 to 25:1 in extreme cases. Typical interstitial sulfide is shown in Fig. 5.4. Pyrrhotite forms irregular grains of varying size up to a maximum of about 5.0 mm. Occasionally a recrystallisation to textural equilibrium with 120^{o} grain-boundary intersections was noted. Using a magnetic colloid (Scott, 1974) the pyrrhotite was identified as dominantly monoclinic, with rare grains of the hexagonal phase.

Fig. 5.4 Photomicrograph of Vakkerlien Interstitial ore (sample 75/27/10.40). Blocky interstitial pentlandite (white) in pyrrhotite (grey). Silicates - dark grey.
Reflected light; ppl; f.o.v. = 1.92 mm.

Fig. 5.5 Photomicrograph of Vakkerlien sulfides (sample 75/27/6.20). Pentlandite exsolution flames in pyrrhotite. Chalcopyrite occurs between two grains of pyrrhotite on right of field of view (c).
Note approximately 120° grain-boundary intersection at bottom right.
Reflected light; slightly uncrossed nicols; f.o.v. = 0.38 mm.

Fig. 5.16 Photomicrograph of Olkar sulfides (sample 77/2/14.90). A euhedral grain of cobaltite in pyrrhotite, with pentlandite (light grey and chalcopyrite (c). Silicates - black.
Reflected light; ppl; f.o.v. = 0.38 mm.

Fig. 5.17 Photomicrograph of Olkar sulfides (sample 77/3/8.65). A molybdenite lath (centre) in pyrrhotite (grey) with tiny pentlandite flames (light grey). Silicates - black.
Reflected light; f.o.v. = 0.38 mm.

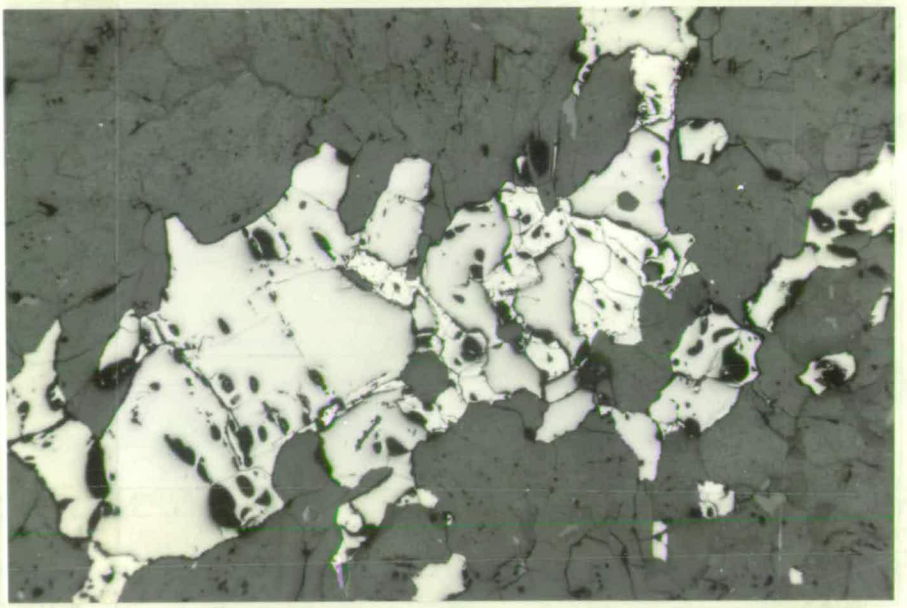

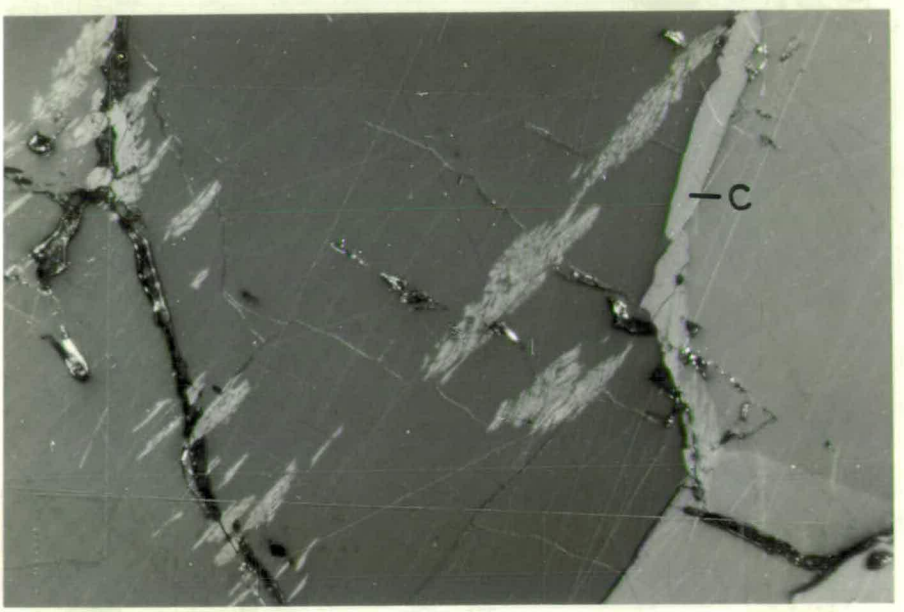
C

Pentlandite occurs as blocky grains, up to 0.5 mm across, commonly interstitial to pyrrhotite (Fig. 5.4). Minor quantities of pentlandite occur as exsolution flames (Fig. 5.5) within pyrrhotite grains, characteristically parallel to (0001).

Chalcopyrite occurs as discrete, generally rounded blebs, commonly located at pyrrhotite/pentlandite grain boundaries or at pyrrhotite/silicate grain boundaries. Chalcopyrite displays much greater concentrations at the margins of massive veins, and in stringer ores, where it may be the dominant sulfide mineral.

Pyrite forms irregular grains interstitial to pyrrhotite, and, according to Thompson (1978), constitutes less than 5% of the sulfide ore as a whole. A small number of euhedral grains of gersdorffite (<0.2 mm) have been recorded, in general included within pentlandite (Fig. 5.6). Thompson (1978) mentions the presence of violarite as an alteration product of pentlandite, but this phase has not been recorded during this study.

Apart from the variation of chalcopyrite concentration, little difference in sulfide mineralogy and microtextures exists between the different ore-types.

5.1.1.2 Olkar - The Olkar metagabbro is situated approximately 4 km to the SE of Kvikne (Map 2). It is poorly exposed in the banks of the River Orkla, and has been the subject of limited exploration activity by A/S Sulfidmalm.

From limited exposure along some 300 m of river bank, and from a single NE-SW drill-hole profile consisting of five holes (Fig. 5.7), the Olkar body appears to consist of a series of discrete lenses of metagabbro enclosed in a black, graphite- and pyrrhotite-bearing schist. Little is known about its lateral extent, but geophysical anomalies suggest a NW-SE elongation parallel to the regional D_1-lineation

Fig. 5.6 Photomicrograph of Vakkerlien sulfides (sample 75/27/6.20). Euhedral gersdorffite in pentlandite. Silicates and pits - black.

Reflected light; ppl; f.o.v. = 0.30 mm.

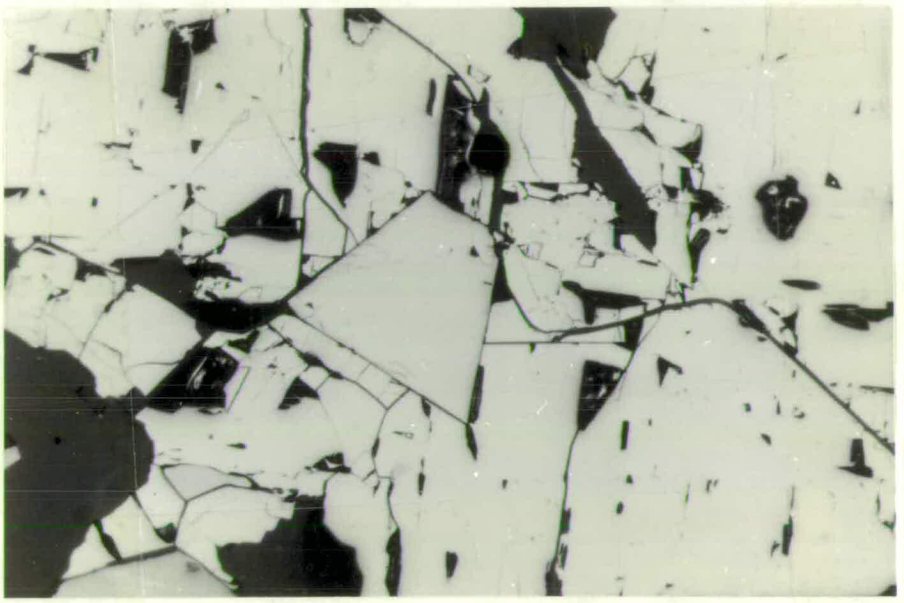

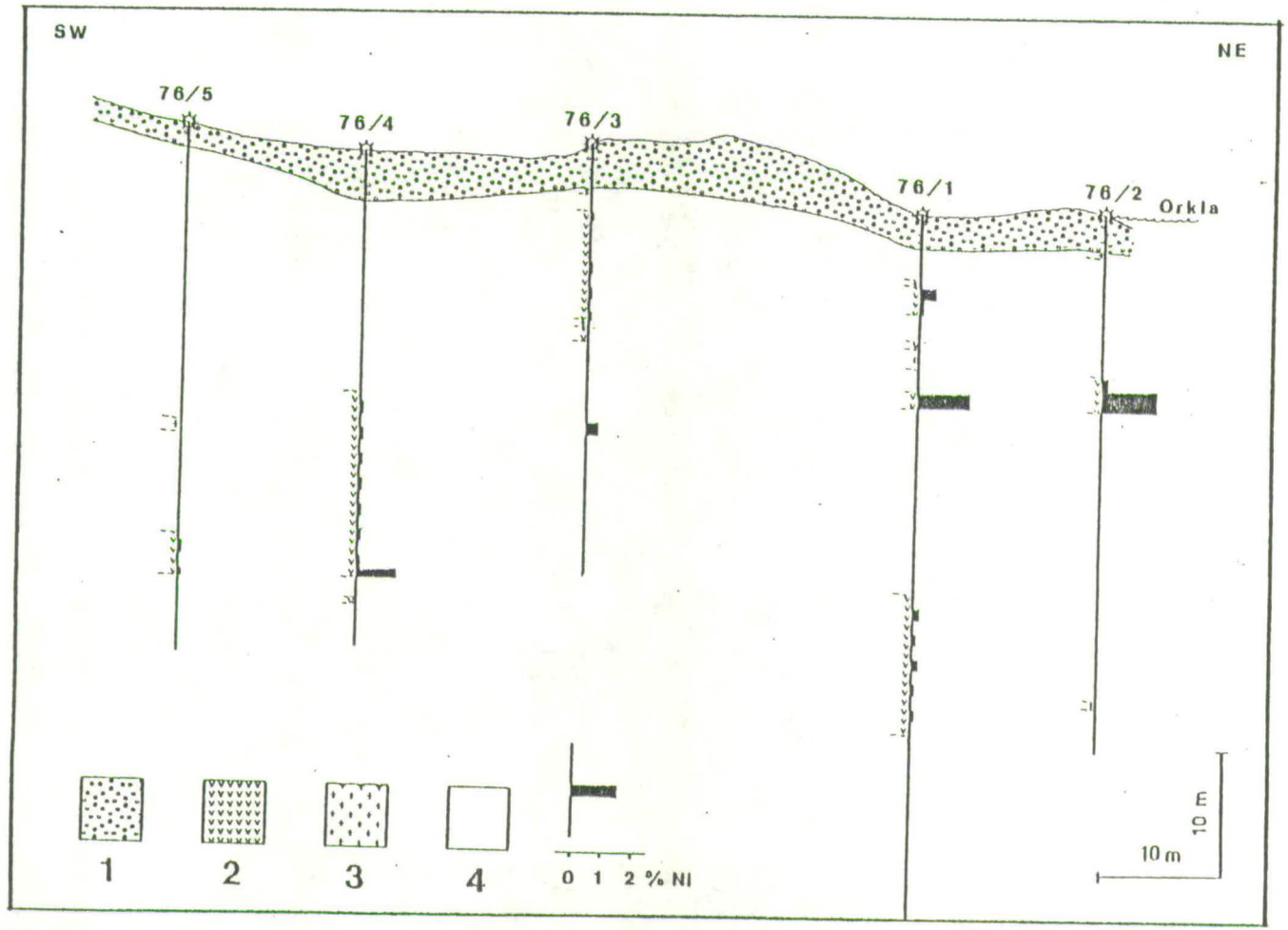

Fig. 5.7 Drill-hole profile at Olkar showing lithological variation and position of sulfide mineralisation as indicated by Ni-assays. 1 - overburden; 2 - metagabbro; 3 - trondhjemite; 4 - schist.

direction in this area. The possibility that the various intersections of metagabbro illustrated in Fig. 5.7 may be related by complex isoclinal folding must also be considered. Sulfide mineralisation occurs at, or close to, the upper and lower margins of the metagabbroic lenses. The Olkar metagabbro is rich in xenoliths, dominantly of country-rock schists, and varying from the mm- to the 10 m-scale. Such xenoliths present obvious problems to drill-core logging and may be responsible for the lenticular appearance of the metagabbro in Fig. 5.7. A typical example of a small schist xenolith is shown in Fig. 5.8.

The metagabbro is similar to that at Vakkerlien, being dominated by plagioclase and amphibole in about equal proportions. Accessory minerals are quartz, zoisite, epidote, biotite, zircon, sphene, chlorite, and sulfides. The amphibole occurs as subhedral grains of average dimension 0.75 mm, but less than 1.5 mm, usually having irregular, ragged edges, and containing numerous inclusions of all other mineral components of the rock. They are commonly zoned from a brown pleochroic core of moderate birefringence, to a pale green, slightly pleochroic rim of high birefringence. Plagioclase is commonly untwinned, and shows a well developed granoblastic texture occasionally with quartz (less than 1.0 mm and average 0.3 mm). A foliation is commonly observed, defined by a preferred orientation of amphibole which may also be lineated parallel to the regional D_1-lineation direction. In more deformed varieties biotite, generally with preferred orientation, increases in importance and may become the dominant mineral phase.

Occasionally small ultramafic pods occur within the metagabbros (Fig. 5.9). They may be several centimetres in largest dimension, and are similar in mineralogy and texture to the metagabbro, except for a plagioclase content of less than 10%, and a somewhat larger amphibole grainsize (average 1.0 mm).

Fig. 5.8 A ground surface of Olkar metagabbro (sample 76.135) with sulfide stringer, and schist xenolith (outlined).

Fig. 5.9 A ground surface of Olkar metagabbro (sample 76.106), with ultramafic xenolith (centre). Light coloured patches in the xenolith are specular reflections from amphibole cleavage surfaces.

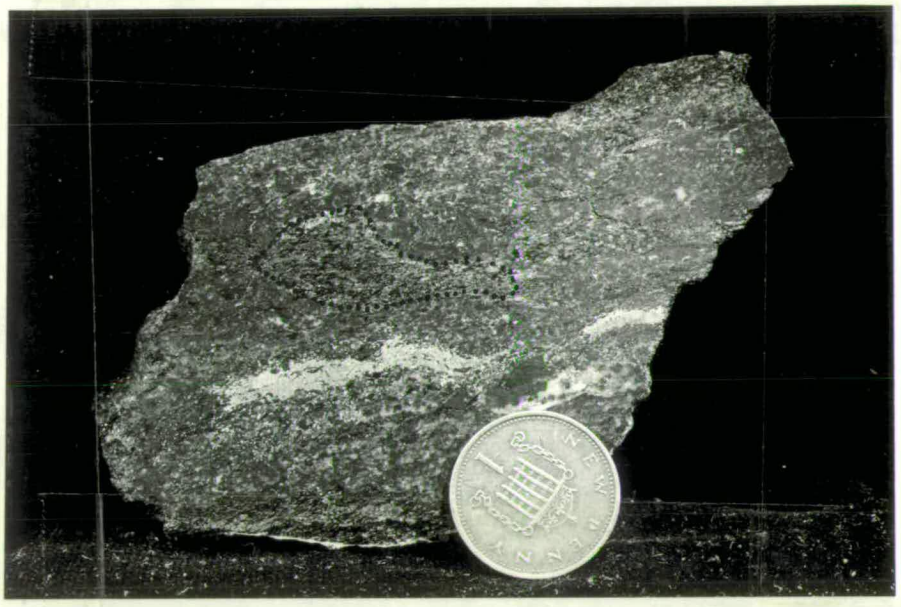

Sulfide mineralisation at Olkar is concentrated at, or close to, the upper and lower margins of the gabbroic lenses. It occurs as massive veins or lenses, which carry fragments of the host silicate rocks as shown in Figs. 5.10 and Fig. 5.11. These ores are therefore classified as Massive-Breccia ores. Stringer, Matrix, Disseminated and Finely Disseminated Breccia and Interstitial ores also occur and are commonly closely associated with the more massive ores, or with xenoliths of country-rock schists (Fig. 5.8).

The mineralogy of the sulfides at Olkar is dominated by pyrrhotite, pentlandite, and chalcopyrite. Pyrite, cobaltite, molybdenite, violarite, and marcasite also occur. Pyrrhotite to pentlandite ratios are variable but average approximately 20:1, while chalcopyrite may be absent (as may be the case in the central parts of massive lenses), or it may be the dominant sulfide present (commonly at the margins of massive lenses, and in fine stringers).

Hexagonal pyrrhotite is the dominant sulfide mineral (monoclinic pyrrhotite occurs in minor amounts), with pentlandite occurring interstitially and as flame-like exsolutions within it (Figs. 5.12 and 5.13). Occasionally an elongation of pyrrhotite grains can be observed as shown in Fig. 5.14. Pyrite replaces pyrrhotite along fractures and grain boundaries (Fig. 5.15) and is therefore probably of secondary origin. Cobaltite has been observed rarely as small, euhedral grains (<0.05 mm) within pyrrhotite (Fig. 5.16). A single lath of molybdenite (0.2 mm in length) has been recorded (Fig. 5.17). The alteration of pyrrhotite to marcasite, and of pentlandite to violarite is the result of supergene processes, and is especially noticeable in surface samples.

5.1.1.3 Gardsjoen - The Gardsjoen showing lies to the west of Orkladalen, some 10 km NW of Kvikne (Map 2). The locality consists of a 10 x 5 m trench cut into a NW-facing slope, together with a dump of

Fig. 5.10 A ground surface of Olkar Massive-Breccia ore (sample 77/2/14.80). The sulfides (light) carry angular fragments of metagabbro (dark).

Fig. 5.11 Photomicrograph of Olkar Massive-Breccia ore (sample 77/1/6.60a). A fragment of metagabbro (amphibole, chlorite, and plagioclase) in sulfide (black).
Transmitted light; ppl; f.o.v. = 0.40 mm.

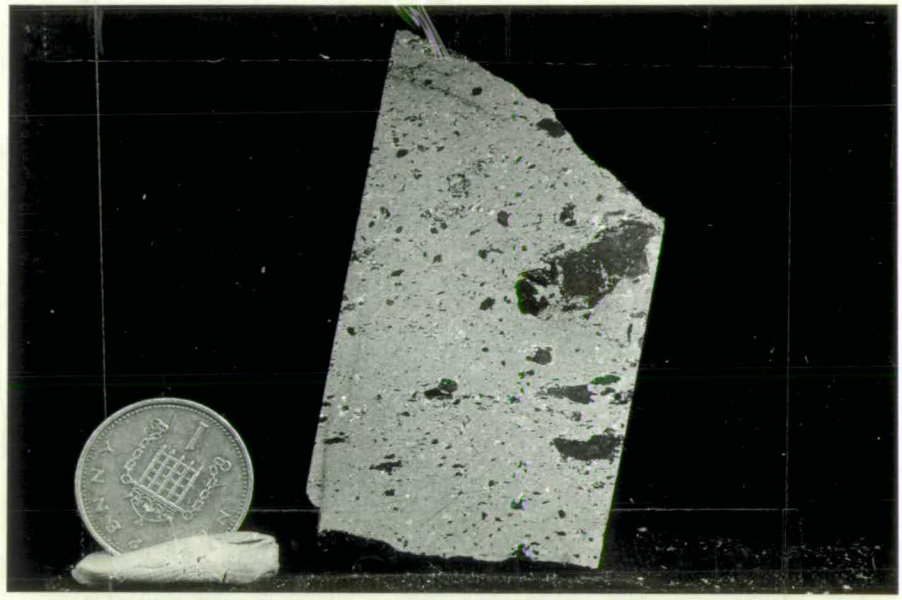

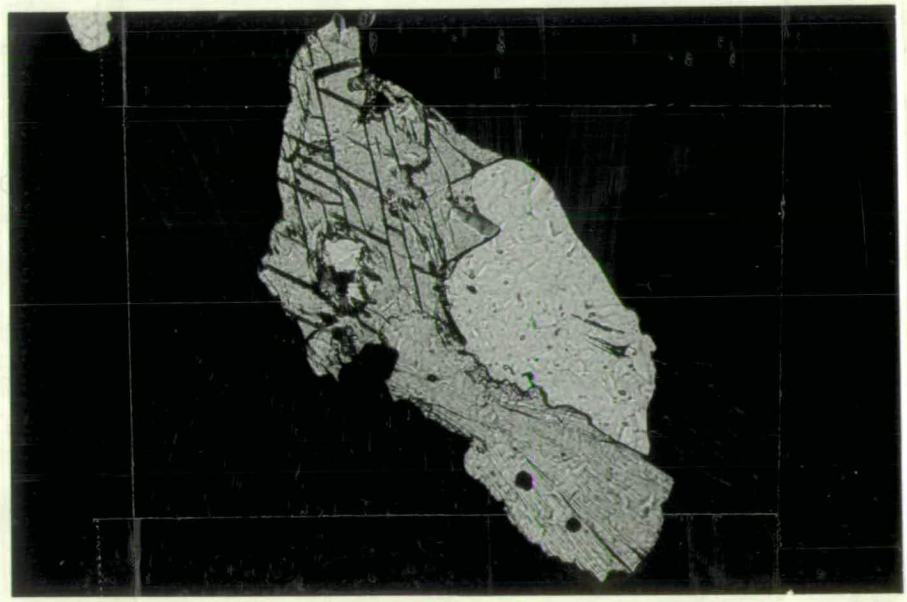

Fig. 5.12 Photomicrograph of Olkar sulfides (sample 77/2/14.90). Blocky pentlandite (light grey) interstitial to pyrrhotite (dark grey), with minor chalcopyrite (c).
Reflected light; ppl; f.o.v. = 0.38 mm.

Fig. 5.13 Photomicrograph of Olkar sulfides (sample 77/2/14.90). Blocky and flame pentlandite (light grey) in pyrrhotite (grey).
Reflected light; ppl - oil immersion; f.o.v. = 0.12 mm.

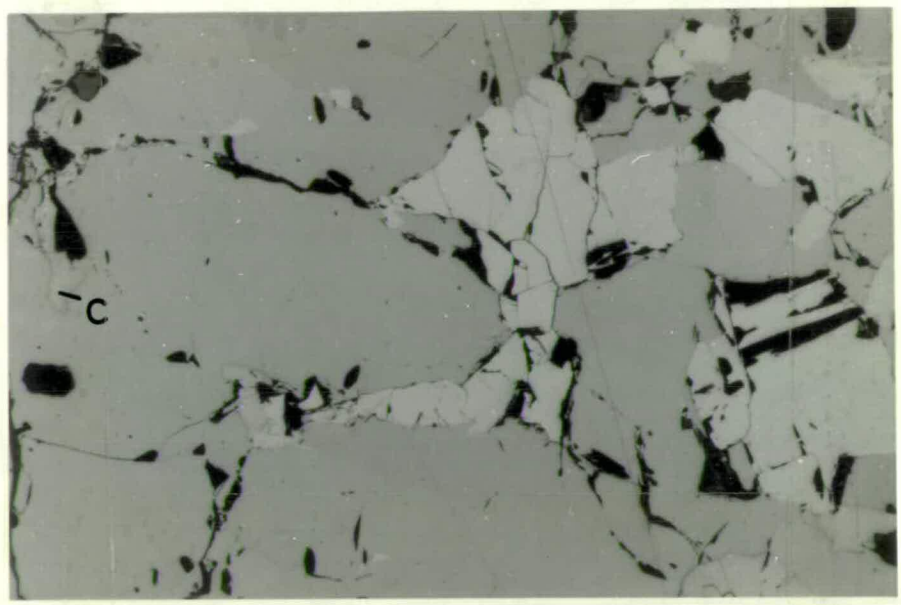
C

Fig. 5.14 Photomicrograph of Olkar sulfides (sample 77/3/8.65). Elongated pyrrhotite grains in Stringer ore.
Reflected light; crossed nicols (x Ni); f.o.v. = 2.40 mm.

Fig. 5.15 Photomicrograph of Olkar sulfides (sample 77/2a/4.85). Pyrite replacing pyrrhotite along grain boundaries. Occasional subhedral grains (e.g. bottom right), suggest a metamorphic rather than a supergene origin.
Reflected light; ppl; f.o.v. = 0.15 mm.

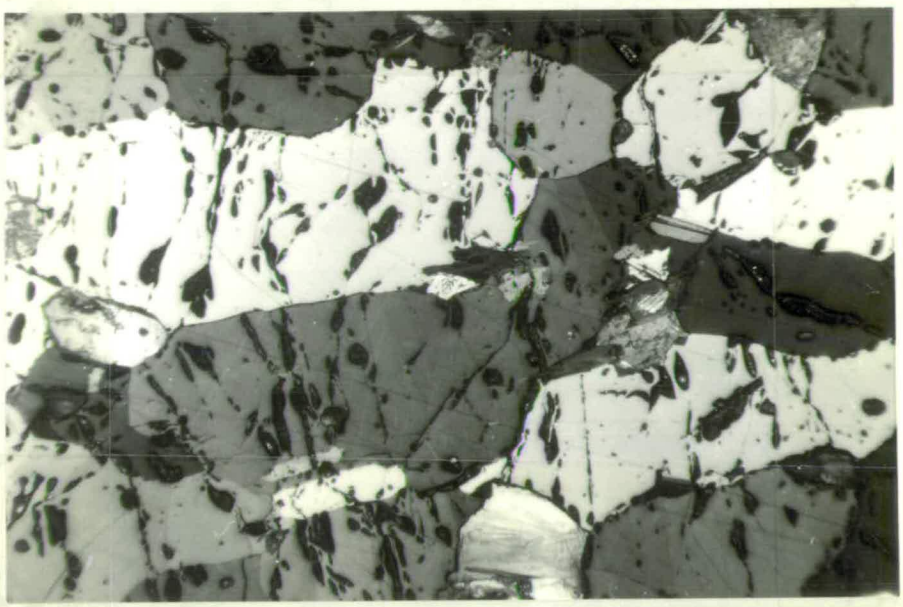

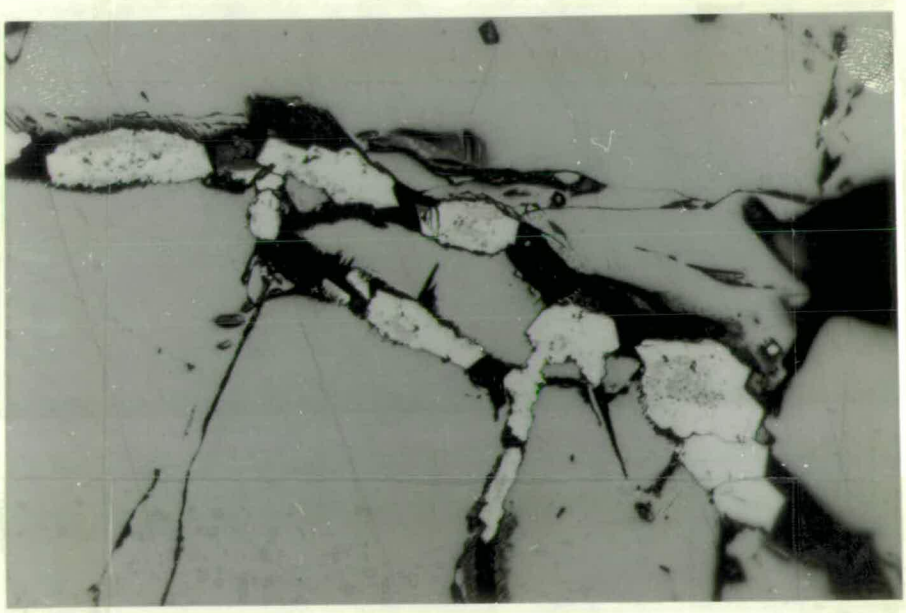

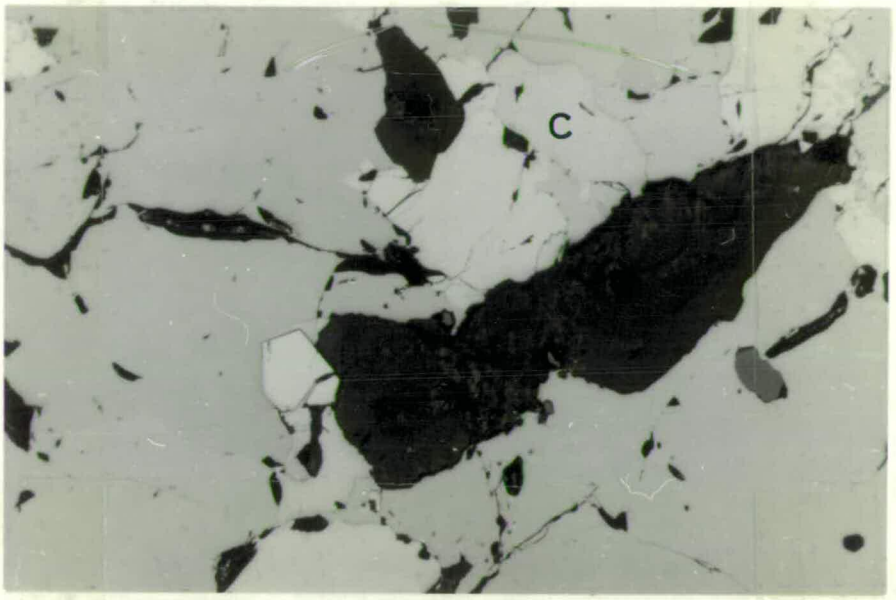
C

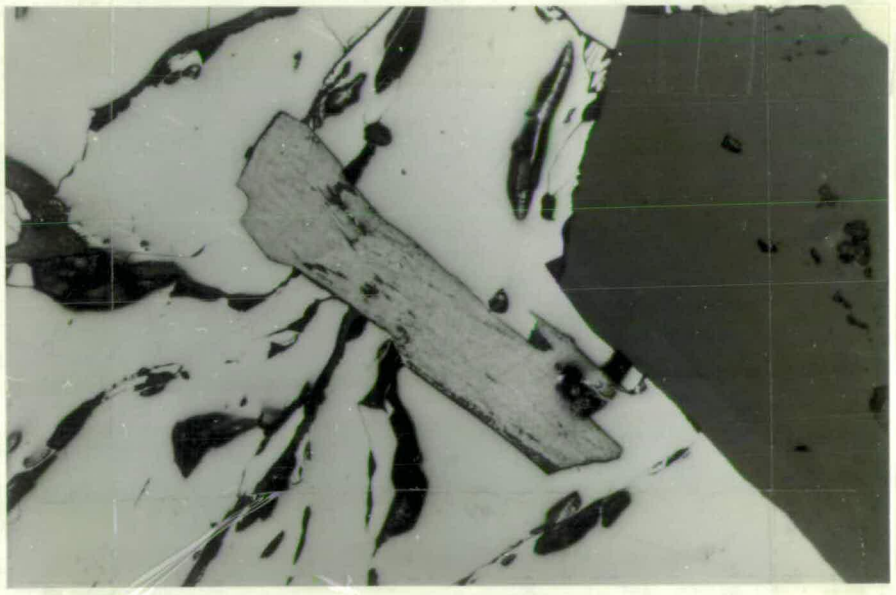

excavated material. Sulfide mineralisation in the dump, and rarely in the walls of the trench, appears to be hosted by a xenolithic metagabbro similar to that at Olkar. Detailed examination of the trench and limited adjacent exposure suggests that the metagabbro is surrounded by a large trondhjemitic mass. The possibility that the metagabbro has an elongated form dipping SE wards into the hill, parallel to the regional lineation, may be discounted by the lack of geophysical evidence. The Gardsjoen showing is therefore thought to be a xenolith, of limited but uncertain extent, and consisting of a mineralised xenolithic metagabbro.

The metagabbroic host rock is similar to that at Olkar and Vakkerlien except that a poikilitic texture, in which large plagioclase grains (<4.0 mm) surround and include zoned amphiboles, is dominant. Occasionally, less mafic varieties occur in which plagioclase may form up to 80% of the rock. This may be the result of assimilation of the gabbro by the enclosing trondhjemite.

Examination of the ore has been restricted to surface and dump samples only, and has revealed Matrix- and Disseminated-Breccia ores. The mineralogy is dominated by pyrrhotite (both hexagonal and monoclinic, and forming approximately 90% of the sulfide phases present), with lesser and variable amounts of pentlandite and chalcopyrite. Textures are similar to those described from Vakkerlien and Olkar. Supergene alteration has resulted in the extensive replacement of pyrrhotite by marcasite, and pentlandite by violarite. Traces of probably secondary pyrite have also been recorded.

5.1.1.4 Skjaekerdalen - The Skjaekerdalen intrusive complex is situated in the northernmost part of the Trondelag region. The complex is intruded into the central parts of the Gula Group approximately 3 km north of Helgaadalen as shown on Map 2.

The intrusion may be described as a lenticular body, elongated in a NE-SW direction, with axial dimensions of 6 x 2 km. The complex has a central core of metagabbroic breccia surrounded by an aureole of unbrecciated metadiorite (Fig. 5.18). The sulfide mineralisation is restricted entirely to the metagabbroic breccia.

The breccia is a complex lithology in which, in general, more mafic fragments occur in a less mafic matrix. Foliated and randomly orientated fragments of country-rock schists have also been recorded. The intrusive rocks vary in composition from ultramafic, through mafic, to more leucocratic. Fig. 5.19 shows a typical exposure in which gabbroic fragments, themselves carrying fragments of ultramafic and schist, are enclosed in a matrix of diorite. Individual fragments may be up to 20 m in greatest dimension, and together usually occupy more than 50% of any one exposure. In many cases the exposure has a "jig-saw puzzle" appearance in which the fragments could be fitted back together as in Fig. 5.20. Fragments are, in general, angular with sharp contacts to the enclosing matrix. Occasional examples of rounded fragments with diffuse contacts suggests partial assimilation. Lieungh (1977) records one instance of an angular fragment with sharp boundaries impacting into a rounded fragment with less clearly defined outlines, the mafic minerals in which can be observed to "flow around" the indentation of the first fragment. Brecciation of partially consolidated material is suggested by this texture. No regular pattern of lithological distribution has been observed. The overall field relationships and large-scale textures suggest successive intrusion of progressively more evolved liquids, perhaps expelled from a fractionating magma chamber at depth.

The metagabbroic lithologies are dominated by amphibole and plagioclase, and vary in average grainsize from less than 0.5 mm to greater than 2.0 mm; the coarse varieties are, however, more common. Amphibole

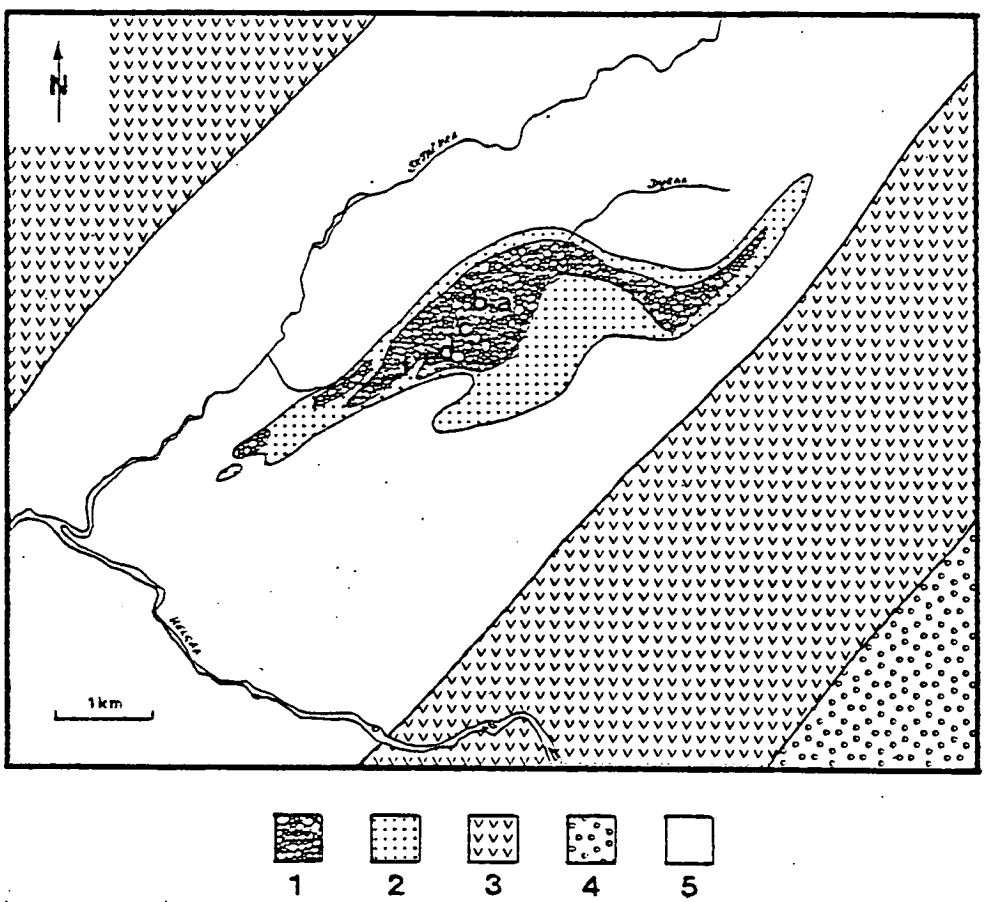

Fig. 5.18 simplified geological map of the area around the Skjaekerdalen intrusive complex (redrawn from Lieungh, 1977). 1 - metagabbro breccia; 2 - metadiorite; 3 - Storen and Fundsjo Groups; 4 - Sulamo Group; 5 - Gula schists. Main showings: a - Archbold; b - Homan; c - St. Olav; d - Anton Bachke; e - Hoved Gruva and Barbara Bachka; f - Slipern.

Fig. 5.19 A typical exposure of Skjaekerdalen metagabbroic breccia (between Archbold and Homan showings). Fragments of metagabbro, carrying fragments of ultramafic (left centre) and schist (upper left), in matrix of metadiorite.

Fig. 5.20 Skjaekerdalen "jig-saw puzzle" breccia (Slipern showing). Ultramafic brecciated by metagabbro.

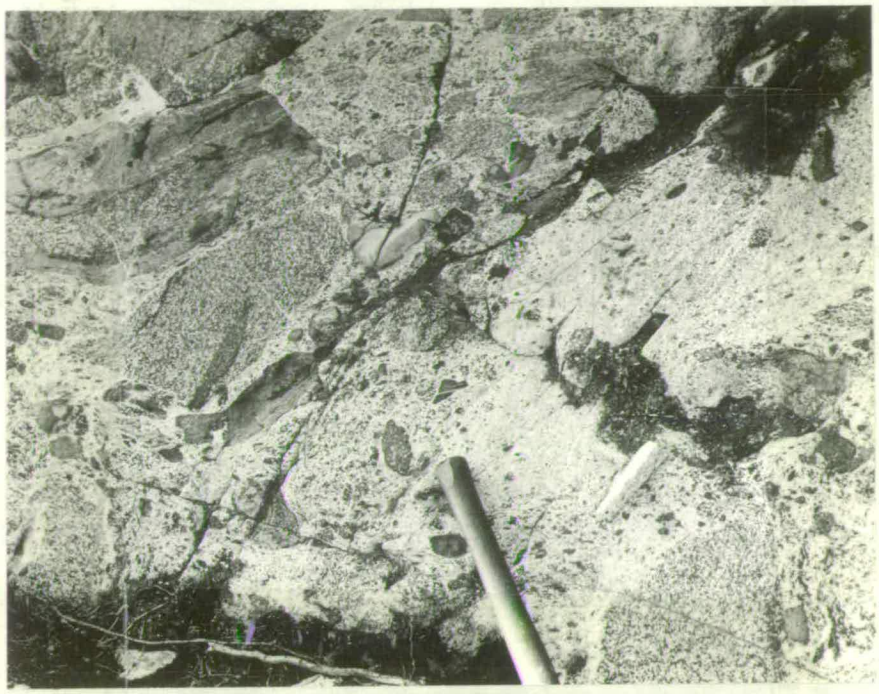

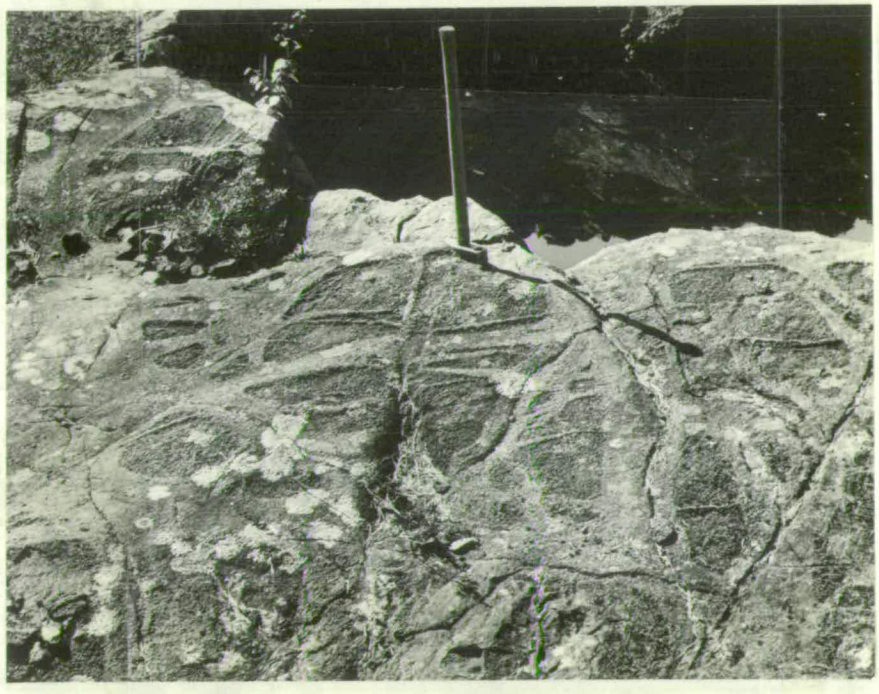

is similar, both in colour and in zoning, to that at Vakkerlien while plagioclase is commonly so intensely saussuritised that its optical properties are obscured. Accessory minerals are sericite, quartz, biotite, chlorite, apatite, epidote, ilmenite, sphene, rutile, and sulfides. The more ultramafic varieties are characterised by a decrease in plagioclase relative to amphibole, while the more leucocratic, dioritic and quartz-dioritic varieties are marked by a decrease in mafic components to less than 30%, of which biotite may form up to a half. In these lithologies, where plagioclase is unsaussuritised, it is optically zoned and commonly untwinned. Quartz occurs interstitially to plagioclase and amphibole or biotite, and may form up to 20% of the total rock components in extreme cases.

The metadiorite of the surrounding unbrecciated aureole is similar to these lithologies except that it tends to be finer grained and more intensely foliated.

Very occasionally primary silicate minerals have been observed in the metagabbros. Olivine, orthopyroxene, and clinopyroxene have all been recorded. In the least altered samples, they occur as glomeroporphyritic aggregates, with individual grains generally less than 2.0 mm, but rarely up to 4.0 mm in diameter. The aggregates are interstitial to plagioclase laths up to 5.0 mm in length as shown in Fig. 5.21. Incipient alteration of pyroxene to amphibole is always present, while olivine is often replaced by talc, carbonate, serpentine, and magnetite or pyrrhotite. Olivine has also been observed as inclusions within orthopyroxene.

At all times, where olivine is in contact with plagioclase the boundary is marked by a kelyphitic reaction rim. An example of such a texture is shown in Figs. 5.22, 5.23, and 5.24. In general, olivine is surrounded by successive zones of orthopyroxene, amphibole, and an

Fig. 5.21 Photomicrograph of Skjaekerdalen metagabbro (sample 77.291a). Glomeroporphyritic aggregate of olivine (upper centre) and two pyroxenes, in plagioclase.
Transmitted light; X Ni; f.o.v. = 2.40 mm.

Fig. 5.22 Photomicrograph of Skjaekerdalen metagabbro (sample 77.300a). Kelyphitic reaction rim between olivine and plagioclase (clinopyroxene also present, e.g. bottom right).
Transmitted light; ppl; f.o.v. = 2.40 mm.

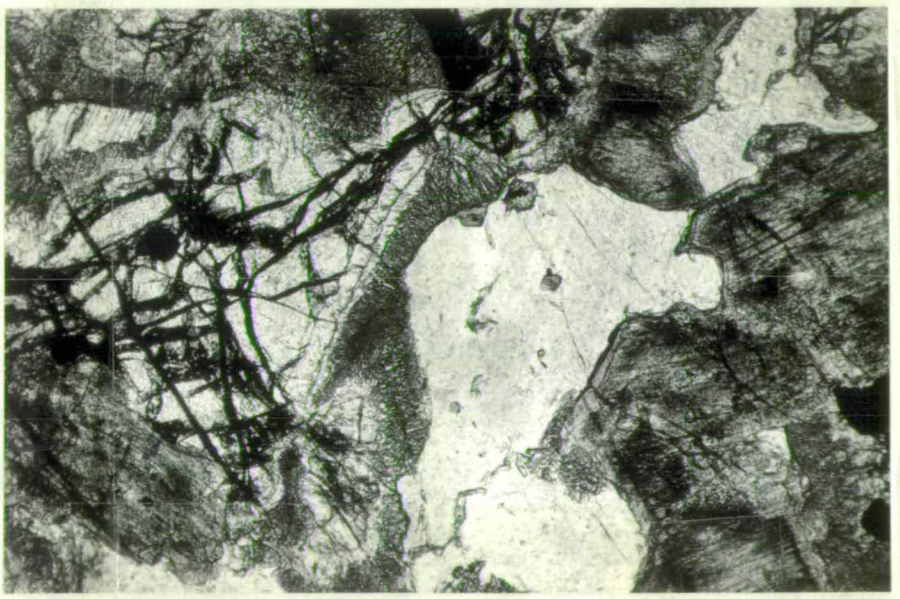

Fig. 5.23 Photomicrograph of Skjaekerdalen metagabbro (sample 77.300a). Close-up of kelyphitic reaction rim shown in Fig. 5.22. From left: olivine; orthopyroxene; amphibole; amphibole-aluminous spinel symplectite; plagioclase.
Transmitted light; ppl; f.o.v. = 0.60 mm.

Fig. 5.24 Photomicrograph of Skjaekerdalen metagabbro (sample 77.300a). Close-up of amphibole (grey) aluminous spinel (light grey) symplectite shown in Figs. 5.22 and 5.23.
Reflected light; ppl; f.o.v. = 0.12 mm.

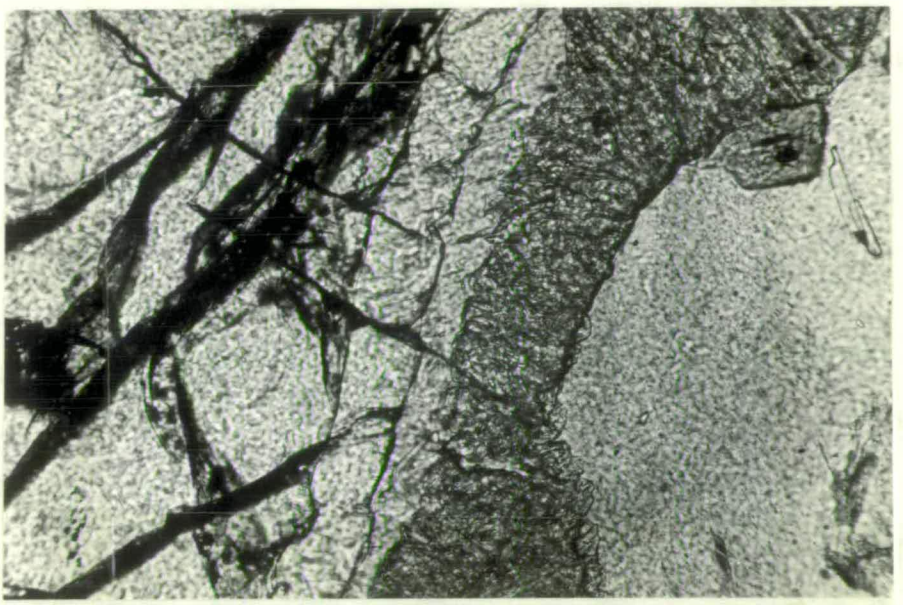

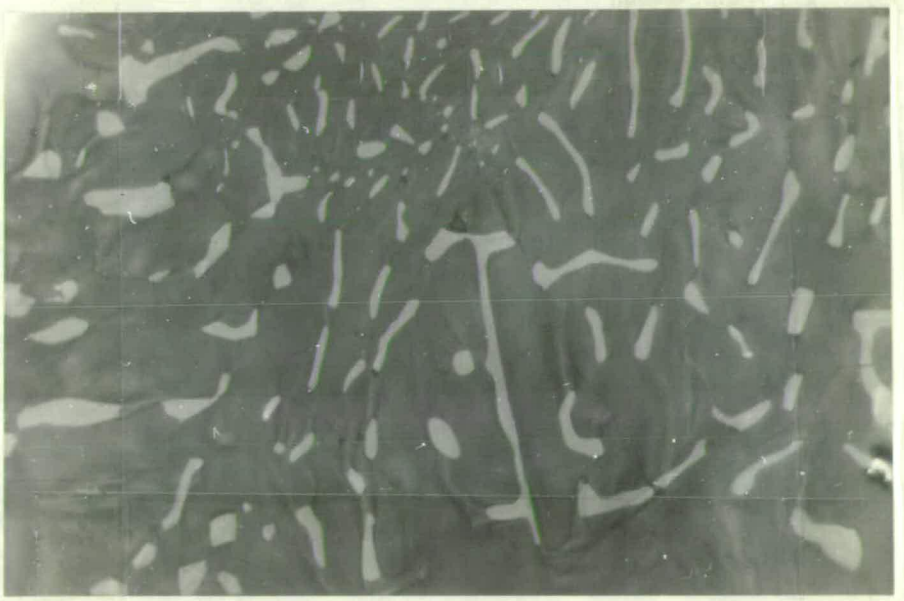

amphibole-aluminous spinel-symplectite. Such textures are probably directly comparable with other olivine-plagioclase bearing rocks of the Norwegian Caledonides (Griffin and Heier, 1973; Gardner and Robins, 1974), in which olivine-plagioclase reaction rims are marked by successive orthopyroxene, clinopyroxene, and clinopyroxene-spinel symplectites. In this instance, however, the clinopyroxene has probably been replaced by amphibole.

According to Herzberg (1976), coronas such as these form as a result of the incompatibility of olivine and plagioclase on crossing the plagioclase-lherzolite to spinel-lherzolite mineral-facies boundary. Experimental data (Herzberg, 1976) indicate that this facies boundary is essentially temperature-independent at low temperatures, and is mildly temperature-dependent at high temperatures. The development of coronas, as described above, by isobaric cooling of olivine-plagioclase bearing igneous assemblages across the facies boundary at high temperatures is restricted to a pressure interval from 8.5 kb to 10 kb. At lower temperatures the reaction proceeds at about 8.5 kb in the pure CaO-MgO-Al_2O_3-SiO_2 system. This implies that the Skjaekerdalen complex was intruded, either during, or prior to a metamorphic event which attained pressures of the order of 8.5 kb. The presence of iron in the system affects the slope of the boundary to greater dT/dP values, thereby allowing isobaric cooling through the facies boundary to lower pressures (Green and Hibberson, 1970), while the presence of sodium transposes the boundary to a divariant zone at higher pressure (Emsli, 1971; Herzberg, 1976).

In more ultramafic lithologies orthopyroxene and clinopyroxene have been recorded and occur as relict cores to amphibole grains. It has not been possible to decide how much, if any, of the amphibole and biotite of the more leucocratic intrusives is of primary magmatic origin.

Sulfide mineralisation at Skjaekerdalen occurs throughout the central intrusive breccia, and is hosted by all lithological types. The locations of the main showings are illustrated in Fig. 5.18. It is noteworthy that most sampling was carried out from dumps and it was therefore difficult to distinguish fragments and matrix. However, there are notable differences in ore textures between the different host lithologies.

Where the host rock is ultramafic, the sulfides have well defined relict interstitial textures, as illustrated in Fig. 5.25. Where metagabbro hosts the ore, sulfides are in part interstitial (Fig. 5.26) but occasionally they take on a blocky fragmental appearance as shown in Fig. 5.27. Such sulfide fragments are commonly several centimetres in maximum dimension. In more leucocratic lithologies, the ores have a strongly fragmental appearance (Fig. 5.28). The sulfide mineralisation hosted by ultramafic lithologies is classified as Interstitial ore, while that occurring in the most leucocratic lithologies is usually Fragmental ore. Mineralisation associated with metagabbroic hosts is commonly of both Interstitial and Fragmental types.

From the limited available information on the sulfide workings (A.S. Bachke, 1880; Rosenlund, 1915; and Lovas, 1970), it appears that most of the ore extracted was of the Interstitial type, in ultramafic and metagabbroic hosts. However, mention is made of sulfide lenses, up to 4 m in length and 20 cm in thickness, occurring in gabbroic and more leucocratic host rocks. Such features presumably represent large-scale examples of the Fragmental ore-type.

The sulfide mineralogy is dominated by pyrrhotite, pentlandite, and chalcopyrite. Pyrrhotite to pentlandite ratios vary from 2:1 to 100:1, and average approximately 20:1. Pyrrhotite to chalcopyrite ratios vary even more widely from 100:1 to 1:8 in extreme cases.

Fig. 5.25 Photomicrograph of Skjaekerdalen Interstitial ore, ultramafic host (sample 77.323). Sulfides (black) are interstitial to amphibole pseudomorphs after pyroxene (and olivine ?). Transmitted light; ppl; f.o.v. = 1.92 mm.

Fig. 5.26 Photomicrograph of Skjaekerdalen Interstitial ore - metagabbroic host (sample 78.67). Sulfides (light) interstitial to silicate (olivine and plagioclase - dark). Sulfide minerals: pyrrhotite (p); pentlandite (pn); and chalcopyrite (c). Reflected light; ppl; f.o.v. = 2.40 mm.

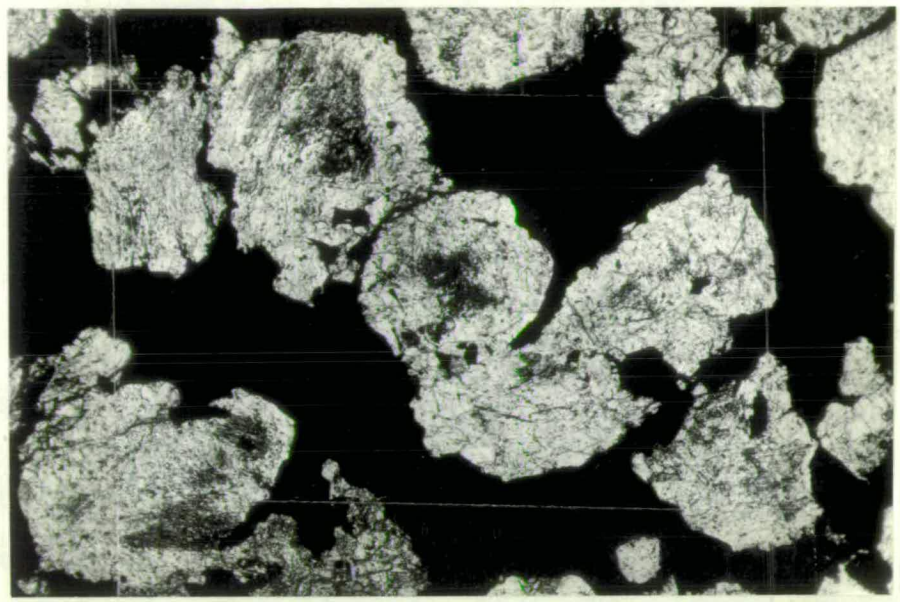

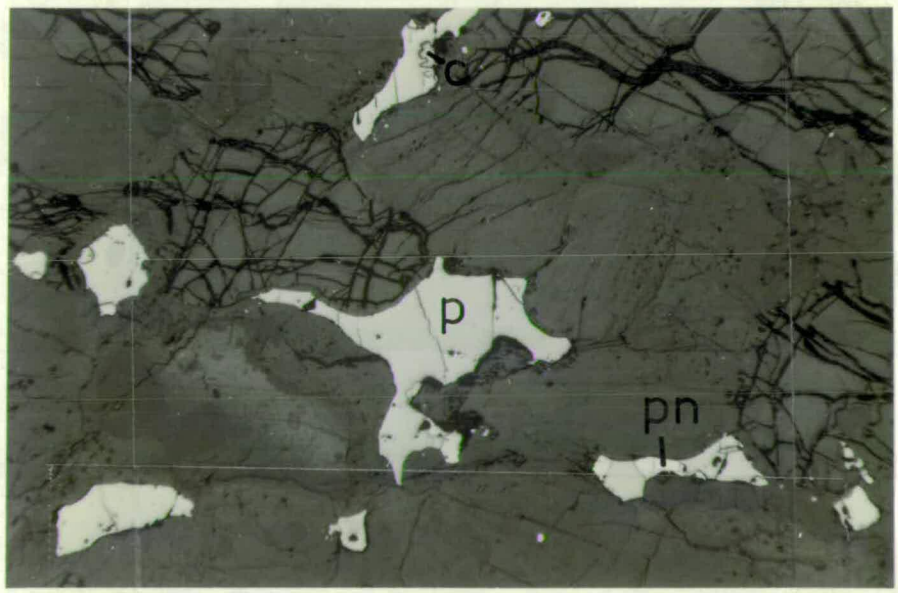
c
p
pn

Fig. 5.27 A ground surface of Skjaekerdalen Interstitial/ Fragmental ore, metagabbroic host (sample 77.307). Interstitial sulfides (light grey) occurring together with sulfide fragments (top).

Fig. 5.28 A ground surface of Skjaekerdalen Fragmental ore, metadiorite host (sample 78.77). Sulfides occur as angular fragments (top - outlined) in silicates.

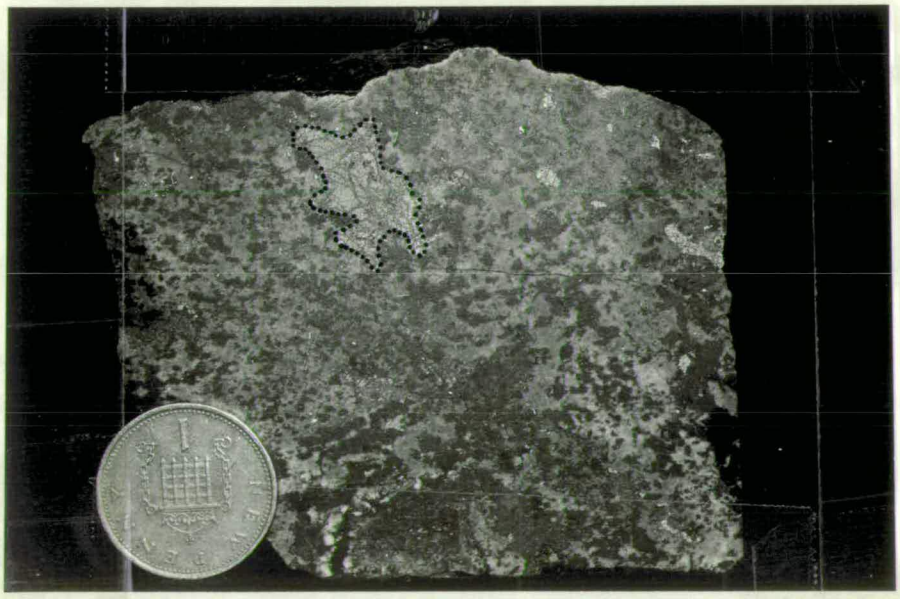

Grainsize is controlled by the ore texture. In brecciated fragments individual pyrrhotite grains may exceed 5 mm in diameter, while in more interstitial ores grainsize is smaller. Both monoclinic and hexagonal pyrrhotite phases are present. Pentlandite occurs as blocky grains and blebs both interstitial to, and within pyrrhotite grains. Grainsize is controlled by ore texture, such that blocky grains in excess of 1.0 mm across occur in coarse sulfide fragments. Exsolution flames of pentlandite in pyrrhotite occur rarely. Chalcopyrite occurs as blebs and broad lamellae marginal to and within pyrrhotite grains. Isolated grains and interstitial patches of chalcopyrite may also occur. In rare instances chalcopyrite may occur with bornite in very small (<0.1 mm) intergrowths. Many samples show supergene replacement of pyrrhotite by marcasite, and of pentlandite by violarite.

5.1.1.5 Undal - The Undal metagabbroic complex is located on the eastern side of Orkladalen, approximately 7 km north of the village of Innset (Map 2). The terrain is heavily forested and the intrusion is only poorly exposed in one NW-SE running stream section of about 5 km, and on a single discontinuous railway cutting of about ½ km which dissects the complex in an E-W direction. No contact relations with the surrounding country-rock schists have been observed, and the poor exposure obscures any internal relationships between different intrusive lithologies. The complex is not associated with any known sulfide mineralisation.

From the limited observations possible the Undal metagabbro is similar lithologically to the Skjaekerdalen complex. However, the following differences have been noted:

1. Sulfide mineralisation is lacking.
2. While a number of exposures reveal ultramafic nodules included in the metagabbroic and dioritic lithologies,

the brecciated nature of the Skjaekerdalen complex is not matched at Undal.

3. Samples of metagabbro from one locality display primary silicate mineralogy and textures identical to those at Skjaekerdalen, with the exception that when olivine and plagioclase are adjacent, the contact is not marked by a kelyphitic reaction rim (Fig. 5.29). The inference is that the Undal metagabbro has not been subjected to such high pressures as the Skjaekerdalen complex.

An ultramafic inclusion in the metagabbro has been found to contain relict olivine, clinopyroxene, and orthopyroxene.

Mesoscopic sulfide mineralisation is absent, but very rare, minute intergrowths of chalcopyrite, bornite, chalcocite, and possibly heazlewoodite have been recorded.

5.1.1.6 Haukfjellet - The Haukfjellet metagabbro lies in mountainous terrain 20 km north of Kvikne (Map 2). The intrusion is barren of sulfide mineralisation.

The metagabbro is similar in mineralogy and texture to those described above, except that a larger grainsize, with amphiboles up to 5 mm in length, is common. Close to the contacts of the intrusion, amphibole may take on a preferred orientation giving rise to a distinct foliation. The matrix is usually finer grained and granular, and appears to be overgrown in part by the porphyroblastic amphiboles. Ultramafic varieties are characterised by large (up to 1 cm) hornblende porphyroblasts in a matrix of chlorite and biotite, occasionally with minor plagioclase. Alternatively, well foliated tremolite-chlorite rocks have been recorded, especially close to the margins of the body. More leucocratic types have not been observed. The spatial distribution of the various lithologies is irregular.

Fig. 5.29 Photomicrograph of Undal metagabbro (sample 77.94). An equilibrium contact between olivine and plagioclase (no kelyphitic reaction rims as at Skjaekerdalen).
Transmitted light; ppl; f.o.v. = 1.50 mm.

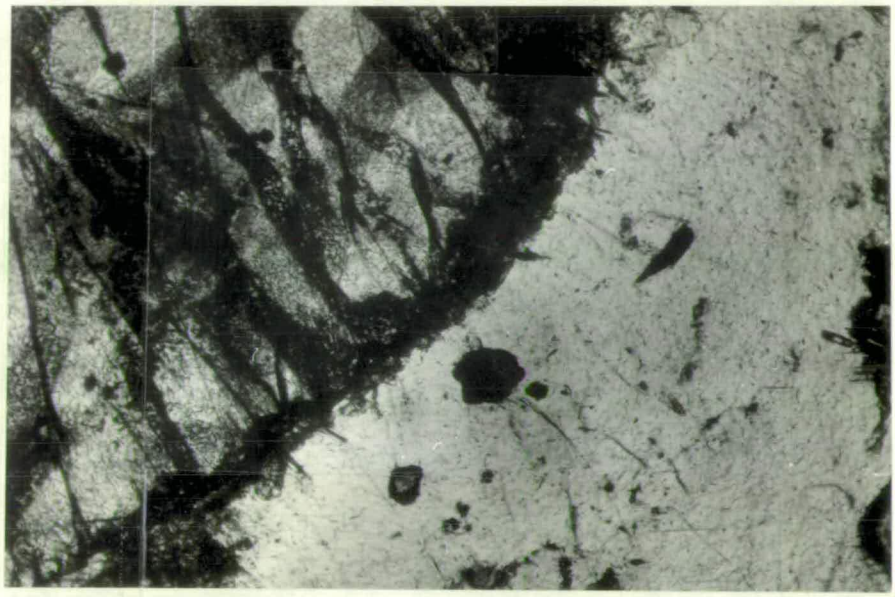

5.1.2 The ultramafics

5.1.2.1 Kaltberget - The Kaltberget ultramafic intrusion lies in a small hollow on the eastern slopes of Orkladalen, about 5½ km SE of Kvikne, as shown on Map 2. Surface exposure is poor, but limited details of the extent and form of the body can be obtained from this, and from drill core obtained by A/S Sulfidmalm. Fig. 5.30 is a simplified map of the area showing the localities of the drill holes discussed below.

The intrusion takes the form of two discrete ultramafic bodies, a Main Body, and a smaller Satellite Body. The Main Body is tabular and may be up to 70 m thick. It extends along strike for at least 500 m, and dips at approximately 30° towards the ESE within the foliation of the country-rock schist. Figs. 5.30 and 5.31 show the relationship between the Main Body and the Satellite Body. The Satellite Body lies above, and to the east of the Main Body; it has a lateral extent of less than 50 m and is approximately 10 m thick. As shown in Fig. 5.31, it pinches out rapidly down-dip.

Petrologically the ultramafics are dominated by a poikilitic, slightly pleochroic amphibole, with the optical properties of actinolite. The amphibole frequently contains well rounded inclusions (0.1 to 0.5 mm across) comprising a felted mass of talc, chlorite and serpentine (Fig. 5.32). In one sample relict olivine was recorded in the cores of such inclusions indicating the original mineralogy (Fig. 5.33). These pseudomorphs are themselves commonly replaced by an actinolitic amphibole which is distinguishable from the surrounding amphibole only by being slightly out of optical continuity (Fig. 5.34). More schistose lithologies are common in which amphibole is subordinant to chlorite, talc, and carbonate. Highly saussuritised plagioclase occurs interstitially to amphibole in the borders of both the Satellite and Main

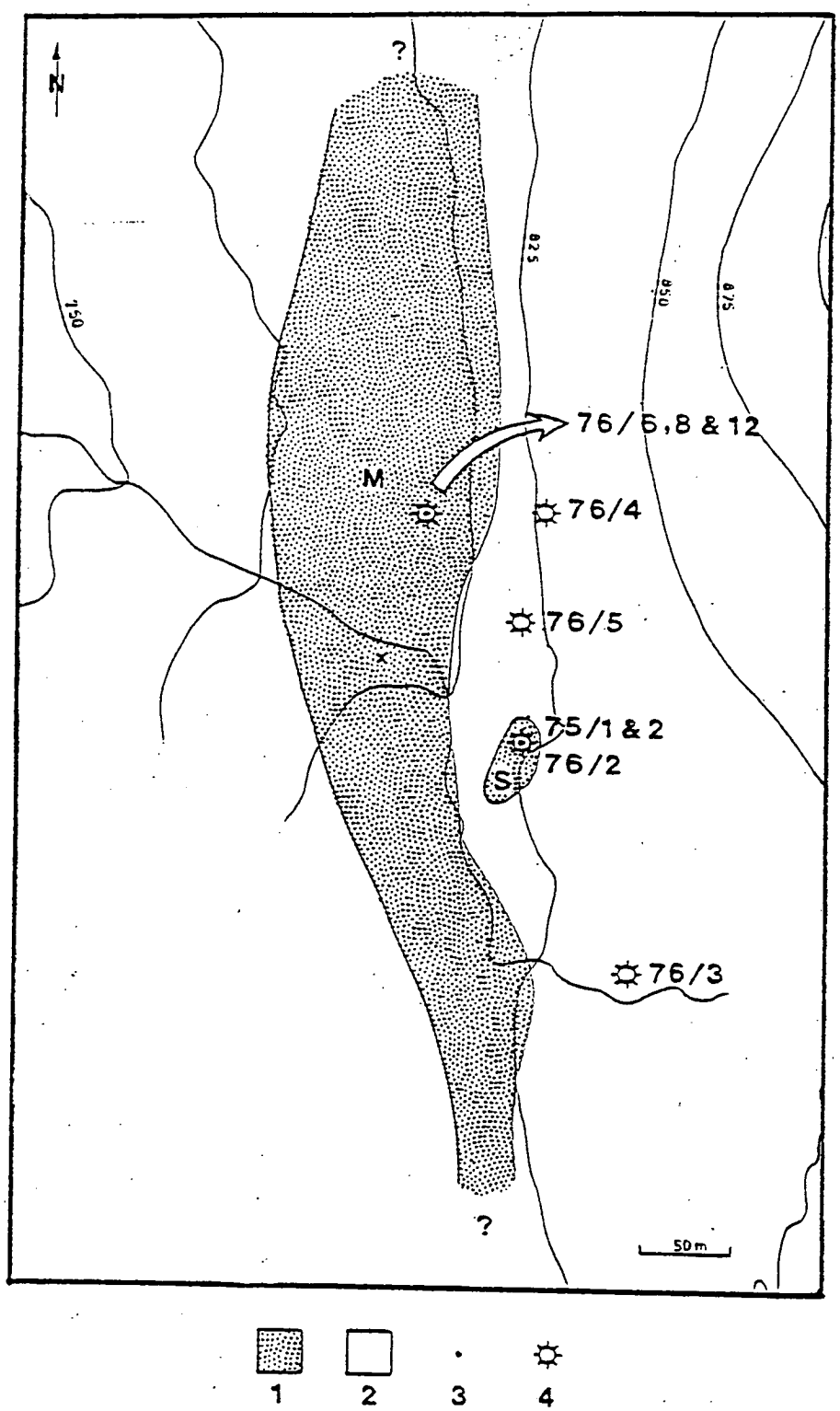

Fig. 5.30 Simplified geological map over the Kaltberget ultramafic bodies. 1 - ultramafic; 2 - schist; 3 - sulfide showing; 4 - drill hole; M - Main Body; S - Satellite Body; X - location of sample 76.245 (Finely Disseminated ore referred to in 6.4.2).

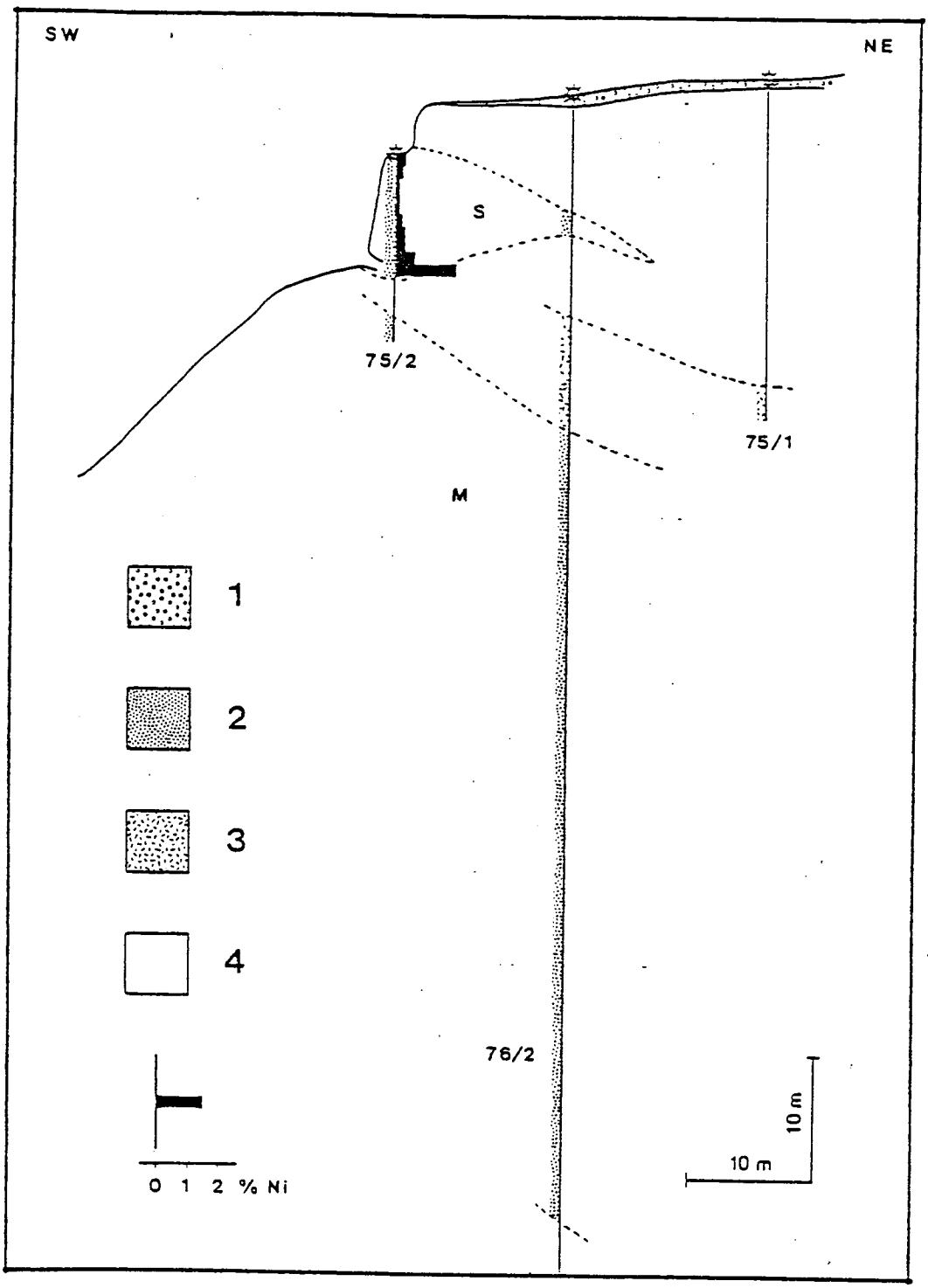

Fig. 5.31 A drill-hole profile showing the relationships between the Kaltberget Main (M) Body and Satellite (S) Body, and the position of sulfide mineralisation as indicated by Ni-assays. 1 - overburden; 2 - ultramafic; 3 - pegmatite; 4 - schist.

Fig. 5.32 A photomicrograph of Kaltberget ultramafic (sample 76/6/2.06). Serpentine, chlorite, and talc pseudomorphing olivine and enclosed in actinolite.
Transmitted light; ppl; f.o.v. = 2.40 mm.

Fig. 5.33 A photomicrograph of Kaltberget ultramafic (sample 77/4/45). Relict olivine (centre), partly replaced by serpentine, in actinolite and chlorite.
Transmitted light; ppl; f.o.v. = 2.40 mm.

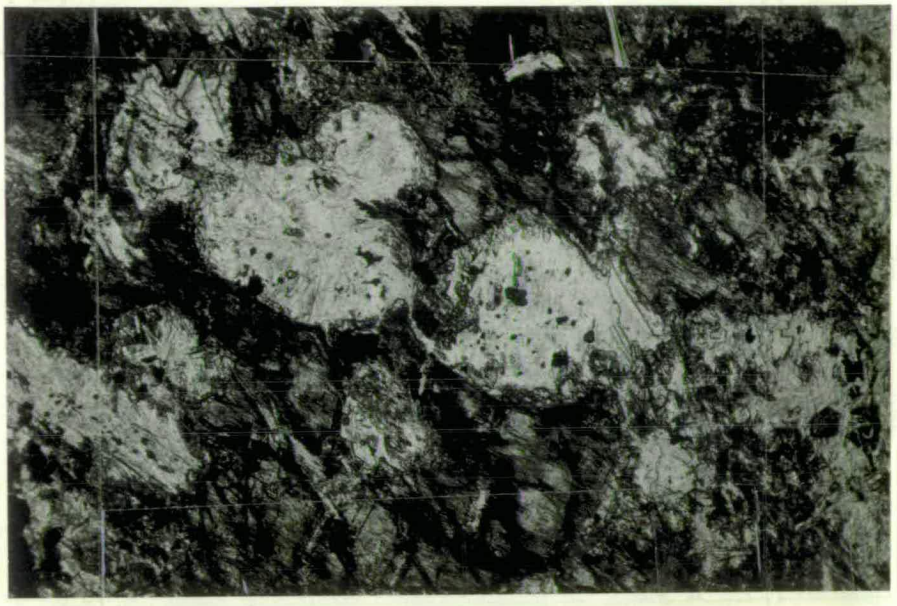

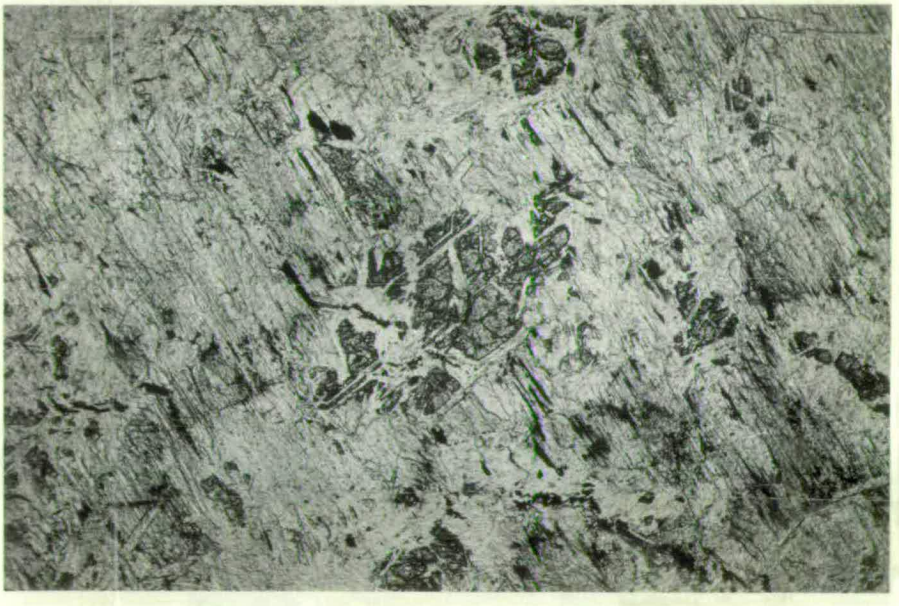

Fig. 5.34 Photomicrograph of Kaltberget ultramafic (sample 76/4/49). Actinolite pseudomorphs after olivine in actinolite. See text for explanation.

Transmitted light; X Ni; f.o.v. = 2.40 mm.

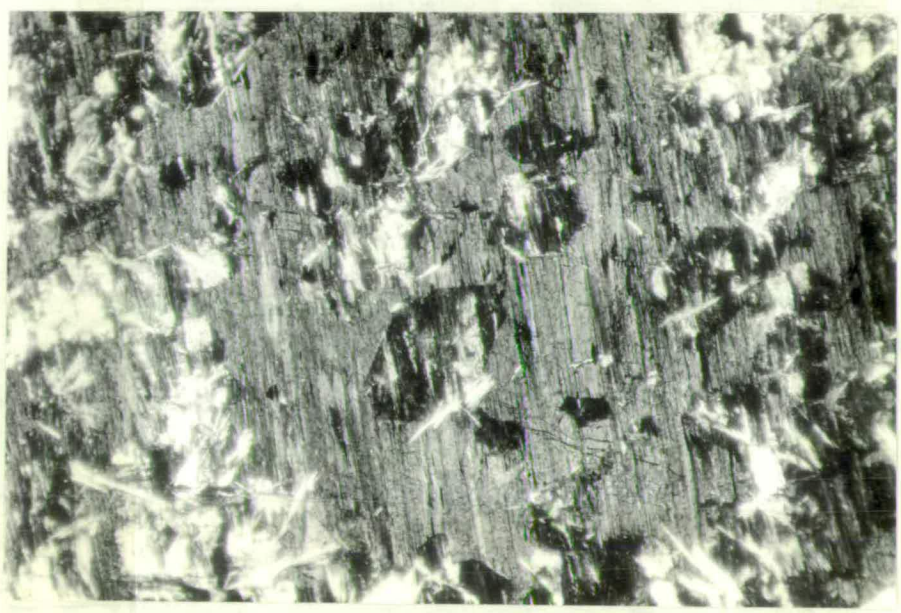

Bodies. Accessory minerals are sphene, apatite, chromite, magnetite, and sulfides. Fig. 5.35 shows the results of systematic modal analyses of drill hole 76-4 (Figs. 5.30 and 5.36). The felspathic border zones, and the differences between amphibole dominated and talc-chlorite-carbonate lithologies are quite evident. Occasionally, very altered, almost opaque, clay-rich patches, less than 3.0 mm across, occur in the felspathic border zones; by comparison with optically similar features in the margins of the Kletten ultramafic, which have been investigated by electron microprobe, these may represent highly altered K-felspar.

Nickel-copper sulfide mineralisation occurs in two sulfide showings as indicated in Fig. 5.30. The first showing is associated with the Satellite Body, where the mineralisation forms stringers up to 1 cm thick in both the upper and lower margins of the ultramafic (Fig. 5.31).

The second showing lies approximately 125 m NNE of the first and consists of a single, roughly elliptical exposure, not more than 5 m in major axis. Figs. 5.30 and 5.36 show that the mineralisation is located towards the centre of the Main Body. As drill holes 76/6 and 76/12 are 1.2 and 2.5 m respectively to the north of the section drawn, it is not possible to decide whether the mineralisation is continuous between these holes and that intersected in drill hole 76/8. Furthermore, it is not known whether the mineralisation is continuous along strike. Fine disseminations have been noted in the central parts of the ultramafic in drill holes 76/4 and 76/5, and in its upper margins in drill hole 76/4 (Fig. 5.30 and 5.36).

Usually the ore at Kaltberget is a complex network of aggregates of sulfide and silicate phases (Fig. 5.37). Sulfide-silicate relationships are most commonly controlled by the crystal form of the silicates

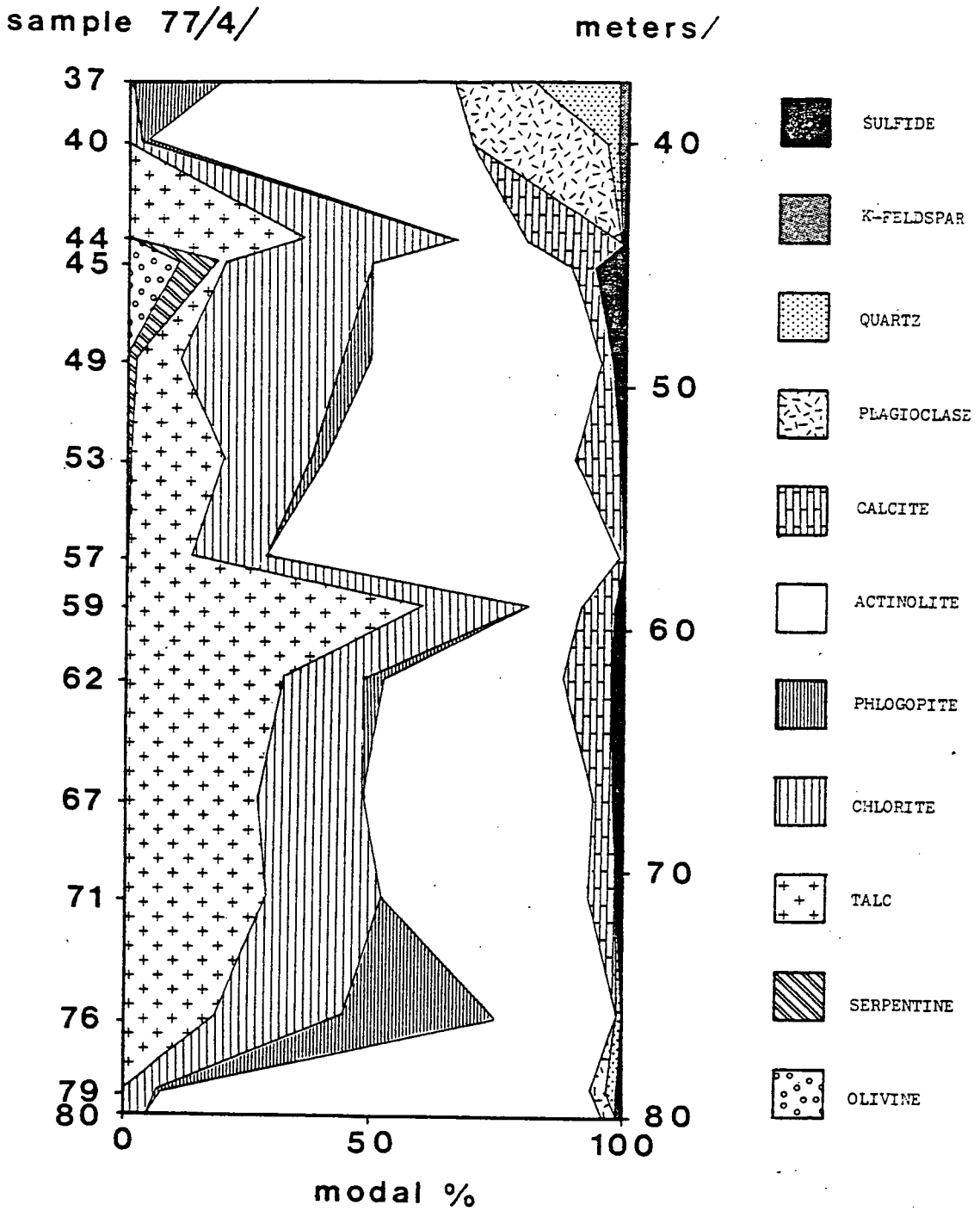

Fig. 5.35 Variation of mineralogy through the Kaltberget Main Body, drill-hole 76/4. All analyses based on at least 333 points.

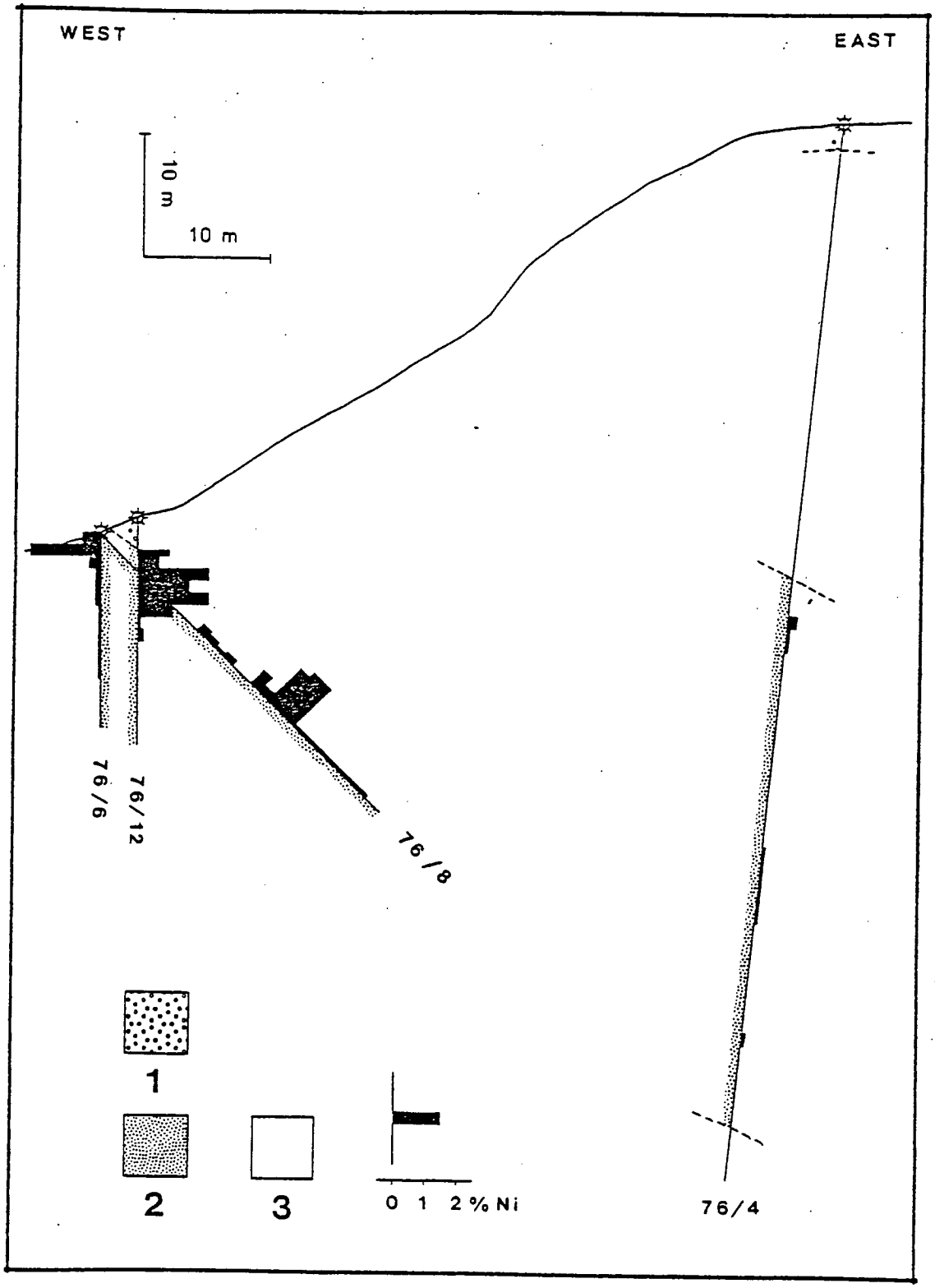

Fig. 5.36 A drill-hole profile through the Kaltberget Main Body (see Fig. 5.30 for location of holes) showing the position of sulfide mineralisation as indicated by Ni-assays. 1 - overburden; 2 - ultramafic; 3 - schist.

Fig. 5.37 A ground surface of typical Kaltberget ore (sample 76.294). Sulfides (grey) occur as a network consisting of aggregates of pyrrhotite, pentlandite, and chalcopyrite. Complex intergrowths of sulfides and silicates are usual (as shown in more detail in Fig. 5.38). According to the classification used in this thesis, these are Interstitial ores, although it is emphasised that, in this context, a metamorphic, rather than a relict igneous texture, is referred to.

Fig. 5.38 Photomicrograph of Kaltberget Interstitial ore (sample 77/6/2.06). Talc and chlorite (dark grey) interfingering with sulfide phases (pyrrhotite - grey; pentlandite - light grey; chalcopyrite - c).
Reflected light; ppl; f.o.v. = 2.40 mm.

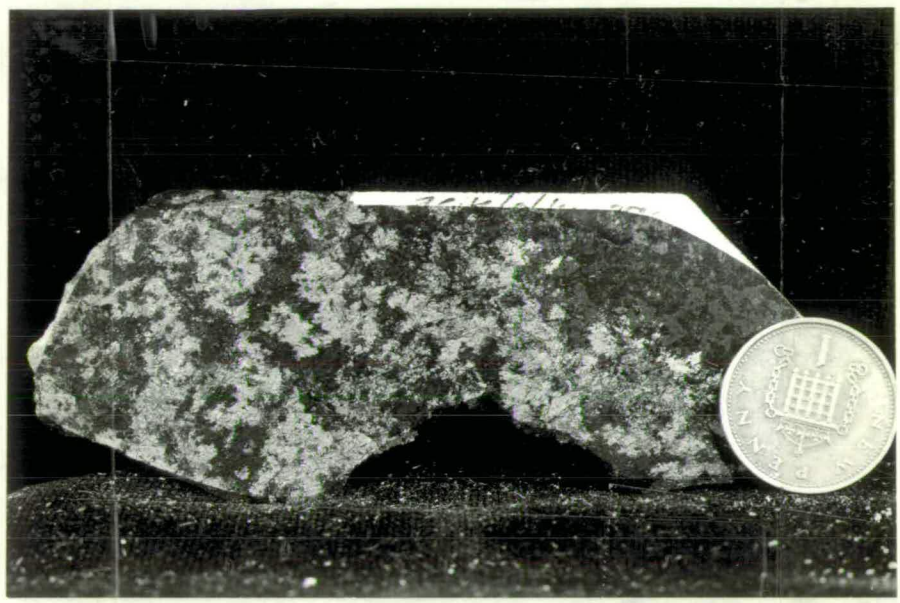

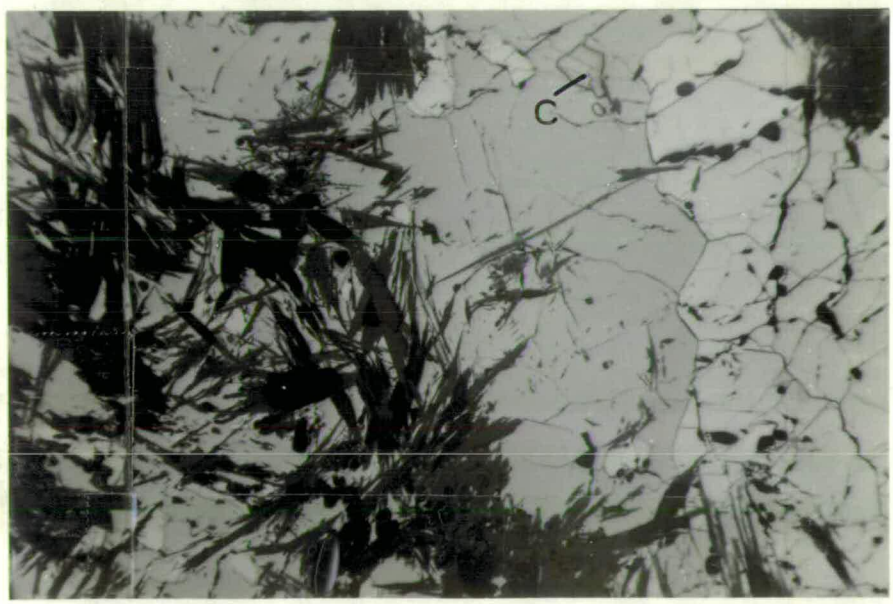
C

(Fig. 5.38). Occasionally, however, the sulfides form almost perfectly rounded globules (less than 10 mm in diameter) within the silicates (Fig. 5.39). The ores are therefore classified as Matrix-, Disseminated-, and Finely Disseminated-Interstitial ores, with rare Disseminated Globular varieties.

Pyrrhotite, pentlandite, and chalcopyrite are the only sulfide minerals present. Pyrrhotite to pentlandite ratios average approximately 7.5:1 and are reasonably consistent. Pyrrhotite to chalcopyrite ratios vary from about 20:1 to 5:1. Pyrrhotite grainsize may approach the size of sulfide blebs and commonly exceeds 5 mm (largest dimension). A finer grained, granular texture is, however, more usual. Only hexagonal pyrrhotite has been recorded in the Main Body and only the monoclinic phase in the Satellite Body. A possible explanation for this difference is suggested later in this chapter. Pentlandite occurs as blocky grains and patches up to 5 mm in extent, and is interstitial to pyrrhotite (Fig. 5.38 and 5.40). Exsolution flames of pentlandite in pyrrhotite are rare, but have been observed. Chalcopyrite occurs as rounded blebs, less than 1 mm in diameter, both interstitial to, and within, pyrrhotite and pentlandite. All three sulfide minerals may be intergrown with silicates at the margins of sulfide blebs, indeed occasionally, the ore as a whole is a complex intergrowth of sulfides and sheet silicates. Samples from dumps or close to the surface may display supergene alteration of pyrrhotite to marcasite, and pentlandite to violarite.

5.1.2.2 Kletten - The Kletten ultramafic body outcrops 10 km south of Kvikne on the eastern slopes of Orkladalen (Map 2). As shown in Fig. 5.41 it has an elongated outline trending approximately N-S, and is exposed to the south in the floor of the valley, and runs northwards up the valley side to the peak of Kletten mountain. The lower ground to the south is densely wooded and hence poorly exposed, but the higher

Fig. 5.39 Photomicrograph of Kaltberget Globular ore (sample 76.296). A globule of sulfide in an ultramafic host. Reflected light; ppl; f.o.v. = 16.0 mm.

Fig. 5.40 Photomicrograph of Kaltberget sulfides (sample 77/6/2.06). Pentlandite (light grey) and chalcopyrite (c) interstitial to pyrrhotite (grey). Silicates - dark grey. Reflected light; ppl; f.o.v. = 2.40 mm.

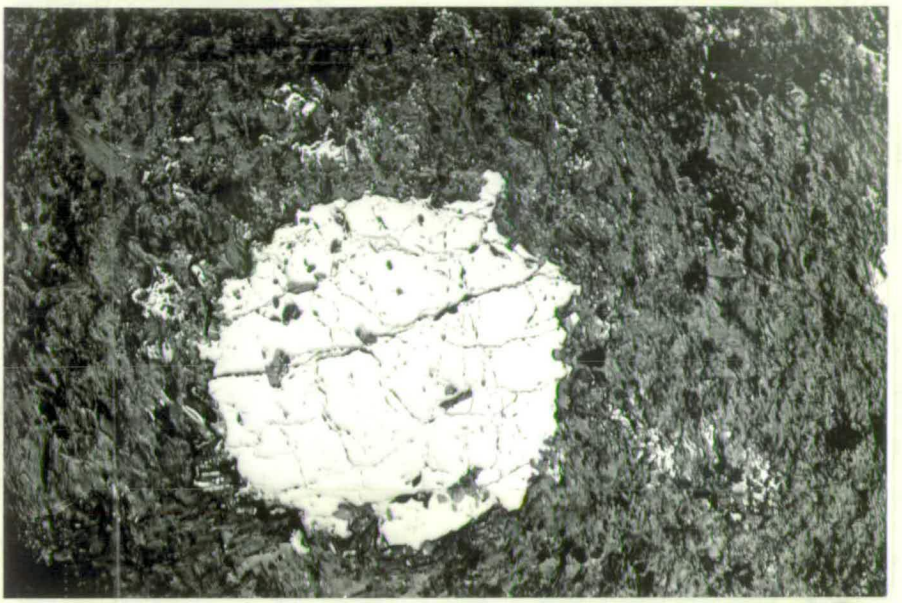

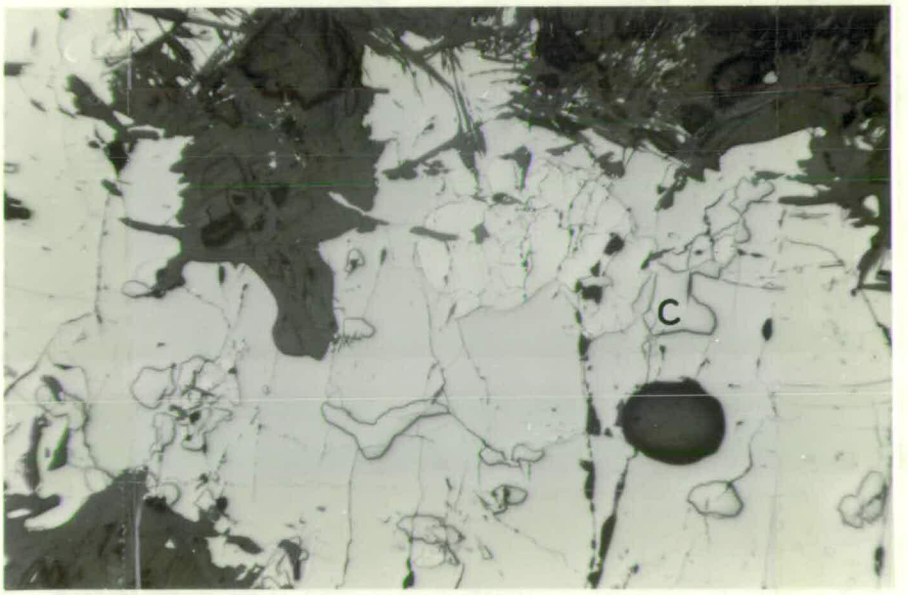
C

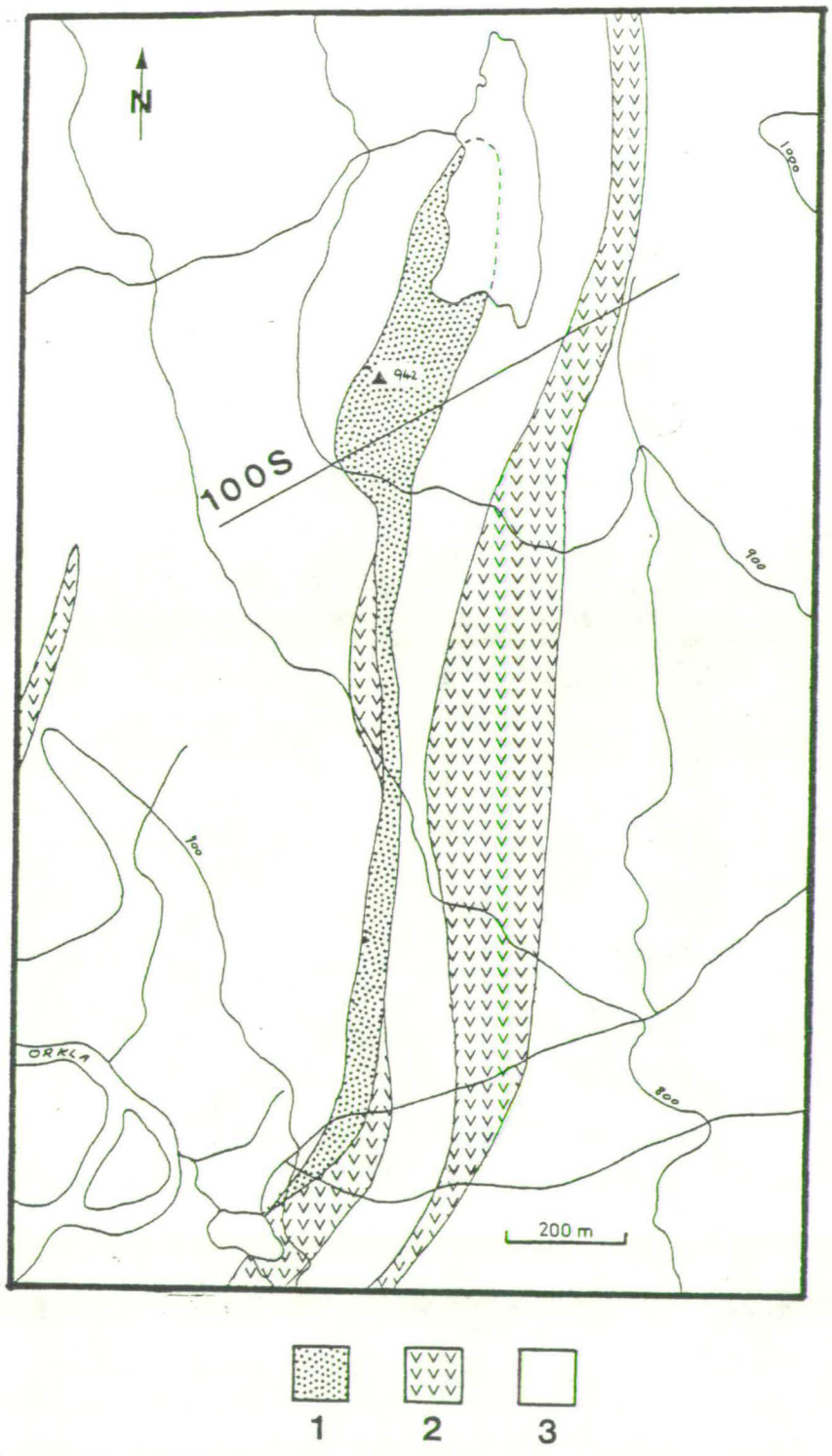

Fig. 5.41 Simplified geological map over the Kletten ultramafic body, showing position of profile 100S. 1 - ultramafic; 2 - amphibolite; 3 - schist.

ground to the north is open and exposure is moderately good.

The intrusion is similar in many respects to the Kaltberget ultramafic. It forms a concordant sheet dipping to the east within the country rock schists. Petrologically it is dominated by stout prisms of an amphibole which may be several centimetres in cross-section. Much of the amphibole has the optical properties of hornblende, but actinolite varieties occur, sometimes rimming the hornblende. In the least metamorphosed samples, from the core of the intrusion, olivine and, to a much lesser extent, clinopyroxene occur as rounded inclusions, generally less than 0.3 mm in diameter, within larger patches of orthopyroxene (less than 5 mm across). The orthopyroxene is surrounded and replaced by the amphibole as shown in Fig. 5.42. Occasionally, rounded olivines, up to 5 mm in diameter, occur between amphibole grains, and traces of interstitial plagioclase have been recorded.

Several stages of replacement have been determined. Olivine is pseudomorphed by serpentine, magnetite, talc, and carbonate, which is often subsequently replaced by tremolite. Actinolite or hornblende may subsequently replace the tremolite such that, in more metamorphosed samples, the texture is one in which large interlocking amphibole poikiloblasts contain small rounded patches in optical discontinuity with the host. This is a texture very similar to that commonly observed at Kaltberget (Fig. 5.34). The original igneous texture was probably one involving olivine and minor clinopyroxene phenocrysts, commonly enclosed in orthopyroxene, with interstitial plagioclase.

Phlogopite is common, replacing amphibole, especially in the margins of the intrusion. The margins also contain greater amounts of plagioclase, and quartz also occurs, commonly in graphic intergrowth with it (Fig. 5.43). As mentioned previously, highly altered, extremely

Fig. 5.42 Photomicrograph of Kletten ultramafic (sample 77.64). Relict orthopyroxene (centre and right) partly replaced by amphibole (left). Partly serpentinised rounded olivine grains are included in both orthopyroxene and amphibole.
Transmitted light; ppl; f.o.v. = 2.40 mm.

Fig. 5.43 Photomicrograph of Kletten felspathic border zone lithology (sample 76.336h). A graphic intergrowth of quartz and plagioclase, interstitial to amphibole.
Transmitted light; X Ni; f.o.v. = 0.60 mm.

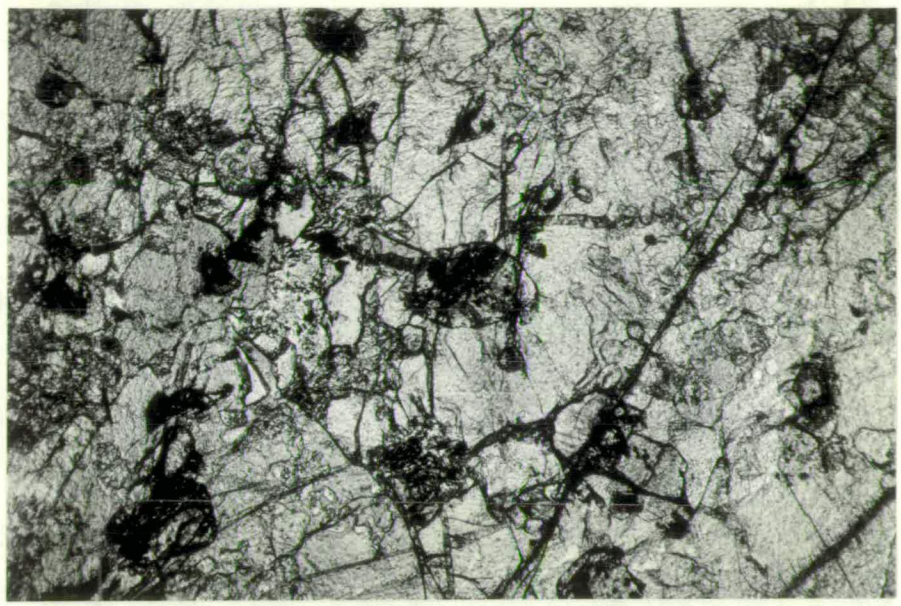

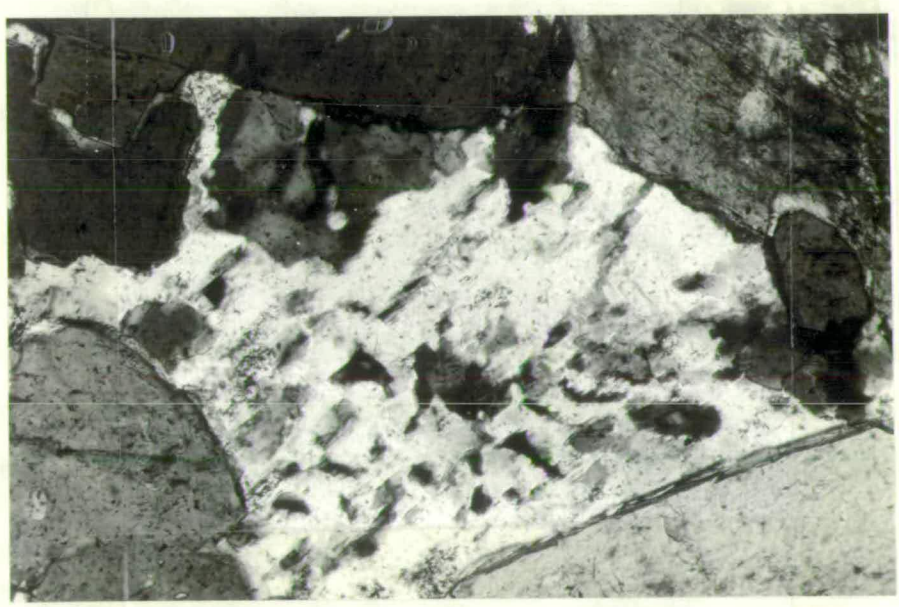

turbid, clay-rich patches occur, and may represent original K-felspar. Accessory minerals are ilmenite, apatite, and sulfides. Fig. 5.44 shows the results of systematic modal analyses across profile 100S (Fig. 5.41).

In the margins of the Kletten ultramafic body, pegmatitic quartzo-felspathic material appears to backvein from the schist into the intrusion. This suggests that the intrusion of the hot ultramafic mass has partially melted the country-rocks, and has itself been intruded by the melt portion. In the immediate vicinity of the contact, veins up to 20 cm across were observed, but thicknesses of less than 5 cm are more usual (Fig. 5.45). Although the contact between the schist and the ultramafic is nowhere exposed, it is estimated that the backveining extends into the ultramafic for a maximum horizontal distance of 50m. Within a horizontal distance of about 10 m of the contact, the enclosing country rocks are characterised by a peculiar tectonic breccia, which probably results from the gentle tectonic disruption of a contact migmatite (the source of the back-veining described above). In this lithology, randomly orientated fragments of quartzo-felspathic pegmatite (melt portion) "float" in a matrix of more micaceous material (residuals) as shown in Fig. 5.46.

Sulfide mineralisation at Kletten is Finely-Disseminated in grade and seems to be randomly distributed throughout the body. Texturally it occurs as large blebs, occasionally several centimetres across. The sulfides surround numerous irregular-shaped inclusions of secondary silicate minerals (less than 1 mm across) and may themselves be brecciated by carbonate veins (Fig. 5.47). It is therefore difficult to classify this mineralisation as globular or interstitial, and it will simply be referred to as Finely-Disseminated Kletten ore.

The sulfide minerals are pyrrhotite, pyrite, pentlandite, and

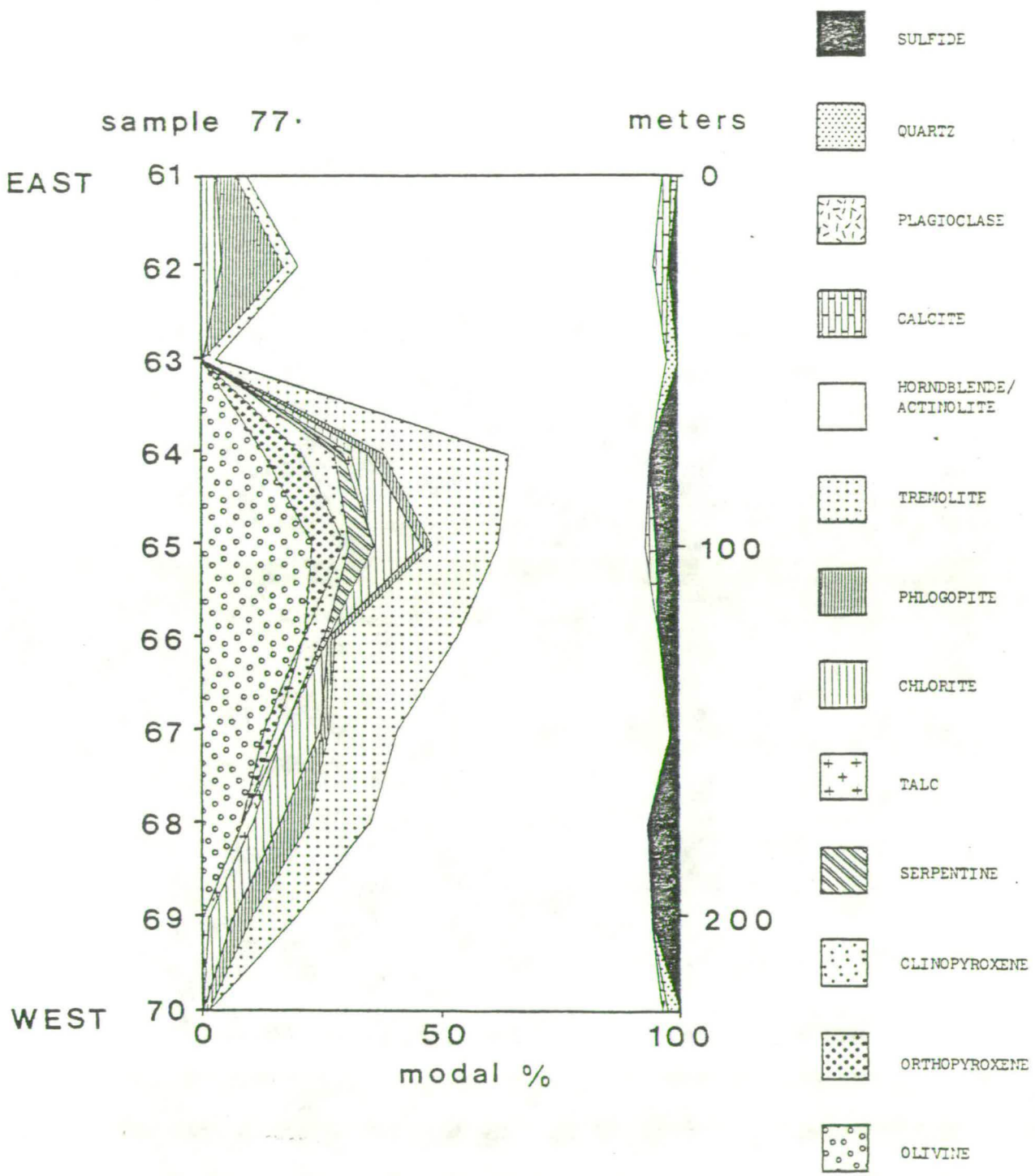

Fig. 5.44 Variation of mineralogy across the Kletten ultramafic body, profile 100S. All analyses based on at least 333 points.

Fig. 5.45 A quartzo-felspathic vein in the margins of the Kletten ultramafic body.
See text for discussion.

Fig. 5.46 Brecciated contact migmatite adjacent to the Kletten ultramafic body. Quartzo-felspathic fragments (melt portion) in a more micaceous matrix (residuals).
See text for discussion.

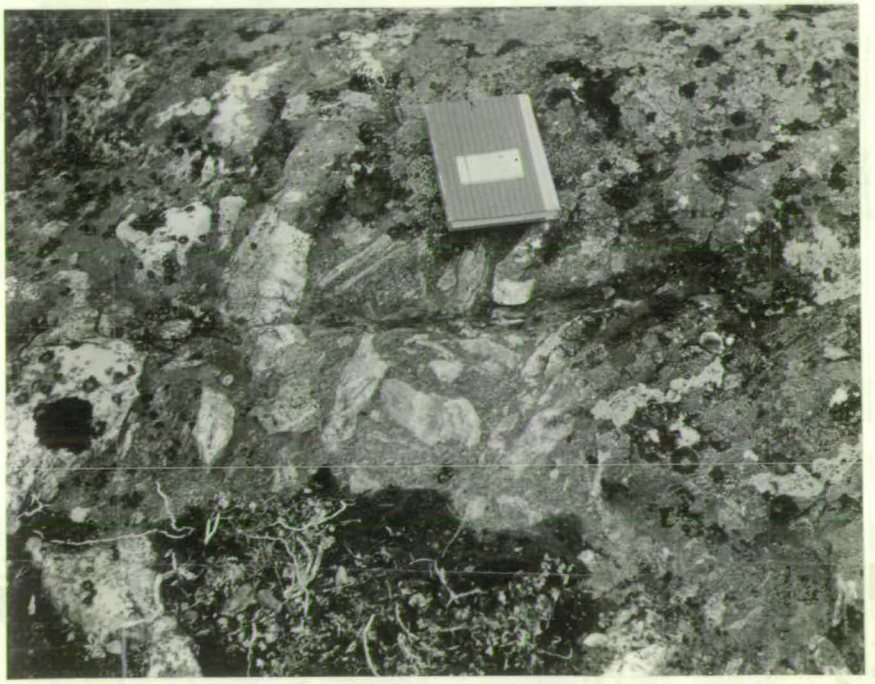

Fig. 5.47 Photomicrograph of Kletten ore (sample 77.52).
A globule of sulfide (pyrrhotite, with pentlandite and chalcopyrite) is brecciated by a carbonate vein, which is itself overgrown by a sub-hedral pyrite grain. The pyrite is largely surrounded by chalcopyrite (c).
Reflected light; ppl; f.o.v. = 20.0 mm.

Fig. 5.48 Photomicrograph of Kletten ore (sample 77.52).
An intergrowth of pyrite (py) and magnetite (m) replacing pyrrhotite (p). Pentlandite is also present (pn).
Reflected light; ppl; f.o.v. = 0.15 mm.


c

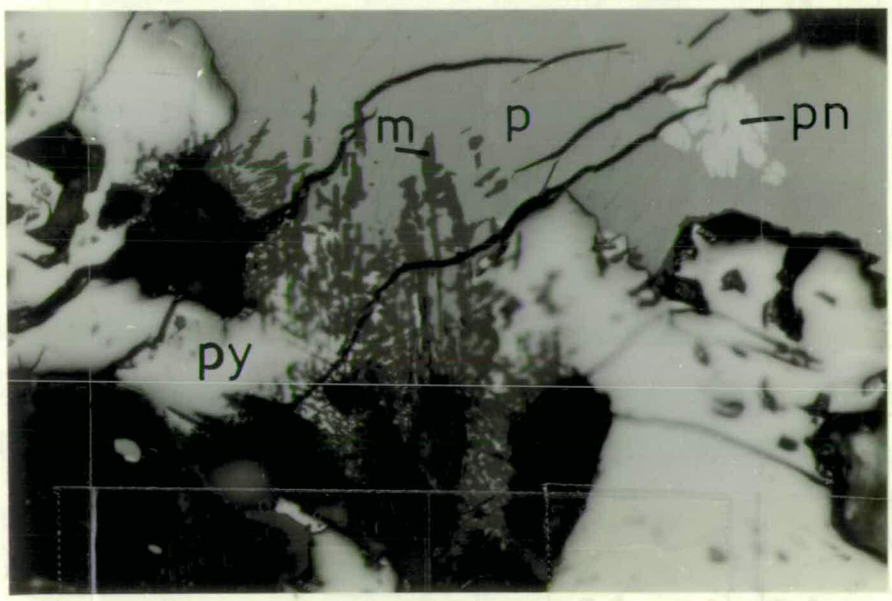
m
p
pn
py

chalcopyrite, and they are always intimately associated with magnetite. Pyrrhotite to pentlandite ratios average about 7.5:1, while pyrrhotite to chalcopyrite ratios vary from 2.5:1 to 39:1. Pyrrhotite forms irregular-shaped grains less than 2 mm in maximum dimension, and is dominantly of the hexagonal type. Pentlandite occurs as blocky grains (less than 0.5 mm) interstitial to pyrrhotite, and as flame-like exsolution lamellae, which commonly emanate from cleavage and other fractures, within pyrrhotite. Chalcopyrite forms rounded blebs, less than 0.5 mm across, interstitial to, and within pyrrhotite. Larger patches of chalcopyrite may surround pyrite grains as shown in Fig. 5.47. Pyrite and magnetite are later metamorphic products of pyrrhotite. The almost euhedral grain of pyrite shown in Fig. 5.47 grows across the carbonate vein which brecciates the sulfide bleb, and is intimately intergrown with both pyrrhotite and magnetite. A typical intergrowth of pyrrhotite with pyrite and magnetite is illustrated in Fig. 5.48. Such alteration of pyrrhotite to pyrite plus magnetite is common in disseminated sulfides in metamorphosed ultramafics where f_{O_2} was high relative to f_{S_2} (Eckstrand, 1975). Some supergene alteration of pentlandite to violarite and pyrrhotite to marcasite is present.

5.1.2.3 Graho - At Graho, some 15 km south of Kvikne (Map 2) a small ultramafic pod is exposed over an area of approximately 50 x 20 m. A contact with the country rock schists is included in this exposure, and is marked by a similar felspathic border zone and tectonic breccia to that at Kletten.

The rock is composed dominantly of serpentine, chlorite, and talc in varying proportions with accessory tremolite, carbonate, sphene, ilmenite, magnetite, and sulfides. Numerous six-sided pseudomorphs of serpentine and chlorite occur (up to 3 mm across), rimmed by magnetite dust, in a matrix dominated by chlorite (Fig. 5.49). The outlines

Fig. 5.49 Photomicrograph of Graho ultramafic (sample 77.197). Serpentine and chlorite pseudomorphs, after olivine, in chlorite.
Transmitted light; X Ni; f.o.v. = 2.40 mm.

suggest primary olivine and, in many cases, such pseudomorphs account for more than 50% of the rock.

Sulfide minerals at Graho are restricted to extremely rare patches of pyrite, up to 1 mm across, complexly intergrown with the silicate minerals. However, Nilsen (1974) has, in addition, recorded rare pyrrhotite, pentlandite, and chalcopyrite.

5.1.2.4 Plassbekken - At Plassbekken, which lies on the densely-wooded southern slopes of Gauldalen, some 6 km ESE of the town of Storen (Map 2), a small ultramafic body, almost barren of sulfides, has been quarried along a trench 70 m long and 5 m wide. The quarry is now densely overgrown and no contact relationships have been observed. The surrounding country rocks however, display well developed D_4 folds (of amplitude and wavelength about 20 m), with upright, NNE-SSW striking axial planes, and variable style from open to tight. The ultramafic is commonly foliated, and consists of varying proportions of serpentine, talc, chlorite, tremolite, and carbonate, which occur as a densely felted mass. The foliation, where present, is upright and of similar orientation to the D_4 axial planes described above. Pseudomorphs after olivine, as at Graho, are only rarely observed. Accessory minerals are sphene, rutile, and pyrite. The latter was observed in the field as small (<5 mm) euhedral porphyroblasts.

5.2 Structural Relationships

The generally poor exposure of both intrusive bodies and country rocks, together with the complex structural history of the area, has limited the extent to which the intrusions can be fitted into a regional tectonic framework. However, the following points are noteworthy.

Where information is available on the three-dimensional form of the smaller metagabbros, either directly from drill-core data (as at

Vakkerlien), or indirectly from geophysical data (as at Olkar), an elongated cylindrical, or "pencil" shape is apparent. At both Vakkerlien and Olkar the orientation of the intrusive bodies is parallel to the direction of the regional D_1 lineation in the area, suggesting intrusion, either before or during the Trondheim Orogeny (Chapter 3).

At Undal, the three-dimensional shape of the intrusion is unknown, while at Skjaekerdalen, the surface outline of the body, as shown in Fig. 5.18, suggests involvement in large-scale folding, but it is not certain at which stage in the structural history of the area this occurred. However, the high pressures (approximately 8.5 kb) required for the development of kelyphitic reaction rims between olivine and plagioclase, as described in 5.1.1.4, are consistent with the Sillimanite-grade regional metamorphism thought to be associated with the Trondheim Orogeny in this area (Fig. 2.1), and suggest intrusion either before or during this event. The lack of kelyphitic reaction rims between olivine and plagioclase in the Undal metagabbro is consistent with the lower metamorphic grade associated with the Trondheim Orogeny along the flanks of the Gula Group.

In contrast to the smaller metagabbros, the ultramafic intrusions retain a sheetlike form. As the concentration of deformation along the margins of ultramafic bodies is well documented (e.g. Jahns, 1967) this cannot be taken as unambiguous evidence for a younger age. However, if such a process had occurred, the preservation of random orientation of fragments in the contact tectonic breccias at Kletten and Graho (Fig. 5.46) would be most unlikely. A post-D_1 intrusion of the ultramafic complexes is therefore suggested. Furthermore, Graho, Kaltberget, and Kletten occur in the central parts of the Gula Group where sphalerite geobarometry indicates pressures associated with the

Trondheim Orogeny of at least 6 kb (Chapter 4), which, with the occurrence of kyanite and staurolite in the country rock schists (Fig. 2.1), suggests temperatures of 550° to 700°C (Winkler, 1976, ch.14). The lack of any textural evidence for the development of bladed, metamorphic olivines, which according to the composition of the fluid phase would develop below 550°C at such pressures (Winkler, 1976, ch.11) together with the igneous composition of olivine relicts at Kletten and Kaltberget (5.3.2) is strong evidence of intrusion after the peak of the metamorphic event associated with the Trondheim Orogeny.

The deformation of the Plassbekken ultramafic, as described in 5.1.2.4, requires that it was intruded prior to D_4. Unfortunately it has not been possible to determine the precise relationship between ultramafic emplacement and D_2 and D_3.

In conclusion it is suggested that the metagabbroic complexes were intruded before or during the Trondheim Orogeny, while the ultramafic bodies were emplaced between this early orogenic event and the end of the main Scandinavian Orogeny (pre-D_4).

As a consequence of this conclusion, Nilsen's (1974) petrogenetic scheme relating all Gula mafic and ultramafic intrusions by crystal fractionation of a basic magma, as described in the introduction to this chapter, cannot be upheld.

5.3 Mineral Chemistry

Thompson (1978) carried out a detailed investigation of the mineral chemistry of the Vakkerlien metagabbro. The essential conclusions of his studies were as follows.

Amphibole. The commonly observed optical zoning of amphibole was reflected in a chemical zonation in which Ti, Al^{IV}, Al^{VI}, Na and K

decrease from cores to margins while Si, Mg/Mg + Fe + Mn, and Ca increase. The overall chemistry of the amphiboles is however controlled by host-rock composition with more ultramafic compositions resulting in increase of Si, Mg/Mg + Fe + Mn, and Ca, and decrease in Ti, Al^{IV}, and Al^{VI}.

Plagioclase. Plagioclase is also compositionally zoned. A maximum of An_{62} was recorded for core compositions while margins fall in the range An_{22}-An_{33}. This zonation was recorded in all plagioclases, including "small recrystallised grains". The anorthite content of plagioclase cores correlates positively with the CaO-content of coexisting amphiboles, and with the CaO, and MgO-content of bulk rocks. Negative correlations with the Na_2O-contents of coexisting amphiboles, and with whole rock Na_2O are also apparent.

Biotite and Chlorite. The chemical compositions of biotite and chlorite are strongly controlled by bulk-rock composition, showing strong positive correlation of Mg/Fe ratios.

Thompson (1978) concluded that whole-rock composition controlled not only the mineral assemblages present, but also the overall chemistry of the various phases. However, he related the chemical zonation of amphibole and plagioclase to the metamorphic history of the intrusion. He discounts the possibility that the core compositions of both phases represent relict igneous chemistries on the grounds of the common structural control of amphibole orientation together with the evidence for recrystallisation of plagioclase. By analogy with other regionally metamorphosed basic rocks (Miyashiro, 1968), he suggests an early upper-amphibolite facies metamorphism, followed by a later, epidote-amphibolite or lower-amphibolite facies event, although he was unable to distinguish between a distinct second metamorphic event and a retrogression from the earlier higher-grade conditions. In the light

of the structural and metamorphic histories presented in Chapters 3 and 4, it is tempting to suggest that the amphibole and plagioclase core compositions relate to the high-grade Trondheim Orogenic event, while the compositions of the rims reflect the lower-grade metamorphism associated with the main Scandinavian event.

A detailed chemical study, such as Thompson's (1978), of all Gula intrusions is beyond the scope of this thesis. Apart from brief qualitative studies, which revealed compositional zoning of amphibole and plagioclase in the Olkar metagabbro (similar to those at Vakkerlien), and confirmed the optical data presented in 5.1, no attempt has been made to investigate their metamorphic chemistry. However, the rare examples of relict igneous mineralogy at Skjaekerdalen, Undal, Kaltberget, and Kletten, have been studied and the results are presented and discussed below.

All mineral analyses were carried out on a Cambridge Microscan V electron microprobe at the University of Edinburgh, using both wavelength and energy dispersive methods. The techniques are described in Appendix B, together with a listing of complete mineral analyses. (Tables B.10-B.17).

5.3.1 The metagabbros

5.3.1.1 Skjaekerdalen - Average wavelength-dispersive analyses of olivines and pyroxenes from Skjaekerdalen are shown in Table 5.2 and all analyses are plotted in Fig. 5.50. Olivine compositions range from Fo_{65} to Fo_{83} and individual grains are unzoned. CaO and Cr_2O_3 are undetectable (typical detection limits are presented in Table B.3, while MnO averages 0.3 wt%. NiO- and CoO-contents average 0.13 and 0.08 wt% respectively.

Clinopyroxenes are diopsides, endiopsides, salites, and augites as shown in Fig. 5.50. They have a narrow range of Mg/Mg + Fe +Mn atomic

	SKJAEKERDALEN			UNDAL			UNDAL INCLUSION		
	Ol	Opx	Cpx	Ol	Opx	Cpx	Ol	Opx	Cpx
SiO_2	38.17	53.41	50.78	37.09	52.39	52.03	38.27	51.83	51.18
TiO_2	nd	0.40	0.74	0.03	0.44	0.63	nd	0.19	0.29
Al_2O_3	nd	1.85	2.80	nd	0.95	1.68	nd	3.46	2.20
Cr_2O_3	nd	0.24	0.53	nd	0.10	0.27	nd	0.14	0.79
FeO	22.92	13.24	5.76	28.96	16.03	7.87	16.25	11.87	4.61
MgO	39.11	28.29	15.76	35.68	26.03	15.51	45.40	29.62	17.11
CaO	nd	1.57	21.25	0.07	2.15	19.86	0.03	1.23	21.30
MnO	0.29	0.28	0.17	0.42	0.35	0.22	0.20	0.25	0.16
NiO	0.13	nd	nd	0.19	nd	nd	0.05	nd	nd
CoO	0.08	0.32	nd	0.12	0.04	nd	nd	nd	nd
Na_2O	ND	0.03	0.42	ND	0.07	0.60	ND	0.04	0.39
K_2O	ND	nd	nd	ND	nd	nd	ND	nd	nd
A:S	6:2	6:2	6:2	4:2	6:2	5:2	3:1	3:1	2:1

	KALTBERGET	KLETTEN		
	Ol	Ol	Opx	Cpx
SiO_2	39.52	40.19	55.17	52.94
TiO_2	nd	nd	0.17	0.30
Al_2O_3	nd	nd	1.38	2.08
Cr_2O_3	nd	0.02	0.23	0.61
FeO	17.21	12.26	8.90	4.36
MgO	42.89	46.40	31.42	17.18
CaO	0.10	0.09	1.10	21.50
MnO	0.22	0.28	0.25	0.17
NiO	0.22	0.08	nd	nd
CoO	0.07	0.03	nd	nd
Na_2O	ND	ND	0.03	0.33
K_2O	ND	ND	nd	nd
A:S	5:1	9:3	8:3	9:3

EXPLANATION

A:S	number of analyses : number of samples
nd	not detectable
ND	not determined
Ol	olivine
Opx	orthopyroxene
Cpx	clinopyroxene

TABLE 5.2 Average wavelength dispersive analyses of olivine, orthopyroxene, and clinopyroxene, from Gula metagabbroic and ultramafic intrusions.

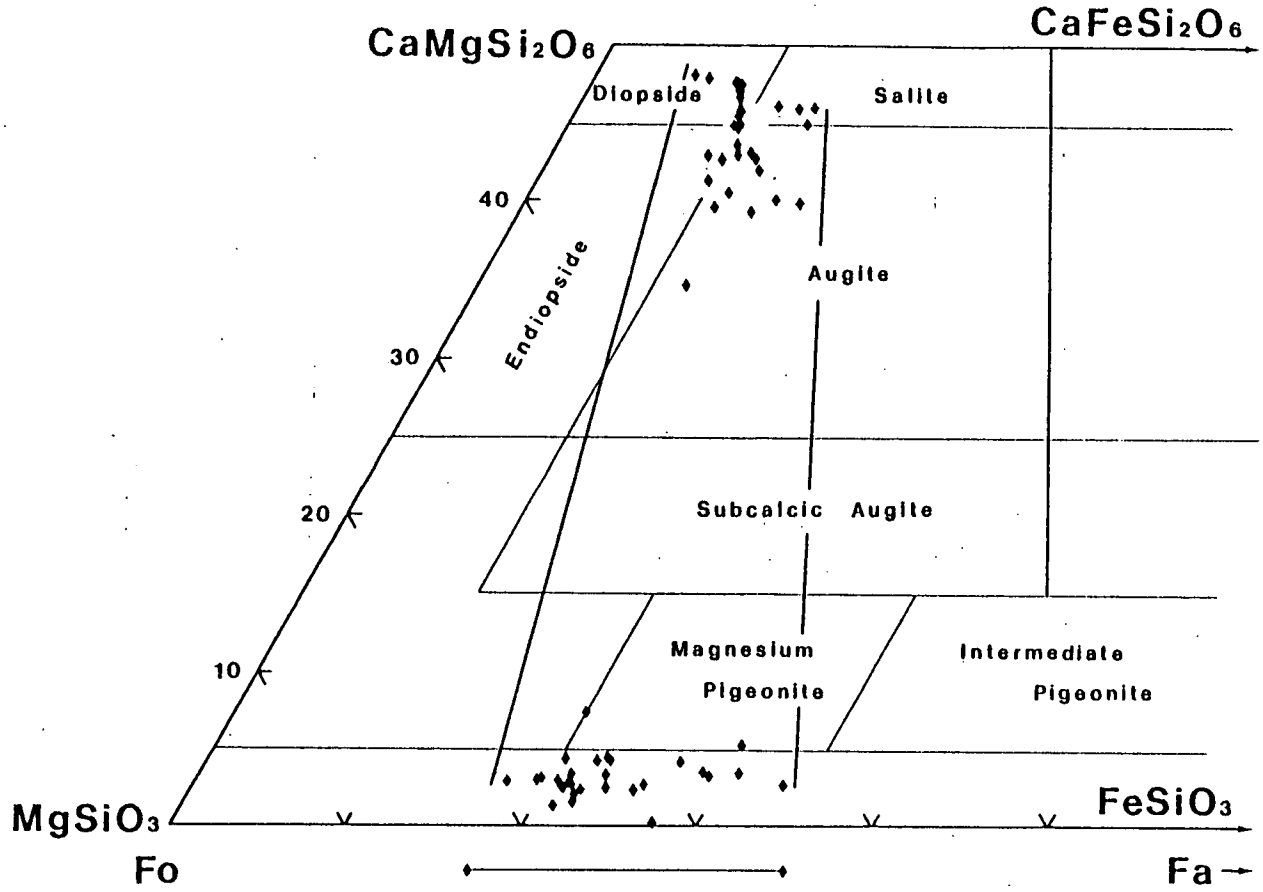

Fig. 5.50 Compositions of olivines and pyroxenes from the Skjaekerdalen metagabbro.

ratio (0.89 to 0.74) and wollastonite-contents vary from Wo_{35} to Wo_{48}. Al_2O_3 averages 2.8 wt% while TiO_2-, Na_2O-, Cr_2O_3-, and MnO-contents are all less than 1.0 wt%. Coexisting orthopyroxenes are bronzites and enstatites with rare magnesium pigeonites. Mg/Mg + Fe + Mn atomic ratios vary from 0.82 to 0.65, and wollastonite contents are usually less than Wo_5. Al_2O_3 averages 1.85 wt%, while TiO_2, Na_2O, Cr_2O_3, and MnO are always less than 1 wt%.

Plagioclase compositions range from An_{90} to An_{43}. Normal zoning is common with a maximum recorded compositional variation of An_{77} to An_{51} from core to margin. Reverse zoning also occurs but is generally associated with kelyphitic olivine-plagioclase reaction rims.

5.3.1.2 Undal - Table 5.2 presents average wave-length dispersive analyses of Undal olivines and pyroxenes. All analyses are plotted in Fig. 5.51. Olivines range in forsterite content from Fo_{84} to Fo_{64}, and fall into two groups. The first group ranges from Fo_{84} to Fo_{82} and represents relict olivines from an ultramafic inclusion in the metagabbro. The second group ranges from Fo_{71} to Fo_{64}, and represents relict olivines from the metagabbro itself. CaO and Cr_2O_3 are always low (<0.1 wt%) while MnO averages 0.4 wt% in the gabbroic rocks and 0.2 wt% in the ultramafic nodule. NiO and CoO average 0.19 and 0.12 wt% respectively in the gabbro and less than 0.1 wt% in the ultramafic.

Clinopyroxenes are endiopsides in the ultramafic nodule and augites in the gabbro. In the ultramafic inclusion the Mg/Mg + Fe + Mn atomic ratio varies from 0.88 to 0.85 and the Ca-content ranges from Wo_{45}-Wo_{43}, while in the gabbro they vary from 0.82 to 0.74 and Wo_{36}-Wo_{44} respectively. Al_2O_3-contents average 1.68 wt% in the gabbro, and 2.20 wt% in the ultramafic inclusion, while Na_2O, TiO_2 and MnO increase, and Cr_2O_3 decreases, from the ultramafic to the metagabbro as shown in Table 5.2

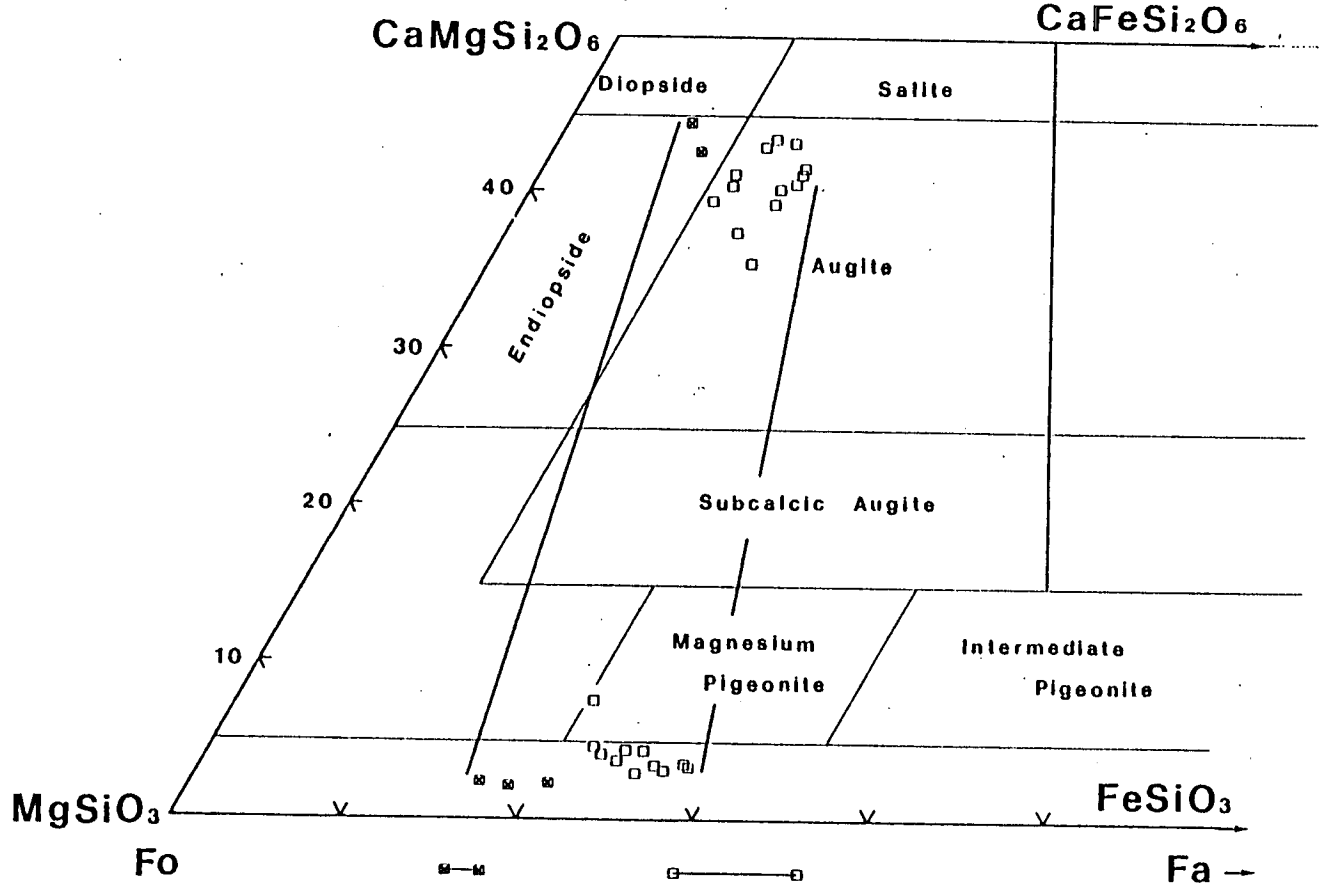

Fig. 5.51 Compositions of olivines and pyroxenes from the Undal metagabbro. Squares - metagabbro; squares with x - ultramafic xenolith.

Orthopyroxenes are usually bronzites (one magnesium pigeonite has been recorded) having a range of Mg/Mg + Fe + Mn atomic ratio of 0.83 to 0.79 in the case of the ultramafic inclusion, and 0.78 to 0.71 in the metagabbro. Ca-contents are less than Wo_3 in the inclusion, and range from this value to Wo_8 in the less mafic host. Al_2O_3-contents are higher in the ultramafic where they average 3.46 wt%, as compared with a value of 0.95 in the gabbro. TiO_2, Cr_2O_3, Na_2O, and MnO behave as in clinopyroxene.

Plagioclase compositions in fresh samples of Undal metagabbro range from An_{60} to An_{50}. Normal zoning commonly occurs with a maximum recorded compositional variation of An_{60}-An_{52}.

5.3.2 The ultramafics

Average olivine and pyroxene analyses (wavelength dispersive) from Kletten, and an average olivine analysis from Kaltberget are listed in Table 5.2, and all analyses are plotted in Fig. 5.52. Forsterite contents at Kletten vary from Fo_{89} to Fo_{84}, while those at Kaltberget vary from Fo_{86}-Fo_{80}. No systemmatic variation of olivine composition across the Kletten body has been defined. Where olivine is enclosed in orthopyroxene at Kletten, a reverse zoning of the olivines is occasionally observed, with differences in composition as much as 2% Fo. Where such zoning is noted in olivine, the associated orthopyroxene displays normal zoning in which enstatite content may decrease by up to 2% towards the olivine. These data suggest that there has been a metamorphic re-equilibration of the two phases. MnO-values are similar at Kaltberget and at Kletten averaging 0.22 and 0.28 wt% respectively. NiO- and CoO-contents vary between the two bodies from 0.22 and 0.07 wt% respectively at Kaltberget, to 0.08 and 0.03 wt% at Kletten. The reasons for this disparity have interesting implications to the origin of the sulfide mineralisation at Kaltberget and will be discussed later in this chapter.

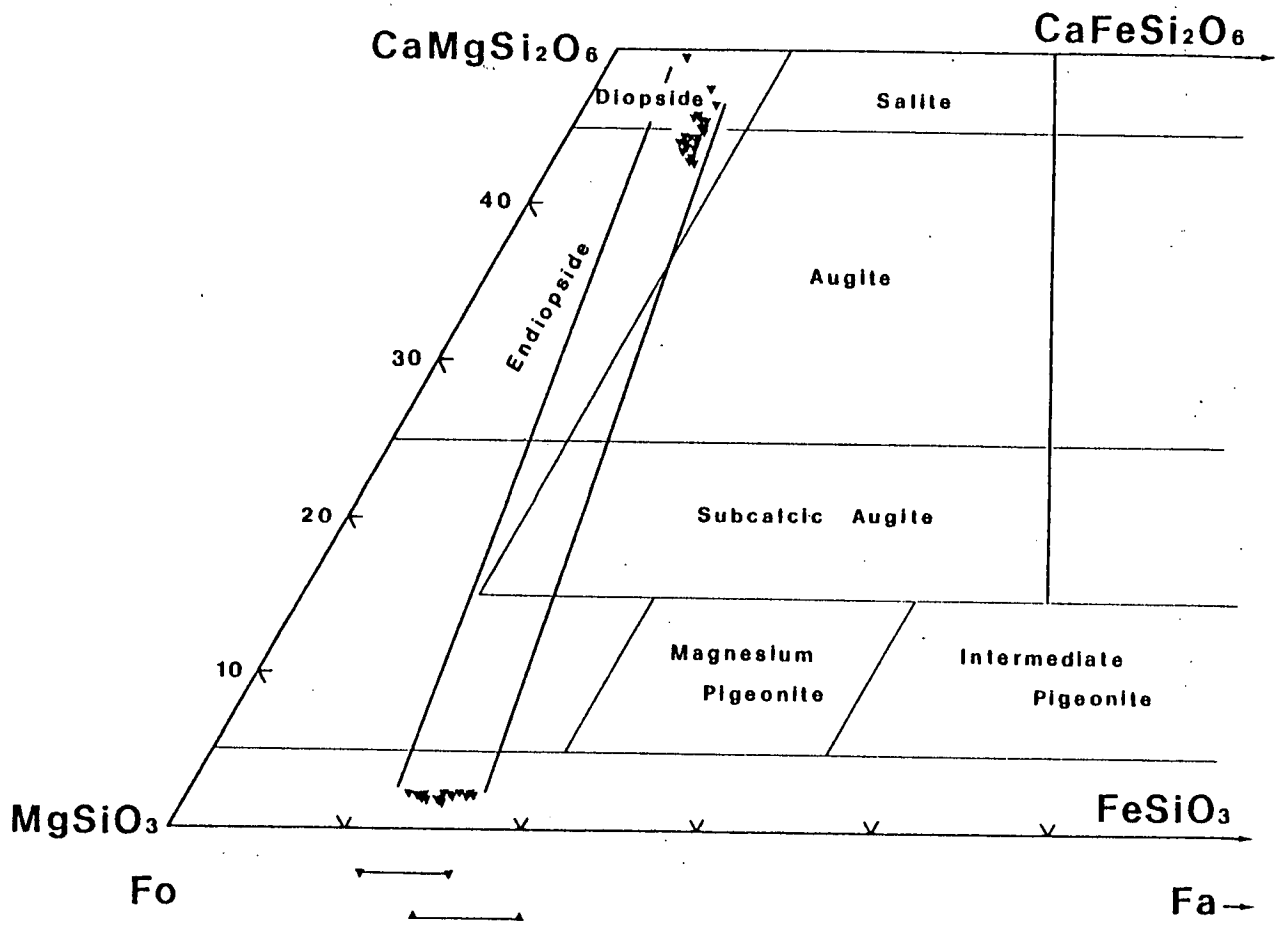

Fig. 5.52 Compositions of olivines and pyroxenes from the Kletten ultramafic body (inverted triangles), and olivines from the Kaltberget body (triangles).

Clinopyroxenes at Kletten are diopsides and endiopsides with Mg/Mg + Fe + Mn atomic ratios varying from 0.92 to 0.86, a range of Ca-contents of Wo_{43} to Wo_{49}, and Al_2O_3 averaging 2.08 wt%. Orthopyroxenes are Mg-rich bronzites varying in Mg/Mg + Fe + Mn atomic ratio from 0.87 to 0.83. Wollastonite-contents are always approximately Wo_2, while the average Al_2O_3-content is 1.38 wt%.

Plagioclase compositions from the felspathic border zones at Kletten and Kaltberget vary from An_{34}-An_{16}. Both normal and reverse zoning are present with a maximum variation between core and rim of 7 mole % anorthite.

5.3.3 Discussion

The mineral compositions from Skjaekerdalen and Undal presented above, are similar to data available from other gabbroic intrusions of tholeiitic affinity. The olivine, pyroxene and plagioclase compositions from Skjaekerdal are similar to the earliest formed phases at the Sudbury (Naldrett et al., 1970); Skaergard (Nwe, 1976); and Dufek (Himmelberg and Ford, 1976) intrusions. Compositions from the ultramafic inclusion at Undal are similarly comparable, while the compositions from the host gabbro suggests crystallisation from a slightly more evolved liquid. As the phases from the ultramafic are not sufficiently magnesian to have been in equilibrium with mantle phases (e.g. Clark and O'Hara, 1979) a cumulate origin is suggested.

The compositions of primary silicate phases at Kletten are, however, considerably more magnesian than the earliest formed phases from many gabbroic intrusions and bear closer resemblance to olivines and pyroxenes crystallising from komatiitic liquids (Arndt and Fleet, 1979), or to early formed phases in the Bushveld complex (Atkins, 1969), for which a picritic parent liquid has recently been suggested (Cawthorne, pers. comm., 1979). A high-Mg parent liquid for the Gula ultramafics must

therefore be considered and will be discussed further in the light of whole-rock geochemistry.

5.4 Whole-rock Geochemistry

Thompson (1978) carried out a systemmatic survey of the whole-rock geochemistry of the Vakkerlien metagabbro complex. The study involved a total of 20 samples from the Main Body (profiles 550S and 950S, Fig. 5.1) and six samples from the Second Body (profile 1400S, Fig. 5.1). He concluded that, although metamorphic effects were probably responsible for the erratic behaviour of the elements when examined in detail, the overall variations of major oxides were consistent with a model involving a differentiated sill-like intrusion, in which olivine was followed by plagioclase fractionation. He suggested that the Shiant Isles Sill of N.W. Scotland (Drever, 1953) was a possible analogy.

Drill-core intersections at Kaltberget, and moderately good exposure at Kletten have allowed the systematic collection and analyses of samples from these ultramafic bodies. The results of this study are presented below. However, the limited exposure and highly xenolithic nature of the Olkar and Gardsjoen metagabbros, the poor exposure at Undal, and the obviously cumulate and complexly brecciated nature of the Skjaekerdalen complex have precluded similar investigations of these bodies.

Samples from Kletten were collected approximately every 25 m across profile 100S (Fig. 5.41). While the western contact of the intrusion is exposed in the vicinity of this profile, the eastern boundary is not, and lies in a gap in exposure of about 100 m. At Kaltberget, samples were selected every 4 m through drill-hole 76/4 (Figs. 5.30 and 5.36). Details of analytical techniques are given in Appendix A, and Tables A.7 and A.8 list full analyses.

Variation diagrams for ten major elements, using MgO as abscissa, are presented in Fig. 5.53. This figure also includes a small number of analyses of Graho and Plassbekken ultramafic rocks. While accepting the possibility of metamorphic modification of bulk chemistries, the following points are noted.

On the SiO_2, CaO, Na_2O, and Al_2O_3 diagrams the compositions from Kaltberget and Kletten plot in, or close to a polygon defined by the average olivine composition from Kletten and Kaltberget, the average orthopyroxene and clinopyroxene analyses from Kletten, and a typical calcic plagioclase of approximately An_{80} (Deer, Howie, and Zussman, 1963, page 119, analyses 9). At Kaltberget, and at Kletten the variation within each body projects towards the olivine apex, suggesting control by varying proportions of olivine in the rock. These characteristics are consistent with petrological observations which indicate a dominance of olivine phenocrysts (with minor clinopyroxene) in a matrix of orthopyroxene and plagioclase.

The variation between Kletten and Kaltberget, especially well demonstrated by the SiO_2 diagram in Fig. 5.53, may be explained either by phenocryst mixing with a slightly more evolved liquid at Kletten, or by removal of late-stage interstitial liquid (perhaps by filter pressing) from Kaltberget. This between-intrusion variation is also displayed by the P_2O_5, TiO_2, and MnO diagrams. On the Fe_2O_3 diagram, analyses commonly plot on the iron-rich side of the polygon outlined above, presumably as a result of the presence of minor amounts of sulfide phases. However, the within-, and between-intrusion variations are still obvious. The occurrence of phlogopite, especially in the contacts of both Kaltberget and Kletten, suggests the metamorphic introduction of K, which perhaps explains the irregular distribution of points on the K_2O-variation diagram.

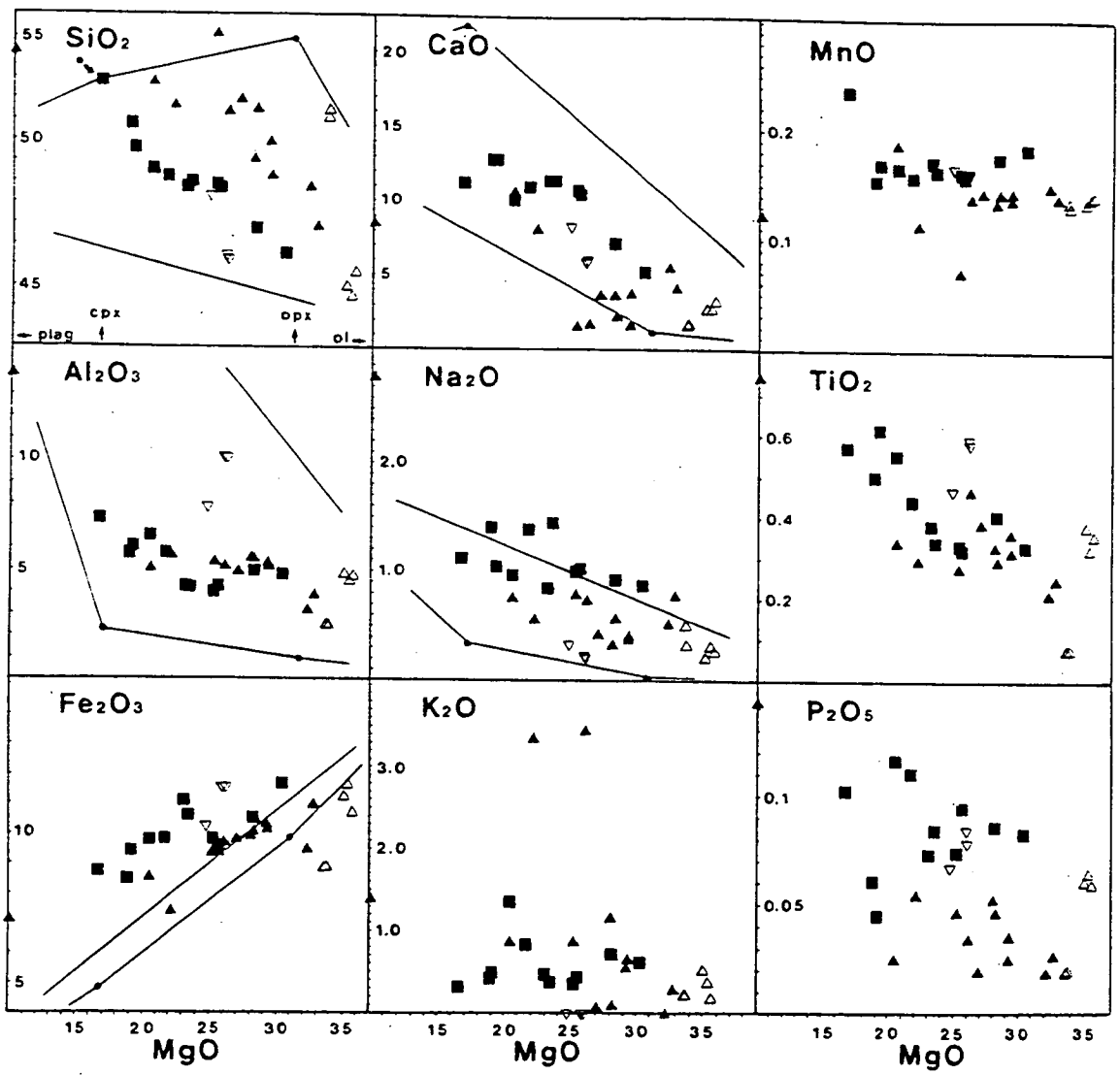

Fig. 5.53 Variation of major oxides in Gula ultramafic intrusions. Solid triangle - Kaltberget; solid square - Kletten; open triangle - Graho; inverted open triangle - Plassbekken.

Insufficient data, to allow meaningful interpretation, are available from Plassbekken or Graho, where the small size of the bodies would increase the likelihood of metasomatic alteration. However, it is noticeable that analyses from Graho commonly plot close to the olivine apex, which agrees favourably with the high proportion of olivine pseudomorphs observed in thin-section.

The variation of MgO-content as a function of position within the intrusives is shown in Fig. 5.54. At Kaltberget a saw-tooth effect is obvious, in which MgO-content increases rapidly from the top, decreases gradually towards the central parts of the body, increases rapidly downwards again, and finally decreases gradually towards the base of the intrusion. Patterns such as this in the ultramafic lenses at Yakabindi, Western Australia, have been taken by Naldrett and Turner (1977) to indicate successive influxes of phenocryst (olivine) - rich magma, which subsequently underwent gravitational settling. If such a process occurred at Kaltberget, two phases of magma input are indicated, together with structural inversion of the intrusion as a whole (Fig. 5.54).

While the development of metasomatic reaction zones around ultramafic bodies is well documented (Read, 1934; Curtis and Brown, 1969), the assymmetric pattern displayed by the MgO-variation through Kaltberget suggests a primary igneous origin.

At Kletten, the pattern is more obscure. The eastern contact of the intrusion is not exposed on profile 100S. However, it is well seen along the shores of the lake which marks the northern-most extent of the intrusion, and is marked there by a felspathic border zone similar to that occurring on the western boundary. MgO should therefore decrease outwards towards the eastern contact as indicated by the dashed line in Fig. 5.54. The pattern then displayed is more symmetrical than that at Kaltberget, and might suggest a two-phase input of phenocryst-rich magma

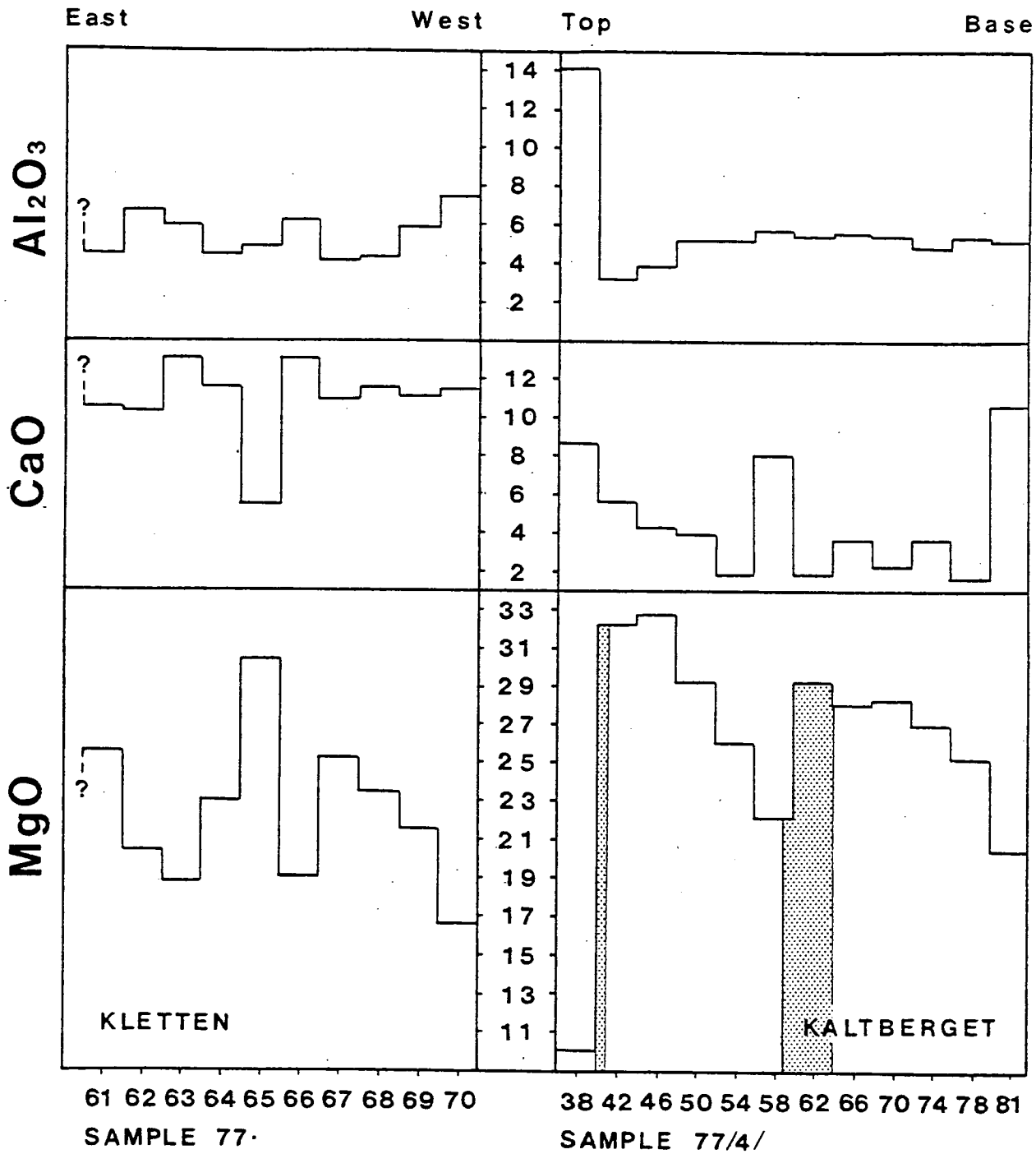

Fig. 5.54 Chemical variation along Kletten profile 100S, and Kaltberget drill hole 76/4. Stippled area - disseminated mineralisation as indicated by Ni-assays greater than 0.1 wt %.

in which the differentiation process was flow, rather than gravity controlled (Bhattachargi and Smith, 1964). Alternatively, as sample spacing was so much greater than at Kaltberget, some detail of the variation may be lost, and a multiple intrusion controlled by either flow or gravity differentiation might also explain the pattern.

The variations of CaO and Al_2O_3 are also presented in Fig. 5.54. At both Kaltberget and Kletten, CaO, in general, varies inversely with MgO, while Al_2O_3 behaves similarly at Kletten. At Kaltberget, however, Al_2O_3 shows little variation across the body, perhaps as a result of metamorphic mobility. The sharp increase in Al_2O_3 and CaO towards the top of Kaltberget, corresponding to a rapid decrease in MgO, presumably related to contamination of the intrusion by the country-rock schists.

If the intrusion of an olivine-liquid crystal mush is accepted for the origin of the ultramafic bodies, then it is possible to make some suggestions as to the possible composition of the parent liquid involved.

Samples 77.63 and 77.66 at Kletten, and sample 77/4/58 at Kaltberget have the lowest MgO-contents with the exception of contact lithologies; they should therefore be the least phenocryst enriched. Furthermore they occur in the centres of the intrusions and are the least likely to have suffered contamination from the country rocks. These samples should therefore represent the closest approximation available to the composition of the parent liquid.

Roeder (1974) and Roeder and Emslie (1970) have shown experimentally that the composition of olivine, with regard to its Mg- and Fe-contents, is independent of other elements in the liquid; of temperature and pressure; and is solely dependent on the abundance of these elements in the liquid. Furthermore, they showed that the distribution coefficient (where X = mole fraction):

$$K_D = \frac{X^{ol}_{FeO} \cdot X^{liq}_{MgO}}{X^{ol}_{MgO} \cdot X^{liq}_{FeO}}$$

for Fe and Mg between olivine (ol) and liquid (liq) was constant, and independent of temperature or liquid composition, with a value of 0.30. More recent experimental data, however, suggests that this value is slightly low, and a value of 0.33 is now preferred (O'Hara et al., 1975). The composition of olivine can therefore be used to predict the Mg/Fe ratio of the liquid from which it crystallised, or conversely, the composition of olivine which would crystallise from a liquid of known composition may be calculated.

If samples 77.63 and 77.66 approximate to the composition of the liquid at Kletten, then the predicted composition of olivine in equilibrium with this "liquid" should correspond to the observed olivine compositions.

Carrying out the calculations outlined above on samples 77.63 and 77.66 predicts equilibrium olivine compositions of between Fo_{92} (ferric/ferrous ratio in "liquid" = 0) and Fo_{94} (ferric/ferrous ratio in "liquid" = 0.2). In view of the probable mantle source of high-Mg liquids, and the further evidence presented below, and in Chapter 6, for such parent liquids at Kaltberget and Kletten, it is likely that original ferric/ferrous ratios were negligible. The lower value of forsterite-content is therefore favoured, and is in reasonable agreement with the most magnesian olivine-core composition of Fo_{89} recorded at Kletten. Sample 77/4/58 from Kaltberget, however, predicts equilibrium olivine compositions of at least Fo_{95}, and therefore requires some phenocryst (olivine) enrichment.

Theoretical (Usselman et al., 1979) and experimental (Campbell, 1978) investigations of cumulate rocks have shown that close packing of

olivine phenocrysts allows a minimum of 40 vol% intercumulus liquid. The application of this constraint to the approximate liquid compositions suggested by samples 77.63 and 77.66, and the average olivine composition from Kaltberget and Kletten, gives a calculated "cumulate rock" composition very similar to the most magnesian sample at Kaltberget (77/4/46). The calculation is illustrated in Table 5.3. Column 1 is the average composition of samples 77.63 and 77.66, and column 2 is the average olivine composition (wavelength dispersive methods) from Kaltberget and Kletten. Column 3 is the calculated composition of a hypothetical cumulate rock composed of 40% liquid (as in column 1) and 60% olivine (as in column 2). Column 4 is the analysis of sample 77/4/46, which is regarded as the basal, and most phenocryst-enriched part of one of two intrusive phases at Kaltberget. The close agreement between columns 3 and 4 supports the possibility that samples 77.63 and 77.66 represent close approximations to liquid compositions.

The composition of the parent liquid for these ultramafic intrusions will be discussed further in the light of details of sulfide chemistry presented in Chapter 6.

5.5 Discussion - The Origin of Gula Ni-Cu Sulfide Deposits.

On a world-wide basis it is now generally accepted that Ni-Cu sulfide ores associated with mafic and ultramafic igneous rocks are, at least originally, of magmatic origin, although metamorphic processes may be responsible for their concentration to form economic ore bodies (e.g. Barrett et al., 1976, 1977). Three lines of evidence have lead to this conclusion and are outlined below.

a) The single most striking piece of evidence is found where ores are located in relatively undeformed rocks. In such examples the ores are almost always localised towards the stratigraphic base of the magmatic

Table 5.3 Mixing calculation for Gula ultramafic intrusions. See text for details.

	1	2	3	4
SiO_2	50.34	39.94	44.10	45.94
Al_2O_3	6.04	-	2.42	3.91
FeO	8.13	14.23	11.67	9.94
MgO	19.00	45.14	34.68	32.79
CaO	12.96	0.09	5.24	4.29
Na_2O	1.25	-	0.50	0.80
K_2O	0.48	-	0.19	0.31
TiO_2	0.57	-	0.23	0.25
MnO	0.16	0.26	0.22	0.14
P_2O_5	0.05	-	0.02	0.03
TOTAL	98.98	99.46	99.27	98.40

1. average composition of samples 77.63 and 77.66
2. average olivine from Kaltberget and Kletten
3. hypothetical rock consisting of 40 vol% of column 1 and 60 vol% of column 2
4. sample 77/4/46

unit with which they are associated. This is true of the ores of the Sudbury, Ungava, and Timmins Ni-camps of Canada (Naldrett, 1979), of the ores of the Kambalda, Scotia, Widgiemooltha district of Western Australia (Hudson, 1972, 1973), of most of the ores of the Duluth complex (Bonnichson, 1974) and of the majority of deposits in the Noril'sk and Pechenga mining camps of the U.S.S.R. (Godlevskii, 1959; Haapala, 1969). As Naldrett (1979) points out, such a spatial relationship between ores and host rocks is entirely expected in view of the magmatic model which predicts that an immiscible sulfide liquid of density 3.9 g/cc will migrate downwards through a silicate melt of density 2.6-3.0 g/cc.

b) Further compelling arguments in favour of the magmatic model are found in the chemistry of the sulfide ores, which show concentrations of exactly those elements (Ni, Cu, Co, and platinum-group (P.G.) elements) experimentally predicted to partition into a sulfide phase under magmatic conditions (MacLean and Shimazaki, 1976; Fleet et al., 1977; Rajamani and Naldrett, 1978). Furthermore, zinc, which is known to be concentrated, transported, and precipitated by hydrothermal solutions is almost totally absent from Ni-Cu ores, yet present in their host rocks, while Ni and PG elements are absent in massive sulfide deposits of known hydrothermal origin.

c) The third convincing line of evidence for a magmatic origin of Ni-Cu ores is the textural relationship between the sulfides and the host silicates. The sulfides commonly form a network interstitial to, and enclosing, the silicate minerals. Such textures are especially common in relatively undeformed ores, and would require somewhat unlikely conditions of selective mineral replacement if they were to be of secondary, non-magmatic origin.

5.5.1 The metagabbros.

It is clear from their very definition that the Ni-Cu deposits associated with Gula metagabbroic complexes fulfill the chemical requirements of magmatic sulfide ores.

At Skjaekerdalen, a basal accumulation of sulfides is not apparent. However, consideration of sulfide-silicate textural relationships may help to explain this. Where mineralisation is hosted by ultramafic lithologies, sulfides are always interstitial to silicate minerals. In more gabbroic lithologies interstitial textures occur together with fragments of massive sulfide, while in more leucocratic hosts, sulfides occur largely as angular fragments.

If the model of successive intrusion of progressively more evolved liquids (perhaps from a fractionating magma chamber at depth) is accepted as accounting for the field relations, and large scale textures of the Skjaekerdalen complex as a whole, a situation could be envisaged in which the earliest intrusion involved both a basic silicate magma and an immiscible sulfide liquid. The sulfide magma would settle downwards through the silicate liquid to form an accumulation of massive sulfide at the base of the intrusion. Ultramafic cumulates crystallising from the silicate magma would be pressed downwards (Hudson, 1972; Naldrett, 1973) into this basal pool of sulfide liquid (Kullerud, Yund and Moh, 1969 , have shown that a sulfide liquid of the composition of a typical Ni-Cu ore would solidify at about 1050^{o}C). The resulting stratigraphic sequence would be one in which massive sulfide was overlain by a matrix ore in which silicate minerals float in an interstitial network of sulfides. This zone should pass gradually upwards through disseminated interstitial ore to barren ultramafic and mafic cumulates. Consider now a second input of gabbroic magma, which disrupts the sequence established above. Large scale textures in which fragments of massive

sulfides are included in a gabbroic host, together with fragments of ultramafic cumulates which may themselves carry interstitial sulfides would result. Provided that the temperature of the second intrusion was greater than 1050°C, at least partial melting of the disrupted massive sulfides should occur, giving rise to further interstitial ores in gabbroic hosts (and possibly a second generation of basal massive sulfide), together with partially "assimilated" fragments of massive sulfide. The model is completed by the further influx of a more evolved silicate liquid at a temperature below 1050°C. Ultramafic fragments carrying interstitial ores, together with gabbroic fragments carrying both interstitial and fragmental ores, and fragments of massive sulfide would be included in this rock on solidification.

Therefore, the full range of ore textures, together with the large scale spatial distribution of rock types at Skjaekerdalen, can be satisfactorily explained by assuming a magmatic origin for the sulfides, indeed, they would be difficult to explain by any other process. It is noteworthy that the above sequence of events might also occur within the limits of a single magma chamber, undergoing crystal fractionation and disruption of cumulate portions by the evolving liquid.

The apparently unmineralised nature of the Undal intrusion, when compared with the Skjaekerdalen complex, poses an intriguing problem. Consideration of olivine compositions provides a possible explanation.

Duke and Naldrett (1978) modelled, by computer, the differentiation of a komatiitic magma by the fractional crystallisation of olivine in the presence and absence of an immiscible sulfide liquid. They demonstrated that the Ni-content of olivine crystallising from such magmas decreases rapidly when the magma becomes saturated with respect to sulfur (i.e. when an immiscible sulfide liquid is precipitated). The

modelling, demonstrated in Fig. 5.55a, is based on an initial liquid composition which is the average of several published analyses of spinifex-textured komatiite flows from Yakabindi, Western Australia.

In Fig. 5.55b curves marking the maximum Ni-values for given Fo-contents of olivines from the Rhum layered intrusion of the British Tertiary igneous province (unpublished data, McClurg, 1980), and from ultramafic nodules of mantle (Hamad, 1963; Frey and Green, 1974; Boyd et al., 1976; Danchin and Boyd, 1976) and cumulate (Dawson and Smith, 1973) origin, are superimposed on the calculated data of Duke and Naldrett (1978). The discrepancy between the modelled sulfur-undersaturated curve, and the data from Rhum (where liquid compositions are believed to be controlled by olivine fractionation - McClurg, pers. comm., 1980) and the ultramafic nodules suggests either, that Duke and Naldrett's (1978) initial liquid composition was unrealistically low in Ni, or that their assumptions with regard to the partitioning behaviour of Ni were in error. In this context, it is interesting to note that the initial silicate liquid assumed by Duke and Naldrett (1978) contained 32.0 wt% MgO and 1600 ppm Ni. investigation of published analyses reveals that spinifex-textured komatiite flows of comparable MgO-content may contain as much as 1900 ppm Ni (Nesbitt and Sun, 1976). However, the overall similarity in geometry between the calculated sulfur-undersaturated curve and the natural data (Fig. 5.55b) suggests that the modelling itself is reasonable, and there is certainly no justification to doubt the general relationships between the compositions of olivines crystallising from sulfur-undersaturated, and sulfur-saturated magmas.

With regard to the sulfur-saturated trends, Duke (1979) demonstrated the considerable effects of varying the ratio of olivine to sulfide magma being removed from the silicate liquid, with a decrease in this

Fig. 5.55 a) Composition of olivines fractionating from sulfur-undersaturated (heavy solid line) and sulfur- saturated (light solid lines) komatiitic liquids, where the silicate magmas become saturated with respect to sulfur after various degrees of olivine fractionation (redrawn from Duke and Naldrett, 1978).

b) As a), but with data from Rhum (dot-dashed line) and ultramafic nodules (dotted line) superimposed. See text for details.

c) As b), but with average compositions of olivines from Undal (square - metagabbro; square with x - ultramafic xenolith), Skjaekerdalen (diamond), Kaltberget (triangle), and Kletten (inverted triangle).

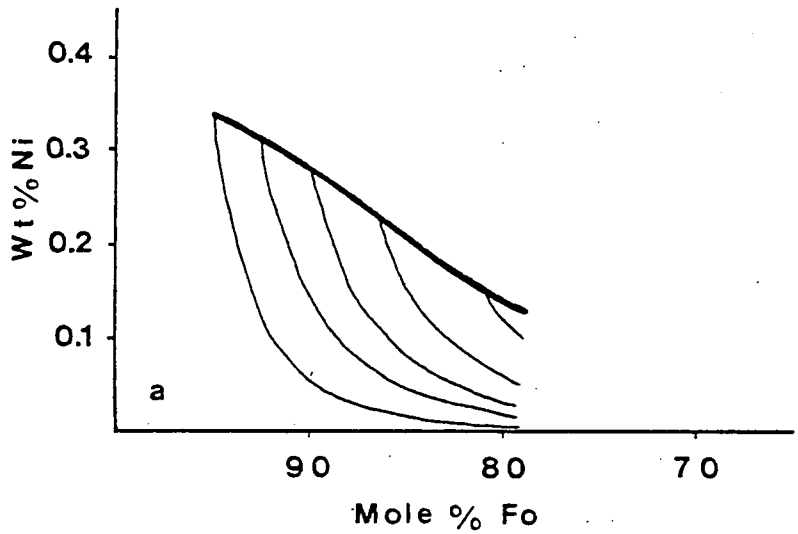
0.4
0.3
0.2
0.1
Wt % Ni
a
90
80
70
Mole % Fo

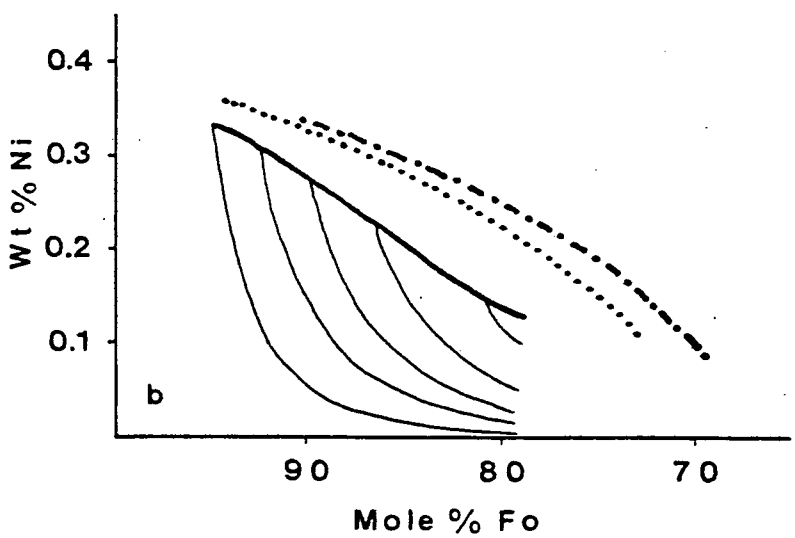
0.4
0.3
0.2
0.1
Wt % Ni
b
90
80
70
Mole % Fo

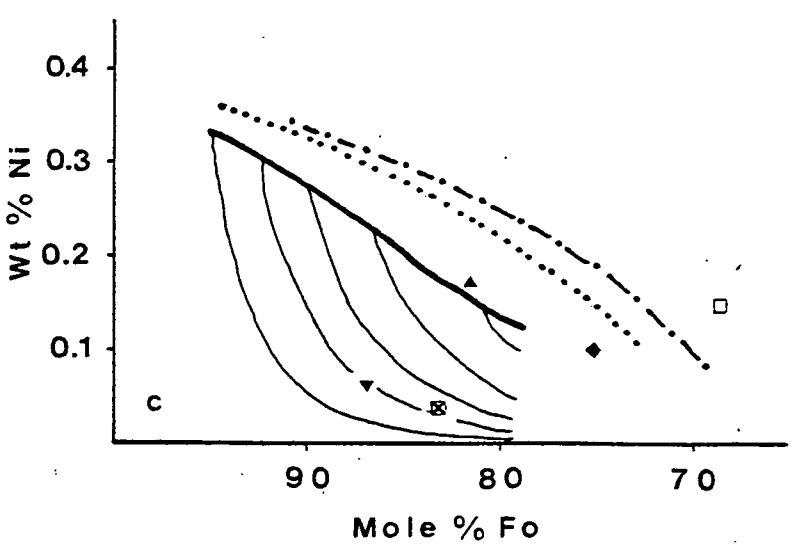
0.4
0.3
0.2
0.1
Wt % Ni
c
90
80
70
Mole % Fo

value leading to enhanced Ni-depletion trends. The ratio is controlled by the solubility of sulfur in the silicate liquid, which, on the basis of experimental investigations (Haughton et al., 1974; Shima and Naldrett, 1975), is expected to decrease with ongoing olivine fractionation, as the liquid becomes less mafic, and the temperature drops. Duke and Naldrett (1978) included these experimental data in their computer modelling and showed that errors in estimates of sulfur solubility of as much as 25% had little effect on the sulfur-saturated trends.

A further complication, involving the possible fractionation of pyroxene in addition to olivine, must be considered. As the Ni partition coefficients for pyroxenes and basic silicate liquids are much lower than for olivines (Duke, 1976; Gill, 1978), fractionation of both olivine and pyroxene will produce less pronounced Ni depletion trends than those resulting from separation of olivine only.

In conclusion, the discussions below, and in the following section, regarding the composition of olivine, and its relationship to the presence of an immiscible sulfide liquid, involve the following assumptions:

1. The data from Rhum and ultramafic nodules presented in Fig. 5.55b, are representative of natural sulfur-undersaturated compositions.
2. While accepting the possibility of modification of the sulfur-saturated trends by fractionation involving varying ratios of olivine to sulfide magma (Duke, 1979), the modelling of Duke and Naldrett (1978) involved realistic estimates of this ratio, and the general relationships between sulfur-undersaturated and sulfur-saturated systems illustrated in Fig. 5.55a, are therefore considered valid.

3. Crystallisation and separation of both olivine and pyroxene as compared with fractionation of olivine alone, will result in less pronounced Ni-depletion trends in both sulfur-undersaturated and sulfur-saturated situations.

4. While sub-solidus re-equilibration of orthopyroxene and olivine rims has been observed at Kletten, only analyses of olivine cores are considered below, and these are assumed to approximate closely to primary magmatic compositions.

Olivines from the metagabbros at Undal average $Fo_{68.7}$ and 0.15 wt% Ni (Table 5.2), and imply equilibration with a sulfur-undersaturated silicate magma, derived by the fractionation of both olivine and pyroxene (Fig. 5.55c). These observations are consistent with the unmineralised character of the intrusion, as presently known, and suggest that further exploration would be unlikely to reveal any significant concentrations of sulfide mineralisation.

In contrast, olivines from the ultramafic xenolith at Undal have average Fo- and Ni-contents of 83.3 mole% and 0.04 wt% respectively (Table 5.2), requiring equilibration with a silicate magma, saturated with respect to sulfur (Fig. 5.55c). It has previously been proposed that this xenolith is of cumulate origin (5.3.3). In view of the evidence suggesting crystallisation from a sulfur-saturated and Ni-depleted silicate liquid, a cognate relationship with the metagabbros is unlikely, and it is therefore concluded that the xenolith was accidently included at some stage prior to the intrusion of the sulfur-undersaturated Undal magma.

Olivines from the Skjaekerdalen complex average $Fo_{75.2}$ and 0.10 wt% Ni. According to Fig. 5.55c, these values suggest equilibration with a sulfide liquid, in agreement with the observed mineralised character of the intrusion.

Spatial and textural relationships at Vakkerlien and Olkar are difficult to explain, probably because of the intense deformation suffered by these intrusions. Further comment on these bodies will be deferred until Chapter 6.

5.5.2 The ultramafics.

As with the metagabbros, the chemical characteristics of nickel-copper ores associated with ultramafic intrusions within the Gula Group are typical of magmatic sulfide deposits. The central location of the high-grade mineralisation at Kaltberget Main Body (drill-holes 76/6, 76/8, and 76/12, Fig. 5.36), together with the locations of sulfide disseminations at the upper margin, and in the central parts of the ultramafic in drill hole 76/4, are perhaps somewhat puzzling. However, when viewed in the light of Fig. 5.54, these relationships not only provide strong evidence of a magmatic origin for the ores themselves, but strongly support the earlier suggestion of an inverted, two-phase intrusion of an olivine-rich crystal mush which underwent gravitational differentiation. The sulfides would percolate downwards through the crystal mush to collect at the base of each intrusive cycle.

However, the occasional globular textures observed in the high-grade ore at Kaltberget Main Body are inconsistent with this hypothesis. Such textures are thought to be the result of the sulfides crystallising before the surrounding silicate minerals (Naldrett, 1969).

In a dry environment it is unlikely that the silicate liquidus would not have been attained before the sulfides finally solidified at about 1050°C (Kullerud et al., 1969). However, it is possible that a high water pressure, which would not affect the sulfide melting temperature, might lower the silicate liquidus sufficiently to allow the sulfides to solidify first (Naldrett, 1969). Such high water pressures would stabilise amphibole at an early stage of silicate

crystallisation, and indeed, the classical "buck-shot" ore at Sudbury is confined to a hornblende-quartz-diorite, and is never found in the sub-layer norite (Naldrett, 1969). At Kaltberget, the abundant petrological and chemical evidence for the intrusion of a crystal mush, involving olivine and a high-Mg liquid, is incompatible with such an explanation. It must therefore be concluded that the Globular ores are the result of a metamorphic coagulation of sulfides, originally interstitial to primary igneous silicate phase.

The mineralisation associated with the Satellite Body at Kaltberget is of more problematical origin. However, the dominance of Stringer ore-types, together with the occurrence of monoclinic pyrrhotite, which has recently been demonstrated to be preferentially concentrated in zones of high strain (Kubler and Lindqvist, 1979), may indicate that, rather than a passive metamorphic coagulation of sulfides as in the Main Body (containing hexagonal pyrrhotite only), the ores of the Satellite Body have suffered a dynamic deformational remobilisation. It is therefore suggested that the Satellite Body is a small pod, tectonically separated from the adjacent, stratigraphically basal parts of the Main Body.

An explanation for the relatively barren nature of the Kletten ultramafic with regard to sulfide mineralisation, when compared with Kaltberget, may be sought in a comparison of olivine compositions. At Kaltberget, the average olivine has a Fo-content of 81.7 mole% and contains 0.17 wt% Ni. From Fig. 5.55c such a composition is consistent with crystallisation from a sulfur-saturated silicate magma. Furthermore, the average composition of Kletten olivines, $Fo_{87.1}$ and 0.06 wt% Ni, also indicates equilibration with a sulfide liquid. However, the much higher Ni-content of Kaltberget olivines suggests that they crystallised from a silicate melt which had been saturated

with respect to sulfur for a much smaller proportion of its history than the magma fractionating the Kletten olivines. It is possible that the Kletten magma may have separated a sulfide liquid at some time before its final emplacement, which by some means, possibly gravitationally controlled, became separated from its parent silicate melt. In contrast, the Kaltberget magma became sulfur-saturated at a much later stage in its history and may consequently have retained its sulfide melt until introduced to its present position. Alternatively, a flow controlled differentiation at Kletten (5.4) may have prevented concentration of a sulfide magma by gravitational processes (as at Kaltberget) such that the sulfides remain disseminated throughout the ultramafic body. A third possibility is that an unexposed zone of higher-grade sulfide mineralisation exists at Kletten. However, the good exposure over the northern parts of the body, together with the lack of any characteristic geophysical anomalies (unpubl. data - A/S Sulfidmalm) suggests that such an explanation is unlikely.

CHAPTER 6

GEOCHEMISTRY OF THE NICKEL-COPPER SULFIDE MINERALISATION

The geochemistry of the various nickel-copper ores described in Chapter 5 has been investigated. The samples studied are identified and classified according to ore-type and ore-grade in Appendix D. Information on bulk sulfide chemistry has been obtained for the Olkar, Skjaekerdalen, and Kaltberget Main Body prospects using atomic absorption and colorimetric methods (Appendix C). This is supplemented by data on Vakkerlien from Thompson (1978), and by assay analyses of Olkar and Kaltberget drill core made available by A/S Sulfidmalm. Mineral chemistry has been studied using a Cambridge Mark V electron microprobe at the University of Edinburgh (Appendix B).

In this chapter, element abundances are generally quoted as weight percents, or ratios thereof. However, in the case of pentlandite, the recent literature is dominated by the use of atomic percents. This convention is followed here, and where ratios of atomic percents are quoted as absolute values, they are identified as such.

Before entering into a discussion of ore chemistry, a brief summary of phase equilibria relating to magmatic sulfide ores is provided.

6.1 Phase Equilibria Relating to Magmatic Ni-Cu Ores.

It may be said of the vast majority of magmatic sulfide deposits that virtually the entire sulfide mass lies within the system Fe-Ni-Cu-S. In general pyrrhotite is the dominant phase present, with lesser and variable amounts of pentlandite, chalcopyrite, pyrite, and cubanite. Of the four ternary systems forming the boundaries of the Fe-Ni-Cu-S quaternary, Fe-Ni-S is by far the most important with regard to deposits of this nature. The general phase relations within this system were first outlined by Lundqvist (1947), and have since been considerably extended and refined.

Equilibria at high temperatures are dominated by an $(FeNi)_{1-x}S$ solid solution known as the monosulfide solid solution (Mss), which spans the system from a temperature of nearly 1000°C to below 400°C (Naldrett et al., 1967; Misra and Fleet, 1973) and possibly to 300°C (Craig, 1973). Considerable amounts of copper (up to 5% at 700°C, Yund and Kullerud, 1966) and Co may be accommodated in this phase. The bulk compositions of many magmatic sulfide deposits (Skinner and Barton, 1973), and of immiscible sulfide droplets in basaltic lavas (Skinner and Peck, 1969) suggest that they would crystallise initially as Mss, which may remain the only sulfide phase present until considerable cooling has taken place.

As cooling proceeds the sulfur-rich and sulfur-poor boundaries contract inwards until the Mss breaks down below 400°C (Misra and Fleet, 1973; Naldrett et al., 1967), or, as suggested by Craig (1973), below 300°C, to form a central miscibility gap. During this cooling sulfur rich compositions would exsolve pyrite, and eventually pentlandite at 212±13°C (Craig, 1973) while sulfur-poor assemblages will exsolve firstly a $(NiFe)_{3\pm x}S_2$ phase which at 610°C (Kullerud, 1963) reacts with Mss to form pentlandite, which at yet lower temperatures becomes the exsolving phase. Below 250°C the iron-rich portion of Mss in which the bulk compositions of many magmatic sulfide deposits lie, contracts towards pyrrhotite, exsolving pentlandite and pyrite (Craig, 1973; Misra and Fleet, 1973). The limited solid solution towards copper also contracts on cooling by exsolution of chalcopyrite and cubanite (Yund and Kullerud, 1966; Cabri, 1973).

A 400°C isothermal section of the Fe-Ni-S ternary system is presented in Fig. 6.1. The extent of the Mss phase at such temperatures is well demonstrated.

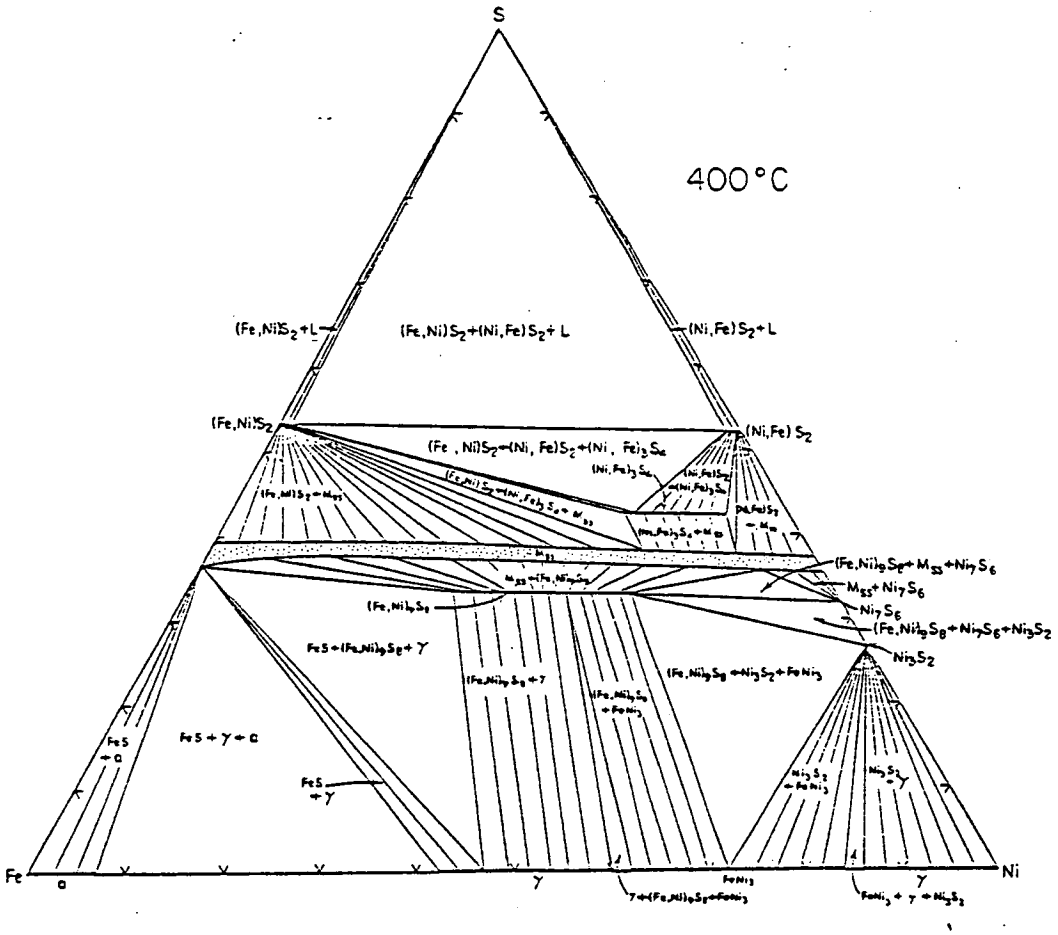

Fig. 6.1 Isothermal diagram of the Fe-Ni-S system at 400°C in the presence of vapour. (From Craig et al., 1967).

6.2 Bulk Sulfide Chemistry.

Table 6.1 presents partial analyses of bulk sulfides from Kaltberget Main Body, Olkar, and Skjaekerdalen, and Table 6.2 lists assay analyses of Ni, Cu, and S obtained by A/S Sulfidmalm.

Cu/Cu + Ni ratios (Table 6.1) are extremely variable at Olkar and at Skjaekerdalen, which agrees with their erratic modal pyrrhotite to chalcopyrite ratios (Chapter 5), and probably reflects secondary remobilisation of chalcopyrite. At Kaltberget however, much more consistent values are observed giving an average Cu/Cu + Ni ratio of 0.13. This is in reasonable agreement with the average of 76 assay analyses giving a value of 0.16. Cu/Cu + Ni ratios of individual samples of Vakkerlien ore are erratic, as at Olkar and Skjaekerdalen (Thompson, 1978), however, A/S Sulfidmalm tonnage calculations suggest an average ore grade of 1.08 %Ni and 0.39%Cu indicating an average Cu/Cu + Ni ratio of 0.26.

Considerable attention has been paid to the relationship between Cu/Ni ratios of magmatic sulfide ores and the composition of the host silicate magma (Wilson and Anderson, 1959; Naldrett and Cabri, 1976; Rajamani and Naldrett, 1978). The relationship has been quantified experimentally by Rajamani and Naldrett (1978) who found reasonable agreement with the reported compositions of naturally occurring magmatic ores and their host rocks, as shown in Fig. 6.2.

The possibility of differential mobility of chalcopyrite at Olkar and Skjaekerdalen limits the usefullness of the observed sulfide Cu/Cu + Ni values to estimates of host rock composition, and as will be shown later, the ores at Vakkerlien are probably considerably enriched in Ni as a consequence of metamorphic processes. However, at Kaltberget (Main Body) the more constant sulfide modal proportions and Cu/Cu + Ni ratios, together with the lack of Vein or Stringer ore-types, suggests

	Ni	Cu	Co	Fe	Cu/Cu+Ni	Ni/Co
OLKAR						
77/2/15.00	2.40	0.59	0.28	56.91	0.20	8.66
77/1/6.60a	1.79	0.06	0.17	58.59	0.03	10.26
77/3/8.65	1.44	0.28	0.12	53.92	0.16	11.89
77/4/31.56	1.01	0.09	0.12	55.93	0.08	8.67
77/4/23.70	0.64	0.19	0.10	43.78	0.23	6.53
77/2/14.90	1.79	0.56	0.19	57.33	0.24	9.21
SKJAEKERDALEN						
78/77	3.30	2.39	0.06	36.00	0.42	51.56
77·330	2.70	0.11	0.11	54.45	0.04	23.94
77·316	3.42	0.46	0.14	49.53	0.12	24.10
78·76	2.87	1.13	0.12	49.48	0.28	23.73
77·307*	0.81	0.82	0.12	53.10	0.50	6.95
78·71	3.22	1.19	0.16	53.63	0.35	20.02
77·300b	2.37	0.98	0.18	51.08	0.29	13.33
KALTBERGET						
77/12/4.30	6.05	1.36	0.23	51.70	0.18	25.88
77/8/21*	3.44	0.31	0.15	53.51	0.08	22.77
77/6/1.5	5.96	0.99	0.24	49.69	0.14	25.27
77/8/17.77	3.14	0.47	0.15	51.71	0.13	21.34
77/12/7.55	4.27	0.64	0.17	54.40	0.13	25.25

* Average of two analyses.

TABLE 6.1 Partial analyses of the sulfide fraction of ores from Olkar, Skjaekerdalen, and Kaltberget (Main Body), with some element ratios. (All values in wt%).

HOLE	DEPTH	Ni	Cu	S
OLKAR				
76/1	5.85 - 7.00	0.47	0.09	7.3
76/1	14.30 - 15.25	1.70	0.01	27.0
76/2	14.00 - 15.50	1.78	1.18	22.5
76/4	33.00 - 33.95	1.33	1.29	23.0
KALTBERGET				
76/6	0.00 - 1.00	0.56	0.04	2.2
76/6	1.00 - 2.00	2.25	0.36	9.2
76/6	2.00 - 3.00	0.44	0.07	1.8
76/12	2.70 - 3.00	1.05	0.23	6.0
76/12	3.00 - 4.00	0.68	0.14	4.0
76/12	4.00 - 5.00	2.25	0.50	10.8
76/12	5.00 - 6.00	1.62	0.32	7.4
76/12	6.00 - 7.00	2.25	0.41	9.9
76/12	7.00 - 8.00	1.15	0.23	5.9

TABLE 6.2 Assay analyses of Olkar and Kaltberget (Main Body) ore (all values in wt %). (Unpublished data - A/S Sulfidmalm).

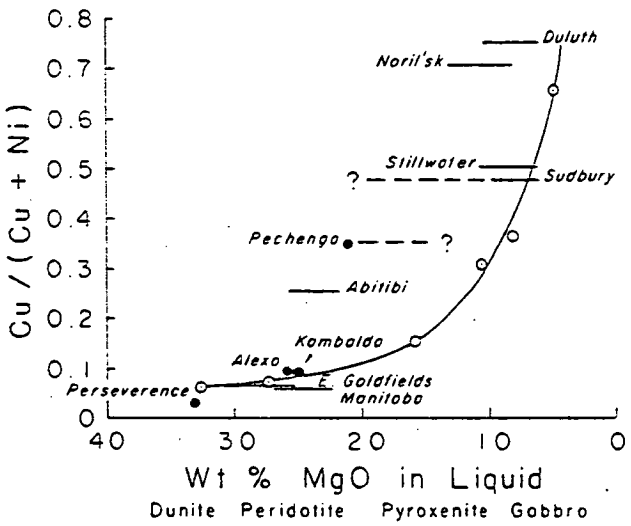

Fig. 6.2 Calculated relationship between Cu/Cu+Ni ratios of sulfide liquids and wt% MgO of komatiitic magmas, and observed compositions of magmatic sulfide deposits and their host rocks. (From Rajamani and Naldrett, 1978).

that little sulfide remobilisation has taken place. Furthermore, as will be explained later in this chapter, the chemistry of these ores probably represents their original magmatic composition. From Fig. 6.2, the compositions of sulfides at Kaltberget are consistent with equilibration with a silicate magma of between 15 and 20% MgO, which agrees well with estimates of liquid composition based on silicate mineral and bulk chemistry (Chapter 5).

Ni- and S-contents of Vakkerlien, Olkar, and Kaltberget ores are shown in Fig. 6.3. Data for Vakkerlien is from Thompson (1978), while for Olkar and Kaltberget the data presented in Table 6.2 are plotted. Average Ni/S ratios are indicated together with the average Ni/S ratio of sulfide ores from the Sudbury intrusive complex, Ontario. The ores at Sudbury are relatively undeformed, are thought to be associated with a basic silicate magma (Rajamani and Naldrett, 1978), and are probably the most intensely studied magmatic sulfide ores in the world. An average composition of the ores has not been published. However, an estimate has been attempted by using the average pyrite + pyrrhotite to pentlandite to chalcopyrite ratios suggested by Hawley (1962), and by assuming mineral compositions of pentlandite - $(Fe\ Ni)_9\ S_8$; chalcopyrite - $Cu\ Fe\ S_2$; and iron sulfides consisting of pyrrhotite and pyrite of average composition $Fe_7\ S_8$. An average composition of 52% Fe; 5% Ni; 5% Cu; and 38% S has been calculated. Fig. 6.3 demonstrates that, when compared with Sudbury, the ores at Kaltberget, and especially at Vakkerlien are considerably enriched in Ni relative to S, while those at Olkar are depleted.

A triangular Fe-Ni-Co diagram is presented in Fig. 6.4. The scaling factors used prevent the various ores from clustering close to the Fe-apex, without altering their relative positions. Average Ni/Co ratios are indicated together with an estimated average Ni/Co ratio for

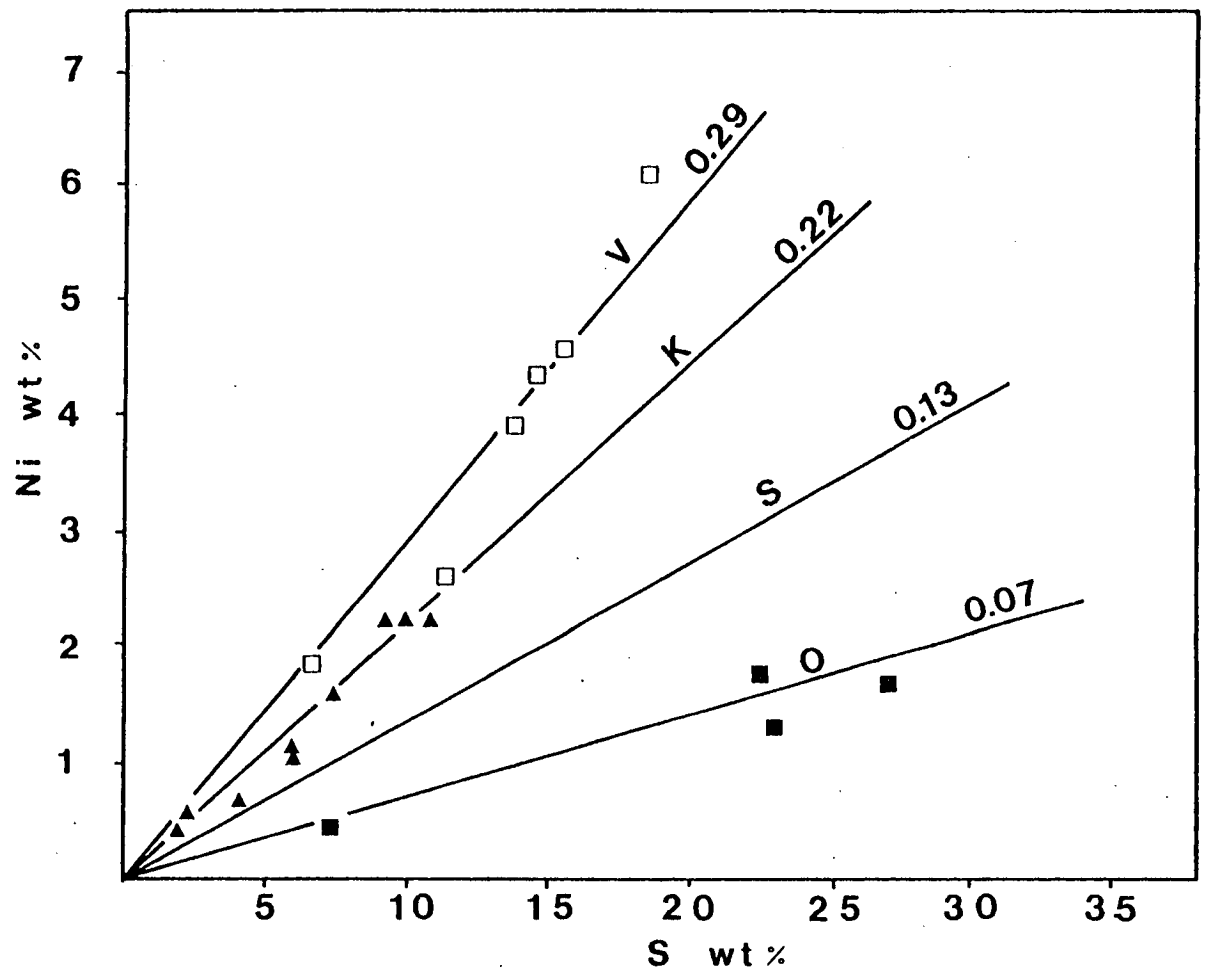

Fig. 6.3 Plot of Ni vs S for Olkar (solid squares); Vakkerlien (open squares); and Kaltberget Main Body (triangles) sulfides. Average Ni/S ratios are indicated (V - Vakkerlien; K - Kaltberget; O - Olkar) together with an average value for Sudbury, Ontario (S). See text for details.

Data from:
Vakkerlien - Thompson (1978)
Sudbury - Green (1975)
Olkar, Skjaekerdalen, and Kaltberget - this study (Table 6.1)

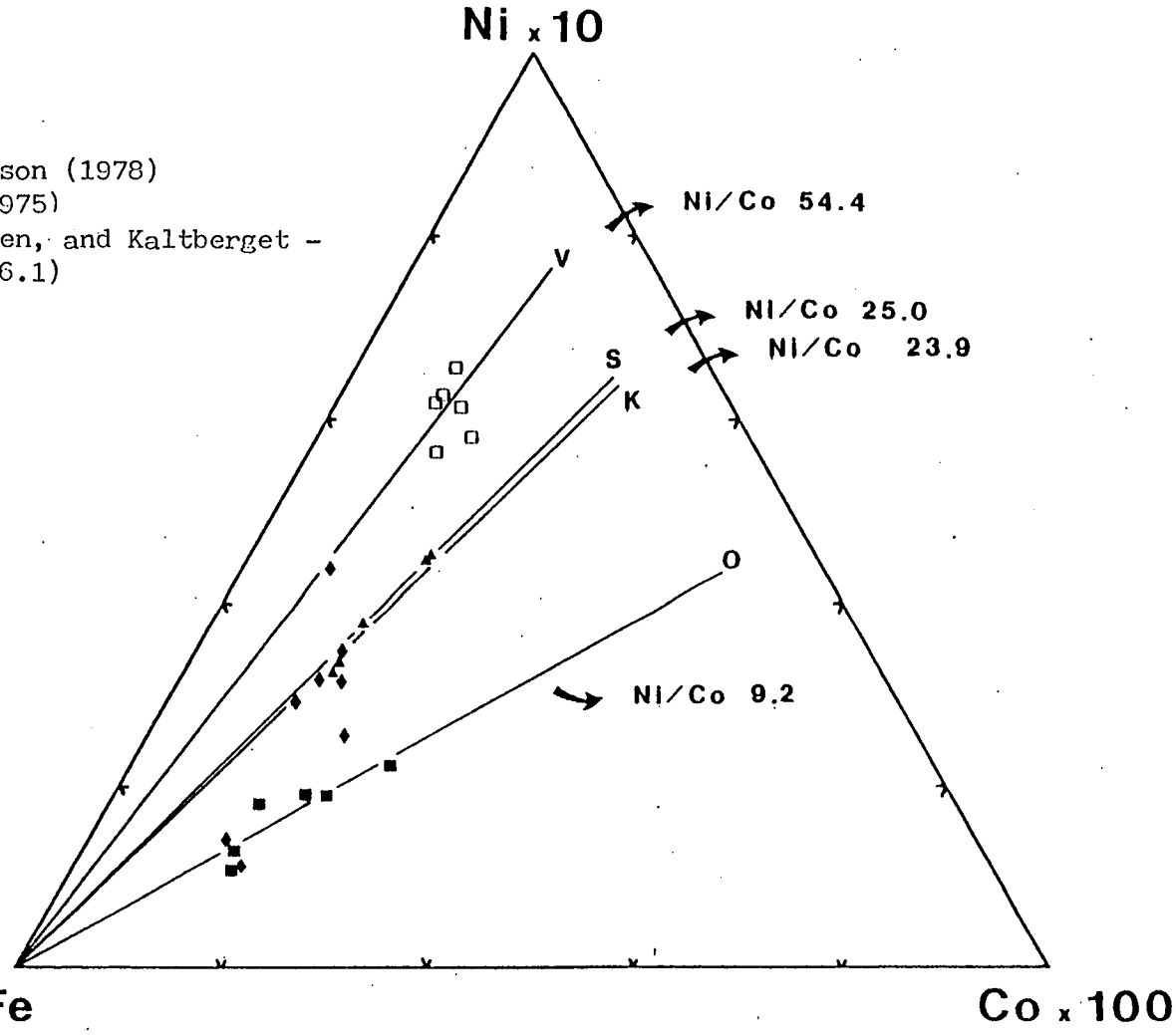

Fig. 6.4 Vakkerlien (open squares), Olkar (solid squares), Skjaekerdalen (diamonds), and Kaltberget Main Body (triangles) sulfides plotted on an Fe-Ni-Co diagram. Average Ni/Co ratios are indicated (V - Vakkerlien, O - Olkar, K - Kaltberget) together with a value for Sudbury sulfides (S).

Sudbury (Green, 1975). At Vakkerlien, considerable enrichment of Ni relative to Co (average Ni/Co ratio - 54.4) is apparent, while at Olkar (average Ni/Co ratio - 9.2) the ores are depleted in Ni when compared with Sudbury. Kaltberget and Skjaekerdalen display average Ni/Co ratios very similar to Sudbury (23.9 and 23.4 respectively), although the range for Skjaekerdalen ores is considerably greater than any of the other prospects, and the average has not been illustrated on the diagram.

Thompson (1978), using data from Green (1975), indicated a relationship between the Ni/Co ratio of sulfide ores and the composition of their host rocks. Such a relationship had previously been noted by Wilson and Anderson (1959) and Haakli (1963). In general Ni/Co in the ores decreases with MgO-content of the host, although the relationship is not nearly so obvious as that for Ni/Cu ratios. Ores associated with basic host rocks have Ni/Co ratios between 10 and 25, while deposits of komatiitic association (MgO > 30%) have values ranging from 75 at Nepean (Western Australia) to approximately 30 at Alexo (Ontario). The enrichment of Ni relative to Co at Vakkerlien is obviously enigmatic, while at Olkar, the Ni/Co ratio is somewhat low when compared with deposits on a world-wide basis. Skjaekerdalen shows highly variable values (Ni/Co ~7 to ~52), and Kaltberget cannot be considered inconsistent with a host silicate magma of 15-20% MgO.

Thompson (1978) suggested that the bulk chemistry of Vakkerlien ores, like that of so many magmatic sulfide deposits, was likely to lie in the field of Mss at 400°C. Although no complete analyses are available, the partial analyses presented in Tables 6.1 and 6.2, together with the pyrrhotite dominated modal compositions described in Chapter 5, would make it unlikely for any of the Gula magmatic sulfide ores to lie off the Mss field at such temperatures.

A discussion of the variation of bulk sulfide chemistry between deposits follows a description of sulfide mineral chemistry.

6.3 Sulfide Mineral Chemistry.

6.3.1 Pyrrhotite.

Pyrrhotite analyses from the various prospects are listed in Table B.18. In ores associated with metagabbroic intrusions, Ni + Co is always less than 1.0 wt%, in agreement with the data (Ni-contents only) of Papunen (1970); Vaughan et al. (1971); Graterol and Naldrett (1971); Harris and Nickel (1972), and Misra and Fleet (1973). Ni/Co varies from 0.3 to 9.2, and at Olkar, shows a tendency to be greater (3.2 to 7.8) in the Massive ores, than in the lower-grade varieties (0.3 to 4.0).

At Kaltberget Ni + Co may reach 1.2 wt% in the monoclinic pyrrhotite of the Satellite Body, but ranges from 0.4 to 0.9 wt% in the hexagonal pyrrhotite of the Main Body; Ni/Co ranges from 2.5 to 8.3. At Kletten Ni + Co is always less than 0.6, and Ni/Co ranges from 1.4 to 4.4.

In no case has it been possible to establish a relationship between Ni/Co ratio and the structure of the pyrrhotite phase.

6.3.2 Pyrite.

Pyrite analyses have been obtained from Olkar and Kletten, and are listed in Table B.21. Ni + Co varies from 0.1 to 4.5 wt%, with Ni generally less than 1.0 wt%, consistent with final equilibration below 143°C (Clark and Kullerud, 1963). Ni/Co ratios are highly variable and either Ni or Co may be dominant. The great variation of pyrite Ni- and Co-content is consistent with the previous data of Misra and Fleet (1973).

6.3.3 Chalcopyrite.

A small number of chalcopyrite analyses have been collected (Table B.20), confirming that this phase invariably approximates to a stoichiometric composition with only variable and trace amounts of Ni and Co.

6.3.4. Gersdorffite and Cobaltite.

Analyses of a single grain of gersdorffite, and of two grains of cobaltite have been obtained from Vakkerlien and Olkar respectively (Table B.22). Their compositions are plotted on Fig. 6.5, together with the limits of solid solution defined by Klemm (1965). Final equilibration at temperatures between 600 and 400°C are indicated.

6.3.5. Pentlandite.

A wide range of pentlandite compositions have been encountered (Table B.19). Harris and Nickel (1972) investigated the compositions of natural pentlandite from a variety of different sulfide assemblages. They showed that the Fe/Ni ratio of the pentlandite was characteristic of the associated sulfide assemblage. This study was extended to include both an experimental investigation of pentlandite phase relations, and a wider range of natural pentlandites by Misra and Fleet (1973). Their experimental study confirmed the conclusions of Harris and Nickel (1972) with regard to the systematic variation of pentlandite Fe/Ni ratio with sulfide assemblage, and described a wide range of Co-content in pentlandites from 0 to 52.6 at%. They interpreted the solid solution between Co-free pentlandite and the isostructural Co-pentlandite (Co_9S_8, Knop and Ibrahim, 1961; Geller, 1962) as a process of substitution of Co for both Fe and Ni in the structure and demonstrated that partition of the Co proportional to the Fe- and Ni-contents of the pentlandites did not significantly alter the variation in pentlandite composition with assemblage. The variation in pentlandite Ni* (where Ni* = Ni + (Ni/(Ni + Fe))x Co) for the different sulfide assemblages in the various Gula prospects are compared with those outlined by Misra and Fleet (1973) in Fig. 6.6, to which has been added the data of Barrett et al. (1976) for the assemblage hexagonal pyrrhotite + pentlandite. Close agreement is demonstrated between the published data and

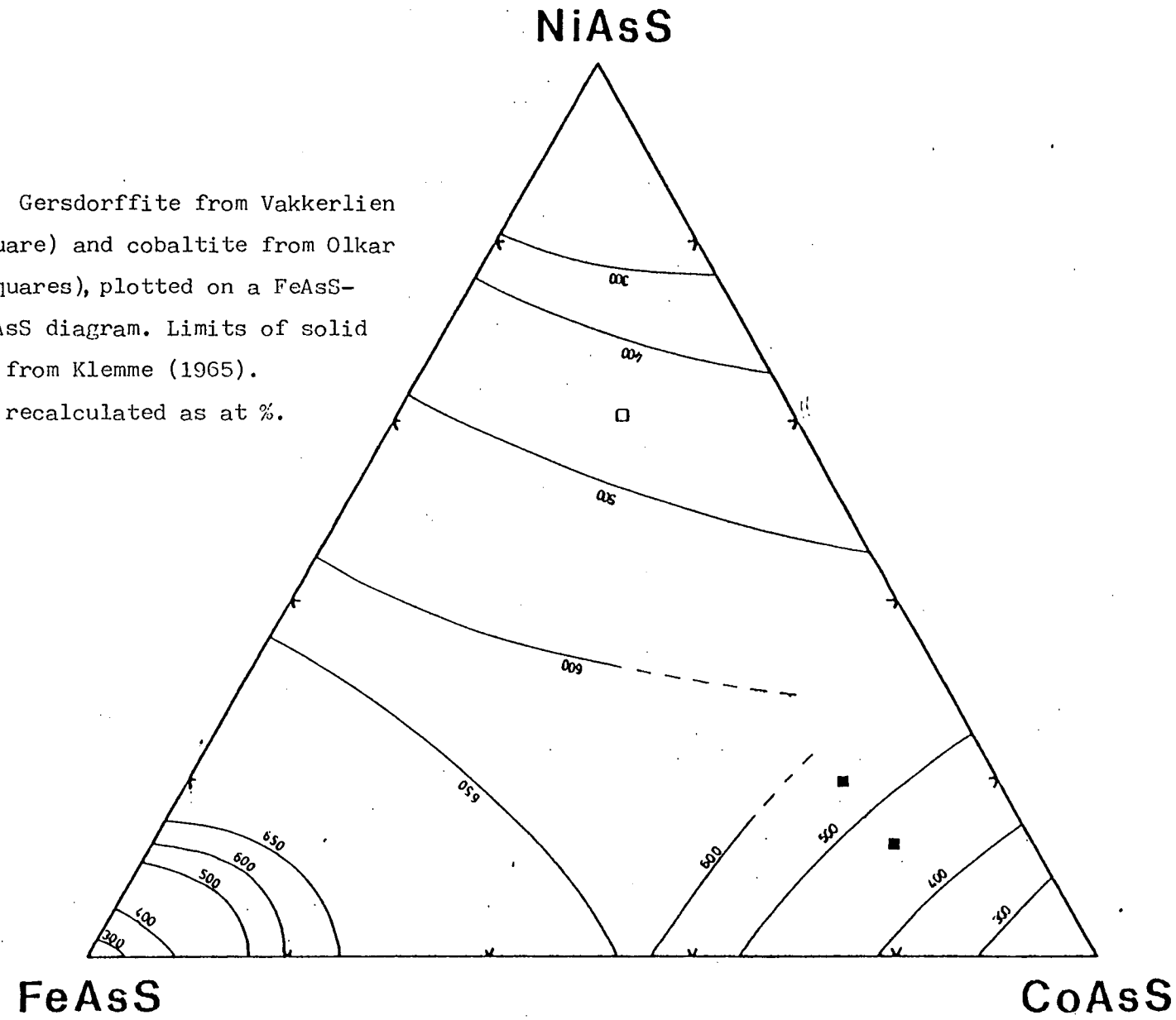

Fig. 6.5 Gersdorffite from Vakkerlien (open square) and cobaltite from Olkar (solid squares), plotted on a FeAsS-NiAsS-CoAsS diagram. Limits of solid solution from Klemme (1965). Analyses recalculated as at %.

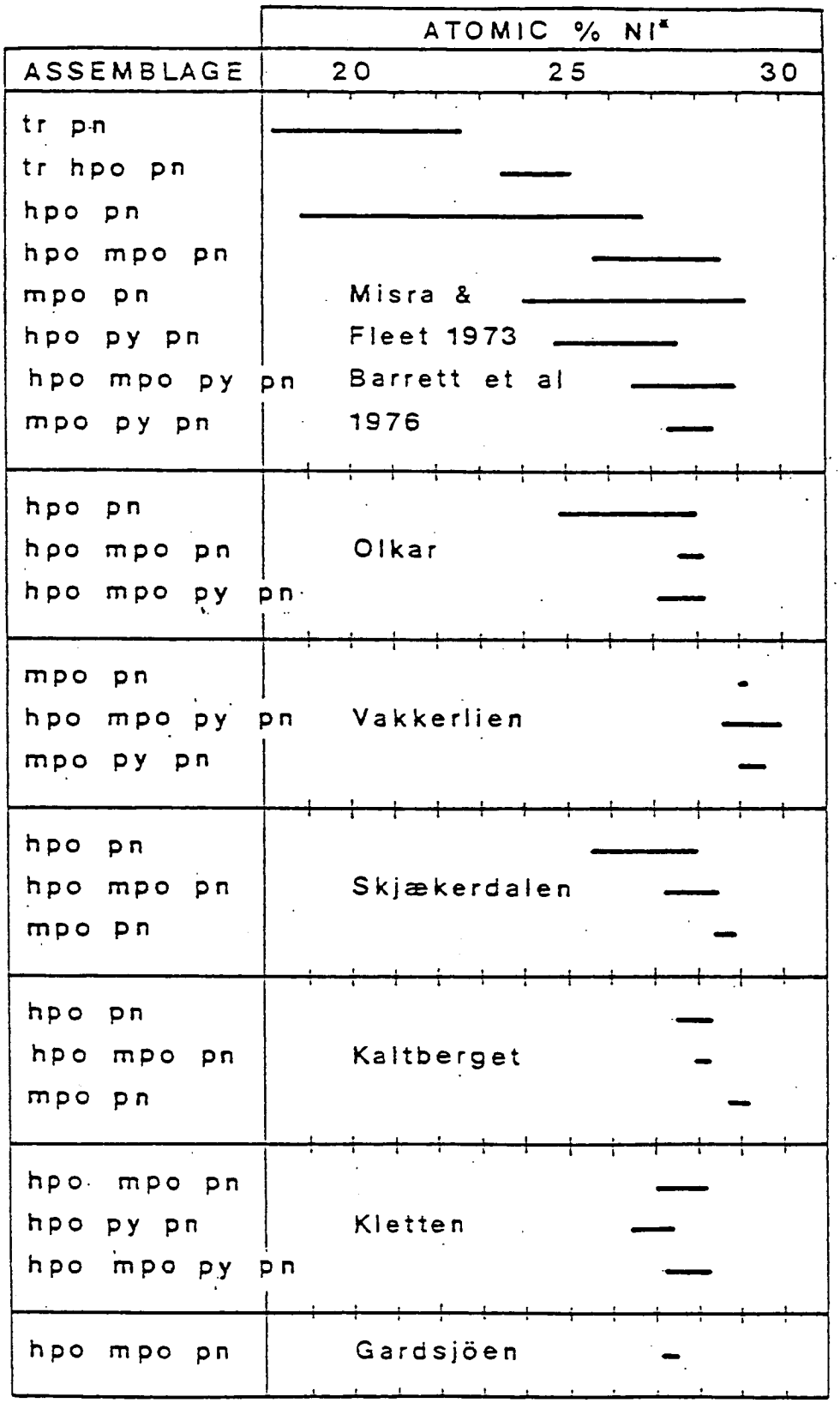

Fig. 6.6 Compositions of pentlandites from Gula mafic and ultramafic hosted magmatic sulfides, compared with data from Misra and Fleet (1973) and Barrett et al (1976). pn - pentlandite; tr - troilite; hpo - hexagonal pyrrhotite; mpo - monoclinic pyrrhotite; py - pyrite.

that obtained in this study, confirming the lack of any optical identification of a troilite phase.

A striking variation of pentlandite Co-content is exhibited both between, and within the Gula prospects. These variations are illustrated in Figs. 6.8-6.13 in which pentlandite compositions are projected from S onto the Fe-Ni-Co side of the Fe-Ni-Co-S tetrahedron (Fig. 6.7). At Vakkerlien the atomic Fe/Ni ratios of pentlandites vary from 0.76 to 0.86, while Co has a fairly restricted range of 0.68 to 1.05 at% (Fig. 6.8). There is little variation in Fe/Ni ratios or in Co-contents between the Matrix and the Disseminated ores. Also shown on Fig. 6.8 is the field of pentlandite compositions obtained by Thompson (1978).

Olkar (Fig. 6.9) shows a much wider range of pentlandite composition. Atomic Fe/Ni ratios are somewhat greater than at Vakkerlien, ranging from 0.87 to 1.18, while Co-contents show a wide range from 3.69 to 13.83 at%, and are obviously related to the grade of the ore in which the pentlandite occurs. Massive ores in general contain the least Co (4.09 to 4.98 at%), while Finely Disseminated ores are the most Co-rich (5.26-13.83 at%). Matrix and Disseminated ores have intermediate Co-contents, while stringer ore has a range of compositions from that typical of Massive ore to that typical of Disseminated ore.

At Gardsjoen, only one sample (Finely Disseminated ore) was found to contain unaltered pentlandite, which has an average atomic Fe/Ni ratio of 0.94 and extremely high Co-contents ranging from 12.60 to 17.09 at% as shown on Fig. 6.10.

Skjaekerdalen is characterised by pentlandites ranging in atomic Fe/Ni ratio from 0.84 to 1.07 and in Co-content from 0.64 to 8.43 at%. However, Fig. 6.11 demonstrates that in this instance there is no systematic variation of composition with ore-grade.

The Kletten ultramafic displays a considerable range of pentlandite

Fig. 6.7 Fe-Ni-Co side of the Fe-Ni-Co-S tetrahedron illustrating the location of the triangle plotted in Figs. 6.8-6.13, and an explanation of the symbols used. Analyses are recalculated as atomic %.

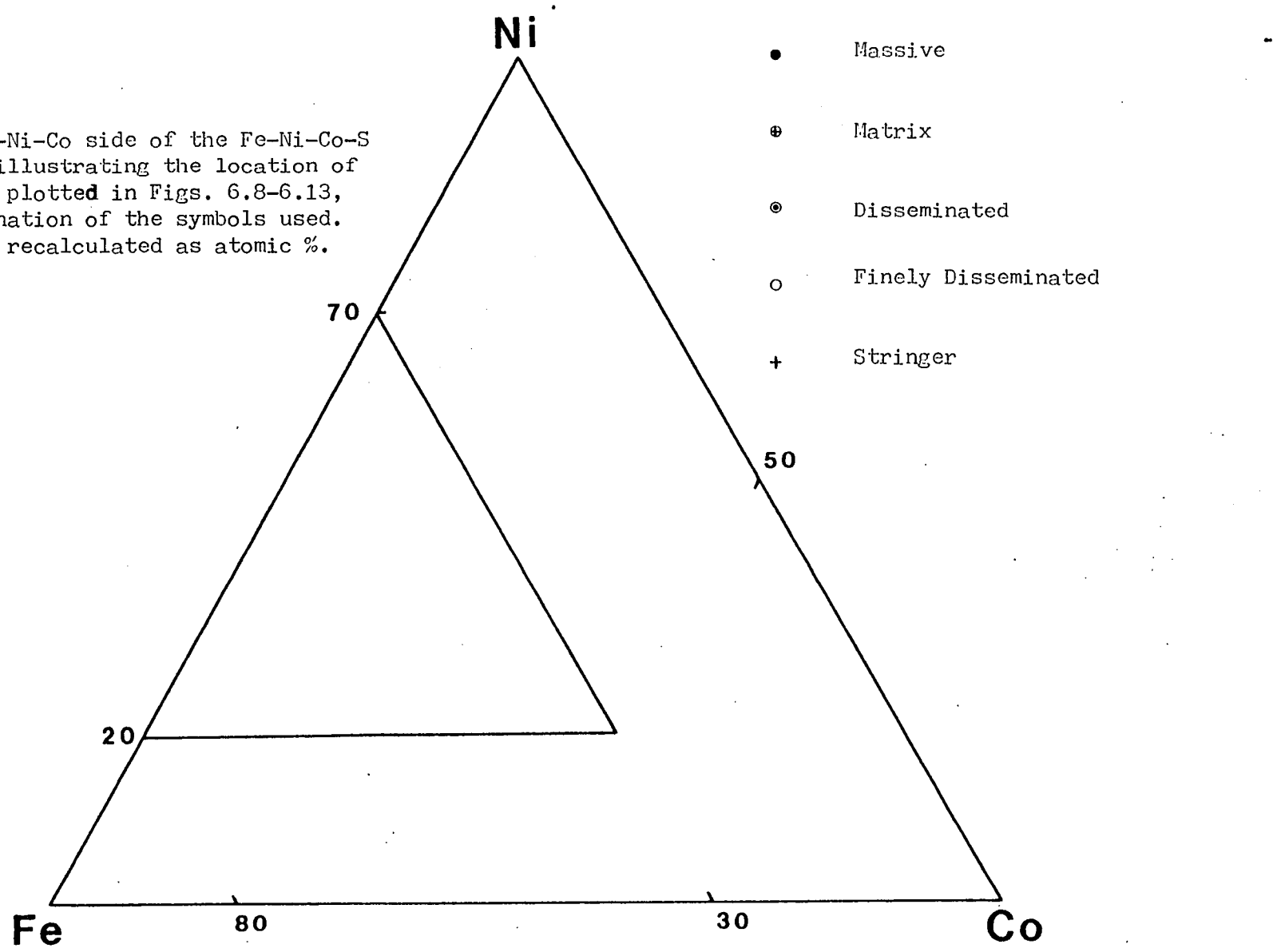

Fig. 6.8 Compositions of Vakkerlien pentlandites. See Fig. 6.7 for explanation. Dotted line encloses analyses from Thompson (1978).

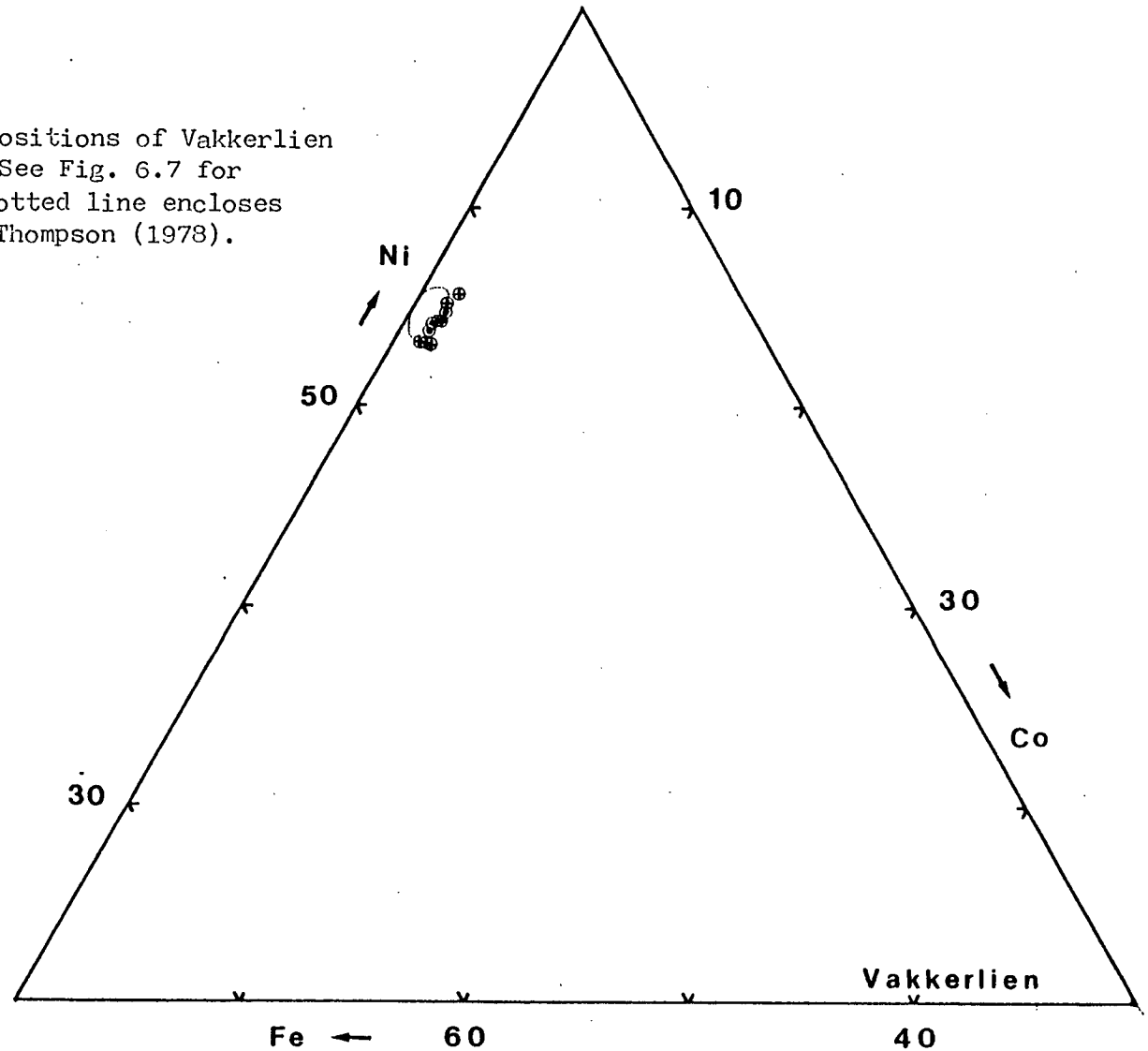

Fig. 6.9 Compositions of Olkar pentlandites. See Fig. 6.7 for explanation.

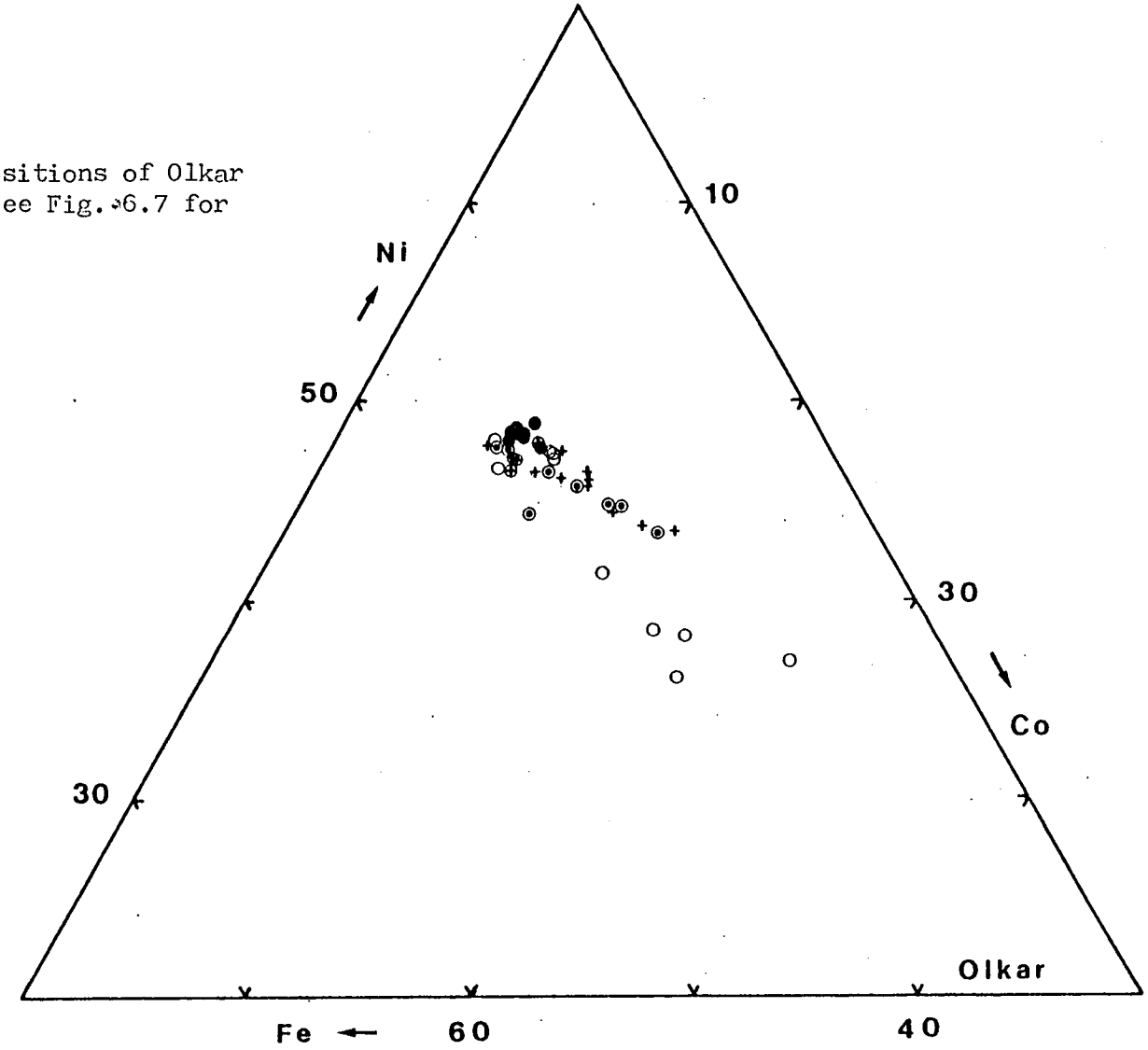

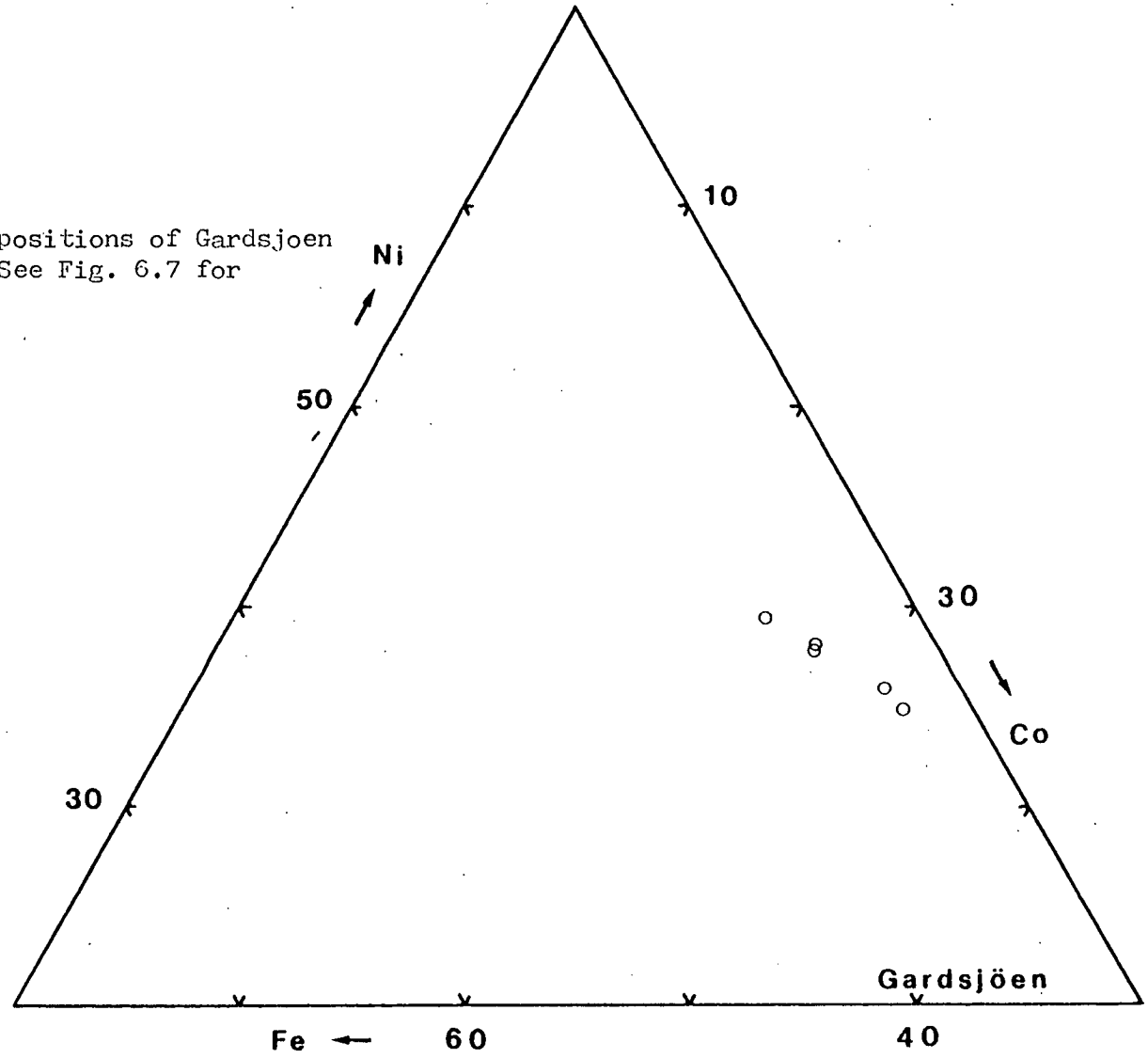

Fig. 6.10 Compositions of Gardsjoen pentlandites. See Fig. 6.7 for explanation.

Fig. 6.11 Compositions of Skjaekerdalen pentlandites. See Fig. 6.7 for explanation.

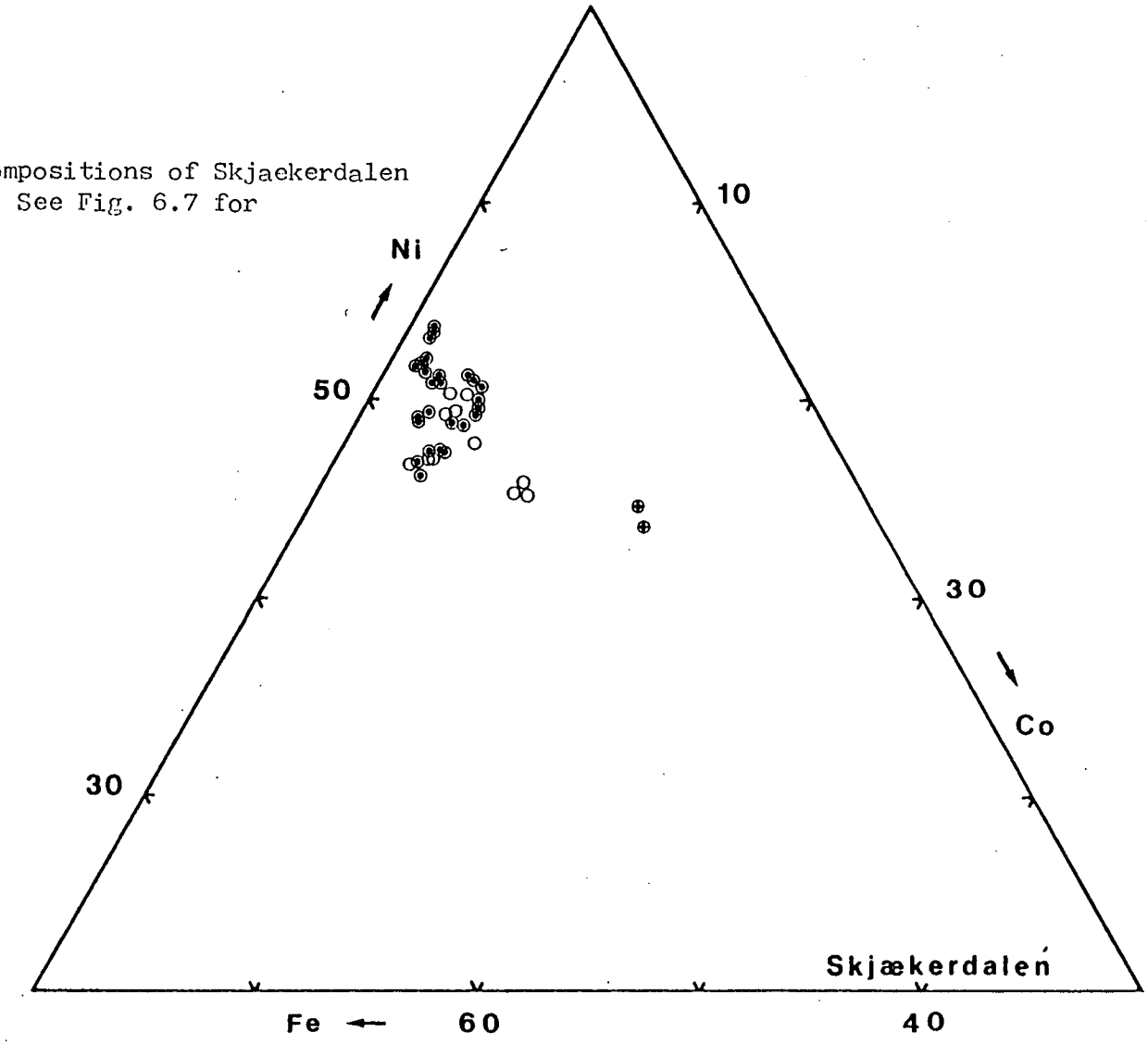

Fig. 6.12 Compositions of Kletten pentlandites. See Fig. 6.7 for explanation.

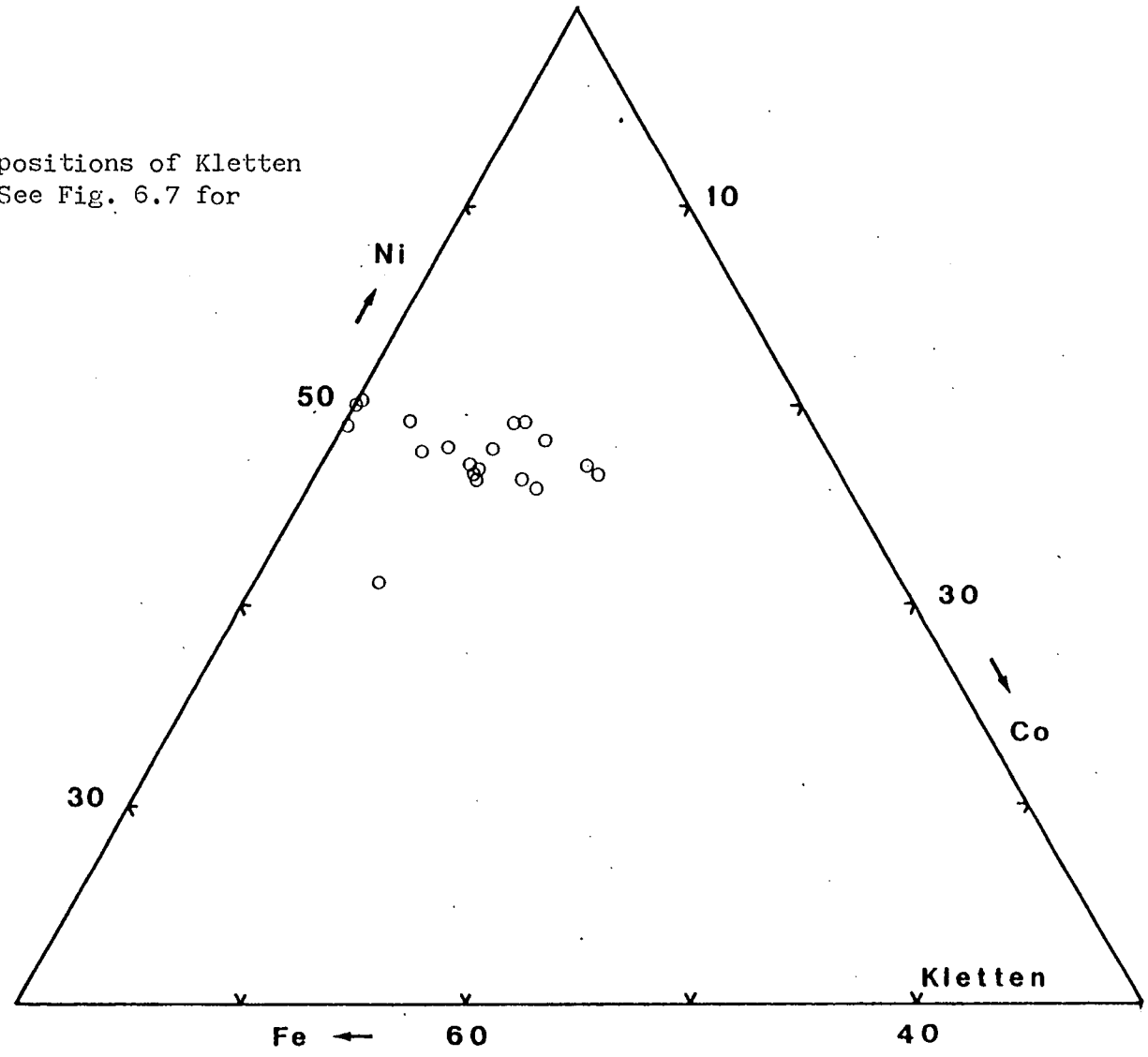

Fig. 6.13 Compositions of Kaltberget pentlandites. See Fig. 6.7 for explanation. Stippled area indicates probable range of Co-contents of original pentlandites in sample 76.245 (see text and Fig. 6.20 for explanation).

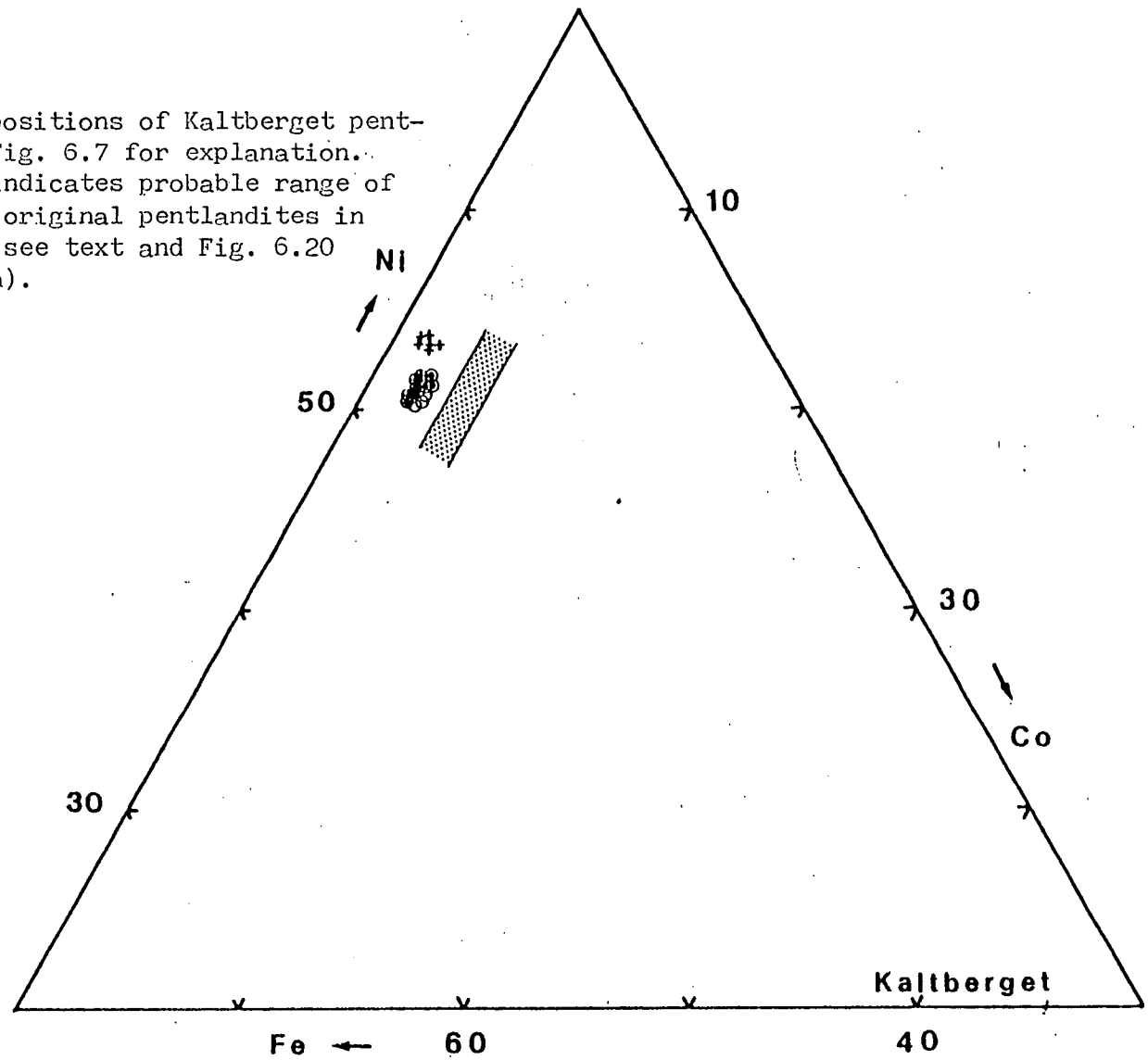

compositions, all of which are associated with Finely Disseminated ore (Fig. 6.12). Atomic Fe/Ni ratios vary from 0.87 to 1.03, while Co-content varies from 0.09 to 6.71 at%. At Kaltberget, pentlandite associated with monoclinic pyrrhotite from the Satellite Body has lower atomic Fe/Ni ratios (0.83 to 0.85) and lower Co-contents 0.64 to 1.17 at%, than pentlandite associated with hexagonal pyrrhotite from the Main Body (0.89 to 0.94 and 1.13 to 1.55 at% respectively). Close inspection of Fig. 6.13 shows that Disseminated and Finely Disseminated ores have slightly higher Co-contents than the Matrix ores.

It is apparent from Figs. 6.8-6.13 that two controls are operating on pentlandite composition. The relationship between Fe/Ni ratio and the coexisting pyrrhotite phase is clearly seen in Fig. 6.14, where pentlandites coexisting with monoclinic pyrrhotite only are obviously enriched in Ni relative to those coexisting with hexagonal pyrrhotite only. Pentlandites coexisting with both hexagonal and monoclinic pyrrhotite are characterised by a wider range of Fe/Ni ratios, almost totally embracing the hexagonal and monoclinic pyrrhotite-only fields.

The second control relates to Co-content, which, with the exception of pentlandites at Vakkerlien, where little variation occurs, and Skjaekerdalen, is controlled to a greater or lesser extent by the grade of the ore with which it is associated (i.e. by the proportion of sulfide to silicate minerals present in the ore). In general, pentlandites associated with Massive ores contain less Co, and have higher Ni/Co ratios, than those from Disseminated ores. Fig. 6.15 demonstrates that the Ni/Co ratio of pentlandites is directly related to Ni/Co in the bulk sulfide.

The majority of pentlandites occurring in magmatic sulfide ores contain less than 2.0 wt% Co. However, Knop and Ibrahim (1961) demonstrated experimentally the existence at room temperature of a pentlandite

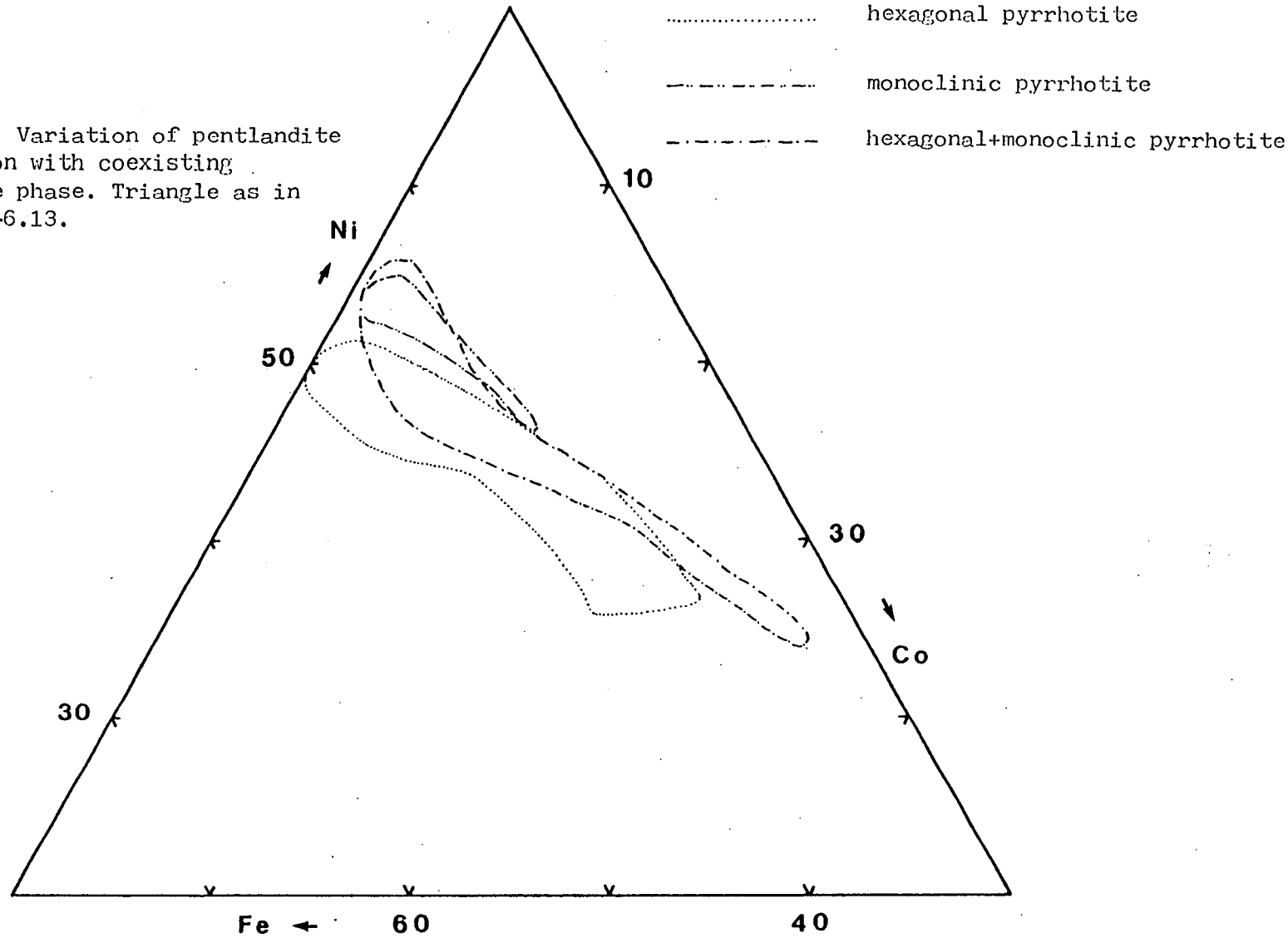

Fig. 6.14 Variation of pentlandite composition with coexisting pyrrhotite phase. Triangle as in Figs. 6.8-6.13.

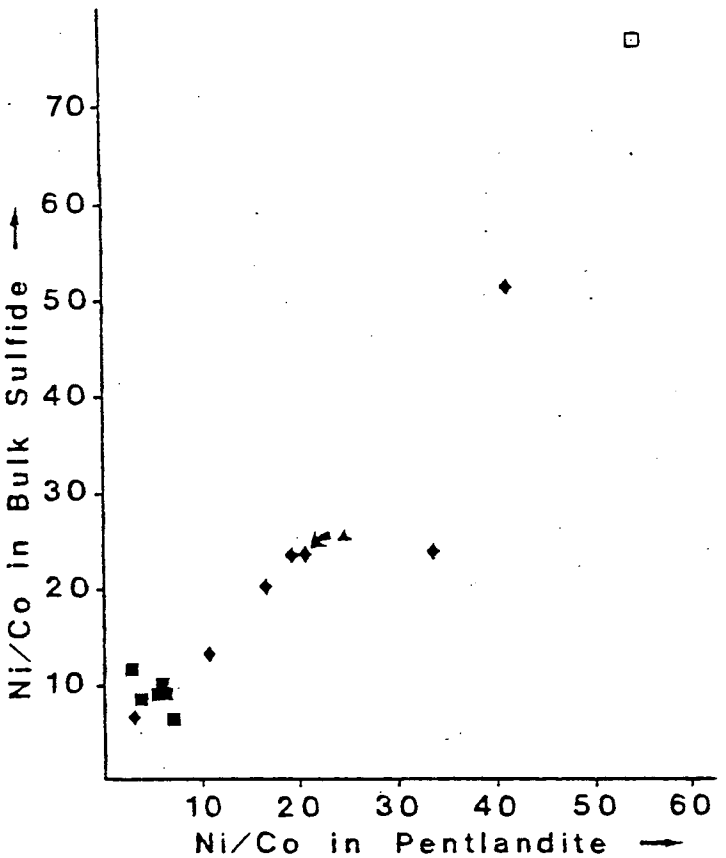

Fig. 6.15 Relationship of pentlandite Ni/Co (weight) ratio to bulk-sulfide Ni/Co (weight) ratio. Individual samples are plotted for Olkar (solid squares) and Skjaekerdalen (diamonds). For Vakkerlien (open square) and Kaltberget (triangle) average values are indicated, but it is emphasised that the pentlandite analyses and the bulk-sulfide analyses were obtained from different samples. Vakkerlien data from Thompson (1978).

solid solution, over wide composition limits, in or close to, the M_9 S_8 - section of the quaternary system Fe-Ni-Co-S. The limits of this solid solution are shown in Fig. 6.17. Natural pentlandites approaching the Co-end member of this solid solution have been recorded (Petruk et al., 1969; Stumpfl and Clark, 1964) but these generally occur in low-temperature, hydrothermal-vein environments. Analyses from the literature of Co-rich pentlandites (>2 wt%) occurring in association with metamorphosed mafic and ultramafic igneous rocks are presented in Fig. 6.16. The sulfide assemblages with which these pentlandites are associated are outlined in Fig. 6.17, from which it is clear that not only are the Fe/Ni ratios of the pentlandites dependent on the sulfide assemblages, as indicated by Harris and Nickel (1972) and Misra and Fleet (1973), but that their Co-contents are also so controlled.

It has been shown by a number of workers (Chamberlain et al., 1965; Ramdohr, 1967; Hudson, 1973; Groves et al., 1974; Eckstrand, 1975; Naldrett, 1966, and subsequent revision 1973), that during the metamorphism of ultramafic rocks, nickel is redistributed amongst the secondary minerals and may be preferentially concentrated into any magmatic sulfide phases present. In each case the evidence cited for Ni-redistribution is the occurrence of unusual, highly nickeliferous opaque mineral assemblages disseminated through the altered ultramafics. Where more massive ores are present in association with the nickeliferous disseminations (Hudson, 1973; Naldrett, 1966, 1973), they are characterised by more Fe-rich assemblages typical of magmatic sulfides. These observations lead Naldrett and Turner (1977) to suggest that the process of Ni-redistribution operates essentially as a closed system, such that the effect on sulfide bulk chemistry, and hence on sulfide mineralogy, is inversely proportional to the amount of sulfide present; large amounts of sulfide "swamping out" the relatively much smaller

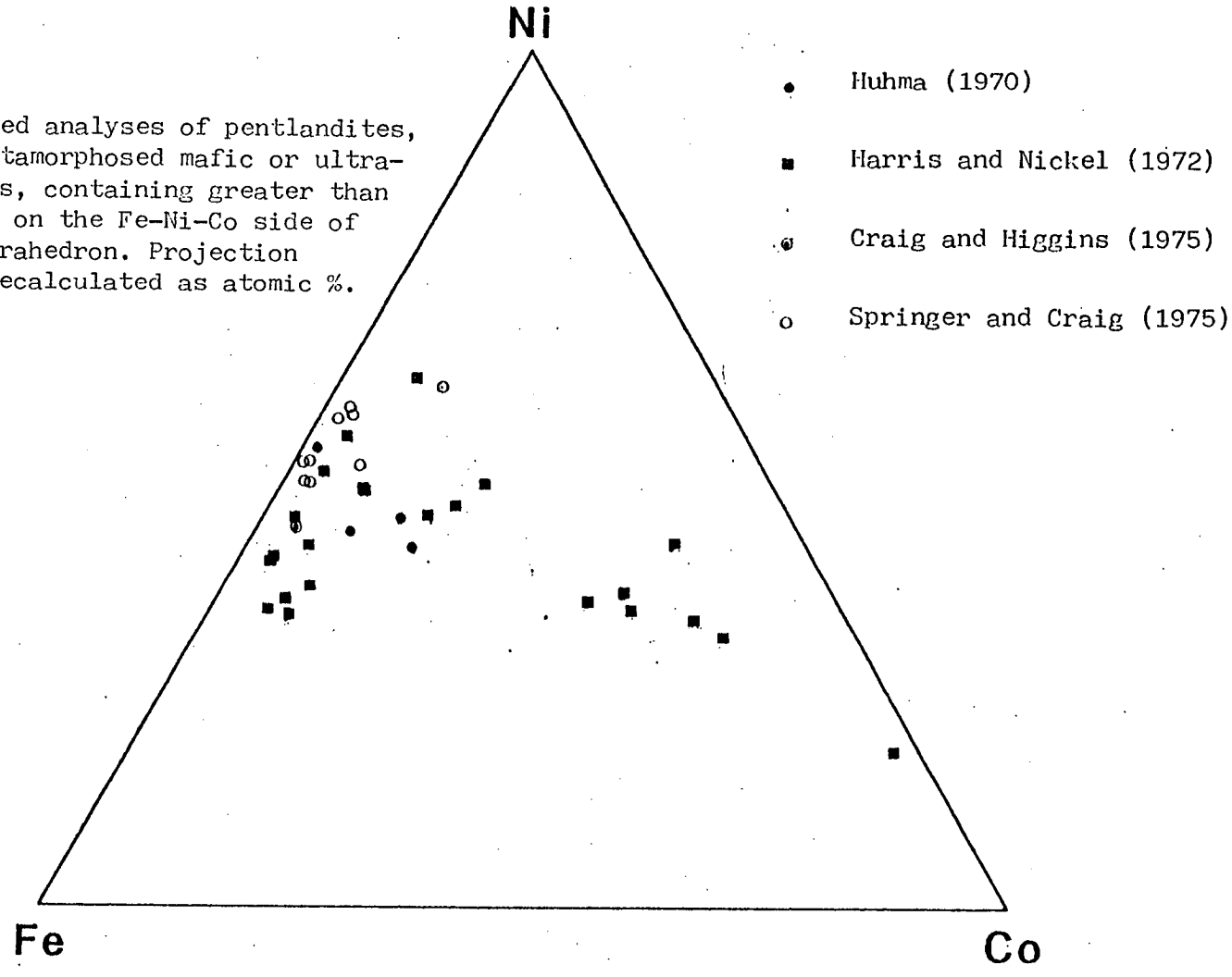

Fig. 6.16 Published analyses of pentlandites, associated with metamorphosed mafic or ultramafic igneous rocks, containing greater than 2 wt % Co, plotted on the Fe-Ni-Co side of the Fe-Ni-Co-S tetrahedron. Projection from S. Analyses recalculated as atomic %.

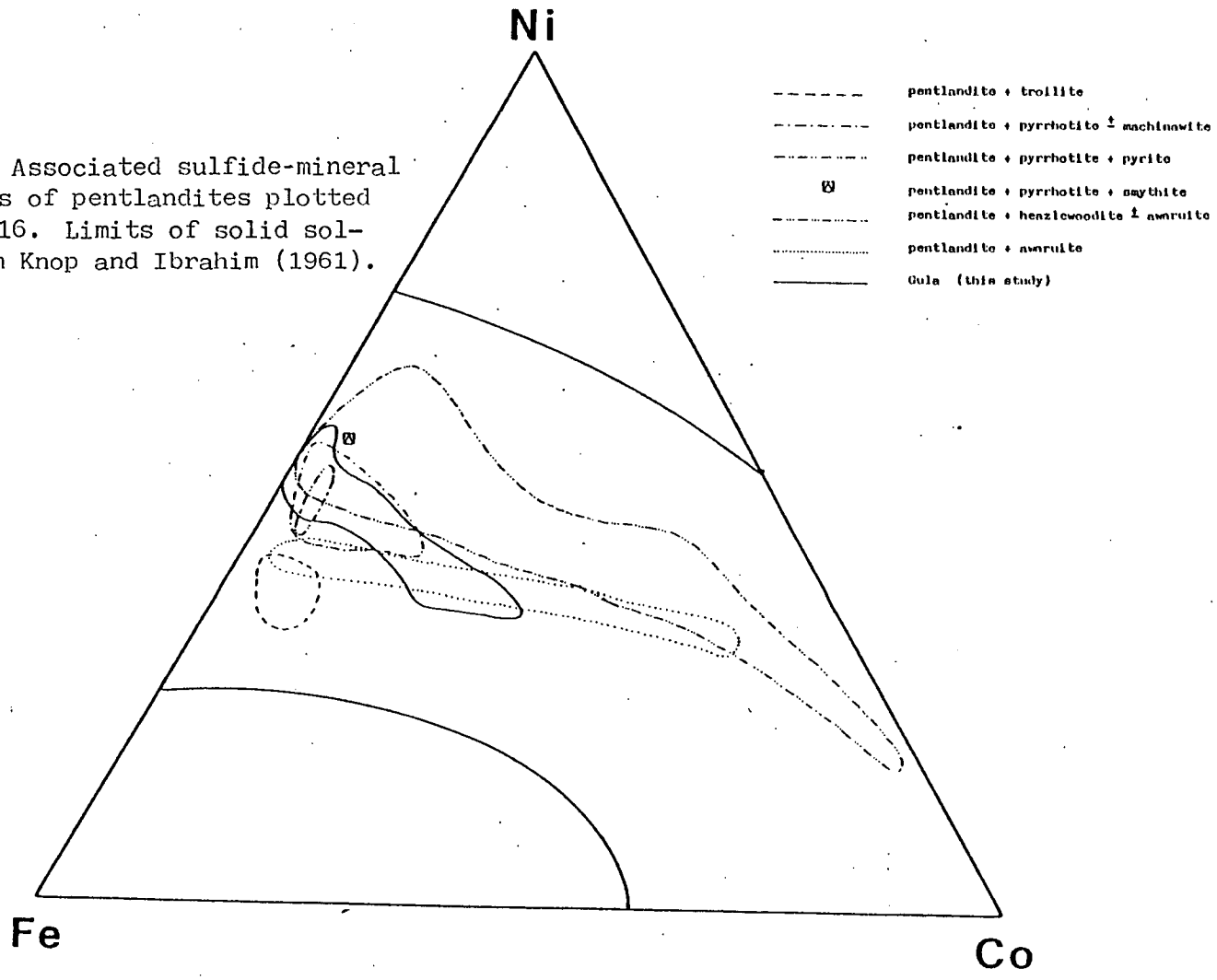

Fig. 6.17 Associated sulfide-mineral assemblages of pentlandites plotted on Fig. 6.16. Limits of solid solution from Knop and Ibrahim (1961).

contribution from the silicates, and suffering little change in composition as a result. However, if only small proportions of sulfides are present, the Ni-content of the bulk sulfides will increase significantly, such that the Fe-Ni sulfide assemblage will change in the following sequence:

pyrrhotite plus pentlandite;
to pentlandite;
to pentlandite plus millerite, or
pentlandite plus millerite plus heazlewoodite;
to pentlandite plux heazlewoodite plus awurite;
to pentlandite plus awurite.

As the Ni-content of the bulk sulfide increases (i.e. as the assemblage changes as described above) so the Ni-content of the associated pentlandite increases as outlined by Harris and Nickel (1972) and Misra and Fleet (1973). Fig. 6.17 suggests that Co sometimes behaves in a similar fashion to Ni. This is supported by the observations of Hudson (1973), who reported variations in sulfide assemblage, and in Co-content of associated pentlandites, through a systematically sampled drill intersection at the Nepean Ni-deposit of metamorphosed komatiitic association in Western Australia. Pentlandites within the basal Main Ore Zone are associated with pyrrhotite and pyrite and contain less than 1.0 wt% Co. On moving upwards through the Disseminated Ore Zone, characterised by pyrrhotite plus pentlandite or pentlandite only assemblages, the pentlandite Co-content increases gradually, over a distance of about 4m, to approximately 2.5 wt%. In the rare disseminations of sulfides in the overlying ultramafic, pentlandite is associated with millerite and heazlewoodite, and may contain more than 10 wt% Co. While Hudson (1973) did not consider any explanation for the variation in pentlandite Co-content, a metamorphic redistribution of this element between silicates

and sulfides must be considered. The possibility that such a process controls the relationship between ore-grade and pentlandite Co-content will be discussed more fully later in this chapter.

6.4 Discussion and Possible Explanation of Sulfide Chemistry.

6.4.1. Ores of metagabbro association.

Any interpretation of the origin of the sulfide ores associated with the metagabbros must account for:

a) the variation in structural relationships between sulfides and host rocks;

b) the variation in bulk sulfide chemistry between deposits;

and c) the variation of mineral chemistry both between, and within deposits.

As will become apparent below, these characteristics may be very much inter-related.

The structural relationships between host rocks and sulfides at Vakkerlien are not easily explained. The mineralisation lies along the centre of the Main Body. It is located in the general vicinity of the contact between the ultramafic and metagabbroic rock types, and may be hosted by either lithology (Fig. 5.3). The Main Body, and the closely associated Second Body, are elongated, pencil-like masses plunging gently towards the SE within the foliation, and parallel to the regional D_1 lineation in this area. This lineation parallels the orientation of D_1-fold hinges (Chapter 3). Thompson (1978) suggested that competence difference between an isoclinally-folded basic intrusive sheet and its enclosing country rocks might result in attenuation of fold limbs, and eventual isolation of hinge zones. He proposed that the Vakkerlien intrusive bodies represented examples of such isolated fold

hinges. This hypothesis is supported by the spatial distribution of metagabbroic and ultramafic lithologies within the Vakkerlien Bodies (Fig. 5.3), and is accepted in this thesis.

With regard to the central location of the ore within the Main Body, Thompson (1978) argued that interstitial textures between sulfides and silicates throughout much of the orebody demands that the sulfides are in their original magmatic position, with Massive-Breccia, and Stringer ores representing limited local remobilisation. He concluded that there was an original magmatic accumulation of sulfides close to the boundary between the ultramafic and metagabbroic lithologies. To explain this he proposed an early input of barren silicate magma followed by a second influx carrying an immiscible sulfide liquid. He further suggested that the Ni-rich nature of the Vakkerlien ore is a result of the metamorphic redistribution of silicate nickel into the sulfides. However, it has been pointed out above (6.3.5) that such processes act essentially as closed systems (Naldrett and Turner, 1977), such that the effect on bulk sulfide chemistry is inversely related to the proportion of sulfide to silicate phases present. If a primary accumulation of magmatic sulfides is accepted, then the Ni-enrichment of the ores remains unexplained.

It has previously been suggested that the bulk compositions of Gula magmatic sulfides are likely to lie on the field of Mss at temperatures above about 400°C. This implies that, throughout at least a proportion of the deformation associated with D_1, the sulfides would have been present as a single phase (Mss). Experimental studies (Clark and Kelly, 1973; Zolotuklein et al., 1972) have shown that pyrrhotite behaves in a ductile fashion at temperatures above 250°C at 1000 bars. Assuming that Mss has similar mechanical properties to pyrrhotite, it is reasonable to suggest that during D_1 the sulfides

would have been less competent than the silicate host rocks. They might, therefore, have been susceptiable to recrystallisation and concentration into structural traps.

There are a number of structures associated with fold hinges to which sulfides might migrate during deformation. Where folding is flexural in character, spaces may develop (Fig. 6.18) between layers on the hinge, if the shapes of layer boundaries are not the same (Spencer, 1969, pp. 185). The separation between the layers may be progressively or subsequently filled by recrystallised material from the surrounding rocks, and the saddle-shaped veins so formed are known as saddle-reefs. Sulfides might also migrate to fill crestal-tension fractures (Fig. 6.18) forming on the outer arches of concentric folds (Sitter, 1956, pp. 199), or to zones of no finite strain (Fig. 6.18), which, according to layer thickness and competence, may occur on fold hinges (e.g. Roberts and Stromgard, 1972).

The development of any one of these features, or a combination thereof, might result in the concentration of originally disseminated sulfides within the Vakkerlien intrusion into a zone at, or close to the boundary between the ultramafic and metagabbroic lithologies.

The relative timing and intensity of deformation and metamorphism would be important in determining the dominant controls on sulfide migration. It might be expected that saddle-reefs and tension fractures would develop only at temperatures at which the metagabbroic and ultramafic lithologies would behave in a brittle fashion. In contrast, the development of zones of no finite strain requires only a competence difference between layers (Roberts and Stromgard, 1972), and might therefore be more important at higher temperatures. In this context the geology of the Central Victorian Goldfields and the Broken Hill Deposit in Australia provide interesting comparisons.

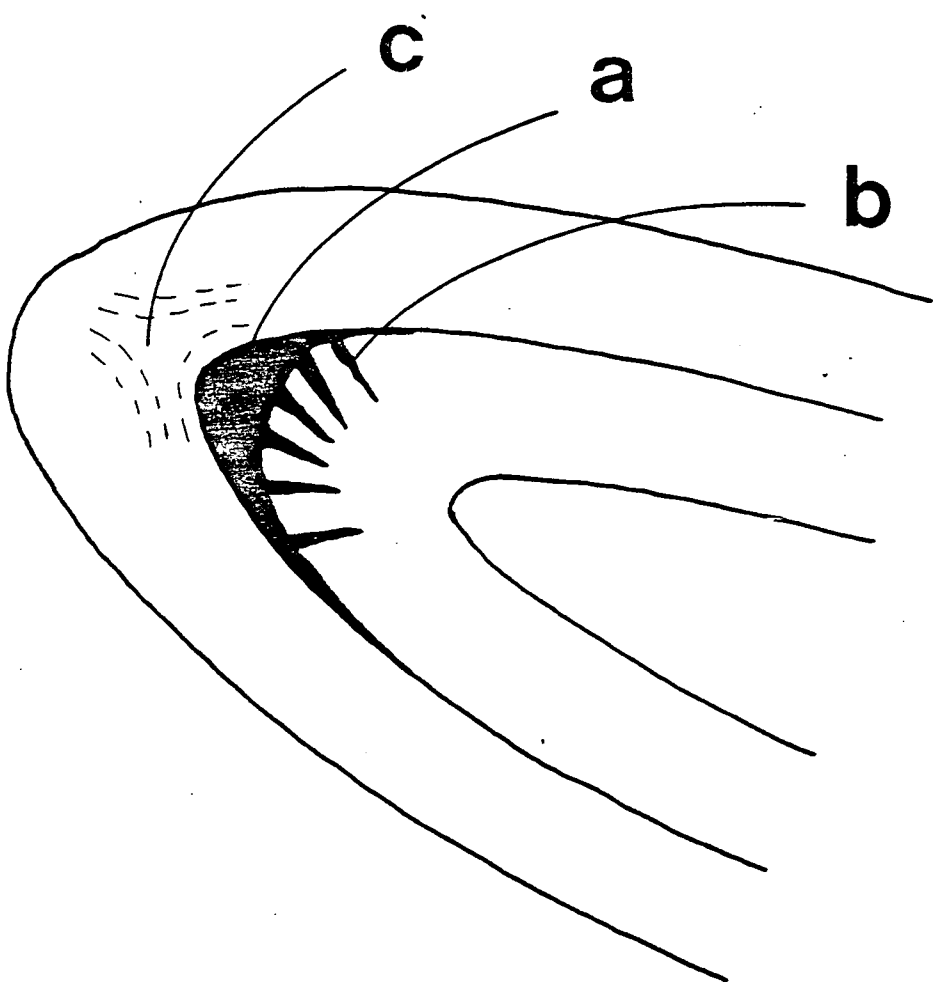

Fig. 6.18 Structures associated with fold hinges to which sulfides might migrate during deformation. a) saddle reef; b) crestal-tension fractures; c) zone of no finite strain (lines indicate long axes of strain-ellipsoids.

The Central Victorian Goldfields occur in a sequence of Lower Palaeozoic sandstones and graptolitic shales (Thomas, 1953; McAndrew, 1965), metamorphosed to 250°-350°C and 1-3 kb (Glasson and Keays, 1978). The mineralisation commonly occurs in crescent-shaped veins at fold hinges, which represent the type-examples of saddle-reefs. Sitter (1956, pp. 220) suggests:

> "that all the reefs are due to recrystallisation of the country rock itself, with concentration of its most mobile elements, the metals, in the reefs."

The Main Broken Hill Orebody is similar to the gold-bearing reefs of Victoria in that it occurs on a fold hinge and has a saddle-shaped cross-section (Andrews, 1908; Mawson, 1912). Until recently most authors have preferred an epigenetic emplacement of the ore, controlled by a pre-existing fold structure (e.g. Andrews, 1922; Kenny, 1932; Gustafson et al., 1950; Lewis et al., 1965; Hobbs, 1966). King and Thomson (1953), however, suggested that the deformation was instrumental in the concentration of original stratabound ores into the fold hinge, as summarised by King and O'Driscoll (1953):

> "The original ore deposit is visualised as a simple stratigraphically-disposed body conformable with the enclosing sediments. Its constituents suffered recrystallisation, concentration, and migration under the influence of severe structural deformation."

This hypothesis has subsequently been expanded by Carruthers and Pratten (1961), and Johnson and Klingner (1976). In the most recent investigation of the structure of the Broken Hill Area, Laing et al. (1978) recognise three fold episodes (F_1, F_2, F_3) of which F_1 and F_2 were associated with sillimanite-grade metamorphism. They define the folds controlling the shape and orientation of the orebodies as F_2 structures, and conclude that "substantial mechanical migrations" of an original syngenetic ore have taken place.

While the actual mechanisms and controls resulting in ore concentration are uncertain, the data from the Victorian Goldfields and from

Broken Hill suggest that ore migration to fold hinges can take place over a wide range of metamorphic conditions. At Vakkerlien it is suggested that sulfide recrystallisation and concentration to the fold hinge now represented by the Main Body, took place synchronously with D_1 and the associated high-grade metamorphism. Interstitial textures between sulfides and silicates might have resulted from subsequent equilibrium recrystallisation of low form strength Mss with higher form strength silicate minerals in a manner similar to that so commonly observed between pyrrhotite and pyrite in metamorphosed volcanogenic massive sulfide deposits (Chapter 4).

The localisation and concentration of ore by migration of originally disseminated sulfides may account for the Ni-enriched nature of the Vakkerlien ores. The process is illustrated below, on a semi-quantitative basis, for a simple silicate-sulfide system.

When considering the formation of a phase A in equilibrium with a liquid B, it is usual to calculate the concentration (X_i^A) of a trace element i in A using the partition coefficient D_i such that

$$X_i^A = D_i X_i^B \qquad (1)$$

where X_i^B is the final concentration of element i in liquid B. The method requires the final liquid concentration to be known, and the value of X_i^A cannot be predicted from the initial liquid composition. However, if D_i is small, and if the volume of B is large relative to that of A, then X_i^B is approximately equal to the initial concentration of i in B ($X_{i(o)}^B$) such that

$$X_i^A \simeq D_i X_{i(o)}^B \qquad (2)$$

In the case of metals such as Ni, Cu, and Co partitioning between immiscible sulfide liquids and silicate melts, the condition that D is

small is not met. In these circumstances the ratio of the mass of the sulfide liquid to the mass of the silicate magma with which it has equilibrated becomes very important.

Campbell and Naldrett (1979) have shown that the initial concentration may be used if equation (1) is modified to read

$$Y_i = \frac{X_i D_i (R + 1)}{(R + D_i)} \qquad (3)$$

where X_i is the initial concentration of i in silicate magma, Y_i is the final concentration of i in the sulfide melt, D_i is the partition coefficient between sulfide and silicate liquids, and R is the ratio of the mass of silicate magma to the mass of sulfide liquid reaching equilibrium with it. It is apparent from equation (3) that if $R >> D$ then

$$\frac{R + 1}{R + D_i} \rightarrow 1$$

and equation (3) assumes the form of equation (2).

A typical basic silicate magma contains approximately 200 ppm Ni (Rajamani and Naldrett, 1978) and 50 ppm Co (Carr and Turekian, 1961; Wager and Brown, 1968, pp. 152). Assuming an initially disseminated ore, say with R = 10000, the composition of the original magmatic sulfide may be calculated using equation (3), and distribution coefficients of $D_{Ni} = 250$ and $D_{Co} = 50$ (Rajamani and Naldrett, 1978) as follows

$$Y_{Ni} = \frac{200 \times 250 \times 10001}{10250} = 4.9 \text{ wt\%}$$

$$Y_{Co} = \frac{50 \times 50 \times 10001}{10050} = 0.2 \text{ wt\%}$$

and a Ni/Co ratio of about 25 may be deduced. These values are in good agreement with the average compositions of Sudbury ores cited earlier and shown on Fig. 6.4.

Under metamorphic conditions, such as those acting during D_1, the contention that redistribution of silicate-system Ni to the sulfide system (Mss) takes place as a closed system, should necessitate a small R-value, even for disseminated ores. The evidence summarised in Fig. 6.17, together with Hudson's (1973) observations on a systematically sample drill hole at Nepean, Western Australia (6.3.5), suggests that similar constraints should apply to the redistribution of silicate Co. However, if the sulfides have migrated through the silicate system, then they have had the opportunity to re-equilibrate with a large volume of silicate rock. At any one instant during the sulfide migration this re-equilibration occurs as a closed system, but overall the process takes place as an open system, such that an unchanged value of R (10000) might result.

Little is known about partitioning of base metals between sulfides and metamorphic silicate assemblages. It is likely, however, that the partition coefficient of Ni between the sulfide system (Mss) and the silicate system as a whole will be greater under metamorphic conditions than under magmatic conditions - the change of sulfide assemblage as a result of uptake of silicate nickel has already been described. Consider an olivine-rich gabbro. The main Ni-bearing phases are olivine and pyroxene. The modelling of Duke and Naldrett (1978) indicates that the Ni-content of olivines varies dramatically according to the presence or absence of a sulfide liquid (Fig. 5.55). However, in an investigation of Finnish nickel-sulfide deposits associated with basic intrusions, Hakli (1963) cited an average olivine Ni -content of 0.15 wt%. He also investigated the Ni -contents of associated pyroxene and metamorphic amphibole, and found average values of approximately 0.05 wt% for both. Assuming that olivine was a major phase in the original Vakkerlien intrusion, as suggested by Thompson (1978), then it is not unreasonable

to suggest that the bulk-sulfide to bulk-silicate partition coefficient would increase by a factor of two giving a value for D_{Ni} of 500.

Even less is known about the behaviour of Co under metamorphic conditions. However, the compositions of olivines from Skjaekerdalen and Undal presented in Chapter 5 (Table 5.2) would suggest an average CoO-content of approximately 0.1 wt%, while amphiboles from the now barren parts of the Vakkerlien metagabbro have similar CoO-contents averaging 0.1 wt% (Thompson, 1978). It would seem that, at the temperatures ambient during the D_1 metamorphic re-equilibration of sulfides and silicates, the partitioning behaviour of Co was similar to that under magmatic conditions. An unchanged Co partition coefficient (D_{Co} = 50) is therefore suggested.

From equation (3) the final composition of the migrated sulfides may be estimated:

$$Y_{Ni} = \frac{200 \times 500 \times 10001}{10500} = 9.5 \text{ wt\%}$$

$$Y_{Co} = \frac{50 \times 50 \times 10001}{10050} = 0.2 \text{ wt\%}$$

which is in excellent agreement with the average bulk composition of Vakkerlien sulfides (10.9 wt% Ni, 0.2 wt% Co - Thompson, 1978).

At Olkar Massive ores are located at, or close to the boundaries between metagabbroic lenses and country-rock schists. It is suggested that originally disseminated sulfides migrated, as Mss, to structural traps at both the upper and lower margins (Chapter 5) of the gabbroic lenses, perhaps in this case representing relicts of attenuated D_1-fold limbs. A similar explanation has been proposed for the occurrence of sulfide concentrations on the hanging walls of ultramafic units at Nepean, Western Australia (Barrett et al., 1976). Enrichment in Ni

should result from the sulfide migration through the metagabbro, as at Vakkerlien, and the Ni-depleted nature of the Olkar ores is therefore problematical. However, consideration of the adjacent country-rock schists provides a possible explanation. These schists contain significant quantities of disseminated pyrrhotite. Analyses of pyrrhotites from three samples of Gula schist are listed in Table B.24 and average 0.23 wt% Ni and 0.14 wt% Co. Migration of country-rock sulfide to the same structural traps as the magmatic sulfides will result in a Ni-depleted bulk chemistry of the resulting ores. Assuming that the magmatic sulfides arrive at the margins of the gabbroic lenses with a Ni-enriched chemistry as described above, mixing of approximately four parts of country-rock sulfide (pyrrhotite) with one part of magmatic sulfide (Mss) would result in a composition similar to the sulfide fraction of Massive ores at Olkar (2.0 wt% Ni; 0.2 wt% Co; Ni/Co = 10)*.

The discussion above, involving a number of assumptions concerning the partitioning behaviour of Ni and Co between sulfide and silicate systems under metamorphic conditions, demonstrates that it is possible to account for the observed bulk sulfide chemistries at Vakkerlien and Olkar, by a process of metamorphic redistribution of Ni and Co between the silicate and sulfide systems, together with, at Olkar, a dilution of the derived sulfides by country-rock pyrrhotite.

The variation of sulfide composition within individual deposits, as illustrated by pentlandite compositions, also requires explanation.

---

* This value has been estimated from the partial analyses of samples 77/2/15.00, 77/1/6.60a, and 77/2/14.90 (Table 6.1) as illustrated below for sample 77/2/15.00.

The pyrrhotite dominated modal composition of the ore ensures a metal to sulfur ratio (M:S) of 0.9. The atomic proportions of Ni,Cu,Co and Fe are calculated and summed, such that M = 1.074 atoms. As M:S is 0.9, S = 1.193 atoms, which gives a S-content of 38.25 wt%. The complete sulfide analyses is then normalised to 100%, resulting in a bulk sulfide composition of 2.44 wt% Ni; 0.59 wt% Cu; 0.28 wt% Co; 57.82 wt% Fe; and 38.86 wt% S.

In the majority of deposits where a variety of ore-grades exist pentlandite shows a decreasing Ni/Co ratio from massive to disseminated ores, implying (Fig. 6.15) a similar change in the composition of the bulk sulfide. In this context, it is interesting to note that, while Vakkerlien pentlandites show little variation in composition, in Fig. 6.4 the three samples lying on the Ni-rich side of the average Ni/Co line are classified by Thompson (1978) as "massive" ore, while those lying on the Co-rich side he classifies as "disseminated". It will be shown below that this decrease in Ni/Co ratio as the ore becomes more disseminated is incompatible with the metamorphic redistribution of Ni and Co as described above, without some variation in the relative partitioning behaviour of the two elements, perhaps at lower metamorphic temperatures.

From equation (3) it can be shown (Campbell and Naldrett, 1979) that the final ratio of two elements (i and j) in a sulfide liquid is given by

$$\frac{Y_i}{Y_j} = \frac{X_i D_i (R + D_j)}{X_j D_j (R + D_i)} \quad \text{or} \quad \frac{Y_i}{Y_j} = A.G \qquad (4)$$

where $A = \frac{X_i}{X_j}$ and $G = \frac{D_i (R + D_j)}{D_j (R + D_i)}$

The application of this equation to metamorphic assemblages requires similar mobilities (or R-values) for the elements involved, in this case for Ni and Co. Such a relationship is assumed hereafter on the basis of the evidence summarised in Fig. 6.17, and the observations of Hudson (1973) regarding the variations of sulfide assemblage and associated pentlandite composition with ore-grade at Nepean, Western Australia. These data suggest that Ni and Co behave similarly under

metamorphic conditions, and that their metamorphic mobilities are not markedly different.

Extrapolating equation (4) to the metamorphic situation, A must be the ratio of i to j in the sulfide and silicate systems combined, and the final ratio of these elements in the sulfide system is controlled by R. Where R is large, and very much greater than D_i and D_j, then A tends to the ratio of the elements i and j in the silicate system, and

$$G \rightarrow \frac{D_i}{D_j}$$

Conversely, where R is small, A tends to the ratio of i to j in the sulfide system and

$$G \rightarrow 1$$

Consider now the situation at Olkar where a variety of ore-grades exist. As the sulfides of the Massive ores exhibit the greatest Ni/Co ratio (Fig. 6.9) it is likely that all ore-types were in equilibrium during the Ni-dilution process outlined above (this is a reasonable suggestion in view of the general association of Disseminated and Stringer ores with Massive types). One possible explanation for the variation of Ni/Co ratio with ore-grade is that this widespread equilibrium was not maintained in a more static, lower temperature environment, such that as R increases, A and G might combine to give a reduced Ni/Co ratio.

Taking the composition calculated above for the sulfide fraction of Olkar Massive ores (2.0 wt% Ni; 0.2 wt% Co; Ni/Co = 10) values of A and G have been calculated for a range of R-values, and for a range of D_{Co} with D_{Ni} = 500. The resulting Ni/Co ratios are shown in Table 6.3. It is evident that by maintaining the values of Ni and Co partition coefficients (500 and 50 respectively) used in the earlier derivation

TABLE 6.3 Calculated Ni/Co ratios (A.G) of Olkar sulfides for a range of R-values, and a range of D_{CO} (50 - 600), with D_{Ni} = 500. See text for explanation.

R	A	G_{50}^{500}(A.G)	G_{100}^{500}(A.G)	G_{200}^{500}(A.G)	G_{300}^{500}(A.G)	G_{400}^{500}(A.G)	G_{500}^{500}(A.G)	G_{600}^{500}(A.G)
1	9.9	1.02(10.1)	1.01(10.0)	1.00(9.9)	1.00(9.9)	1.00(9.9)	1.00(9.9)	1.00(9.9)
10	8.8	1.18(10.4)	1.08(9.5)	1.03(9.1)	1.01(8.9)	1.00(8.8)	1.00(8.8)	1.00(8.8)
100	5.7	2.50(14.2)	1.67(9.5)	1.25(7.1)	1.11(6.3)	1.04(5.9)	1.00(5.7)	0.97(5.5)
1000	4.2	7.00(29.4)	3.67(15.4)	2.00(8.4)	1.44(6.0)	1.17(4.9)	1.00(4.2)	0.89(3.7)
10000	4.0	9.57(38.3)	4.81(19.2)	2.43(9.7)	1.63(6.5)	1.24(5.0)	1.00(4.0)	0.84(3.4)
100000	4.0	9.95(40.0)	4.98(19.9)	2.49(10.0)	1.66(6.6)	1.25(5.0)	1.00(4.0)	0.83(3.3)

of Massive ore sulfide composition, it is impossible to produce a Ni/Co ratio of less than 10. Only by increasing the sulfophile nature of Co relative to Ni is this possible. A small increase in the partition coefficient of Co (D_{Co} = 100) relative to that of Ni will allow a Ni/Co decrease over a small range of R-values (1 to 100); at R-values greater than 100 the Ni/Co ratio increases again to greater than 10. As the ratio of D_{Ni} to D_{Co} decreases, so the range of R over which the final Ni/Co ratio of the sulfides will be less than 10 increases. In higher-grade ores, such as the Massive ores at Olkar and at Vakkerlien, R <1 such that G → 1 and the sulfide composition is unchanged.

As discussed above, the partitioning behaviour of silicate and sulfide systems in metamorphic environments can only be guessed at. A decrease in Ni/Co ratio in the sulfide system could be achieved either by an increased sulfophile nature of Co (as demonstrated in Table 6.3), or by a decreased D_{Ni}, at lower metamorphic temperatures. However, the former possibility is favoured by the evidence presented in Fig. 6.16 and 6.17, which suggests that, in some cases, disseminated sulfides become enriched in both Ni and Co, relative to the magmatic situation, through metamorphic processes.

Evidence, based on natural data, suggesting an inverse relationship between the sulfophile nature of Co and metamorphic temperature, is provided by Springer and Craig (1975). In the western Sierra Nevada foothills of California, the Pine Hill gabbroic complex (Springer, 1974) intrudes and metamorphoses Alpine-type ultramafic rocks. The ultramafics contain disseminations (<½ vol%) of sulfide phases, dominated by pentlandite with rare pyrrhotite or heazlewoodite. Four contact metamorphic zones (I-IV), and one regional metamorphic zone (V) are defined around the Pine Hill complex. The metamorphic grade decreases from Zone I (olivine, orthopyroxene, calcic-amphibole, Fe-Cr spinel,

aluminous spinel; 700°C, 1.5 kb - Springer, 1974) to Zone V (lizardite, clinocrysotile, chromite, magnetite, chlorite). Springer and Craig suggest that the pentlandite dominated sulfide mineralogy results from the sulfurization of original silicate phases, but it is equally possible that it represents a metamorphic Ni-enrichment of a pre-existing pyrrhotite-dominated magmatic sulfide assemblage. Zone I is barren of sulfides. Pentlandites in Zones II and III have Co-contents ranging from 0.6 to 1.6 at% and Ni/Co ratios from 16.2 to 45.8. In contrast, the pentlandites in Zones IV and V range in Co-content from 2.1 to 5.9 at% and in Ni/Co ratio from 5.4 to 14.8. Whatever the origin of the sulfide phases, the higher Co-abundances and lower Ni/Co ratios in pentlandites from the zones of lower-metamorphic grade are notable. The greater sulfophile behaviour of Co at lower temperatures suggested by these observations may be related to the accompanying change in silicate mineral assemblage.

From a more theoretical standpoint, Rajamani (1976) noted a discrepency in the sulfide-silicate partitioning behaviour of Co at magmatic temperatures (as indicated by experimental work and the compositions of most magmatic sulfide deposits) and its behaviour as predicted on purely crystal chemical grounds at low temperature. The natural and experimental data on magmatic environments are in agreement that Co is much less sulfophile than Ni (Rajamani, 1976; MacLean and Shimizaki, 1976; Rajamani and Naldrett, 1978). However, Rajamani (1976) points out that Co is generally present in the low-spin state in the octahedral sites of sulfide structures (Kuznetsov et al., 1965; Pauwels, 1970; Burns and Vaughan, 1970; Vaughan et al., 1971; Rajamani and Prewitt, 1973). He suggests that, as low-spin Co gains higher ligand field stabilisation energy in octahedral co-ordination with S ligands than Ni, and has a smaller radius than Ni, it ought to be the more sulfophile.

As a possible explanation he proposes a conversion of low-spin Co^{2+} to the high-spin state at high temperature, similar to that observed by Bari and Sivardiere (1972) for Co^{3+}, which converts to the high-spin state at approximately 450°C. The larger radius and lower ligand field stabilisation energy of high-spin Co^{2+} would result in a less sulfophile behaviour.

In conclusion, if, as seems likely, the composition of the Massive ores at Vakkerlien and Olkar are the result of a redistribution of silicate Ni and Co at the high metamorphic temperatures associated with D_1, then in order to explain the variation in chemistry between different ore-grades, an increase in the sulfophile nature of Co, relative to Ni, at lower temperatures is required. Natural (Figs. 6.16 and 6.17; and Springer and Craig, 1975) and theoretical (Rajamani, 1976) evidence for an increase in the sulfophile nature of Co from high-temperature (magmatic or metamorphic) to low temperature metamorphic conditions has been described above. However, it is uncertain whether this variation in the partitioning behaviour of Co is related to mineral assemblage in the silicate system (as allowed, but not required, by the observations of Springer and Craig, 1975), or to a fundamental change in the crystal chemical properties of Co itself, as suggested by Rajamani (1976).

At Skjaekerdalen, the variation in ore texture has previously been accounted for without recourse to a metamorphic remobilisation of sulfides (Chapter 5). The sulfides occur in a variety of host rocks, their chemistry of irregular (Fig. 6.4), and shows no relationship to ore-grade (Fig. 6.11). As mentioned previously, the Ni/Co ratio of sulfide liquids equilibrating with silicate magmas decreases as the silicate melt becomes less basic (Wilson and Anderson, 1959; Hakli, 1963; Green, 1975). However, it has been suggested that the Skjaekerdalen ores, although now included in a wide range of host-rock

lithologies, originally equilibrated from a basic silicate magma (Chapter 5). Furthermore, they have experienced the high temperature metamorphic conditions ambient during D_1 and the later, lower-grade metamorphic conditions associated with the Main Scandinavian Orogeny (Chapter 5). It would be expected therefore that a complicated ore chemistry, controlled not only by ore-grade but also by original and final host rock chemistries would be displayed. However, it might be expected that the decrease in Ni/Co ratio as a result of low temperature re-equilibration would depend on the amount of Ni and Co available in the silicate system, in effect on the proportion of mafic minerals present (e.g. Krauskopf, 1967, pp. 589) such that Ni/Co might decrease as the host rock becomes increasingly mafic. Fig. 6.19 presents a plot of Ni/Co ratio of the sulfide fractions of Skjaekerdalen ores, against MgO as a mafic index of the silicate fractions (complete analyses of the silicate fractions are presented in Table A.9, and the separation techniques are described in Appendix C). With one exception, the points lie on a trend of decreasing Ni/Co with increasing MgO-content as predicted. The highest Ni/Co ratio (52) associated with a dioritic host rock suggests Ni-enrichment by high-temperature re-equilibration with more mafic assemblages, before fragmentation and inclusion in the diorite. The exception, a gabbroic rock with a very low Ni/Co ratio (7) is not difficult to account for if the large-scale textures of the intrusive complex at Skjaekerdalen are considered. It is not unlikely that this sample formed the matrix to an ultramafic "jig-saw puzzle" rock (Fig. 5.20) such that the sulfides have re-equilibrated with a more mafic silicate system than is indicated. A control of host-rock composition over ore chemistry, at Skjaekerdalen, may account for the lack of any relationship between ore-grade and pentlandite composition (Fig. 6.11). However, the common

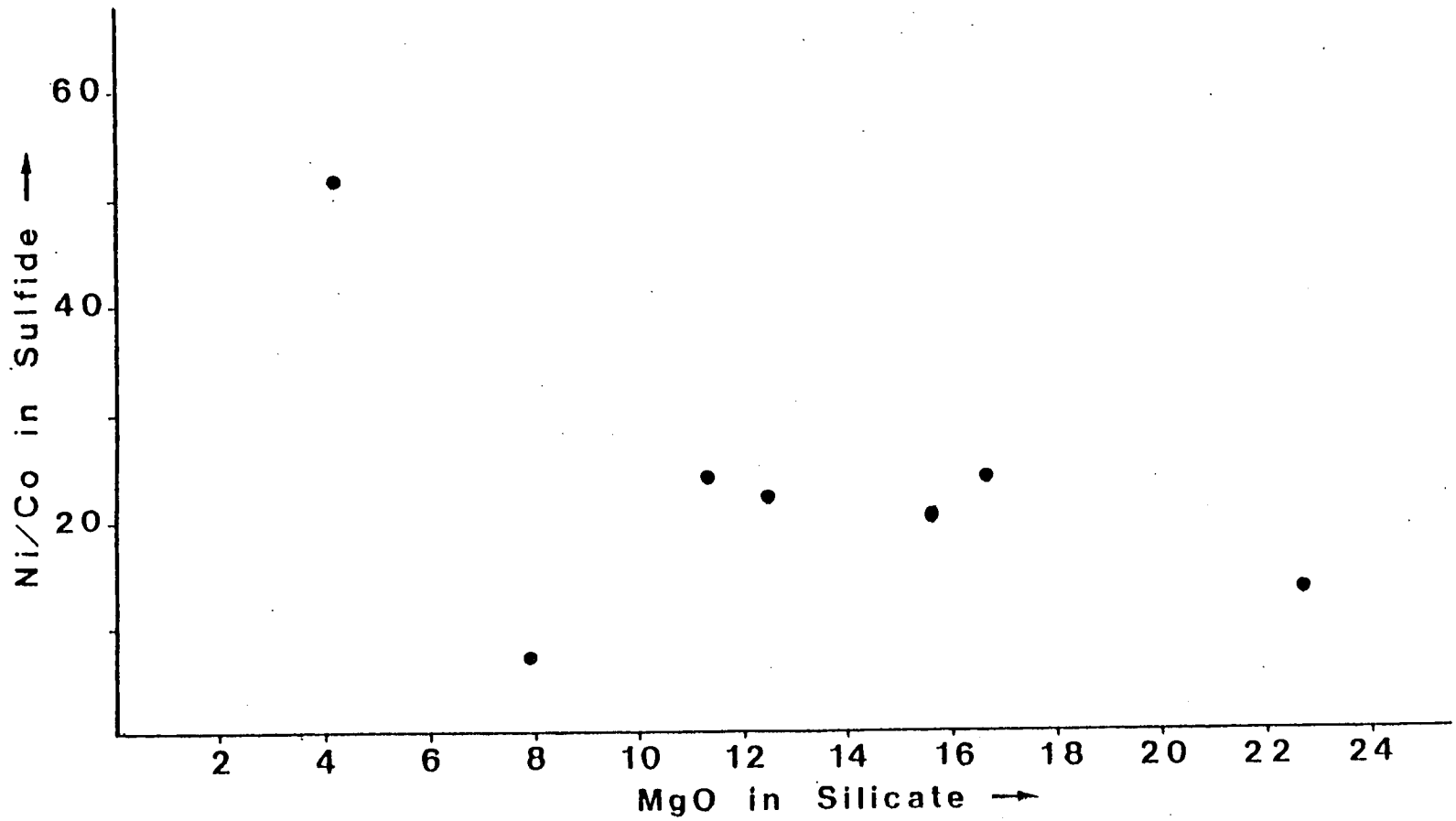

Fig. 6.19 Ni/Co in bulk sulfide fraction of Skjaekerdalen ore plotted against MgO in silicate fraction. (Values in wt %).

occurrence of supergene alteration in samples of Skjaekerdalen ore (5.1.1.4; Appendix D) requires that these suggestions should be treated with caution.

The ores at Gardsjoen have not been studied in as much detail as those previously described. However, the highly xenolithic nature of the host gabbro, itself a xenolith in a large trondhjemitic mass, together with the Co-enriched nature of the ore indicated by the pentlandite compositions shown in Fig. 6.10, suggests a history similar to the ores at Olkar, before incorporation into the trondhjemite.

6.4.2 Ores of ultramafic association.

In Chapter 5 it was demonstrated that the ultramafic intrusives were emplaced after the Trondheim Orogeny (i.e. post D_1) but before the end of the later main Scandinavian event (pre D_4). Furthermore, it was suggested that the ores at Kaltberget (Main Body) represent primary basal accumulations of magmatic sulfides in an inverted intrusion involving an olivine high-Mg liquid-crystal mush. In view of its primary position, and the lack of any chemical or textural evidence for sulfide remobilisation (6.2), it is unlikely that any significant metamorphic upgrading of the ore has taken place, although considerable sulfide recrystallisation has probably occurred (as demonstrated by the globular sulfide textures). Throughout its history therefore the ore has had a small R-value, and hence little chemical modification of the sulfides can have taken place. This is supported by the Cu/Cu + Ni and Ni/Co ratios of the ore which are consistent with equilibration with a silicate magma of 15-20 wt% MgO, as indicated by silicate mineral and bulk chemistry. However, Fig. 6.13 shows a very slight increase in the Co-content of the more disseminated ores, suggesting similar low temperature re-equilibration of sulfides and silicates to that described for the metagabbros. These Disseminated and Finely Disseminated ores

are all drill-core samples and are therefore from within a few metres of, and perhaps from within the "sphere of influence" of, the higher-grade mineralisation. This would account for the limited variation of pentlandite composition between high- and low-grade ores. In surface samples Disseminated ore is extremely rare and where it has been recorded, pentlandite is invariably replaced by violarite. However, in Fig. 6.20, the Co-contents of a number of coexisting pentlandite-violarite pairs, associated with the primary assemblage pyrrhotite, pentlandite, chalcopyrite, (±pyrite), are plotted, and a strong positive correlation observed. The range of Co-content of violarites from a surface sample of Finely Disseminated Kaltberget ore (sample 76.245; see Fig. 5.30) is shown, together with the derived pentlandite composition. This range of pentlandite Co-content is shown in Fig. 6.13 as the stippled area, and indicates a higher Co-content for this sample of Finely Disseminated ore removed from the main zone of mineralisation. If this relationship could be quantified for a variety of environments (gabbroic, komatiitic, etc.) perhaps by a series of continuous drill holes through known ore bodies, it would provide a useful tool for exploration, in which Co-content of pentlandite in disseminated ore would relate to the proximity, or otherwise, of a zone of high-grade mineralisation.

At Kletten the high Co-content of many of the pentlandites shown in Fig. 6.12 are presumably related to their occurrence in Finely Disseminated ores. The observation that Co-enrichment has occurred in Kletten ores, and to a lesser extent at Kaltberget, suggests that the process responsible must, in part at least, be related to the lower-grade metamorphism associated with the main Scandinavian Orogeny.

Pentlandites at Kletten containing little or negligible Co, from ores classified as Finely Disseminated, are problematical. However, in view of the evidence, presented in 5.5.2, arguing against the existence of unexposed zones of high-grade mineralisation, it is suggested

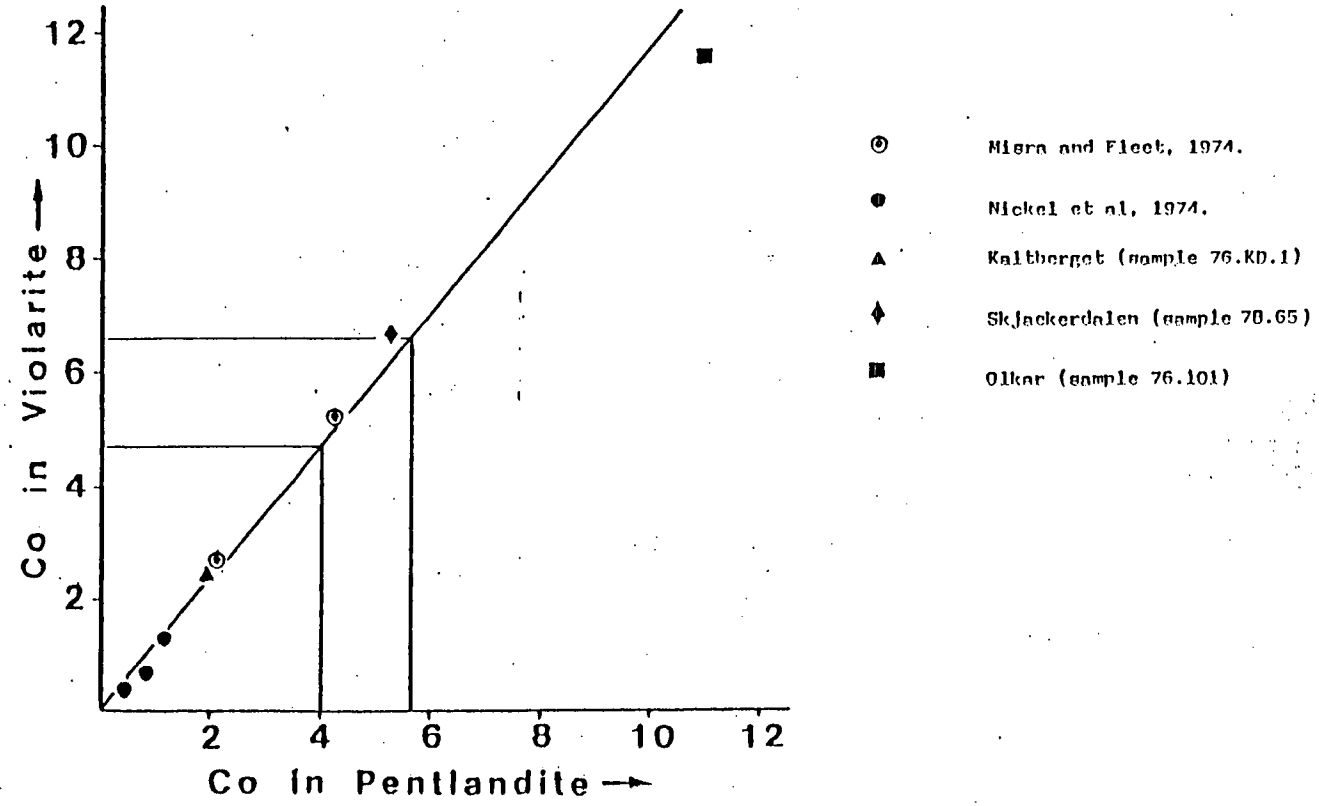

Fig. 6.20 Atomic % Co in coexisting pentlandites and violarites associated with the primary assemblage pyrrhotite, pentlandite, chalcopyrite, (± pyrite). The range of violarite composition from sample 76.245 is shown, together with the probable original pentlandite composition. See text and Fig. 6.13 for explanation.

that the characteristic occurrence of Kletten sulfides as large isolated blebs (5.1.2.2, Fig. 5.47) in some cases dictates that they behave chemically as higher-grade ores.

6.5 The Problem of Sulfur and the Origin of Magmatic Sulfide Deposits.

Consideration of the distribution of magmatic Ni-Cu sulfide deposits throughout geological time reveals a general lack of such ores in rocks younger than 1.7×10^9y. Naldrett (1973) suggested that this might result from a depletion of the mantle in sulfur through repeated partial melting events. Any sulfur present becomes concentrated in the partial melt and is removed, leaving a residue depleted in sulfur. Subsequent partial melts derived from this now depleted mantle will contain much lower concentrations of sulfur and will consequently be much less likely to become sulfur saturated and thereby to produce an immiscible sulfide liquid. The very occurrence of magmatic sulfide deposits in the Gula Group therefore poses a fundamental problem.

However, a key assumption in Naldrett's mantle depletion model is that the sulfur responsible for saturation of a silicate magma is mantle-derived. If an initially sulfur-poor silicate melt assimilates sufficient sulfur from its wallrocks, either before final emplacement or during crystallisation, it may eventually become sulfur-saturated and produce an immiscible sulfide liquid. In this context it is interesting to note that the sulfides of the Duluth and Noril'sk complexes, which are the only major magmatic sulfide deposits younger than 1.7×10^9y, contain sulfide S^{34}/S^{32} ratios typical of crustal rather than mantle derivation (Mainwaring and Naldrett, 1977; Godlevski and Grinenko, 1963). The possibility that the Gula sulfides result from assimilation of wallrock sulfur must therefore be considered.

While the country rocks in the immediate vicinity of Vakkerlien

are essentially barren of sulfides, those adjacent to Olkar, Skjaekerdalen, Kaltberget, and Kletten commonly contain abundant disseminations of pyrrhotite. These observations, and the commonly xenolithic nature of the intrusives, support an assimilation process for sulfur-saturation. Furthermore, the generally sulfide bearing nature of the Gula schists, together with numerous small massive volcanogenic sulfide concentrations commonly associated with the Gula amphibolites (Chapter 4), would allow plenty of opportunity for any silicate magma intruding the environment to assimilate sulfur prior to its final emplacement. The lack of country-rock sulfide in the immediate vicinity of Vakkerlien, and the lack of Fe-oxide phases which might suggest the breakdown of pre-existing sulfides, cannot therefore be regarded as inconsistent with a sulfur-assimilation model.

The ratio of S/Se in bulk sulfides is believed to be characteristic of source environment. Allen et al. (1970) has suggested a chondrite, and hence a possible mantle, S/Se ratio of approximately 2700, while in sediments under oxidising conditions (Hatten, Howard III, 1977; Leuthwein, 1972) Se is depleted relative to S, resulting in very high S/Se ratios in the order of 30000. However, it is not possible to distinguish between magmatic S/Se ratios and those of reducing sedimentary environments which may have similar values (Stanton, 1972, p. 174). Thompson (1978) obtained a small number of Se values for bulk Vakkerlien sulfides, by neutron activation analyses. The average S/Se ratio was approximately 7600, high but not markedly so by chondritic standards. However, the common association of pyrrhotite and black graphitic schist throughout the Gula Group does not allow distinction between a magmatic or a reducing sedimentary source.

In the absence of isotopic data, which might also yield inconclusive results, the commonly sulfide-bearing nature of the Gula schists,

together with the comparatively young age of the region, favours assimilation of country-rock sulfide as the process leading to sulfur-saturation of the silicate magmas, and hence to the precipitation of immiscible sulfide liquids.

6.6 Conclusions.

The chemistry of the various Gula magmatic sulfide deposits has been described. The ores at Vakkerlien are enriched in Ni relative to S and Co, while those at Olkar are depleted. At Skjaekerdalen, the ores display an erratic chemistry, with regard to Ni and Co, while all metagabbroic associated sulfides show irregular copper concentrations, probably as a result of secondary remobilisation of chalcopyrite. The ores at Kaltberget are consistent in all respects with equilibration with a high-Mg silicate liquid of 15-20% MgO, while those at Kletten show considerable enrichment in Co. With the exception of Skjaekerdalen, all prospects show a decrease in Ni/Co ratio as the ore becomes increasingly disseminated.

It is suggested that high temperature metamorphic re-equilibration of sulfides with a large volume of silicates will result in a Ni-enrichment of the ores. The composition of Vakkerlein ore is regarded as an example of such a process, occurring during the high-grade metamorphism of the Trondheim Orogeny, and aided by migration of disseminated sulfides through the metagabbro to give access to a large volume of silicate. The composition of the ore at Olkar was further modified by a process of dilution by country-rock sulfides migrating to the same structural traps as the magmatic sulfides from within the intrusion. It is also proposed that, at lower metamorphic temperatures, the sulfophile nature of Co is greater than in either the high-temperature metamorphic, or the magmatic situation. The composition of more massive

ores, resulting from the migration and concentration of originally disseminated sulfides during the Trondheim Orogeny, was little altered during subsequent lower-grade metamorphism, as a result of their high proportion of sulfide. In contrast, disseminated sulfides became richer in Co, such that observed Ni/Co ratios, in general, decrease from massive to disseminated ores. However, a wide variety of host rock compositions occurs at Skjaekerdalen, and evidence has been presented which suggests that, in this case, the dominant control over lower-temperature metamorphic re-equilibration may be the amount of Ni and Co available in the silicate system, such that Ni/Co decreases as the host rock becomes more mafic.

Kaltberget ores have retained their primary magmatic chemistry, as a consequence of their originally high proportion of sulfide to silicate minerals, resulting from gravity differentiation of an immiscible sulfide magma to the base of the silicate crystal-liquid mush. The finely disseminated sulfides at Kletten, however, have suffered a degree of low-temperature metamorphic re-equilibration, as evidenced by their pentlandite compositions.

The Co-content of pentlandites in disseminated magmatic ores, associated with mafic and ultramafic host rocks, has been shown to be a useful indicator of the proximity of higher-grade mineralisation, and may therefore prove useful to exploration.

CHAPTER 7

CONCLUSIONS

The overall objective of the present study has been to elucidate the origin and subsequent history of the various types of sulfide mineralisation occurring in the Gula Group. However, the controversy surrounding the regional geology of the Trondheim Nappe, particularly with regard to the stratigraphic and structural position of the Gula Group in relation to other units, has necessitated prior investigation of these aspects. The conclusions of the thesis are summarised below.

7.1 Regional Geology of the Trondheim Nappe.

The regional geology of the Trondheim Nappe has been investigated by the examination of five traverses through the Gula Group and adjacent units. The traverses trend NW-SE, and follow major river valleys, allowing utilisation of good exposure provided by road and railway construction.

7.1.1 Outcrop distribution of the Gula Group.

On the southeastern flanks of the Tommeras Antiform, and in western Trondelag, a narrow sliver of Gula Group (less than 1km wide) has been identified, separating low-grade Storen metavolcanics from the garnetiferous Seve amphibolites of the underlying Seve-Koli Nappe Complex. In southern Trondelag, the Gula and Storen Groups are successively thrust out along the western margin of the Trondheim Nappe such that the Hovin Group rests directly on the high-grade Seve.

7.1.2 Stratigraphy.

The stratigraphic correlation of the Eastern Trondelag Succession with the Koli Supergroup of Sweden, as suggested by Gee and Zachrisson (1974), is rejected on the basis that it is incompatible with established details of Trondelag geology. The more widely held correlation of the

Eastern Trondelag Succession with the Western Trondelag Succession is favoured in this thesis. The possibility of a stratigraphic repetition within the Gula Group, involving correlation of the lithologically similar Undal and Asli Formations about the central Singsas Formation has also been suggested.

The Dictyonema-bearing shales at Nordaunevoll, in eastern Trondelag, have been alternatively included in the Sulamo Group (Wolff, 1967b, 1976) and in the Gula Group (Rui, 1972). In view of their close proximity (three hundred metres) to Fundsjo metavolcanics of epidote-amphibolite facies, the conclusions of Wolff (1967b, 1976) are accepted in this thesis, and the boundary between the Fundsjo and Sulamo Groups is regarded as a major non-conformity as originally suggested by Sturt (1975). Stratigraphic correlation of the Eastern and Western Trondelag successions implies a similar relationship between the Storen and Hovin Groups in western Trondelag. As a consequence of these observations both the Storen and Fundsjo Groups are regarded as pre-Tremadocian in age.

7.1.3 Metamorphism.

Previous descriptions of the variation of metamorphic grade throughout the Trondheim Nappe have been summarised, and a compilation map presented (Fig. 2.1). In general, the metamorphic grade decrease symmetrically about the central parts of the Gula Group. Consideration of ore textures in the massive volcanogenic sulfide deposits of the Gula, Storen, and Fundsjo Groups, together with the overall structural control of the orebodies, suggests that this zonation is real, and not an effect of retrogression, related for instance to thrusting at the base of the Trondheim Nappe.

Two discrete metamorphic events have been distinguished. The earliest affected only the Gula, Storen and Fundsjo Groups, and was

associated with the pre-Tremadocian Trondheim Orogeny, tentatively correlated herein with the Finnmarkian Orogeny of north and south west Norway, and the Grampian Orogeny of Scotland. The highest metamorphic grade is found in the central parts of the Gula Group in northern Trondelag, where kelyphitic reaction rims between olivine and plagioclase in the Skjaekerdalen intrusive complex suggest attainment of pressures of at least approximately 8.5 kb (Herzberg, 1976), and with the occurrence of sillimanite in the surrounding schists, temperatures in excess of 700°C (Richardson, et al., 1969; Holdaway, 1971). In southern Trondelag, the central parts of the Gula Group are characterised by the occurrence of kyanite and staurolite restricting temperatures to below 700°C (Winkler, 1976, Chapter 14). Application of the sphalerite geobarometer (at Rostvangen and Kvikne) indicates pressures of at least 6 kb, although complications arising from low pressure re-equilibration have been suggested, and pressures greater than 9 kb may have been reached.

The later metamorphic event was associated with the post-Llandoverian main Scandinavian Orogeny, and effects all stratigraphic units within the Trondheim Nappe. Epidote-amphibolite facies (garnet grade) is attained in parts of the Eastern Trondelag succession, while the Western Trondelag succession is dominated by greenschist-facies assemblages (chlorite grade).

Repetition of isograds established during the Trondheim Orogeny, by deformation associated with the main Scandinavian Orogeny, is responsible for the zonal pattern of metamorphic grade within the Trondheim Nappe.

7.1.4 Structure.

The sequential development of mesoscopic structures within the Gula Group has been described, together with limited observations on

higher stratigraphic units. An early phase of isoclinal deformation (D_1) affects only the Gula, Storen, and Fundsjo Groups, which together with the lineation of high-grade minerals such as sillimanite and kyanite parallel to D_1-fold axes, suggests that this deformation was associated with the Trondheim Orogeny. Two subsequent phases of isoclinal deformation (D_2 and D_3), and later, less intense deformation (D_4 and D_5), were associated with the main Scandinavian Orogeny.

An interpretation of the regional structure is presented. The model, demonstrated in Figs. 3.8 and 3.9, is regionally consistent, and accounts for: the outcrop distribution of the various stratigraphic units; the variation in orientation of the regional foliation; many of the stratigraphic and structural observations of previous workers; and the zonation of metamorphic grade about the central parts of the Gula Group.

7.1.5 Tectonic setting.

While the Hovin and Horg Groups, and their eastern correlatives are generally accepted as having been deposited in a fossil volcanic arc - marginal basin system, the original tectonic environments of the Gula, Storen, and Fundsjo Groups are much less certain. A reconnaissance geochemical investigation of the basic metavolcanics of these units, together with consideration of the composition of associated volcanogenic sulfide deposits, provides valuable insight to this problem. The metamorphosed nature of the volcanics is acknowledged and only those elements generally regarded as relatively stable are considered. However, the possibility of metamorphic mobilisation of even these elements must be borne in mind.

The geochemistry of the Gula amphibolite horizons suggests that they may represent original low-k tholeiites of island-arc affinity. While massive sulfide deposits have not previously been recorded in

association with volcanics of this type, the average composition of the Rostvangen deposits fulfills the predictions of previous workers that such ores would have similar bulk chemistries to those formed at sites of sea-floor spreading. It is suggested that gravity sliding of the dense mafic volcanics and associated massive sulfides, away from their source region, into an essentially sedimentary environment, may explain many of the general geological features of the Gula Group.

The geological and geochemical characteristics of the Storen and Fundsjo metabasics suggest an origin at a submarine spreading centre. Associated sediments imply deposition in shallow water, while a common geochemical depletion of the metabasics in Nb may favour a marginal-basin environment. The average bulk compositions of the Lokken and Tverfjellet massive sulfide deposits are consistent with these proposals. However, the ores at Killingdal have chemical affinities to deposits of volcanic-arc association.

The apparently contrasting palaeoenvironments of the Gula Group, and the Storen and Fundsjo Groups, probably requires their juxtaposition by tectonic processes, presumably during the Trondheim Orogeny. Subsequent to this event, the volcanic arc - marginal basin sequences of the overlying units of the Eastern and Western Trondelag successions were deposited. The North American faunas of the Lower Hovin Group requires that the entire Trondheim Supergroup was derived from the Greenland-Laurentian continental margin. Emplacement of the Trondheim Nappe onto the Baltoscandian platform took place during the main Scandinavian Orogeny, as a result of closure of the Iapetus Ocean.

7.2 Copper-Zinc Mineralisation.

In common with most recent investigations a volcanogenic origin for the Gula copper-zinc sulfide mineralisation is accepted. Deposits

intimately associated with amphibolite horizons probably represent in situ deposition. Those with no such relationship may have become separated from their volcanic host rocks by tectonic processes, or they may have formed by migration of ore-forming fluids away from volcanic sources, or by transport and resedimentation of the sulfides themselves. The possibility that at least a proportion of the Gula schist lithologies represents original intermediate and more evolved volcanics, may also account for deposits with no close spatial relationship to amphibolites.

The Kvikne and Rostvangen deposits in the central parts of the Gula Group in southern Trondelag have been compared with the Lokken and Tverfjellet deposits in the Storen Group, and the Killingdal deposit in the Fundsjo Group.

Consideration of the structural control of the deposits, and of the textures of the ores themselves has important implications for the regional geology of the Trondheim Nappe, as previously described. The average bulk compositions of the ores have also been mentioned.

7.2.1 Application of the sphalerite geobarometer.

The application of the sphalerite geobarometer requires equilibration of sphalerite with pyrite and hexagonal pyrrhotite. This requirement is not satisfied at Lokken where no pyrrhotite has been recorded. However, mean pressures of 4.5, 5.2, 6.0 and 6.2 kb were obtained for the Tverfjellet, Killingdal, Kvikne, and Rostvangen deposits respectively. The higher pressures obtained from deposits in the central parts of the Gula Group suggest that these values relate to the Cambro-Ordovician Trondheim Orogeny.

Bristol (1979) suggested that anomalously high pressures result from the re-equilibration of sphalerite with monoclinic pyrrhotite, when this phase becomes stable below 253°C. No evidence for such a

process has been observed in this study. To the contrary, the possibility of a re-equilibration to lower pressure, with pyrite and hexagonal pyrrhotite, during the main Scandinavian Orogeny is suggested. Pressures greater than 9 kb may have been attained in the central parts of the Gula Group (Rostvangen deposit).

7.3 Nickel-Copper Mineralisation.

A small number of basic intrusions within the Gula Group are associated with nickel-copper sulfide mineralisation. The intrusions are divided into two groups - metagabbros and ultramafics.

The metagabbroic complexes were intruded before or during the Trondheim Orogeny. Original magmatic silicate assemblages have been found at Skjaekerdalen and Undal, and their mineral chemistry is consistent with available data from other gabbroic intrusions of tholeiitic character.

The ultramafic bodies were emplaced after the metamorphic peak associated with the Trondheim Orogeny, but before the end of the main Scandinavian Orogeny (pre-D_4). Petrological observations, together with consideration of whole-rock and mineral chemistry, suggest intrusion of a crystal-liquid mush containing olivine (with minor clinopyroxene) and a highly-magnesian liquid.

A magmatic origin for the Gula nickel-copper sulfide mineralisation is favoured, and it is suggested that assimilation of country-rock sulfur was responsible for saturation of the silicate magmas with respect to sulfur, and hence for the precipitation of immiscible sulfide liquids. However, it has been demonstrated that metamorphism and deformation have in many cases resulted in considerable chemical and textural modification of the original ores.

At metamorphic temperatures above about 400°C, the pyrrhotite

dominated sulfide assemblages would revert to a single phase - Mss. Accompanying deformational processes might result in migration and concentration of this phase to structural traps.

Metamorphic re-equilibration of the sulfides with the host silicate assemblage has been discussed. On the basis of published data, and data obtained in this study, the following general observations are noted. At low metamorphic temperatures both Ni and Co are more sulfophile than under magmatic conditions, and sulfide enrichment in both elements results. At higher temperatures, however, the sulfophile nature of Co decreases, and the sulfides become preferentially enriched in Ni. At what temperature, and by what mechanism, the behaviour of Co changes is uncertain.

The effects of such metamorphic redistributions of Ni and Co on sulfide chemistry are inversely related to the modal proportion of sulfide present, such that sulfides in Massive ores are little altered, while those in more disseminated ores are increasingly susceptible to chemical modification. However, where disseminated sulfides occur in proximity to large volumes of more massive ores, an equilibrium may exist, and the disseminated sulfides suffer little change in chemistry. The composition of disseminated sulfides in mafic and ultramafic intrusions is consequently a useful indicator of their proximity, or otherwise, to zones of higher-grade mineralisation. A strong positive correlation between bulk sulfide Ni/Co ratio, and that of the associated pentlandite has been demonstrated, and the composition of pentlandite in Disseminated ores is therefore an alternative exploration tool.

7.3.1 Prospects of metagabbroic association.

7.3.1.1 Vakkerlien - Sulfide mineralisation at Vakkerlein lies along the centre of the Main Body, in the general vicinity of the contact between metagabbroic and ultramafic lithologies. When compared with

the observed and calculated compositions of magmatic sulfides in equilibrium with basic silicate magmas, the Vakkerlien sulfides are considerably enriched in Ni.

Thompson (1978) suggested that the original Vakkerlien complex had a tabular form, and that the present Vakkerlien Main and Second Bodies represent isolated fold hinge zones, resulting from the isoclinal deformation of this intrusion. This hypothesis is accepted herein. However, his proposal that the localisation of the sulfide mineralisation is an original magmatic feature is refuted on the basis that it is incompatible with the Ni-enriched nature of the sulfides. The following explanation is preferred.

The Vakkerlien bodies are elongated parallel to the D_1-lineation direction. It is suggested that, during D_1 and the associated high-grade metamorphism of the Trondheim Orogeny, sulfides, originally disseminated throughout the Vakkerlien intrusion, migrated, as Mss, into structural traps such as the fold-hinge zone now represented by the Vakkerlien Main Body. High temperature metamorphic re-equilibration of the disseminated sulfides with large volumes of silicate host rock resulted in their Ni-enrichment. The high sulfide to silicate ratio resulting from concentration of the sulfides to the fold hinge prevented any significant modification of sulfide chemistry during subsequent lower temperature metamorphism (retrogressive or associated with the main Scandinavian Orogeny). Thompson's data, however, indicates a slight lowering of the Ni/Co ratio from "massive" to "disseminated" ores.

7.3.1.2 Olkar - The sulfide mineralisation at Olkar occurs at, or close to, the boundaries between metagabbroic lenses and country-rock schists. The sulfides are depleted in Ni when compared with the observed and calculated compositions of magmatic sulfides associated with

basic silicate liquids. During the high-temperature metamorphism associated with the Trondheim Orogeny, originally disseminated magmatic sulfides may have migrated, as Mss, to structural traps at the margins of the gabbroic lenses, which perhaps represent relicts of attenuated D_1-fold limbs. A Ni-enrichment of the sulfides presumably resulted. However, migration of country-rock pyrrhotite to the same structural traps lead to an overall depletion of the ores in Ni. The wide range of ore-grades at Olkar demonstrates the effects of lower temperature re-equilibration between sulfides and silicates, with a decreasing ore-grade corresponding to a decreasing pentlandite, and hence bulk-sulfide, Ni/Co ratio.

7.3.1.3 Gardsjoen - The Gardsjoen showing is a xenolith of mineralised metagabbro, enveloped in a large trondhjemitic mass. Limited petrological and chemical data suggest an early history similar to the ores at Olkar, prior to incorporation into the Trondhjemite.

7.3.1.4 Skjaekerdalen - The Skjaekerdalen intrusive complex consists of a central core of metagabbroic breccia, surrounded by an aureole of unbrecciated metadiorite. The breccia is a complex lithology in which, in general, more mafic fragments occur in a less mafic matrix. The overall field relations and large-scale textures suggest successive intrusion of progressively more evolved liquids.

Relict igneous silicate assemblages have been recorded as mentioned above. Olivine compositions suggest equilibration with a sulfur-saturated silicate liquid, in keeping with the mineralised nature of the intrusion.

Sulfide mineralisation at Skjaekerdalen is restricted to the central breccia, and is hosted by all lithologies therein. A variety of ore-types exist, and have been explained by assuming a magmatic origin for the sulfides. Ni/Co ratios of the sulfides are highly variable

and show no systematic relationship to ore-grade. Instead, the dominant control appears to be the wide range of host rock compositions, such that Ni/Co ratios in general decrease as the host rock becomes more mafic. However, the possibility of supergene alteration of ore chemistry has been mentioned.

7.3.2 Prospects of ultramafic association.

7.3.2.1 Kaltberget - Systematic sampling and analysis of drill core through the Kaltberget Main Body suggests two influxes of olivine-rich magma followed by gravitational differentiation, and subsequent inversion of the intrusion as a whole. Accompanying immiscible sulfides percolated downwards through the olivine-liquid mush to collect at the base of each intrusive cycle. The compositions of relict olivines suggest crystallisation from a sulfur-saturated magma, and are therefore consistent with these proposals.

Little metamorphic alteration of sulfide chemistry has taken place as a result of the originally high proportion of sulfide to silicate phases in the ore. The bulk composition of the sulfides is consistent with equilibration with a silicate liquid of between 15 and 20% MgO. In view of this, and the additional evidence of silicate whole-rock and mineral chemistry supporting such a highly-magnesian parent liquid, the occasional globular textures of Kaltberget ores are thought to have developed by metamorphic recrystallisation of original interstitial ores.

The Kaltberget Satellite Body is a small pod, tectonically separated from the adjacent, stratigraphically basal parts of the Main Body.

7.3.2.2 Kletten - A two phase intrusion in which the differentiation was flow controlled, or a multiple intrusion in which differentiation was controlled by either flow or gravity, is suggested by the variation of whole-rock composition across the Kletten ultramafic body. Wide sample spacing prevents any more precise definition of the intrusive history.

The composition of relict olivines at Kletten suggest fractionation from a sulfur-saturated silicate melt. When compared with Kaltberget olivines, a much longer history of sulfur-saturation, and hence sulfide precipitation, is indicated. Separation of the dence immiscible sulfides from the Kletten magma, before its final emplacement may account for the poorly mineralised nature of the intrusion. Alternatively, flow differentiation at Kletten may have prevented concentration of an immiscible sulfide liquid (as at Kaltberget) by gravitational processes.

Sulfide mineralisation is Finely-Disseminated and pentlandite compositions suggest a degree of low-temperature metamorphic re-equilibration with the host ultramafics.

7.3.3 Unmineralised intrusions.

The Undal and Haukfjellet metagabbros, and the Graho and Plassbekken ultramafics have been described. On the basis of available exposure, these intrusions are barren of sulfide mineralisation.

Olivine compositions suggest that the Undal metagabbros crystallised from a sulfur-undersaturated magma. It is therefore unlikely that further exploration would reveal any significant concentrations of sulfide mineralisation.

At Haukfjellet, Graho, and Plassbekken, insufficient data is available to allow similar comment.

ACKNOWLEDGEMENTS

I gratefully acknowledge Dr. Roy Gill for his supervision, interest, and encouragement throughout all stages of this work.

The research would not have been possible without the co-operation and assistance, both logistical and financial, of A/S Sulfidmalm. I thank Dr. John Gammon for initiating the project, and Frank Nixon, Ronny Sivertsen, Bjarna Lieungh, and Dr. Colin Coats (of Falconbridge Nickel Mines Ltd.) for many interesting and fruitful discussions on all aspects of the topic, and for permission to use their unpublished data in the thesis.

Professors Sir Frederick Stewart and G. Y. Craig made available the excellent research facilities of the Grant Institute, and I am most grateful to them. I acknowledge the receipt of a post graduate studentship from the Department of Education, Northern Ireland.

The project has benefited from the interest and guidance of Dr. David Gee, of the Swedish Geological Survey, who was also instrumental in arranging the initial contact with A/S Sulfidmalm.

Professor A. J. Naldrett, of the University of Toronto, displayed a continuing interest in this research. I thank him for his hospitality in Canada, and for many stimulating discussions there, in Norway, and in the U.K.

I am particularly grateful to John Thompson, also of the University of Toronto. A number of the conclusions presented herein depend on the data collected and made available by him, and benefited from his careful and constructive criticism. I thank him also for his hospitality in Toronto, and for his companionship in Kvikne.

I acknowledge the people of Kvikne, and especially the families Grotli and Skogstad, for welcoming me into their valley and into their homes.

I am indebted to many of the staff and students of the Grant Institute of Geology, Edinburgh. In particular I would mention the following:

Mr. Colin Chaplin and his staff for their unfailing and expert assistance in all aspects of this work.

Dr. Peter Hill, Dr. Susan O'Hara, and Mr. Cameron Begg for their instruction in the operation of an extremely reliable electron microprobe, and especially for their prompt assistance at any hour in the event of machine or, more usually, operator malfunction.

Dr. Godfrey Fitton, Dr. Matthew Thirlwall, and Mr. Geoff Angell, for assistance and advice on X-ray fluorescence techniques.

Michael Saunders for patient instruction in wet chemical analyses.

Dr. Matthew Thirlwall and Dr. Alastair Graham for guidance in computing procedures.

Mrs. Thea Grieve for her excellent administration of the Geology Department Library.

Dr. Colin Graham, Dr. Jeff Harris and Mr. Andy Barnicoat for their careful and critical reading of thesis chapters or parts thereof.

My fellow research students, and especially Andy Barnicoat, Alastair Graham, Peter Jackson, Janet McClurg, and Matthew Thirlwall, for academic and other discussion, and for their friendship during the course of this work.

Samples of ore were provided by the managements of A/S Orkla Industrier (Lokken Mine), A/S Folldal Verk (Tverfjellet Mine), and Killingdal Grubeselskap A/S (Killingdal Mine). I am particularly grateful to resident geologists G. Grammeltvedt and M. Motyse for their discussion and instruction on the geology of the Lokken and Tverfjellet deposits respectively.

This thesis has been patiently, and expertly typed by Mrs. Lucian Begg, whom I thank, and to whom I apologise for my frequent "editorial" alterations.

Without the continual support of my family and friends I could not even have contemplated this project. I thank especially my father and mother for their encouragement, not only during the course of this work, but throughout the last twenty years - I owe them an incalculable debt. Finally, I regret that I shall be unable to provide as much support for Janet in the months to come, as she has provided for me, during the seemingly interminable final stages of this thesis.

REFERENCES

GFF = Geologiska Foreningens i Stockholm Forhandlingar.

NGT = Norsk Geologisk Tidsskrift.

NGU = Norsk Geologiske Undersokelse.

SGU = Sveriges Geologiska Undersokning.

ALLEN, R. C., HASKINS, L. A., ANDERSON, M. R., and MULLER, C., 1970. Neutron activation analysis for 39 elements in small or precious geological samples. Jour. Radioanal. Chem., 6, 116-137.

ANDREASSON, P. G., 1978. Aspects of the lithology and structure of the Lekstalsvann Group, Tommeras window, central Norwegian Caledonides. NGT, 58, 109-112.

ANDREASSON, P. G., GEE, D. G., and KUMPULAINEN, R., 1978. Some remarks on the Steinkjer Mega-Boudin. NGT, 58, 305-307.

ANDREWS, E. C., 1908. Broken Hill silver mine. Econ. Geol., 3, 644-646.

ANDREWS, E. C., 1922. The geology of the Broken Hill district: New South Wales Geol. Survey Mem. 8, 432 pp.

ANNERSTEN, L., 1973. The Swedish National Programme for the Geodynamics Project, GFF, 95, 311-316.

ANTUN, P., EL GORSEY, A., and RAMDOHR, P., 1966. Ein neuartiger Typ "hydrothermaler" Cu-Ni-Lagerstatten mit Bemerkungen uber die Mineralien : Valleriit, Mackinawit, Oregonit. Mineralium Deposita, 2, 113-132.

ARNDT, N. T., and FLEET, M. E., 1979. Stable and metastable pyroxene crystallisation in layered komatiite lava flows. Amer. Mineral., 64, 856-864.

ATKINS, F. B., 1969. Pyroxenes of the Bushveld Intrusion. Jour. Pet., 10, 222-249.

BACHKE, A. S., 1880. The Vaerdals Nickel-Mines (report). "Bergarkivet", NGU.

BARI, R. A., and SIVARDIERE, J., 1972. Low-spin - high-spin transitions in transition metal ion compounds. Phys. Rev. B, 5, 4466-4471.

BARRETT, F. M., GROVES, D. I., and BINNS, R. A., 1976. Importance of metamorphic processes at the Nepean nickel deposit, Western Australia. Trans. Inst. Min. Metall., 85, B252-273.

BARRETT, F. M., BINNS, R. A., GROVES, D. I., MARSTON, R. J., and McQUEEN, K. G., 1977. Structural history and metamorphic modification of Archean volcanic-type nickel deposits, Yilgarn Block, Western Australia. Econ. Geol., 72, 1195-1224.

BARTON, P. B., and TOULMIN, P., III, 1966. Phase relations involving sphalerite in the Fe-Zn-S system. Econ. Geol., 61, 815-849.

BERRY, W. B. N., 1968. Age of Bogo Shah and western Ireland graptolite faunas and their bearing on dating early Ordovician deformation and metamorphism in Norway and Britain. NGT, 48, 217-230.

BERTHOMIER, A. L., LEUTWEIN, F., MAILLOT, J., and SONET, J., 1972. Sur quelques trondhjemites de Norvege : etude geochronologique et geochimique. Sci. de la Terre, 17, 343-351.

BERTHOMIER, C., MAILLOT, J., and ROLLET, M., 1972. Etude du massif de gabbro et diorites du Hog-Gia. Sci. de la Terre, 17, 331-340.

BHATTACHARGI, S., and SMITH, C. H., 1964. Flowage differentiation, Science, 145, 150-153.

BIRKELAND, T., and NILSEN, O., 1972. Contact metamorphism associated with gabbros in the Trondheim Region. NGU, 273, 13-22.

BJORLYKKE, K., 1974. Glacial striations on clast from the Molev tillite of the late Precambrian of Southern Norway. Amer. Jour. Sci., 274, 443-448.

BLAKE, D. H., 1962. A new Lower Ordovician graptolite fauna from the Trondheim Region. NGT, 42, 223-238.

BLOXAM, T. W., and LEWIS, A. D., 1972. Ti, Zr, and Cr in some British pillow lavas and their petrogenetic affinities. Nature Phys. Sci., 237, 134-136.

BONNICHSEN, B., 1974. Copper and nickel resources in the Duluth complex, Northeastern Minnesota. Minnesota Geol. Surv. Information Circ., 10.

BOWES, D. R., BAROOAH, B. C., and KHOURY, S. G., 1971. Original nature of Archaean rocks of North-West Scotland. Spec. Publ. Geol. Soc. Aust., 3, 77-91.

BOYD, F. R., FUJII, T., and DANCHIN, R. V., 1976. A noninflected geotherm for the Udachnaya Kimberlite Pipe, U.S.S.R.. Carnegie Inst. Wash. Year Book, 75, 523-531.

BOYLE, R. W., 1968. The geochemistry of silver and its deposits with notes on geochemical prospecting for the element. Bull. Geol. Surv. Can., 160, 264 pp.

BRISTOL, C. C., 1979. Application of sphalerite geobarometry to ores from the Ruttan Mine. Econ. Geol., 74, 1496-1503.

BUCHANAN, D. L., and NOLAN, J., 1979. Solubility of sulfur and sulfide immiscibility in synthetic tholeiitic melts and their relevance to Bushveld-complex rocks. Can. Mineral., 17, 483-494.

BUGGE, C., 1910. Rennebu. NGU, 56.

BUGGE, C., 1912. Lagfolgen i Trondhjemsfeltet. NGU, 61. Arbok 1912.

BUGGE, C., 1954. Den Kaledonske fjellkjede i Norge. NGU, 189.

BURNS, R. G., and VAUGHAN, D. J., 1970. Interpretation of the reflectivity behaviour of ore minerals. Amer. Mineral., 55, 1576-1586.

CABRI, J. L., 1973. New data on phase relations in the Cu-Fe-S system. Econ. Geol., 68, 443-454.

CAMPBELL, I. H., 1978. Some problems with the cumulus theory. Lithos, 11, 311-323.

CAMPBELL, I. H., and NALDRETT, A. J., 1979. The influence of silicate: sulfide ratios on the geochemistry of magmatic sulfides. Econ. Geol., 74, 1503-1506.

CANN, J. R., 1969. Spilites from the Carlsberg Ridge, Indian Ocean. Jour. Pet., 10, 1-19.

CARR, M. H., and TUREKIAN, K. K., 1961. The geochemistry of cobalt. Geochim. et Cosmochim. Acta, 23, 9-60.

CARRUTHERS, D. S., and PRATTEN, R. D., 1961. The stratigraphic succession and structure in the Zinc Corporation Ltd., and New Broken Hill Consolidated Ltd., Broken Hill, New South Wales. Econ. Geol., 56, 1088-1102.

CARSTENS, H., 1958. Layered basic xenoliths in some Norwegian gabbros. Beitrage zur Mineralogie und Petrographie, Bd. 6, 139-146.

CHALOUPSKY, J., and FEDIUK, F., 1967. Geology of the western and north eastern part of the Meraker area. NGU, 245, 9-21.

CHAMBERLAIN, J. A., 1967. Sulfides of the Muskox intrusion. Can. Jour. Earth Sci., 4, 105-153.

CHAMBERLAIN, J. A., McLEOD, C. R., TRAILL, R. J., and LACHANCE, G. R., 1965. Native metals in the Muskox intrusion. Can. Jour. Earth Sci., 2, 188-215.

CLARK, B. R., and KELLY, W. C., 1973. Sulfide deformation studies: I. Experimental deformation of pyrrhotite and sphalerite to 2000 bars and 500°C. Econ. Geol., 68, 332-352.

CLARKE, D. B., and O'HARA, M. J., 1979. Nickel, and the existence of high-MgO liquids in nature. Earth Planet. Sci. Lett., 44, 153-158.

CLARK, L. A., 1960a. The Fe-As-S system: phase relations and applications. Econ. Geol., 55, 1345-1381; 1631-1652.

CLARK, L. A., 1960b. Arsenopyrite As:S ratio as a possible geobarometer (abst.). Bull. Geol. Soc. Amer., 71, 1894.

CLARK, L. A., and KULLERUD, G., 1963. The sulfur-rich portion of the Fe-Ni-S system. Econ. Geol., 58, 853-885.

COWAN, J. C., 1968. Geology of the Strathcona ore deposit. Can. Inst. Min. Metall. Bull., 61, 38-54.

CRAIG, J. R., 1973. Pyrite-pentlandite assemblages and other low temperature relations in the Fe-Ni-S system. Amer. Jour. Sci., 273A, 496-510.

CRAIG, J. R., and HIGGINS, J. B., 1975. Cobalt- and iron-rich violarites from Virginia. Amer. Mineral., 60, 35-38.

CRAIG, J. R., NALDRETT, A. G., and KULLERUD, G., 1967. The Fe-Ni-S system - 400°C isothermal diagram. Carnegie Inst. Wash. Year Book, 66, 440-441.

CURTIS, C. D., and BROWN, P. E., 1969. The metasomatic development of zoned ultrabasic bodies in the Unst, Shetland. Contribs. Min. Pet., 24, 275-292.

DANCHIN, R. V., and BOYD, F. R., 1976. Ultramafic nodules from the Premier Kimberlite Pipe, South Africa. Carnegie Inst. Wash. Year Book, 75, 531-538.

DAWSON, J. B., and SMITH, J. V., 1973. Alkalic pyroxenite xenoliths from the Lashaine volcano, Northern Tanzania. Jour. Pet., 14, 113-131.

DEER, W. A., HOWIE, R. A., and ZUSSMAN, J., 1963. Rock-forming minerals: Vol. 4; framework silicates. Longmans, Green, and Co. Ltd., London, 435 pp.

DEWEY, J. F., and PANKHURST, R. J., 1970. The evolution of the Scottish Caledonides in relation to their isotopic age pattern. Trans. Roy. Sco. Edinburgh, 68, 361-389.

DEWEY, J. F., RICKARDS, R. B., and SKEVINGTON, D., 1970. New light on the age of Dalradian deformation and metamorphism in western Ireland. NGT, 50, 19-44.

DOLEZAL, J., POVONDRA, P., and SULCEK, Z., 1968. Decomposition techniques in inorganic analysis. London Iliffe Books Ltd., London, 224 pp.

DREVER, H. I., 1953. A note on the field relations of the Shiant Isles picrite. Geol. Mag., 90, 159-160.

DUDEK, A., FEDIUK, F., SUK, M., and WOLFF, F. C., 1973. Metamorphism of the Faeren Area, Central Norwegian Caledonides. NGU, 289, 1-14.

DUKE, J. M., 1976. Distribution of the period four transition elements among olivine, calcic clinopyroxene, and mafic silicate liquid: experimental results. Jour. Pet., 17, 499-521.

DUKE, J. M., 1979. Computer simulation of the fractionation of olivine and sulfide from mafic and ultramafic magmas. Can. Mineral., 17, 507-514.

DUKE, J. M., and NALDRETT, A. J., 1978. A numerical model of the fractionation of olivine and molten sulfide from komatiite magma. Earth Planet. Sci. Lett., 39, 255-266.

DUNCUMB, P., and JONES, E. M., 1969. Electron probe microanalysis: an easy to use computer program for correcting quantitative data. Tube Investments Research Laboratories, Saffron Walden, Cambridge.

EAKLE, A. S., 1922. Massive troilite from Del Norte County, California, Amer. Mineral., 7, 77-80.

ECKSTRAND, O. R., 1971. The mineralogy, geochemistry and texture of a low-grade nickeliferous serpentinite. Presented at Ann. Mtg. Geol. Assoc. Can.-Min. Assoc. Can., Sudbury, Ontario, May, 1971.

ECKSTRAND, O. R., 1975. The Dumont serpentinite: A model for the control of nickeliferous opaque mineral assemblages by alteration reactions in ultramafic rocks. Econ. Geol., 70, 183-201.

EMSLIE, R. F., 1971. Liquidus relations and subsolidus reactions in some plagioclase-bearing systems. Carnegie Inst. Wash. Year Book, 69, 148-155.

ENMO, L., 1935. Budalen Kapparverk, Gauldalsminne 1, 630-634.

ERLANK, A. J., and KABLE, E. J. D., 1976. The significance of incompatible elements in Mid-Atlantic Ridge basalts from 45°N with particular reference to Zr/Nb. Contrib. Min. Pet., 54, 281-291.

ERNST, W. G., 1973. Interpretive synthesis of metamorphism in the Alps. Geol. Soc. Amer. Bull., 84, 2053-2078.

FALCK-MUUS, R., 1932. Kvikne kobberverk 1631-1931, Sven. Bergs- & Brukstidning, 6-8, 65-72, 77-82.

FITTON, J. G., and GILL, R. C. O., 1970. The oxidation of ferrous iron in rocks during mechanical grinding. Geochim. et Cosmochim. Acta, 34, 518-524.

FLEET, M. E., MacREA, N. D., and HERZBERG, C. T., 1977. Partition of nickel between olivine and sulfide: A test for immiscible sulfide liquids. Contribs. Min. Pet., 65, 191-197.

FLOYD, P. A., and WINCHESTER, J. A., 1975. Magma type and tectonic setting discrimination using immobile elements. Earth Planet. Sci. Lett., 27, 211-218.

FOSLIE, S., 1926. Norges svovelkisforekomster. (Norwegian pyrite deposits). NGU, 127, 122 pp.

FREY, F. A., and GREEN, D. H., 1974. The mineralogy, geochemistry, and origin of lherzolite inclusions in Victorian basanites. Geochim. et Cosmochim. Acta, 38, 1023-1059.

GABRIELSE, H., 1963. McDame map-area. Cassiar district, British Columbia Geol. Surv. Can. Mem., 319.

GALE, G. H., and ROBERTS, D., 1974. Trace element geochemistry of the Norwegian Lower Palaeozoic basic volcanics and its tectonic implications. Earth Planet. Sci. Lett., 22, 380-390.

GARDNER, P. M., and ROBINS, B., 1974. The olivine-plagioclase reaction. Contribs. Min. Pet., 44, 149-156.

GAVELIN, S., and KULLING, O., 1955. Beskrivning till Berggrundskarta over Vasterbottens lan. SGU, Ca 37.

GEE, D. G., 1974. Comments on the metamorphic allochthon in northern Trondelag, Central Scandinavian Caledonides. NGT, 74, 435-440.

GEE, D. G., 1975a. A Geotraverse Through the Scandinavian Caledonides - Osterund to Trondheim, SGU C., 717, 66 pp.

GEE, D. G., 1975b. A tectonic model for the central part of the Scandinavian Caledonides, Amer. Jour. Sci., 275A, 468-515.

GEE, D. G., 1977. Extension of the Offerdal and Sarv Nappes and the Seve Supergroup into northern Trondelag. NGT, 57, 163-170.

GEE, D. G., 1978. Nappe displacement in the Scandinavian Caledonides, Tectonophysics, 47, 393-419.

GEE, D. G., and WILSON, M. R., 1974. The age of orogenic deformation in the Swedish Caledonides. Amer. Jour. Sci., 274, 1-9.

GEE, D. G., and ZACHRISSON, E., 1974. Comments on stratigraphy, faunal provinces and structure of the metamorphic allochthon, central Scandinavian Caledonides. GFF, 96, 61-66.

GELLER, S., 1962. Refinement of the crystal structure of $Co_9 S_8$. Acta Crystallogr., 15, 1195-1198.

GILL, J. B., 1976. Composition and age of Lau Basin and Ridge volcanic rocks: implications for evolution of an interarc basin and remnant arc. Bull. Geol. Soc. Amer., 87, 1384-1395.

GILL, J. B., 1978. Role of trace element partition coefficients in models of andesite genesis. Geochim. et Cosmochim. Acta, 42, 709-724.

GLASSON, M. J., and KEAYS, R. R., 1978. Gold mobilization during cleavage development in sedimentary rocks from the auriferous slate belt of Central Victoria, Australia: some important boundary conditions. Econ. Geol., 73, 496-511.

GODLEVESKII, M. N., 1959. Traps and ore-bearing intrusions of the Noril'sk region. Gosgeoltekhizdat, Moscow, pp. 69.

GODLEVESKII, M. N., and GRINENKO, L. N., 1963. Some data on the isotopic composition of sulfur in the sulfides of Noril'sk deposit. Geochemistry, No. 1, 35-41.

GOLDSCHMIDT, V. M., 1915. Die Kalksilikatgneise und Kalksilikatglimmerschiefer des Trondhjem-Gebietes. Skr. Vidensk Selsk. Christ., No. 10, 37 pp.

GRAHAM, A. MacL., 1980. Genesis of the igneous rock suite of Grenada, Lesser Antilles. Unpubl. Ph.D. thesis, Univ. Edinburgh.

GRAHAM, C. M., 1976. Petrochemistry and tectonic setting of Dalradian metabasaltic rocks of the S. W. Scottish Highlands. Jour. Geol. Soc., 132, 61-84.

GRATEROL, M., and NALDRETT, A. J., 1971. Mineralogy of the Marbridge No. 3 and No. 4 nickel-iron sulfide deposits. Econ. Geol., 66, 866-900.

GREEN, A. H., 1975. Nickel sulfide deposits. Unpubl. report, University of Toronto.

GREEN, D. H., and HIBBERSON, W., 1970. The instability of plagioclase in peridotite at high pressure. Lithos, 3, 209-221.

GRENNE, T., GRAMMELTVEDT, G., and VOKES, F. M., in prep.. Cyprus-type sulfide deposits in the Western Trondheim District, central Norwegian Caledonides.

GRIFFIN, W. L., and HEIER, K. S., 1973. Petrologic implications of some corona structures. Lithos, 6, 315-335.

GROVES, D. I., HUDSON, D. R., and HACK, T. B. C., 1974. Modification of iron-nickel sulfides during serpentinization and talc-carbonate alteration at Black Swan, Western Australia. Econ. Geol., 69, 1265-1281.

GUEZOU, J. C., 1977. Histoire Paleozoique d'un segment central des Caledonides Scandinaves internes. Rev. Geog. Phys. Geol. Dynamique (2), XIX, 453-470.

GUEZOU, J. C., 1978. Geology and structure of the Dombas-Lesja area, Southern Trondheim region, south-central Norway. NGU, 340, 1-34.

GUSTAFSON, J. K., BURRELL, H. C., and GARRETY, M. D., 1950. Geology of the Broken Hill ore deposit, Broken Hill, N.S.W., Australia. Bull. Geol. Soc. Amer., 61, 1369-1438.

HAAPALA, P. S., 1969. Fennoscandian nickel deposits. In, H. D. B. Wilson (ed.), Magmatic Ore Deposits. Econ. Geol. Monograph 4, 262-275.

HAKLI, A., 1963. Distribution of nickel between the silicate and sulphide phases in some basic intrusions in Finland. Comm. geol. Finlande Bull., 209, 54 pp.

HAMAD, El, D., 1963. The chemistry and mineralogy of the olivine nodules of Calton Hill, Derbyshire. Min. Mag., 33, 483-497.

HARRIS, D. C., and NICKEL, E. H., 1972. Pentlandite compositions and associations in some mineral deposits. Can. Mineral., 11, 861-878.

HART, S. R., 1970. Chemical exchange between sea water and deep ocean basalts. Earth Planet. Sci. Lett., 9, 269-279.

HART, S. R., GLASSLEY, W. E., and KARIG, D. E., 1972. Basalts and sea-floor spreading behind the Mariana island arc. Earth Planet. Sci. Lett., 15, 12-18.

HATTON, HOWARD III, 1977. Geochemistry of Selenium. Geochim. et Cosmochim. Acta, 41, 1665-1678.

HAUGHTON, D., ROEDER, P. L., and SKINNER, B. J., 1974. Solubility of sulfur in mafic magmas. Econ. Geol., 69, 451-467.

HAWLEY, J. E., 1962. The Sudbury ores: Their mineralogy and origin. Can. Mineral., 7, pt. 1, 207 pp.

HELLAND, A., 1902. Norges land og folk: Hedemarkens Amt, bd. II. Kristiania (Oslo), 728 pp.

HELLMAN, P. L., SMITH, R. E., and HENDERSON, P., 1979. The mobility of the rare earth elements: evidence and implications from selected terrains affected by burial metamorphism. Contrib. Min. Pet., 71, 23-44.

HERRMANN, A. G., POTTS, M. J., and KNAKE, D., 1974. Geochemistry of the rare earth elements in spilite from the oceanic and continental crust. Contrib. Min. Pet., 44, 1-16.

HERZBERG, C. T., 1976. The plagioclase-lherzolite to spinel-lherzolite facies boundary; its bearing on corona structure formation and tectonic history in the Norwegian Caledonides. Progress in Experimental Petrology, N.E.R.C., Third Report, 233-235.

HIMMELBERG, G. R., and FORD, A. B., 1976. Pyroxenes of the Dufek intrusion, Antarctica. Jour. Pet., 17, 219-243.

HOBBS, B. E., 1966. The structural environment of the northern part of the Broken Hill orebody. Geol. Soc. Aust. Jour., 13, 315-338.

HOGBOM, A. G., 1909. Studies in the post-Silurian thrust region of Jamtland, GFF, 31, 289-346.

HOLDAWAY, M. J., 1971. Stability of andalusite and the aluminium-silicate phase diagram. Amer. Jour. Sci., 271, 97-131.

HUDSON, D. R., 1972. Evaluation of genetic models for Australia sulfide nickel deposits. Australas. Inst. Min. Metall. Ann. Conference, Newcastle, 59-68.

HUDSON, D. R., 1973. Genesis of Archaean ultramafic - associated nickel-iron sulfide at Nepean, Western Australia. Australas. Inst. Min. Metall., Western Australian Conference, 99-109.

HUHMA, M., 1970. Nickel, cobalt, and copper in some rocks of the Outokumpu region. Bull. Geol. Soc. Finland, 42, 67-88.

JAANUSSON, V., 1973. Aspects of carbonate sedimentation in the Ordovician of Baltoscandia. Lethaia, 6, 11-34.

JAHNS, R. H., 1967. Serpentinites of the Roxbury district, Vermont. In: Wyllie, P. J. (ed.), Ultramafic and related rocks, John Wiley and Sons, Inc., New York, 137-160.

JENKS, W. F., 1971. Tectonic transport of massive sulfides in submarine volcanic and sedimentary host rocks. Econ. Geol., 66, 1215-1224.

JOHNSON, I. R., and KLINGNER, G. D., 1976. Broken Hill ore deposit and its environment. In: Knight, C. L. (ed): Economic geology of Australia and Papua New Guinea, 1. Metals: Australasian Inst. Min. Metall., Monograph 5, 476-491.

KAUP-MOLLER, S., and BRUMMER, J. J., 1970. Geology and sulfide deposits of the Bird River claim group of Maskwa Nickel Chrome Mines Ltd., Southeastern Manitoba. Presented at Ann. Mtg. Geol. Assoc. CAN.-MIN. ASSOC. CAN., Winnipeg, Manitoba, Sept., 1970.

KEILHAU, B. M., 1850. Gaea Norvegica, Chra. (J. Dahl).

KENNY, E. J., 1932. The Broken Hill lode - its geological structure: Australas. Inst. Min. Metall. Proc., No. 87, 217-245.

KIAER, J., 1932. The Hovin Group in the Trondheim area. With Paleontological contributions by O. A. Hoeg, A. Hadding, F.R.C. Reed, T. Strand, Leif Stormer and the author. Skr. norske Videnske Akad., No. 4, 176 pp.

KING, H. F., and O'DRISCOLL, E. S., 1953. The Broken Hill Lode. In: Edwards, A. B., (ed.): Geology of Australian ore deposits. Fifth Empire Mining and Metallurgical Congress, 578-600.

KING, H. F., and THOMSON, B. P., 1953. The geology of the Broken Hill District. In: Edwards, A. B. (ed.): Geology of Australian ore deposits. Fifth Empire Mining and Metallurgical Congress, 533-577.

KISSIN, S. A., 1974. Phase relations in a portion of the Fe-S system. Unpubl. Ph.D. thesis, University of Toronto, Canada.

KISSIN, S. A., and SCOTT, S. D., 1972. Phase relations of intermediate pyrrhotites (abstr.). Geol. Soc. Amer. Abstr. Progr. 4., 562 (also in Econ. Geol., 67, 1007).

KJERULF, Th., 1871. Om Trondhjems Stifts geologi. Chra. Nyt Mag. for Naturv. Bd. 18.

KJERULF, Th., 1878. Udsigt over det sydlige Norges Geologi. Chra.

KLEMM, D. D., 1965. Synthesen und Analysen in den Dreickdiagrammen FeAsS-CoAsS-NiAsS und FeS_2-CoS_2-NiS_2. Neues Jahrb. Mineral. Abh., 103, 205-255.

KNOP, O., and IBRAHIM, M. A., 1961. Chalcogenides of the transition elements II. Existence of the π phase in the M_9 S_8 section of the system Fe-Co-Ni-S. Can. Jour. Chem., 39, 297-317.

KOLDERUP, C. F., and KOLDERUP, N. H., 1940. Geology of the Bergen Arc System. Bergens Mus. Skr., no. 20, 137 pp.

KOLJONEN, T., and ROSENBERG, R. J., 1975. Rare earth elements in middle precambrian volcanic rocks of Finland, with a discussion of the origin of the rocks. Bull. Geol. Soc. Finland, 47, 127-138.

KRAUSKOPF, K. B., 1967. Introduction to geochemistry. McGraw-Hill Book Company, New York, 721 pp.

KUBLER, L., and LINDQVIST, B., 1979. Tectonic control of pyrrhotite phase distribution studied on a fold structure. Lithos, 12, 241-249.

KULLERUD, G., 1963. Thermal stability of pentlandite. Can. Mineral., 7, 353-366.

KULLERUD, G., and YODER, H. S., 1959. Pyrite stability relations in the Fe-S system. Econ. Geol., 54, 533-572.

KULLERUD, G., YUND, R. A., and MOH, G. H., 1969. Phase relations in the Cu-Fe-S, Cu-Ni-S, and Fe-Ni-S system. In: H. D. B. Wilson (ed.), Magmatic Ore Deposits. Econ. Geol. Monograph 4, 323-343.

KULLING, O., 1961. On the age and tectonic position of the Valdres Sparagmite, GFF, 83, 210-214.

KUZNETSOV, V. G., SOKOLOVA, M. A., PALKINA, K. K., and POPOVA, Z. V., 1965. The cobalt-sulfur system. Izvestiya Akademii Nauk SSSR Neoorganicheskie Materialy, 1(5), 675-689.

LAING, W. P., MARJORIBANKS, R. W., and RUTLAND, R. W. R., 1978. Structure of the Broken Hill Mine Area and its significance for the genesis of the orebodies. Econ. Geol., 73, 1112-1136.

LAMBERT, R. St. J., and McKERROW, W. S., 1976. The Grampian Orogeny. Scott. Jour. Geol., 12, 271-292.

LEUTHWEIN, F., 1972. Selenium, 34. In: Wedepohl, K. H. (ed.), Handbook of Geochemistry. Springer-Verlag, Berlin.

LEWIS, B. R., FORWARD, P. S., and ROBERTS, J. B., 1965. Geology of Broken Hill lode, reinterpreted. In: McAndrew, J. (ed.): Geology of Australian Ore Deposits. Eighth Commonwealth Mining and Metallurgical Congress, Vol. 1, 319-338.

LIEUNGH, B., 1977. Geological report of the Skjaekerdalen-Helgadalen area with special respect to the Dyrhaugen Gabbro breccia and Ni-deposits. Unpubl. report. A/S Sulfidmalm, Report No. 462/77/24.

LOVAS, L. B., 1970. En malmgeologisk undersokelse av Skjaekerdalens Ni-Cu forekomst. Unpubl. thesis, NTH, Trondheim.

LUNDQVIST, D., 1947. X-ray studies in the ternary system Fe-Ni-S. Ark. Kemi. Mineral. Geol., 24A, no. 22.

LUSK, J., and FORD, C. E., 1978. Experimental extension of the sphalerite geobarometer to 10 kbar. Amer. Mineral., 63, 516-519.

LUSK, J., CAMPBELL, F. A., and KROUSE, H. R., 1975. Application of sphalerite geobarometry and sulfur-isotope geothermometry to ores of the Quemont Mine, Noranda, Quebec. Econ. Geol., 70, 1070-1083.

LUYENDYK, B. P., CANN, J. R., and SHARMAN, G. S., 1979. Introduction and site reports: Site 410. Initial Repts. DSDP, 49, 227-313.

MAINWARING, P. R., and NALDRETT, A. J., 1977. Country rock assimilation and the genesis of Cu-Ni sulfides in the Water Hen intrusion, Duluth Complex, Minnesota. Econ. Geol., 72, 1269-1284.

MANSON, V., 1967. Geochemistry of Basaltic rocks : major elements. In: Hess, H. H., and Poldervaart, A. (eds.), Basalts: the Poldervaart Treatise on Rocks of Basaltic Composition; Vol. 1, 215-269. John Wiley and Sons, N.Y., 862 pp.

MATTHEWS, D. H., 1971. Weathered basalts from Swallow Bank, an abyssal hill in the NE Atlantic. Philos. Trans. Roy. Soc. (London), Ser. A, 268, 551-571.

MAWSON, Sir Douglas, 1912. Geological investigations in the Broken Hill Area. Roy. Soc. S. Aust., Mem. 2.

MELSON, W. G., and VAN ANDEL, T. H., 1966. Metamorphism in the Mid-Atlantic Ridge, 22°N latitude. Mar. Geol., 4, 165-186.

MISRA, K. C., and FLEET, M. E., 1973. The chemical composition of synthetic and natural pentlandite assemblages. Econ. Geol., 68, 518-539.

MITCHELL, A. H., and BELL, J. D., 1973. Island-arc evolution and related mineral deposits. Jour. Geol., 81, 381-405.

MIYASHIRO, A., 1968. Metamorphism of mafic rocks. In: Hess, H. H., and Poldervaart, A., (eds.), Basalts: the Poldervaart Treatise on rocks of basaltic composition, Vol. 2, 799-834. John Wiley and Sons, N.Y., 862 pp.

MIYASHIRO, A., 1973. Metamorphism and metamorphic belts. George Allen & Unwin, 492 pp.

McANDREW, J., 1965. Gold deposits of Victoria. In: McAndrew J. (ed.): Geology of Australian ore deposits. Eighth Commonwealth Mining and Metallurgical Congress, Vol., 1, 450-456.

MacLEAN, W. H., and SHIMAZAKI, H., 1976. The partition of Co, Ni, Cu, and Zn between sulfide and silicate liquids. Econ. Geol., 71, 1049-1057.

NALDRETT, A. J., 1966. The role of sulphurization in the genesis of iron-nickel sulfide deposits of the Porcupine district, Ontario. Trans. Can. Inst. Min. Metal., 69, 147-155.

NALDRETT, A. J. 1969. A portion of the system Fe-S-O and its application to sulfide ore magmas. Jour. Pet., 10, 171-201.

NALDRETT, A. J., 1973. Nickel sulfide deposits - Their classification and genesis, with special emphasis on deposits of volcanic association. Bull. Can. Inst. Min. and Metall., 76, 45-63.

NALDRETT, A. J., 1979. Partitioning of Fe, Co, Ni, and Cu between sulfide liquid and basaltic melts and the composition of Ni-Cu sulfide deposits - a reply and further discussion. Econ. Geol., 74, 1520-1528.

NALDRETT, A. J., and CABRI, L. J., 1976. Ultramafic and related mafic rocks: Their classification and genesis with special reference to the concentration of nickel sulfides and platinum-group elements. Econ. Geol., 71, 1131-1158.

NALDRETT, A. J., and TURNER, A. R., 1977. The geology and petrogenesis of a greenstone belt and related nickel-sulfide mineralisation at Yakabindie, Western Australia. Precamb. Research, 5, 43-103.

NALDRETT, A. J., CRAIG, J. R. and KULLERUD, G., 1967. The central portion of the Fe-Ni-S system and its bearing on pentlandite exsolution in iron-nickel sulfide ores. Econ. Geol., 62, 826-847.

NALDRETT, A. J., BRAY, J. G., GASPARRINI, E. L., PODOLSKY, T., and RUCKLIDGE, J. C., 1970. Cryptic variation and the petrology of the Sudbury Nickel Irruptive. Econ. Geol., 65, 122-155.

NESBITT, R. W., and SUN, S. S., 1976. Geochemistry of Archean spinifex-textured peridotites and magnesian and low-magnesian tholeiites. Earth Planet. Sci. Lett., 31, 433-453.

NEUMAN, R. B., and BRUTON, D. L., 1974. Early Middle Ordovician (Whiterock) fossils from the Holana area, Trondheim Region, West Central Norway. NGT, 54, 69-115.

NICHOLLS, I. A., and RINGWOOD, A. E., 1972. Production of silica-saturated tholeiitic magmas in island arcs. Earth Planet. Sci. Lett., 17, 243-246.

NILSEN, O., 1971. Sulfide mineralisation and wall-rock alteration at Rodhammeren mine, Sor-Trondelag, Norway. NGT, 51, 329-354.

NILSEN, O., 1974. Mafic and ultramafic inclusions from the initial (Cambrian?) volcanism in the central Trondheim region, Norway, NGT, 54, 337-359.

NILSEN, O., 1978. Caledonian sulfide deposits and minor iron-formations from the southern Trondheim region, Norway, NGU, 340, 35-85.

NILSEN, O., and MUKHERJEE, A. D., 1972. Geology of the Kvikne mines with special reference to the sulfide ore mineralisation. NGT, 52, 151-192.

NORRISH, K., and HUTTON, J. T., 1969. An accurate X-ray spectrographic method for the analysis of a wide range of geological samples. Geochim. et Cosmochim. Acta, 33, 431-453.

NWE, Y. Y., 1976. Electron microprobe studies of the earlier pyroxenes and olivines from the Skaergaard Intrusion, East Greenland. Contrib. Min. Pet., 55, 105-126.

OFTEDAHL, C., 1958. On exhalative-sedimentary ores. GFF, 80, 1-19.

OFTEDAHL, C., 1967. A manganiferous chert in the Caledonian greenstone of Trondheim. Kgl. Norske Vidensk. Selskabs Forhandl., 40, 48-54.

OFTEDAHL, C., 1968. Greenstone volcanoes in the central Norwegian Caledonides. Geol. Rdsch., 57, 920-930.

OFTEDAHL, C., 1969. One-day excursion through the Horg syncline: In Excursion guide to the central parts of the Trondheim region. NGU, 14 pp.

O'HARA, M. J., SAUNDERS, M. J., and MERCY, E. L. P., 1975. Garnet-peridotite, primary ultrabasic magma and eclogite: interpretation of upper mantle processes in Kimberlites. Phys. Chem. Earth., 9, 571-604.

OLESEN, N. O., HANSEN, E. S., KRISTENSEN, L. H., and THYRSTED, T., 1973. A preliminary account of the geology of the Selbu-Tydal area, the Trondheim Region, Central Norwegian Caledonides. Leidse. geol. Meded., 49, 259-276.

OLSEN, J., in press. Genesis of the Joma stratiform sulfide deposit, Central Norwegian Caledonides. Proceedings of the V. IAGOD-meeting.

PAPUNEN, H., 1970. Sulfide mineralogy of the Kotalahti and Hitura nickel-copper ores, Finland. Annales Acad. Sci. Fennicae, ser. A, III. Geologica-Geographica, 109, 74 pp.

PAUWELS, L. J., 1970. Energy level diagrams of the "NiAs" pyrite and spinel type sulfides of Fe, Co, and Ni. Soc. Chim.Bulges Bull., 79, 549-566.

PEARCE, J. A., 1975. Basalt geochemistry used to investigate past tectonic environment on Cyprus. Tectonophysics, 25, 41-68.

PEARCE, J. A., and CANN, J. R., 1973. Tectonic setting of basic volcanic rocks determined using trace element analyses. Earth Planet. Sci. Lett., 19, 290-300.

PEARCE, J. A., and GALE, G. H., 1977. Identification of ore-deposition encironment from trace-element geochemistry of associated igneous host rocks. In: Volcanic processes in ore genesis. Geol. Soc. London Publ. 7, 14-24.

PEARCE, J. A., and NORRY, M. J., 1979. Petrogenetic implications of Ti, Zr, Y, and Nb variations in volcanic rocks. Contrib. Min. Pet., 69, 33-47.

PETRUK, W., HARRIS, D. C., and STEWART, J. M., 1969. Langisite, a new mineral, and the rare minerals cobalt pentlandite, siegenite, parkerite, and bravoite from the Langis Mine, Cobalt-Gowganda area, Ontario. Can. Mineral., 9, 597-616.

PETTIJOHN, F. J., 1975. Sedimentary rocks. Harper and Row, New York, 628 pp.

PINNA, P., 1973. Etude geologique du Dovrefjell meridional. These, Lab. Geol. Structurale, Univ. Paris, Orsay, 85 pp.

PRINGLE, I. R., and STURT, B. A., 1969. The age of the peak of the Caledonian orogeny in west Finnmark, north Norway. NGT, 49, 435-436.

RAJAMANI, V., 1976. Distribution of iron, cobalt, and nickel between synthetic sulfide and orthopyroxene at 900°C. Econ. Geol., 71, 795-802.

RAJAMANI, V., and NALDRETT, A. J., 1978. Partitioning of Fe, Co, Ni, and Cu between sulfide liquid and basaltic melts and the composition of Ni-Cu sulfide deposits. Econ. Geol., 73, 82-93.

RAJAMANI, V., and PREWITT, C. T., 1973. Crystal chemistry of natural pentlandites. Can. Mineral., 12, 178-187.

RAMDOHR, P., 1967. A widespread mineral association, connected with serpentinization; with notes on some new or insufficiently defined minerals. Neues Jahrbuch Mineral. Abh., 107, 241-265.

RASCHKA, H., and ECKHARDT, F. J., 1976. Geochemistry of basalts from the Norwegian-Greenland Sea, Leg 38, DSDP. Initial Repts. D.S.D.P., 38, 719-730.

READ, H. H., 1934. On zoned associations of talc, actinolite, chlorite, and biotite in Unst, Shetland Islands. Min. Mag., 23, 519-540.

RICHARDSON, S. W., GILBERT, M. C., and BELL, P. M., 1969. Experimental determination of kyanite-andalusite and andalusite-sillimanite equilibria; the aluminium silicate triple point. Amer. Jour. Sci., 267, 259-272.

ROBERTS, D., 1967. Structural observations from the Koppera-Riksgrense area and discussion of the tectonics of the Stjordalen and the N.E. Trondheim region. NGU, 245, 64-120.

ROBERTS, D., 1968. On the occurrence of sillimanite in the Gula Schist Group, Trondheim region. NGT, 48, 171-177.

ROBERTS, D., 1978. Caledonides of south central Norway. Geol. Surv. Canada, Paper 78-13, 31-37.

ROBERTS, D., and STROMGARD, K.-E., 1972. A comparison of natural and experimental strain patterns around fold hinge zones. Tectonophysics, 14, 105-120.

ROBERTS, D., SPRINGER, J., and WOLFF, F. C., 1970. Evolution of the Caledonides in the northern Trondheim region, Central Norway: a review, Geol. Mag., 107, 133-145.

ROEDER, P. L., 1974. Activity of iron and olivine solubility in basaltic liquids. Earth Planet. Sci. Lett., 23, 397-410.

ROEDER, P. L., and EMSLIE, R. F., 1970. Olivine-liquid equilibrium, Contrib. Min. Pet., 29, 275-289.

ROHR-TORP, E., 1972. A major inversion of the Western part of the Trondheim Nappe. NGT, 52, 453-458.

ROHR-TORP, E., 1974. Contact metamorphism around the Innset massif. NGT, 54, 13-33.

ROSENLUND, A. L., 1915. Meddelelse vedrorende Vaerdalens eller Skjaekerdalens gruver (report).

RUI, I. J., 1972. Geology of the Roros district, south-eastern Trondheim region with a special study of the Kjoliskarvene-Holtsjoen area. NGT, 52, 1-21.

RUI, I. J., 1973a. Geology and structures of the Rostvangen sulphide deposit in the Kvikne district, central Norwegian Caledonides. NGT, 53, 433-442.

RUI, I. J., 1973b. Structural control and wall-rock alteration at Killingdal mine, central Norwegian Caledonides. Econ. Geol., 68, 859-883.

SANDELL, E. B., 1959. Colorimetric determination of traces of metals. Interscience Publishers, Inc., New York, 1032 pp.

SANGSTER, D. F., and SCOTT, S. D., 1976. Precambrian, stratabound, massive, Cu-Zn-Pb sulfide ores of North America. In: Wolff, K. H. (ed.): Handbook of stratabound and stratiform ore deposits, Vol. 6, Elsevier, N.Y., 129-222.

SATO, T., 1972. Behaviours of ore-forming solutions in seawater. Mining Geology, Jour. Soc. Min. Geol. Japan, 22, 31-42.

SAUNDERS, A. D., and TARNEY, J., 1979. The geochemistry of basalts from a back-arc spreading centre in the East Scotia Sea. Geochim. et Cosmochim. Acta, 43, 555-572.

SAUNDERS, A. D., TARNEY, J., and WEAVER, S. D., in press. Traverse geochemical variations across the Antarctic Peninsula: implications for the genesis of calc-alkaline magmas. Earth Planet. Sci. Lett., in press.

SAUNDERS, A. D., TARNEY, J., STERN, C., and DALZIEL, I. W. D., 1979. Geochemistry of Mesozoic marginal basin floor igneous rocks from southern Chile. Bull. Geol. Soc. Amer. 90, 237-258.

SAWKINS, F. J., 1976. Massive sulfide deposits in relation to geotectonics. IN: Strong, D. F. (ed.): Metallogeny and plate tectonics. Geol. Assoc. Can., Spec. Pap. 14, 221-240.

SCOTT, S. D., 1973. Experimental calibration of the sphalerite geobarometer. Econ. Geol., 68, 466-474.

SCOTT, S. D., 1974. Experimental methods in sulfide synthesis. In: Ribbe (ed.), Sulfide Mineralogy. Min. Soc. Amer. Short Course Notes, Vol. 1, S1-S38.

SCOTT, S. D., 1976. Application of the sphalerite geobarometer to regionally metamorphosed terrains. Amer. Mineral., 61, 661-670.

SCOTT, S. D., and BARNES, H. L., 1971. Sphalerite geothermometry and geobarometry. Econ. Geol., 66, 653-669.

SCOTT, S. D., and KISSIN, S. A., 1973. Sphalerite composition in the Zn-Fe-S system below 300°C. Econ. Geol., 68, 475-479.

SHIMA, H., and NALDRETT, A. J., 1975. Solubility of sulfur in an ultramafic melt and the relevance of the system Fe-S-O. Econ. Geol., 70, 960-967.

SIEDLECKA, A., 1967. Geology of the eastern part of the Meraker area. NGU, 245, 22-58.

SIEDLECKA, A., and SIEDLECKI, S., 1967. Geology of the northernmost part of the Meraker area. NGU, 245, 59-63.

SILLITOE, R. H., 1972. Formation of certain massive sulfide deposits at sites of sea-floor spreading. Trans. Inst. Min. Metall, 81, B141-B148.

SILLITOE, R. H., 1973. Environments of formation of volcanogenic massive sulfide deposits. Econ. Geol., 68, 1321-1325.

SITTER, L. U. De., 1956. Structural geology. McGraw-Hill Publishing Company Limited, New York, 552 pp.

SKINNER, B. J., and BARTON, P. B., 1973. Genesis of mineral deposits. Ann. Rev. Earth Sci., 1, 183-211.

SKINNER, B. J., and PECK, D. L., 1969. An immiscible sulfide melt from Hawaii. In: H. D. B. Wilson (ed.), Magmatic Ore Deposits. Econ. Geol. Monograph 4, 310-322.

SKJESETH, S., 1963. Contributions to the geology of the Mjosa district and the classical sparagmite area in southern Norway. NGU, 220.

SPENCER, E. W., 1969. Introduction to the structure of the earth. McGraw-Hill Book Company, New York, 597 pp.

SPRINGER, R. K., 1974. Contact metamorphosed ultramafic rocks in the western Sierra Nevada foothills, California. Jour. Pet., 15, 160-195.

SPRINGER, R. K., and CRAIG, J. R., 1975. Sulfide mineralogy of metamorphosed ultramafic rocks, western Sierra Nevada foothills, California. Econ. Geol., 70, 1478-1483.

SPRINGER-PEACEY, J., 1964. Reconnaissance of the Tommeras Anticline, NGU, 227, 13-84.

STANTON, R. L., 1972. Ore Petrology. McGraw-Hill Book Company, 713 pp.

STATHAM, P. J., 1975. Quantitative X-ray energy spectrometry: the application of a Si(Li) detector to electron microprobe analysis. Unpubl. Ph.D. thesis, Univ. Cambridge.

STOREN, R., 1951. Kvikne Koparverk. Kvikne Bygdebok, Bd. II, Oslo, 414-460.

STORMER, L., 1941. Dictyonema shales outside the Oslo region. NGT, 20.

STRAND, T., 1948. New trilobites from the Holanda limestone (Trondheim Region, Southern Norway). NGT, 27, 74-88.

STRAND, T., 1951. The Sel and Vaga map areas. NGU, 178, 116 pp.

STRAND, T., 1960. The pre-Devonian rocks and structures in the region of Caledonian deformation. In: Holtedahl, O. (ed.), Geology of Norway, 170-284.

STRAND, T., and KULLING, O., 1972. Scandinavian Caledonides. Wiley and Sons, London, 302 pp.

STRAUSS, G. K., and MADEL, J., 1974. Geology of massive sulphide deposits in the Spanish-Portuguese pyrite belt. Geol. Rdsch., 63, 191-211.

STUMPFL, E. F., and CLARK, A. M., 1964. A natural occurrence of $Co_9 S_8$, identified by X-ray microanalysis. Neues. Jahr. Min., heft 8, 240-245.

STURT, B. A., 1975. Preliminary report on the Geology of the Vakkerlien prospect. Unpubl. report to A/S Sulfidmalm, Kristiansand, Norway.

STURT, B. A., 1978. The Norwegian Caledonides - Introduction. Geol. Surv. Canada, Paper 78-13, 13-15.

STURT, B. A., and ROBERTS, D., 1978. Caledonides of Northernmost Norway (Finnmark). Geol. Surv. Canada, Paper 78-13, 17-24.

STURT, B. A., and THON, A., 1976. Discussion: The age of Orogenic Deformation in the Swedish Caledonides. Amer. Jour. Sci., 276, 385-390.

STURT, B. A., MILLER, J. A., and FITCH, F. J., 1967. The age of alkaline rocks from west Finnmark, northern Norway, and their bearing on dating the Caledonian Orogeny. NGT, 47, 255-273.

STURT, B. A., PRINGLE, I. R., and ROBERTS, D., 1975. Caledonian nappe sequence of Finnmark, northern Norway, and the timing of Orogenic deformation and metamorphism. Bull. Geol. Soc. Amer., 86, 710-718.

SUGISAKI, R., MIZUTANI, S., HATTORI, H., ADACHI, M., and TANAKA, T., 1972. Late Paleozoic geosynclinal basalt and tectonism in Japanese Islands: Tectonophysics, 14, 35-56.

SVENONIUS, F., 1885. Nagra profiler inom mellersta Skandinaviens skifferomrade. GFF, no. 95. Bd. VII, Hft. 11.

SWEATMAN, T. R., and LONG, J. V. P., 1969. Quantitative electron-probe microanalysis of rock-forming minerals. Jour. Pet., 10, 332-379.

TARNEY, J., SAUNDERS, A. D., and WEAVER, S. D., 1977. Geochemistry of volcanic rocks from the island arcs and marginal basins of the Scotia Sea region. In: Talwani, M., and Pitman, W. C., III (eds.), Island Arcs, Deep Sea Trenches and Back-arc Basins, Maurice Ewing series, Vol. 1: Washington, D. C., American Geophysical Union, 367-378.

TARNEY, J., SAUNDERS, A. D., WEAVER, S. D., DONNELLAN, N. C. B., and GRAHAM, L. H., 1979. Minor-element geochemistry of basalts from Leg 49, North Atlantic Ocean. Initial Repts. DSDP, 49, 657-691.

TEMPLEMAN-KLUIT, D. J., 1970. The relationship between sulfide grain size and metamorphic grade of host rocks in some strata-bound pyritic ores. Can. Jour. Earth Sci., 7, 1339-1345.

THIRLWALL, M. F., 1979. The petrochemistry of the British Old Red Sandstone volcanic province. Unpubl. Ph.D. thesis, Univ. Edinburgh.

THOMAS, D. E., 1953. The Bendigo Goldfield. In: Edwards, A. B. (ed.): Geology of Australian Ore Deposits. Fifth Empire Mining and Metallurgical Congress, 1011-1027.

THOMPSON, J. F., 1978. The geology of the Vakkerlien nickel deposit, Kvikne, Norway. Unpubl. M.Sc. thesis, Univ. Toronto.

THOMPSON, K. C., and REYNOLDS, R. J., 1970. Atomic Absorption, fluorescence and flame emission spectroscopy. Charles Griffin and Company Ltd., High Wycombe, England, 319 pp.

TILLEY, C. E., 1935. Metasomatism associated with greenstone hornfelses of Kenidjack and Botallack, Cornwall, Min. Mag., 24, 181-202.

TOULMIN, P. III, 1960. Effect of Cu on sphalerite phase equilibria - a preliminary report (abstr.). Bull. Geol. Soc. Amer., 71, 1993.

TURNER, J. S., and GUSTAFSON, L. B., 1978. The flow of hot saline solutions from vents in the sea floor - Some implications for exhalative massive sulfide and other ore deposits. Econ. Geol., 73, 1082-1100.

USSELMAN, T. M., HODGE, D. S., NALDRETT, A. J., and CAMPBELL, I. H., 1979. Physical constraints on the characteristics of nickel sulfide ore in ultramafic lavas. Can. Mineral., 17, 361-372.

VAUGHAN, D. J., BURNS, R. G., and BURNS, V. M., 1971. Geochemistry and bonding of thiospinel minerals. Geochim.et Cosmochim. Acta, 35, 365-381.

VAUGHAN, D. J., SCHWARZ, E. J., and OWENS, D., 1971. Pyrrhotite from Strathcona mine, Sudbury, Canada; a thermal magnetic mineralogical study. Econ. Geol., 66, 1131-1144.

VOGT, J. H. L., 1889. Funn av Dictyonema ved Holsjoen, Holtalen. Vid selsk. Christiania Forh. Oversikt over Videnskabs-Selskabets Moder I 1888.

VOGT, T., 1928. Den norske fjellkjedes revolusjonshistorie. NGT, 25, 449-528.

VOGT, T., 1941. Geological notes on the Dictyonema locality and the upper Gauldal District in the Trondheim Area, NGT, 20, 171-192.

VOGT, T., 1945. The geology of part of the Holanda-Horg District, a type area in the Trondheim Region, NGT, 25, 449-528.

VOKES, F. M., 1968. Regional metamorphism of the Palaeozoic geosynclinal sulfide ore deposits of Norway. Trans. Inst. Min. Metall., 77, B53-B59.

VOKES, F. M., 1969. A review of the metamorphism of sulfide deposits. Earth-Sci. Rev., 5, 99-143.

VOKES, F. M., 1970. Discussion: Aspects of wall rock alteration associated with some Finnish sulfide deposits; a Review (by A. Mikkola). Trans. Inst. Min. Metall., 79, B99-B100.

VOKES, F. M., 1974. Structural control and wall rock alteration at Killingdal mine, central Norwegian Caledonides: Discussion. Econ. Geol., 69, 706-708.

VOKES, F. M., 1976. Caledonian massive sulfide deposits in Scandinavia: A comparative review. In: Wolf, K. H. (ed.): Handbook of strata-bound and stratiform ore deposits, Vol. 6, Elsevier, N.Y., 79-127.

VOKES, F. M., and GALE, G. H., 1976. Metallogeny relatable to global tectonics in southern Scandinavia. In: Strong, D. F. (ed.), Metallogeny and plate tectonics. Geol. Assoc. Can., Spec. Pap. 14, 413-441.

VOKES, F. M., and MORTON, R. D., 1973. A discussion: Geology of the Kvikne Mines with special reference to the sulfide ore mineralis-ation. NGT, 53, 333-336.

VOSS, J. F., 1783-1790. Forsog til en norsk bergverkshistorie. Kristiana (Oslo) 1911(-12), 156 pp.

WAGER, L. R., and BROWN, G. M., 1968. Layered igneous rocks. Oliver and Boyd, Edinburgh, 588 pp.

WAGNER, P. A., 1929. Platinum deposits and mines of South Africa. Oliver and Boyd, London, 71-79.

WALTHAM, A. C., 1968a. Classification and genesis of some massive sulfide deposits in Norway. Trans. Inst. Min. Metall., 77, B153-B161.

WALTHAM, A. C., 1968b. The geology of the Folldal massive sulfide deposits, Norway. Unpubl. Ph.D. Thesis, R.S.M., Imp. Coll., London.

WEAVER, S. D., SAUNDERS, A. D., PANKHURST, R. J., and TARNEY, J., 1979. A geochemical study of magmatism associated with the initial stages of back-arc spreading. Contrib. Min. Pet., 68, 151-169.

WEGMANN, E., 1925. Sur le lambeau de recouvrement de la Gula (Chaine Caledonienne Scandinave). C. R. Somm. des Scieances de la Soc. geol. de Fr., 1925, 158-159.

WIGGINS, L. B., and CRAIG, J. R., 1975. A reconnaissance investigation of chalcopyrite-sphalerite relationships in the Cu-Fe-Zn-S system (abstr.). Geol. Soc. Amer. Abstr. Progr. 7, 1317.

WILSON, H. D. B., and ANDERSON, D. T., 1959. The composition of Canadian sulfide ore deposits. Trans. Can. Inst. Min. Metall., 62, 325-337.

WILSON, M. R., ROBERTS, D., and WOLFF, F. C., 1973. Age determination from the Trondheim Region Caledonides, Norway: a preliminary report. NGU, 288, 53-63.

WINKLER, H. G. F., 1976. Petrogenesis of metamorphic rocks. Springer-Verlag, New York, Inc., 334 pp.

WOLFF, F. C., 1960. Foreløpige meddelelser fra Kartbladet Verdal. NGU, 211, 212-230.

WOLFF, F. C., 1964. Stratigraphical position of the Guda conglomerate zone. NGU, 227, 85-91.

WOLFF, F. C., 1967a. Geology of the Meraker area as a key to the eastern part of the Trondheim region, NGU, 245, 123-142.

WOLFF, F. C., 1967b. Geological map of the Trondheim Region. In: Wolff, F. C. (ed.), Studies in the Trondheim Region, Central Norwegian Caledonides II. NGU, 245, 146 pp.

WOLFF, F. C., 1976. Geologisk Kart over Norge, bergerunnskart Trondheim 1:250000. NGU.

WOOD, D. A., in press. A variably veined sub-oceanic upper mantle: genetic significance for MORB from geochemical evidence. Geology, in press.

WOOD, D. A., JORON, J.-L., and TREUIL, M., 1979. A re-appraisal of the use of trace elements to classify and discriminate between magma series erupted in different tectonic settings. Earth Planet. Sci. Lett., 45, 326-336.

WOOD, D. A., TARNEY, J., VARET, J., SAUNDERS, A. D., BOUGAULT, H., JORON, J.-L., TREUIL, M., and CANN, J. R., 1979. Geochemistry of basalts drilled in the north Atlantic by IPOD leg 49: implications for mantle heterogeneity. Earth Planet. Sci. Lett., 42, 77-97.

WRIGHT, A. E., 1976. Alternating subduction direction and the evolution of the Atlantic Caledonides. Nature, 264, 156-160.

YUND, R. A., and KULLERUD, G., 1966. Thermal stability of assemblages in the Cu-Fe-S system. Jour. Pet., 7, 454-488.

ZACHRISSON, E., 1964. The Remdalen Syncline. SGU, C596, 1-53.

ZACHRISSON, E., 1969. Caledonian geology of Northern Jamtland - Southern Vasterbotten. SGU, C644, 1-33.

ZACHRISSON, E., 1971. The structural setting of the Stekenjokk Ore Bodies, central Swedish Caledonides. Econ. Geol., 66, 641-652.

ZOLOTUKHIN, V. V., USHAKAV, G. D., and RYABOVE, V. V., 1972. Mechanical activity of sulphide material in massive Noril'sk ores. Docklady Akad. Nauk, U.S.S.R., 216, 91-93.

ADDENDA

GETZ, A., 1890. Graptolitforende skiferzoner i det trondhjemske. Nyt. Mag. Naturv. 3, 31-42.

HALLS, C., REINSBAKKEN, A., FERRIDAY, I., HAUGEN, A., and RANKIN, A., 1977. Geological setting of the Skorovos orebody within the allochthonous volcanic stratigraphy of the Gjersvik Nappe, Central Norway. In: Volcanic processes in ore genesis. Geol. Soc. London Publ. 7, 128-151.

MISRA, K. C., and FLEET, M. E., 1974. Chemical composition and stability of violarite. Econ. Geol., 69, 391-403.

NICKEL, E. H., ROSS, J. R., and THORNBER, M. R., 1974. The supergene alteration of pyrrhotite-pentlandite ore at Kambalda, Western Australia. Econ. Geol., 69, 93-107.

RHODES, J. M., BLANCHARD, D. P., RODGERS, K. V., JACOBS, J. W. and BRANNER, J. C., 1976. Petrology and chemistry of basalts from the Nazca plate: Part 2. Major and trace element chemistry. Initial Repts., D.S.D.P, 34, 239-244.

STURT, B. A., PRINGLE, I. R., and RAMSAY, D. M., 1978. The Finnmarkian phase of the Caledonian Orogeny. Jour. Geol. Soc., 135, 597-610.

APPENDIX A

X-RAY FLUORESCENCE ANALYSIS

A.1 Preparation of Rock Powders.

Since the Gula, Storen, and Fundsjo Group metabasics are fine-grained and generally homogenous, only small sample weights (about 200 g) are thought to be required to obtain a representative analysis (Thirlwall, 1979). However, where possible, samples of at least 500 g were used for these rocks, and correspondingly larger samples were processed for the more coarse-grained metagabbroic and ultramafic lithologies.

The samples were trimmed of weathered surfaces using a diamond saw, and washed thoroughly in clean running water. A pre-contaminated Sturtevant open-door roll jaw-crusher reduced the samples to 0.5 mm chips, and powder, which were subsequently split by the "cone and quarter" method. A proportion of the chips and powder were then ground in a Tema tungsten-carbide swing-mill to <100 mesh. Partial oxidation of iron (Fitton and Gill, 1970) and contamination by Co and W are probably caused by grinding. The latter two elements were not analysed in this study.

A.2 Analytical Procedure.

All elements were determined using the Philips PW 1450/20 spectrometer at the Grant Institute of Geology, Edinburgh. A brief summary of the techniques is presented below, and full details are given by Thirlwall (1979).

A.2.1 Preparation

A.2.1.1 Major elements - Fused glass discs, prepared by a method similar to that of Norrish and Hutton (1969), were used for major element analyses. Sample powders (in small glass jars) were dried over-

night at 110°C to remove adsorbed water (H_2O-). Approximately 1 g of sample, accurately weighed into a clean Pt-5%Au crucible, was ignited at 1100°C in a Gallenkamp furnace for 30 minutes, allowed to cool, and reweighed. Wt.% loss on ignition (LOI), consisting of a combination of the weight loss due to loss of volatile constituents, and the weight gain due to the almost total oxidation of iron, was calculated. A consequence of the oxidation of iron is that total iron may be determined as Fe_2O_3. The generally high values of LOI reflect the metamorphosed nature of the samples.

A lithium tetraborate-lithium oxide-lanthanum oxide flux was added to the ignited sample in a fixed sample:flux ratio. The mixture was then fused at 1100°C until the sample had completely dissolved (usually about 20 minutes) and cooled rapidly to a glass. The crucible was reweighed to determine the flux volatile loss, and a small amount of flux added to make up the constant sample:flux weight ratio. The mixture was re-fused, swirled gently to ensure homogeneity, and cast into a glass disc.

A.2.1.2 Trace elements - The fused disc preparation outlined above involves a high degree of dilution and hence leads to difficulty in the analysis of trace elements. Consequently, trace elements were analysed using pressed pellets. A sample weight of approximately 7 g (calculated by Fitton, pers. comm., 1979, to allow 99% of NbK radiation in a matrix of very low absorption) was used. The sample, mixed with 6 drops of a 2% aqueous solution of polyvinyl alcohol as a binding agent, was transferred to a polished tungsten-carbide pressing apparatus, and hand pressed. Powdered boric acid was added as a backing, and the complete pellet compressed to about 10 ton/in^2 for about 1 minute using a hydraulic press.

A.2.2 The Philips PW 1450/20 Spectrometer.

As the choice of high-voltage X-ray tube is the only analytical condition which must be manually selected, the PW 1450/20 spectrometer at Edinburgh runs on three programs.

Program 90: measures counts for major elements (Na, Mg, Al, Si, P, K, Ca, Ti, Mn, Fe) using a Cr-anode X-ray tube in an evacuated X-ray path.

Program 91, Cr-tube: measures counts for the trace elements Sc, V, Cu, Ba, and La, using a Cr-anode X-ray tube in an evacuated X-ray path.

Program 91, W-tube: measures counts for the trace elements Ni, Zn, Th, Rb, Sr, Y, Zr, Nb, Cr, Ce, Sm, and Nd using a W-anode X-ray tube in an evacuated X-ray path.

Although the metamorphosed nature of the Gula, Store, and Fundsjo Group metabasics restricts the usefulness of all but a small number of elements to petrogenetic considerations, all elements mentioned above were determined in order that mass absorption and interference corrections could be carried out. For samples of the Kletten, Kaltberget, and Skjaekerdalen intrusives, however, only major elements have been determined. Analytical conditions are summarised in Table A.1, while the various interferences between analytical lines, and their treatment are shown in Table A.2.

A.3 Data Processing

A.3.1 Major elements.

Major element calibrations were based on international standards. As samples have similar mass absorption coefficients as a result of the presence of the heavy absorber La in the flux, no corrections for mass absorption differences were made. Averaging of count ratios and

TABLE A.1 XRF analytical conditions.

Line	Crystal	kV	mA	Collimator	Counter	Background offset 2θ°	Lower Level	Windo
SiK_α	PE	50	45	C	F	+ 4.40	25%	60%
AlK_α	PE	60	45	C	F	- 5.75	25%	60%
FeK_α	LiF200	50	45	F	F	- 1.63	20%	60%
MgK_α	TlAP	60	45	C	F	+ 2.70	25%	50%
CaK_α	LiF200	50	30	F	F	- 3.00	25%	60%
NaK_α	TlAP	60	45	C	F	- 2.25	30%	50%
KK_α	LiF200	50	45	F	F	- 4.55	25%	60%
TiK_α	LiF200	50	45	F	F	+ 4.74	30%	50%
MnK_α	LiF200	60	45	F	F	- 1.00	15%	70%
PK_α	Ge	50	45	C	F	+ 3.14	35%	40%
ScK_α	LiF200	60	45	F	F	- 1.59	25%	60%
VK_α	LiF220	60	45	F	F	- 2.62	30%	50%
CuK_α	LiF200	60	45	C	F	+ 1.01	39%	26%
BaL_{β_2}	LiF220	60	45	F	F	+ 1.75	15%	60%
LaL_{α_1}	LiF200	60	45	C	F	- 1.08	30%	50%
NiK_α	LiF200	60	45	F	F	+ 1.33	25%	50%
ZnK_α	"	60	45	F	F	+ 0.80	25%	50%
ThL_{α_1}	"	90	30	F	FS	-	20%	60%
RbK_α	"	90	30	F	FS	+ 2.09	20%	60%
SrK_α	"	90	30	F	FS	-	20%	60%
YK_α	"	90	30	F	FS	+ 0.48	20%	60%
ZrK_α	"	90	30	F	FS	-	20%	60%
NbK_α	"	90	30	F	FS	- 0.40	20%	60%
CrK_α	"	60	45	F	F	+ 1.44 - 0.74	15%	60%
CeL_{β_1}	"	60	45	F	F	-	15%	60%
SmL_{α_1}	"	60	45	F	FS	- 0.48	20%	60%
NdL_{α_1}	"	60	45	F	F	- 1.34	15%	60%
TiK_β	"	60	45	F	F	- 1.54	30%	50%
CaK_β	"	60	45	F	F	-	25%	60%

Crystals

PE = Pentaerythritol, TlAP = Thallium acid phthalate
Ge = Germanium, LiF = Lithium Fluoride

Collimators

C = coarse, F = fine

Counters

F = gas flow proportional counter
FS = flow counter and scintillation counter.

TABLE A.2 Interferences on chosen analytical lines and backgrounds, and their treatments.

Line	Interference	Approx extent of Interference	Correction made
Mn K_α	Cr K_β	Unimportant for Cr <1500 ppm	None
P K_α	Ca K_β (2nd order)	Unimportant for CaO <20%	Narrow energy window
Mg K_α	Ca K_α (3rd order)	? 0.1% MgO for 20% CaO	None
Sc K_α	Ca K_β	1 ppm. Sc per % CaO	Regression
V K_α	Ti K_β	180 ppm. V per % TiO_2	Regression
La $L\alpha_1$	Ti K_α	5 ppm. La per % TiO_2	Regression
Ti K_β	Ba $L\beta_3$	0.00004 % TiO_2 per ppm. Ba	Yes
	V K_α	0.0004 % TiO_2 per ppm. V	Yes
Ni K_α	Y K_α (2nd order)	Unimportant for Y <400 ppm.	Narrow energy window
Y K_α	Rb K_α	0.22 ppm. Y per ppm. Rb	Regression
Zr K_α	Sr K_α	0.07 ppm. Zr per ppm. Sr	Regression
Nb K_α	La K_α (2nd order)	0.01 ppm. Nb per ppm. La	Regression
	Y K_β	Unimportant for Y <1000 ppm.	None
	U $L\beta_{2,4}$	Unimportant for U<50 ppm.	None
Cr K_α	V K_β	0.05 ppm. Cr per ppm. V	Regression
Ce $L\beta_1$	Nd $L\alpha_1$	Probably unimportant?	None
Nd $L\alpha_1$	Ce $L\beta_1$	0.01 ppm. Nd per ppm. Ce	Regression
Sm $L\alpha_1$	Ce $L\beta_2$	0.02 ppm. Sm per ppm. Ce	Regression
Cu background	Hf $L\alpha_1$	Unimportant for Zr <800 ppm	None
	Zr K_α (2nd order)		
Y, Zr, Nb backgrounds	U, Th	Unimportant for <500 ppm U, Th	None
Ce, Nd background	Cr K_α	Unimportant for Cr <800 ppm	None

calibration regressions were carried out using the computer programs RATMAJ and MAJORS respectively (written by Thirlwall, 1979).

A.3.2 Trace elements

Trace element calibrations were based on international standards and synthetic spiked standards (Thirlwall, 1979). Mass absorption coefficients were calculated for each sample on the basis of the major element analyses. Averaging of count ratios, calibration regressions, and interference and matrix corrections were carried out using the computer programs CRTRACE, WTRACE, and TRACE, written by Thirlwall (1979). A flow diagram of computer processing of the raw data produced by the three spectrometer programs outlined in A.2.2 is presented in Fig. A.1.

A.4. Reproducibility, Repeatability, Precision, and Accuracy.

The reproducibility of fused disc and pressed pellet preparation has been investigated by Thirlwall (1979) by the preparation and analysis of six discs and pellets of one sample. The results of this study are summarised in Table A.3. Table A.4. presents data on the repeatability, or analytical precision, of the method, investigated by the repeated analyses of one disc and pellet (Thirlwall, 1979). Accuracy (Table A.5) has been estimated by analysis of standard samples (Thirlwall, 1979), while a comparison of trace element data obtained on the Edinburgh PW 1450/20 spectrometer, with those obtained from the same samples by other techniques is presented in Table A.6 (Graham, 1980).

A.5 Analysis of Silicate Fraction of Skjaekerdalen Ores.

Prior to the preparation of fused discs, the sulfide components of these ores were removed by the separation techniques described in Appendix C. To facilitate separation the samples were ground to pass

Fig. A.1 Flow diagram of data processing computer programs (from Thirlwall, 1979).

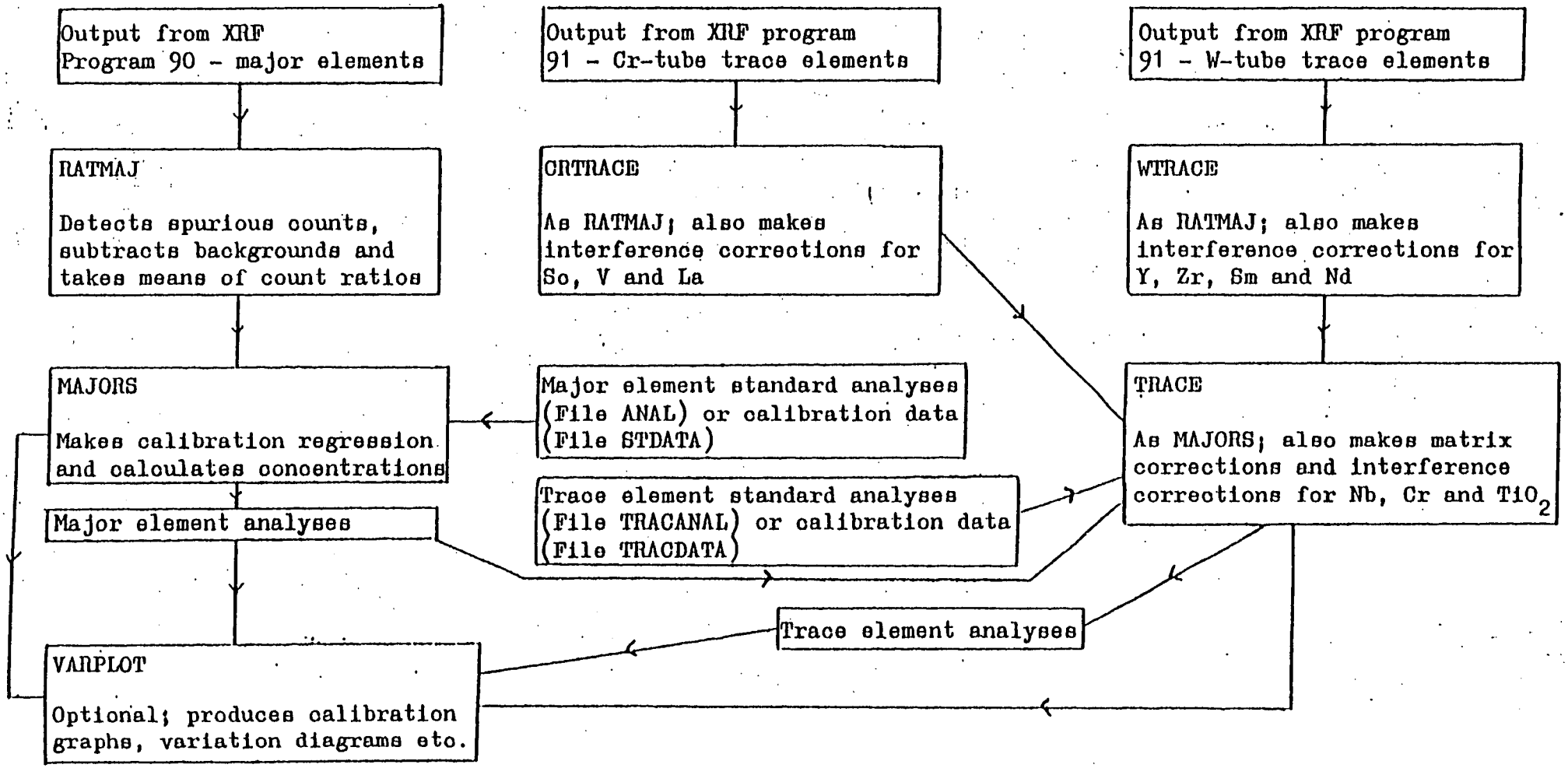

TABLE A.3 Reproducibility of disc and pellet production.

Six discs and six pellets of sample MT45

Data from Thirlwall (1979)

	mean	$\pm 2\sigma$
SiO_2	54.529	0.342
Al_2O_3	15.589	0.114
Fe_2O_3	8.248	0.101
MgO	6.743	0.069
CaO	8.023	0.025
Na_2O	3.317	0.104
K_2O	1.356	0.011
TiO_2	1.281	0.007
MnO	0.115	0.016
P_2O_5	0.347	0.004
LOI	1.542	0.100
Ni	138.3	0.8
Cr	289.8	4.0
V	167.0	4.6
Sc	24.4	0.4
Cu	49.9	1.2
Zn	67.9	1.1
Sr	601.1	4.5
Rb	17.3	0.9
Zr	249.1	1.5
Nb	12.4	0.9
Ba	543.6	8.5
Th	10.6	2.3
La	31.1	2.1
Ce	73.3	2.3
Nd	34.1	1.7
Sm	8.8	4.6
Y	25.8	0.8
TiO_2CR	1.309	0.036
TiO_2W	1.331	0.016

TABLE A.4 Analytical precision/repeatability data. Data from Thirlwall (1979).

	G2		AGV1		DTS1	
	Mean	± 2σ	Mean	± 2σ	Mean	± 2σ
SiO_2	69.32	0.210	59.62	0.240	40.57	0.146
Al_2O_3	15.48	0.058	17.12	0.062	0.40	0.006
Fe_2O_3	2.74	0.015	6.92	0.035	8,93	0.036
MgO	0.84	0.038	1.59	0.030	49.89	0.253
CaO	1.92	0.010	4.96	0.020	0.17	0.002
Na_2O	4.30	0.060	4.37	0.124	0.11	0.057
K_2O	4.49	0.014	2.96	0.013	(-0.02)	0.001
TiO_2	0.49	0.004	1.06	0.006	0.02	0.002
MnO	0.03	0.010	0.10	0.009	0.13	0.008
P_2O_5	0.13	0.005	0.48	0.007	0.01	0.003

16 CYCLES PER SAMPLE

	SR6		S32		JB1	
	Mean	± 2σ	Mean	± 2σ	Mean	± 2σ
Sc	15.7	0.4	21.7	0.6	26.2	0.5
V	162.7	3.1	133.1	4.5	194.0	2.8
Cu	29.9	0.5	22.2	1.0	53.9	0.8
Ba	893.7	7.0	408.2	4.1	554.1	5.7
La	44.9	2.0	30.6	2.8	40.2	2.0
TiO_2CR	0.73%	0.003	1.18%	0.003	1.27%	0.007%

19 CYCLES PER SAMPLE

	MT45	
	Mean	± 2σ
Ni	138.9	1.5
Zn	68.6	1.7
Th	4.6	2.2
Rb	16.7	1.2
Sr	603.6	2.0
Y	25.5	0.5
Zr	249.8	1.7
Nb	12.7	1.1
Cr	290.0	1.7
Ce	71.7	3.8
Sm	8.7	2.8
Nd	34.1	1.6
TiO_2W	1.34%	0.014

12 CYCLES

Oxides in wt.%; trace elements in p.p.m.

G2, AGV1, DTS1 and JB1 are international standards

S32, MT45 are samples from the present study

SR6 is a basaltic andesite from the volcano Stromboli, Italy

TABLE A.5 Analytical accuracy. Data from Thirlwall (1979).

Analyses of standard samples run as unknowns, not included in calibrations, compared with values from Abbey (1977). Major elements in wt.%, trace elements in ppm.

Major elements: sample GS-N

	SiO_2	Al_2O_3	Fe_2O_3*	MgO	CaO	Na_2O	K_2O	TiO_2	MnO	P_2O_5
XRF	66.09	14.81	3.82	2.30	2.45	3.60	4.687	0.662	0.060	0.269
Abbey (1977)	65.98	14.71	3.75	2.31	2.51	3.78	4.64	0.68	0.06	0.28

	XRF						Abbey (1977)					
	DR-N	FK-N	UB-N	W1	SY2	TB	DR-N	FK-N	UB-N	W1	SY2	TB
Sc	34	0	14	37	6	21	-	-	-	?35	?7	13.5
V	224	2	68	264	50	121	220	-	75	240	50	105
Cu	44	4	20	102	3	32	52	?3	30	110	4	50
Ba	398	198	40	175	460	777	380	?210	?45	160	460	720
La	20	2	3	12	67	51	-	-	-	?12	?85	?56

		Ni	Zn	Th	Rb	Sr	Y	Zr	Nb	Cr	Ce	Sm	Nd
XRF	W1	74	84	2	22	196	24	107	9	128	19	3	11
	SY2	11	260	427	226	270	124	288	37	9	157	13	72
	TB	44	98	19	189	164	33	188	20	107	103	7	43
Abbey (1977)	W1	78	86	2	21	190	25	105	?10	120	?23	?4	15
	SY2	10	250	?370	220	270	130	270	?25	10	?210	?16	?70
	TB	40	95	?19	180	155	?39	175	-	80	?115	?9	-

TABLE A.6 Comparison of XRF data with other published analyses. Data from Graham (1980).

	Th		La		Ce		Nd		Sm	
	XRF	INAA	XRF	ID	XRF	ID	XRF	ID	XRF	ID
43	2.8	2.45	9.6	-	21.5	19.0	7.0	10.8	2.1	2.85
225B	6.6	-	17.6	17.6	42.5	41.2	21.6	22.4	7.9	4.72
239	4.7	-	34.6	-	36.5	33.9	21.5	21.8	3.5	5.28
266	11.6	-	27.3	27.3	56.4	53.0	24.2	28.8	6.3	6.19
286	12.5	9.01	28.8	-	58.5	52.4	23.0	25.0	4.9	5.26
314	8.4	8.40	25.5	21.4	48.8	45.4	20.6	22.8	3.0	4.93
380	5.7	-	20.7	18.3	35.1	41.5	20.6	24.3	4.4	5.51
449	3.7	5.10	17.2	-	32.7	31.4	13.0	16.7	7.5	3.93
450	2.6	-	10.4	8.59	20.1	20.9	11.8	14.6	0.4	3.61
454	0.0	-	7.8	8.19	18.7	20.8	10.7	14.5	5.8	3.64
500	1.5	1.25	6.1	5.52	14.2	13.5	4.7	8.96	3.0	2.49
507	1.1	1.65	6.4	-	19.8	15.8	6.8	11.0	7.7	3.07
509	9.8	10.6	32.7	-	58.0	57.4	24.2	29.3	8.2	5.78

ID analyses from Shimizu and Arculus (1975) and Hawkesworth et al. (1979b)

INAA analyses from Minster and Allegre (1978)

80 mesh. As the silicate powders fused easily at this grainsize, it was not thought necessary to recrush to 100 mesh.

TABLE A.7 Analyses of Kletten Ultramafic Body - Profile 100s.

Sample	77.61	77.62	77.63	77.64	77.65	77.66	77.67	77.68	77.69	77.70
SiO_2	47.86	48.82	50.93	47.88	44.73	49.75	48.07	48.18	48.49	53.01
Al_2O_3	4.38	6.67	5.89	4.36	4.92	6.19	4.10	4.26	5.89	7.49
Fe_2O_3T	9.55	9.91	8.56	11.20	11.81	9.52	9.92	10.71	9.92	8.82
MgO	25.62	20.48	18.85	23.11	30.40	19.15	25.29	23.47	21.64	16.66
CaO	10.53	10.26	12.96	11.51	5.45	12.97	10.91	11.52	11.09	11.40
Na_2O	1.07	1.00	1.43	0.88	0.91	1.08	1.03	1.48	1.42	1.15
K_2O	0.48	1.40	0.45	0.52	0.66	0.52	0.39	0.41	0.87	0.35
TiO_2	0.33	0.56	0.51	0.39	0.34	0.63	0.35	0.35	0.45	0.58
MnO	0.16	0.17	0.16	0.18	0.19	0.17	0.17	0.17	0.16	0.24
P_2O_5	0.10	0.12	0.06	0.07	0.08	0.05	0.08	0.09	0.11	0.10
TOTAL	100.07	99.40	99.81	100.10	99.50	100.03	100.31	100.64	100.05	99.84
L.O.I.	2.84	4.09	2.88	2.75	3.42	4.08	2.66	3.08	3.66	1.81

TABLE A.8 Analyses of Kaltberget Ultramafic Body - Drill Hole 76/4

Sample	77/4/38	77/4/42	77/4/46	77/4/50	77/4/54	77/4/58	77/4/62	77/4/66	77/4/70	77/4/74	77/4/78	77/4/81
SiO_2	54.32	47.89	45.94	48.46	51.50	51.77	50.09	49.22	51.70	52.13	55.33	52.92
Al_2O_3	14.09	3.21	3.91	5.24	5.22	5.68	5.37	5.57	5.53	4.95	5.36	5.17
Fe_2O_3T	7.20	9.53	11.05	10.26	9.79	7.46	10.39	9.97	10.09	9.85	9.40	8.58
MgO	10.14	32.25	32.79	29.33	26.13	22.17	29.27	28.10	28.27	27.04	25.28	20.49
CaO	8.58	5.63	4.29	3.92	1.78	8.14	1.78	3.73	2.35	3.70	1.69	10.67
Na_2O	2.81	0.54	0.80	0.41	0.75	0.58	0.43	0.35	0.58	0.44	0.80	0.79
K_2O	1.41	0.00	0.31	0.67	3.47	3.37	0.57	1.18	0.11	0.07	0.89	0.88
TiO_2	0.74	0.22	0.25	0.32	0.47	0.30	0.37	0.33	0.30	0.39	0.28	0.35
MnO	0.12	0.15	0.14	0.15	0.14	0.12	0.14	0.14	0.14	0.15	0.07	0.19
P_2O_5	0.14	0.02	0.03	0.04	0.04	0.06	0.03	0.05	0.05	0.02	0.05	0.03
TOTAL	99.57	99.44	99.51	98.79	99.28	99.64	98.43	98.66	99.14	98.74	99.17	100.07
L.O.I.	1.58	13.39	5.34	8.30	3.93	2.57	7.26	7.51	6.06	5.47	4.76	2.74

TABLE A.9 Analyses of Skjaekerdalen Host Rocks

Sample	78.77	77.330	77.316	78.76	77.307	78.71	77.300b
SiO_2	51.07	51.42	50.92	45.91	49.07	51.83	46.26
Al_2O_3	23.29	12.52	12.91	12.03	18.62	4.63	7.29
Fe_2O_3T	5.74	7.40	9.14	12.86	9.97	12.95	12.63
MgO	4.18	12.52	11.30	16.66	7.95	15.59	22.74
CaO	9.83	12.92	11.23	8.96	10.75	12.85	8.90
Na_2O	3.75	1.69	2.04	1.62	2.07	0.55	0.76
K_2O	0.44	0.20	0.46	0.16	0.45	0.34	0.06
TiO_2	0.35	0.45	0.57	0.45	0.29	0.71	0.54
MnO	0.07	0.17	0.18	0.18	0.17	0.23	0.21
P_2O_5	0.03	0.01	0.05	0.01	0.03	0.03	0.02
TOTAL	98.76	99.30	98.82	98.85	99.38	99.70	99.41
L.O.I	0.73	1.91	1.73	0.91	1.10	1.37	0.45

APPENDIX B

ELECTRON MICROPROBE ANALYSIS

All mineral analyses presented in this thesis were obtained using the Cambridge Instruments Microscan 5 electron microprobe at the Grant Institute of Geology, Edinburgh. Wavelength-dispersive and energy-dispersive systems are available, and have been used in this study. The methods are described below.

After preparation and petrological examination of polished thin sections, a vacuum-deposited carbon film was added to provide a conductive coating. Samples and standards were coated simultaneously.

B.1 Wavelength-Dispersive Spectrometry.

Analyses by wavelength-dispersive spectrometry were carried out using an accelerating potential of 20 kV, and a probe current of 30 nA. The beam diameter was approximately 1μm. The probe current was monitored using a Faraday Cage, and flow counters were used for all elements. Elements may be determined in groups of four, such that relocation of the electron beam is required for successive groups. The method is therefore slightly more time consuming than energy-dispersive analysis, but has the advantage of yielding better precision for minor and trace elements.

Backgrounds were counted only on standards and on one example of each phase, unless large compositional variations of a phase occurred. Where possible, background counts were measured on either side of the peak. However, in some cases, interference from other elements restricted background readings to one side only.

Deadtime correction and calculation of apparent concentrations were carried out using the computer program APPCONC written by D. J. Humphries. In general, apparent concentrations were calculated relative to an

average of standard counts measured before and after each set of unknowns. Rarely, where significant drift in standard count rates occurred, only one set of standard measurements was used. Atomic number, matrix absorption, and enhancement (ZAF) corrections were made using the computer program PROBE, written by D. J. Humphries, based on the program of Duncumb and Jones (1969), and using the correction procedures of Sweatman and Long (1969).

Analytical conditions and standards used during the analysis of sulfide and silicate minerals are presented in Tables B.1 and B.2, respectively. Table B.3 illustrates typical precisions and detection limits for the various minerals analysed.

B.2 Energy-Dispersive Spectrometry.

Analyses by energy-dispersive methods were obtained using the Si (Li) Link Systems detector fitted to the Edinburgh Microscan. Accelerating potential and probe current were 20 kV and 6 nA respectively. Livetimes were 100 seconds and spectrum processing was carried out on-line by a Data General Nova Computer, using a program written by Statham (1975), and utilising the ZAF correction procedures of Sweatman and Long (1969).

Full calibration of the energy-dispersive system is necessary only at infrequent intervals, while short-term drift is corrected by reference to a Co metal monitor.

TABLE B.1 Analytical Conditions Used During Wavelength-Dispersive Electron Microprobe Analyses of Sulfide Minerals.

Element & Line	Crystal	Background Offset 2θ	Peak Time	Background Time	Standard
S Kα	PET	+ 2	40	40	Pyrite
Mn Kα	LiF	± 2	40	40	Element
Fe Kα	LiF	± 2	40	40	Element OR Pyrite*
Co Kα	LiF	± 2	40	40	Element
Ni Kα	LiF	± 2	40	40	Element
Cu Kα	LiF	± 2	40	40	Element
Zn Kα	LiF	- 2	40	40	Element
As Lα	KAP	+ 2	40	40	Galium Arsenide**
As Kα	LiF	± 2	40	40	Galium Arsenide***
Ag Lα	Quartz	± 1	40	40	Element
Cd Lα	Quartz	+ 1	40	40	Element
Pb Mα	PET	- 2	40	40	Galena

* In general sulfide minerals of massive volcanogenic sulfide deposits were analysed using a pyrite standard while for those of magmatic association iron element was used as standard.

** For analyses of sulfide minerals of massive volcanogenic sulfide deposit

*** For analyses of sulfide minerals of magmatic origin.

TABLE B. 2 Analytical Conditions Used During Wavelength-Dispersive Electron Microprobe Analyses of Silicate Minerals

Element & Line	Crystal	Background Offset 2θ	Peak Time	Background Time	Standard
Si Kα	RAP	+ 1.5	40	40	Wollastonite
Na Kα	RAP	+ 1.5	40	40	Jaedite
Mg Kα	RAP	+ 1.5	40	40	Olivine OR Periclase*
Al Kα	RAP	+ 1.5	40	40	Corundum
K Kα	PET	± 1.75	40	40	Orthoclase
Ca Kα	LiF	± 2	40	40	Wollastonite
Ti Kα	PET	± 2	40	40	Rutile
Cr Kα	Quartz	± 2	40	40	Element
Mn Kα	Quartz	± 2	40	40	Element
Fe Kα	LiF	± 2	40	40	Element
Co Kα	LiF	± 2	40	40	Element
Ni Kα	LiF	± 2	40	40	Element

* An olivine standard was used for analyses of olivines while periclase was used for pyroxene analyses.

TABLE B.3 Precision and Detection Limits of Typical Wavelength-Dispersive Microprobe Analyses

Olivine 1			
oxide	analysis	precision (±2σ)	detection limit
SiO_2	40.19	0.192	0.019
TiO_2	0.00	-	0.023
Al_2O_3	0.01	0.008	0.009
Cr_2O_3	0.01	0.015	0.020
FeO	13.04	0.153	0.026
MgO	45.45	0.177	0.012
CaO	0.02	0.017	0.021
MnO	0.33	0.023	0.021
NiO	0.04	0.023	0.033
CoO	0.03	0.020	0.029

Orthopyroxene 1			
oxide	analysis	precision (±2σ)	detection limit
SiO_2	56.01	0.233	0.021
TiO_2	0.09	0.017	0.022
Al_2O_3	0.82	0.023	0.009
Cr_2O_3	0.09	0.017	0.020
FeO	8.70	0.125	0.024
MgO	32.08	0.134	0.010
CaO	1.04	0.062	0.018
MnO	0.25	0.021	0.019
NiO	0.01	0.022	0.032
CoO	0.01	0.020	0.029
Na_2O	0.02	0.007	0.008
K_2O	0.01	0.008	0.011

Clinopyroxene 9			
oxide	analysis	precision (±2σ)	detection limit
SiO_2	52.62	0.233	0.021
TiO_2	0.28	0.022	0.022
Al_2O_3	2.15	0.036	0.011
Cr_2O_3	0.84	0.032	0.020
FeO	4.53	0.090	0.027
MgO	17.20	0.098	0.010
CaO	20.53	0.274	0.029
MnO	0.17	0.018	0.021
NiO	0.02	0.023	0.034
CoO	0.02	0.020	0.029
Na_2O	0.32	0.017	0.009
K_2O	0.00	-	0.013

Pyrite 43			
element	analysis	precision (±2σ)	detection limit
S	52.75	0.230	0.013
Pb	0.25	0.047	0.056
Fe	46.49	0.280	0.032
Zn	0.04	0.039	0.057
Cu	0.04	0.028	0.039
Ni	0.01	0.023	0.033
Ag	0.08	0.048	0.063
Cd	0.00	-	0.072
Co	0.21	0.027	0.031
Mn	0.00	-	0.026
As	0.27	0.035	0.026

TABLE B.3 (continued)

Pyrrhotite 23			
element	analysis	precision (±2σ)	detection limit
S	38.72	0.193	0.013
Pb	0.15	0.041	0.052
Fe	60.65	0.323	0.033
Zn	0.32	0.049	0.058
Cu	0.06	0.029	0.040
Ni	0.01	0.024	0.035
Ag	0.02	0.045	0.065
Cd	0.05	0.047	0.064
Co	0.09	0.024	0.032
Mn	0.00	-	0.025
As	0.00	-	0.023

Chalcopyrite 37			
element	analysis	precision (±2σ)	detection limit
S	34.58	0.182	0.012
Pb	0.13	0.042	0.055
Fe	30.76	0.238	0.032
Zn	0.00	-	0.064
Cu	33.81	0.258	0.045
Ni	0.00	-	0.039
Ag	0.04	0.048	0.068
Cd	0.00	-	0.071
Co	0.07	0.024	0.032
Mn	0.02	0.018	0.026
As	0.00	-	0.023

Sphalerite 29			
element	analysis	precision (±2σ)	detection limit
S	33.31	0.171	0.011
Pb	0.15	0.039	0.049
Fe	8.36	0.128	0.032
Zn	56.73	0.418	0.068
Cu	0.03	0.032	0.046
Ni	0.00	-	0.039
Ag	0.08	0.047	0.061
Cd	0.29	0.063	0.064
Co	0.01	0.023	0.034
Mn	0.13	0.022	0.027
As	0.00	-	0.022

Galena 12			
element	analysis	precision (±2σ)	detection limit
S	12.96	0.124	0.016
Pb	85.72	0.593	0.112
Fe	1.36	0.063	0.051
Zn	0.00	-	0.099
Cu	0.10	0.049	0.069
Ni	0.00	-	0.060
Ag	0.28	0.076	0.090
Cd	0.07	0.068	0.096
Co	0.00	-	0.051
Mn	0.02	0.026	0.039
As	0.11	0.026	0.019

TABLE B.3 (continued)

Arsenopyrite 1			
element	analysis	precision (±2σ)	detection limit
S	22.14	0.135	0.011
Pb	0.14	0.036	0.046
Fe	35.57	0.254	0.035
Zn	0.00	-	0.062
Cu	0.04	0.032	0.046
Ni	0.03	0.027	0.040
Ag	0.00	-	0.068
Cd	0.06	0.050	0.068
Co	0.14	0.027	0.034
Mn	0.01	0.019	0.028
As	41.57	0.385	0.036

Cobaltite 1			
element	analysis	precision (±2σ)	detection limit
S	19.63	0.132	0.011
Pb	0.00	-	0.050
Fe	5.26	0.105	0.034
Zn	0.01	0.049	0.073
Cu	0.21	0.047	0.063
Ni	7.20	0.122	0.040
Co	23.51	0.202	0.039
As	44.63	0.596	0.174

Pentlandite 10			
element	analysis	precision (±2σ)	detection limit
S	32.75	0.176	0.012
Pb	0.14	0.043	0.056
Fe	25.34	0.202	0.029
Zn	0.00	-	0.065
Cu	0.00	-	0.053
Ni	29.74	0.226	0.034
Co	11.96	0.136	0.034
As	0.10	0.106	0.154

Formula used:

$$\text{detection limit} = S \times \frac{3\sqrt{C_b}}{(C_{sp}-C_{sb})} \text{ wt \%}$$

$$\text{precision } \sigma = S \times \frac{\sqrt{C_p}}{(C_{sp}-C_{sb})} \text{ wt \%}$$

where S = standard composition in wt%

C_{sp} = total counts on standard peak

C_{sb} = total counts on standard background

C_p = total counts on sample peak

C_b = total counts on sample background.

TABLE B.4 Pyrite Analyses - Massive Volcanogenic Sulfide Deposits

Deposit	TVERFJELLET										
Sample	78.FM.1(G1)			78.FM.3(G2)			78.FM.6(G3)		78.FM.7(G4)		
PYRITE	1	2	3	4	5	6	8	9	10	11	12
S	53.70	53.45	53.82	53.60	53.56	53.68	53.61	53.31	53.31	53.47	53.44
Pb	0.19	0.11	0.17	0.24	0.14	0.18	0.17	0.18	0.12	0.08	0.06
Fe	47.06	46.32	46.67	47.48	47.34	47.63	47.48	47.45	47.94	47.53	47.70
Zn	0.00	0.00	0.04	0.00	0.00	0.00	0.02	0.00	0.00	0.01	0.00
Cu	0.09	0.07	0.10	0.06	0.05	0.05	0.08	0.06	0.00	0.07	0.06
Ni	0.00	0.00	0.02	0.05	0.03	0.01	0.00	0.03	0.00	0.01	0.04
Ag	0.02	0.00	0.00	0.00	0.00	0.02	0.02	0.00	0.00	0.00	0.00
Cd	0.05	0.06	0.04	0.04	0.02	0.03	0.06	0.04	0.00	0.00	0.05
Co	0.29	0.95	0.95	0.16	0.12	0.18	0.09	0.18	0.17	0.11	0.24
Mn	ND	ND	ND	ND	ND	ND	ND	ND	ND	ND	ND
As	ND	ND	ND	ND	ND	ND	ND	ND	ND	ND	ND
Total	101.40	100.97	101.83	101.64	101.26	101.79	101.54	101.25	101.55	101.28	101.60

Deposit				LOKKEN								
Sample	78.FM.8(G5)			78.LM.1(G6)		78.LM.2(G7)		78.LM.3(G8)			78.LM.4(G9)	
PYRITE	13	14	15	16	17	19	21	22	23	24	25	26
S	53.28	53.07	52.99	52.48	52.92	53.75	53.80	53.74	53.87	53.50	53.17	53.53
Pb	0.14	0.05	0.18	0.06	0.09	0.17	0.20	0.16	0.14	0.15	0.27	0.18
Fe	47.77	47.85	47.39	47.28	47.55	47.25	47.29	47.01	47.45	47.40	46.80	47.29
Zn	0.14	0.08	0.01	0.16	0.30	0.00	0.02	0.00	0.00	0.00	0.00	0.00
Cu	0.03	0.05	0.02	0.09	0.01	0.19	0.06	0.06	0.17	0.15	0.07	0.08
Ni	0.03	0.03	0.00	0.03	0.04	0.00	0.00	0.01	0.00	0.00	0.00	0.01
Ag	0.00	0.00	0.00	0.00	0.02	0.02	0.00	0.01	0.10	0.02	0.00	0.00
Cd	0.00	0.02	0.02	0.01	0.00	0.00	0.00	0.02	0.00	0.00	0.04	0.01
Co	0.09	0.07	0.08	0.05	0.07	0.18	0.14	0.11	0.23	0.15	0.42	0.16
Mn	ND	ND	ND	ND	ND	0.02	0.00	0.01	0.00	0.14	0.00	0.01
As	ND	ND	ND	ND	ND	ND	ND	ND	ND	ND	ND	ND
Total	101.47	101.21	100.68	100.16	100.99	101.57	101.52	101.13	101.97	101.51	100.78	101.26

TABLE B.4 (continued) Pyrite Analyses - Massive Volcanogenic Sulfide Deposits

Deposit	KILLINGDAL												
Sample	78.LM.8(G10)				78.KM.1(G11)			78.KM.2(G12)			78.KM.4(G13)		
PYRITE	28	29	30	37	31	32	33	34	35	36	38	39	40
S	53.15	53.37	53.25	51.77	53.63	53.39	53.16	53.51	53.78	53.50	53.42	53.79	53.83
Pb	0.19	0.19	0.21	0.06	0.19	0.18	0.20	0.19	0.21	0.23	0.12	0.27	0.19
Fe	47.16	49.98	47.28	45.83	47.49	47.59	47.44	47.33	47.16	47.24	46.96	46.67	46.53
Zn	0.00	0.05	0.02	0.00	0.05	0.06	0.00	0.01	0.09	0.10	0.00	0.03	0.00
Cu	0.07	0.11	0.10	0.91	0.03	0.05	0.11	0.12	0.03	0.04	0.05	0.15	0.08
Ni	0.00	0.01	0.00	0.01	0.00	0.00	0.00	0.01	0.00	0.01	0.02	0.02	0.00
Ag	0.00	0.08	0.00	0.04	0.04	0.00	0.00	0.00	0.00	0.01	0.06	0.00	0.04
Cd	0.14	0.05	0.07	0.05	0.11	0.07	0.11	0.10	0.08	0.12	0.00	0.00	0.00
Co	0.09	0.10	0.10	0.48	0.11	0.08	0.12	0.14	0.19	0.11	0.09	0.13	0.14
Mn	0.00	0.01	0.09	0.00	0.00	0.00	0.00	0.00	0.00	0.00	0.00	0.00	0.00
As	ND	ND	ND	ND	ND	ND	ND	ND	ND	ND	0.00	0.00	0.00
Total	100.81	100.95	101.14	99.17	101.65	101.41	101.15	101.41	101.55	101.36	100.72	101.06	100.80

Deposit	ROSTVANGEN											
Sample	78.KM.5(G14)			78.KM.8(G15)			77.RD.1(F1)			77.RD.2(F2)		
PYRITE	41	42	43	44	45	46	47	48	49	50	51	52
S	53.73	53.49	52.75	53.31	53.36	53.44	53.56	53.85	54.41	53.70	53.32	53.35
Pb	0.15	0.21	0.25	0.20	0.22	0.17	0.16	0.19	0.15	0.14	0.20	0.17
Fe	46.69	46.89	46.49	46.78	46.82	49.94	46.72	45.95	46.53	46.47	46.82	46.86
Zn	0.28	0.06	0.04	0.00	0.06	0.01	0.0	0.95	0.00	0.00	0.00	0.00
Cu	0.09	0.03	0.04	0.06	0.04	0.10	0.07	0.05	0.07	0.07	0.08	0.05
Ni	0.05	0.00	0.01	0.03	0.01	0.02	0.00	0.00	0.02	0.00	0.00	0.01
Ag	0.01	0.02	0.08	0.00	0.03	0.03	0.00	0.00	0.00	0.00	0.00	0.00
Cd	0.00	0.00	0.00	0.00	0.00	0.00	0.09	0.07	0.00	0.10	0.06	0.13
Co	0.13	0.12	0.21	0.15	0.15	0.17	0.28	0.16	0.23	0.10	0.14	0.13
Mn	0.00	0.00	0.00	0.00	0.00	0.00	0.00	0.00	0.00	0.00	0.00	0.01
As	0.00	0.00	0.27	0.00	0.00	0.00	ND	ND	ND	ND	ND	ND
Total	101.13	100.82	100.16	100.53	100.71	100.89	100.88	101.23	101.40	100.59	100.63	100.71

TABLE E.4 (continued) Pyrite Analyses - Massive Volcanogenic Sulfide Deposits

Deposit									
Sample	78.RD.10(G16)								
PYRITE	53	54	55	56	57	58	59	60	61
S	53.46	53.75	53.53	53.39	53.33	53.45	53.49	53.47	53.27
Pb	0.14	0.24	0.22	0.17	0.19	0.22	0.20	0.22	0.24
Fe	46.41	46.46	46.67	46.29	46.59	46.73	46.67	46.52	46.61
Zn	0.00	0.00	0.00	0.00	0.00	0.00	0.00	0.00	0.00
Cu	0.06	0.07	0.05	0.04	0.05	0.05	0.04	0.05	0.03
Ni	0.00	0.00	0.00	0.00	0.00	0.00	0.00	0.00	0.01
Ag	0.00	0.00	0.00	0.00	0.05	0.01	0.02	0.01	0.08
Cd	0.05	0.11	0.07	0.02	0.05	0.03	0.04	0.06	0.07
Co	0.21	0.20	0.16	0.03	0.05	0.15	0.11	0.07	0.08
Mn	0.00	0.00	0.00	0.01	0.01	0.00	0.01	0.01	0.02
As	ND	ND	ND	ND	ND	ND	ND	ND	ND
Total	100.35	100.84	100.69	99.97	100.32	100.64	100.58	100.43	100.40

Deposit	KVIKNE											
Sample	78.KVD.1(G19)			78.KVD.2(G20)			78.KVD.6(G21)			78.KVD.7(G22)		
PYRITE	62	63	64	65	66	67	68	69	70	71	72	73
S	53.37	53.44	53.43	53.55	53.63	53.58	53.52	53.31	53.18	53.50	53.11	53.21
Pb	0.19	0.20	0.16	0.23	0.18	0.17	0.23	0.22	0.21	0.20	0.19	0.24
Fe	46.54	46.79	46.78	46.72	46.47	46.67	46.88	46.86	46.71	46.66	46.71	46.55
Zn	0.00	0.00	0.00	0.00	0.00	0.00	0.00	0.00	0.00	0.00	0.01	0.00
Cu	0.02	0.02	0.04	0.03	0.00	0.00	0.01	0.03	0.01	0.03	0.01	0.03
Ni	0.00	0.00	0.01	0.02	0.00	0.01	0.01	0.01	0.01	0.00	0.02	0.01
Ag	0.00	0.00	0.01	0.00	0.00	0.00	0.00	0.00	0.00	0.00	0.02	0.01
Cd	0.01	0.02	0.03	0.04	0.00	0.16	0.08	0.13	0.04	0.10	0.00	0.13
Co	0.08	0.08	0.05	0.06	0.13	0.09	0.10	0.08	0.09	0.10	0.09	0.07
Mn	0.00	0.00	0.00	0.00	0.00	0.00	0.00	0.00	0.00	0.00	0.00	0.00
As	ND	ND	ND	ND	ND	ND	ND	ND	ND	ND	ND	ND
Total	100.20	100.54	100.51	100.65	100.41	100.67	100.82	100.64	100.26	100.60	100.14	100.26

TABLE B.5 Pyrrhotite Analyses - Massive Volcanogenic Sulfide Deposits

Deposit	TVERFJELLET						KILLINGDAL					
Sample	78.FM.6(G3)		78.FM.3(G2)			78.FM.1(G1)	78.KM.1(G11)			78.KM.2(G12)		
PYRRHOTITE	1	3	4	5	6	8	10	11	12	13	14	15
S	39.63	39.40	39.34	39.22	39.26	39.34	38.55	39.14	39.06	38.56	38.60	38.95
Pb	0.51	0.47	0.49	0.46	0.49	0.52	0.08	0.12	0.16	0.09	0.10	0.11
Fe	60.88	61.10	60.79	60.53	61.22	61.12	61.58	60.62	60.79	61.40	61.29	60.55
Zn	0.66	0.63	0.62	0.64	0.60	0.59	0.03	0.00	0.00	0.00	0.14	0.27
Cu	0.11	0.13	0.02	0.04	0.22	0.06	0.05	0.09	0.09	0.10	0.05	0.05
Ni	0.04	0.05	0.03	0.01	0.01	0.01	0.02	0.01	0.01	0.00	0.02	0.00
Ag	0.00	0.00	0.03	0.00	0.00	0.00	0.04	0.00	0.00	0.06	0.02	0.02
Cd	0.01	0.00	0.00	0.00	0.06	0.05	0.00	0.05	0.00	0.08	0.00	0.00
Co	0.14	0.11	0.13	0.12	0.10	0.14	0.10	0.10	0.11	0.10	0.11	0.12
Mn	ND	ND	ND	ND	ND	ND	0.00	0.01	0.00	0.01	0.00	0.01
As	ND	ND	ND	ND	ND	ND	ND	ND	ND	ND	ND	ND
Total	101.98	101.90	101.45	101.03	101.98	101.83	100.45	100.14	100.21	100.39	100.33	100.07

Deposit										ROSTVANGEN		
Sample	78.KM.4(G11)			78.KM.5(G14)			78.KM.8(G15)			77.RD.1(F1)		
PYRRHOTITE	16	17	18	19	20	21	22	23	24	25	26	27
S	39.59	40.05	39.80	40.28	39.76	39.89	39.12	38.72	39.30	38.85	39.23	38.96
Pb	0.14	0.17	0.18	0.21	0.17	0.22	0.18	0.15	0.18	0.11	0.23	0.16
Fe	60.47	60.59	60.72	60.05	59.98	59.95	60.95	60.65	60.78	60.46	59.65	59.98
Zn	0.06	0.04	0.14	0.05	0.02	0.09	0.02	0.32	0.28	0.13	0.42	0.00
Cu	0.05	0.09	0.07	0.08	0.07	0.07	0.09	0.06	0.07	0.09	0.11	0.06
Ni	0.02	0.00	0.00	0.01	0.02	0.00	0.00	0.01	0.01	0.00	0.01	0.01
Ag	0.09	0.01	0.00	0.05	0.04	0.00	0.00	0.02	0.00	0.00	0.00	0.00
Cd	0.05	0.00	0.07	0.01	0.09	0.06	0.04	0.05	0.01	0.13	0.04	0.12
Co	0.11	0.11	0.12	0.12	0.08	0.08	0.10	0.09	0.08	0.09	0.10	0.07
Mn	0.01	0.00	0.01	0.00	0.00	0.01	0.00	0.00	0.01	0.00	0.00	0.00
As	0.00	0.00	0.00	0.00	0.00	0.00	0.00	0.00	0.00	ND	ND	ND
Total	100.57	101.08	101.13	100.87	100.24	100.38	100.50	100.09	100.72	99.86	99.80	99.37

TABLE B.5 (continued) Pyrrhotite Analyses - Massive Volcanogenic Sulfide Deposits

Deposit												
Sample	77.RD.2(F2)			78.RD.10(G16)			78.RD.14(G17)			78.RD.15(G18)		
PYRRHOTITE	28	29	30	31	32	33	34	35	36	37	38	39
S	38.43	38.52	37.84	39.66	39.03	39.50	38.89	38.90	38.93	38.98	38.54	39.35
Pb	0.14	0.18	0.19	0.17	0.20	0.12	0.04	0.08	0.09	0.12	0.15	0.11
Fe	60.54	60.15	61.08	59.06	60.14	59.46	60.71	60.89	60.88	60.19	61.03	59.32
Zn	0.00	0.00	0.00	0.37	0.19	0.21	0.00	0.00	0.00	0.01	0.00	0.06
Cu	0.03	0.00	0.01	0.07	0.15	0.08	0.08	0.06	0.06	0.25	0.05	0.40
Ni	0.02	0.00	0.02	0.00	0.01	0.00	0.05	0.05	0.03	0.02	0.06	0.00
Ag	0.00	0.03	0.01	0.00	0.00	0.00	0.01	0.01	0.00	0.00	0.00	0.00
Cd	0.10	0.09	0.16	0.14	0.06	0.07	0.08	0.08	0.08	0.09	0.11	0.09
Co	0.09	0.13	0.12	0.08	0.11	0.10	0.07	0.09	0.04	0.05	0.04	0.03
Mn	0.00	0.01	0.00	0.00	0.01	0.00	0.02	0.00	0.00	0.00	0.00	0.00
As	ND	ND	ND	ND	ND	ND	ND	ND	ND	ND	ND	ND
Total	99.34	99.11	99.43	99.56	99.92	99.54	99.95	100.16	100.11	99.70	99.98	99.35

Deposit	KVIKNE											
Sample	78.KVD.1(G19)			78.KVD.2(G20)			78.KVD.6(G21)			78.KVD.7(G22)		
PYRRHOTITE	41	42	43	44	45	46	47	48	49	50	51	52
S	38.81	38.73	38.16	38.92	39.38	39.25	39.08	39.06	39.03	39.15	38.98	39.09
Pb	0.14	0.12	0.12	0.08	0.12	0.05	0.08	0.08	0.11	0.11	0.10	0.10
Fe	60.72	60.93	60.79	61.13	60.78	60.71	60.24	60.80	60.93	61.15	60.78	60.64
Zn	0.00	0.00	0.27	0.00	0.00	0.00	0.66	0.00	0.00	0.00	0.00	0.00
Cu	0.11	0.03	0.21	0.07	0.04	0.06	0.04	0.03	0.02	0.04	0.03	0.04
Ni	0.06	0.03	0.00	0.02	0.00	0.04	0.00	0.01	0.03	0.06	0.04	0.02
Ag	0.01	0.04	0.00	0.00	0.00	0.02	0.00	0.03	0.00	0.01	0.00	0.06
Cd	0.06	0.06	0.03	0.06	0.03	0.01	0.00	0.08	0.07	0.00	0.00	0.09
Co	0.04	0.02	0.02	0.07	0.08	0.08	0.06	0.08	0.06	0.06	0.06	0.07
Mn	0.00	0.00	0.00	0.00	0.00	0.00	0.00	0.00	0.00	0.00	0.00	0.00
As	ND	ND	ND	ND	ND	ND	ND	ND	ND	ND	ND	ND
Total	99.96	99.97	99.61	100.35	100.43	100.22	100.16	100.17	100.27	100.58	99.99	100.12

TABLE B.6 Chalcopyrite Analyses - Massive Volcanogenic Sulfide Deposits

Deposit	TVERFJELLET										
Sample	78.FM.1 (G1)			78.FM.3 (G2)			78.FM.6 (G3)			78.FM.8 (G5)	
CHALCOPYRITE	1	2	3	4	5	6	7	8	9	13	14
S	34.35	34.54	34.35	34.37	34.47	34.39	34.04	34.22	34.05	34.91	34.80
Pb	0.03	0.13	0.09	0.10	0.06	0.10	0.07	0.06	0.15	0.12	0.21
Fe	31.40	31.41	31.39	31.22	31.72	31.26	31.11	31.01	31.12	30.82	30.96
Zn	0.05	0.04	0.02	0.05	0.02	0.04	0.06	0.03	0.12	0.08	0.00
Cu	33.58	33.29	33.51	33.61	33.08	33.53	33.32	33.49	33.64	33.95	34.18
Ni	0.00	0.00	0.00	0.00	0.00	0.00	0.00	0.00	0.00	0.02	0.01
Ag	0.12	0.06	0.09	0.00	0.09	0.04	0.06	0.12	0.11	0.02	0.05
Cd	0.10	0.13	0.04	0.04	0.10	0.04	0.10	0.07	0.13	0.12	0.00
Co	0.06	0.05	0.07	0.07	0.05	0.07	0.07	0.07	0.05	0.06	0.03
Mn	ND	ND	ND	ND	ND	ND	ND	ND	ND	ND	ND
As	ND	ND	ND	ND	ND	ND	ND	ND	ND	ND	ND
Total	99.70	99.66	99.57	99.47	99.60	99.48	98.82	99.07	99.38	100.12	100.23

Deposit				LOKKEN						
Sample	78.FM.7 (G4)			78.LM.1 (G6)			78.LM.4 (G9)			78.LM.3 (G8)
CHALCOPYRITE	16	17	18	10	11	12	19	20	21	22
S	34.45	34.52	34.51	34.32	34.31	35.13	35.16	35.20	35.18	35.09
Pb	0.16	0.17	0.15	0.10	0.18	0.10	0.06	0.10	0.06	0.06
Fe	30.14	31.06	30.92	30.25	30.69	31.03	30.53	31.19	30.46	30.81
Zn	0.02	0.03	0.03	0.83	0.68	0.23	0.00	0.00	0.02	0.00
Cu	33.67	33.90	33.57	32.94	33.47	33.88	33.23	33.34	34.02	34.10
Ni	0.03	0.03	0.00	0.01	0.01	0.01	0.00	0.00	0.00	0.00
Ag	0.00	0.00	0.05	0.01	0.00	0.02	0.04	0.04	0.00	0.05
Cd	0.10	0.04	0.01	0.00	0.05	0.05	0.08	0.02	0.04	0.02
Co	0.07	0.02	0.03	0.04	0.04	0.04	0.05	0.07	0.05	0.05
Mn	ND	ND	ND	ND	ND	ND	0.00	0.00	0.00	0.00
As	ND	ND	ND	ND	ND	ND	ND	ND	ND	ND
Total	98.64	99.78	99.29	98.52	99.43	100.29	99.15	99.97	99.82	100.18

TABLE 5.6 (continued) Chalcopyrite Analyses - Massive Volcanogenic Sulfide Deposits

Deposit	KILLINGDAL										
Sample	78.LM.2 (G7)			78.LM.8 (G10)		78.KM.8 (G15)			78.KM.5 (G14)		
CHALCOPYRITE	25	26	27	34	35	37	38	39	40	41	42
S	35.04	35.51	35.28	34.52	34.39	34.58	34.59	34.53	34.56	34.50	34.35
Pb	0.07	0.05	0.04	0.12	0.09	0.13	0.15	0.08	0.11	0.10	0.11
Fe	30.70	30.45	30.96	30.74	30.77	30.76	30.63	30.47	30.38	30.48	30.77
Zn	0.00	0.03	0.00	0.03	0.06	0.00	0.04	0.07	0.07	0.16	0.15
Cu	34.36	34.33	33.53	33.83	33.97	33.81	34.14	34.05	33.97	33.78	33.03
Ni	0.00	0.00	0.00	0.00	0.00	0.00	0.00	0.00	0.00	0.00	0.00
Ag	0.00	0.03	0.07	0.00	0.01	0.04	0.01	0.00	0.00	0.01	0.05
Cd	0.01	0.00	0.05	0.01	0.00	0.00	0.00	0.05	0.00	0.03	0.00
Co	0.03	0.05	0.04	0.05	0.04	0.07	0.05	0.05	0.05	0.06	0.03
Mn	0.00	0.00	0.01	0.01	0.00	0.02	0.02	0.01	0.01	0.03	0.00
As	ND	ND	ND	ND	ND	0.00	0.00	0.00	0.00	0.00	0.00
Total	100.20	100.43	100.02	99.32	99.34	99.41	99.63	99.32	99.15	99.15	98.50

Deposit									
Sample	78.KM.4 (G13)			78.KM.2 (G12)			78.KM.1 (G11)		
CHALCOPYRITE	43	44	45	28	29	30	31	32	33
S	34.41	34.68	35.42	34.52	34.44	34.35	34.58	34.73	34.65
Pb	0.10	0.07	0.08	0.10	0.04	0.07	0.09	0.08	0.07
Fe	30.37	30.71	30.72	31.20	31.06	30.82	31.21	21.27	30.80
Zn	0.03	0.00	0.03	0.02	0.04	0.00	0.09	0.09	0.88
Cu	34.05	33.95	34.10	33.53	33.28	33.30	33.35	32.80	33.10
Ni	0.00	0.00	0.00	0.00	0.00	0.00	0.00	0.00	0.00
Ag	0.01	0.03	0.04	0.00	0.00	0.00	0.00	0.00	0.00
Cd	0.00	0.01	0.00	0.00	0.00	0.00	0.00	0.00	0.00
Co	0.06	0.03	0.05	0.05	0.05	0.06	0.06	0.08	0.05
Mn	0.02	0.01	0.01	0.01	0.00	0.01	0.01	0.01	0.00
As	0.00	0.00	0.00	ND	ND	ND	ND	ND	ND
Total	99.05	99.50	100.45	99.44	98.91	98.61	99.39	99.05	99.56

TABLE B.6 (continued) Chalcopyrite Analyses - Massive Volcanogenic Sulfide Deposits

Deposit	ROSTVANGEN											
Sample	78.RD.10 (G16)			77.RD.2 (F2)			77.RD.1 (F1)			78.RD.15 (G18)		
CHALCOPYRITE	46	47	48	49	50	51	52	53	54	58	59	60
S	34.72	34.69	34.63	35.06	34.94	35.03	34.72	34.97	34.78	34.66	34.64	34.81
Pb	0.14	0.16	0.14	0.15	0.09	0.12	0.15	0.11	0.10	0.11	0.10	0.12
Fe	30.37	29.93	30.11	30.58	30.44	30.14	30.56	30.03	30.68	30.53	30.36	30.76
Zn	0.24	0.15	0.07	0.05	0.00	0.00	0.01	0.02	0.01	0.00	0.00	0.00
Cu	34.62	34.15	34.52	34.15	34.44	34.40	34.48	34.75	34.36	34.26	34.23	34.20
Ni	0.03	0.03	0.00	0.01	0.00	0.02	0.03	0.02	0.01	0.00	0.00	0.00
Ag	0.09	0.03	0.10	0.00	0.04	0.05	0.06	0.01	0.00	0.04	0.06	0.05
Cd	0.00	0.00	0.01	0.09	0.08	0.03	0.05	0.00	0.02	0.00	0.01	0.10
Co	0.05	0.05	0.06	0.04	0.05	0.05	0.07	0.05	0.06	0.05	0.03	0.02
Mn	0.00	0.00	0.00	0.00	0.00	0.00	0.00	0.01	0.00	0.00	0.00	0.00
As	ND	ND	ND	ND	ND	ND	ND	ND	ND	ND	ND	ND
Total	100.25	99.19	99.64	100.14	100.08	99.85	100.15	99.97	100.04	99.68	99.44	100.07

Deposit				KVIKNE											
Sample	78.ED.14 (G17)			78.KVD.1 (G19)			78.KVD.7 (G22)			78.KVD.6 (G21)			78.KVD.2 (G20)		
CHALCOPYRITE	61	63	64	55	56	57	65	66	67	68	69	70	71	72	73
S	34.86	35.04	34.94	34.57	34.49	34.85	34.90	35.21	35.00	34.88	34.85	34.72	34.97	34.87	35.04
Pb	0.11	0.11	0.14	0.12	0.00	0.10	0.19	0.17	0.16	0.14	0.18	0.16	0.18	0.20	0.13
Fe	30.57	30.23	30.48	29.89	30.38	30.79	30.52	30.60	30.67	30.59	30.55	30.70	30.60	30.05	30.18
Zn	0.00	0.00	0.00	0.00	0.00	0.00	0.08	0.11	0.09	0.10	0.07	0.10	0.06	0.03	0.05
Cu	34.00	34.55	34.15	34.14	34.26	34.30	33.91	33.92	34.35	34.29	34.10	34.18	34.24	34.12	34.39
Ni	0.01	0.00	0.00	0.00	0.00	0.00	0.01	0.02	0.00	0.00	0.00	0.01	0.03	0.01	0.02
Ag	0.05	0.04	0.02	0.00	0.02	0.07	0.04	0.00	0.00	0.00	0.03	0.07	0.00	0.03	0.00
Cd	0.00	0.01	0.00	0.00	0.05	0.01	0.07	0.12	0.09	0.07	0.06	0.05	0.04	0.10	0.07
Co	0.04	0.04	0.02	0.04	0.02	0.03	0.05	0.03	0.00	0.04	0.03	0.04	0.05	0.05	0.03
Mn	0.00	0.00	0.00	0.00	0.00	0.00	0.00	0.00	0.00	0.00	0.02	0.00	0.00	0.01	0.00
As	ND	ND	ND	ND	ND	ND	ND	ND	ND	ND	ND	ND	ND	ND	ND
Total	99.65	100.02	99.76	98.76	99.24	100.16	99.68	100.18	100.36	100.11	99.88	100.04	100.16	99.47	99.92

TABLE B.7 Sphalerite Analyses - Massive Volcanogenic Sulfide Deposits.

Deposit	TVERFJELLET										
Sample	78.FM.7(G4)										
Sphalerite	3	425E	426E	427E	428E	429E	430E	431E	432E	433E	434E
S	33.28	33.46	33.28	33.32	33.30	33.34	33.08	34.10	33.45	33.25	33.26
Pb	0.12	ND	ND	ND	ND	ND	ND	ND	ND	ND	ND
Fe	8.88	8.02	9.34	9.30	8.46	7.18	7.61	9.25	7.84	9.00	8.66
Zn	55.41	59.04	58.38	58.11	58.61	60.21	58.92	57.64	59.38	58.08	57.96
Cu	0.04	0.02	nd	nd	nd	nd	nd	nd	nd	nd	nd
Ni	0.00	nd	nd	nd	nd	nd	nd	nd	nd	nd	nd
Ag	0.00	ND	ND	ND	ND	ND	ND	ND	ND	ND	ND
Cd	0.33	ND	ND	ND	ND	ND	ND	ND	ND	ND	ND
Co	0.04	0.11	nd	nd	nd	nd	nd	nd	nd	0.17	nd
Mn	ND	nd	nd	nd	nd	nd	nd	nd	nd	nd	nd
As	ND	nd	nd	nd	nd	nd	nd	nd	nd	nd	nd
Total	98.10	100.83	101.00	100.73	100.37	100.74	99.61	100.98	100.67	100.50	99.98

Deposit						LOKKEN				
Sample	78.FM.6(G5)					78.LM.1(G6)		78.LM.2(G7)		
Sphalerite	5	6	435E	436E	437E	8	9	10	11	12
S	33.94	33.93	33.41	33.10	32.91	33.74	33.68	33.69	33.67	34.03
Pb	0.15	0.19	ND	ND	ND	0.13	0.19	0.14	0.12	0.09
Fe	5.03	4.93	5.60	4.80	5.05	2.36	2.28	3.15	3.53	3.28
Zn	59.09	59.53	61.40	62.05	62.16	63.13	62.27	64.36	63.30	63.67
Cu	0.04	0.02	nd	nd	nd	0.03	0.05	0.14	0.21	0.12
Ni	0.01	0.00	nd	nd	nd	0.02	0.00	0.01	0.01	0.02
Ag	0.06	0.00	ND	ND	ND	0.00	0.00	0.00	0.00	0.00
Cd	0.22	0.26	ND	ND	ND	0.18	0.23	0.36	0.29	0.21
Co	0.02	0.03	nd	nd	nd	0.04	0.02	0.02	0.00	0.02
Mn	ND	ND	nd	nd	nd	ND	ND	0.00	0.00	0.00
As	ND	ND	nd	nd	nd	ND	ND	ND	ND	ND
Total	98.56	98.90	100.41	99.96	100.12	99.64	98.71	101.86	101.14	101.45

TABLE B.7 (continued) Sphalerite Analyses - Massive Volcanogenic Sulfide Deposits

Deposit	KILLINGDAL										
Sample	78.LM.3(G8)			78.LM.8(G10)	78.KM.8(G15)						
	13	14	15	22	25	26	27	375E	376E	377E	378E
S	33.57	33.44	33.61	32.69	33.53	33.59	33.58	33.13	32.98	33.10	33.19
Pb	0.13	0.16	0.12	0.14	0.25	0.13	0.22	ND	ND	ND	ND
Fe	2.49	3.76	3.40	3.62	8.38	8.15	7.94	7.92	7.88	8.16	7.92
Zn	64.22	62.84	64.18	61.32	55.54	56.11	56.04	59.46	58.61	58.10	59.09
Cu	0.01	0.53	0.18	0.48	0.06	0.04	0.07	nd	nd	0.22	0.23
Ni	0.02	0.02	0.00	0.01	0.00	0.00	0.01	nd	nd	nd	nd
Ag	0.00	0.00	0.04	0.00	0.03	0.07	0.05	ND	ND	ND	ND
Cd	0.09	0.08	0.21	0.30	0.31	0.26	0.38	ND	ND	ND	ND
Co	0.00	0.00	0.01	0.01	0.00	0.00	0.00	nd	nd	nd	0.16
Mn	0.00	0.00	0.00	0.01	0.16	0.19	0.17	0.17	0.20	0.15	0.25
As	ND	ND	ND	0.00	0.00	0.00	0.00	nd	nd	nd	nd
Total	100.53	100.54	101.76	98.59	98.25	98.53	98.46	100.68	99.68	99.72	100.83

Deposit											
Sample						78.KM.5(G14)					
	379E	380E	382E	383E	384E	28	29	385E	386E	387E	388E
S	33.20	33.77	33.51	33.34	33.27	33.49	33.31	33.37	33.35	33.41	33.19
Pb	ND	ND	ND	ND	ND	0.26	0.15	ND	ND	ND	ND
Fe	7.95	7.82	7.87	8.04	7.68	8.52	8.36	8.05	8.11	8.89	7.94
Zn	58.98	59.08	58.91	58.41	59.12	55.43	56.73	58.39	59.00	57.62	59.10
Cu	0.29	nd	nd	nd	nd	0.14	0.03	nd	nd	nd	nd
Ni	nd	nd	nd	nd	nd	0.00	0.00	nd	nd	nd	nd
Ag	ND	ND	ND	ND	ND	0.08	0.08	ND	ND	ND	ND
Cd	ND	ND	ND	ND	ND	0.23	0.29	ND	ND	ND	ND
Co	nd	nd	nd	0.13	nd	0.00	0.01	0.13	nd	nd	nd
Mn	0.22	nd	0.24	0.21	nd	0.11	0.13	0.12	0.12	0.14	nd
As	nd	nd	nd	nd	nd	0.00	0.00	nd	nd	nd	nd
Total	100.64	100.66	100.53	100.14	100.07	98.25	99.09	100.06	100.59	100.06	100.23

TABLE B.7 (continued) Sphalerite Analyses - Massive Volcanogenic Sulfide Deposits

Deposit												
Sample						78.KM.4(G13)						
SPHALERITE	389E	390E	391E	392E	393E	31	33	395E	396E	397E	398E	399E
S	33.34	33.20	33.57	32.58	33.32	33.56	34.39	33.34	33.43	33.32	33.49	33.29
Pb	ND	ND	ND	ND	ND	0.24	0.18	ND	ND	ND	ND	ND
Fe	8.95	7.51	7.96	8.33	8.02	8.00	7.72	8.04	8.14	8.07	7.79	8.05
Zn	57.76	59.77	58.76	58.72	58.89	56.71	59.09	59.52	58.92	58.58	59.05	59.15
Cu	nd	nd	nd	nd	nd	0.05	0.07	nd	0.21	0.62	nd	nd
Ni	nd	nd	nd	nd	nd	0.00	0.00	nd	nd	nd	nd	nd
Ag	ND	ND	ND	ND	ND	0.13	0.08	ND	ND	ND	ND	ND
Cd	ND	ND	ND	ND	ND	0.25	0.21	ND	ND	ND	ND	ND
Co	0.11	0.11	nd	nd	nd	0.01	0.01	nd	nd	nd	nd	nd
Mn	0.20	0.20	0.16	0.12	nd	0.11	0.09	0.13	0.12	nd	0.18	0.16
As	nd	nd	nd	nd	nd	0.00	0.00	nd	nd	nd	nd	nd
Total	100.37	100.79	100.45	99.75	100.23	99.06	101.85	101.02	100.82	100.58	100.51	100.65

Deposit												
Sample						78.KM.2(G12)						
SPHALERITE	400E	401E	402E	403E	404E	20	21	405E	406E	407E	408E	409E
S	33.20	33.59	33.41	33.37	33.22	32.81	33.04	33.10	33.49	33.17	33.05	33.26
Pb	ND	ND	ND	ND	ND	0.12	0.17	ND	ND	ND	ND	ND
Fe	7.76	7.88	8.09	7.92	8.14	8.78	7.22	8.05	8.18	8.14	7.97	8.21
Zn	59.25	59.40	59.18	59.55	59.56	56.00	57.34	58.13	59.08	59.08	58.45	58.74
Cu	nd	nd	nd	nd	nd	0.28	0.06	nd	nd	nd	nd	nd
Ni	nd	nd	nd	nd	nd	0.01	0.02	nd	nd	nd	nd	nd
Ag	ND	ND	ND	ND	ND	0.00	0.00	ND	ND	ND	ND	ND
Cd	ND	ND	ND	ND	ND	0.00	0.07	ND	ND	ND	ND	ND
Co	0.17	nd	nd	nd	nd	0.01	0.02	nd	nd	0.12	nd	nd
Mn	0.15	nd	nd	0.14	nd	0.14	0.11	0.18	0.34	0.18	0.34	0.25
As	nd	nd	nd	nd	nd	ND	ND	nd	nd	nd	nd	nd
Total	100.54	100.87	100.69	100.97	100.92	98.16	98.04	99.47	101.10	100.69	99.82	100.46

TABLE B.7 (continued) Sphalerite Analyses - Massive Volcanogenic Sulfide Deposits

Deposit												
Sample						78.KM.1(G11)						
SPHALERITE	410E	411E	412E	413E	414E	19	415E	416E	417E	418E	419E	420E
S	33.20	33.10	33.44	33.23	33.34	33.23	33.34	33.40	33.02	33.24	33.24	33.29
Pb	ND	ND	ND	ND	ND	0.11	ND	ND	ND	ND	ND	ND
Fe	8.03	8.17	8.15	8.09	8.18	6.57	6.74	6.66	7.32	6.59	7.42	8.09
Zn	58.10	58.82	58.55	58.63	59.07	58.42	60.60	60.52	59.85	60.53	59.91	58.43
Cu	nd	nd	nd	nd	nd	0.03	0.19	nd	nd	nd	nd	0.22
Ni	nd	nd	nd	nd	nd	0.00	nd	nd	nd	nd	nd	nd
Ag	ND	ND	ND	ND	ND	0.02	ND	ND	ND	ND	ND	ND
Cd	ND	ND	ND	ND	ND	0.12	ND	ND	ND	ND	ND	ND
Co	nd	0.12	nd	0.14	nd	0.01	nd	nd	nd	0.15	nd	0.13
Mn	0.17	0.26	0.21	0.24	0.25	0.12	nd	nd	nd	0.12	0.20	nd
As	nd	nd	nd	nd	nd	ND	nd	nd	nd	nd	nd	nd
Total	99.51	100.47	100.34	100.32	100.83	98.62	100.88	100.57	100.20	100.63	100.77	100.17

Deposit					ROSTVANGEN							
Sample					78.RD.10(G16)							
SPHALERITE	421E	422E	423E	424E	35	36	353E	354E	355E	356E	357E	358E
S	33.33	33.09	33.22	33.55	33.15	33.61	33.25	33.29	33.39	333.37	33.60	33.39
Pb	ND	ND	ND	ND	0.12	0.10	ND	ND	ND	ND	ND	ND
Fe	7.78	6.67	8.12	8.38	6.65	8.92	8.03	7.70	8.10	8.01	8.11	8.17
Zn	59.08	60.03	58.95	58.48	59.62	57.50	59.12	58.66	57.81	59.49	59.18	58.81
Cu	nd	0.32	0.19	0.23	0.07	0.56	nd	nd	nd	nd	nd	nd
Ni	nd	nd	nd	nd	0.01	0.01	0.12	nd	nd	nd	nd	nd
Ag	ND	ND	ND	ND	0.00	0.01	ND	ND	ND	ND	ND	ND
Cd	ND	ND	ND	ND	0.17	0.19	ND	ND	ND	ND	ND	ND
Co	nd	0.16	nd	nd	0.00	0.04	0.15	nd	nd	nd	nd	0.12
Mn	nd	0.16	0.17	nd	0.03	0.00	nd	nd	nd	0.15	nd	nd
As	nd	nd	nd	nd	ND	ND	nd	nd	nd	nd	nd	nd
Total	100.19	100.42	100.65	100.64	99.82	100.96	100.67	99.65	99.30	101.02	100.89	100.49

TABLE B.7 (continued) Sphalerite Analyses - Massive Volcanogenic Sulfide Deposits

Deposit															
Sample															
SPHALERITE	359E	360E	362E	364E	493E	494E	495E	496E	497E	498E	499E	500E	501E	502E	509E
S	33.59	33.51	33.43	33.42	32.80	32.73	32.72	32.77	32.85	32.92	32.65	32.64	32.72	32.90	32.81
Pb	ND	ND	ND	ND	ND	ND	ND	ND	ND	ND	ND	ND	ND	ND	ND
Fe	7.73	7.42	8.26	7.87	8.43	7.44	7.45	7.65	7.57	7.96	7.88	7.70	7.99	7.85	7.84
Zn	59.34	59.91	58.27	59.43	59.26	60.04	59.25	59.04	59.82	58.36	59.46	58.88	58.80	59.15	59.49
Cu	nd	nd	0.27	nd	nd	0.19	nd	0.86	nd	nd	0.17	nd	0.17	nd	0.17
Ni	nd	nd	nd	nd	nd	nd	nd	nd	nd	nd	nd	nd	nd	nd	nd
Ag	ND	ND	ND	ND	ND	ND	ND	ND	ND	ND	ND	ND	ND	ND	ND
Cd	ND	ND	ND	ND	ND	ND	ND	ND	ND	ND	ND	ND	ND	ND	ND
Co	0.12	nd	nd	nd	nd	nd	nd	nd	0.26	nd	nd	nd	0.24	nd	nd
Mn	nd	nd	nd	nd	nd	nd	nd	0.15	nd	0.16	nd	nd	nd	nd	nd
As	nd	nd	nd	nd	nd	nd	nd	nd	nd	nd	nd	nd	nd	nd	nd
Total	100.66	100.84	100.23	100.73	100.49	100.40	99.42	100.47	100.51	99.39	100.17	99.23	99.92	99.89	100.32

Deposit															
Sample	77.HD.1(P1)														
SPHALERITE	39	40	41	366E	367E	368E	369E	370E	371E	372E	373E	374E	472E	473E	474E
S	33.97	33.67	33.86	32.82	33.22	33.24	33.00	33.21	33.03	33.15	33.16	33.26	32.68	32.63	32.77
Pb	0.10	0.10	0.09	ND	ND	ND	ND	ND	ND	ND	ND	ND	ND	ND	ND
Fe	7.33	6.49	6.72	7.17	6.66	7.58	7.45	7.80	7.14	6.99	6.60	7.95	6.87	8.26	8.57
Zn	60.25	60.57	60.75	59.62	59.78	59.00	60.04	58.78	60.25	60.62	60.75	59.14	60.53	59.82	58.58
Cu	0.06	0.09	0.07	nd	nd	nd	nd	nd	nd	nd	nd	0.25	nd	nd	nd
Ni	0.01	0.03	0.00	nd	0.12	nd	nd	nd	nd	nd	nd	nd	nd	nd	nd
Ag	0.00	0.04	0.00	ND	ND	ND	ND	ND	ND	ND	ND	ND	ND	ND	ND
Cd	0.21	0.24	0.28	ND	ND	ND	ND	ND	ND	ND	ND	ND	ND	ND	ND
Co	0.02	0.04	0.02	nd	nd	nd	0.11	nd	nd	nd	nd	0.13	nd	nd	nd
Mn	0.01	0.01	0.01	nd	nd	nd	nd	nd	nd	nd	nd	nd	nd	nd	nd
As	ND	ND	ND	nd	nd	nd	nd	nd	nd	nd	nd	nd	nd	nd	nd
Total	101.95	101.26	101.79	99.61	99.77	99.83	100.60	99.79	100.42	100.77	100.51	100.74	100.08	100.71	99.92

TABLE E.7 (continued) Sphalerite Analyses - Massive Volcanogenic Sulfide Deposits

Deposit															
Sample															
SPHALERITE	475E	476E	477E	478E	479E	480E	481E	482E	483E	484E	485E	486E	487E	488E	489E
S	32.46	32.59	32.48	33.07	32.61	32.86	32.62	32.82	32.73	32.83	32.78	32.66	32.80	32.69	32.80
Pb	ND	ND	ND	ND	ND	ND	ND	ND	ND	ND	ND	ND	ND	ND	ND
Fe	7.59	7.87	6.92	7.50	6.78	6.56	6.14	6.98	9.17	8.32	6.94	6.60	9.29	5.90	6.06
Zn	59.61	58.72	60.57	59.73	61.01	61.23	61.77	59.74	57.20	59.59	60.63	60.19	57.71	62.35	60.16
Cu	nd	nd	nd	0.29	0.18	nd	nd	nd	nd	nd	nd	0.18	0.31	nd	0.21
Ni	nd	nd	nd	nd	nd	nd	nd	nd	nd	nd	nd	nd	nd	nd	nd
Ag	ND	ND	ND	ND	ND	ND	ND	ND	ND	ND	ND	ND	ND	ND	ND
Cd	ND	ND	ND	ND	ND	ND	ND	ND	ND	ND	ND	ND	ND	ND	ND
Co	0.14	nd	nd	nd	nd	nd	nd	nd	nd	0.13	nd	0.12	nd	nd	nd
Mn	nd	nd	nd	nd	nd	nd	nd	nd	0.16	nd	nd	nd	nd	nd	nd
As	nd	nd	nd	nd	nd	nd	nd	nd	nd	nd	nd	nd	nd	nd	nd
Total	99.81	99.18	99.98	100.58	100.59	100.64	100.53	99.53	99.26	100.87	100.35	99.76	100.11	100.94	100.22

Deposit															
Sample															
SPHALERITE	490E	491E	492E	510E	511E	512E	513E	514E	515E	516E	517E	518E	519E	520E	521E
S	32.66	32.78	32.81	32.71	32.94	33.07	32.97	32.87	32.55	32.66	32.56	32.75	32.62	32.57	32.59
Pb	ND	ND	ND	ND	ND	ND	ND	ND	ND	ND	ND	ND	ND	ND	ND
Fe	6.18	7.46	8.73	8.27	6.46	7.66	7.51	7.57	5.90	6.33	7.53	7.18	6.88	7.95	7.35
Zn	61.40	59.62	57.62	58.90	61.31	59.96	59.65	59.62	61.38	60.35	59.55	59.65	60.72	59.38	60.17
Cu	nd	0.23	nd	0.21	nd	nd	0.62	0.40	nd	nd	0.17	nd	0.19	nd	0.19
Ni	nd	nd	nd	nd	nd	nd	nd	nd	nd	nd	nd	nd	nd	nd	nd
Ag	ND	ND	ND	ND	ND	ND	ND	ND	ND	ND	ND	ND	ND	ND	ND
Cd	ND	ND	ND	ND	ND	ND	ND	ND	ND	ND	ND	ND	ND	ND	ND
Co	nd	nd	nd	nd	nd	nd	nd	0.14	nd	nd	nd	0.13	nd	nd	nd
Mn	nd	nd	nd	nd	nd	nd	nd	nd	nd	nd	nd	nd	nd	nd	nd
As	nd	nd	nd	nd	nd	nd	nd	nd	nd	nd	nd	nd	nd	nd	nd
Total	100.25	100.09	99.16	100.10	100.73	100.69	100.75	100.90	99.83	99.34	99.81	99.70	100.41	99.90	100.30

TABLE B.7 (continued) SPHALERITE ANALYSES - Massive Volcanogenic Sulfide Deposits

Deposit														
Sample				78.KD.15(G18)										
SPHALERITE	522E	523E	524E	46	47	48	345E	346E	347E	348E	349E	350E	351E	352E
S	32.70	32.62	32.83	32.29	33.66	33.50	33.79	32.96	33.18	33.10	33.28	33.26	33.20	33.10
Pb	ND	ND	ND	0.11	0.08	0.08	ND	ND	ND	ND	ND	ND	ND	ND
Fe	9.13	7.75	7.70	7.76	7.27	7.79	7.44	7.83	7.07	7.39	7.99	7.66	7.94	8.43
Zn	58.33	59.12	59.47	59.46	59.89	58.86	58.93	59.41	59.84	59.15	59.15	59.80	59.22	58.59
Cu	nd	nd	0.20	0.38	0.21	0.42	0.32	nd	0.27	0.55	0.18	0.28	nd	nd
Ni	nd	nd	nd	0.00	0.00	0.00	nd	nd	nd	nd	nd	nd	nd	nd
Ag	ND	ND	ND	0.00	0.02	0.00	ND	ND	ND	ND	ND	ND	ND	ND
Cd	ND	ND	ND	0.25	0.23	0.28	ND	ND	ND	ND	ND	ND	ND	ND
Co	nd	nd	nd	0.04	0.03	0.03	0.14	0.14	0.14	0.14	0.13	nd	nd	nd
Mn	nd	nd	nd	0.02	0.02	0.01	nd	nd	nd	nd	nd	nd	nd	nd
As	nd	nd	nd	ND	ND	ND	0.36	nd	nd	nd	nd	nd	nd	nd
Total	100.16	99.49	100.20	101.32	101.41	100.96	100.98	100.34	100.50	100.33	100.72	101.00	100.37	100.12

Deposit									KVIKNE					
Sample	78.KD.14(G17)								78.KVD.1(G19)					
SPHALERITE	49	50	503E	504E	505E	506E	507E	508E	42	43	44	45	338E	339E
S	33.48	33.26	32.70	32.82	32.53	32.56	32.59	32.26	33.55	33.61	33.40	33.36	33.29	33.35
Pb	0.10	0.10	ND	ND	ND	ND	ND	ND	0.09	0.07	0.10	0.08	ND	ND
Fe	6.39	6.46	6.53	8.11	7.65	8.04	7.22	7.59	9.54	9.20	7.14	7.56	7.23	7.08
Zn	59.66	59.84	60.01	58.10	58.62	58.30	58.36	58.35	56.65	57.53	59.54	59.33	59.78	59.70
Cu	0.21	0.12	0.17	0.31	0.67	0.88	0.78	0.64	0.10	0.06	0.05	0.05	nd	nd
Ni	0.00	0.00	nd	nd	nd	nd	nd	nd	0.00	0.00	0.00	0.02	nd	nd
Ag	0.00	0.00	ND	ND	ND	ND	ND	ND	0.00	0.00	0.00	0.00	ND	ND
Cd	0.21	0.25	ND	ND	ND	ND	ND	ND	0.34	0.31	0.32	0.27	ND	ND
Co	0.03	0.01	nd	0.16	nd	0.13	nd	nd	0.02	0.01	0.02	0.02	nd	nd
Mn	0.25	0.26	0.27	0.15	0.24	0.21	0.18	nd	0.22	0.19	0.16	0.11	0.20	nd
As	ND	ND	nd	nd	nd	nd	nd	nd	ND	ND	ND	ND	nd	nd
Total	100.34	100.29	99.67	99.65	99.72	100.13	99.12	99.84	100.52	100.99	100.72	100.79	100.50	100.14

TABLE B.7 (continued) Sphalerite Analyses - Massive Volcanogenic Sulfide Deposits

Deposit														
Sample						78.KVD.7(G22)								
SPHALERITE	340E	341E	342E	343E	344E	51	53	306E	307E	309E	311E	312E	313E	314E
S	33.34	33.34	32.89	33.35	33.02	33.59	33.50	33.60	33.37	33.37	33.26	33.41	33.21	33.35
Pb	ND	ND	ND	ND	ND	0.18	0.11	ND	ND	ND	ND	ND	ND	ND
Fe	7.31	6.97	7.36	6.96	7.84	7.47	7.76	7.30	7.85	7.86	6.56	6.65	7.64	7.31
Zn	58.80	59.29	60.18	59.11	58.57	59.98	59.51	59.80	58.80	59.08	60.98	60.63	59.25	59.60
Cu	0.17	nd	0.21	nd	0.24	0.02	0.00	nd	nd	nd	nd	nd	0.17	nd
Ni	nd	nd	nd	nd	nd	0.02	0.02	nd	nd	nd	nd	nd	0.14	nd
Ag	ND	ND	ND	ND	ND	0.00	0.00	ND	ND	ND	ND	ND	ND	ND
Cd	ND	ND	ND	ND	ND	0.33	0.35	ND	ND	ND	ND	ND	ND	ND
Co	nd	nd	nd	nd	0.14	0.01	0.00	nd	nd	nd	nd	nd	nd	nd
Mn	0.26	0.14	0.21	0.20	0.29	0.04	0.06	nd	nd	nd	nd	nd	0.11	0.12
As	nd	nd	nd	nd	nd	ND	ND	nd	nd	nd	nd	nd	nd	nd
Total	99.89	99.73	100.84	99.62	100.11	101.63	101.31	100.70	100.02	100.32	100.80	100.70	100.52	100.38

Deposit														
Sample						78.KVD.6(G21)								
SPHALERITE	315E	316E	317E	318E	319E	54	55	56	320E	321E	322E	323E	324E	325E
S	33.52	33.51	33.40	33.26	33.27	33.34	33.45	33.50	33.23	33.49	33.39	33.43	33.22	33.18
Pb	ND	ND	ND	ND	ND	0.20	0.15	0.15	ND	ND	ND	ND	ND	ND
Fe	8.17	8.31	7.30	7.35	8.10	7.15	7.37	7.35	7.55	7.22	7.86	7.61	7.39	7.72
Zn	58.50	57.95	59.98	59.96	59.14	59.82	59.84	59.83	58.46	59.63	59.30	59.17	59.09	59.17
Cu	nd	0.16	nd	nd	nd	0.04	0.05	0.03	nd	nd	nd	nd	nd	nd
Ni	nd	nd	nd	nd	nd	0.01	0.00	0.03	nd	nd	nd	nd	nd	nd
Ag	ND	ND	ND	ND	ND	0.00	0.00	0.00	ND	ND	ND	ND	ND	ND
Cd	ND	ND	ND	ND	ND	0.27	0.21	0.20	ND	ND	ND	ND	ND	ND
Co	0.15	nd	nd	nd	nd	0.00	0.00	0.00	nd	0.15	0.11	nd	nd	nd
Mn	0.14	0.18	nd	0.13	nd	0.13	0.11	0.13	0.21	0.21	0.16	0.15	0.22	0.22
As	nd	nd	nd	nd	nd	ND	ND	ND	nd	nd	nd	nd	nd	nd
Total	100.48	100.11	100.69	100.70	100.61	100.95	101.19	101.22	99.44	100.69	100.82	10037	99.92	100.29

TABLE B.7 (continued) Sphalerite Analyses - Massive Volcanogenic Sulfide Deposits

Deposit							
Sample				78.KVD.2(G20)			
SPHALERITE	326E	327E	328E	57	58	59	329E
S	33.26	33.44	33.46	33.78	33.59	33.15	33.28
Pb	ND	ND	ND	0.16	0.18	0.14	ND
Fe	7.50	7.58	7.73	8.62	7.59	7.79	7.23
Zn	58.65	59.67	59.01	58.48	59.50	58.54	60.09
Cu	nd	nd	nd	0.02	0.04	0.01	nd
Ni	nd	nd	nd	0.02	0.00	0.01	nd
Ag	ND	ND	ND	0.00	0.00	0.00	ND
Cd	ND	ND	ND	0.28	0.24	0.27	ND
Co	nd	nd	nd	0.00	0.00	0.00	nd
Mn	nd	0.27	0.15	0.24	0.19	0.21	0.20
As	nd	nd	nd	ND	ND	ND	nd
Total	99.40	100.96	100.36	101.60	101.33	100.13	100.80

Deposit								
Sample								
SPHALERITE	330E	331E	332E	333E	334E	335E	336E	337E
S	33.24	33.41	33.30	33.30	33.26	33.38	33.21	33.27
Pb	ND	ND	ND	ND	ND	ND	ND	ND
Fe	7.56	7.16	8.39	8.15	7.68	8.46	7.73	8.05
Zn	59.61	60.24	57.83	58.07	58.70	58.14	58.69	58.18
Cu	nd	nd	0.18	nd	nd	nd	nd	0.29
Ni	nd	nd	nd	nd	nd	nd	nd	nd
Ag	ND	ND	ND	ND	ND	ND	ND	ND
Cd	ND	ND	ND	ND	ND	ND	ND	ND
Co	nd	0.12	nd	nd	nd	0.15	0.11	nd
Mn	0.26		0.27	0.29	0.25	0.32	0.15	0.34
As	nd	nd	nd	nd	nd	nd	nd	nd
Total	100.66	100.93	99.98	99.82	99.89	100.45	99.90	100.12

TABLE B.7 (continued) Sphalerite Analyses - Massive Volcanogenic Sulfide Deposits

Deposit	ROSTVANGEN					
Sample	77.RD.1(F1)					
SPHALERITE	472RE	477RE	478RE	479RE	480RE	481RE
S	32.55	32.65	33.04	32.89	32.61	32.31
Pb	ND	ND	ND	ND	ND	ND
Fe	7.51	7.17	9.02	7.23	7.65	7.36
Zn	59.29	60.53	58.03	60.44	59.71	59.45
Cu	nd	nd	nd	nd	nd	nd
Ni	nd	nd	nd	nd	nd	nd
Ag	ND	ND	ND	ND	ND	ND
Cd	ND	ND	ND	ND	ND	ND
Co	nd	nd	0.15	0.22	0.17	nd
Mn	nd	nd	nd	nd	nd	nd
As	nd	nd	nd	nd	nd	nd
Total	99.35	100.35	100.24	100.78	100.14	99.12

TABLE B.8 Arsenopyrite Analyses - Massive Volcanogenic Sulfide Deposits

Deposit	KILLINGDAL				
Sample	78.KM.5(G14)			78.KM.4(G13)	
	1	2	3	4	5
S	22.14	22.24	22.05	21.33	22.04
Pb	0.14	0.12	0.12	0.11	0.13
Fe	35.57	35.73	36.20	35.68	35.70
Zn	0.00	0.02	0.02	0.06	0.06
Cu	0.04	0.08	0.05	0.09	0.14
Ni	0.03	0.01	0.00	0.00	0.03
Ag	0.00	0.00	0.02	0.00	0.04
Cd	0.06	0.02	0.05	0.00	0.00
Co	0.14	0.10	0.09	0.07	0.14
Mn	0.01	0.00	0.00	0.01	0.00
As	41.57	41.59	41.81	42.66	41.63
Total	99.69	99.91	100.42	100.01	99.91

TABLE B.9 Galena Analyses - Massive Volcanogenic Sulfide Deposits

Deposit	KILLINGDAL			
Sample	78.KM.4(G13)	78.KM.5(G14)		
	8	10	11	12
S	12.94	12.97	13.02	12.96
Pb	86.76	84.68	85.27	85.72
Fe	0.35	0.77	1.96	1.36
Zn	0.00	0.00	0.00	0.00
Cu	0.10	0.10	0.13	0.10
Ni	0.00	0.00	0.00	0.00
Ag	0.55	0.33	0.33	0.28
Cd	0.02	0.02	0.00	0.07
Co	0.00	0.02	0.00	0.00
Mn	0.01	0.03	0.02	0.02
As	0.13	0.14	0.11	0.11
Total	98.86	99.06	100.84	100.63

TABLE B.10 Olivine Analyses - Ultramafics

Intrusion	KALTBERGET									
Sample	76/4/45									
OLIVINE	10	11	12	13	14	128E	129E	130E	135E	137E
SiO_2	39.05	40.13	39.33	39.68	39.42	39.87	39.83	40.20	39.85	40.55
TiO_2	0.00	0.00	0.00	0.00	0.00	nd	nd	nd	nd	nd
Al_2O_3	0.00	0.00	0.00	0.00	0.00	nd	nd	nd	nd	nd
Cr_2O_3	0.04	0.00	0.06	0.01	0.01	ND	ND	ND	ND	ND
FeO	18.41	14.36	18.56	17.24	17.47	16.75	17.24	14.06	13.69	13.51
MgO	41.95	45.36	42.03	42.31	42.80	43.50	43.92	45.29	45.13	47.03
CaO	0.01	0.00	0.00	0.47	0.01	nd	nd	0.11	0.37	nd
MnO	0.23	0.16	0.24	0.24	0.22	0.26	0.22	0.22	0.21	0.12
NiO	0.31	0.20	0.18	0.21	0.18	nd	0.16	0.29	nd	0.29
CoO	0.07	0.04	0.06	0.08	0.08	ND	ND	ND	ND	ND
Na_2O	ND	ND	ND	ND	ND	ND	ND	ND	ND	ND
K_2O	ND	ND	ND	ND	ND	ND	ND	ND	ND	ND
Total	100.07	100.26	100.48	100.26	100.19	100.38	101.36	100.18	99.24	101.49
Fo	80	85	80	81	81	82	81	85	85	86

Intrusion	KLETTEN											
Sample	76.336e								77.64			
OLIVINE	7	8	9	51E	54E	56E	72E	84E	1	2	3	152E
SiO_2	40.40	40.02	40.21	39.71	39.58	40.40	41.53	41.53	40.19	40.01	40.30	39.78
TiO_2	0.00	0.00	0.00	nd	nd	nd	nd	0.11	0.00	0.00	0.00	nd
Al_2O_3	0.00	0.00	0.00	nd	nd	nd	nd	nd	0.01	0.00	0.00	nd
Cr_2O_3	0.02	0.00	0.01	ND	ND	ND	ND	ND	0.01	0.00	0.04	ND
FeO	11.50	12.39	12.57	12.08	13.03	13.18	10.99	10.23	13.04	12.70	11.67	13.38
MgO	46.96	46.57	46.02	47.55	46.55	46.87	48.79	48.35	45.45	46.33	46.62	46.17
CaO	0.02	0.01	0.20	0.08	nd	nd	nd	0.21	0.02	0.05	0.33	nd
MnO	0.33	0.27	0.24	0.25	0.25	0.23	0.39	0.40	0.33	0.28	0.33	0.38
NiO	0.07	0.06	0.08	nd	nd	nd	nd	nd	0.04	0.03	0.08	nd
CoO	0.04	0.05	0.03	ND	ND	ND	ND	ND	0.03	0.01	0.03	ND
Na_2O	ND	ND	ND	ND	ND	ND	ND	ND	ND	ND	ND	ND
K_2O	ND	ND	ND	ND	ND	ND	ND	ND	ND	ND	ND	ND
Total	99.35	99.38	99.37	99.67	99.41	100.69	101.69	100.87	99.13	99.41	99.39	99.72
Fo	88	87	87	88	87	86	88	89	86	87	88	85

TABLE B.10 (continued) Olivine Analyses - Ultramafics

Intrusion										
Sample	77.64 (continued)				77.66					
OLIVINE	153E	155E	156E	157E	4	5	6	165E	158E	159E
SiO_2	40.05	40.74	40.30	40.09	40.21	40.16	40.22	39.56	39.97	39.69
TiO_2	nd	nd	nd	nd	0.00	0.00	0.00	nd	nd	nd
Al_2O_3	nd	nd	nd	nd	0.00	0.00	0.00	nd	nd	nd
Cr_2O_3	ND	ND	ND	ND	0.04	0.01	0.00	ND	ND	ND
FeO	14.26	14.18	13.69	13.94	12.41	12.59	11.44	12.99	12.89	13.03
MgO	33.89	45.05	44.77	46.23	46.38	46.31	47.00	45.77	44.94	44.69
CaO	0.15	0.33	0.81	nd	0.12	0.02	0.02	nd	nd	0.21
MnO	0.34	0.39	0.23	0.29	0.27	0.22	0.26	0.22	0.25	0.40
NiO	nd	nd	nd	nd	0.06	0.21	0.08	nd	0.27	0.24
CoO	ND	ND	ND	ND	0.04	0.03	0.04	ND	ND	ND
Na_2O	ND	ND	ND	ND	ND	ND	ND	ND	ND	ND
K_2O	ND	ND	ND	ND	ND	ND	ND	ND	ND	ND
Total	99.69	100.69	99.80	100.55	99.54	99.56	99.08	98.54	98.33	98.26
Fo	84	84	84	85	87	87	88	86	86	85

Intrusion								
Sample	77.68							
OLIVINE	167E	169E	171E	173E	175E	177E	179E	182E
SiO_2	40.96	40.36	40.70	40.70	40.63	40.52	41.12	40.79
TiO_2	nd	nd	nd	nd	nd	nd	nd	nd
Al_2O_3	nd	nd	nd	nd	nd	nd	nd	nd
Cr_2O_3	ND	ND	ND	ND	ND	ND	ND	ND
FeO	11.28	13.27	11.59	11.49	12.09	12.07	10.92	13.13
MgO	47.68	46.53	47.13	47.49	46.90	47.96	48.01	46.98
CaO	0.13	nd	0.24	0.10	0.13	0.12	0.21	nd
MnO	0.47	0.44	0.42	0.60	0.49	0.41	0.63	0.31
NiO	nd	nd	nd	nd	nd	nd	nd	nd
CoO	ND	ND	ND	ND	ND	ND	ND	ND
Na_2O	ND	ND	ND	ND	ND	ND	ND	ND
K_2O	ND	ND	ND	ND	ND	ND	ND	ND
Total	100.51	100.60	100.09	100.38	100.24	101.09	100.89	101.23
Fo	88	86	87	87	87	87	88	86

TABLE B.11 Olivine Analyses - Metagabbros

Intrusion	UNDAL												
Sample	77.94									77.91	77.148(inclusion)		
OLIVINE	15	16	17	139E	140E	141E	142E	143E	144E	21	25	26	27
SiO_2	37.34	36.78	37.23	38.12	37.68	37.79	37.31	37.56	37.79	36.94	36.61	38.13	37.77
TiO_2	0.06	0.05	0.03	nd	nd	nd	0.11	nd	nd	0.00	0.00	0.00	0.00
Al_2O_3	0.01	0.00	0.00	nd	nd	nd	nd	nd	nd	0.03	0.00	0.00	0.01
Cr_2O_3	0.03	0.02	0.03	ND	ND	ND	ND	ND	ND	0.00	0.00	0.00	0.00
FeO	26.54	31.25	29.86	28.60	30.65	30.72	30.11	29.84	29.05	26.19	16.61	15.09	17.04
MgO	34.08	31.88	32.91	34.60	32.79	32.86	33.65	33.60	33.50	36.01	44.15	45.11	43.97
CaO	0.06	0.08	0.06	nd	nd	nd	nd	0.14	0.11	0.09	0.03	0.04	0.03
MnO	0.41	0.45	0.46	0.50	0.52	0.44	0.47	0.46	0.43	0.36	0.21	0.18	0.21
NiO	0.19	0.19	0.17	0.18	nd	nd	nd	0.15	nd	0.21	0.05	0.04	0.06
CoO	0.14	0.12	0.14	ND	ND	ND	ND	ND	ND	0.06	0.01	0.00	0.02
Na_2O	ND	ND	ND	ND	ND	ND	ND	ND	ND	ND	ND	ND	ND
K_2O	ND	ND	ND	ND	ND	ND	ND	ND	ND	ND	ND	ND	ND
Total	100.88	100.84	100.88	101.99	101.64	101.82	101.65	101.75	100.88	99.89	99.68	98.59	99.11
Fo	68	64	66	68	65	65	66	66	67	71	82	84	82

Intrusion	SKJAEKERDALEN												
Sample	77.299							78.67			77.300b		
OLIVINE	18	19	20	145E	147E	206E	207E	22	23	24	184E	186E	188E
SiO_2	38.25	38.44	38.63	38.28	38.48	38.74	39.9	37.55	37.89	37.97	38.54	39.53	38.71
TiO_2	0.01	0.00	0.00	nd	nd	nd	nd	0.00	00.00	0.00	nd	nd	nd
Al_2O_3	0.00	0.00	0.00	nd	nd	nd	nd	0.00	0.00	0.00	nd	nd	nd
Cr_2O_3	0.03	0.02	0.01	ND	ND	ND	ND	0.00	0.00	0.00	ND	ND	ND
FeO	23.52	22.88	22.73	23.39	23.46	23.69	15.25	22.79	23.20	22.40	23.81	19.85	22.55
MgO	37.90	38.72	38.75	38.78	38.98	37.94	43.65	38.67	38.61	39.37	38.54	41.71	38.97
CaO	0.01	0.02	0.00	nd	nd	0.09	nd	0.00	0.02	0.03	nd	nd	nd
MnO	0.28	0.29	0.25	0.33	0.27	0.26	nd	0.30	0.31	0.31	0.38	0.32	0.33
NiO	0.15	0.16	0.13	nd	0.17	nd	0.17	0.11	0.11	0.14	nd	nd	nd
CoO	0.10	0.10	0.10	ND	ND	ND	ND	0.07	0.05	0.05	ND	ND	ND
Na_2O	ND	ND	ND	ND	ND	ND	ND	ND	ND	ND	ND	ND	ND
K_2O	ND	ND	ND	ND	ND	ND	ND	ND	ND	ND	ND	ND	ND
Total	100.24	100.62	100.60	100.78	101.36	100.72	99.01	99.52	100.20	100.27	101.26	101.41	100.56
Fo	74	75	75	74	74	74	83	75	75	76	74	79	75

TABLE B.11 (continued) Olivine Analyses - Metagabbros

Intrusion											
Sample	78.76		78.72		77.291b			77.291a		77.299	
OLIVINE	197E	199E	200E	201E	203E	204E	205E	208E	209E	190E	192E
SiO_2	38.33	39.77	37.82	37.46	39.52	39.13	38.74	37.07	37.53	38.89	39.05
TiO_2	nd	nd	nd	0.21	nd	nd	nd	0.20	nd	nd	nd
Al_2O_3	nd	nd	nd	nd	nd	nd	nd	nd	nd	nd	nd
Cr_2O_3	ND	ND	ND	ND	ND	ND	ND	ND	ND	ND	ND
FeO	26.50	19.62	26.98	26.55	18.80	18.79	19.14	30.67	30.81	23.17	23.05
MgO	36.04	41.74	35.92	35.26	42.55	42.16	42.63	32.92	32.76	38.98	39.01
CaO	nd	nd	nd	nd	nd	nd	nd	0.19	nd	nd	nd
MnO	0.35	0.34	0.31	0.34	0.13	0.26	0.16	0.46	0.28	0.33	0.27
NiO	0.17	0.16	nd	nd	nd	nd	nd	nd	nd	0.29	nd
CoO	ND	ND	ND	ND	ND	ND	ND	ND	ND	ND	ND
Na_2O	ND	ND	ND	ND	ND	ND	ND	ND	ND	ND	ND
K_2O	ND	ND	ND	ND	ND	ND	ND	ND	ND	ND	ND
Total	101.39	101.62	101.03	99.83	101.01	100.35	100.68	101.52	101.38	101.67	101.38
Fo	70	79	70	70	80	80	79	65	65	74	75

TABLE B.12 Orthopyroxene Analyses - Ultramafics

Intrusion	KLETTEN								
Sample	76.336e								
PYROXENE	1	2	3	2E	3E	6E	14E	21E	30E
SiO_2	56.01	55.36	54.85	54.86	55.83	54.93	55.47	57.04	56.88
TiO_2	0.09	0.18	0.17	0.13	nd	nd	0.14	0.12	nd
Al_2O_3	0.82	1.32	1.90	1.89	1.57	1.84	1.23	1.38	1.86
Cr_2O_3	0.09	0.28	0.21	0.36	0.21	0.16	0.20	0.12	0.12
FeO	8.70	8.43	8.77	9.49	9.60	9.35	8.84	9.24	9.47
MgO	32.08	31.72	31.56	31.58	31.85	31.32	31.76	31.65	31.95
CaO	1.04	1.07	1.05	1.00	0.94	0.93	1.10	1.04	0.92
MnO	0.25	0.24	0.26	0.26	0.14	0.30	0.25	0.20	0.29
NiO	0.01	0.01	0.03	nd	nd	nd	nd	nd	nd
CoO	0.01	0.01	0.01	ND	ND	ND	ND	ND	ND
Na_2O	0.02	0.03	0.03	nd	nd	nd	nd	nd	nd
K_2O	0.01	0.00	0.00	ND	ND	ND	ND	ND	ND
Total	99.13	98.65	98.86	99.57	100.13	98.82	99.00	100.79	101.50
Wo	2.0	2.1	2.0	1.9	1.8	1.8	2.1	2.0	1.8
En	84.8	84.9	84.4	83.6	83.7	83.7	84.3	84.9	83.8
Fs	13.3	13.0	13.6	14.5	14.4	14.5	13.6	14.1	14.4

Intrusion											
Sample	77.64										
PYROXENE	6	7	8	51E	52E	53E	54E	4	5	55E	56E
SiO_2	55.00	55.24	54.56	55.52	55.12	55.08	56.06	55.56	54.75	54.57	55.54
TiO_2	0.15	0.19	0.18	0.20	0.17	0.16	0.30	0.19	0.24	0.22	0.18
Al_2O_3	1.12	1.35	1.35	1.65	1.90	2.10	1.85	1.47	1.90	2.26	1.54
Cr_2O_3	0.12	0.21	0.10	nd	0.15	nd	0.27	0.39	0.44	0.42	0.31
FeO	9.56	9.47	9.71	10.47	10.28	10.37	10.05	8.10	8.47	8.92	8.73
MgO	30.71	31.18	30.82	31.34	30.52	30.59	30.95	31.77	31.56	31.69	31.96
CaO	1.13	1.22	1.09	1.12	1.12	1.15	1.19	1.15	1.07	1.01	1.09
MnO	0.28	0.26	0.25	0.33	0.33	0.34	0.32	0.24	0.23	0.22	0.23
NiO	0.01	0.03	0.01	nd	nd	nd	nd	0.00	0.02	nd	nd
CoO	0.02	0.02	0.01	ND	ND	ND	ND	0.01	0.00	ND	ND
Na_2O	0.03	0.03	0.05	nd	nd	nd	nd	0.03	0.04	nd	nd
K_2O	0.00	0.00	0.01	ND	ND	ND	ND	0.01	0.00	ND	ND
Total	98.14	99.19	98.14	100.62	99.59	99.79	100.99	98.93	98.74	99.31	99.58
Wo	2.2	2.3	2.1	2.1	2.2	2.2	2.3	2.2	2.1	2.0	2.1
En	82.9	83.1	82.8	82.0	81.8	81.6	82.2	85.2	84.8	84.3	84.5
Fs	14.9	14.6	15.0	15.9	16.0	16.1	15.4	12.6	13.1	13.7	13.3

TABLE B.13 Orthopyroxene Analyses - Metagabbros

Intrusion	UNDAL														
Sample	77.94									77.91			77.148(inclusion)		
PYROXENE	18	19	20	39E	40E	41E	42E	43E	44E	30	31	32	36	37	38
SiO_2	53.38	53.25	53.15	54.17	54.09	54.56	54.62	53.90	54.08	51.16	52.01	51.40	52.73	50.88	51.89
TiO_2	0.53	0.50	0.53	0.51	0.57	0.43	0.43	0.48	0.47	0.47	0.23	0.40	0.15	0.33	0.10
Al_2O_3	0.61	0.55	1.06	1.81	1.66	1.73	0.87	1.72	1.47	1.60	1.40	1.48	2.30	4.81	3.26
Cr_2O_3	0.06	0.07	0.12	0.23	0.16	0.23	nd	0.17	0.12	0.09	0.13	0.13	0.21	0.07	0.12
FeO	17.50	17.62	14.94	15.32	15.70	14.42	16.98	14.02	15.29	16.74	13.13	16.23	10.83	12.98	11.78
MgO	25.06	24.93	26.48	26.35	25.74	27.13	25.87	27.05	26.53	26.03	26.88	26.77	30.89	28.22	29.76
CaO	1.81	1.73	2.01	2.14	2.26	2.25	1.57	2.40	2.27	1.77	4.03	1.57	1.35	1.22	1.11
MnO	0.41	0.42	0.34	0.22	0.36	0.25	0.44	0.32	0.30	0.36	0.26	0.31	0.23	0.26	0.25
NiO	0.06	0.05	0.07	nd	nd	nd	nd	nd	nd	0.06	0.09	0.05	0.03	0.05	0.03
CoO	0.03	0.05	0.03	ND	ND	ND	ND	ND	ND	0.05	0.03	0.05	0.02	0.02	0.00
Na_2O	0.07	0.07	0.07	nd	nd	nd	nd	nd	nd	0.05	0.12	0.05	0.03	0.04	0.04
K_2O	0.00	0.00	0.00	ND	ND	ND	ND	ND	ND	0.00	0.00	0.00	0.00	0.00	0.00
Total	99.55	99.24	98.81	100.76	100.54	100.99	100.78	100.06	100.53	98.39	98.31	98.44	98.80	98.89	98.34
Wo	3.6	3.4	4.0	4.2	4.4	4.4	3.1	4.7	4.4	3.5	7.8	3.0	2.5	2.4	2.1
En	66.8	68.7	72.6	71.9	70.8	73.3	70.3	73.4	71.8	70.6	72.1	72.0	81.1	77.3	79.8
Fs	27.6	27.9	23.5	23.8	24.8	22.3	26.6	21.9	23.7	26.0	20.2	25.0	16.3	20.3	18.1

Intrusion	SKJAEKERDALEN													
Sample	77.299											78.67		
PYROXENE	21	22	23	45E	46E	47E	48E	49E	50E	81E	82E	33	34	35
SiO_2	53.99	54.08	53.96	53.07	55.34	54.54	54.31	54.33	54.01	54.07	54.11	52.42	53.32	52.68
TiO_2	0.19	0.22	0.41	0.29	nd	0.17	0.27	0.27	0.57	0.46	0.30	0.76	0.40	0.42
Al_2O_3	1.27	1.88	1.52	1.76	2.07	2.04	2.59	2.25	2.05	2.00	2.14	1.78	2.36	2.29
Cr_2O_3	0.17	0.24	0.21	0.25	nd	0.18	0.21	0.26	0.22	0.30	0.29	0.25	0.32	0.26
FeO	13.62	13.53	13.43	15.01	14.22	13.63	13.77	14.33	12.75	13.50	13.91	13.32	12.84	12.72
MgO	28.38	27.72	28.24	27.08	28.47	28.47	28.34	28.30	26.54	28.31	28.19	27.89	28.66	28.84
CaO	0.77	1.71	1.52	1.27	1.03	1.19	1.52	0.91	3.76	1.28	1.43	2.25	1.59	1.58
MnO	0.27	0.30	0.30	0.35	0.46	0.42	0.26	0.29	0.27	0.31	0.29	0.29	0.25	0.27
NiO	0.04	0.07	0.05	nd	nd	nd	nd	nd	nd	nd	nd	0.05	0.01	0.01
CoO	0.01	0.04	0.04	ND	ND	ND	ND	ND	ND	ND	ND	0.03	0.04	0.02
Na_2O	0.01	0.05	0.02	nd	nd	nd	nd	nd	nd	nd	nd	0.03	0.04	0.03
K_2O	0.00	0.02	0.00	ND	ND	ND	ND	ND	ND	ND	ND	0.00	0.00	0.00
Total	98.73	99.86	99.71	99.10	101.60	100.64	101.28	100.94	100.20	100.24	100.66	99.07	99.83	99.14
Wo	1.5	3.4	3.0	2.5	2.0	2.3	2.9	1.8	7.4	2.5	2.8	4.4	3.1	3.0
En	77.3	75.5	76.2	73.9	75.9	76.5	75.9	76.1	72.6	76.5	75.8	75.1	77.1	77.4
Fs	21.2	21.2	20.8	23.6	22.0	21.2	21.1	22.1	20.0	21.0	21.4	20.5	19.8	19.6

TABLE B.13 (continued) Orthopyroxene Analyses - Metagabbros

Intrusion												
Sample	77.307			78.71		78.76	78.72			77.326		
PYROXENE	64E	65E	66E	67E	69E	72E	74E	75E8	76E	77E	78E	79E
SiO_2	51.80	53.37	53.25	53.81	53.29	55.11	53.51	52.97	53.24	54.59	54.54	54.48
TiO_2	0.50	0.37	0.25	0.23	0.18	nd	0.30	0.84	0.16	0.49	0.37	0.20
Al_2O_3	2.14	2.58	2.55	1.41	2.45	0.73	2.40	2.20	2.37	1.88	2.47	1.92
Cr_2O_3	0.12	0.40	0.28	nd	nd	nd	nd	nd	nd	0.12	0.19	nd
FeO	18.95	18.35	16.74	21.39	18.75	18.08	15.98	18.01	16.06	14.33	15.04	14.38
MgO	23.38	24.51	24.43	23.14	23.19	27.30	26.11	24.34	25.78	27.18	27.20	28.09
CaO	1.74	1.65	2.06	1.35	2.54	0.15	1.21	1.76	1.35	2.17	1.76	1.26
MnO	0.55	0.44	0.30	0.42	0.33	0.32	0.30	0.28	0.37	0.25	0.31	0.32
NiO	nd	nd	nd	nd	nd	nd	nd	nd	nd	nd	nd	nd
CoO	ND	ND	ND	ND	ND	ND	ND	ND	ND	ND	ND	ND
Na_2O	nd	nd	nd	nd	nd	nd	nd	nd	nd	nd	nd	nd
K_2O	ND	ND	ND	ND	ND	ND	ND	ND	ND	ND	ND	ND
Total	99.17	101.67	99.86	101.76	100.74	101.70	99.82	100.40	99.33	101.02	101.88	100.65
Wo	3.5	3.3	4.2	2.7	5.1	0.3	2.5	3.5	2.7	4.2	3.4	2.5
En	65.7	67.6	68.8	63.6	64.9	72.3	72.2	67.8	71.6	73.6	73.3	75.3
Fs	30.8	29.1	27.0	33.7	30.0	27.4	25.3	38.6	25.6	22.2	23.2	22.2

Intrusion			
Sample	77.291b	77.291a	
PYROXENE	80E	83E	84E
SiO_2	55.04	54.41	53.99
TiO_2	0.54	0.63	0.50
Al_2O_3	2.38	1.44	1.51
Cr_2O_3	nd	0.21	0.30
FeO	11.44	14.85	14.87
MgO	29.52	27.05	26.96
CaO	1.55	2.25	2.19
MnO	0.37	0.31	0.30
NiO	nd	nd	nd
CoO	ND	ND	ND
Na_2O	nd	nd	nd
K_2O	ND	ND	ND
Total	100.85	101.16	100.63
Wo	3.0	4.3	4.3
En	79.1	72.8	72.7
Fs	17.8	22.9	23.0

TABLE B.14 Clinopyroxene Analyses - Ultramafics

Intrusion	KLETTEN														
Sample	76.336e									77.64					
PYROXENE	15	16	17	4E	10E	12E	14E	19E	23E	9	10	11	39E	40E	41E
SiO_2	53.34	53.38	53.18	52.24	52.50	53.70	52.77	54.36	53.16	52.62	52.98	51.78	53.00	53.28	53.73
TiO_2	0.26	0.26	0.26	0.30	0.25	0.21	0.15	nd	0.19	0.28	0.36	0.28	0.38	0.34	0.18
Al_2O_3	1.98	1.80	1.67	2.09	2.22	1.56	1.57	1.50	1.96	2.15	2.37	2.02	1.90	2.18	1.03
Cr_2O_3	0.65	0.57	0.30	0.82	0.64	0.49	0.37	0.52	0.87	0.84	0.62	0.46	0.73	0.46	0.34
FeO	4.28	4.29	4.52	4.27	4.25	4.10	3.99	3.63	4.19	4.53	4.70	4.56	4.57	4.54	4.41
MgO	17.37	17.61	16.78	16.84	17.27	17.49	16.78	17.02	16.82	17.20	17.10	17.01	17.25	16.52	17.34
CaO	21.50	21.58	22.46	22.06	21.80	21.66	22.36	23.40	22.34	20.53	20.78	21.56	21.35	23.07	22.82
MnO	0.17	0.16	0.16	0.17	0.15	nd	0.16	nd	0.18	0.17	0.16	0.17	0.20	0.19	0.19
NiO	0.01	0.00	0.00	nd	nd	nd	nd	nd	nd	0.02	0.00	0.01	nd	nd	nd
CoO	0.03	0.01	0.03	ND	ND	ND	ND	ND	ND	0.02	0.05	0.03	ND	ND	ND
Na_2O	0.32	0.29	0.27	nd	nd	nd	nd	nd	nd	0.32	0.33	0.37	nd	nd	nd
K_2O	0.00	0.00	0.00	ND	ND	ND	ND	ND	ND	0.00	0.00	0.00	ND	ND	ND
Total	99.91	99.96	99.64	98.80	99.08	99.20	98.16	100.43	99.70	98.69	99.46	98.25	99.39	100.58	100.05
Wo	43.8	43.5	45.4	45.0	44.2	44.0	45.7	46.9	45.4	42.7	43.0	44.2	43.5	46.3	45.2
En	49.2	49.4	47.2	47.8	48.7	49.4	47.7	47.4	47.6	49.7	49.2	48.4	48.9	46.2	47.7
Fs	7.1	7.0	7.4	7.1	7.0	6.5	6.7	5.7	7.0	7.6	7.8	7.5	7.6	7.5	7.1

Intrusion										
Sample			77.66					77.68		
PYROXENE	42E	43E	12	13	14	45E	46E	47E	48E	49E
SiO_2	53.73	52.75	52.67	53.38	53.16	52.45	52.20	54.60	52.83	52.18
TiO_2	0.18	0.17	0.33	0.32	0.35	0.32	0.32	nd	0.27	0.35
Al_2O_3	1.28	1.95	2.42	2.01	2.30	1.90	2.15	nd	1.79	2.64
Cr_2O_3	0.74	1.06	0.92	0.47	0.61	0.95	0.98	0.14	0.81	0.58
FeO	3.83	4.83	3.90	4.21	4.29	3.99	4.28	2.53	4.42	4.70
MgO	16.32	17.53	16.57	17.53	17.42	17.20	17.29	17.18	16.76	16.83
CaO	23.51	21.24	21.87	21.76	21.47	21.64	21.43	25.60	22.06	22.01
MnO	0.17	0.22	0.17	0.27	0.18	0.14	0.15	0.17	0.21	nd
NiO	nd	nd	0.01	0.03	0.00	nd	nd	nd	nd	nd
CoO	ND	ND	0.01	0.02	0.02	ND	ND	ND	ND	ND
Na_2O	nd	nd	0.43	0.32	0.38	nd	nd	nd	nd	nd
K_2O	ND	ND	0.00	0.00	0.00	ND	ND	ND	ND	ND
Total	99.75	99.74	99.31	100.22	100.18	98.59	98.81	100.22	99.15	99.29
Wo	47.6	42.8	45.5	43.9	44.0	44.3	43.8	49.6	45.0	44.8
En	46.0	49.2	47.9	49.2	48.5	49.0	49.1	46.3	47.6	47.7
Fs	6.4	8.00	6.6	6.9	7.5	6.7	7.1	4.1	7.4	7.5

TABLE B.15 Clinopyroxene Analyses - Metagabbros

Intrusion	UNDAL												
Sample	77.94									77.91		77.148(inclusion)	
PYROXENE	24	25	26	28E	29E	30E	31E	32E	33E	40	41	45	46
SiO_2	52.16	52.54	51.06	52.11	50.71	51.92	52.11	52.15	52.69	51.84	52.52	50.71	51.65
TiO_2	0.55	0.34	1.17	0.68	1.33	0.80	0.72	1.19	0.91	0.60	0.49	0.37	0.21
Al_2O_3	1.02	0.75	2.00	2.31	4.29	2.26	1.88	2.23	2.58	2.54	2.10	2.45	1.94
Cr_2O_3	0.11	0.17	0.37	0.84	0.69	0.46	0.27	0.27	0.36	0.23	0.45	0.71	0.86
FeO	8.96	8.18	8.41	6.55	7.09	8.87	9.04	8.56	7.75	7.41	6.38	5.07	4.16
MgO	15.07	14.85	15.63	17.38	14.99	15.32	15.06	15.73	16.99	15.14	16.86	17.27	16.95
CaO	19.64	20.75	18.47	19.12	19.91	19.45	19.86	19.26	17.96	20.79	19.65	20.99	21.61
MnO	0.24	0.21	0.24	0.12	nd	0.31	0.23	0.20	0.29	0.21	0.20	0.15	0.18
NiO	0.04	0.06	0.06	nd	nd	nd	nd	nd	nd	0.05	0.04	0.00	0.04
CoO	0.01	0.03	0.00	ND	ND	ND	ND	ND	ND	0.03	0.01	0.02	0.00
Na_2O	0.66	0.49	0.68	nd	0.96	0.49	nd	nd	nd	0.64	0.52	0.36	0.42
K_2O	0.00	0.00	0.00	ND	ND	ND	ND	ND	ND	0.00	0.00	0.00	0.00
Total	99.45	98.36	98.09	99.11	99.97	99.89	99.17	99.59	99.54	99.46	99.24	98.09	98.03
Wo	41.1	43.3	39.3	39.4	43.0	40.6	41.4	40.1	37.5	43.5	40.7	42.8	44.5
En	43.9	43.1	46.3	49.8	45.0	44.4	43.6	45.6	49.3	44.1	48.6	48.9	48.5
Fs	15.0	13.7	14.4	10.8	12.0	15.0	15.0	14.3	13.1	12.4	10.6	8.3	7.0

Intrusion			SKJAEKERDALEN									
Sample	77.96		77.299									
PYROXENE	68E	70E	27	28	29	34E	335E	36E	37E	38E	77E	78E
SiO_2	52.87	51.20	51.36	51.23	52.36	52.04	51.92	57.52	52.23	52.80	52.63	52.09
TiO_2	0.72	0.89	0.74	0.60	0.35	0.56	0.54	0.45	0.62	0.44	0.49	0.66
Al_2O_3	1.80	2.89	2.89	2.33	1.31	2.66	2.95	2.47	2.53	1.49	2.29	2.82
Cr_2O_3	0.43	1.35	0.42	0.46	0.46	0.40	0.51	0.45	0.46	0.47	0.36	0.51
FeO	9.06	6.64	4.78	6.13	5.30	5.86	5.75	3.33	3.84	5.32	5.73	5.12
MgO	17.15	16.37	15.11	15.98	15.42	15.92	15.73	15.48	16.39	15.57	15.72	15.20
CaO	17.04	19.68	22.50	20.99	22.24	21.49	22.05	22.26	23.83	23.10	21.54	22.65
MnO	0.16	0.13	0.15	0.15	0.17	0.13	nd	nd	0.16	0.12	0.18	0.13
NiO	0.21	nd	0.07	0.05	0.06	nd	nd	nd	0.15	nd	0.14	nd
CoO	ND	ND	0.00	0.01	0.01	ND	ND	ND	ND	ND	ND	ND
Na_2O	nd	0.52	0.39	0.42	0.32	nd	nd	nd	nd	nd	nd	nd
K_2O	ND	ND	0.01	0.00	0.00	ND	ND	ND	ND	ND	ND	ND
Total	99.45	99.68	97.92	98.37	97.94	99.18	99.41	101.97	100.22	99.32	99.07	99.19
Wo	35.4	41.2	47.5	43.6	46.5	44.4	45.5	48.0	47.9	47.1	44.8	47.3
En	49.6	47.7	44.4	46.2	44.7	45.8	45.2	46.4	45.8	44.2	45.5	44.1
Fs	15.0	11.1	8.1	10.2	8.9	9.7	9.3	5.6	6.3	8.7	9.7	8.6

TABLE B.15 (continued) Clinopyroxene Analyses - Metagabbros

Intrusion															
Sample	78.67			77.300b			78.71				78.68			78.72	
PYROXENE	42	43	44	50E	52E	54E	56E	57E	58E	59E	60E	62E	64E	65E	66E
SiO_2	50.10	50.14	49.47	51.22	52.76	53.23	52.08	53.94	53.16	52.29	51.66	52.19	51.62	51.51	51.86
TiO_2	1.04	1.00	0.70	0.72	0.51	0.41	0.41	nd	0.38	0.46	0.63	0.45	0.42	0.65	0.49
Al_2O_3	3.60	3.56	3.63	3.25	2.59	1.86	3.56	0.51	1.42	1.77	2.84	2.55	2.66	3.44	2.12
Cr_2O_3	0.68	0.53	0.67	1.02	0.83	0.49	0.94	nd	0.24	0.35	0.78	0.88	0.80	0.32	nd
FeO	6.24	5.46	6.79	6.34	5.00	5.63	6.59	8.13	8.35	7.52	5.89	5.48	6.72	4.72	6.64
MgO	16.00	15.37	16.78	16.30	15.17	16.08	15.54	14.46	14.70	14.44	16.23	15.59	17.03	15.19	14.72
CaO	20.49	21.69	19.60	20.78	22.35	21.77	20.31	22.68	22.10	22.13	20.27	21.97	18.93	22.60	22.00
MnO	0.18	0.19	0.18	0.21	0.21	0.23	0.13	0.31	0.24	0.24	0.15	0.25	nd	0.20	0.19
NiO	0.03	0.03	0.04	nd	nd	nd	nd	nd	nd	nd	nd	nd	nd	nd	nd
CoO	0.00	0.01	0.02	ND	ND	ND	ND	ND	ND	ND	ND	ND	ND	ND	ND
Na_2O	0.44	0.53	0.44	nd	nd	nd	nd	nd	nd	nd	nd	nd	nd	nd	nd
K_2O	0.00	0.00	0.00	ND	ND	ND	ND	ND	ND	ND	ND	ND	ND	ND	ND
Total	98.81	98.52	98.33	99.84	99.43	99.70	99.58	100.05	100.59	99.19	98.45	99.36	98.18	98.63	98.02
Wo	42.9	45.7	40.5	42.8	47.0	44.7	43.0	45.9	44.9	45.8	42.6	45.7	39.5	47.5	46.0
En	46.6	45.0	48.2	46.7	44.4	45.9	45.8	40.7	41.5	41.6	47.5	45.0	49.5	44.4	42.8
Fs	10.5	9.3	11.3	10.6	8.6	9.4	11.2	13.4	13.6	12.6	9.9	9.3	11.0	8.1	11.2

Intrusion								
Sample	77.326			77.291b			77.291a	
PYROXENE	71E	72E	73E	74E	75E	76E	79E	80E
SiO_2	51.57	51.51	51.68	51.86	52.20	51.86	52.20	52.03
TiO_2	0.70	0.78	0.71	0.51	0.43	0.66	0.68	0.93
Al_2O_3	3.63	3.94	3.55	4.50	4.01	3.79	2.51	2.02
Cr_2O_3	0.18	0.20	0.26	0.70	0.40	0.26	0.69	0.20
FeO	7.20	6.93	7.91	5.23	7.23	5.88	8.40	9.56
MgO	15.77	15.60	16.72	16.62	16.91	16.62	15.57	15.54
CaO	20.12	20.30	19.18	20.61	16.99	19.44	18.91	19.25
MnO	0.26	0.12	0.21	0.19	0.22	nd	0.20	0.24
NiO	0.18	nd	nd	0.19	nd	nd	nd	nd
CoO	ND	ND	ND	ND	ND	ND	ND	ND
Na_2O	nd	nd	nd	nd	nd	nd	nd	nd
K_2O	ND	ND	ND	ND	ND	ND	ND	ND
Total	99.61	99.38	100.24	100.41	100.39	98.52	99.16	99.78
Wo	42.0	42.7	39.3	42.9	34.6	41.2	40.0	39.7
En	45.8	45.6	47.6	48.2	52.5	49.0	45.8	44.5
Fs	12.2	11.6	13.1	8.9	11.9	9.7	14.2	15.8

TABLE B.16 Plagioclase Analyses - Ultramafics (all analyses by E.D.S.)

	KALTBERGET											
Sample	76.254											
PLAGIOCLASE	26C	26R	28C	28R	30C	30R	32C	32R	34C	34R	36C	36R
SiO_2	60.54	61.45	59.51	61.10	60.43	59.89	59.85	61.76	59.91	59.79	59.55	60.70
TiO_2	nd	nd	nd	nd	nd	0.12	nd	nd	nd	nd	nd	nd
Al_2O_3	24.70	23.73	24.90	24.61	25.14	25.22	24.80	23.64	25.87	24.47	25.48	24.98
Cr_2O_3	ND	ND	ND	ND	ND	ND	ND	ND	ND	ND	ND	ND
FeO	nd	nd	nd	nd	nd	0.17	nd	nd	nd	nd	nd	0.11
MgO	nd	nd	nd	nd	nd	nd	nd	nd	nd	nd	nd	nd
CaO	6.26	5.29	6.76	5.95	6.62	6.92	6.41	5.29	7.06	6.20	6.98	6.34
MnO	ND	ND	ND	ND	ND	ND	ND	ND	ND	ND	ND	ND
NiO	ND	ND	ND	ND	ND	ND	ND	ND	ND	ND	ND	ND
CoO	ND	ND	ND	ND	ND	ND	ND	ND	ND	ND	ND	ND
Na_2O	7.93	8.15	7.23	8.13	7.97	7.97	7.49	8.53	7.72	7.79	7.62	7.53
K_2O	nd	nd	nd	nd	nd	nd	0.10	nd	0.07	nd	nd	nd
Total	99.43	98.62	98.40	99.79	100.15	100.28	98.65	99.22	100.63	98.24	99.63	99.67
An	30.4	26.4	34.1	28.8	31.5	32.4	31.9	25.5	33.5	30.6	33.6	32.1
Ab	69.6	73.6	65.9	71.2	68.5	67.6	67.5	74.5	66.1	69.4	66.4	67.9
O_r							0.6		0.4			

	KLETTEN														
Sample	76.336h														
PLAGIOCLASE	42	43	44	45	46C	46R	48R	50C	50R	52C	52R	54C	54R	56C	56R
SiO_2	63.57	64.20	64.93	63.74	62.70	63.52	63.43	64.86	63.89	63.31	64.19	64.19	64.70	63.72	63.22
TiO_2	nd	nd	nd	nd	0.13	nd	nd	nd	nd	nd	nd	nd	nd	nd	nd
Al_2O_3	22.79	22.28	22.36	22.43	22.12	22.89	22.26	22.28	22.27	22.51	22.42	22.74	22.00	22.23	22.51
Cr_2O_3	ND	ND	ND	ND	ND	ND	ND	ND	ND	ND	ND	ND	ND	ND	ND
FeO	nd	nd	0.14	nd	nd	nd	0.16	0.13	nd	nd	nd	nd	nd	nd	0.23
MgO	nd	nd	nd	nd	nd	nd	nd	nd	nd	nd	nd	nd	nd	nd	nd
CaO	3.85	3.34	3.37	3.75	3.99	4.04	3.52	3.30	3.51	3.21	3.57	3.60	3.24	3.42	3.53
MnO	ND	ND	ND	ND	ND	ND	ND	ND	ND	ND	ND	ND	ND	ND	ND
NiO	ND	ND	ND	ND	ND	ND	ND	ND	ND	ND	ND	ND	ND	ND	ND
CoO	ND	ND	ND	ND	ND	ND	ND	ND	ND	ND	ND	ND	ND	ND	ND
Na_2O	9.03	9.06	9.64	9.06	8.39	9.26	9.34	9.57	9.30	9.37	9.08	8.82	9.35	9.13	8.97
K_2O	nd	nd	nd	nd	1.24	nd	nd	nd	nd	0.15	nd	nd	0.08	nd	0.07
Total	99.24	98.88	100.44	98.99	98.57	99.71	98.71	100.15	98.98	98.54	99.27	99.34	99.37	98.49	98.55
An	19.1	16.9	16.2	18.6	19.3	19.4	17.2	16.5	17.3	15.8	17.9	18.4	16.0	17.1	18.6
Ab	80.9	83.1	83.8	81.3	73.5	80.6	82.7	83.5	82.7	83.3	82.1	81.6	83.5	82.8	81.0
O_r					7.2					0.9			0.5		0.5

TABLE B.17 Plagioclase Analyses - Metagabbros (all analyses by E.D.S.)

	SKJAERKERDALEN													
Sample	77.299													
PLAGIOCLASE	78C	78R	80C	80R	82C	82R	84C	84R	86	87	119C	119R	120C	120R
SiO_2	46.91	47.34	48.01	48.39	48.40	47.77	48.29	47.75	47.28	47.26	48.05	46.12	48.11	48.09
TiO_2	nd	nd	nd	nd	nd	0.12	nd	nd	nd	nd	nd	nd	nd	nd
Al_2O_3	33.41	32.59	32.90	32.50	32.51	33.12	32.34	33.12	32.70	33.31	32.77	34.06	33.59	33.40
Cr_2O_3	ND	ND	ND	ND	ND	ND	ND	ND	ND	ND	ND	ND	ND	ND
FeO	nd	0.16	nd	0.19	0.12	nd	nd	0.23	nd	nd	0.11	nd	nd	0.10
MgO	nd	nd	nd	nd	nd	nd	nd	nd	nd	nd	nd	nd	nd	nd
CaO	17.13	16.42	16.34	15.83	16.40	16.22	15.97	16.28	16.47	16.38	15.98	18.09	16.93	16.54
MnO	ND	ND	ND	ND	ND	ND	ND	ND	ND	ND	ND	ND	ND	ND
NiO	ND	ND	ND	ND	ND	ND	ND	ND	ND	ND	ND	ND	ND	ND
CoO	ND	ND	ND	ND	ND	ND	ND	ND	ND	ND	ND	ND	ND	ND
Na_2O	1.69	1.83	2.15	2.43	2.43	2.22	1.91	2.10	1.79	1.94	2.36	1.15	1.25	2.16
K_2O	nd	nd	nd	nd	nd	nd	nd.	nd	nd	nd	nd	nd	nd	nd
Total	99.15	98.34	99.39	99.36	99.85	99.45	98.51	99.47	98.25	98.89	99.27	99.43	99.88	100.29
An	84.9	83.3	80.8	78.4	79.0	80.2	82.2	81.1	83.5	82.4	78.9	89.6	88.2	80.9
Ab	15.1	16.7	19.2	21.6	21.0	19.8	17.8	18.9	16.5	17.6	21.1	10.3	11.8	19.1
O_r														

Sample	77.300b								77.307						
PLAGIOCLASE	68C	68R	71	72	73C	73R	75C	75R	88C	88R	89C	89R	90	91C	91R
SiO_2	51.71	47.91	48.23	51.20	49.12	51.96	52.12	51.13	50.34	52.55	48.89	54.86	52.12	49.44	53.34
TiO_2	nd	0.15	nd	nd	nd	0.12	nd	0.17	nd	nd	nd	nd	nd	nd	nd
Al_2O_3	30.45	32.83	32.27	30.63	31.76	29.84	30.00	30.19	30.99	29.48	32.54	27.70	30.00	31.48	28.81
Cr_2O_3	ND	ND	ND	ND	ND	ND	ND	ND	ND	ND	ND	ND	ND	ND	ND
FeO	nd	0.11	0.19	nd	nd	nd	nd	0.17	nd	0.22	nd	nd	0.43	nd	0.21
MgO	nd	nd	nd	nd	nd	nd	nd	nd	nd	nd	nd	nd	nd	nd	nd
CaO	13.50	16.22	15.80	13.92	15.26	12.94	12.65	13.47	14.24	12.14	15.49	10.43	13.01	14.52	11.60
MnO	ND	ND	ND	ND	ND	ND	ND	ND	ND	ND	ND	ND	ND	ND	ND
NiO	ND	ND	ND	ND	ND	ND	ND	ND	ND	ND	ND	ND	ND	ND	ND
CoO	ND	ND	ND	ND	ND	ND	ND	ND	ND	ND	ND	ND	ND	ND	ND
Na_2O	3.62	1.51	2.68	3.34	2.08	4.05	4.10	4.05	3.88	3.91	2.57	5.44	4.16	2.97	5.19
K_2O	nd	nd	nd	nd	nd	nd	nd	nd	nd	nd	nd	nd	nd	nd	nd
Total	99.28	98.73	99.17	99.09	98.23	98.92	98.87	99.18	99.44	98.30	99.50	98.44	99.72	98.41	99.15
An	67.3	85.6	76.5	69.7	80.2	63.8	63.0	64.8	67.0	63.5	76.9	51.4	63.9	73.0	55.6
Ab	32.7	14.4	23.5	30.3	19.8	36.2	37.0	35.2	33.0	36.5	23.1	48.6	36.0	27.0	44.4
O_r															

TABLE B.17 (continued) Plagioclase Analyses - Metagabbros (all analyses by E.D.S.)

Sample	78.76						78.72					
PLAGIOCLASE	93C	93R	94C	94R	95C	95R	96C	96R	98C	98R	100C	100R
SiO_2	53.21	54.15	53.29	54.60	52.36	52.29	52.88	53.01	51.34	53.41	50.34	45.72
TiO_2	0.27	nd	nnd	nd	nd	nd	nd	nd	nd	nd	nd	nd
Al_2O_3	30.23	29.51	30.14	29.00	30.61	31.30	29.36	29.37	29.93	26.58	30.88	33.82
Cr_2O_3	ND	ND	ND	ND	ND	ND	ND	ND	ND	ND	ND	ND
FeO	nd	0.16	0.11	0.20	0.14	nd	nd	nd	nd	nd	nd	nd
MgO	nd	nd	nd	nd	nd	nd	nd	nd	nd	nd	nd	nd
CaO	12.52	12.03	12.42	11.00	13.26	13.05	12.11	11.89	12.82	11.12	13.49	17.44
MnO	ND	ND	ND	ND	ND	ND	ND	ND	ND	ND	ND	ND
NiO	ND	ND	ND	ND	ND	ND	ND	ND	ND	ND	ND	ND
CoO	ND	ND	ND	ND	ND	ND	ND	ND	ND	ND	ND	ND
Na_2O	5.04	5.07	4.55	5.27	4.33	3.98	4.58	4.58	4.24	4.88	3.65	1.50
K_2O	nd	nd	nd	nd	nd	nd	nd	nd	nd	nd	nd	nd
Total	101.27	100.92	100.51	100.07	100.70	100.62	98.92	98.85	98.33	97.99	98.36	98.47
An	57.8	57.0	60.3	53.9	63.1	64.4	59.4	58.9	62.5	55.7	67.1	86.5
Ab	42.2	43.0	39.7	46.0	36.9	35.6	40.6	41.1	37.4	44.3	32.9	13.5
O_r												

Sample	77.326						77.291b					
PLAGIOCLASE	107C	107R	109C	109R	111C	111R	113C	113R	115C	115R	117C	117R
SiO_2	51.12	52.85	52.98	53.32	56.48	57.22	50.64	50.11	48.12	52.00	52.77	51.06
TiO_2	nd	nd	nd	nd	nd	0.13	nd	nd	nd	nd	nd	nd
Al_2O_3	31.36	29.24	29.82	29.66	27.04	26.71	31.42	31.54	32.44	30.15	29.22	30.92
Cr_2O_3	ND	ND	ND	ND	ND	ND	ND	ND	ND	ND	ND	ND
FeO	nd	0.79	nd	nd	nd	nd	0.10	nd	nd	nd	nd	0.12
MgO	nd	0.38	nd	nd	nd	nd	nd	nd	nd	nd	nd	nd
CaO	14.20	11.87	12.74	12.15	9.23	8.75	13.90	14.62	15.73	12.92	12.13	13.82
MnO	ND	ND	ND	ND	ND	ND	ND	ND	ND	ND	ND	ND
NiO	ND	ND	ND	ND	ND	ND	ND	ND	ND	ND	ND	ND
CoO	ND	ND	ND	ND	ND	ND	ND	ND	ND	ND	ND	ND
Na_2O	3.28	4.19	4.18	4.64	6.50	6.38	3.53	3.53	2.23	4.21	4.50	3.20
K_2O	nd	nd	0.15	0.07	nd	nd	nd	nd	nd	nd	nd	nd
Total	99.98	99.32	99.87	99.83	99.26	99.19	99.61	99.81	98.53	99.28	98.63	99.12
An	70.5	61.0	62.2	58.9	44.0	43.1	68.5	69.6	79.6	62.9	59.8	70.5
Ab	29.5	39.0	36.9	40.7	56.0	56.9	31.5	30.4	20.4	37.1	40.2	29.5
O_r			0.9	0.4								

TABLE B.17 (continued) Plagioclase Analyses - Metagabbros (all analyses by E.D.S.)

					UNDAL								
Sample	77.291a				77.94							77.96	
PLAGIOCLASE	121C	121R	122C	122R	58C	58R	60C	60R	62C	62R	64	102	103C
SiO_2	53.13	53.14	53.12	55.30	52.46	53.87	53.55	55.28	53.25	55.41	53.25	54.37	53.10
TiO_2	nd	nd	nd	0.11	nd	nd	nd	nd	nd	nd	0.17	nd	0.11
Al_2O_3	29.01	29.36	28.90	28.22	29.40	28.37	29.28	28.20	29.46	27.81	29.29	29.01	29.64
Cr_2O_3	ND	ND	ND	ND	ND	ND	ND	ND	ND	ND	ND	ND	ND
FeO	0.21	0.20	0.29	0.14	0.12	0.21	0.18	0.12	0.16	0.17	nd	0.11	0.21
MgO	nd	nd	nd	nd	nd	nd	nd	nd	nd	nd	nd	nd	nd
CaO	12.12	11.86	11.52	10.53	12.15	10.83	11.75	10.53	12.06	10.37	11.97	11.53	11.99
MnO	ND	ND	ND	ND	ND	ND	ND	ND	ND	ND	ND	ND	ND
NiO	ND	ND	ND	ND	ND	ND	ND	ND	ND	ND	ND	ND	ND
CoO	ND	ND	ND	ND	ND	ND	ND	ND	ND	ND	ND	ND	ND
Na_2O	4.11	4.40	4.31	5.30	4.53	5.39	4.32	5.28	4.86	5.82	4.76	4.80	4.76
K_2O	0.15	0.10	0.63	0.42	0.12	0.27	0.21	0.26	0.24	nd	0.15	nd	nd
Total	98.73	99.07	98.77	100.03	98.79	98.95	99.29	99.68	100.04	99.59	99.60	99.83	99.80
An	61.4	59.4	57.4	51.0	59.4	52.2	59.6	51.9	57.3	50.0	57.6	57.0	58.2
Ab	37.6	40.0	38.8	46.5	39.8	46.3	39.1	46.6	41.3	50.0	41.5	43.0	41.8
O_r	0.9	0.6	3.8	2.4	0.7	1.5	1.2	1.5	1.4		0.9		

				OLKAR								
Sample				76.94								
PLAGIOCLASE	103R	105C	105R	17C	17R	19C	19R	21C	21R	23C	23R	13C	13R
SiO_2	54.59	53.14	55.46	58.20	59.40	58.54	60.04	58.54	59.75	57.53	58.17	58.41	60.65
TiO_2	nd	nd	0.10	nd	nd	nd	nd	nd	nd	nd	nd	nd	nd
Al_2O_3	28.62	29.92	28.30	25.53	25.18	25.09	24.70	25.95	24.55	26.38	25.26	26.17	23.89
Cr_2O_3	ND	ND	ND	ND	ND	ND	ND	ND	ND	ND	ND	ND	ND
FeO	nd	nd	0.16	nd	nd	nd	nd	nd	nd	nd	nd	nd	nd
MgO	nd	nd	nd	nd	nd	nd	nd	nd	nd	nd	nd	nd	nd
CaO	11.06	12.23	10.51	7.69	7.11	7.36	6.70	8.17	6.56	8.56	7.77	8.14	5.52
MnO	ND	ND	ND	ND	ND	ND	ND	ND	ND	ND	ND	ND	ND
NiO	ND	ND	ND	ND	ND	ND	ND	ND	ND	ND	ND	ND	ND
CoO	ND	ND	ND	ND	ND	ND	ND	ND	ND	ND	ND	ND	ND
Na_2O	4.83	5.00	5.22	7.03	7.27	6.92	7.64	6.19	7.78	6.53	7.20	7.13	8.18
K_2O	nd	0.06	nd	0.08	nd	0.17	0.08	nd	0.15	0.10	0.10	0.08	nd
Total	99.10	100.36	99.75	98.55	98.96	98.09	99.16	98.85	98.80	99.12	98.51	99.93	98.24
An	55.9	57.2	52.7	37.5	35.1	36.7	32.5	42.2	31.5	41.8	37.2	38.5	27.2
Ab	44.1	42.4	47.3	62.0	64.9	62.3	67.0	57.8	67.6	57.6	62.3	61.0	72.8
O_r		0.4		0.5		1.0	0.5		0.9	0.6	0.6	0.5	

TABLE B.18 Pyrrhotite Analyses - Magmatic Sulfides

Prospect	VAKKERLIEN									OLKAR		
Sample	75/27/620			75/27/10.40			75/27/6.60			77/2/14.90		
PYRRHOTITE	95	96	97	98	99	100	101	102	103	53	54	55
Fe	60.13	59.62	59.34	60.72	60.77	59.76	60.54	60.41	60.43	59.65	59.51	60.25
Ni	0.22	0.29	0.65	0.62	0.27	0.95	0.32	0.79	0.41	0.54	0.51	0.51
Co	0.12	0.10	0.14	0.12	0.12	0.11	0.10	0.12	0.09	0.11	0.11	0.12
Cu	0.07	0.04	0.02	0.06	0.01	0.02	0.04	0.06	0.02	0.05	0.09	0.05
Pb	0.16	0.14	0.12	0.13	0.13	0.11	0.21	0.18	0.14	0.17	0.18	0.17
Zn	0.00	0.00	0.00	0.00	0.04	0.05	0.00	0.07	0.01	0.00	0.00	0.00
As	0.00	0.07	0.06	0.09	0.17	0.07	0.17	0.11	0.06	0.00	0.04	0.00
S	37.95	38.17	38.30	38.48	38.75	38.98	38.90	38.86	38.92	38.10	38.24	38.53
Total	98.65	98.43	98.64	100.23	100.27	100.05	100.27	100.60	100.08	98.62	98.64	99.63

Prospect												
Sample	77/1/6.60a			77/2/15.00			77/3/8.65			77/4/23.70		
PYRRHOTITE	56	57	58	59	60	61	62	63	64	65	66	67
Fe	59.39	59.68	60.19	59.61	59.42	60.42	60.98	60.88	61.22	60.77	60.65	61.35
Ni	0.62	0.62	0.59	0.34	0.47	0.52	0.39	0.46	0.55	0.46	0.48	0.40
Co	0.11	0.08	0.10	0.11	0.11	0.11	0.16	0.14	0.14	0.12	0.13	0.15
Cu	0.03	0.05	0.06	0.03	0.02	0.04	0.06	0.02	0.02	0.05	0.04	0.03
Pb	0.15	0.20	0.15	0.08	0.12	0.12	0.17	0.17	0.16	0.15	0.17	0.18
Zn	0.00	0.00	0.00	0.00	0.00	0.00	0.00	0.00	0.00	0.02	0.00	0.03
As	0.08	0.03	0.00	0.00	0.00	0.00	0.11	0.24	0.10	0.18	0.12	0.23
S	38.24	38.48	38.38	38.57	38.27	38.25	38.43	38.14	38.08	38.35	38.52	38.31
Total	98.62	99.14	99.47	98.74	98.41	99.47	100.29	100.05	100.26	100.11	100.11	100.68

TABLE B.18 (continued) Pyrrhotite Analyses - Magmatic Sulfides

Prospect												
Sample	77/1/10.60			77/4/31.56			77/5/32.84			77/4/27.56		
PYRRHOTITE	68	69	70	71	72	73	74	75	76	77	78	79
Fe	60.16	60.69	60.21	61.07	61.31	60.71	60.54	60.33	60.95	60.60	60.51	60.58
Ni	0.30	0.48	0.60	0.47	0.47	0.47	0.06	0.11	0.08	0.48	0.54	0.57
Co	0.14	0.12	0.16	0.14	0.14	0.12	0.20	0.25	0.20	0.23	0.20	0.23
Cu	0.02	0.03	0.04	0.08	0.10	0.05	0.04	0.06	0.06	0.07	0.06	0.08
Pb	0.20	0.15	0.13	0.16	0.11	0.14	0.18	0.20	0.13	0.14	0.14	0.15
Zn	0.00	0.02	0.00	0.00	0.00	0.00	0.00	0.00	0.04	0.00	0.00	0.00
As	0.19	0.10	0.26	0.00	0.00	0.00	0.00	0.00	0.00	0.00	0.00	0.00
S	39.20	38.45	38.47	37.62	37.22	37.38	37.97	38.03	37.87	37.85	37.64	37.82
Total	100.20	100.05	99.87	99.54	99.45	98.87	98.99	98.98	99.33	99.37	99.10	99.44

Prospect												
Sample	77/2a/4.85			77/4/33.23c			77/4/20.48			77/2/3.26		
PYRRHOTITE	80	81	82	83	84	85	86	87	88	89	90	91
Fe	60.25	60.50	60.89	60.62	60.43	60.23	60.68	60.68	60.65	59.93	60.08	59.93
Ni	0.35	0.50	0.44	0.43	0.48	0.45	0.16	0.17	0.38	0.31	0.23	0.39
Co	0.14	0.14	0.11	0.12	0.12	0.11	0.19	0.21	0.13	0.13	0.11	0.13
Cu	0.07	0.02	0.01	0.03	0.04	0.08	0.06	0.07	0.05	0.07	0.07	0.03
Pb	0.16	0.09	0.10	0.15	0.13	0.15	0.07	0.11	0.12	0.15	0.18	0.14
Zn	0.00	0.00	0.00	0.00	0.03	0.02	0.02	0.03	0.00	0.02	0.00	0.01
As	0.00	0.05	0.11	0.08	0.11	0.16	0.09	0.15	0.17	0.03	0.00	0.00
S	38.73	38.55	38.86	38.61	38.92	38.86	38.63	38.46	38.42	38.18	37.94	37.66
Total	99.71	99.85	100.52	100.04	100.25	100.07	99.91	99.88	99.91	98.82	98.62	98.30

TABLE B.18 (continued) Pyrrhotite Analyses - Magmatic Sulfides

Prospect	SKJAEKERDALEN										
Sample	77/3/14.60		78.71			78.64			78.76		
PYRRHOTITE	92	93	134	135	136	137	138	139	140	141	142
Fe	60.54	60.35	60.81	61.05	61.18	60.29	60.59	59.95	60.47	60.40	60.01
Ni	0.41	0.33	0.40	0.48	0.46	0.52	0.50	0.55	0.73	0.50	0.66
Co	0.11	0.15	0.13	0.00	0.12	0.15	0.15	0.14	0.16	0.11	0.15
Cu	0.07	0.07	0.05	0.00	0.00	0.04	0.02	0.04	0.05	0.04	0.05
Pb	0.17	0.16	0.14	0.13	0.17	0.15	0.11	0.18	0.12	0.14	0.12
Zn	0.00	0.00	0.00	0.00	0.00	0.00	0.00	0.00	0.00	0.00	0.00
As	0.00	0.01	0.00	0.00	0.00	0.00	0.00	0.00	0.00	0.00	0.00
S	37.55	37.30	38.50	38.53	38.34	38.64	38.41	38.19	38.57	38.51	38.61
Total	98.86	98.38	100.03	100.19	100.27	99.79	99.77	99.05	100.10	99.70	99.61

Prospect												
Sample	78.65			78.68			78.67			78.72		
PYRRHOTITE	143	144	145	146	147	148	149	150	151	152	153	154
Fe	59.89	60.38	60.41	60.26	60.15	60.61	60.89	60.82	60.95	61.07	61.04	61.19
Ni	0.45	0.46	0.53	0.42	0.42	0.45	0.29	0.23	0.25	0.23	0.27	0.26
Co	0.17	0.13	0.16	0.18	0.20	0.17	0.12	0.16	0.14	0.13	0.12	0.11
Cu	0.04	0.04	0.07	0.07	0.05	0.07	0.08	0.06	0.12	0.12	0.07	0.09
Pb	0.10	0.11	0.14	0.15	0.13	0.16	0.10	0.10	0.12	0.16	0.21	0.12
Zn	0.00	0.00	0.00	0.00	0.00	0.00	0.00	0.00	0.00	0.00	0.00	0.00
As	0.06	0.06	0.05	0.04	0.00	0.00	0.06	0.05	0.19	0.07	0.00	0.01
S	38.33	38.26	38.65	38.31	38.33	38.30	37.91	38.28	37.54	37.62	37.89	37.88
Total	99.05	99.43	100.02	99.43	99.27	99.77	99.46	99.70	99.33	99.41	99.60	99.65

TABLE B.18 (continued) Pyrrhotite Analyses - Magmatic Sulfides

Prospect												
Sample	78.77			77.304			77.339					
PYRRHOTITE	155	156	157	158	159	160	171	172	173	174	175	176
Fe	59.70	60.07	59.74	59.95	60.31	60.39	60.48	60.48	60.49	60.52	60.05	60.40
Ni	0.45	0.50	0.56	0.13	0.19	0.23	0.40	0.58	0.40	0.55	0.80	0.38
Co	0.12	0.09	0.09	0.11	0.13	0.12	0.14	0.12	0.10	0.12	0.10	0.12
Cu	0.10	0.07	0.08	0.12	0.14	0.11	0.07	0.09	0.04	0.04	0.04	0.07
Pb	0.18	0.19	0.14	0.12	0.18	0.13	0.06	0.07	0.13	0.12	0.10	0.14
Zn	0.00	0.00	0.00	0.00	0.00	0.00	0.00	0.00	0.00	0.00	0.00	0.00
As	0.02	0.00	0.00	0.00	0.00	0.05	0.11	0.00	0.00	0.00	0.00	0.05
S	38.74	38.77	38.84	38.56	38.96	38.42	38.47	38.17	38.15	38.05	38.11	38.73
Total	99.31	99.69	99.46	99.00	99.90	99.45	99.72	99.51	99.31	99.40	99.20	99.90

Prospect	SKJAEKERDALEN						GARDSJOEN			KALTBERGET		
Sample	77.316			77.330			77.34			76.KD.1		
PYRRHOTITE	197	198	199	200	201	202	104	105	106	107	108	109
Fe	59.52	60.03	59.56	60.08	60.16	60.30	61.07	60.49	61.09	59.89	59.69	59.54
Ni	0.70	0.64	0.67	0.39	0.45	0.43	0.46	0.21	0.42	0.70	0.87	1.11
Co	0.14	0.12	0.14	0.12	0.12	0.14	0.20	0.22	0.18	0.14	0.13	0.14
Cu	0.16	0.13	0.08	0.12	0.12	0.11	0.03	0.03	0.03	0.07	0.03	0.05
Pb	ND	ND	ND	ND	ND	ND	0.20	0.15	0.13	0.13	0.20	0.13
Zn	ND	ND	ND	ND	ND	ND	0.04	0.05	0.01	0.00	0.00	0.02
As	0.00	0.00	0.02	0.00	0.00	0.00	0.08	0.11	0.17	0.00	0.10	0.03
S	38.88	39.07	38.64	38.87	39.10	39.02	38.69	38.71	38.25	38.88	39.05	38.63
Total	99.41	99.99	99.10	99.59	99.95	100.01	100.76	99.97	100.28	99.82	100.08	99.64

TABLE B.16 (continued) Pyrrhotite Analyses - Magmatic Sulfides

Prospect												
Sample	77/12/5.50			77/12/6.10			76.294			76.293		
PYRRHOTITE	110	111	112	113	114	115	116	117	118	119	120	121
Fe	61.02	60.84	60.78	60.95	61.05	60.85	60.06	60.83	60.48	61.50	61.14	61.46
Ni	0.52	0.53	0.54	0.71	0.51	0.62	0.63	0.61	0.72	0.43	0.46	0.52
Co	0.12	0.10	0.12	0.13	0.10	0.11	0.12	0.13	0.16	0.14	0.16	0.11
Cu	0.05	0.04	0.04	0.03	0.06	0.05	0.06	0.05	0.05	0.02	0.04	0.05
Pb	0.18	0.14	0.14	0.16	0.20	0.14	0.19	0.22	0.24	0.17	0.20	0.21
Zn	0.00	0.00	0.00	0.00	0.00	0.00	0.00	0.04	0.01	0.00	0.00	0.00
As	0.00	0.13	0.02	0.00	0.06	0.05	0.04	0.00	0.10	0.00	0.00	0.00
S	38.03	38.36	38.28	38.06	37.96	38.17	38.20	37.76	38.15	37.87	37.97	37.80
Total	99.92	100.12	99.92	100.04	99.94	100.00	99.33	99.64	99.92	100.13	99.98	100.15

Prospect										KLETTEN		
Sample	77/8/19.55			77/6/2.06			77/12/7.30			76.336e		
PYRRHOTITE	177	178	179	180	181	182	183	184	185	122	123	124
Fe	60.12	59.99	59.72	60.11	60.27	60.79	60.84	60.50	60.60	60.44	61.44	61.05
Ni	0.37	0.33	0.48	0.67	0.61	0.69	0.28	0.44	0.47	0.26	0.42	0.33
Co	0.12	0.11	0.13	0.10	0.15	0.11	0.11	0.13	0.14	0.17	0.16	0.14
Cu	0.08	0.09	0.07	0.06	0.08	0.08	0.13	0.10	0.05	0.02	0.04	0.03
Pb	0.07	0.09	0.10	0.10	0.08	0.09	0.08	0.09	0.06	0.18	0.14	0.18
Zn	0.00	0.01	0.00	0.02	0.00	0.00	0.00	0.00	0.03	0.03	0.02	0.06
As	0.05	0.05	0.04	0.11	0.01	0.05	0.09	0.09	0.11	0.10	0.11	0.13
S	38.83	38.55	38.92	37.98	38.07	38.30	38.02	38.49	38.52	38.67	37.65	37.68
Total	99.65	99.22	99.46	99.16	99.27	100.11	99.55	99.85	99.98	99.89	99.98	99.61

TABLE B.18 (continued) Pyrrhotite Analyses - Magmatic Sulfides

Prospect									
Sample	77.64			77.66			77.68		
PYRRHOTITE	125	126	127	128	129	130	131	132	133
Fe	61.58	61.50	61.24	62.34	61.27	61.23	60.39	59.99	60.16
Ni	0.19	0.25	0.18	0.12	0.19	0.33	0.46	0.29	0.31
Co	0.10	0.10	0.10	0.08	0.11	0.11	0.10	0.17	0.15
Cu	0.10	0.05	0.09	0.06	0.09	0.02	0.07	0.05	0.04
Pb	0.13	0.16	0.16	0.18	0.18	0.14	0.13	0.13	0.11
Zn	0.00	0.00	0.00	0.00	0.00	0.00	0.00	0.00	0.00
As	0.02	0.03	0.13	0.00	0.03	0.08	0.03	0.08	0.00
S	37.98	37.93	37.43	37.60	37.96	37.77	38.19	38.92	39.25
Total	100.11	100.02	99.32	100.40	99.83	99.69	99.36	99.63	100.03

TABLE B.19 Pentlandite Analyses - Magmatic Sulfides

Prospect	VAKKERLIEN											
Sample	75/27/6.20						75/27/10.40			75/27/6.60		
PENTLANDITE	32	33	34	38E	55E	70E	35	36	37	38	39	40
Fe	27.91	29.01	28.48	27.53	29.72	29.13	29.22	29.25	29.26	28.36	28.86	29.14
Ni	37.41	35.85	36.85	38.05	36.45	36.19	36.86	37.43	37.10	37.50	37.25	36.90
Co	1.03	1.06	1.17	1.21	0.88	1.35	0.98	0.91	0.96	1.09	1.05	1.03
Cu	0.00	0.01	0.01	nd	nd	nd	0.00	0.04	0.01	0.06	0.06	0.09
Pb	0.05	0.09	0.08	ND	ND	ND	0.17	0.17	0.13	0.11	0.17	0.15
Zn	0.00	0.00	0.00	nd	nd	nd	0.02	0.00	0.00	0.00	0.00	0.00
As	0.00	0.00	0.00	ND	ND	ND	0.08	0.00	0.00	0.00	0.06	0.02
S	32.47	32.24	32.36	32.95	32.98	32.83	32.65	33.03	33.07	32.73	32.82	32.89
Total	98.87	98.26	98.96	99.74	100.03	99.50	99.99	100.85	100.53	99.86	100.27	100.23

Prospect	OLKAR											
Sample	77/2/14.90			77/1/6.60a			77/2/15.00			77/3/8.65		
PENTLANDITE	1	2	3	4	5	6	7	8	9	10	11	12
Fe	27.68	27.80	27.79	28.39	27.42	28.32	28.28	28.56	28.17	25.34	26.19	27.07
Ni	32.60	32.46	32.52	32.96	33.16	33.25	32.88	33.08	33.18	29.74	30.06	30.67
Co	5.60	5.58	6.40	5.15	5.75	5.48	5.29	5.23	5.30	11.96	10.93	9.78
Cu	0.00	0.01	0.00	0.00	0.00	0.00	0.02	0.00	0.00	0.00	0.00	0.00
Pb	0.11	0.18	0.10	0.12	0.20	0.15	0.16	0.14	0.15	0.14	0.14	0.14
Zn	0.00	0.00	0.00	0.00	0.00	0.00	0.00	0.00	0.00	0.00	0.00	0.00
As	0.04	0.04	0.00	0.12	0.03	0.01	0.02	0.00	0.11	0.10	0.00	0.00
S	32.67	32.79	33.00	32.87	32.78	32.81	32.67	32.55	32.93	32.75	32.52	32.60
Total	98.71	98.86	99.82	99.60	99.34	100.03	99.31	99.57	99.86	100.03	99.83	100.27

TABLE B.19 (continued) Pentlandite Analyses - Magmatic Sulfides

Prospect											
Sample	77/4/23.70		77/1/10.60			77/4/31.56			77/2a/4.85		
PENTLANDITE	13	15	16	17	18	19	20	21	22	23	24
Fe	27.50	26.85	27.52	27.43	27.77	26.86	27.17	27.05	28.82	27.36	27.96
Ni	31.43	30.71	32.45	32.67	32.15	31.68	31.44	31.48	32.20	30.99	31.28
Co	8.24	9.46	7.08	7.12	6.75	8.26	8.61	8.53	4.74	7.47	6.55
Cu	0.00	0.00	0.00	0.00	0.00	0.00	0.02	0.00	0.01	0.04	0.04
Pb	0.15	0.09	0.10	0.13	0.13	0.12	0.07	0.18	0.17	0.15	0.10
Zn	0.00	0.00	0.00	0.00	0.00	0.00	0.00	0.00	0.00	0.00	0.00
As	0.01	0.00	0.00	0.00	0.00	0.13	0.00	0.00	0.00	0.07	0.06
S	32.65	32.53	32.59	32.54	32.68	32.33	32.11	32.29	32.84	32.83	32.89
Total	99.99	99.65	99.75	99.90	99.48	99.39	99.43	99.53	98.78	98.92	98.90

Prospect													
Sample	77/4/33.23						77/3/14.60	76.94					
PENTLANDITE	25	26	27	28	29	30	31	101E	107E	109E	113E	117E	121E
Fe	28.53	28.39	28.30	27.63	27.52	27.79	27.82	29.15	24.36	26.79	27.47	27.98	27.15
Ni	31.32	31.84	31.65	32.29	32.10	32.28	31.48	32.74	25.38	26.12	24.51	28.00	25.91
Co	5.92	5.89	5.79	6.73	7.06	6.83	6.99	4.83	17.92	14.10	14.46	10.34	12.77
Cu	0.01	0.01	0.06	0.00	0.00	0.00	0.00	nd	nd	nd	nd	nd	nd
Pb	0,14	0.14	0.18	0.05	0.07	0.11	0.09	ND	ND	ND	ND	ND	ND
Zn	0.00	0.00	0.00	0.00	0.00	0.01	0.00	nd	nd	nd	nd	0.21	0.28
As	0.00	0.01	0.06	0.00	0.00	0.00	0.00	ND	ND	ND	ND	ND	ND
S	32.89	32.76	32.66	32.35	32.02	32.45	32.40	32.74	32.90	32.89	33.42	33.17	33.13
Total	98.81	99.03	98.71	99.05	98.77	99.47	98.79	99.47	100.55	99.90	99.86	99.71	99.24

TABLE B.19 (continued) Pentlandite Analyses - Magmatic Sulfides

Prospect	SKJAERFJORDALEN											
Sample	76.101						78.71			78.76		
P	7E	11E	13E	14E	15E	16E	68	69	70	71	72	73
Fe	29.50	26.76	26.23	28.86	28.17	29.29	31.49	31.35	30.97	30.24	30.39	30.31
Ni	30.70	30.95	29.99	33.36	33.01	32.79	33.60	33.54	33.90	34.93	34.75	35.00
Co	7.24	9.90	11.56	5.40	6.34	5.01	1.98	1.95	2.13	1.87	1.72	1.86
Cu	0.33	nd	nd	0.23	0.23	nd	0.02	0.04	0.06	0.03	0.08	0.05
Pb	ND	ND	ND	ND	ND	ND	0.12	0.19	0.14	0.19	0.15	0.13
Zn	nd	nd	0.26	0.43	nd	nd	0.00	0.00	0.01	0.01	0.00	0.00
As	nd	nd	nd	nd	nd	nd	0.07	0.00	0.00	0.00	0.00	0.00
S	33.01	32.84	32.58	32.81	32.88	32.66	33.21	32.91	32.74	32.82	33.02	33.02
Total	100.79	100.44	100.62	101.09	100.63	99.78	100.49	99.99	99.94	100.07	100.12	100.37

Prospect													
Sample	78.67			78.72			78.77			77.339			
PENTLANDITE	74	75	76	472E	473E	474E	475E	476E	477E	83	84	85	86
Fe	30.76	31.65	31.79	29.07	29.48	29.43	29.64	29.39	29.33	30.24	30.35	30.81	29.46
Ni	31.36	31.31	30.85	30.61	30.70	31.62	36.39	35.96	36.72	32.83	33.93	33.97	35.22
Co	3.10	2.42	2.83	6.65	6.15	6.28	0.91	0.88	0.85	4.11	2.93	2.74	2.69
Cu	0.07	0.05	0.06	0.35	0.18	nd	0.24	nd	0.28	0.00	0.00	0.00	0.00
Pb	0.14	0.09	0.20	ND	ND	ND	ND	ND	ND	0.15	0.16	0.17	0.14
Zn	0.00	0.00	0.05	0.19	0.22	nd	nd	0.19	nd	0.00	0.00	0.00	0.00
As	0.06	0.16	0.12	0.35	nd	nd	nd	nd	nd	0.00	0.00	0.00	0.00
S	32.82	32.91	32.51	32.61	32.78	32.85	32.93	32.89	32.86	32.42	32.69	32.56	32.55
Total	98.30	98.59	98.42	99.83	99.51	100.18	100.11	99.31	100.04	99.75	100.07	100.25	100.07

TABLE B.19 (continued) Pentlandite Analyses - Magmatic Sulfides

Prospect												
Sample			77.299					77.300b			77.307	
PENTLANDITE	87	88	150E	152E	154E	160E	162E	206E	209E	216E	220E	227E
Fe	29.19	29.12	31.61	32.37	31.56	30.66	30.98	31.29	31.66	32.60	26.58	26.31
Ni	35.03	34.85	32.53	32.46	32.86	33.94	33.97	32.60	32.50	31.88	30.90	29.71
Co	3.00	3.28	2.83	2.70	3.13	3.49	3.08	3.27	2.81	3.04	10.31	10.85
Cu	0.00	0.01	nd	nd	nd	nd	nd	0.58	0.41	0.19	0.29	0.20
Pb	0.17	0.15	ND	ND	ND	ND	ND	ND	ND	ND	ND	ND
Zn	0.00	0.00	nd	0.36	0.21	0.27	nd	nd	nd	nd	nd	0.37
As	0.00	0.00	nd	nd	nd	nd	nd	nd	nd	nd	nd	nd
S	32.67	32.83	32.55	32.83	32.82	32.90	32.76	32.74	32.91	32.83	32.59	32.73
Total	100.07	100.24	99.52	100.72	100.58	101.26	100.78	100.48	100.29	100.54	100.67	100.19

Prospect										
Sample	78.64	78.65			77.330			77.316		
PENTLANDITE	456E	459E	460E	462E	100	101	102	103	104	105
Fe	29.40	29.67	29.46	29.29	30.12	30.44	29.97	30.25	30.54	30.14
Ni	33.60	33.71	33.97	34.23	34.78	35.15	34.96	35.43	35.24	35.49
Co	2.49	3.69	3.59	3.44	1.94	1.39	1.89	1.10	0.95	1.10
Cu	nd	nd	0.25	nd	0.11	0.08	0.10	0.04	0.11	0.06
Pb	ND	ND	ND	ND	ND	ND	ND	ND	ND	ND
Zn	nd	nd	nd	nd	ND	ND	ND	ND	ND	ND
As	nd	nd	nd	nd	0.05	0.11	0.03	0.04	0.03	0.00
S	32.75	32.73	32.97	32.99	32.93	32.89	33.04	32.93	32.84	32.85
Total	98.23	99.80	100.25	99.95	99.93	100.07	99.99	99.79	99.71	99.64

TABLE B.19 (continued) Pentlandite Analyses - Magmatic Sulfides

Prospect	GARDSJOEN					KALTBERGET					
Sample	77.36					76.KD.1					
PENTLANDITE	451E	452E	453E	454E	455E	41	42	43	441E	443E	445E
Fe	24.37	23.59	22.17	21.78	23.54	29.00	29.42	29.34	29.21	29.49	29.50
Ni	27.26	26.14	24.65	24.00	26.39	36.74	37.04	37.18	37.01	36.54	37.36
Co	16.37	18.52	21.41	22.15	18.52	0.98	0.84	1.00	1.53	1.42	1.17
Cu	0.25	0.19	0.19	nd	0.20	0.05	0.06	0.07	nd	nd	nd
Pb	ND	ND	ND	ND	ND	0.04	0.09	0.03	ND	ND	ND
Zn	nd	nd	nd	nd	nd	0.00	0.00	0.00	nd	0.36	0.25
As	nd	nd	nd	nd	0.28	0.12	0.04	0.13	nd	nd	nd
S	33.01	33.23	32.71	32.86	32.97	32.59	32.88	32.68	33.37	32.86	33.30
Total	101.26	101.68	101.14	100.81	101.90	99.53	100.36	100.43	101.12	100.68	101.58

Prospect											
Sample			77/12/5.50			77/12/6.10					
PENTLANDITE	447E	449E	44	45	46	47	48	49	78E	84E	86E
Fe	29.49	29.58	30.42	30.93	30.54	30.13	31.04	30.67	29.68	29.35	30.82
Ni	36.81	36.68	35.07	35.16	35.10	35.48	34.82	34.82	35.22	34.51	35.53
Co	1.32	0.89	1.57	1.58	1.69	1.76	1.55	1.52	1.47	1.92	1.54
Cu	nd	nd	0.07	0.05	0.03	0.06	0.03	0.07	nd	nd	nd
Pb	ND	ND	0.10	0.08	0.08	0.06	0.03	0.03	ND	ND	ND
Zn	0.20	nd	0.00	0.00	0.00	0.00	0.00	0.00	nd	nd	nd
As	nd	nd	0.04	0.00	0.00	0.03	0.04	0.08	ND	ND	ND
S	33.03	33.01	32.75	32.92	32.87	32.83	32.66	32.64	33.68	32.91	32.06
Total	100.85	100.17	100.02	100.74	100.31	100.36	100.16	99.83	100.06	98.70	99.95

TABLE B.19 (continued) Pentlandite Analyses - Magmatic Sulfides

Prospect												
Sample	76.294			76.293			77/8/19.55			77/6/2.06		
PENTLANDITE	50	51	52	53	54	55	89	90	91	92	93	94
Fe	29.81	30.04	29.99	30.59	30.51	30.15	29.85	30.13	29.89	30.40	30.41	30.26
Ni	35.34	35.22	35.31	34.39	34.77	34.89	35.71	35.12	35.09	35.52	35.63	35.13
Co	1.48	1.59	1.60	1.79	1.93	1.90	1.83	1.75	1.99	1.64	1.49	1.79
Cu	0.10	0.08	0.08	0.12	0.05	0.11	0.09	0.12	0.08	0.09	0.11	0.14
Pb	0.18	0.13	0.11	0.13	0.17	0.15	0.13	0.08	0.11	0.07	0.11	0.03
Zn	0.00	0.00	0.00	0.00	0.00	0.00	0.00	0.00	0.00	0.00	0.00	0.00
As	0.13	0.08	0.05	0.02	0.08	0.03	0.00	0.00	0.05	0.00	0.10	0.00
S	32.73	32.45	32.72	32.76	32.66	32.86	32.86	32.94	32.82	32.86	32.91	32.65
Total	99.79	99.58	99.88	99.80	100.17	100.08	100.47	100.13	100.04	100.58	100.77	100.00

Prospect				KLETTEN								
Sample	77/12/7.30			76.336e			77.64					
PENTLANDITE	95	96	97	56	57	58	59	60	61	171E	173E	177E
Fe	30.91	30.59	30.80	28.19	27.83	28.73	32.02	31.04	30.07	32.80	32.30	33.32
Ni	34.67	34.96	34.83	33.72	33.65	31.58	33.87	33.71	31.72	35.10	34.54	33.92
Co	1.80	1.45	1.49	5.26	5.56	6.98	0.07	2.05	5.09	0.23	0.24	0.15
Cu	0.07	0.11	0.09	0.07	0.14	0.06	0.10	0.09	0.13	nd	0.29	nd
Pb	0.04	0.10	0.13	0.12	0.14	0.13	0.17	0.12	0.19	ND	ND	ND
Zn	0.00	0.00	0.00	0.00	0.00	0.00	0.00	0.01	0.00	nd	nd	00.27
As	0.04	0.00	0.00	0.06	0.00	0.02	0.11	0.00	0.00	ND	ND	ND
S	32.79	32.91	32.78	32.83	32.78	32.86	32.93	32.93	32.39	33.14	32.65	32.57
Total	100.31	100.12	100.12	100.26	100.11	100.37	99.25	99.95	99.59	101.27	100.01	100.22

TABLE B.19 (continued) Pentlandite Analyses - Magmatic Sulfides

Prospect											
Sample	77.66				77.68						
PENTLANDITE	62	63	64	187E	65	66	67	194E	198E	200E	203E
Fe	28.75	29.90	29.04	31.24	27.33	26.49	26.70	30.53	30.52	29.92	34.13
Ni	31.70	32.11	32.72	32.66	32.76	31.79	32.15	32.41	32.98	32.20	27.78
Co	6.45	4.61	5.02	2.91	6.47	8.63	8.19	4.93	3.65	4.98	3.76
Cu	0.12	0.13	0.09	nd	0.15	0.10	0.14	nd	0.32	0.30	0.26
Pb	0.11	0.13	0.15	ND	0.09	0.11	0.16	ND	ND	ND	ND
Zn	0.03	0.00	0.02	nd	0.00	0.01	0.03	0.25	nd	0.24	0.37
As	0.06	0.00	0.07	ND	0.01	0.09	0.04	0.39	nd	nd	nd
S	32.87	32.69	32.92	32.55	32.89	32.58	32.82	32.50	32.74	32.67	33.52
Total	100.09	99.57	100.03	99.36	99.71	99.79	100.23	101.01	100.22	100.31	99.83

TABLE B.20 Chalcopyrite Analyses - Magmatic Sulfides

Prospect	VARKERLIEN			OLKAR							
Sample	75/27/6.20	75/27/10.40	75/27/6.60	77/2/14.90	77/1/6.60a	77/2/15.00	77/3/8.65	77/4/23.70	77/1/10.60	77/4/31.56	77/5/32.04
CHALCOPYRITE	86	90	89	76	75	74	79	78	77	82	81
Fe	29.85	30.67	30.40	30.27	30.42	30.18	29.60	29.61	29.30	29.53	29.80
Ni	0.01	0.03	0.02	0.06	0.03	0.09	0.00	0.00	0.09	0.01	0.02
Co	0.09	0.05	0.06	0.03	0.04	0.07	0.05	0.04	0.05	0.05	0.04
Cu	34.57	34.42	34.40	34.21	34.53	33.84	34.40	34.18	34.27	34.58	34.42
Pb	0.10	0.21	0.13	0.15	0.15	0.08	0.18	0.22	0.18	0.14	0.15
Zn	0.05	0.09	0.17	0.00	0.02	0.00	0.00	0.00	0.02	0.01	0.04
As	0.00	0.18	0.07	0.00	0.00	0.00	0.10	0.10	0.00	0.00	0.43
S	34.11	34.35	34.47	34.46	34.39	34.23	34.71	34.54	34.65	34.40	34.46
Total	98.78	100.00	99.71	99.18	99.57	98.50	99.05	98.70	98.56	98.72	99.38

Prospect						SKJAERFJELLEN					
Sample	77/4/27.56	77/2e/4.05	77/4/33.23	77/2/3.26	77/3/14.60	78.71	78.64	78.76	78.65	78.68	78.67
CHALCOPYRITE	80	85	84	83	87	102	101	100	105	104	103
Fe	29.65	29.65	29.86	29.97	29.74	30.76	30.29	30.46	30.31	30.68	30.41
Ni	0.02	0.00	0.00	0.01	0.02	0.02	0.01	0.03	0.03	0.03	0.03
Co	0.05	0.06	0.08	0.04	0.07	0.05	0.04	0.06	0.07	0.08	0.05
Cu	34.42	33.94	34.67	34.48	34.40	34.23	34.25	34.53	34.16	33.74	34.13
Pb	0.06	0.16	0.25	0.22	0.12	0.07	0.08	0.02	0.12	0.13	0.22
Zn	0.03	0.05	0.10	0.13	0.12	0.01	0.08	0.05	0.08	0.06	0.00
As	0.14	0.05	0.05	0.00	0.00	0.11	0.04	0.06	0.01	0.15	0.14
S	34.32	34.80	34.76	34.58	34.17	34.52	34.65	34.50	34.33	34.29	34.56
Total	98.70	98.71	99.77	99.43	98.65	99.78	99.43	99.70	99.11	99.17	99.53

TABLE B.20 (continued) Chalcopyrite Analyses - Magmatic Sulfides

Prospect					GARDSJOEN	KALTBERGET			
Sample	78.72	78.77	77.304	77.339	77.34	76.KD.1	77/12/5.50	77/12/6.10	76.294
CHALCOPYRITE	109	108	106	110	88	93	92	91	96
Fe	30.68	30.68	30.11	31.11	31.06	30.96	30.78	31.10	30.36
Ni	0.02	0.02	0.02	0.00	0.00	0.02	0.04	0.01	0.00
Co	0.06	0.06	0.08	0.05	0.03	0.04	0.02	0.05	0.05
Cu	34.02	34.02	33.36	33.89	33.97	34.90	34.43	34.50	34.50
Pb	0.13	0.13	0.07	0.14	0.16	0.16	0.14	0.16	0.15
Zn	0.10	0.10	0.05	0.02	0.08	0.06	0.02	0.09	0.01
As	0.00	0.00	0.00	0.00	0.00	0.21	0.03	0.14	0.03
S	34.27	34.27	34.53	34.06	34.46	34.00	34.27	34.20	33.90
Total	99.27	99.27	98.23	99.28	99.77	100.34	99.74	100.25	99.01

Prospect					KLETTEN			
Sample	76.293	77/8/19.55	77/6/2.06	77/12/7.30	76.336e	77.64	77.66	77.68
CHALCOPYRITE	95	114	113	112	94	99	98	97
Fe	30.68	30.98	30.77	30.25	30.70	31.10	31.16	30.85
Ni	0.04	0.03	0.01	0.01	0.03	0.00	0.00	0.00
Co	0.05	0.06	0.03	0.04	0.05	0.07	0.08	0.12
Cu	34.72	34.33	34.23	34.19	34.55	33.59	33.57	34.08
Pb	0.16	0.05	0.14	0.08	0.11	0.21	0.18	0.11
Zn	0.00	0.04	0.01	0.10	0.03	0.13	0.02	0.07
As	0.07	0.06	0.09	0.00	0.17	0.01	0.02	0.00
S	34.34	34.53	34.20	34.61	34.27	34.09	34.24	34.51
Total	100.04	100.08	99.49	99.28	99.91	99.19	99.27	99.74

TABLE B.21 Pyrite Analyses - Magmatic Sulfides

Prospect	OLKAR			KLETTEN									
Sample	77/1/10.60	77/2a/4.85		76.336e				77.66			77.64		
PYRITE	74	75	76	77	78	79	80	81	82	83	84	85	86
Fe	45.98	44.89	46.37	45.39	46.85	46.76	46.90	46.23	45.65	44.80	46.04	43.06	47.25
Ni	0.15	1.13	0.03	0.04	0.03	0.03	0.06	0.00	0.00	0.00	0.00	0.00	0.11
Co	0.11	0.12	0.08	1.97	0.35	1.04	0.95	1.43	1.81	2.32	1.28	4.56	0.12
Cu	0.05	0.04	0.08	0.01	0.06	0.01	0.04	0.04	0.04	0.12	0.02	0.11	0.02
Pb	0.24	0.16	0.21	0.24	0.22	0.24	0.20	0.14	0.19	0.26	0.25	0.22	0.20
Zn	0.00	0.00	0.00	0.00	0.00	0.00	0.00	0.03	0.00	0.00	0.01	0.00	0.03
As	0.00	0.00	0.00	0.17	0.16	0.13	0.00	0.14	0.14	0.14	0.08	0.17	0.00
S	53.03	52.61	53.43	53.29	53.32	53.29	53.44	53.52	53.57	53.40	53.79	53.14	53.54
Total	99.57	98.96	100.20	101.11	101.04	101.50	101.58	101.55	101.40	101.03	101.47	101.26	101.28

TABLE B.22 Gersdorffite and Cobaltite Analyses - Magmatic Sulfides

Prospect	VAKKERLIEN	OLKAR	
Sample	75/27/6.20	77/2/14.90	77/1/6.60a
	45E (Gersdorffite)*	1 (Cobaltite)	2 (Cobaltite)
Fe	6.17	5.26	4.81
Ni	23.02	7.20	4.71
Co	8.55	23.51	26.65
Cu	nd	0.21	0.00
Pb	nd	0.00	0.06
Zn	nd	0.01	0.00
As	ND	44.63	43.97
S	17.00	19.63	19.46
Total	54.75	100.46	99.68

* partial analysis

TABLE B·23 Violarite Analyses - Magmatic Sulfides

Prospect	OLKAR				SKJAERDALEN				KALTBERGET				
Sample	76.101				78.64	78.65	77.307		76.KD.1				
VIOLARITE	8aE	10aE	12aE	17aE	458E	461E	228	235	442E	444E	446E	448E	45(
Fe	24.04	27.32	23.48	26.22	22.50	26.12	26.90	19.91	31.14	30.95	31.30	33.01	31.
Ni	24.91	21.49	26.07	22.58	27.16	24.78	20.27	28.66	24.33	22.43	23.37	22.78	23.
Co	6.80	6.72	6.55	6.42	3.19	3.78	10.02	8.91	1.37	1.43	1.44	1.38	1.
Cu	0.22	nd	0.25	0.20	nd	0.20	nd	0.36	nd	nd	nd	nd	nd
Pb	ND	ND	ND	ND	ND	ND	ND	ND	ND	ND	ND	ND	ND
Zn	nd	0.25	0.23	nd	nd	0.27	0.20	nd	0.23	0.27	nd	nd	nd
As	nd	nd	nd	nd	nd	nd	nd	nd	nd	nd	nd	nd	nd
S	41.16	41.75	41.59	41.32	37.67	39.82	40.40	39.01	40.68	40.05	40.21	39.09	40.
Total	97.13	97.54	98.17	96.74	90.52	94.99	97.80	97.05	97.76	95.13	96.33	96.26	96.

							KLETTEN		
Sample	76.245						76.300b		
	1aE	2aE	3aE	4aE	5aE	6aE	a5	a6	21E
Fe	23.98	27.24	24.40	23.34	24.67	24.80	10.79	10.46	12.50
Ni	29.32	25.71	28.26	30.77	27.87	28.60	25.52	25.65	26.06
Co	2.72	3.62	3.85	3.23	3.75	3.24	20.22	21.90	20.40
Cu	nd	nd	0.28	0.32	nd	nd	0.00	0.12	0.18
Pb	ND	ND	ND	ND	ND	ND	ND	ND	ND
Zn	0.20	nd	nd	nd	nd	nd	ND	ND	ND
As	nd	nd	nd	nd	nd	nd	ND	ND	ND
S	42.41	41.52	41.71	41.34	41.23	41.42	42.16	42.05	40.66
Total	98.64	98.09	98.51	99.00	97.52	98.06	98.71	100.18	99.80

TABLE B.24 Pyrrhotite Analyses - Gula Schists

Sample	78.84					78.59					76.9				
PYRRHOTITE	161	162	163	164	165	166	167	168	169	170	192	193	194	195	196
Fe	60.51	60.76	60.42	59.50	61.03	61.12	61.15	61.19	61.36	61.48	61.19	61.19	61.33	61.34	60.86
Ni	0.37	0.42	0.20	0.13	0.31	0.11	0.09	0.11	0.11	0.11	0.34	0.30	0.27	0.29	0.30
Co	0.15	0.17	0.11	0.13	0.14	0.13	0.14	0.12	0.13	0.13	0.19	0.15	0.12	0.16	0.11
Cu	0.04	0.09	0.12	0.07	0.07	0.02	0.07	0.05	0.03	0.07	0.04	0.07	0.06	0.02	0.08
Pb	0.12	0.07	0.09	0.11	0.14	0.13	0.09	0.09	0.10	0.05	ND	ND	ND	ND	ND
Zn	0.00	0.00	0.00	0.00	0.00	0.00	0.00	0.00	0.00	0.00	ND	ND	ND	ND	ND
As	0.00	0.00	0.00	0.00	0.01	0.00	0.00	0.00	0.00	0.00	0.09	0.00	0.03	0.00	0.00
S	37.87	37.75	38.78	38.40	38.10	38.03	37.99	38.20	38.02	38.15	38.27	38.31	38.20	38.24	38.31
Total	99.06	99.25	99.73	98.34	99.81	99.55	99.54	99.75	99.75	100.01	100.11	100.02	100.01	100.04	99.66

APPENDIX C

WET-CHEMICAL ANALYSIS OF MAGMATIC SULFIDE ORES

In order to allow analysis of the silicate component of Skjaekerdalen ores, and to ensure the greatest possible dissolution of the sulfides during preparation of the sample solutions, a rough separation of the silicate and sulfide fractions was performed.

C.1 Separation of Sulfide and Silicate Fractions.

Trimmed and washed samples were reduced to 0.5 mm chips and powder by a pre-contaminated Sturtevant open-door roll jaw-crusher as described in A.1. The samples were then split by the "cone and quarter" method. To facilitate separation, and to prevent contamination of the sulfide fraction by Co, the samples were ground slowly in a Fritsch automatic agate mortar and pestel. Sieving was carried out frequently, at 80 mesh, to prevent the excessive reduction of the sulfide fractions to dust. When all of the sample had passed 80 mesh, it was washed repeatedly to remove dust.

The sulfide and silicate fractions were separated using the heavy liquids di-iodomethane and Clerici solution. Di-iodomethane was usually sufficiently dense to produce a good separation. However, where olivine and pyroxene occurred, a further separation using Clerici solution was required.

While the separation of silicates from sulfides was usually good (>95% optically), the sulfide fraction usually contained greater proportions of entrained silicate phases (generally less than 15% optically, but approximately 30% in one sample). However, as the ratio of silicates to sulfides in the samples is usually large (the one example of a Matrix ore gave a 90% pure sulfide separate, all other samples were of Disseminated or Finely Disseminated ores), it is believed that this will have

had little effect on the major element analyses presented in Table A.9.

C.2. Preparation of Sample Solutions.

Approximately 0.5 g of sample were accurately weighed into a glass beaker. The sulfide phases were decomposed by attack with nitric acid and bromine (Dolezal et al., 1968, pp. 57). When activity had ceased, the solution was warmed gently on an asbestos plate over a steam bath to evaporate the bromine. Any globules of sulfur which formed were broken up. A second attack with nitric acid and bromine was carried out, and the solution evaporated to dryness to remove the nitric acid. The beakers were then thoroughly washed down, a little hydrochloric acid added, and the solutions evaporated to dryness (this operation was repeated once). After addition of a little water, hydrochloric acid is added, and the salts dissolved. The solution is then carefully washed into a flask and diluted to 100 ml. The undissolved residue was examined optically in a refractive index oil, and mounted and polished on an araldite block, and found to consist only of silicate and oxide minerals.

C.3. Determination of Ni, Cu, and Co by Atomic Absorption Spectrophotometry.

The instrument used was a Varian Techtron Model AA-4 Atomic Absorption Spectrophotometer. The sample solutions were diluted to the range 0-5 ppm, and calibrated against working standard solutions containing 0, 1, 2, 3, 4, and 5 ppm of Ni, Cu, and Co. The instrument conditions were as recommended in the makers handbook, and the wavelengths used were as follows:

Ni - 232.0 n m

Cu - 324.7 n m

Co - 240.7 n m.

Interference effects were assumed to be minimal (Thompson and Reynolds, 1970, pp. 48, 49, and 60), while the degree of non-specific background absorption was investigated by use of a Hydrogen Continuum lamp, and found to be negligible. On the instrument used, a precision of better than 5% (standard deviation as % of amount of element present) is usual (Saunders, pers. comm., 1979).

C.4 Determination of Fe by Colorimetric Spectrophotometry.

The instrument used was a Perkin-Elmer Model 550 (UV-VIS) Spectrophotometer, and the method was essentially that outlined by Sandell (1959, pp. 542), using ammonium thiologlycolate solution. The sample solutions were diluted to the range 0-15 ppm. Before addition of the colorimetric solution, sodium citrate solution was added to prevent the precipitation of metal hydroxides. The colour was compared soon after development with that produced by standard solutions containing 0, 5, 10, and 15 ppm of Fe, using 1 cm cells in the spectrophotometer at wavelength 540 n m.

The colour is independent of the exact concentration of thiologlycolate solution used, and of pH in the range 6-11. Sandell (1959, pp. 543) notes the possibility of interference by Co and Ni. However, for analysis of magmatic sulfides, the extreme dilution of these elements relative to Fe allow such effects to be ignored. On the instrument used, a precision of better than 1% (standard deviation as % of amount of element present) is usual (Saunders, pers. comm., 1979).

APPENDIX D

EXPLANATION OF ANALYSIS TABLES IN APPENDICES A-C.

D.1 Samples.

Sample numbers such as 77/12/6.10 refer to drill core samples. The first group of characters indicates the year of sampling; the second group indicates A/S Sulfidmalm drill-hole number; and the third gives depth in metres. At Kaltberget, all samples referred to are from drill holes prefaced by 76/-, such that sample 77/12/6.10 is from drill hole 76/12.

All other sample numbers refer to mine, surface-exposure, or dump samples.

D.1.1 Massive volcanogenic ores.

Samples of ore from Lokken, Tverfjellet, and Killingdal deposits were provided by the operating companies.

Samples from Kvikne and Rostvangen were collected by the author from dumps.

Characters in parenthesis in Tables B.4-B.9 refer to sample names used in Table 4.6.

D.1.2 Magmatic ores.

See Table D.1.

D.2 Mineral Analyses.

Unless otherwise specified, all analyses represent core compositions. The letter "R" following the analysis number denotes a rim composition.

Energy-dispersive analyses are distinguished by the letter "E" following the analysis number; all others by wavelength-dispersive methods.

Other symbols used: ND - not determined

nd - not detectable.

D.3 Metagabbroic and Ultramafic Intrusions and Associated Magmatic Sulfide Mineralisation.

Samples of metagabbroic and ultramafic intrusives, and associated magmatic sulfide mineralisation referred to in this thesis are described below (Table D.1), according to the following characteristics.

SAMPLE: E - surface-exposure

D - dump

C - drill core

HOST: The silicate fraction of the rock is classified on a hand specimen basis, according to the proportion of leucocratic minerals present. The classification corresponds to a field-based rock nomenclature as shown

I - <10% - ultramafic

II - >10<50% - metagabbro

III - >50% - metadiorite

RELICT IGNEOUS SILICATE MINERALOGY (MIN):

1 - olivine

2 - orthopyroxene

3 - clinopyroxene

ORE-TYPE (as described in Chapter 5):

abbreviations INT - interstitial

FRAG - fragmental

ORE-GRADE (as described in Chapter 5):

abbreviations DISS - disseminated

F.DISS - finely disseminated

SUPERGENE ALTERATION (ALT): The presence of supergene alteration of pyrrhotite to marcasite, and pentlandite to violarite is indicated as follows:

alteration	pyrrhotite to marcasite	pentlandite to violarite
<25%	mc	vl
>25<75%	mc	vl
>75<100%	MC	VL
100%	MC	VL

ACCESSORY SULFIDE MINERALS (ASM): The following abbreviations denote the presence of sulfide minerals other than pyrrhotite, pentlandite, and chalcopyrite.

py - pyrite

ge - gersdorffite

Co - cobaltite

bn - bornite

cc - chalcocite

hz - heazlewoodite

mo - molybdenite

gn - galena

Where magnetite occurs as a metamorphic product of pyrrhotite, it is recorded as,

mt - magnetite.

TABLE D.1 Description of samples of metagabbroic and ultramafic intrusions, and associated magmatic sulfide mineralisation.

SAMPLE No.	SAMPLE	HOST	MIN	ORE-TYPE	ORE-GRADE	ALT	ASM	COMMENTS
VAKKERLIEN								
75/27/6.20	C	II	-	INT	MATRIX		py,ge	
75/27/6.60	C	II	-	INT	DISS			
75/27/10.40	C	II	-	INT	DISS		py	
OLKAR								
77/1/6.60a	C	-	-	BRECCIA	MASSIVE			
77/1/10.60	C	II	-	BRECCIA	STRINGER		Co,py	
77/2/3.26	C	III	-	INT	F.DISS			
77/2/14.80	C	-	-	BRECCIA	MASSIVE			
77/2/14.90	C	-	-	BRECCIA	MASSIVE		Co	
77/2/15.00	C	-	-	BRECCIA	MASSIVE		Co	
77/2a/4.85	C	II	-	BRECCIA	STRINGER		py	
77/3/8.65	C	II	-	BRECCIA	STRINGER		mo	
77/3/14.60	C	III	-	INT	DISS			
77/4/20.48	C	III	-	BRECCIA	STRINGER			
77/4/23.70	C	II	-	BRECCIA	DISS			
77/4/27.56	C	II	-	INT	DISS			
77/4/31.56	C	II	-	BRECCIA	STRINGER			
77/4/33.23c	C	III	-	BRECCIA	MATRIX		gn	
77/5/32.84	C	II	-	INT	F.DISS			no pentlandite
76.94	E	II	-	INT	F.DISS	mc		
76.101	E	II	-	BRECCIA	DISS	mc,VL		
76.106	E	II	-	BARREN	-			ultramafic xenolith
76.135	E	II	-	BRECCIA	STRINGER			
SKJAEKERDALEN								
(ARCHBOLD)								
78.64	E	I	-	INT	F.DISS	mc,VL		
78.65	E	I	-	INT	DISS	VL		
78.67	D	II	1,2,3,	INT	F.DISS	vl		
77.300a	D	II	1,2,3,	INT	DISS	vl		
77.300b	D	II	1,3,	INT	DISS	vl		
(HOMAN)								
78.68	D	I	3,	INT	MATRIX	VL		
77.304	E	III	-	INT	F.DISS			also chalcopyrite-rich vein (<1mm)
77.307	D	II	2,	FRAG+INT	MATRIX	mc,VL		
(St. OLAV)								
77.316	D	II	-	FRAG/INT?	DISS	vl		

TABLE D.1 (continued) Description of samples of metagabbroic and ultramafic intrusions, and associated magmatic sulfide mineralisation.

SAMPLE No.	SAMPLE	HOST	MIN	ORE-TYPE	ORE-GRADE	ALT	ASM	COMMENTS
SKJAEKERDALEN								
(ANTON BACHKE)								
78.71	D	I	2,3,	INT	DISS			
78.72	D	II	1,2,3,	FRAG+INT	F.DISS			
77.323	E	I	-	INT	DISS	vl		
(HOVED GRUVA)								
78.76	D	I	1,2,	INT	DISS	vl		
78.77	D	III	-	FRAG	DISS	vl		
(BARBARA BACHKE)								
77.291a	E	III	1,2,3,	BARREN	-			
77.291b	E	II	1,2,3,	INT	F.DISS			
77.339	E	II	-	INT	F.DISS			xenolith
	E	III	-	INT	DISS	vl		matrix
(SLIPERN)								
77.299	E	II	1,2,3	INT	DISS	vl		
77.326	E	II	2,3,	INT	F.DISS	vl		
77.330	D	II	-	INT	DISS	vl		
GARDSJOEN								
77.34	D	II	-	BRECCIA	MATRIX	VL		
77.36	D	II	-	BRECCIA	DISS	mc		
UNDAL								
77.91	E	II	1,2,3	BARREN	-			bn,cc,hz?,as minute (<0.02mm) intergrowths with chalcopyrite
77.94	E	II	1,2,3	BARREN	-			
77.96	E	II	3,	BARREN	-			
77.148	E	I	1,2,3	BARREN	-			
KALTBERGET								
MAIN BODY								
76/4/45	C	I	1,	BARREN	-			
76/4/49	C	I	-	BARREN	-			
77/6/1.5	C	I	-	INT	MATRIX			
77/6/2.06	C	I	-	INT	MATRIX			
77/8/17.77	C	I	-	INT	DISS			
77/8/19.55	C	I	-	INT	DISS	vl		
77/8/21	C	I	-	INT	MATRIX			
77/12/4.30	C	I	-	INT	MATRIX			
77/12/5.50	C	I	-	INT	MATRIX			
77/12/6.10	C	I	-	INT	MATRIX			
77/12/7.30	C	I	-	INT	DISS			

TABLE D.1 (continued) Description of samples of metagabbroic and ultramafic intrusions, and associated magmatic sulfide mineralisation.

SAMPLE No.	SAMPLE	HOST	MIN	ORE-TYPE	ORE-GRADE	ALT	ASM	COMMENTS
KALTBERGET								
MAIN BODY cont.								
77/12/7.55	C	I	-	INT	DISS			
76.245	E	I	-	INT	F.DISS	VL		
76.254	E	II	-	BARREN	-			felspathic border zone
76.293	E	I	-	INT	F.DISS			
76.294	E	I	-	INT	MATRIX	vl		
76.296	E	I	-	GLOBULAR	DISS			
SATELLITE BODY								
76.KD.1	D	I	-	BRECCIA	STRINGER	mc,vl		
KLETTEN								
76.300b	E	I		KLETTEN	F.DISS	VL	py,mt	
76.336e	E	I	1,2,3	KLETTEN	F.DISS		py,mt	
76.336h	E	II		KLETTEN	F.DISS		py	- no pyrrhotite, pentlandite or chalcopyrite; felspathic border zone.
77.52	E	I	1,2,3	KLETTEN	F.DISS		py,mt	
77.64	E	I	1,2,3	KLETTEN	F.DISS		py,mt	
77.66	E	I	1,3	KLETTEN	F.DISS		py,mt	
77.68	E	I	1,3	KLETTEN	F.DISS		mt	
GRAHO								
77.197	E	I	-	BARREN	-			

TRONDELAG

Localities & Place Names

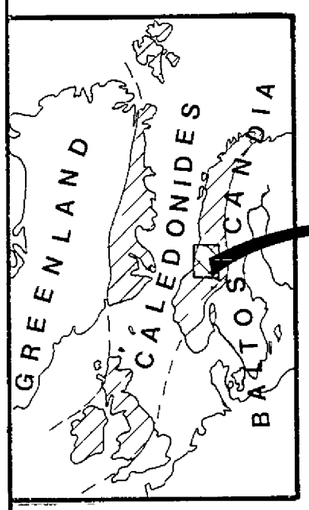

TRONDHEIMSFJORDEN

TRONDHEIM

STJØRDALEN

INNDALEN

HELGAADALEN

GAULDALEN

ORKLADALEN

LOKKEN

HOLONG

BULKA

OPPDAL

RENNEBU

UNDAL

HAUKFJELLET

INNSE

TVERFJELLET

DROYA

FLOTTUM

0 10 20 30 40 Km

LEGEND

MAPPED — UNMAPPED — TRAVERSE

MASSIVE ULTRAMAFIC DEPOSIT

METAGABBRO

ULTRAMAFIC

PLACE NAMES

OTHER SYMBOLS AS ON MAP 1

MAP 2 TRONDELAG - LOCALITIES AND PLACE NAMES

GEOLOGICAL MAP OF THE TRONDELAG REGION

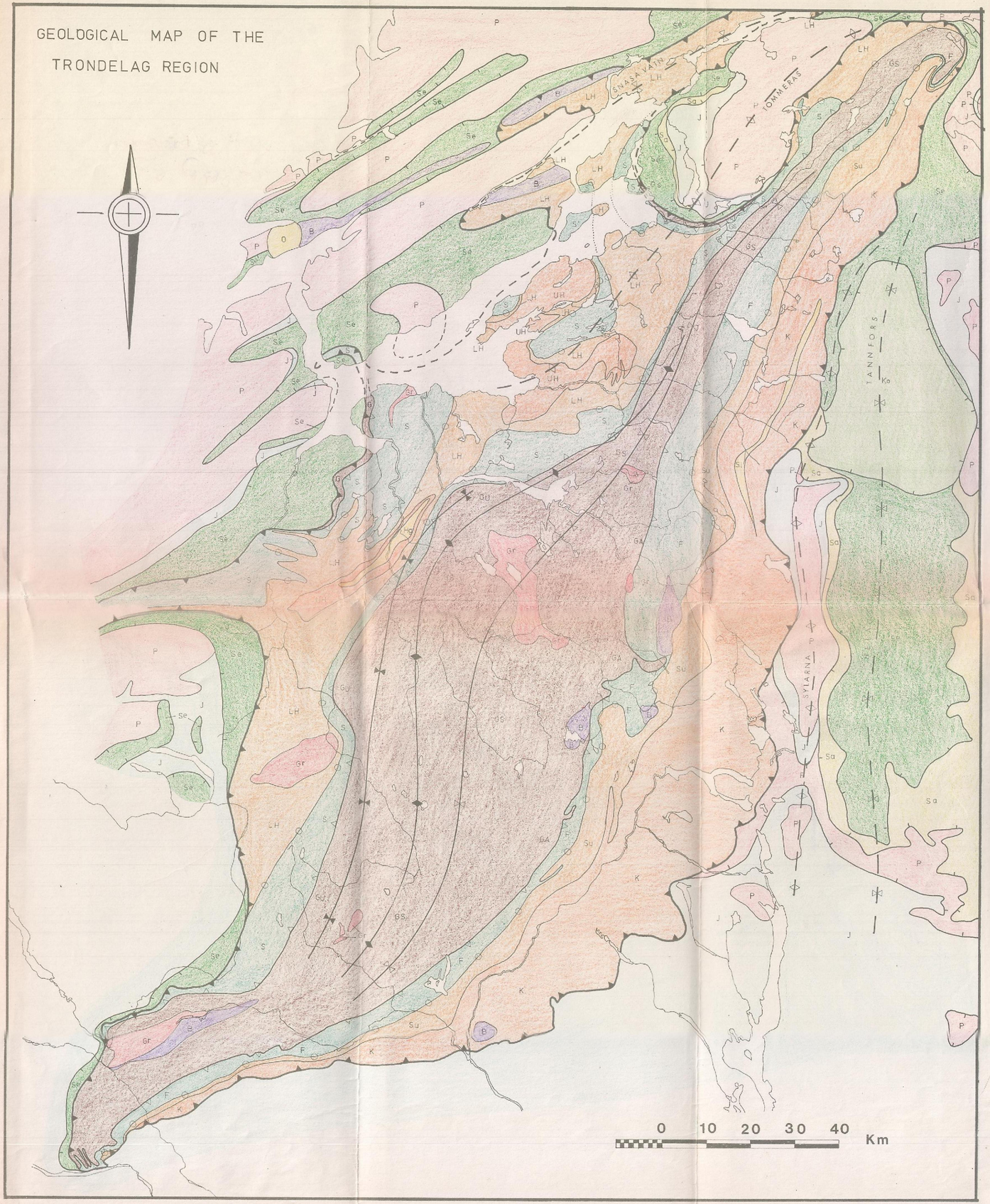

LEGEND

Geological boundary

Thrusts

Unconformity

D_4 Folds

GARDSJOEN SYNFORM — GROTLI ANTIFORM — SINGSAS SYNFORM — OTHER

O — LATE OROGENIC SEDIMENTS

Gr — GRANITE

Ub — GABBRO / ULTRABASIC

WESTERN TRONDELAG			EASTERN TRONDELAG
HORG GROUP	Hg	LLANDOVERIAN — Sl	SLAGAN GROUP
UPPER HOVIN GROUP	UH	K	KJOLHAUGEN GROUP
LOWER HOVIN GROUP	LH	CARADOCIAN / TREMADOCIAN — S	SULAMO GROUP
STOREN GROUP	St	? — Fu	FUNDSJO GROUP
GULA GROUP	Gu	? — Gu/As	UNDAL and ASLI FORMATIONS / SINGSAS FORMATION
SEVE-KOLI NAPPE COMPLEX	Ko		KOLI SUPERGROUP
	Se		SEVE SUPERGROUP
SARV NAPPE	Sa		SARV GROUP
	J		JAMTLAND SUPERGROUP
	P		PRECAMBRIAN BASEMENT

TRONDHEIM NAPPE COMPLEX

TRONDHEIM SUPERGROUP

WESTERN COMPLEX

EASTERN COMPLEX